

CR-183781

P-460

Fluctuating Pressures
in
Pump Diffuser
and
Collector Scrolls

Part I

Final Report

NASA Contract Number
NAS8-36223

(NASA-CR-183781) FLUCTUATING PRESSURES IN
PUMP DIFFUSER AND COLLECTOR SCROLLS, PART I
Final Report (Ingersoll-Rand Co.) 460 p
CSCL 200

N91-24554

Unclas
63/34 0019898

By

Donald P. Sloteman

Ingersoll-Rand Company
Research & Development Department
Pump Group
942 Memorial Parkway
Phillipsburg, New Jersey 08865

Prepared for George C. Marshall Space Flight Center
Marshall Spaceflight Center, Alabama 35812

Date of general release

06-91

DISCLAIMER NOTICE

This report was prepared as an account of work sponsored by the United States Government. Neither the employees, nor any contractors, subcontractors, or their employees make any warrant, expressed or implied, or assume any legal liability or responsibility for the accuracy, completeness, or usefulness of any information, apparatus, product, or process disclosed, or represent that its use would not infringe privately owned rights.

ABSTRACT

The cracking of scroll liners on the SSME High Pressure Fuel Turbo Pump (HPFTP) on hot gas engine test firings has prompted a study into the nature of pressure fluctuations in centrifugal pump stages. This study will quantify the amplitudes of these fluctuations and where they originate in the pump stage. To accomplish this, a test program has been conducted to map the pressure pulsation activity in a centrifugal pump stage. This stage is based on typical commercial (or generic) pump design practice and not the specialized design of the HPFTP. Measurements made in the various elements comprising the stage indicate that pulsation activity is dominated by synchronous related phenomena. Pulsation amplitudes measured in the scroll are low, on the order of 2% to 7% of the impeller exit tip speed velocity head. Significant non-synchronous pressure fluctuations occur at low flow, and while of interest to commercial pump designers, have little meaning to the HPFTP experience. Results obtained with the generic components do provide insights into possible pulsation related scroll failures on the HPFTP, and provide a basis for further investigation.

ACKNOWLEDGEMENTS

The results of the test work described in this report provide a unique contribution to the understanding of pressure pulsation activity in a centrifugal pump stage. Many individuals have contributed to the success of this program. Thanks must first go to Heinz Struck and the staff at Marshall Space Flight Center for originating the concept for the program, and providing the support and financial resources necessary to complete the work.

At Ingersoll-Rand, Dr. Paul Cooper, Director of Research, Pump Group provided the technical guidance and inspiration which made it possible to attempt this project. Walter J. Schmidt, Vice-President and General Manager, of Ingersoll-Rand's Engineered Pump Division provides the facility and administrative support which allows the R&D Department to pursue and execute programs such as this. Dr. Pawan Singh, Assistant Director of Research, contributed technical consultation on specific areas of fluid dynamic behavior. Mr. Kim Horten, R&D Technician, made sure that the hardware (both mechanical and electronic) was ready to operate in a reliable and consistent manner. Mr. Dave Varley put his efforts into generating a practical and flexible test vehicle design configuration.

The responsibility for instrumentation, data collection and data reduction belonged to Liberty Technology Inc. Thanks must first go to Mr. Robert Leon, who participated in the initial conceptualization of the program and was responsible (along with Kulite Corp.) for arriving at a successful pressure sensor configuration. Mr. Marty Dowling managed the instrumentation and data processing details (with support from Mr. Pete Phillips). The actual work of wiring up instrumentation, collecting and reducing data was done by Mr. Dave Powell, whose devotion of time and energy to the project was greatly appreciated.

EXECUTIVE SUMMARY

Background

Extensive cracking in the volute scroll liner of the Space Shuttle Main Engine (SSME) High Pressure Fuel Turbo Pump (HPFTP) during hot gas test firings has been observed. During the post test damage assessment, it was realized that little was known about the flow behavior past the impeller exit. Literature searches revealed little. A test effort would be required to measure the fluctuation pressures present in the various elements of the pump stage. The work should be general enough to be applicable to pumps of similar geometrical configuration.

Objective

The objective of the investigation is to quantify the fluctuating pressure behavior in the various stage elements (impeller, diffuser and collector scroll). The causes of pulsation activity must be determined and their dependence on specific pump geometry investigated. The effects of speed on scalability of these pulsations will also be established.

Test Hardware and Relationship to HPFTP Design

The pump geometry used in the HPFTP varies from commercial practice (which is referred to as generic design practice). The physical size limitations imposed by flight hardware, result in a design with higher head and flow coefficients than would be found on generic machines of similar stage size. This approach has undoubtedly been the reason for design features on the HPFTP which would not be found on its commercial brothers. The use of multiple length splitter blades in the impeller to

reduce blade loading is one example. Another is the unusual diffuser vane design where the vanes are configured to not diffuse, but to turn the flow in a more tangential direction. The scroll design is unusual in that the throat area at the exit of the scroll is not sized to match the flow exiting the third stage diffuser. The pump stage elements used in the test rig are either taken from or derived from commercial design practice. The configuration is the same as the HPFTP in that a last stage impeller (2 stages on this tester as opposed to 3 stages on the HPFTP) precedes a vaned diffuser, which in turn discharges into a single throat (or discharge) volute type scroll. The test hardware is equipped with a multitude of pressure sensors in these three key stage elements, to measure the instantaneous pressures at a variety of flows and speeds.

Test Results

Three different configurations of the generic design hardware were tested. Two diffuser designs (a 9-vane and an 11-vane design), and 3 impeller to diffuser clearance ratios (achieved by reducing the impeller diameter) were tested within these three configurations. The test results showed that the dominant pulsation activity occurred at synchronous frequencies (or at integer orders of running speed). The source of these pulsations is traced to the interaction of the impeller blades and diffuser vanes. The pulsations are largest in the vicinity of the interaction, and can be as high as 20% to 30% of the impeller tip speed velocity head. These values are a function of diffuser and impeller blade loading, impeller to diffuser clearance ratio, and flow rate (affecting the angle of attack to the diffuser vane leading edge). Pulsation values measured in the scroll never exceeded 7% of the impeller exit tip speed

velocity head. The 7% value was for the case where the impeller to diffuser clearance ratio was .021 of the impeller radius and the flow was at a quarter of the design condition. At higher flows and larger clearances this amplitude is decreased to about 3%. This amplitude, scaled to HPFTP conditions would result in a peak-to-peak pulsation of about 53 psi. Some non-synchronous pulsation events were encountered in the diffuser and impeller. However, these occurred at very low flow rates and so are not considered directly applicable to the HPFTP experience.

Conclusions

1. The combination of vane numbers of the impeller (24) and diffuser (13) in the HPFTP is favorable for minimizing synchronous pulsations arising from impeller to diffuser interaction. However, this is true only if the 12 exit splitter vanes are effective at sharing the blade loading (ie. separation has not occurred upstream of the splitters, rendering them ineffective). If the splitters are ineffective, the impeller exit blade number becomes 12 and is likely to cause strong synchronous pulsations.
2. The mismatch of scroll exit area to the diffuser exit area, and the resulting circumferential pressure gradient may be the source for unsteady flow and pressure fluctuations.
3. The presence of even low level pulsations in the scroll can excite the natural frequency of that component. The presence of a multitude of balance holes communicating to the surrounding chamber may also affect the phase of pulsations in the scroll liner. These out of phase pulsations

could result in larger forces on the scroll liner and cause alternating stresses on local sections.

4. The change in pump rpm in going from 100% to 109% thrust results in a 12.5% increase in pulsation amplitude. Assuming that pulsation amplitudes in the HPFTP scroll are approximately 3% of the impeller exit tip speed velocity head, the peak-to-peak amplitude in the scroll is 22 psi at 100% thrust condition. At 109% thrust, this amplitude would be about 27 psi.

Questions raised by this study include how effective are the impeller splitter blades at sharing the impeller blade loading at the exit of the impeller, what impact does the design of the diffuser guide vanes have on flow entering the scroll and on the interactions with the exit flow field of the impeller and finally what are the vibratory modes for the scroll liner and could it be excited by low level pulsations which are synchronous in nature?

TABLE OF CONTENTS

PAGE NUMBER

Disclaimer Notice	i
Abstract	ii
Acknowledgements	iii
Executive Summary	iv
Table of Contents	viii
List of Figures	x
List of Tables	xi
Nomenclature	xii
Introduction	1
Literature Survey	4
Discussion of Hardware Design Approaches	7
Experimental Techniques	19
Validation and Comparison of Test Data	26
Data Analysis and Interpretation	33
Synchronous Data	49
Unsteady, Non-Synchronous Data	169
Conclusions	191
References	198

TABLE of CONTENTS

cont'd

PAGE NUMBER

Appendices

A - Literature Search	A1
B - Test Hardware Design Details	B1
C - "Fluctuating Pressures in Pump Diffusers and Collector Scrolls"	C1
D - Summary of Steady State Test Data	D1
E - Summary of Synchronous Pulsation Test Data	E1

LIST OF TABLES

PAGE NUMBER

Table 1 - Comparison of Operating Conditions for the HPFTP and the Generic Design Test Hardware	9
Table 2 - Configuration Guide	17
Table 3 - Operating Condition Guide	36
Table 4 - Synchronous Pressure Pulsation Amplitudes	47
Table 5 - Table of Impeller/Diffuser Interactions	93

LIST OF FIGURES

	PAGE NUMBER
Figure 1 - Comparison of Velocities in Generic Design and in the HPFTP	11
Figure 2 - Configuration C, Cutwater Extension Modification	14
Figure 3 - Performance Curves and Operating Characteristics of the HPFTP	16
Figure 4 - Cross-section of Test Pump	18
Figure 5 - Comparison of Pressure Pulsations Measured on the Impeller O.D.	27
Figure 6 - Comparison of Pressure Pulsations Measured Along the Diffuser Vane	29
Figure 7 - Comparison of Pressure Pulsations from Test and from Analysis	31
Figure 8 - Definition of Nomenclature Used on Synchronous, Time-Averaged, Pressure Waveform Plot	34
Figure 9 - Definition of Nomenclature Used on Plots Showing the Rotation Based Frequency Components of the Pressure Waveform	35
Figure 10 - Pressure Sensor Mounting Locations	37
Figure 11 - Scroll Sensor Mounting Locations	38
Figure 12 - Sidewall Sensor Mounting Locations	39
Figure 13 - Diffuser Passage Sensor Locations	40
Figure 14 - Diffuser Passage Sensor Locations	41
Figure 15 - Impeller Sensor Mounting Locations	42
Figure 16 - Impeller Sensor Mounting Locations	43

NOMENCLATURE

A = Area

D = Diameter

D_3/D_2 = Diffuser to Impeller Clearance Ratio

g = Gravitational Constant

H = Head per Unit Mass

P = Pressure

Q = Volumetric Flow Rate

r = Radius

U = Peripheral Velocity of Impeller

V = Velocity

Ω = Angular Velocity

Φ = Flow Coefficient

ρ = Fluid Density

Subscripts

a,b,c,d Locations Between Impeller Exit and Diffuser Exit

m Meridional Component

th Scroll Throat

2 Impeller Exit Location

3 Diffuser Inlet Location

- Fluctuation Component

θ Tangential Component

INTRODUCTION

Concern over cracking of the volute/scroll liner on the Space Shuttle Main Engine (SSME), High Pressure Fuel Turbo Pump (HPFTP) which has occurred during hot gas test firings, has caused the initiation of a program to obtain information regarding the flow behavior in the vicinity of the diffuser exit and scroll passage of that pump. Specifically, the fluctuating pressures present in this region are of primary interest since the interaction of these fluctuations with the mechanical response of the scroll liner determines the structural integrity of scroll itself. The influence of the various hydraulic design parameters, on these fluctuating pressures, is another area of interest. The investigation of the nature of these fluctuating pressures, or pressure pulsations, were conducted on a pump than can be characterized as being of generic design. The term generic means a pump of configuration similar to that of the SSME HPFTP but of commercial design practice. This configuration consists of a multistage diffuser pump with a single volute type scroll collector around the final stage. The elements of the pump test rig include the impeller, diffuser and collector, and are based on typical commercial design practice. Two of the three elements are actual production designs. The various components of the test pump are instrumented with pressure sensors to obtain the static as well as the fluctuating (or dynamic) components of the pressure signal at each sensor location. This fluctuating data was synchronized to the shaft position, so that information from all sensors is in phase.

Prior to testing, a literature search was conducted to identify previous test efforts, and incorporate ideas coming from those sources into this test program. It was found that no published work attempted to measure fluctuating pressures in a centrifugal pump stage in as comprehensive a manner as that defined here. Some test results do exist in the literature and provide a means to validate and a comparison with the results from this program.

Three different configurations of hardware were tested in a closed loop (having a total system volume of 2500 gallons). Tests were conducted at constant speed, with de-aerated cold water, at an NPSH high enough to suppress cavitation. Parameters which vary with each configuration include three different impeller to diffuser clearance ratios and two different diffuser vane numbers. Results unique to each configuration have been identified. For each configuration the scroll was instrumented with eight pressure sensors; each diffuser passage contained a minimum of two pressure sensors (at inlet and discharge) and each impeller passage was equipped with a minimum of one pressure sensor. Extra sensors were mounted on suction and pressure surfaces of an impeller vane, on the stationary sidewalls adjacent to the rotating impeller, and in one diffuser passage an array of three sensors at three radii were installed. Not all configurations utilized these extra sensors.

FM tape is used to record pressure signals from each sensor simultaneously, for later analysis. This allows the pressure waveforms for each location to be displayed in phase with the other sensors. Data was obtained over a range of flows (25% to 125% of design flow) and for

two or three speeds. The data reduction included presentation of the data in three different formats. First, all sensors were synchronous time averaged over a minimum of 700 shaft revolutions. This technique eliminates noise and random events, and leaves an average waveform from which the frequency spectrum can be obtained. This presentation includes synchronous pulsation data only. Secondly, the frequency spectrum for specifically selected sensors were obtained without synchronous averaging in order to identify pulsation activity not related to rotation (or non-synchronous hydraulic behavior). This type of presentation shows information related to piping resonances and structural vibrations which induce pulsations. Thirdly, the basic pressure waveforms can be examined over many rotations to identify pressure fluctuations which are not periodic and best described as random.

A separate section is devoted to the display and explanation of results from the test data. The details regarding the generation, the frequency and amplitude of the pressure pulsations are given in this section. Information on scaling with speed is also presented.

Since the test work here is conducted on generically designed hardware, and not on models of the HPTFP, some interpretation is necessary to relate these results to the SSME experience. The test work has led to some ideas relating to the problem of scroll cracking on the HPFTP. A section of this report includes a discussion of the applicability of these test results to HPFTP hardware.

LITERATURE SURVEY

In accordance with the contract, a literature search was conducted to identify sources of information regarding pressure pulsation activity in centrifugal pumps. This search was conducted by Ingersoll-Rand corporate library staff, using the Dialog data base. An internal review of known references relating to pressure pulsations in commercially derived pumps was also conducted. The internal review utilized references produced in the Technical Proposal for this contract. One reason for conducting this search was to provide some guidance in the formulation of a test program to meet the contractual goals for the program. The result of the computer search is included in Appendix B. These references were of little help since they really do not address the detailed measurement of pulsation activity in the various components of the centrifugal pump (impeller, diffuser and volute scroll). References (1) thru (5) are relevant in terms of understanding and quantifying pulsation activity. However, not even these sources provide a complete mapping of pressure pulsation activity in all parts of the pump.

References (1) thru (5) are useful in comparison with data collected in this program. A summary of these references follow.

Ref 1. Kanki, et al. The purpose of this paper is to investigate the various radial forces imposed on the pump rotor and their effects on rotordynamics. In determining these forces (synchronous in nature) the writers have collected pressure pulsation data from single sensors located on the impeller, in a diffuser, and in the collector. No comprehensive

mapping of pulsation activity was done. The experimenters do show that low flow conditions result in higher, poorly defined low frequency pulsation activity, the result of possible rotating diffuser stall. They also show that for their hardware, the amplitudes of synchronous pulsations decrease with decreasing flow rate. Details of these results are included in a later section, where comparison with this program's test data are made.

Ref 2. Bolleter. In this paper, the author presents an approach used to understanding the interaction of the impeller vanes with stator vanes. This resulting synchronous behavior can take the form of pressure pulsations, radial forces, torsional forces and impeller structural excitation. The simple analysis procedure provides guidance in selection of proper combinations for impeller and stator vane numbers. Reference to this procedure is made in the Data Analysis and Interpretation section of this report.

Ref 3. Sano. The data included in this paper shows that piping resonances are a source of pressure pulsations measured in the discharge of a volute type pump. This behavior is non-synchronous and similar results will be observed in the test results described later.

Ref 4. Iino. This analytical study was conducted to examine the effects of interaction between impeller and diffuser on dynamic radial loads exerted on a pump rotor. The analysis utilizes a two-dimensional potential flow model. Viscous effects are ignored. The conclusions reached are 1) the pulsation amplitudes decrease with increased

impeller/diffuser clearance and 2) the pulsation amplitude is highly dependent on the load distribution imposed on the diffuser blades. Comparison of these results with test data from this program indicate that the model predicts higher pulsation amplitudes than actually exist.

Ref 5. Brennan et al. The work described in this paper includes testing of a model of the SSME oxygen pump (with a reduced number of diffuser vanes) in a sub-speed water test rig. The SSME HPOTP diffuser appears to be of similar design to the HPFTP and so pulsation data collected here is of interest since it can be compared to the data collected from this program on hardware based on typical, generic design practices. The comparison of the data can be found in the section titled Validation and Comparison of Test Data.

The testing carried out in this program includes a comprehensive mapping of pressure pulsation activity in the impeller, diffuser and collector scroll. The pulsation data are in phase so that relationships between sensor locations can be observed. Several geometric configurations are included in the test program. No literature has been found which provides the complete data base of pressure pulsation information (synchronous, non-synchronous, and non-periodic) which has been gathered through this testing. In the following sections, reference will be made to the work just described when presenting this program's test results. A special section is included which will make direct comparisons between the test data and data contained in the above references.

DISCUSSION OF HARDWARE DESIGN APPROACHES (HPFTP & Generic)

The design of the test rig used for this program utilizes the same basic configuration as that found on the SSME HPFTP. It is a two-stage centrifugal pump with a single volute type scroll around the vaned diffuser of the last stage. The HPFTP configuration differs only in having an extra stage. This difference is not relevant to this investigation. The focus of this work is to study the fluctuating pressures associated with the last stage and the discharge scroll. The hydraulic designs (impeller, diffuser and volute scroll) used for the test rig are considered generic to the commercial pump industry. They are typical, and are the product of commercial design evolution over many years. The evolution of the design approach has included optimization of stage efficiency, providing a suitable head-flow characteristic which allows stable operation in a variety of system requirements and eliminating or minimizing hydraulic instabilities (synchronous and non-synchronous) at the design point which result in system pressure pulsations and adverse mechanical response. In the past decade, commercial pump users have been requiring their pumping machinery to operate over a wider range of flow rates. This has created an ongoing design challenge to improve the generic design in terms of reducing its minimum continuous stable flow. Development to meet this challenge is progressing, however, it is not entirely relevant to the hardware used in this program. The generic impeller and diffuser are fabricated from existing designs. The volute scroll was designed using criteria established by Ingersoll-Rand.

The operating condition of the generic design was selected to match the operating conditions of the HPFTP as closely as possible. A comparison of operating parameters is found in Table 1. A summary of stage performance for the various geometric configurations is found in Appendix D. The design condition for both stages, as defined by pump specific speed is similar. However, the hydraulic design approach to achieve this condition varies. The impeller head coefficient (gH/U_2^2) for the HPFTP is .615. For the generic design it is .49. The generic design is intended for operation over a wide flow range with a variety of system head, flow characteristics. For this reason the head coefficient is kept low to assure a constantly rising slope to the pump characteristic. The rise to shutoff is necessary to ensure stable operation during system transients. The HPFTP design apparently provides sufficient negative slope to the head, flow characteristic over its operating range to maintain system stability. The impeller exit flow coefficients vary also. The generic design has a flow coefficient ($V_{m,exit}/U_2$) of .08 at its design point. The HPFTP flow coefficient is .12. It is obvious that the HPFTP design is required to provide a larger flow rate at higher stage head rise than the generic design of similar physical size. Size and weight considerations for flight hardware must influence this design condition. While this approach is necessary, it creates higher internal pressure loading of mechanical components and leads to more problems involving system stability and unsteady hydraulic behavior.

The variation in diffuser design between the HPFTP and generic is quite apparent. The 3rd stage diffuser of the HPFTP appears to be less of a diffuser and more a set of guide vanes. An analysis using the PANEL

COMPARISON
OF
OPERATING CONDITIONS

	IR GENERIC TEST PUMP	SSME HPFTP (APPROXIMATE)	
SPEED	2,300	36,000	RPM
FLOW	700	15,150	GPM
HEAD/STAGE	190	65,000	FT
PRESSURE RISE/STAGE	82	2,100	PSI
STAGE SPECIFIC SPEED	1,190	1,090	$\text{RPM-GPM}^{1/2}/\text{FT}^{3/4}$
STAGE REYNOLDS NO.	5×10^6	400×10^6	$\Omega R^2/u$
STAGE DENSITY RATIO	1.00	1.04	
IMPELLER HEAD COEF.	.49	.615	gH/U_2^2
IMPELLER FLOW COEF.	.080	.120	$V_{m,exit}/U_2$

Comparitson of operating conditions for the HPFTP
and the generic design test hardware.

TABLE 1

code (an inviscid, 2-dimensional flow code,) (Reference 7) provides the information shown in Figure 1. regarding flow through this diffuser. This vane design accelerates the flow from inlet to discharge, as seen by the velocities shown in Figure 1. This design approach creates thin boundary layers, and discourages separation and stall behavior often found in the diffusers characterized by the generic design. The HPFTP design reduces the efficiency potential of the stage because of its lack of pressure recovery, however it is not subject to the blade-to-blade pressure loading of more conventional diffuser designs. The generic diffuser is intended to provide an area ratio from inlet to discharge of about 1.75 (V_b to V_c in Figure 1). The number of vanes is selected from experience, with the major concern being the maintenance of a suitably rising head, flow characteristic. A high vane number usually means better pressure recovery and a high overall head coefficient. Since the shutoff head coefficient is between .6 and .65 for typical commercial machines, head coefficients at design point are usually kept at .5 or less to ensure a 1.25 ratio of shutoff to design head coefficients. The generic diffuser selected has 9 vanes, and is based on an existing production diffuser. A detailed drawing of this design can be found in Appendix B. An alternate diffuser (Configuration C) for use in this program is not based on typical commercial design practice. A total of eleven vanes is used in this alternate design, with the intention of increasing the exit velocity from the diffuser and forcing a mismatch with the existing scroll design. The mismatch would be similar to that found on the HPFTP when analyzing flow velocities leaving the diffuser and velocities in the scroll throat. A table showing these velocities can be found in Figure 1. The extra diffuser vanes also serve to reduce the

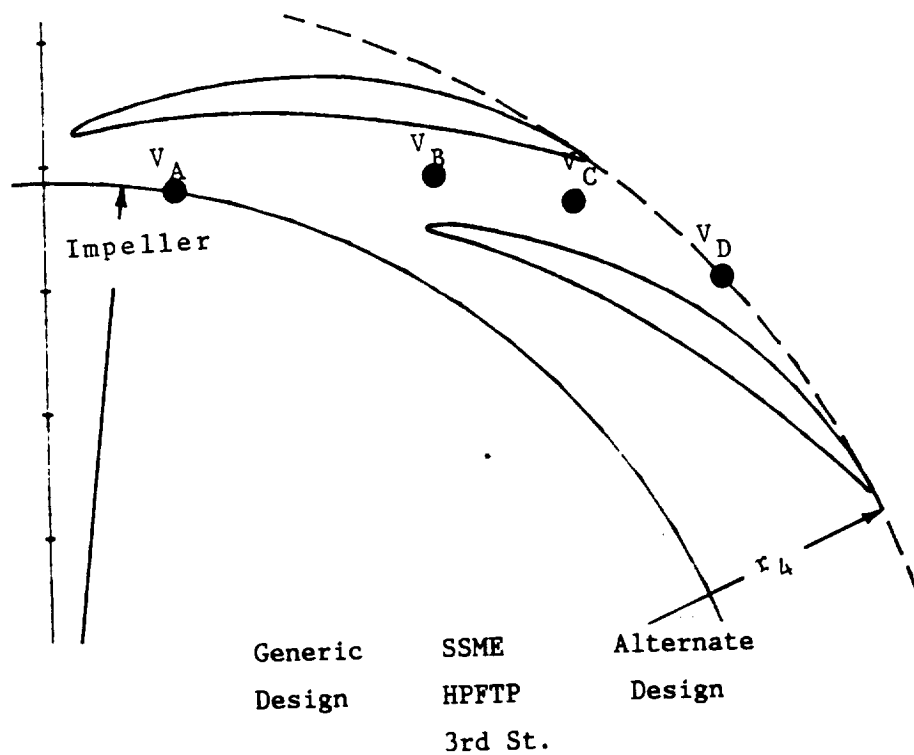


Figure 1. Comparison of Velocities in Generic Design and HPFTP.

Summary of diffuser and volute velocities at nominal design flow (550 gpm @ 1780 rpm for generic and alternate design), at various locations in the diffuser and volute scroll,

blade-to-blade pressure loading found on the 9-vane diffuser. Details of this design can also be found in Appendix B.

The scroll for the test program follows the basic sizing and configuration guidelines used for Ingersoll-Rand commercial designs. A detail drawing, including development of the sectional areas, is found in Appendix B. The sectional shape is based on design experience, which dictates a side wall angle of 22 degrees to the centerline of the volute section. The areas are scheduled linearly with circumferential position, from cutwater to the outside wall of the throat (throat being defined as the location where the full flow of the stage has been collected, and the diffusion process begins). The process used to determine the throat area is covered in Reference 6. This reference is found, in it's entirety, in Appendix C. To describe it simply, the throat area must be sized to provide an integrated thru-flow velocity which conserves the angular momentum present at the diffuser discharge (less flow losses in the collector). The aspect ratio of the sections of the generic volute scroll appear unusual because the throat area is uncommonly large. For commercial machines of this size, a double volute is used, which provides two throats, 180 degrees apart. Since it is the purpose of this program to use the basic configuration of the HPFTP, a single throat scroll was designed using the basic commercial guidelines. As described in Reference (6), the scroll of the HPFTP appears to be too large to conform to commercial guidelines. This results in a deceleration of the flow as it enters the throat, with an accompanying increase in static pressure. This creates a circumferential distribution of pressure around the OD. of the diffuser stage which upsets the flow entering the diffuser and ultimately

the flow exiting the impeller. A correctly matched scroll provides a uniform circumferential distribution of pressure around the diffuser OD. which reduces the radial load on the rotor and eliminates the possibility of unsteady flow due to the rapid diffusion occurring near the scroll throat. The impact of the scroll mismatch may be lessened by the addition of a multitude of radially drilled holes around the HPFTP's scroll. These holes no doubt pass flow from high to low pressure regions of the scroll, helping to balance any circumferential pressure distribution around the OD of the diffuser. Another aspect of the scroll design of the HPFTP is in the extending of the scroll cutwater to form one of the diffuser vanes. This configuration would increase the circumferential pressure variation around the diffuser OD., by eliminating the clearance between diffuser OD. and volute cutwater. This clearance performs a function similar to the multitude of holes already mentioned, in that it helps to balance any pressure difference caused by mismatched velocities between diffuser and scroll. The effectiveness of using these holes and cutwater extension in balancing pressures is unknown. The application of the cutwater extension is made to the alternated diffuser design (known as Configuration C). A sketch of this extension as applied to the alternate diffuser can be found in Figure 2.

A major difference in the design requirements between the HPFTP and commercially available pumps involves the operating flow range which the pumps encounter. Commercially, it is not uncommon for a single pump to be required to operate over a flow range of 25% to 125% of its design flow point. This is true of machines in fixed speed and variable speed applications. At these extremes, stall, flow separation and angle of

CONFIGURATION 'C' CUTWATER EXTENSION MODIFICATION

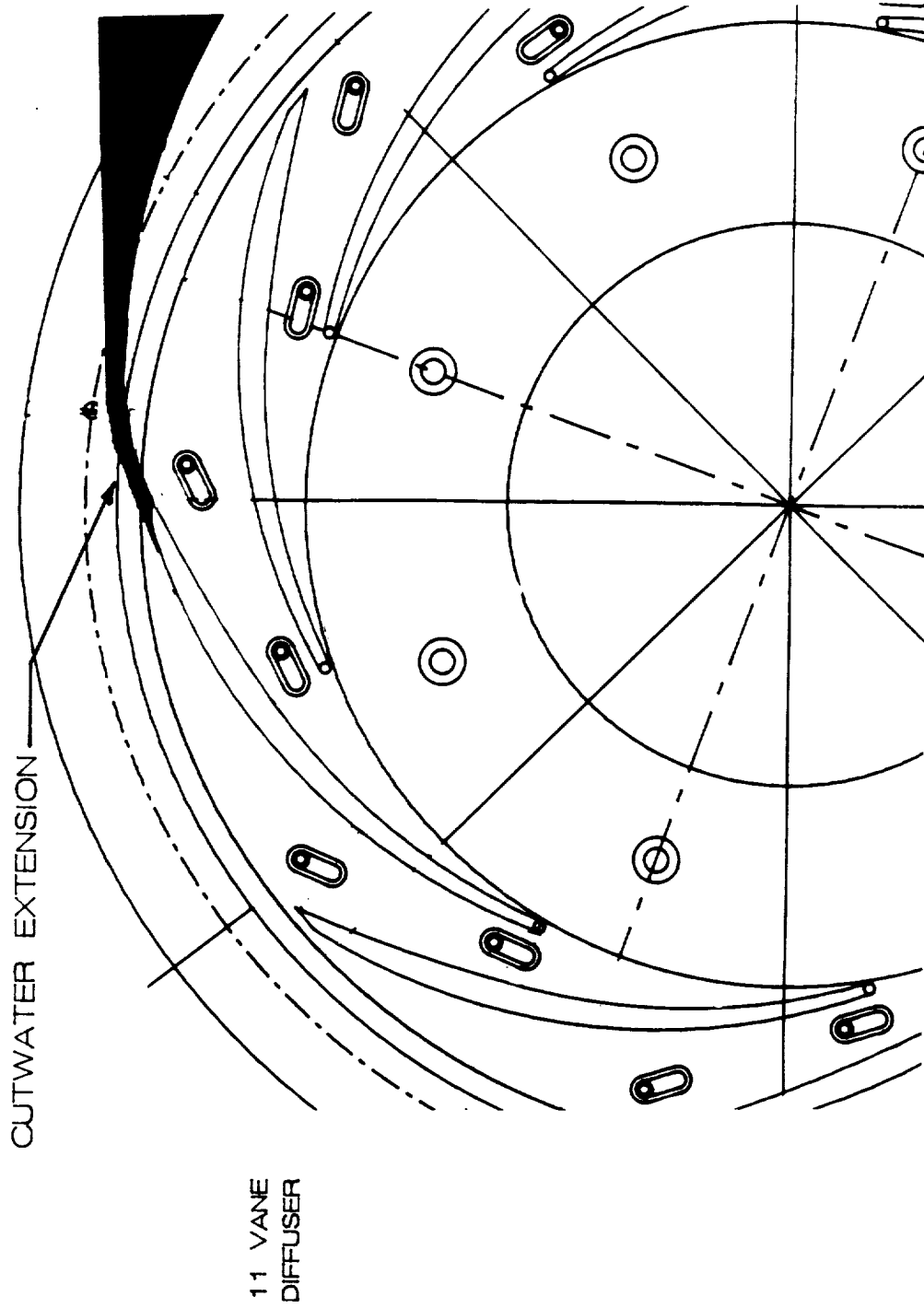


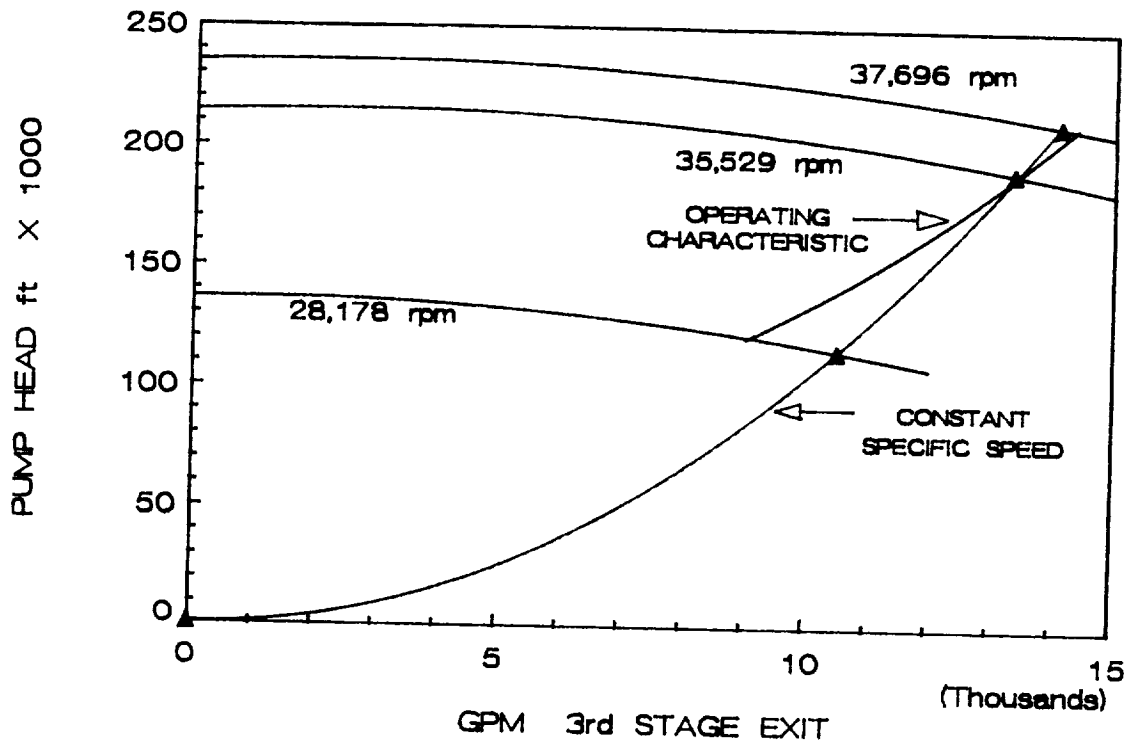
Figure 2. Configuration C Cutwater Extension Modification.

This modification simulates the cutwater extension used on the 3rd stage of the HPTTP.

incidence variations result in unsteady flow behavior (in impellers and diffusers) which are manifested in fluctuating pressures and flows, and in adverse mechanical responses which cause component failures. The typical operating range of the HPFTP is shown in Figure 3. This pump is required to operate at only 85% of its design point when at its minimum speed (encountered at the minimum engine thrust condition of 65%). Detailed analysis and test of the HPFTP design would be necessary to fully identify any occurrence of unsteady behavior which could be related to the commercial experience (which includes a wider flow range). For the purposes of this program, a flow range consistent with commercial practice is investigated. A performance map of the generic hardware can be found in Appendix D, along with a compilation of other performance data accumulated during the course of the testing.

A cross-section of the test rig can be found in Figure 4. All of the elements are present in this figure, impeller, diffuser and volute scroll (showing the development of the various sections). The test rig has been configured in a manner to facilitate the installation and routing of pressures sensing transducers and the resulting cabling. The cabling is needed to provide excitation voltage and sensing outputs. Pressure sensors mounted on the impeller have their leads routed through the shaft to a slipring assembly located between the pump and drive motor. The rig itself is modular, meaning that components can be easily interchanged if desired. This feature has allowed for relatively easy integration of the alternate diffuser design. A description of the key geometric parameters tested is found in the top half of Table 2.

SSME HPTFP PERFORMANCE CURVES



HPTFP OPERATING CONDITIONS

% THRUST	RPM	GPM	Q/Q _{100%}	Q/Q _{despt}	V _{maxit} / U ₂
109	37,696	14,369	1.08	1.01	.119
100	35,529	13,355	1.00	1.00	.117
65	28,178	9,014	0.68	0.85	.099

V_{maxit} / U₂ - 3rd STAGE IMPELLER EXIT COEFFICIENT

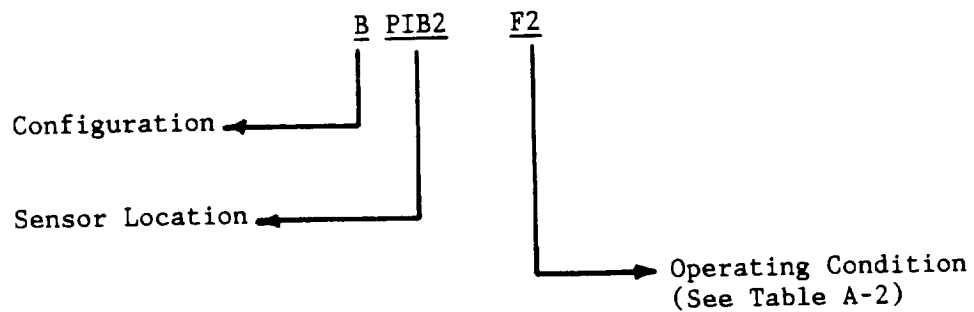
Figure 3. Performance Curves and Operating Characteristics of the HPFTP.

At the reduced thrust level of 65%, the HPFTP is operating at only 85% of its design point. At 109% thrust the pump is at 101% of its design flow.

	<u>CONFIGURATION</u>		
	<u>"A"</u>	<u>"B"</u>	<u>"C"</u>
Impeller Dia (in)	11.02	10.62	10.62
Diffuser ID (in)	11.25	11.25	11.12
Clearance Ratio	1.021	1.059	1.047
# Impeller vanes	5	5	5
# Diffuser vanes	9	9	11

DATA IDENTIFICATION SCHEME

example



Configuration Guide

Table 2

IR
GENERIC
DIFFUSER PUMP

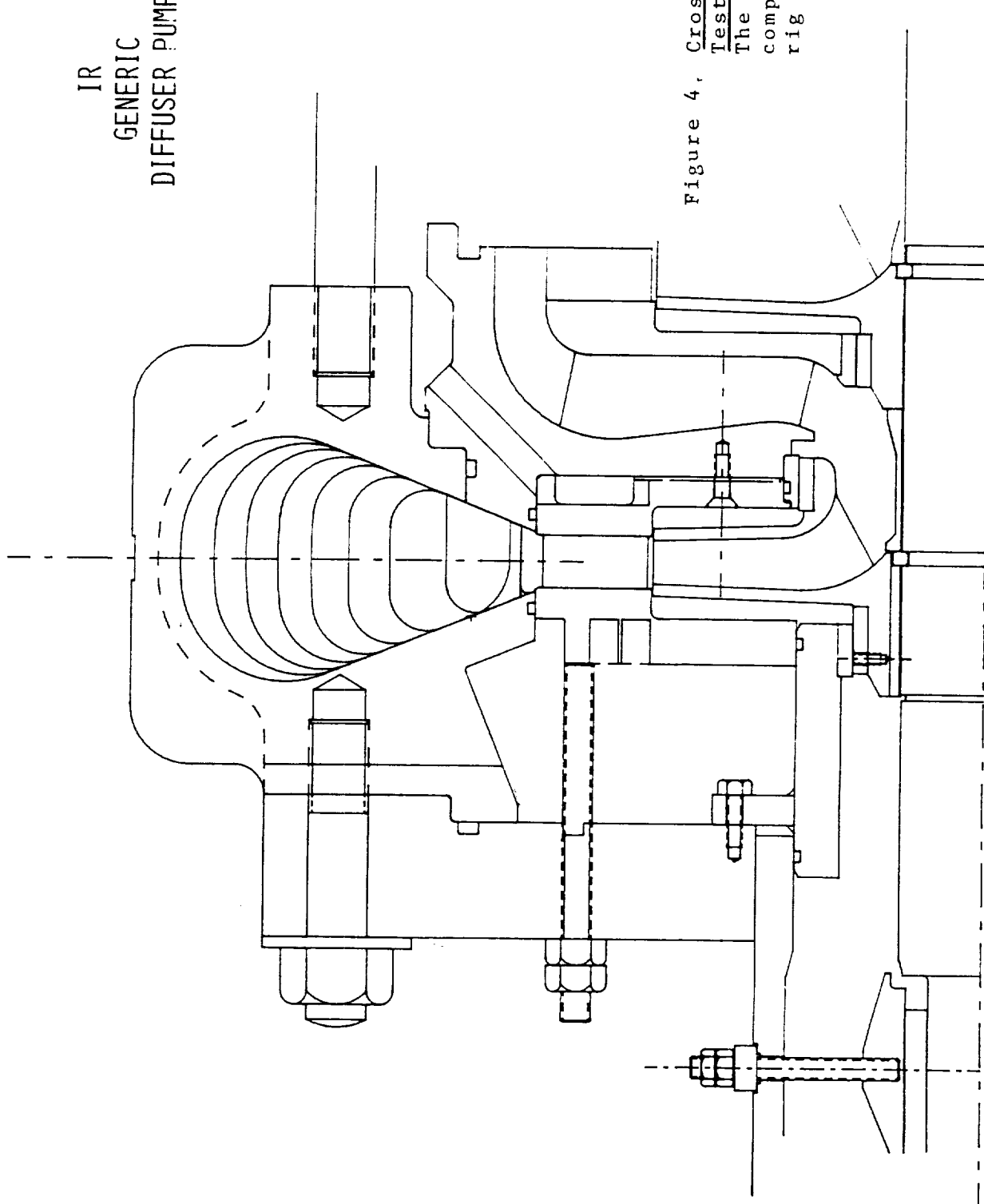


Figure 4. Cross-Section of
Test Pump.
The various components
comprising the test
rig are shown here.

EXPERIMENTAL TECHNIQUES

To properly investigate the fluctuating pressure behavior in the test pump, detailed pressure mapping of the internal components is necessary. Transducers must be selected for installation into the major components of the test pump (impeller, sidewalls, diffuser and scroll). Installation techniques must be perfected to assure trouble free operation of the sensors. The data from the planned 66 sensor locations has to be collected in a manner which allows for suitable interpretation of the pressure signals. The data, once collected, must then be put into a form for presentation. To perform these tasks, the services of Liberty Technology Inc. of Conshohocken, Pennsylvania were used. Based on their past experience, Liberty is qualified to carry out all of the above mentioned tasks.

The selection of the specific transducers was made on the basis of their capability of providing DC (steady state pressure component) and AC (fluctuating pressure component) response. This fact, along with the requirements of high sensitivity, good frequency response (5 KHZ minimum with a possible requirement to 50 KHZ), and miniature packaging suggested the use of Piezoresistive sensors. Kulite Model LQ-125-500 sensors were selected where space was at a premium. To insure they would function in a pressurized water environment they were conformally coated by the manufacturer, and samples pretested in water. Where space was not critical, Kulite model XT-140 and XT-190 pressure transducers were used (these sensors also allowed for removal from these locations for replacement or for future use). The transducers have four active arms,

temperature compensation, and closed strain gage bridges, making them insensitive to noise resulting from connector contact resistance. All of the transducers were conditioned using Vishay Instruments Model 2100 series strain gage conditioners. Data sheets describing these sensors can be found in Appendix B.

Other sensors employed during the course of testing included accelerometers and a once-per-rev tachometer. The accelerometers (B&K 4370) were used to assist, if required, in the analysis of the pressure data. They help to detect structure borne signals from purely fluid generated pulsations. The optical tachometer used was a Monarch SPS-5, employing a tach probe detecting the passage of a shaft mounted reflective tape segment. This provides a phase reference as well as a once-per-rev clock to trigger synchronous averaging of the data.

The pressure transducers were installed flush with the flow passage surfaces so as not to disrupt the continuity of flow along the wall. This required machining a recessed bed for the flat mounted LQ-125 sensors, with a through hole provided for passing wire leads of the sensors to the outside environment. A shoulder was provided to seat a small thin metal plate to cover the transducer (except for the sensing diaphragm). Before the cover was seated, the void around the transducer was filled with a waterproofing compound. The cover was then spot welded in place. The other two types of sensors were threaded into position via a tapped hole in the side walls. They were sealed by conformal coating over the sensing area, by O-ring, by silicone grease and finally by a waterproofing compound to fill any voids and to penetrate the threaded

areas. Where wire leads were required to be extracted to the outside environment, epoxy filler was used to plug the holes containing the leads. Photos which show details of the sensor installation can be found in Appendix B. This Appendix contains drawings of the test equipment used in this program, including machining details for each sensor location..

According to the original plan, eight rotating sensors and 58 stationary sensors were to be utilized in the test pump. In actuality, several sensors failed before testing began and so the full complement of 66 was never achieved. The peak number of sensors was 50, as used in configurations A and B. When sensors failed in key locations, other sensors in less important positions were shifted to fill their position, if possible.

The leads of the rotating sensors were passed through the hollow center of the shaft and connected to signal conditioning by means of a slip ring assembly mounted between the pump drive coupling and the motor coupling. To minimize noise from variations in resistance of ring contacts, slip rings with four brush contacts per ring were employed. Each piezoresistive pressure transducer has four leads, so a 26 ring assembly was utilized as follows:

- (3) rings per transducer (total 24 rings)
- (1) common ring
- (1) spare

The instrumentation was very successful in avoiding random and 60 Hz electrical noise.

It was expected that the synchronously averaged signals could contain frequencies as high as 100 orders of running speed, thus requiring bandwidths up to 5 KHz ($2500 \text{ RPM} / 60 \times 100 = 4167 \text{ Hz}$). This information was used to determine the instrumentation bandwidth. The test was conducted using instrumentation recorders operating at $7\frac{1}{2}$ inches per second. IRIG Wideband I format tape was used as the recording media. This captures signals with frequency components up to 5 KHz. Altogether, eight 14-channel instrumentation FM tape recorders were utilized to capture all data channels simultaneously for configurations A and B. Because of reduced sensor requirements, only four recorders were used for configuration C. Six channels on each tape recorder were reserved for common channels as follows:

- 1 Channel Voice and synchronization signals
- 2 Channels Once-per-rev tachometer (odd & even heads)
- 1 Channel Rotating pressure sensor
- 1 Channel Stationary pressure sensor
- 1 Channel Accelerometer

The accelerometer channel was dispensed with on configuration C. The other channels on the recorders were available for collection of actual test data. Use of the six common channels on all eight recorders provides for synchronization between any two pressure channels, regardless of tape location. Additionally, simultaneous broadband noise, recorded on all channels of each tape recorder, enabled transfer functions to be determined. These transfer functions are useful in correcting interchannel time delays caused by variations in tape head alignment encountered when playing data recorded on a different recorder.

For each test, at least one calibration was performed to check continuity and provide calibration factors for each pressure channel including sensor, conditioner, and recorder. Prior to all tests, compressed air was used for this calibration, and was measured via a precision test gauge. Data from this calibration was recorded and used to determine calibration factors and offset values. For configurations A and B the calibration was performed at the end of the test as well as at the beginning.

The pressure fluctuations expected to occur are of two types. First are order-related pulsations occurring at integer multiples (or orders) of rotation frequency. The second type includes periodic events, not order-related and random fluctuations of pressure levels not associated with any particular periodicity. The techniques utilized to acquire and process data associated with each of these two types differ.

The non order-related signals were captured in the time domain by means of two techniques. In the first case, global synchronizing signals were injected onto the voice tracks of all tape recorders, simultaneously at known instances of time during the tests. The pressure vs time waveforms of any sensor can be observed (initially on strip chart recorders) to identify significant fluctuations in pressure levels which are not periodic in nature. The synchronizing signals allow multiple sensors to be displayed, in phase. Since the pressure histories are in phase, correlation of events between one sensor and another is possible. Secondly, in the frequency domain, periodic but non order-related signals are best identified by use of a power or auto (real) spectrum in which a free-run trigger is used. This does not improve the signal to noise ratio

but does better define the signals (and unfortunately any noise). Once an event is identified, averaging of the data is used to obtain the final spectrum. In this vein, auto-spectra were produced for specific sensor locations covering a bandwidth of 0-6.4 KHz.

The order-related signals repeat exactly in each shaft revolution, and are phase locked to the once-per-rev tach signal. The once-per-rev tach serves as a common trigger for data collection and the synchronous time averaging process. This process separates the order-related and non order-related fluctuations, with the end result being a order related waveform minus noise and any periodic, non order-related signals. Synchronous averaging improves the signal-to-noise ratio (SNR) of order related signals. For this data, 700 averages were used, which improves the SNR by a factor of 26. The spectra of such synchronous averaged signals contain only order-related components. It was found that an averaged waveform record of two revolutions and a spectrum containing the first 64 orders of running speed were sufficient to obtain any significant synchronous data.

All order related records were phase corrected. It was not necessary to do this for non order-related signals because the time delay error is small in comparison with the time scale of the pulsation events. To allow for phase correction, white noise was recorded on each tape track on each recorder. In playback, any phase shift that showed up between channels was due to tape recorder time delay errors. To be able to measure this time delay or phase shift, tracks 7 and 8, which were used for the tachometer during tesing, were used as reference tracks during the white

noise tests. The transfer function between each channel and track 7 and 8 (the former was used for odd, the latter of even, channels was obtained. Since the transfer function is a complex function, it yields a magnitude and phase as a function of frequency. In this manner it was possible to obtain a phase correction for each channel. A transfer function was also obtained between tracks 7 and 8 so that odd and even channels could be compared. Odd and even tracks are on different heads.

The data from the analog, FM tape, was digitized on HP 5423 spectrum analyzers and stored as raw data. Phase corrections and calibration factors (slope and intercept of the linear calibration curve) were applied. The resultant data was stored separately as corrected data. Both raw and corrected data are stored on hard disk and backed up on magnetic tape cartridge. In order to expedite the massive data reduction and storage tasks, a computer program was written, using an HP 9816 desktop computer. This program manages the data handling between instruments, stores calibration factors, labels, phase correction data and sensor and test condition information. The program also performs statistical manipulation of the data and provides the overall control needed to automate the data reduction process. Another program was designed to analyze the synchronous data. This program allows for graphic display of waveforms and spectra, in a real time display or generates hardcopy plots using a digital plotter. The results of the various data display methods are found in the Data Analysis and Interpretation section which follows later in this report.

VALIDATION AND COMPARISON OF TEST DATA

In order to establish confidence in the accuracy of the test data obtained during the course of this program, it is desirable to make comparisons with results from similar investigations found in literature. Three of the references mentioned in the literature survey will be used for this comparison. References (1) and (5) offer experimental results while Reference 4 presents numerical results based on an analytical model used to predict pressure pulsations from impeller/diffuser interaction.

The work of Kanki, et al (Ref. 1) includes the measuring of unsteady pressures at the discharge of a 2000 specific speed pump impeller. His work was focused on measuring the fluctuating radial loads on a pump rotor due to the synchronous interactions of an impeller and a diffuser or volute scroll. The comparison of Kanki's data with data from this program can be found in Figure 5. Kanki's results are plotted against the discharge flow coefficient from the impeller. Data for configurations A and B are shown. These amplitudes include only those orders of pulsation activity greater than or equal to blade pass frequency. This is done to filter out pulsation activity not associated with impeller/diffuser interaction. Good correlation is observed with Kanki's two data points. Also notice the variation in the clearance ratio between impeller OD. and diffuser ID. Kanki's data with a ratio of 1.03 falls between the two test configuration ratios of 1.02 and 1.06.

IMPELLER PRES PULSATIONS COMPARISON WITH KANKI *etal*

○ I7 CL=1.02 △ I7 CL=1.06 ◆ KANKI/
MITSUBISHI

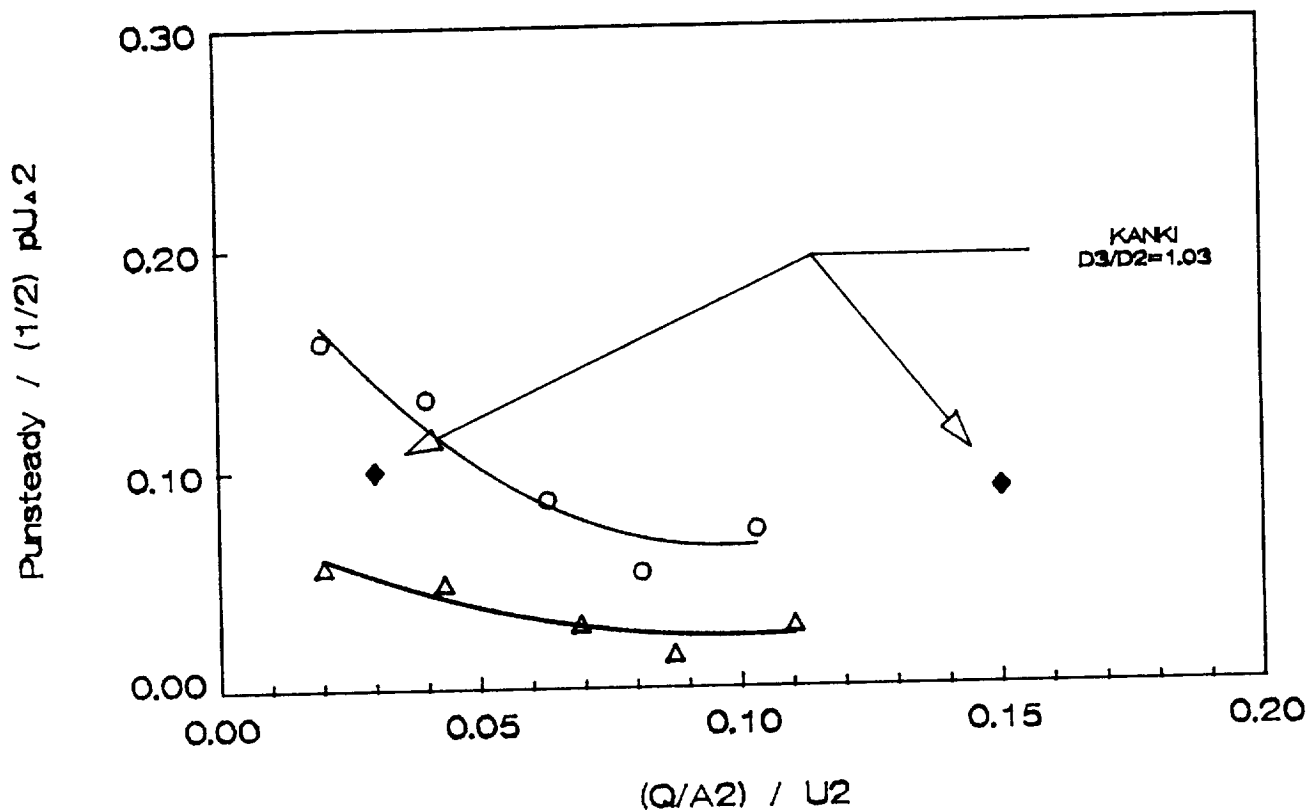


Figure 5, Comparison of Pressure Pulsations Measured on the Impeller O.D.

This data compares test results from sensor location I7 with results from Kanki (Ref. 1).

Data from Brennen et al (Ref. 5) was obtained on a sub-speed test rig utilizing modified hydraulics from the SSME High Pressure Oxygen Turbo Pump (HPOTP). Pressures were measured on the diffuser vane surface by piezo-electric transducers. Pressure pulsation levels are plotted in a nondimensional form versus the diffuser vane length. A comparison of this data with test data from Configurations A and B is found in Figure 6. The data is for impeller exit flow coefficients of between .110 and .100. Brennan does measure higher pulsation levels near the leading edge and along the pressure surface. Good agreement is found along the suction surface. The discrepancies may be due to the different blade loading characteristics of the two designs. In the Brennen test rig, eight of the seventeen diffuser vanes of the HPOTP design are removed. The impeller/diffuser clearance ratios are similar, falling between 1.02 and 1.06. Brennen does report higher pulsation levels at higher flow coefficients. The generic test configurations were tested over their intended flow range, which produces a maximum flow coefficient of .110 at the maximum flow condition which is 125% of design. Our test data show that pulsation activity in some of the components begins to increase as flow is increased beyond the design point of the machine.

The work of Iino (Ref.4) provides the results using an analytical model to predict dynamic loads on impeller blades due to impeller/diffuser interaction. His model utilizes two-dimensional potential flow theory. The singularity method is used to analyze the unsteady velocity field in the impeller. A Fourier series is used to express unsteady flow quantities, and the unsteady Bernoulli equation for a rotating coordinate system is applied to solve the unsteady pressure

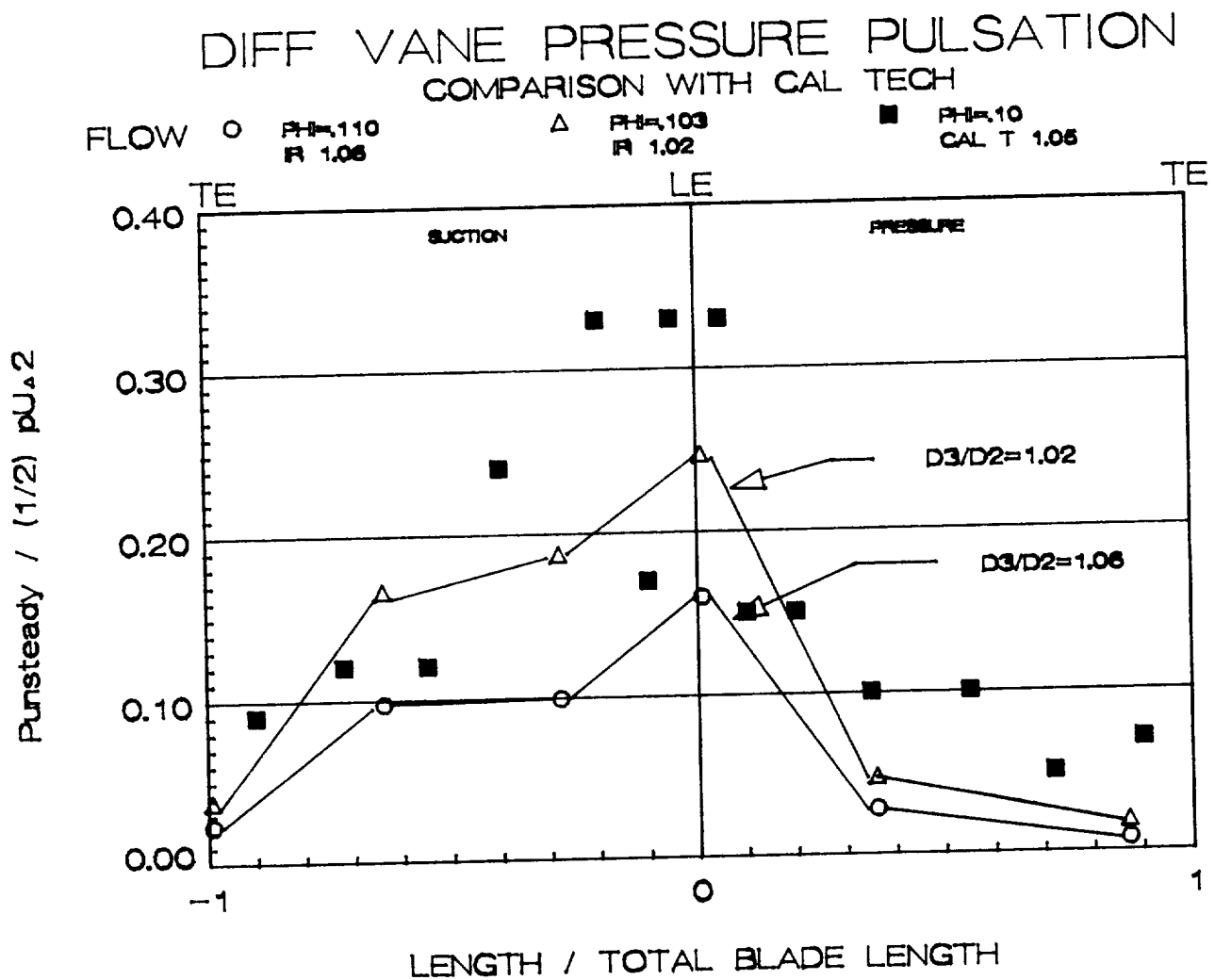


Figure 6. Comparison of Pressure Pulsations Measured Along the Diffuser Vane.

This data compares test results from the diffuser passage sensors with results from Brennan (Ref. 5).

field. Numerical results are provided for specific configurations. One of these configurations is close to our generic design and can be used for comparison purposes. The result of this comparison can be found in Figure 7. The diffuser inlet and impeller exit angles are similar, as is the clearance ratio between the impeller and diffuser. Iino calculates results only at the impeller exit radius (radius number $K=20$). The pressure side transducer location in the test case (configuration A) is closer to his radius number of 16 (with $K=1$ being the inlet radius). In order to determine the exact correlation with Iino's model, the complete analysis would have to be installed on a computer and the solution found for the other impeller radius numbers. The comparison presented is still interesting. If the analytical results are accurate, one would expect an increase of pulsation activity between our test location and the impeller exit of between 300% and 500% depending on flow coefficient. At a flow coefficient of .20, the increase in pulsation level (normalized to impeller exit velocity head) would be from .25 to .75 (if the Iino curve is extrapolated). At a flow coefficient of .100, the pulsation levels would increase from .085 to .430. It is difficult to totally accept the Iino result due to the complicated fluid dynamic activity occurring as the result of impeller and diffuser flow, including viscous effects. The work is still valuable since it does identify key elements of the causes of synchronous pulsation activity, these being the clearance between impeller and diffuser and the load distribution on the diffuser blades. Both of these conclusions are verified in the test data obtained in this program.

COMPARISON OF UNSTEADY PRESSURES IMPELLER PRESSURE SURFACE

+ TEST
DATA

Δ Iino
NUMERICAL

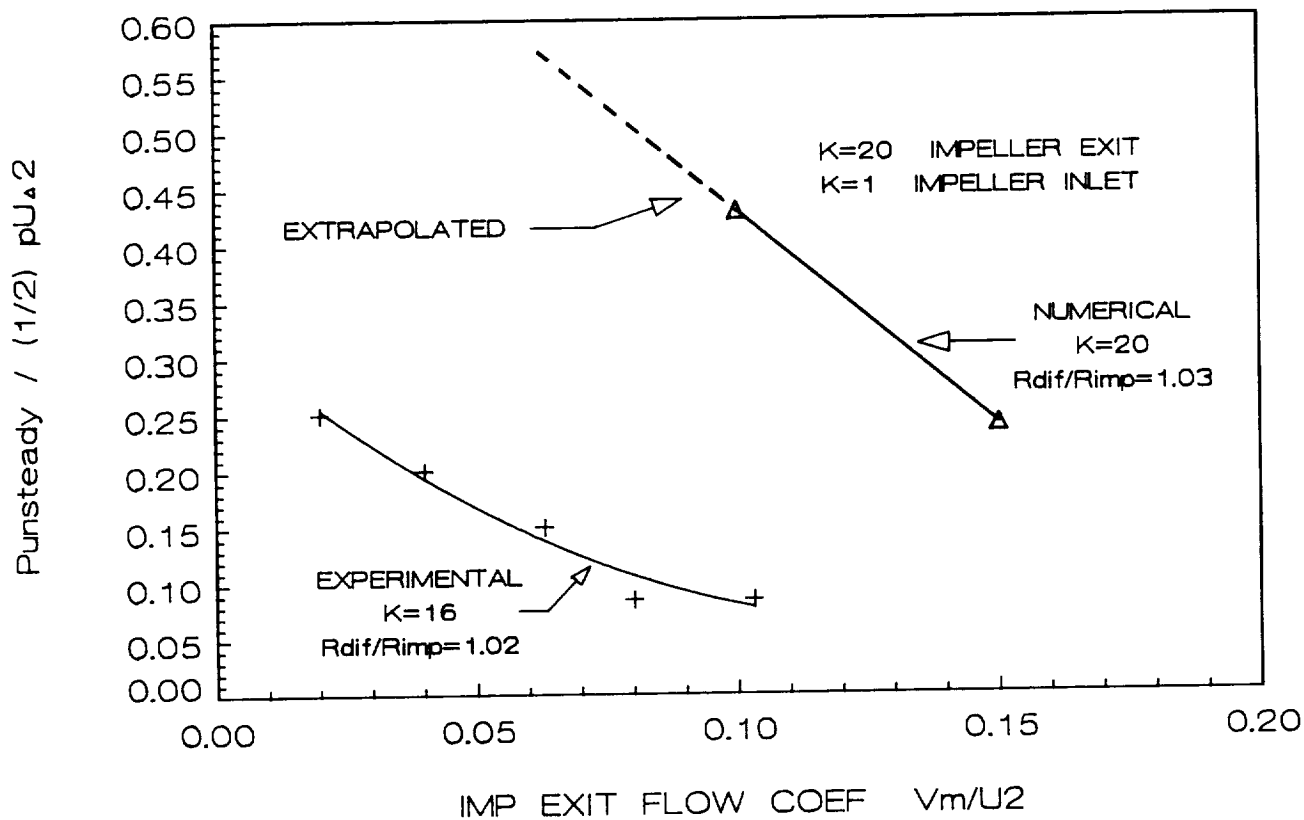


Figure 7. Comparison of Pressure Pulsations From Test and From Analysis.

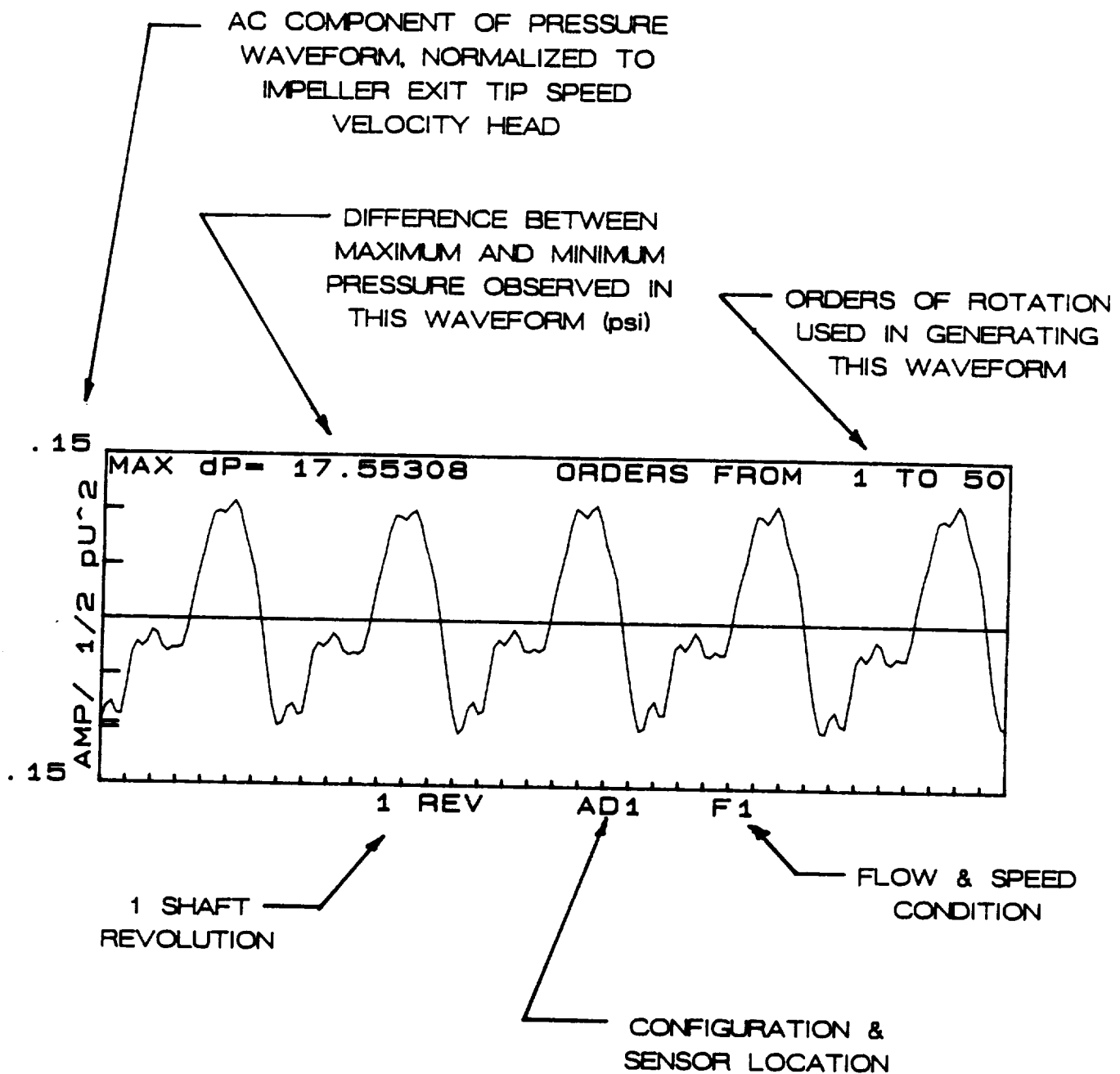
This data compares test results with calculated pulsations from Iino (Ref, 4),

A final point of test data validation concerns the comparison of one of the test pressure sensors (Kulite XT-190 piezo-resistive type) with a piezo-electric type (Kistler 211B). Each sensor was installed in the discharge head of a reciprocating pump operating at a speed which created discharge valve opening and closing at a frequency of 60 Hz. The resulting pressure waveforms were compared for frequency and amplitude and found to be identical.

DATA ANALYSIS and INTERPRETATION

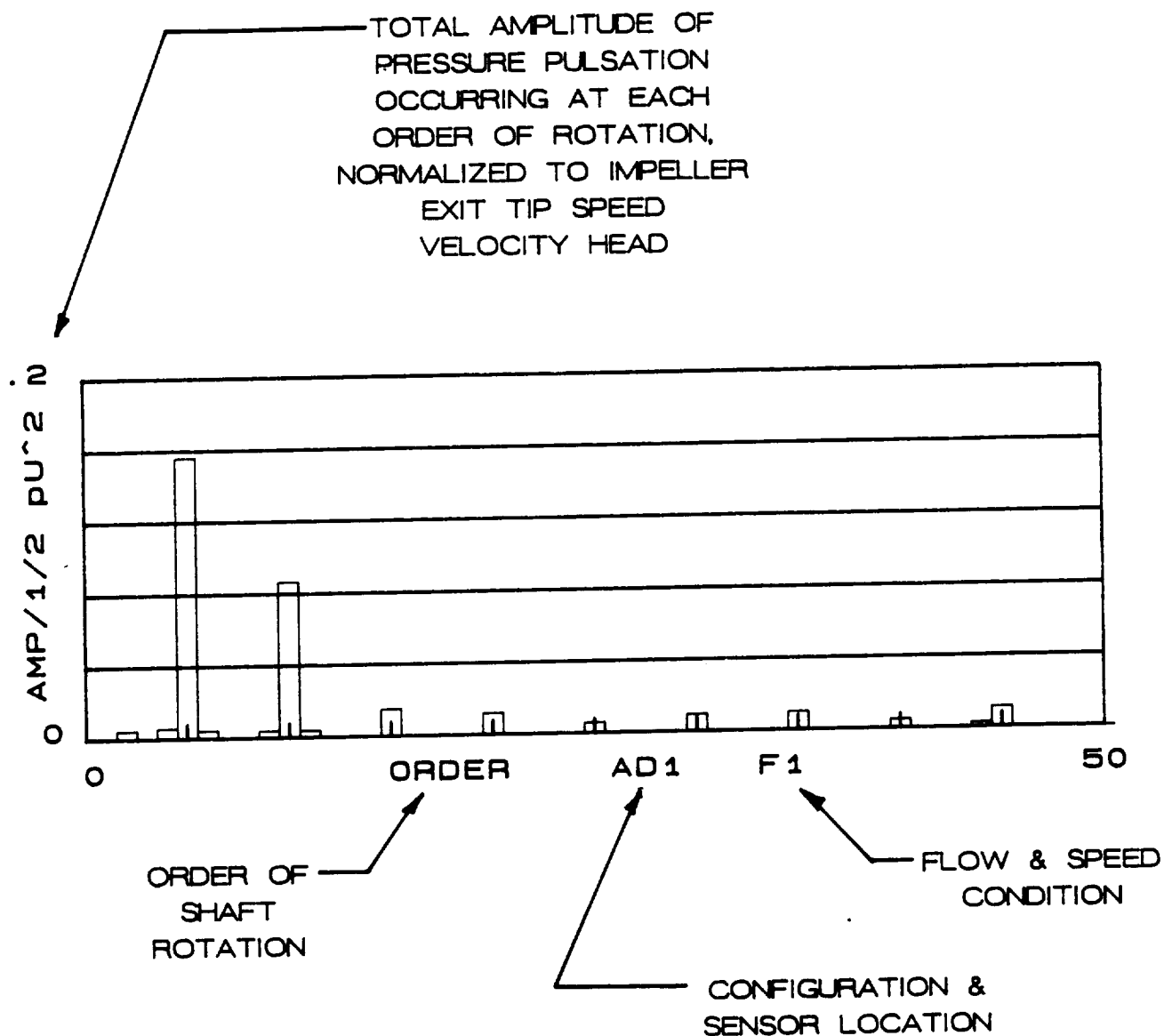
The question of how to organize and display the large amount of information produced by this test program in a logical and informative manner is an important one. The format uses discrete plots of data combined with a description of how the plots (or group of plots) contribute to an understanding of the nature of fluctuating pressures in the pump components. Topics covered in this section include the effect of impeller to diffuser clearance, diffuser vane loading, interaction between impeller and diffuser vane number, attenuation of fluctuating pressures through the stage, non-synchronous pulsation behavior, and scaling of pulsations with speed.

To facilitate the study of the plots, Figures 8 and 9 are provided to describe the nomenclature used in the presentation of the synchronous plots. When reviewing the plots, an awareness of the sensor location and flow condition is necessary. Information on operating conditions can be found in Table 3. This information includes pump speed, fraction of design flow and exit flow coefficient. Reference must also be made to the figures identifying the location of sensors installed in the various pump components (Figures 10 thru 16). A configuration guide summarizing the key geometrical parameters for each configuration can be found in Table 2. The data are organized into two sub-sections. The first includes synchronous pulsation data only, this information coming from the synchronous time averaged pressure waveforms and spectral analysis. The second section includes non-synchronous and non-periodic type fluctuating pressure activity.



EXAMPLE OF SYNCHRONOUS, TIME-AVERAGED, PRESSURE WAVEFORM
(200 REVOLUTIONS IN AVG)

Figure 8. Definition of Nomenclature Used on Synchronous, Time-Averaged, Pressure Waveform Plot



ORDER OF ROTATION BASED FREQUENCY COMPONENTS
OF SYNCHRONOUS, TIME-AVERAGED PRESSURE WAVEFORM
(200 REVOLUTIONS IN AVG)

Figure 9. Definition of Nomenclature Used on Plots
Showing the Rotation Based Frequency
Components of the Pressure Waveform

<u>OPERATING CONDITION</u>	<u>RPM</u>	<u>APPROXIMATE FRACTION OF DESIGN FLOW</u>	<u>EXIT FLOW COEFFICIENT FOR EACH CONFIGURATION</u>		
			<u>"A"</u>	<u>"B"</u>	<u>"C"</u>
F1	2300	.25	.020	.020	.019
F2	2300	.50	.040	.043	.042
F3	2300	.75	.063	.069	.068
F4	2300	1.00	.081	.087	.087
F5	2300	1.25	.103	.110	.107
F6	1780	1.25	.105	.112	.108
F7	1780	1.00	.081	.087	.087
F8	1780	.25	.016	.018	.018
F9	2700	.25	-	-	.019

EXIT FLOW COEFFICIENT = C_m/U_2

Operating Condition Guide

Table 3

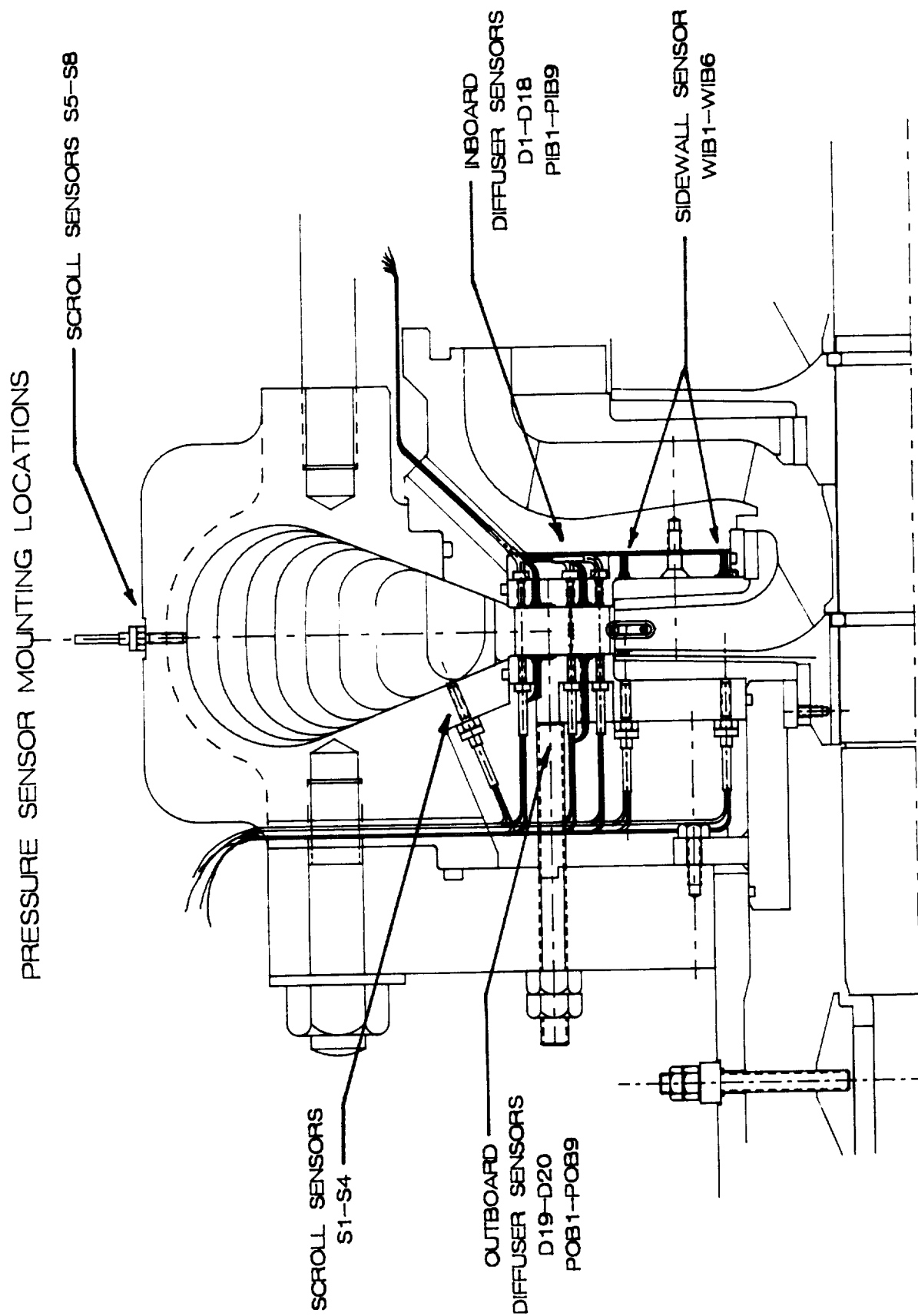


Figure 10. Pressure Sensor Mounting Locations.

This cross-sectional view of the major pump components shows the locations of the various pressure sensor groups.

SCROLL SENSOR LOCATIONS

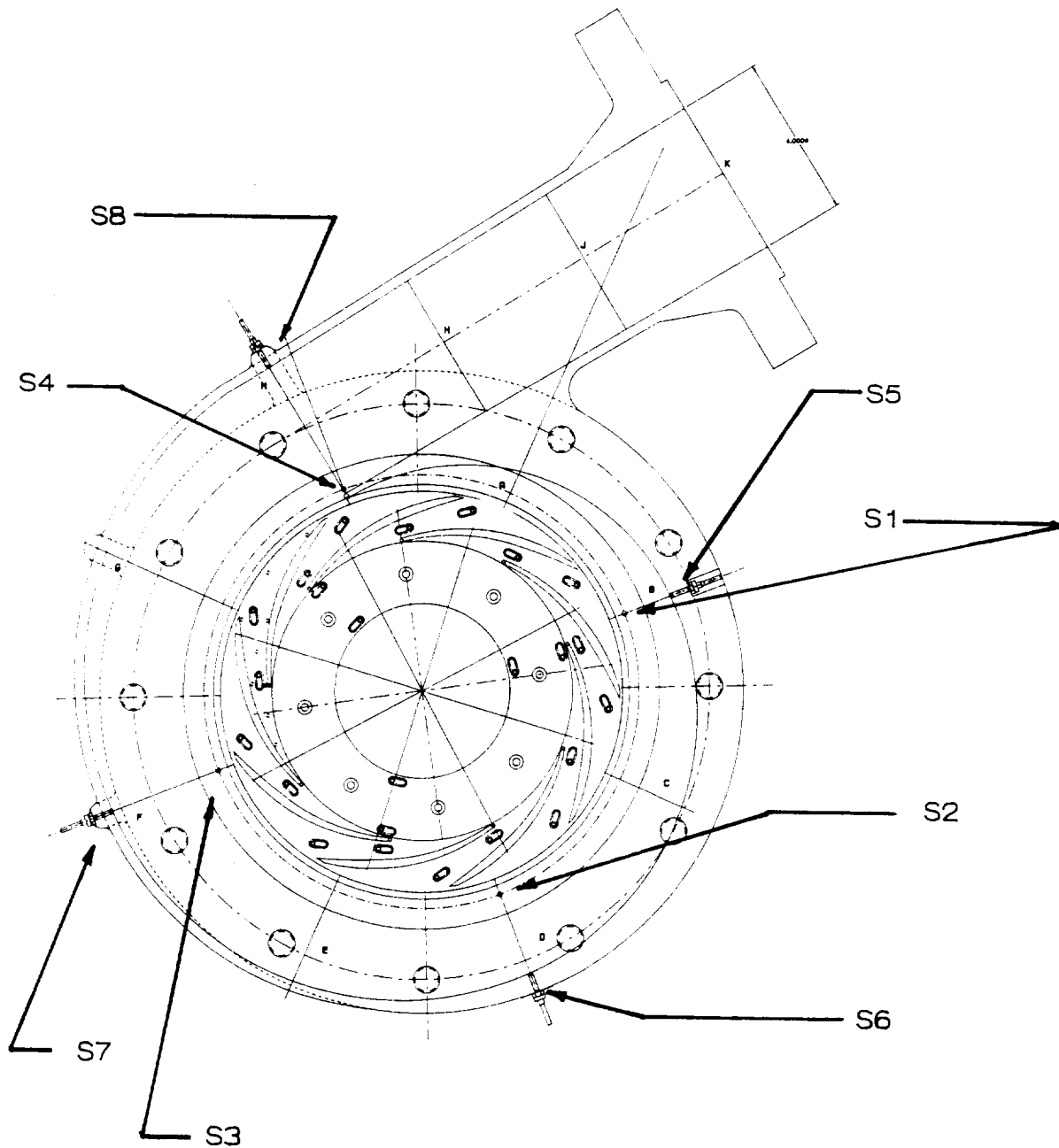


Figure 11. Scroll Sensor Mounting Locations.

The diagram illustrates a complex circular structure, possibly a ship's hull or a large vessel, with various components and labels. The central area is marked with concentric circles and radial lines. Labels include WIB1, WIB2, WIB3, WIB4, WIB5, and WIB6, pointing to specific locations on the structure. Other labels include J, K, L, M, N, O, P, Q, R, S, T, U, V, W, X, Y, Z, and A through I. The diagram is oriented with the top of the structure towards the upper right.

39

DIFFUSER PASSAGE SENSOR LOCATIONS

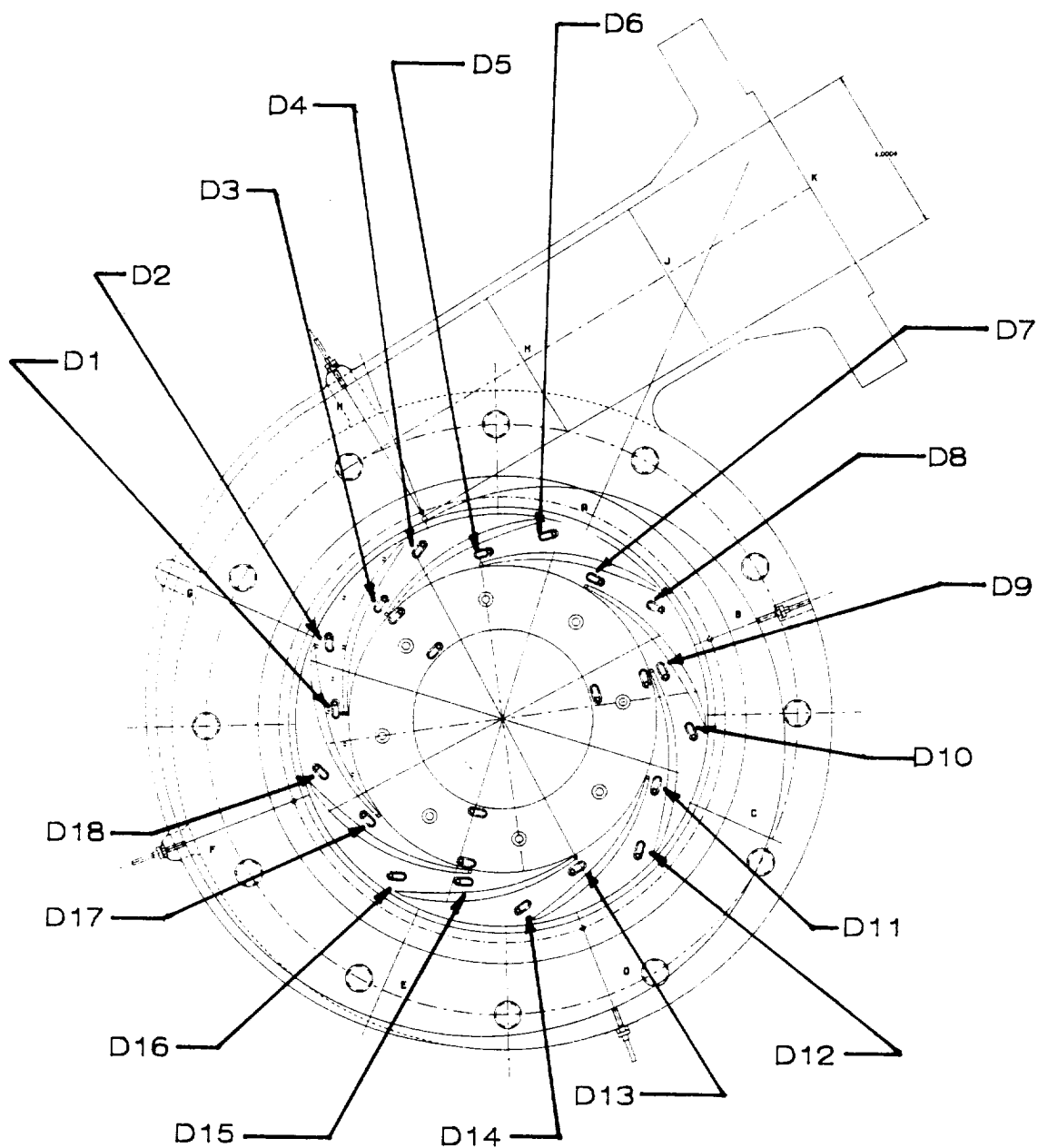


Figure 13. Diffuser Passage Sensor Locations.

The passage containing sensors D1 and D2 has two additional sensors, D19 and D20, mounted opposite D1 and D2,

DIFFUSER PASSAGE SENSOR LOCATIONS

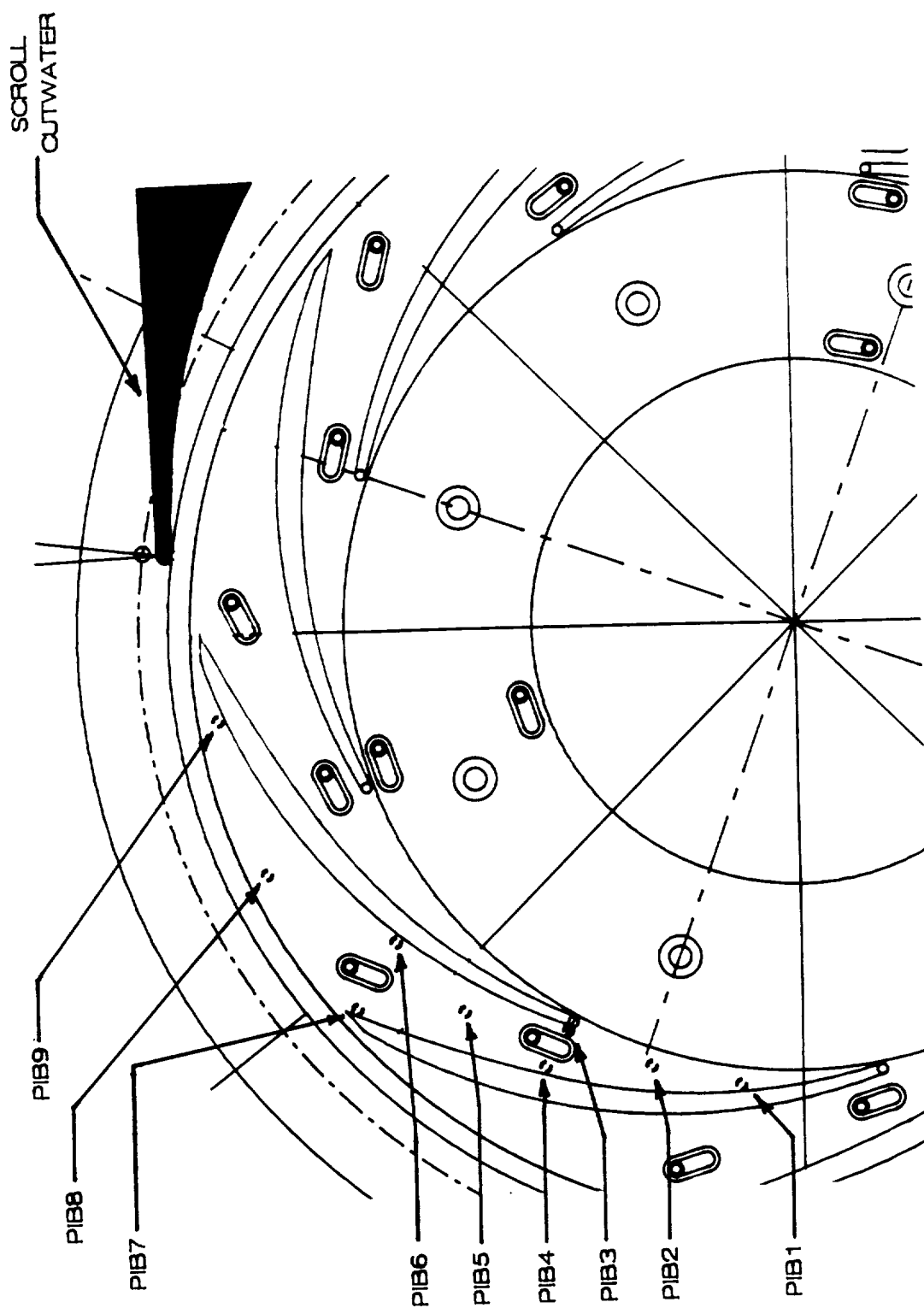


Figure 14. Diffuser Passage Sensor Locations.
 These sensors are referred to as the inboard sensors. Directly opposite each of these sensors, in the outboard wall, these sensors identified as POB1, POB2, etc.

IMPELLER SENSOR LOCATIONS

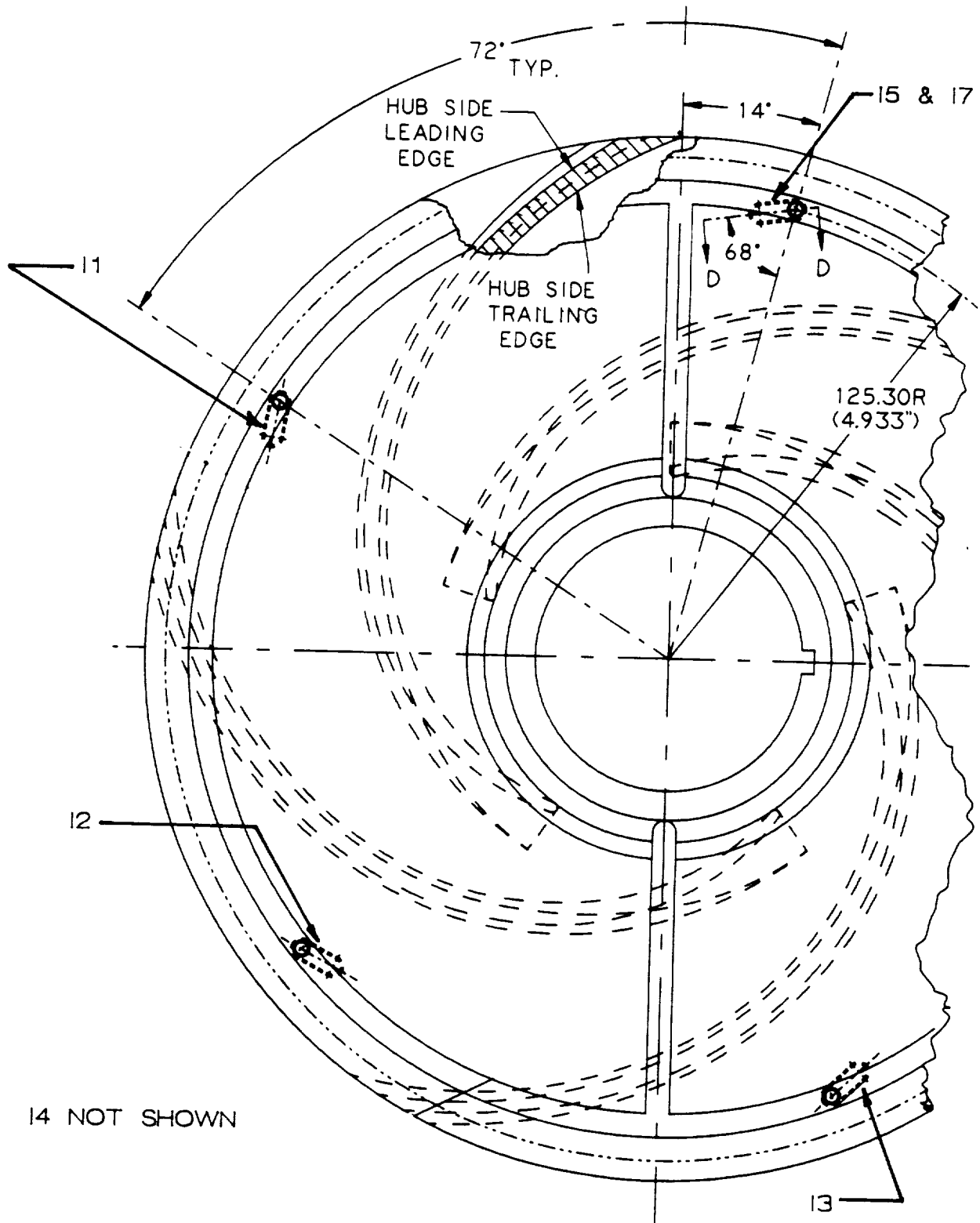


Figure 15, Impeller Sensor Mounting Locations,
Locations I5 and I7 are directly across
from each other.

IMPELLER PASSAGE SENSOR LOCATIONS

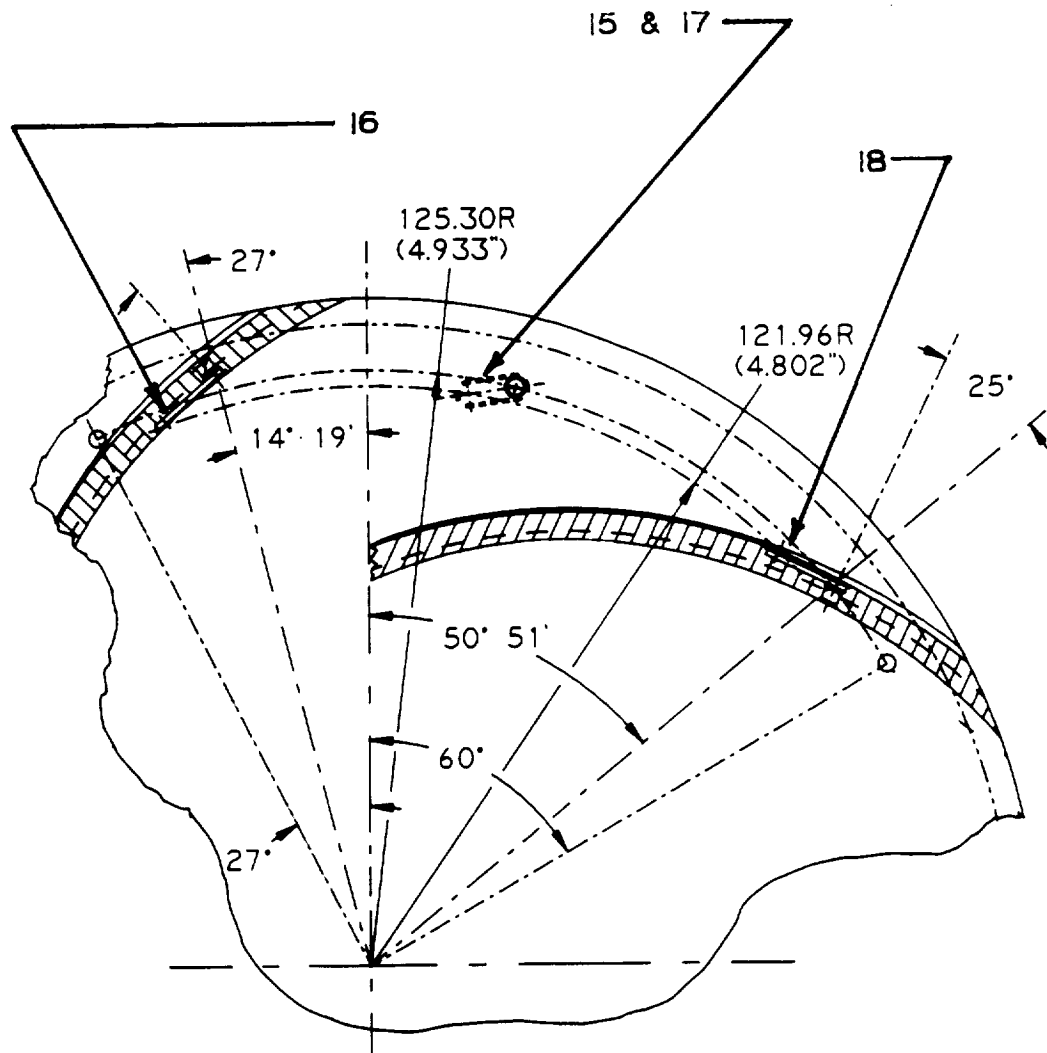


Figure 16. Impeller Sensor Mounting Locations on Suction and Pressure Side Surfaces.

The dominant activity observed is synchronous in nature and is related to impeller/diffuser interaction. Other observed phenomena were related to system piping configuration, low flow unsteadiness due to boundary layer growth and separation and to structural resonance which is excited by the synchronous pulsation behavior. The influence of synchronous pulsation behavior is important in all pumping turbomachinery, regardless of application or energy levels. Of course as energy levels increase, the severity and impact of the fluctuations on structural integrity are of more concern.

Pressure pulsations are indications of acceleration and deceleration of the local flow velocity. A number of causes exist for this variation in flow velocity.

1. To a stationary observer located just outside the impeller OD, the absolute flow velocity observed varies with each impeller vane pass. This variation is due to the addition of torque to the fluid within the impeller passage. The larger the torque change (which is the case at low flow rates), the greater the variation in relative velocity and also the variation in static pressure across the passage. The variation in velocity is attenuated as the reference position is moved farther from the impeller discharge. This also attenuates the resultant pressure pulsations.
2. From a location on the rotating impeller, variations in the relative through flow velocity also occur. These variations are caused by the presence of the diffuser vanes downstream

of the impeller exit. Diffuser vanes (or volute cutwaters) are used to turn the absolute flow from a tangential direction to a more radial direction. This reduces the absolute velocity thereby converting the potential energy of the absolute flow into static pressure. In doing this, a torque is exerted on the flow field and like the impeller, creates a circumferential pressure variation across the diffuser passage. Flow in the impeller responds to this variation in back pressure and correspondingly speeds up or slows down according to the exit condition at the particular location. The pressure variation is dependent on the diffuser design (how much torque is being removed from the flow) and the degree of incidence to the vane leading edge. The degree of response of the flow in the impeller is also dependent on the distance the impeller is from the leading edge of the diffuser and its accompanying pressure field.

3. Half and quarter-wave pipe or passage resonances will also cause variations in flow velocity and resultant pressure oscillations.
4. Unsteady flow in passages due to boundary layer growth, separation and re-attachment causes fluctuations in flow velocity and pressure pulsations. This behavior can be found in diffuser and impeller passages. Severe changes in velocity can be found in these cases, since it is common for flow to actually reverse before recovery in the passage occurs and correct through flow is resumed.
5. Structural resonances impart motion to fluid adjacent to the vibrating element. This motion radiates through the liquid and

is another source of pressure pulsation.

All of the above phenomena have been observed through the course of this testing. At times all these elements exist together, with the result being a complicated time record of pressure behavior. By using techniques such as synchronous time averaging and FFT analysis the different components of the waveform can be separated and identified as resulting from one of the above phenomena.

A summary of synchronous pressure pulsation levels (normalized to the impeller exit velocity head) is shown in Table 4. The levels are peak-to-peak amplitudes and are representative of activity in the three major elements in the pump; impeller, diffuser and volute scroll. The value of the peak-to-peak amplitude at a specific location is important in that it determines the variation of the forces acting upon the local structure. The average pressure (referred to as the DC component of the pressure waveform), when added to the alternating component is used to determine the total force applied at that location. The largest amplitudes are found in configuration A (AI5, APIB3, AS7) which is the configuration with the smallest clearance ratio between impeller and diffuser. The location where the largest amplitudes occur is on the diffuser vane pressure surface, near the leading edge. Pulsation amplitudes are somewhat attenuated in the scroll area (AS7, BS7, CS7) with the peak-to-peak amplitudes 15 to 30 percent less than those found at the diffuser vane. Flow condition has a large effect on pulsation levels. Three flow conditions are shown on Table 4, F1 is 25% of design flow, F4

ELEMENT	LOCATION	CONDITION		
		F1	F4	F5
SCROLL	AS7	.07	.05	.05
	BS7	.05	.045	.03
	CS7	.02	.01	.01
DIFFUSER	APIB3	.21	.23	.30
	BPIB3	.11	.14	.17
IMPELLER	AI5	.17	.06	.08
	BI5	.07	.03	.03
	CI5	.07	.03	.03

ALL VALUES NORMALIZED TO IMPELLER VELOCITY HEAD

$$\Delta P / \frac{1}{2} \rho U_2^2$$

TABLE 4
Synchronous Pressure Pulsation Amplitudes

is the design flow and F5 is 125% of design. The scroll locations "see" decreasing pulsation activity as flow rate is increased. The impeller locations have minimum activity at the design condition (F4), which indicates that matching of the absolute flow angle to the diffuser vane angle minimizes the pressure field disturbance around the leading edge of the diffuser. The pulsation activity continues to increase as flow rate is increased. A nearly periodic, rotating stall exists in configurations B and C, at the low flow condition. The magnitude of the pressure variation caused by the stall is about 20% of the impeller exit velocity head. This value is measured at the diffuser inlet. Pressure fluctuations measured in the scroll during this phenomenon are less than half of those measured in the diffuser itself. Pulsations measured due to the vibrations of the impeller shrouds are only 2.5% of the impeller exit velocity head. These pulsations are not measurable in the collector scroll.

The following subsections provide details regarding the fluctuating pressures observed and recorded throughout the course of the test program.

SYNCHRONOUS DATA

Typical Selection of Sensors

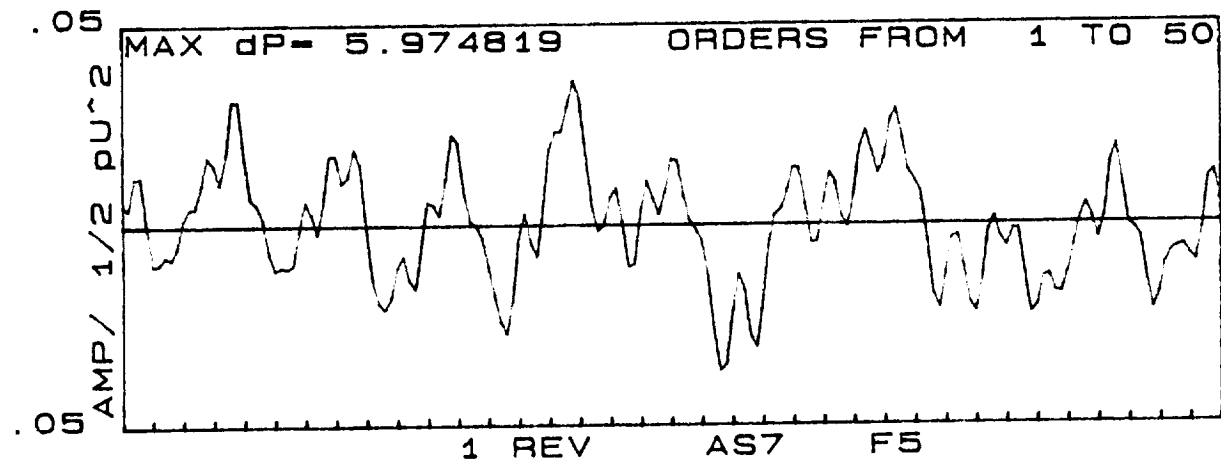
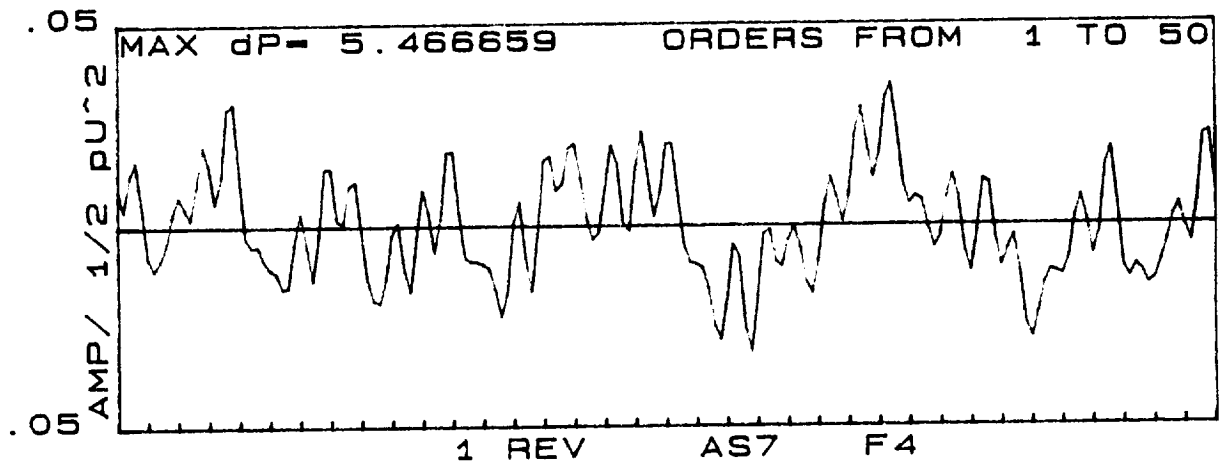
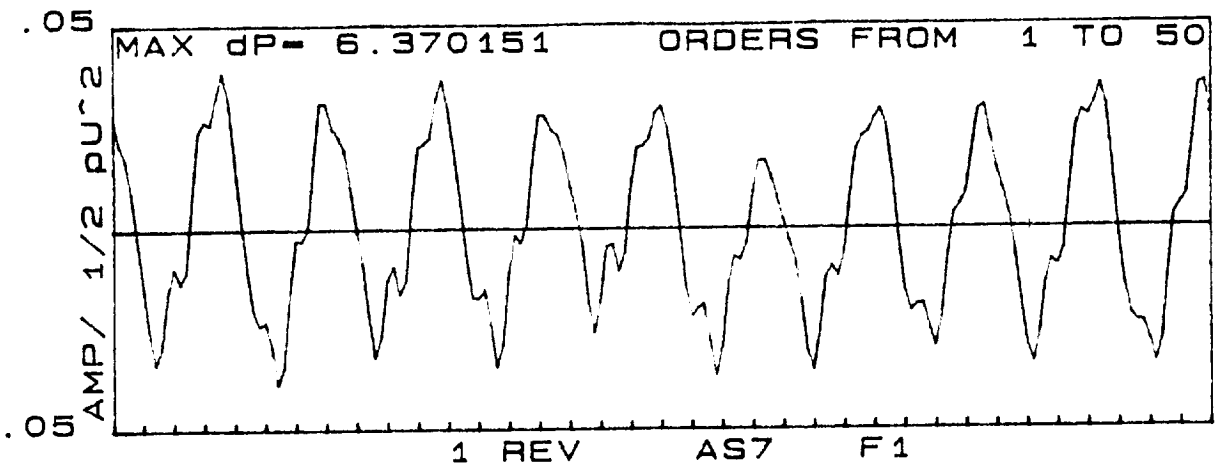
Locations: AS7, APIB3, AI5

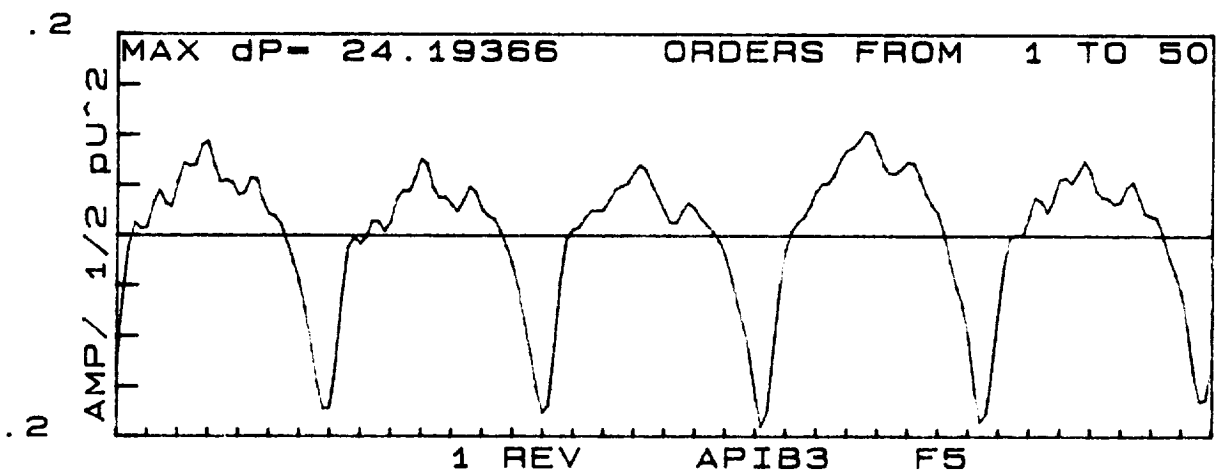
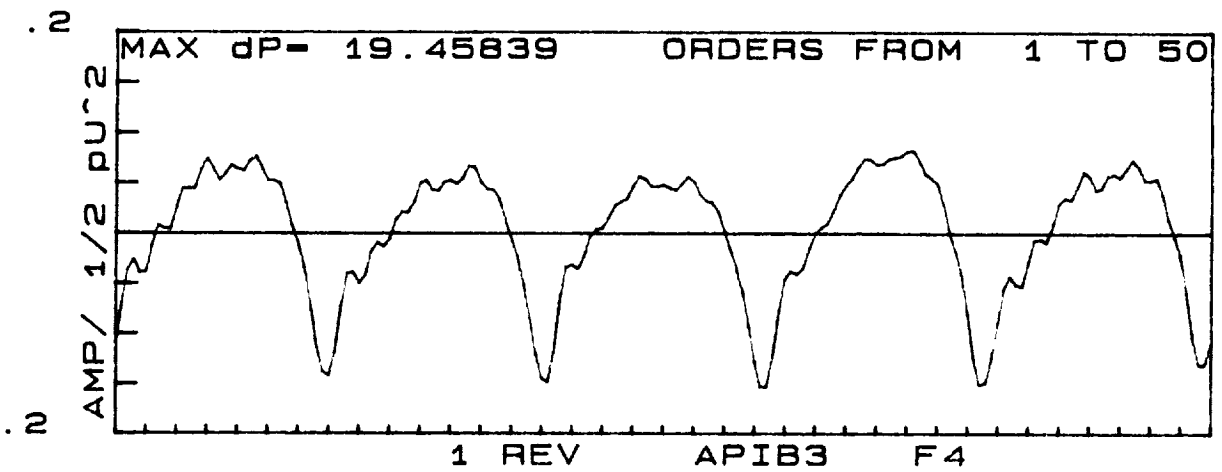
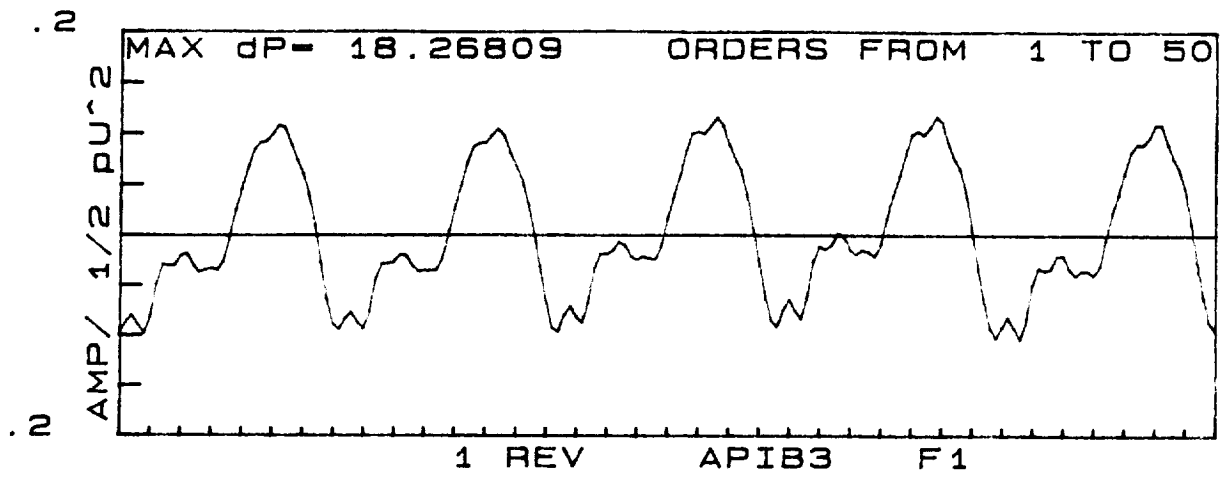
BS7, BPIB3, BI5

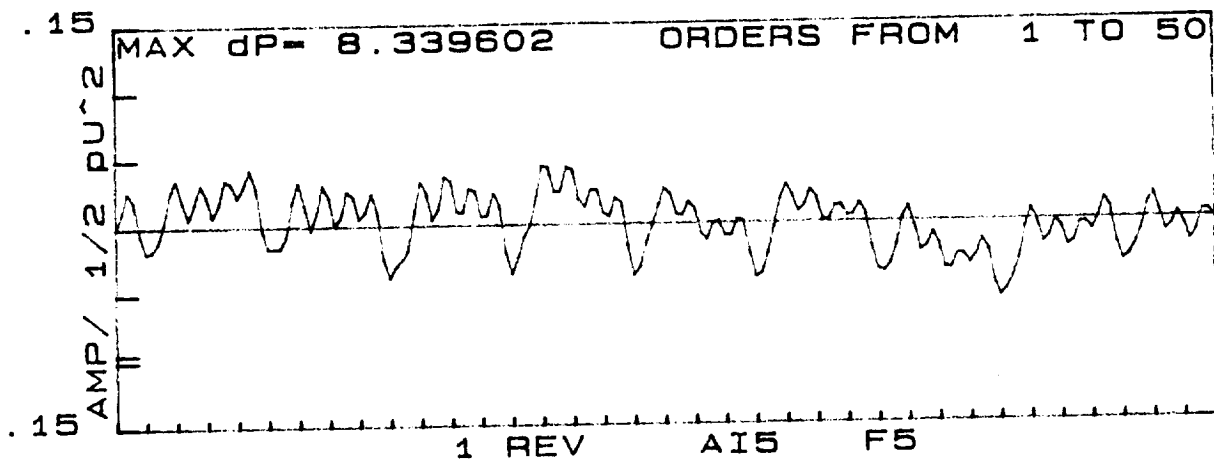
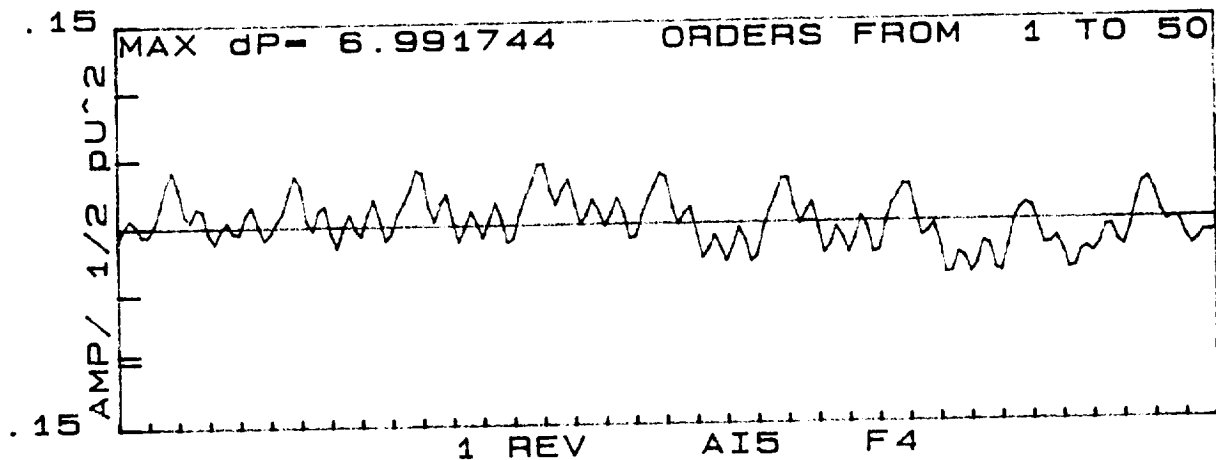
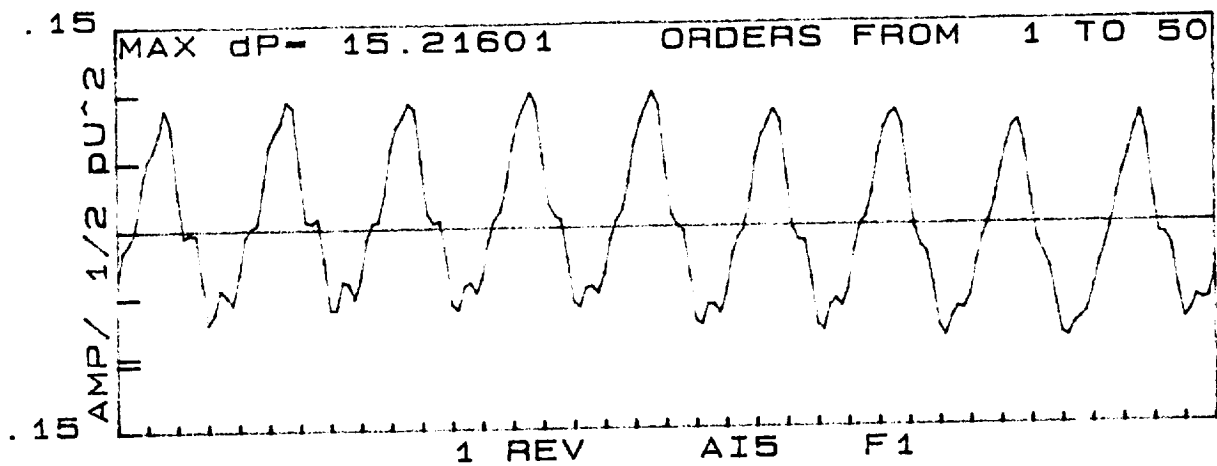
CS7, CI5

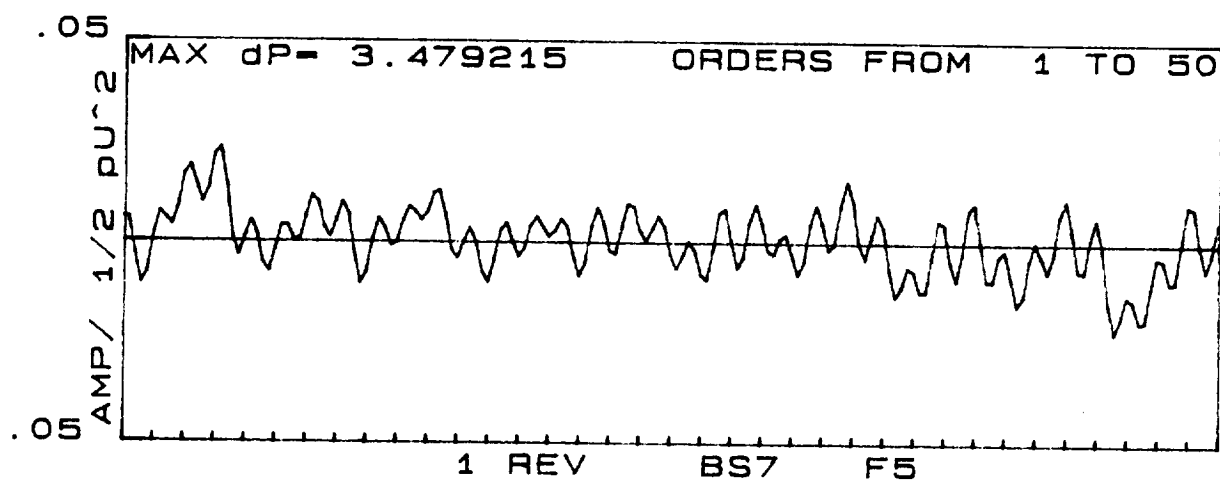
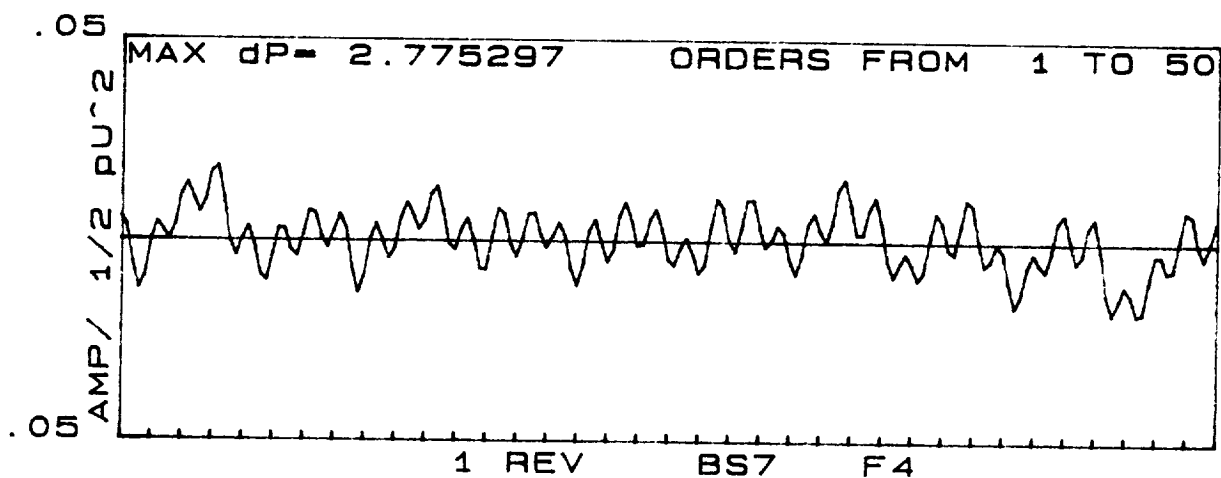
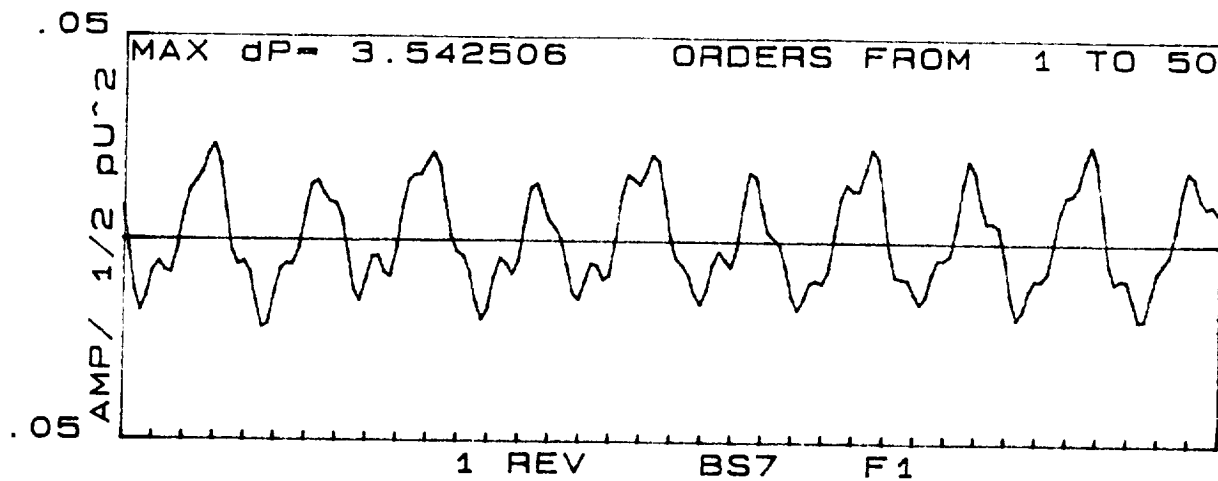
Conditions: F1, F4, F5

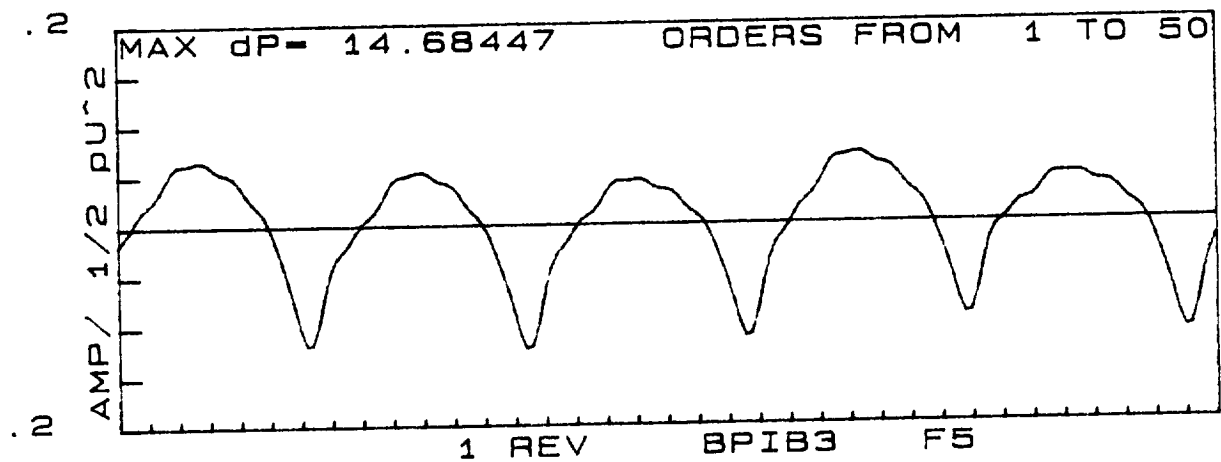
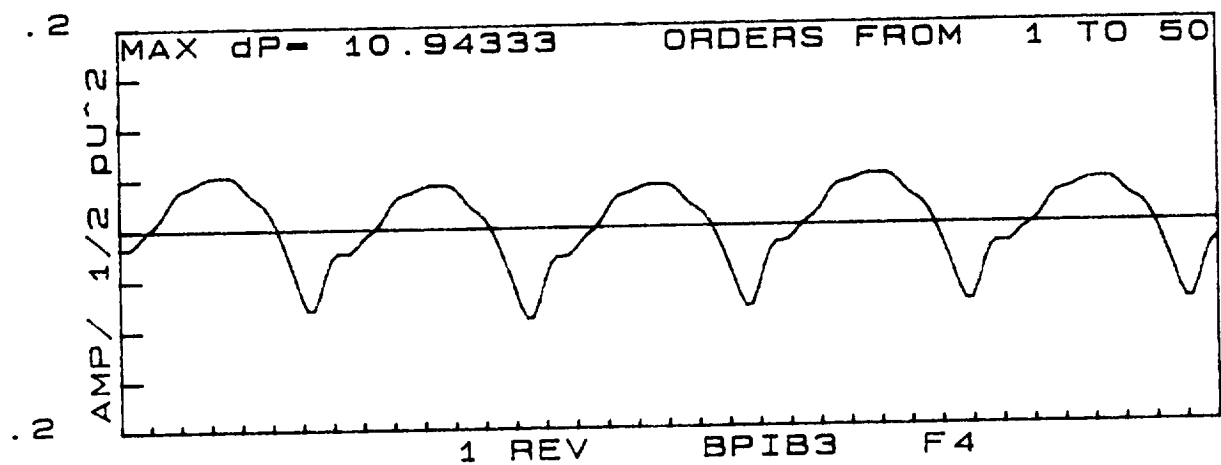
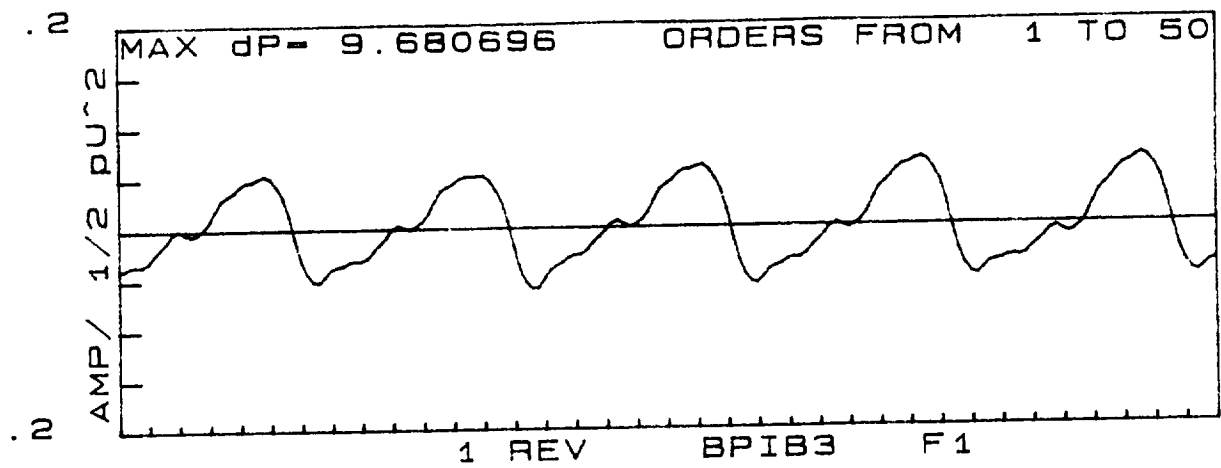
The information shown on these plots is used to generate Table 4. These are synchronous waveforms, the result of synchronous time averaging. They are representative of the pulsation activity occurring in the various components of the pump.

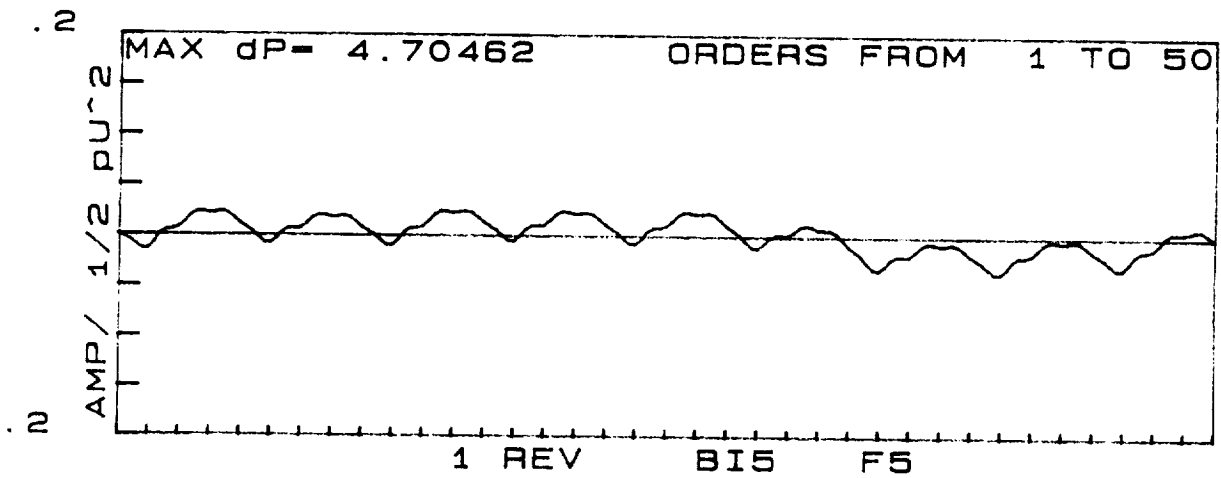
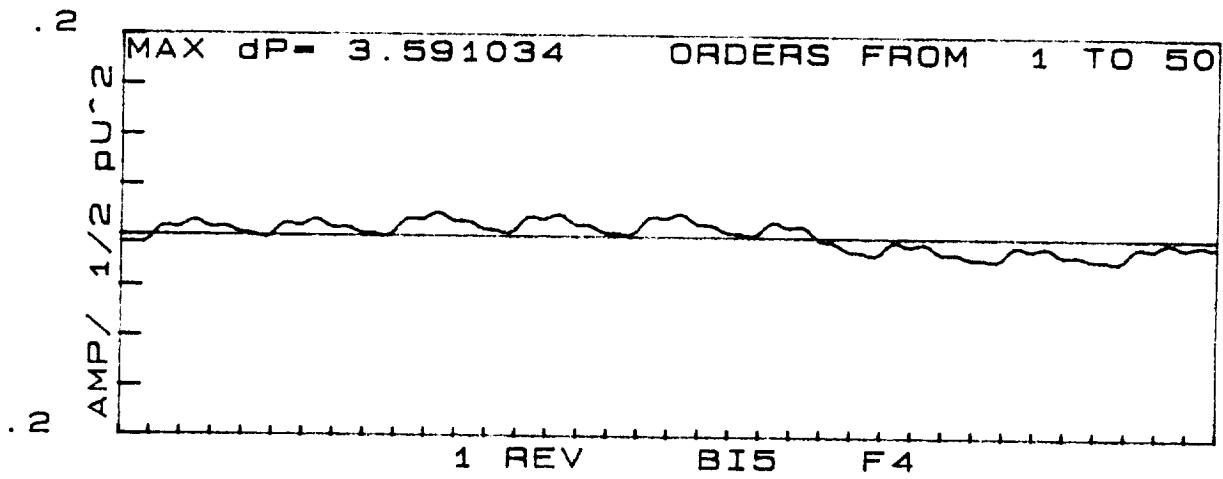
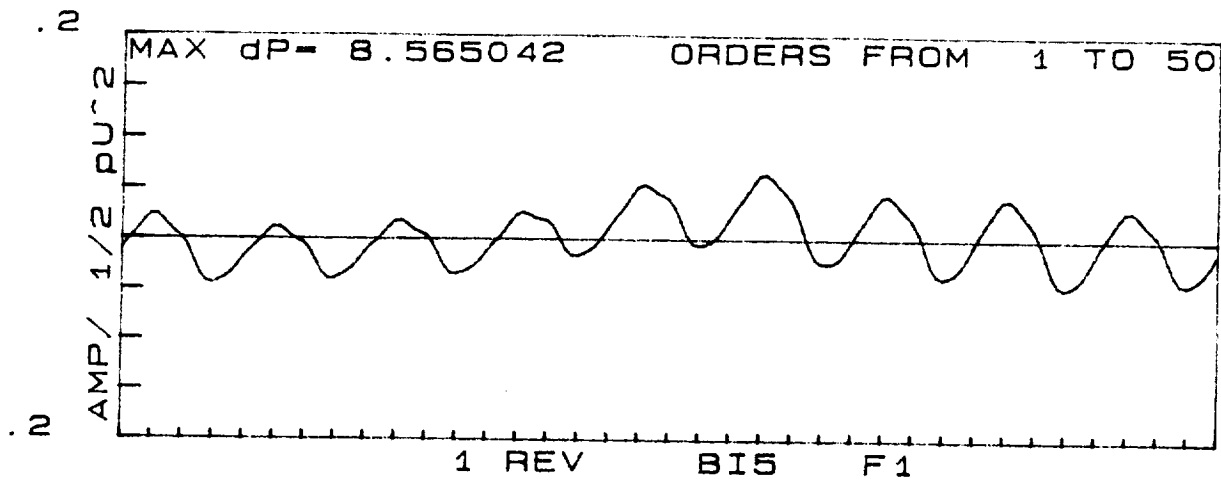


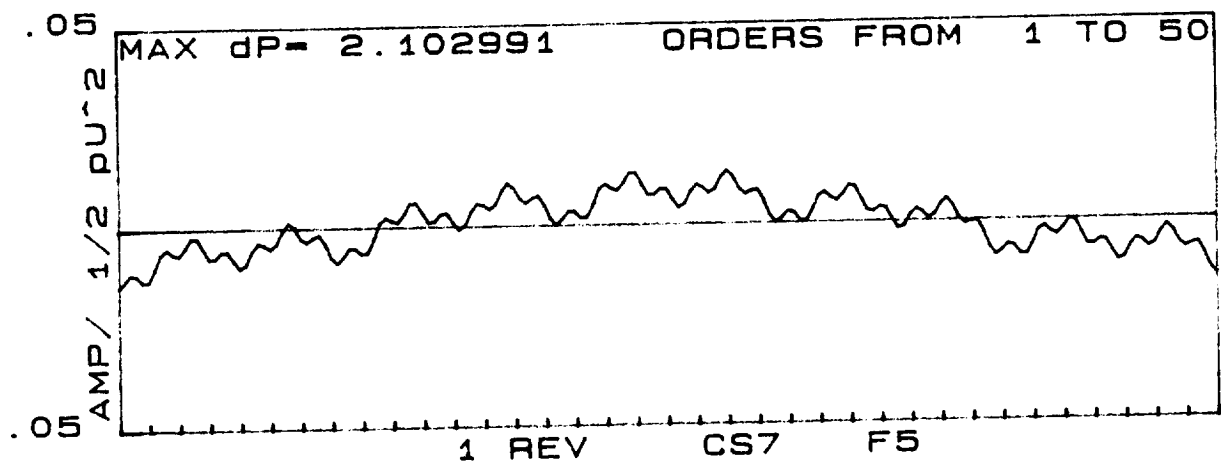
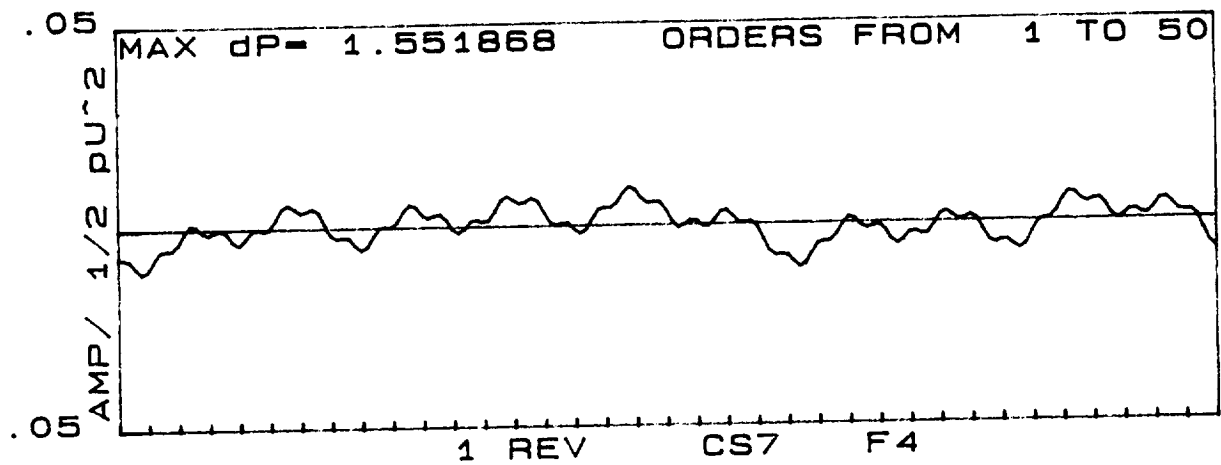
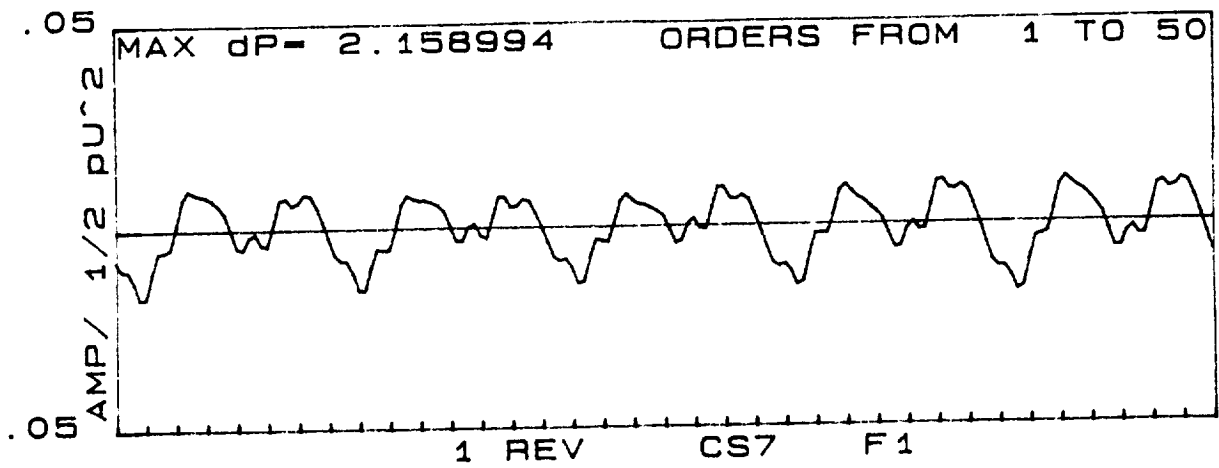


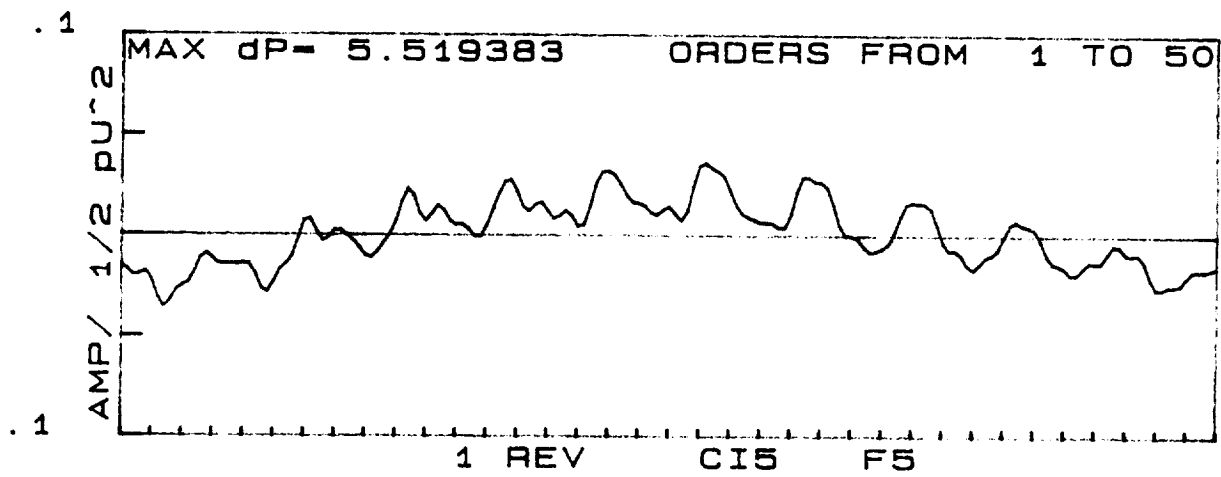
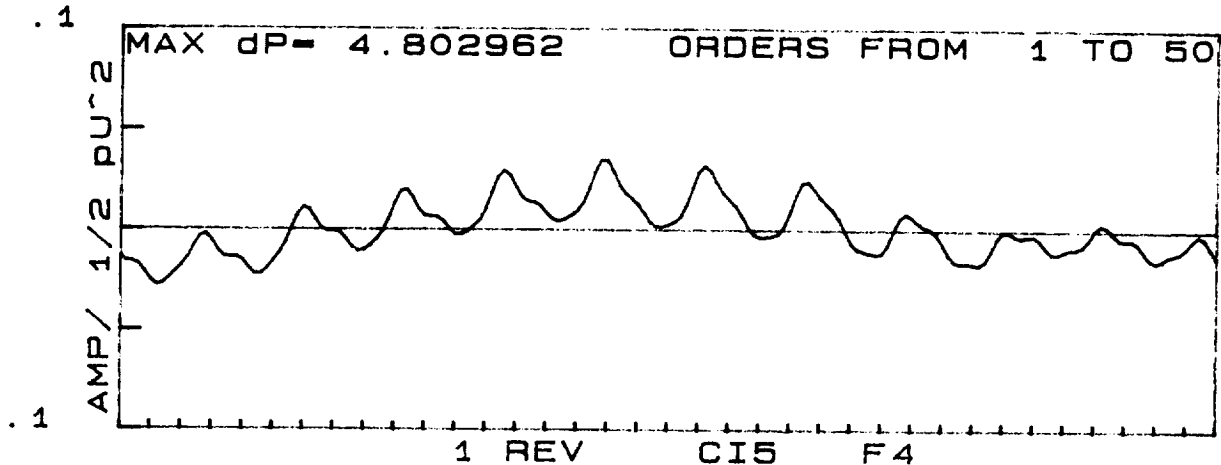
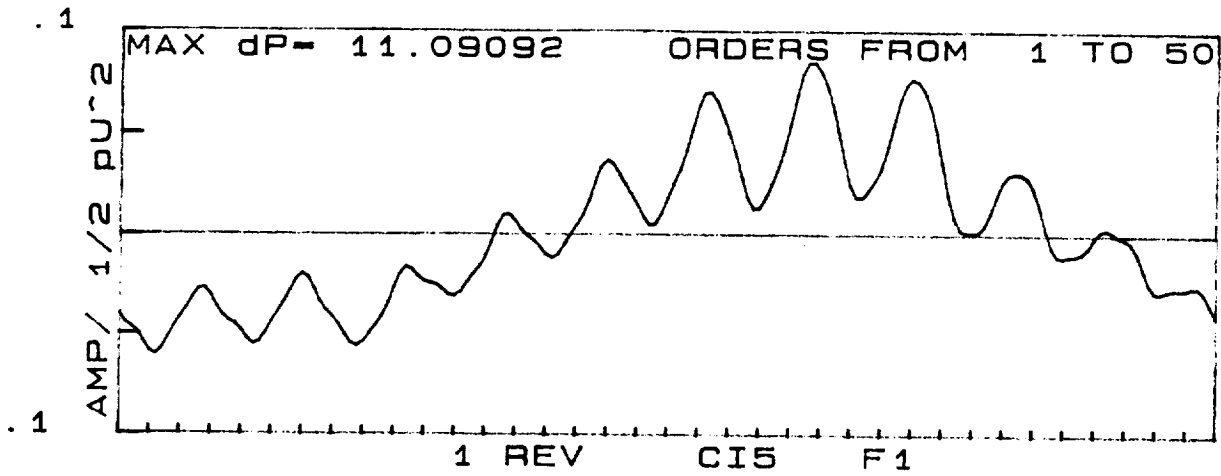










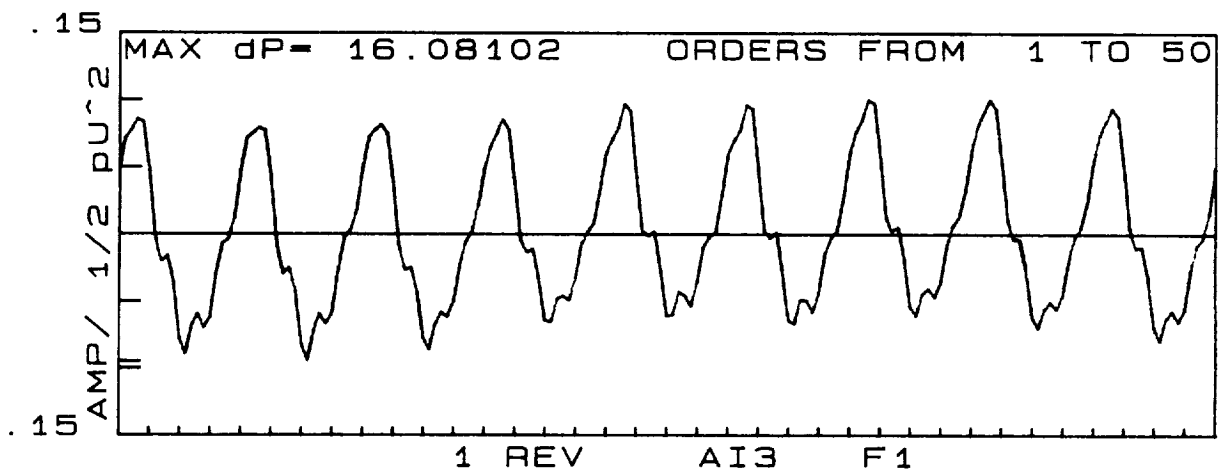
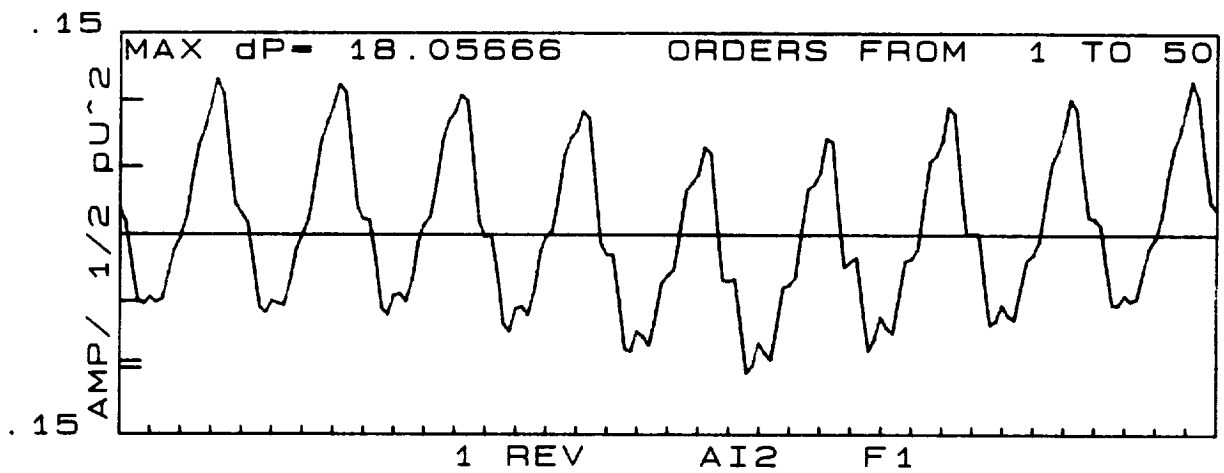
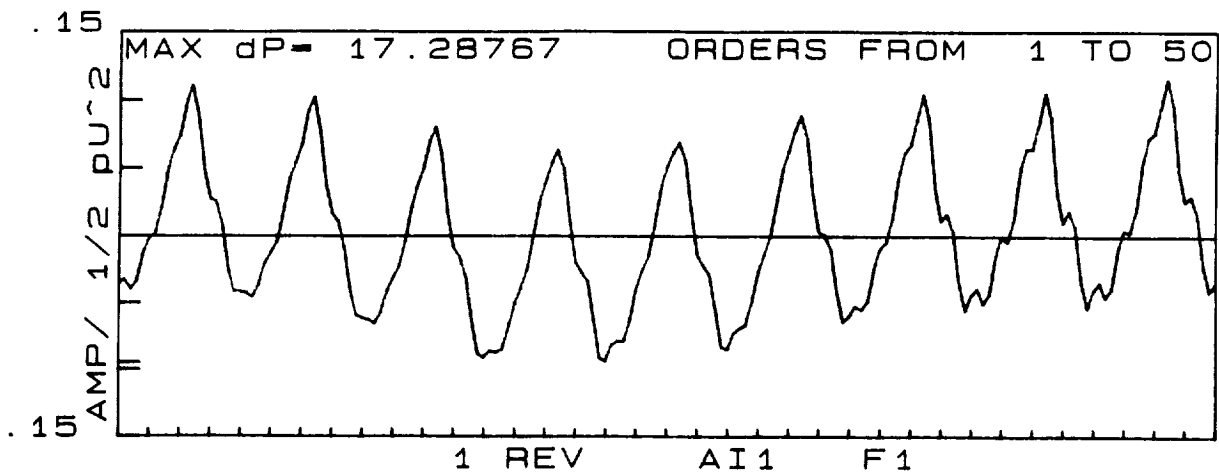


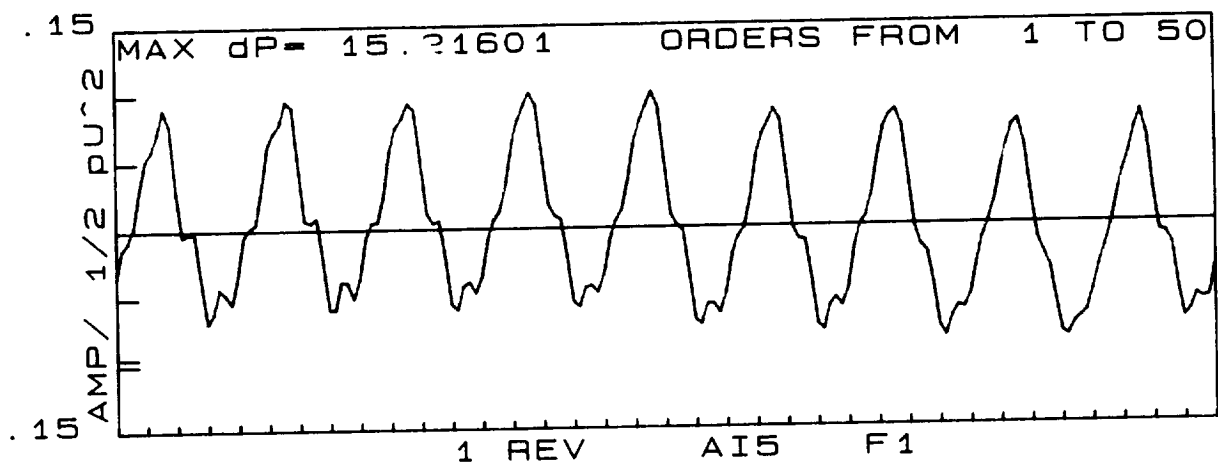
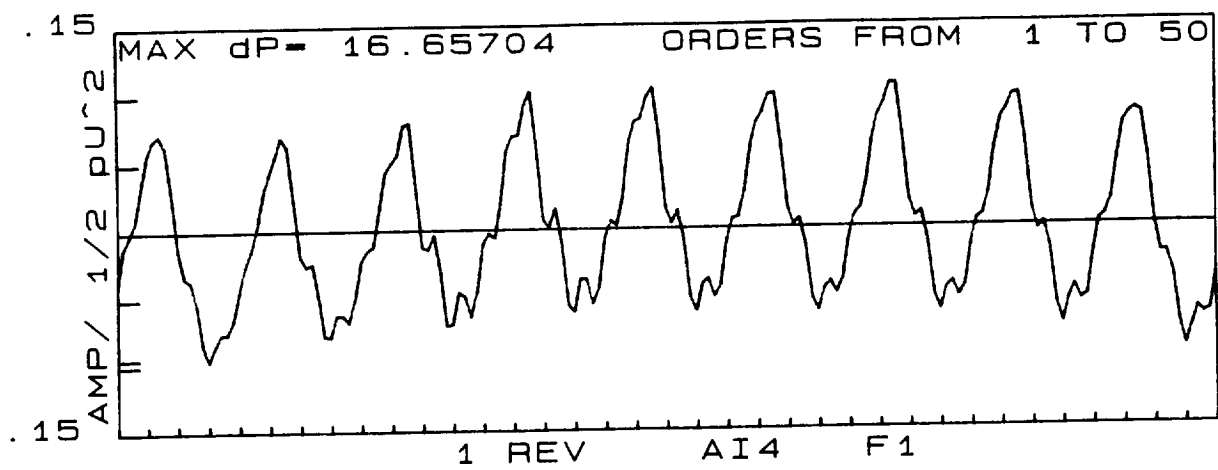
Circumferential Uniformity of Impeller Exit Sensors

Locations: AI1,...,AI5

Condition: F1

The uniformity of the pressure waveform (synchronously averaged) data from one impeller sensor to another is shown in this series of plots. The sensors are equally spaced in each of the 5 impeller passages. The magnitude and characteristic shape of each waveform are essentially identical. These plots help serve to establish the reliability of sensors, data collection and data reduction procedures.





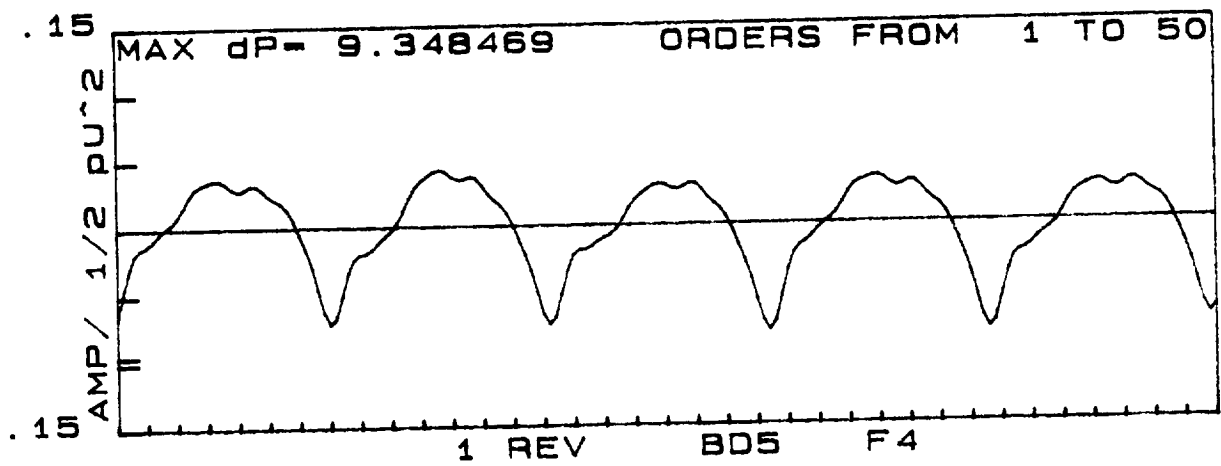
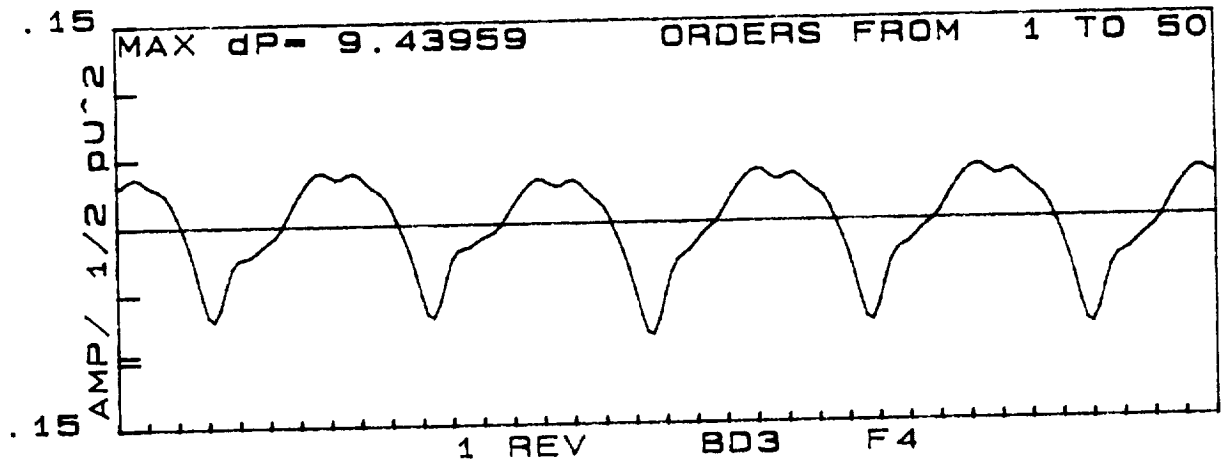
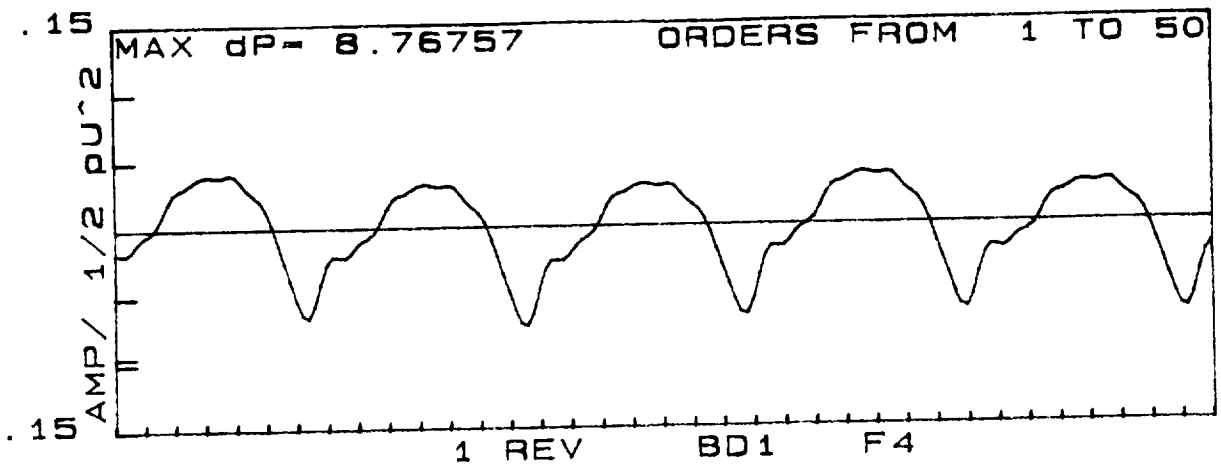
Circumferential Uniformity of Diffuser Throat Sensors

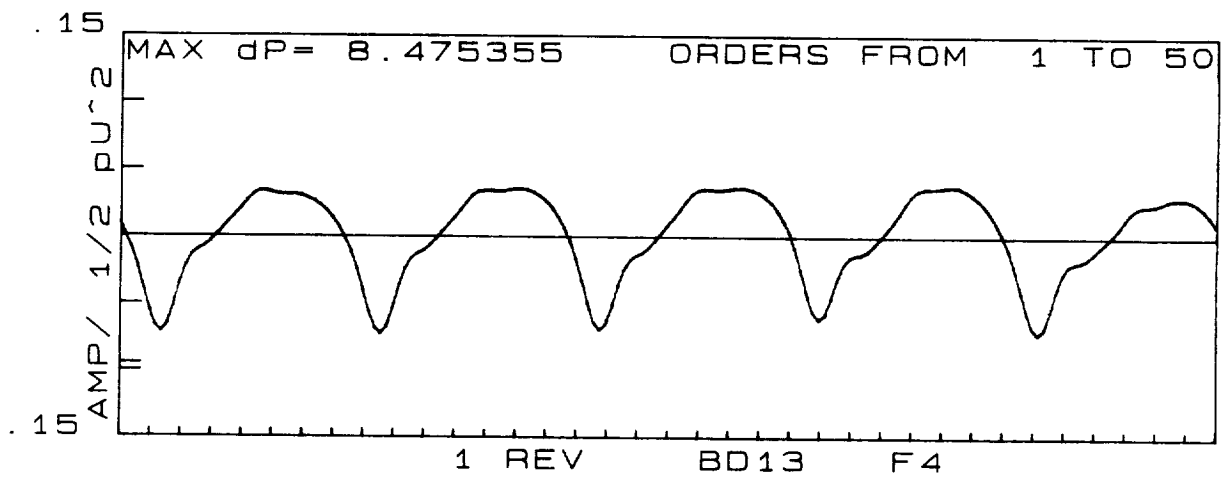
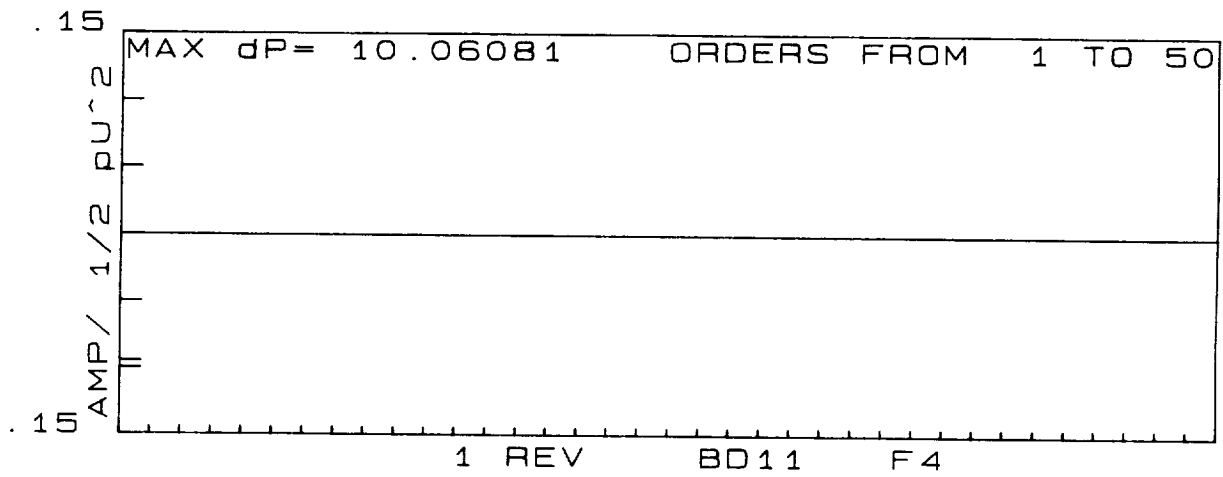
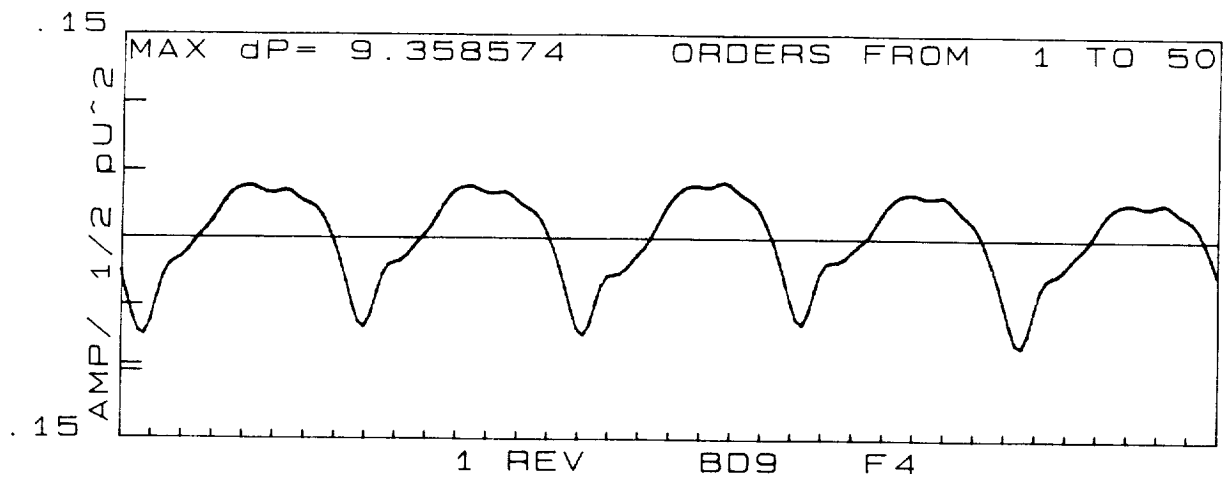
Locations: BD1,...,BD17

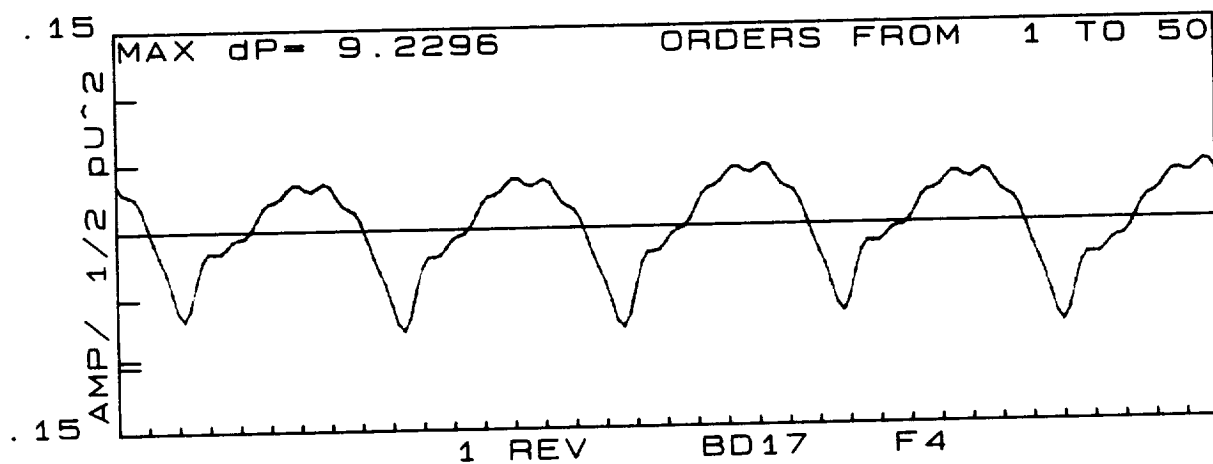
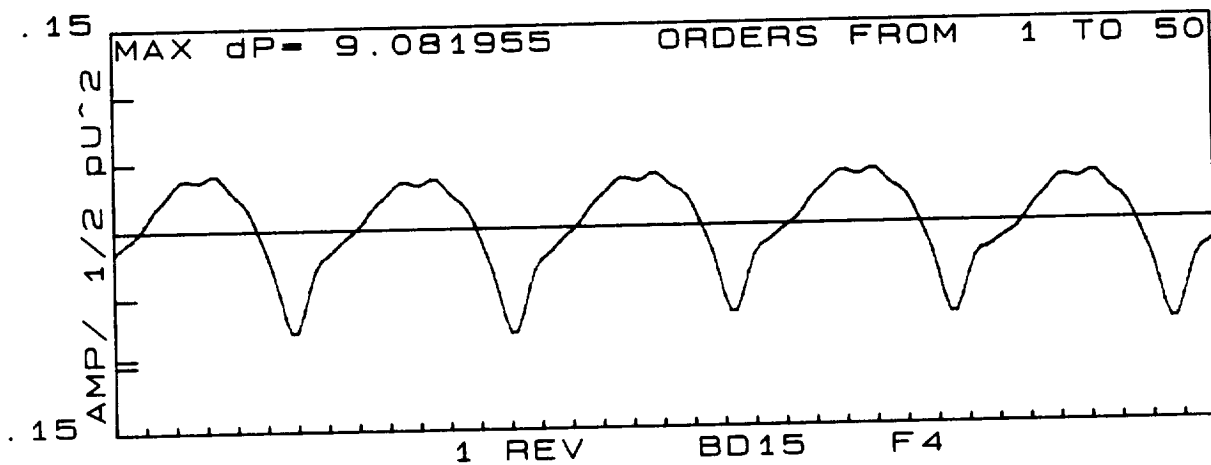
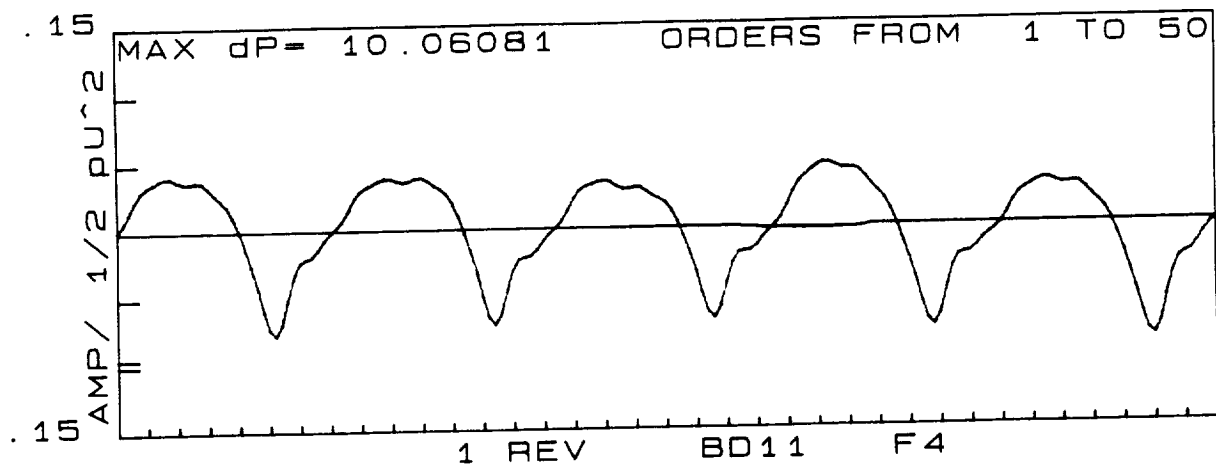
CD1,...,CD21

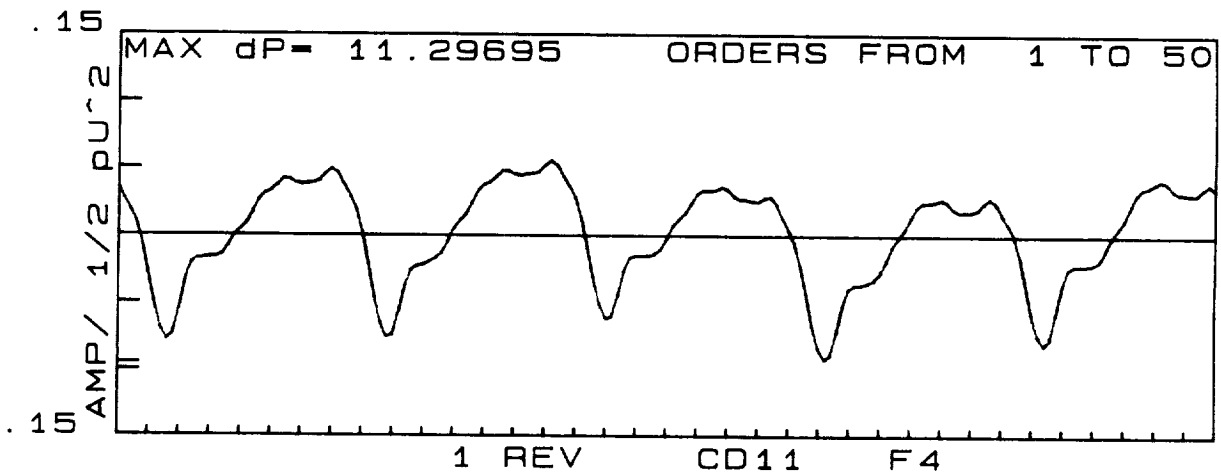
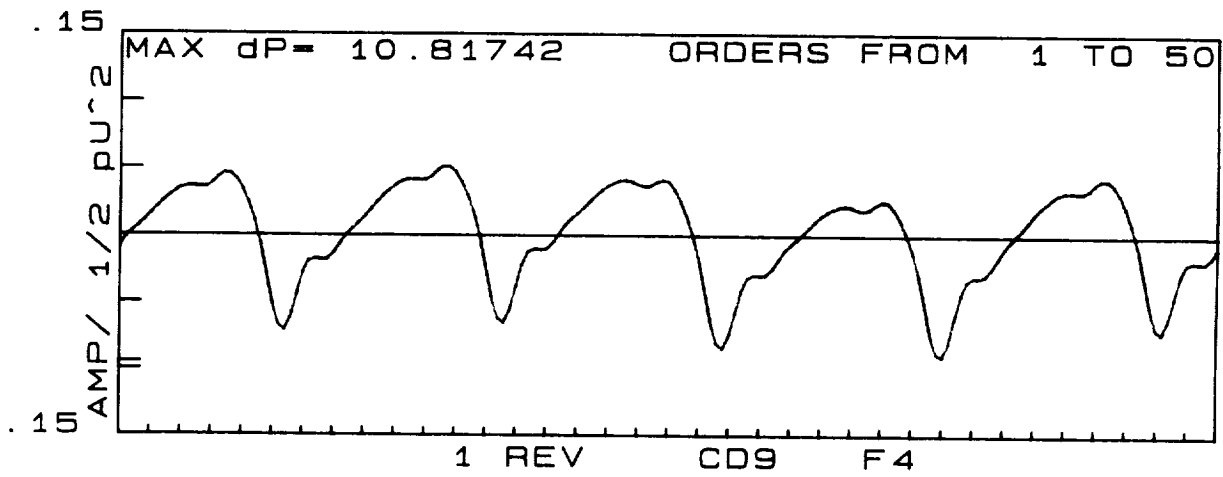
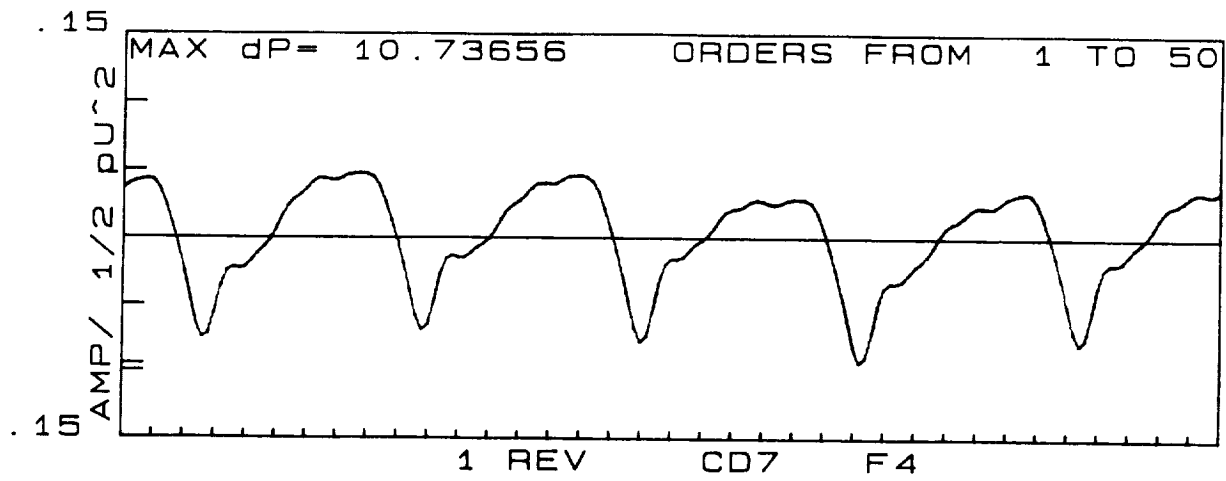
Condition: F4

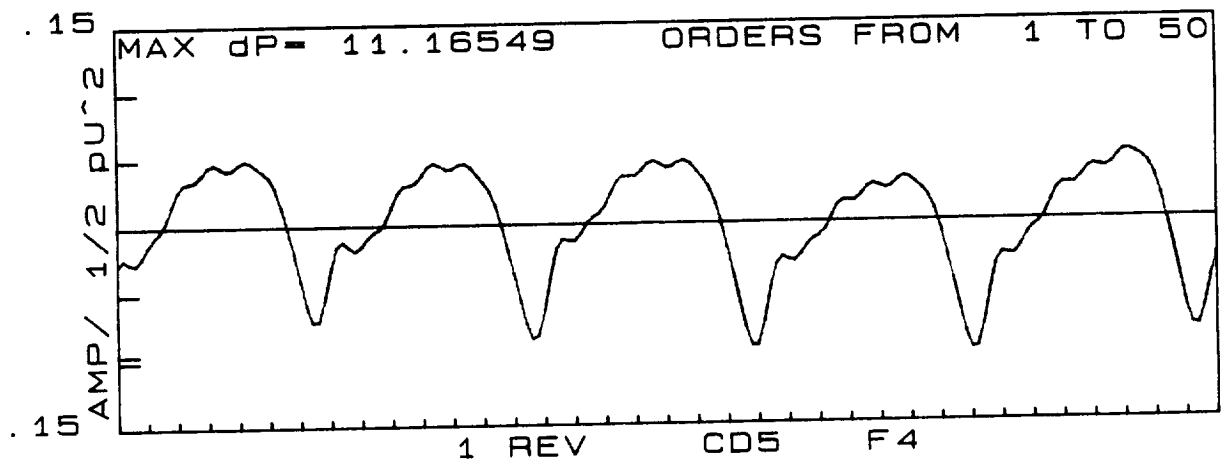
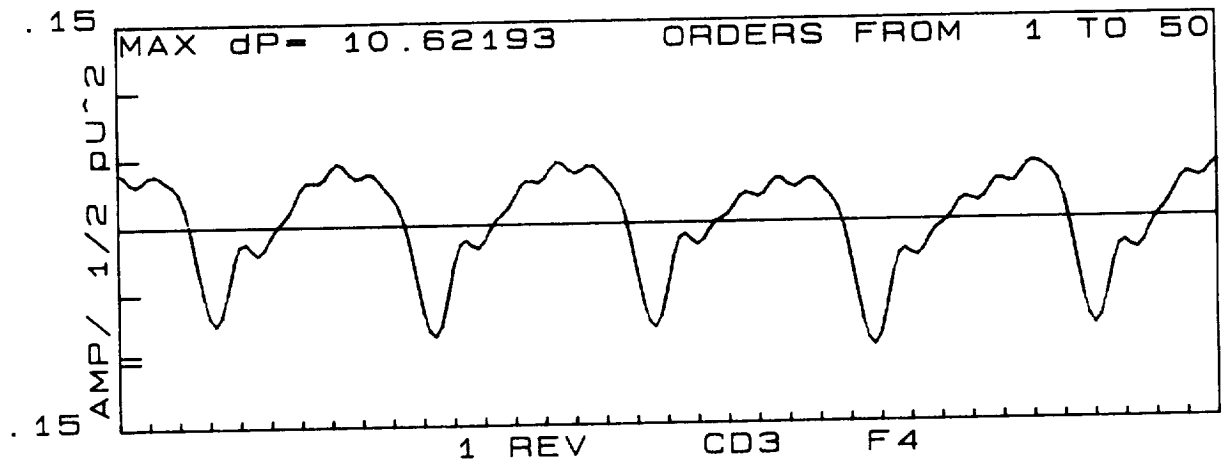
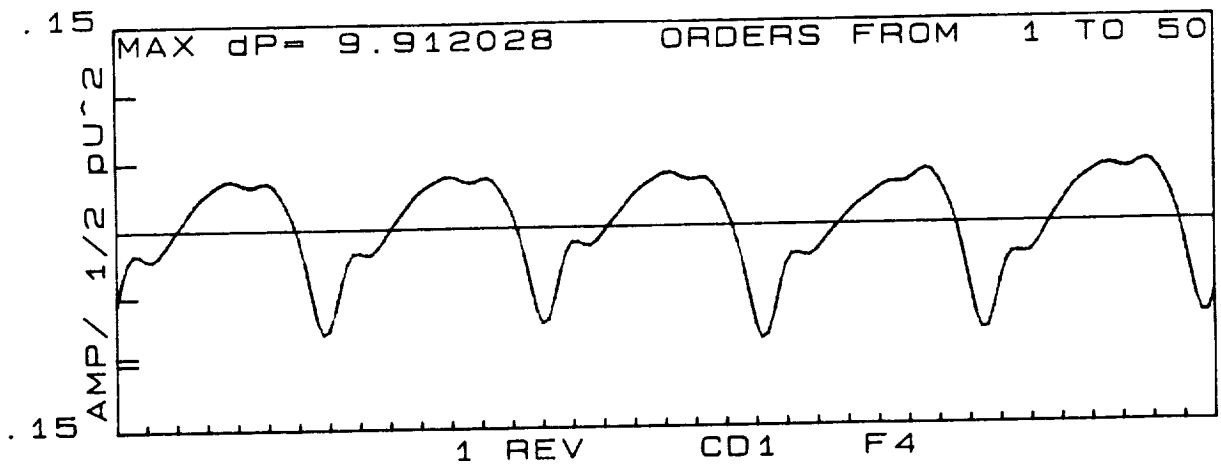
The circumferential uniformity of the synchronous pressure pulsation waveforms for configurations B and C are shown in this series of plots. The magnitude and characteristic shapes of the waveforms are essentially identical. These plots serve to establish the reliability of the sensors, data collection and data reduction technique. Each waveform is the synchronous pressure history at a different diffuser inlet location.

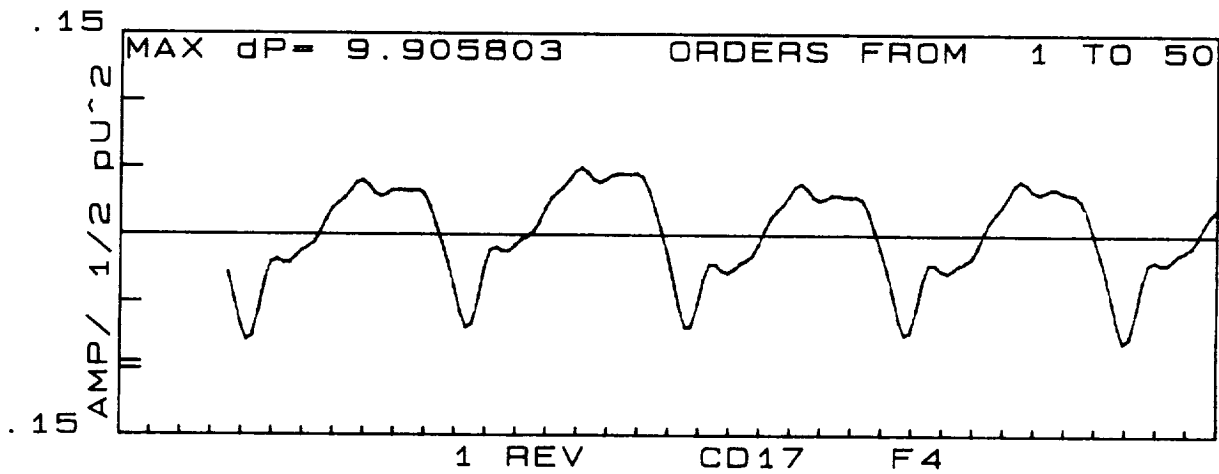
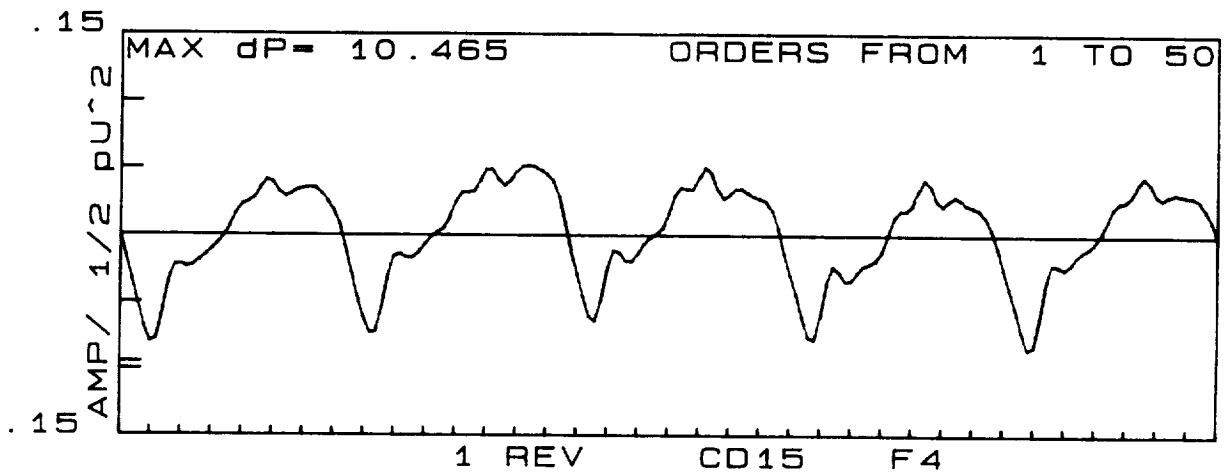
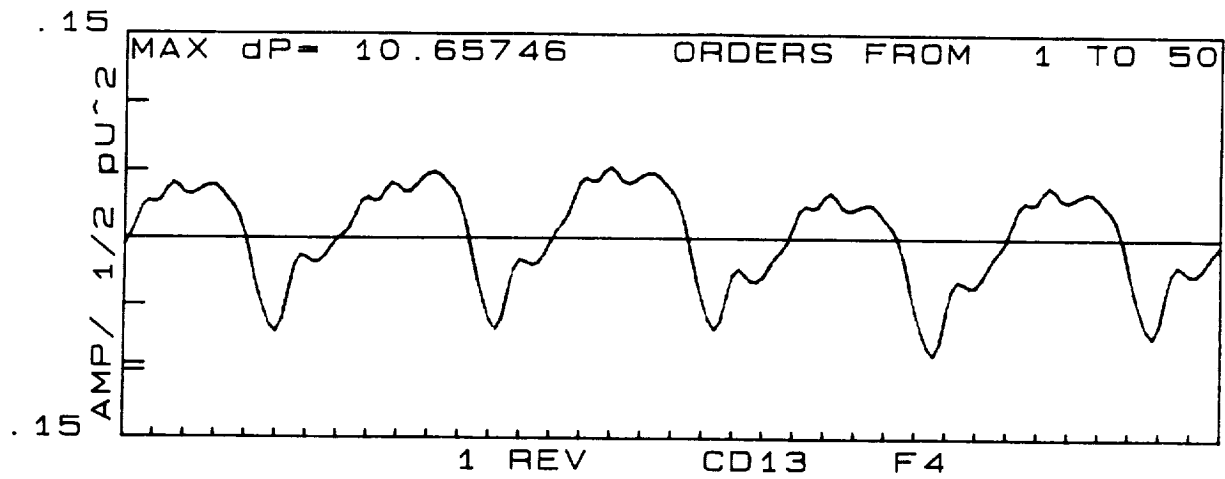


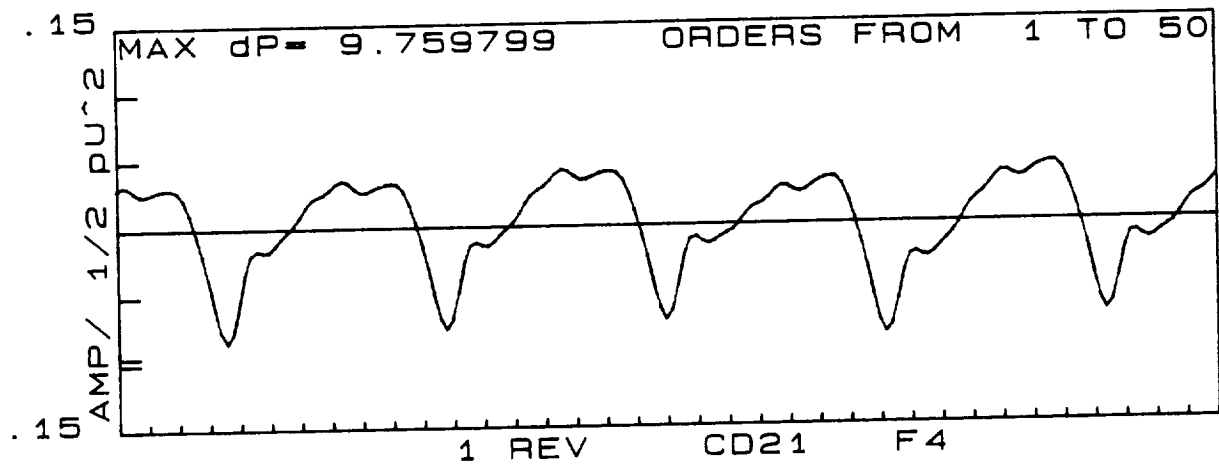
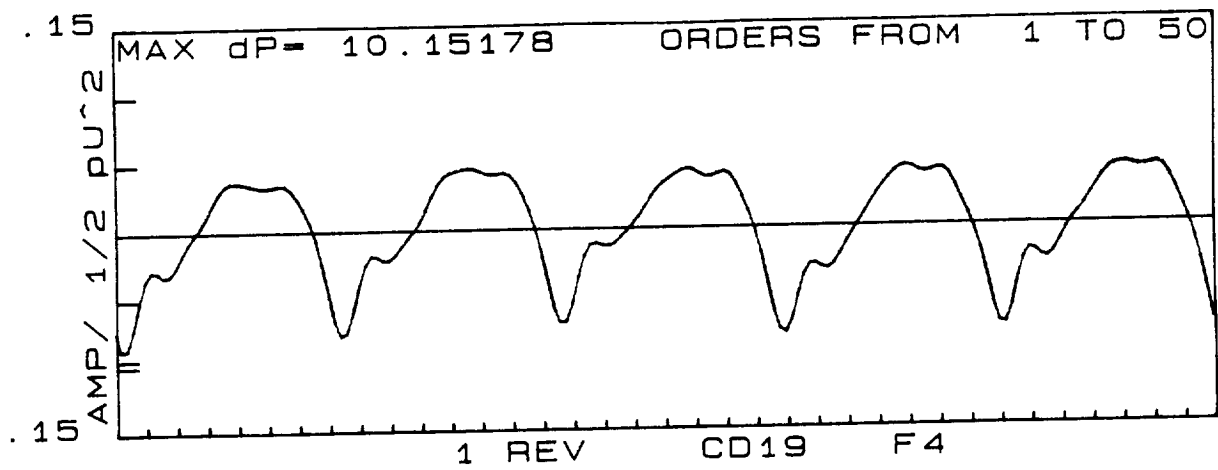










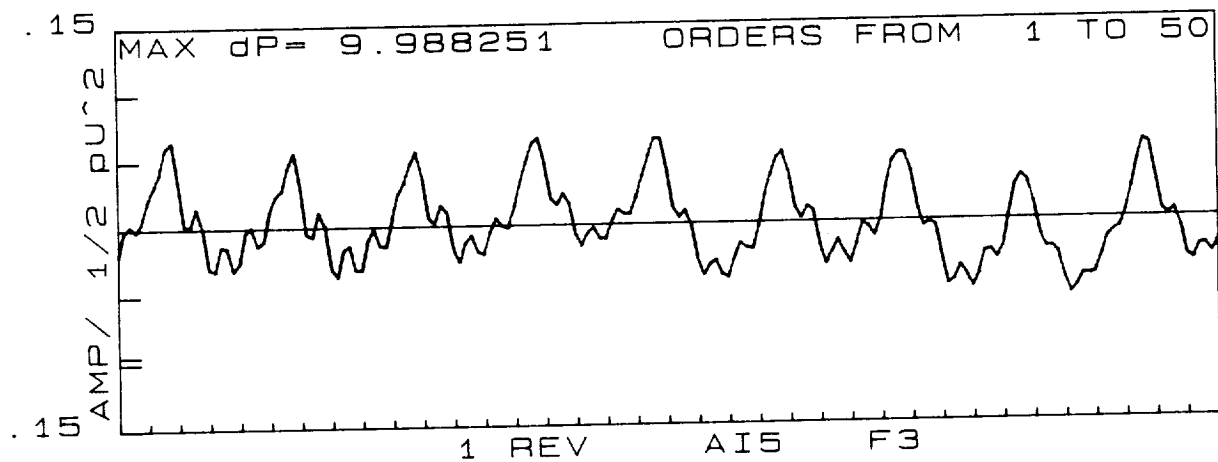
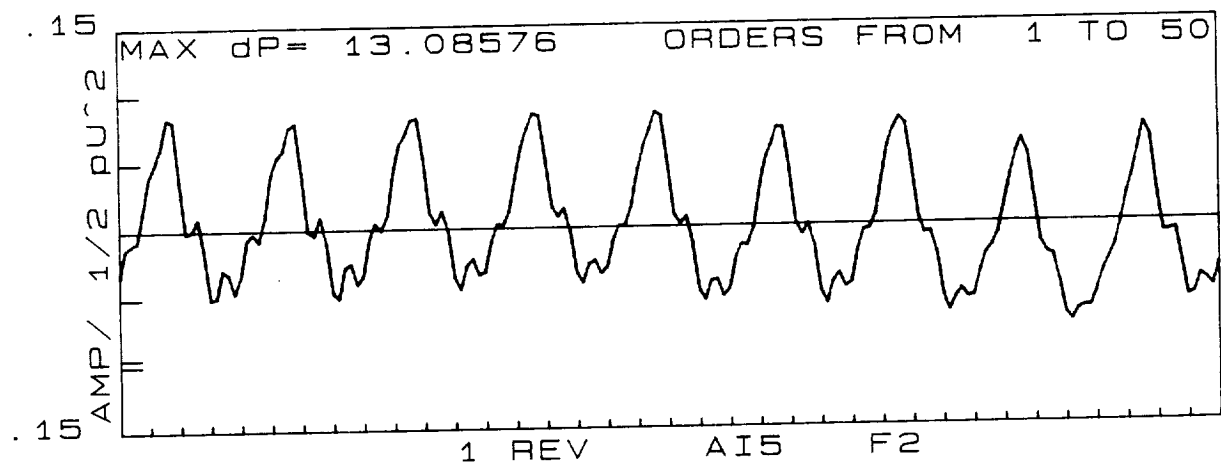
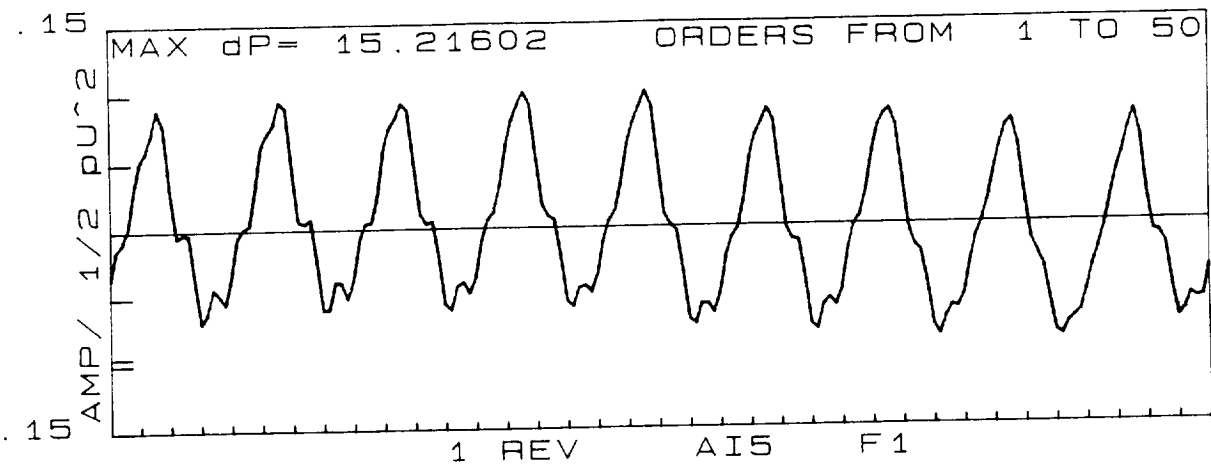


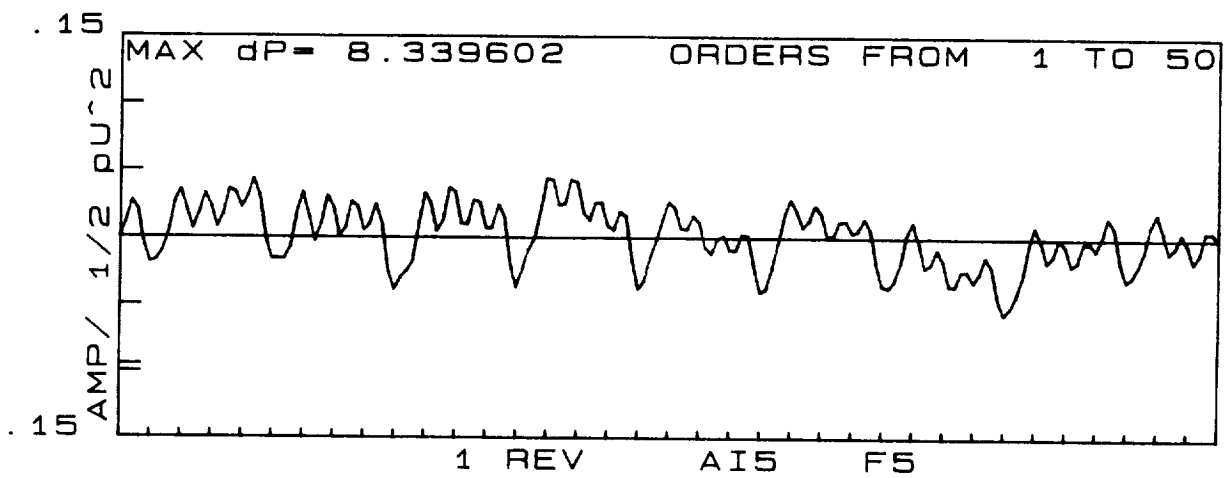
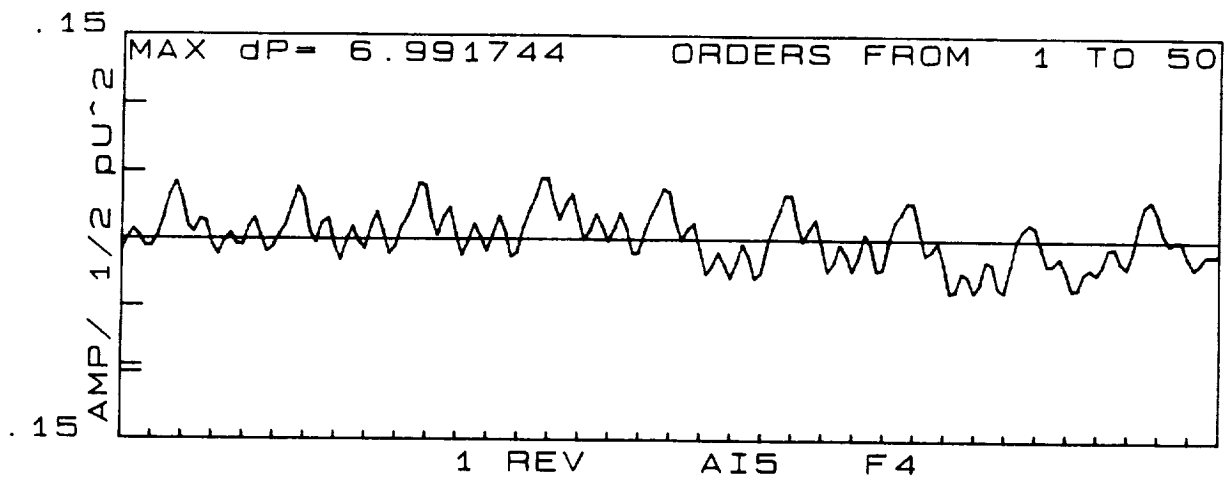
Effect of Clearance and Diffuser Vane # in Impeller Exit Sensors

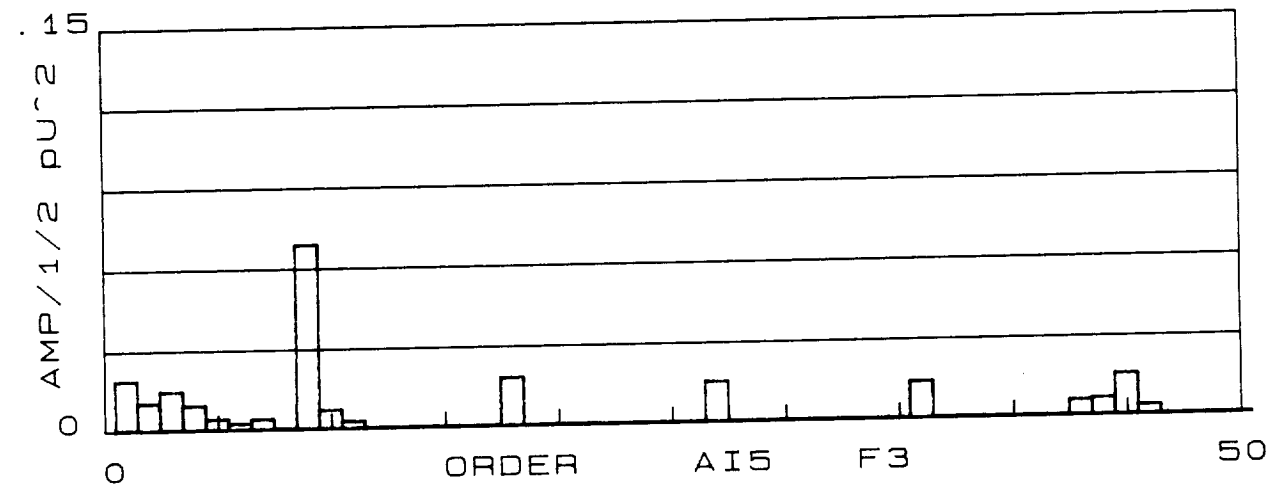
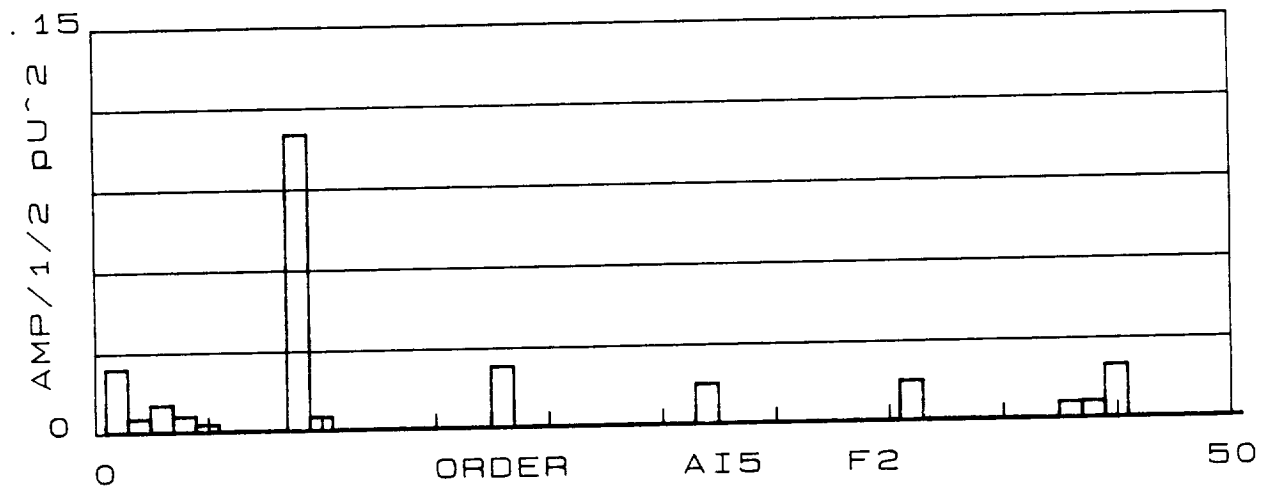
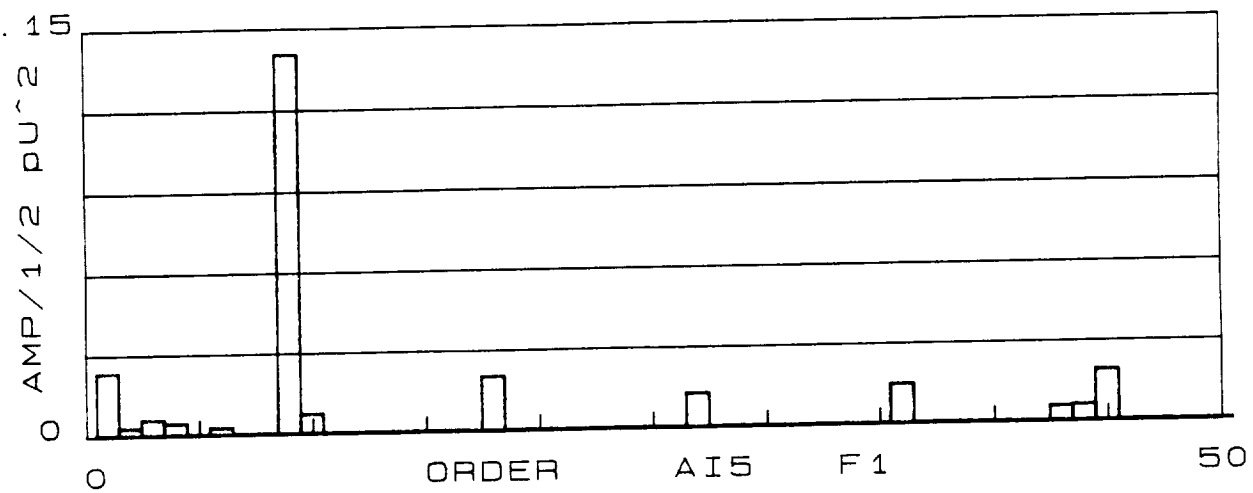
Locations: AI5, CI5, BI5

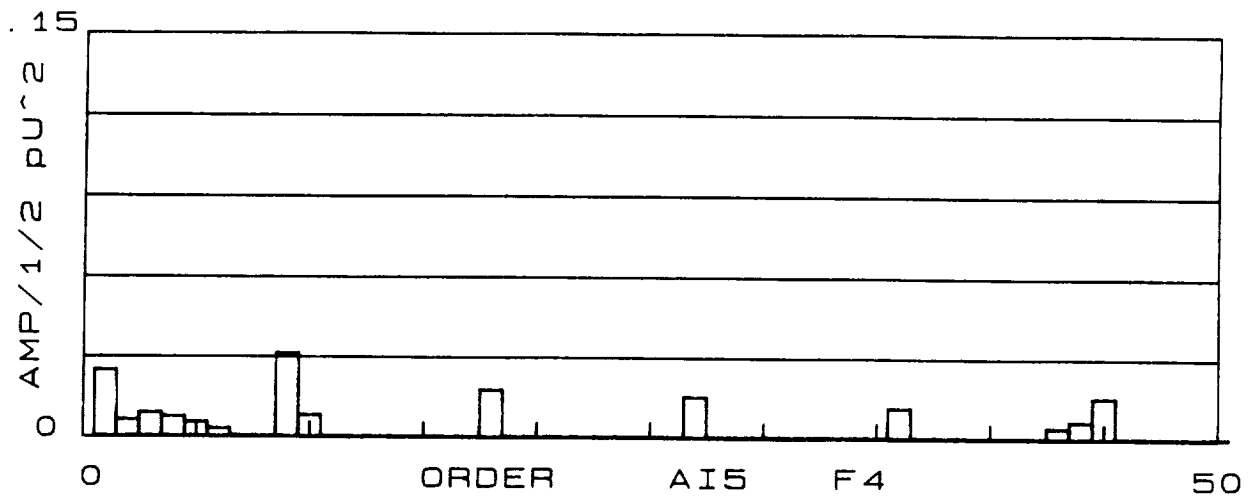
Conditions: F1, F2, F3, F4, F5

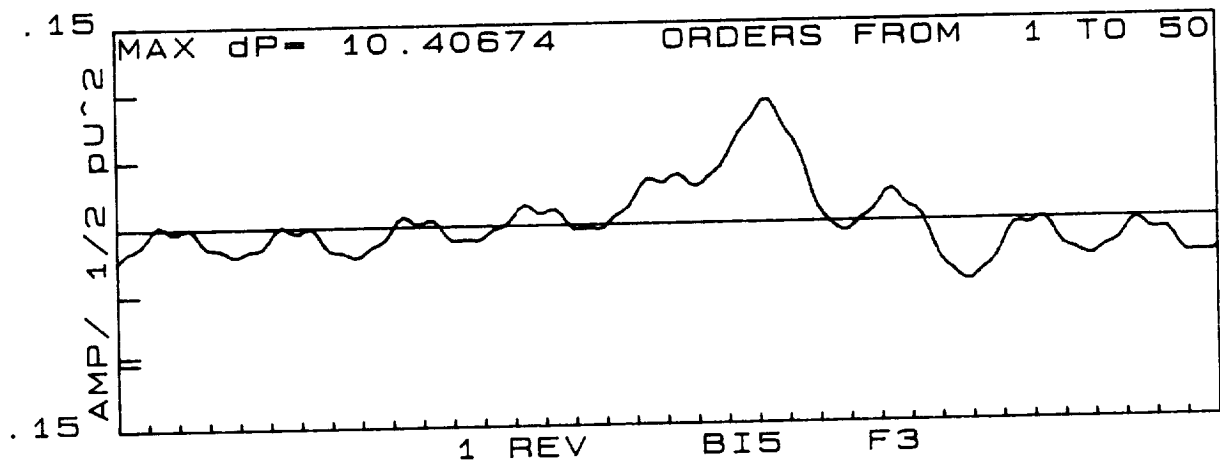
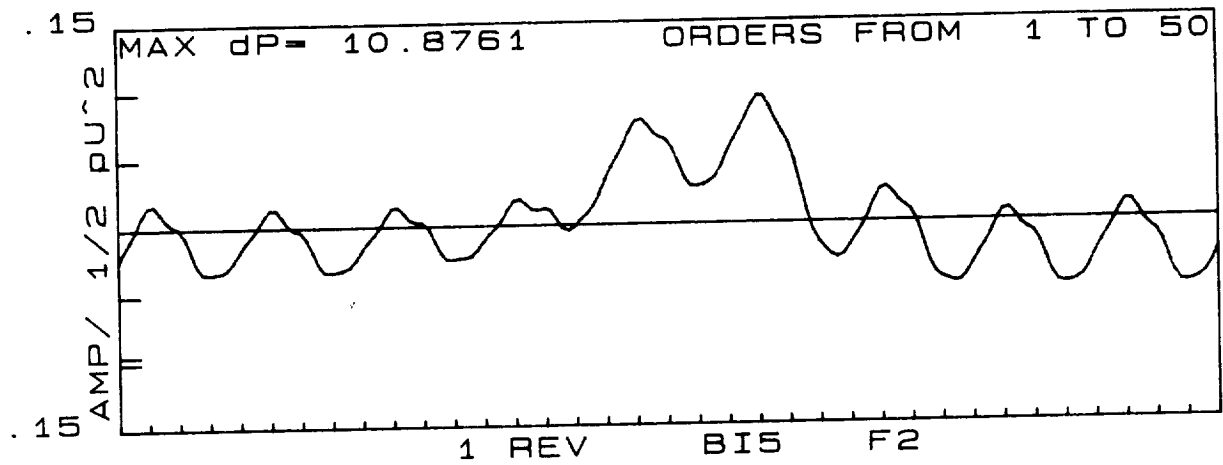
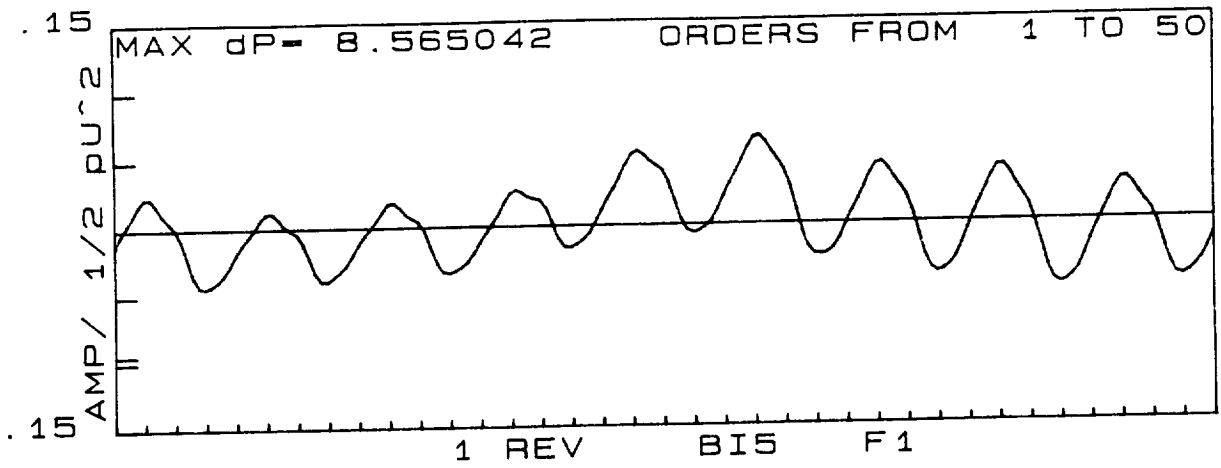
The changes in pressure pulsation amplitudes at the impeller exit for varying impeller/diffuser clearance and two different diffuser vane numbers are shown in this group of plots. The amplitudes for CI5 (11 vane diffuser) are actually less than for BI5 in spite of the larger clearance ratio of BI5 (1.059 vs 1.041). As expected, the increase in clearance ratio between AI5 and BI5 (9 vane diffuser, ratio change from 1.021 to 1.059) results in a reduction in pulsation amplitudes. Notice the large 1st order component of CI5 at F1 (25%Q). This configuration (C) incorporates an extension of a diffuser vane to the scroll cutwater, in a fashion similar to the HPTFP. This appears to have an effect at low flow, but no effect at the higher flows tested (75% to 125% Q).

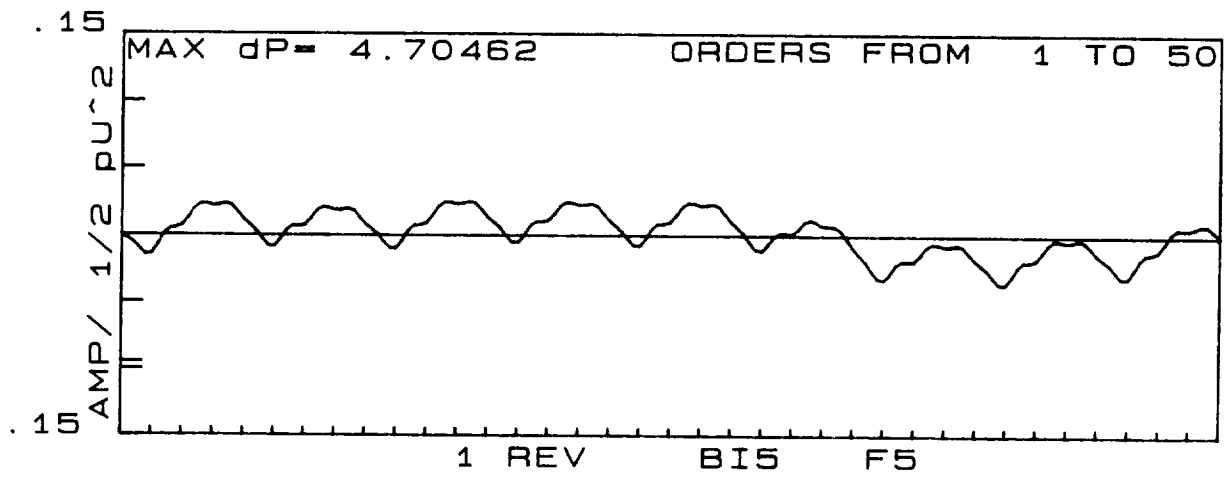
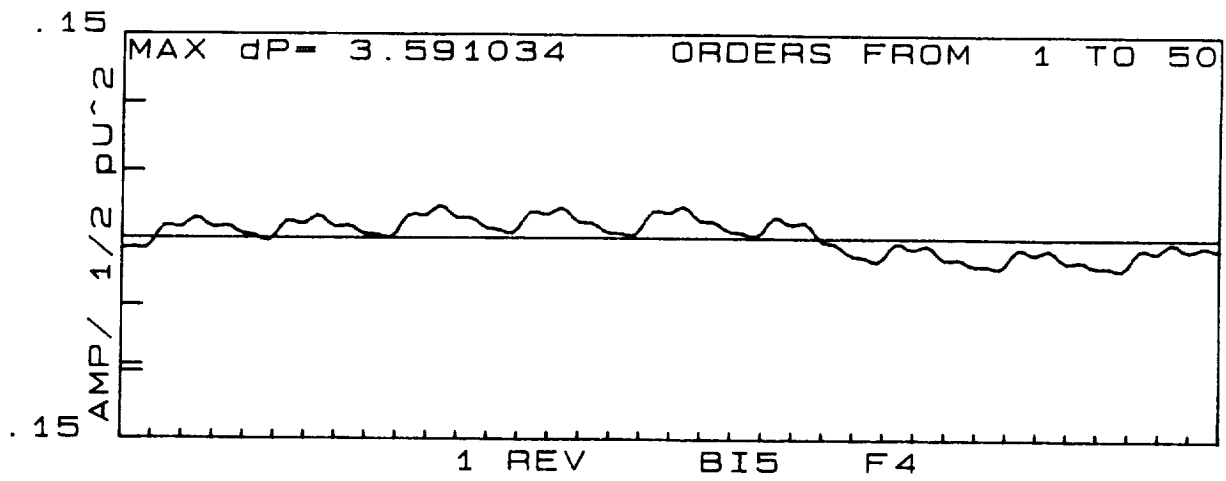


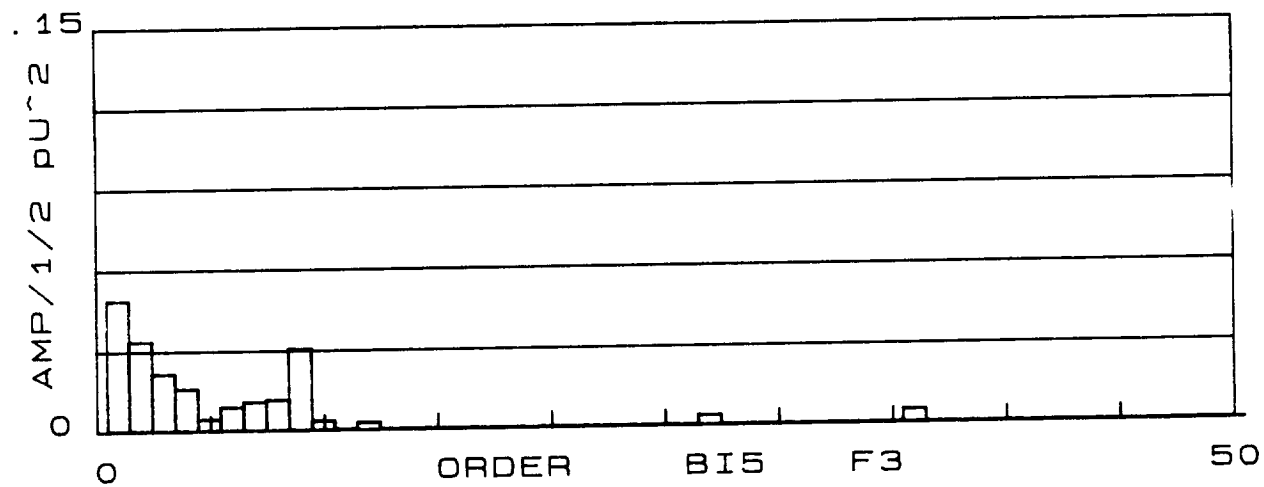
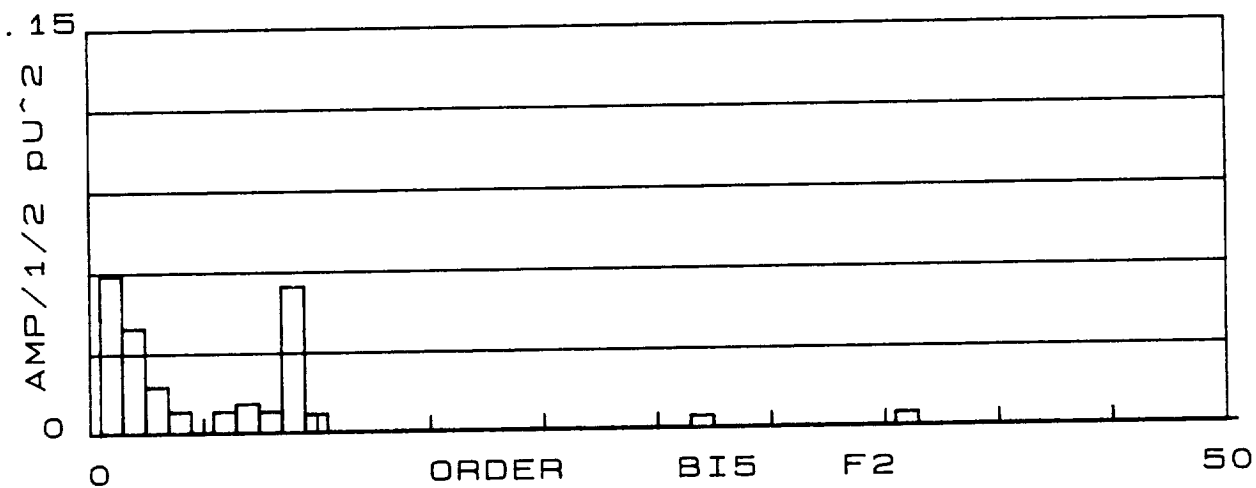
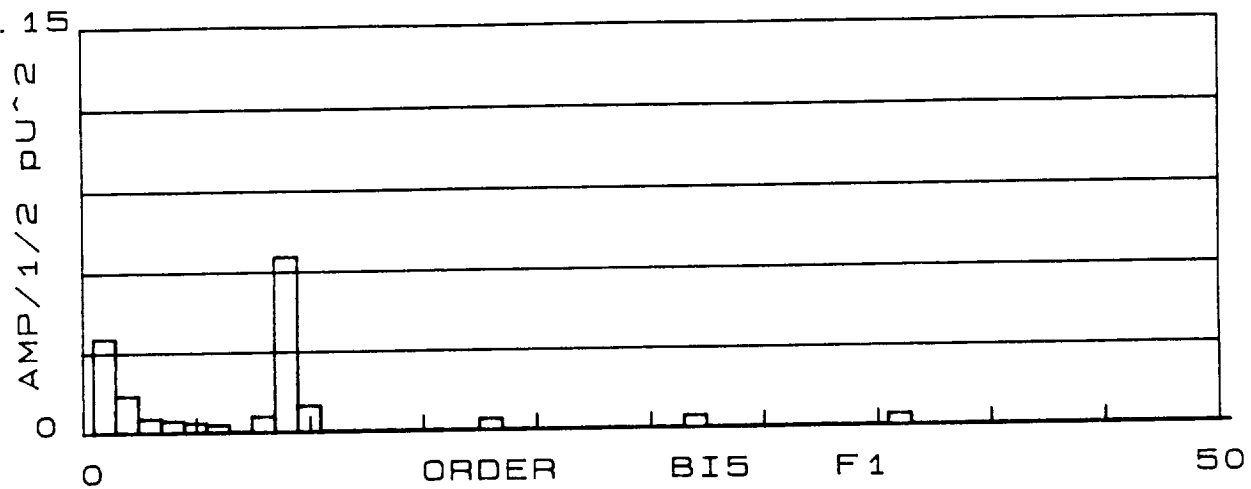


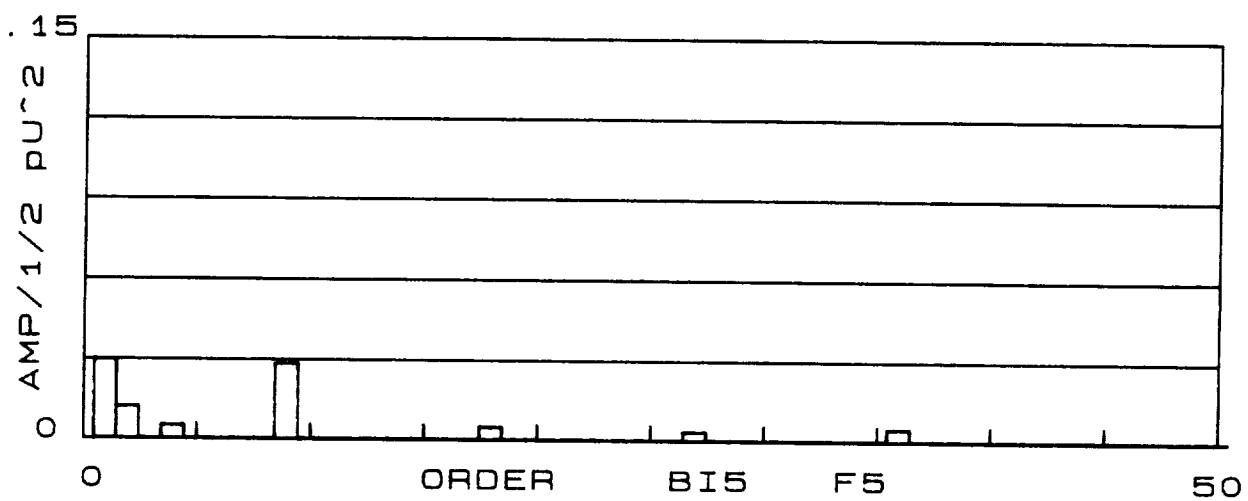
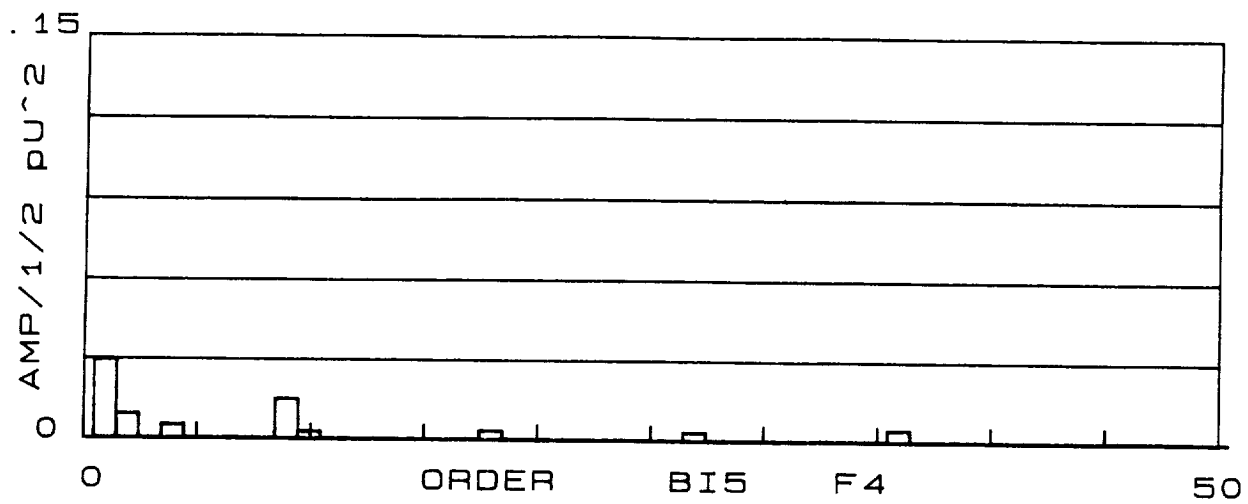


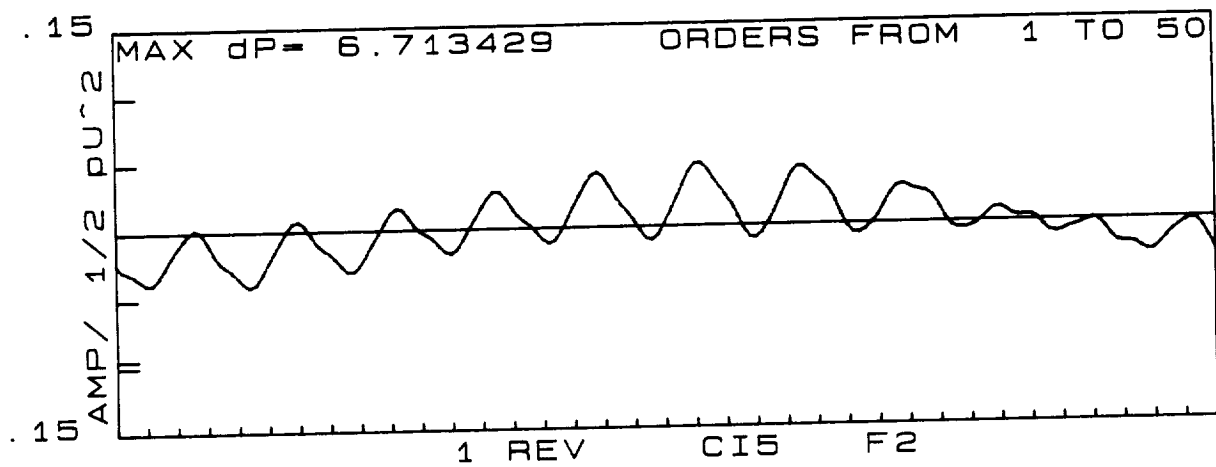
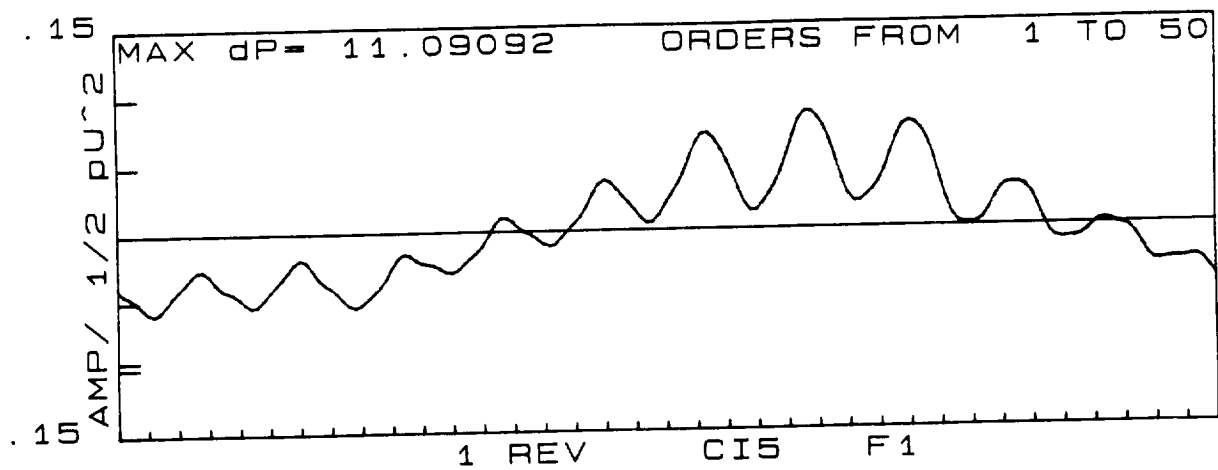


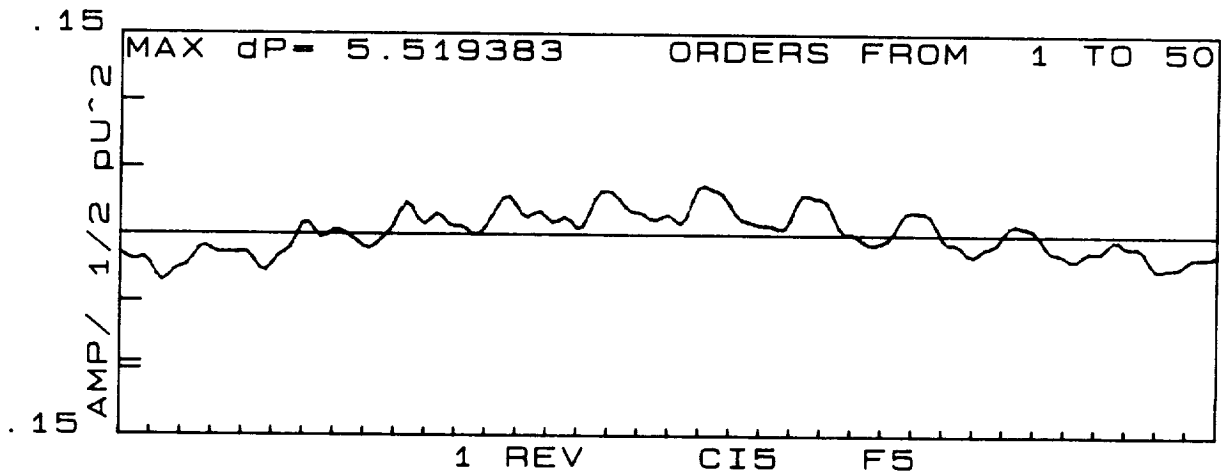
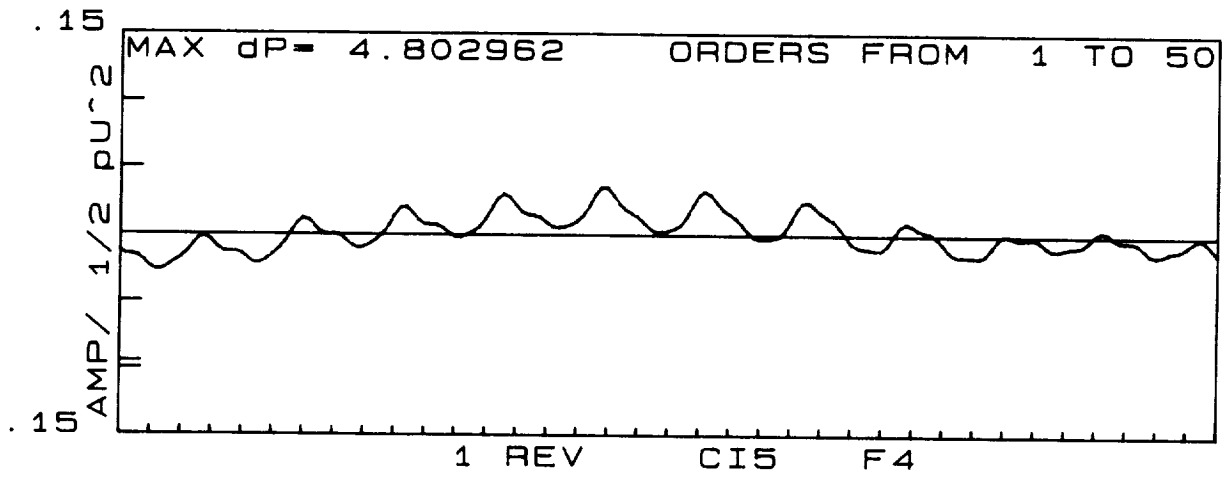
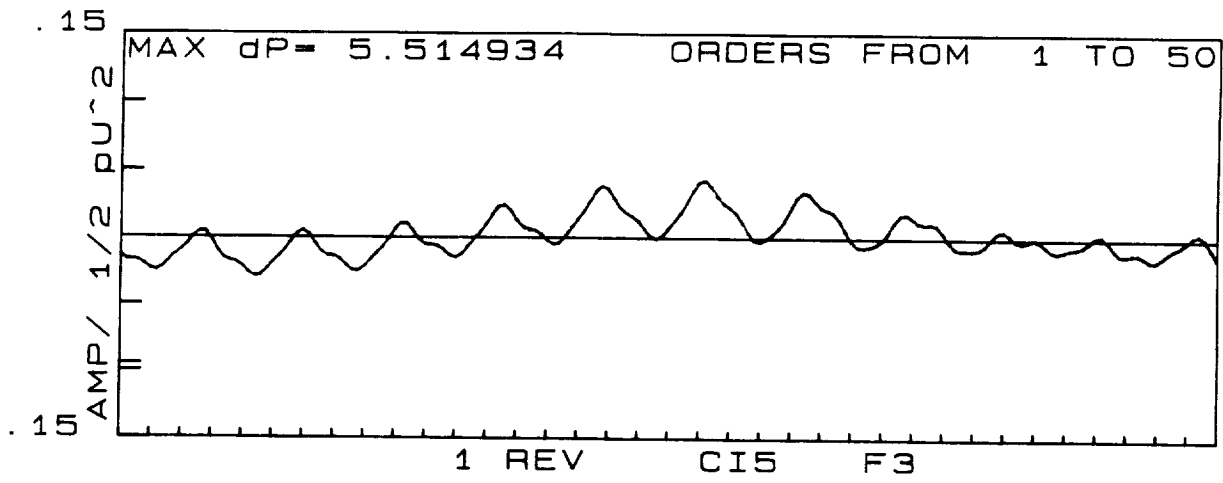


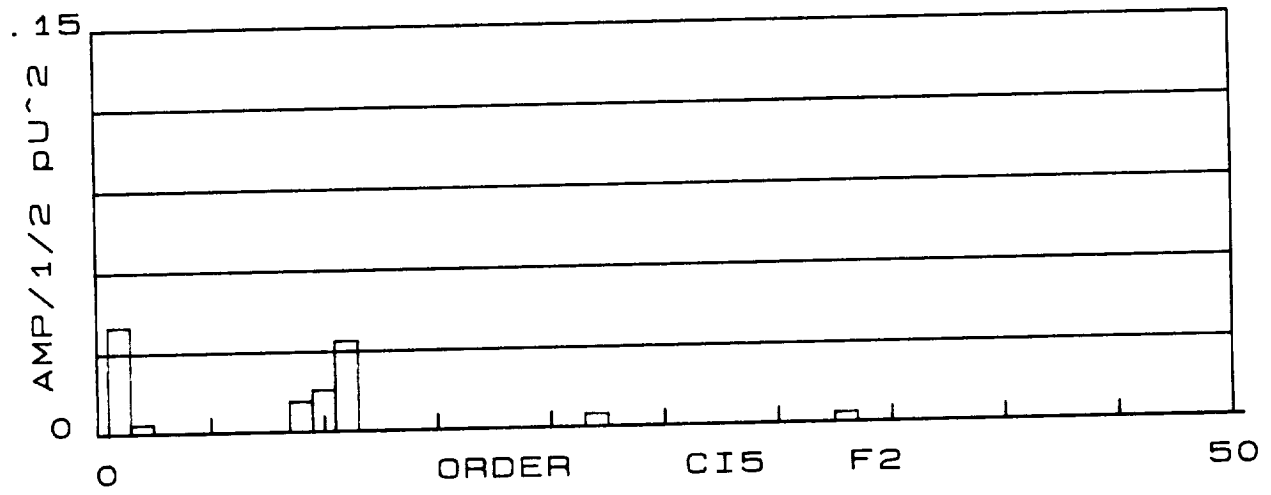
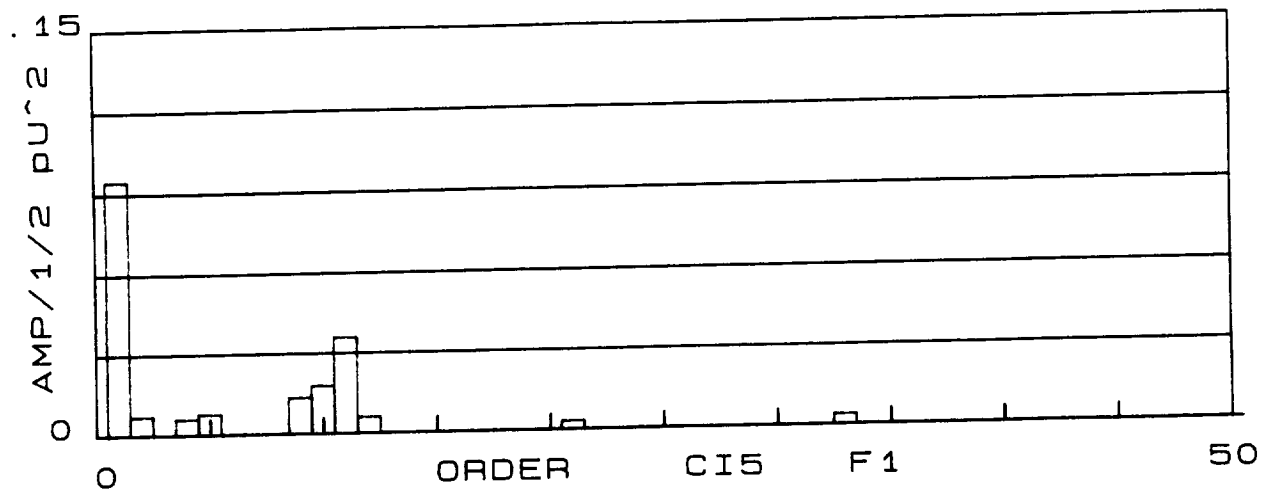


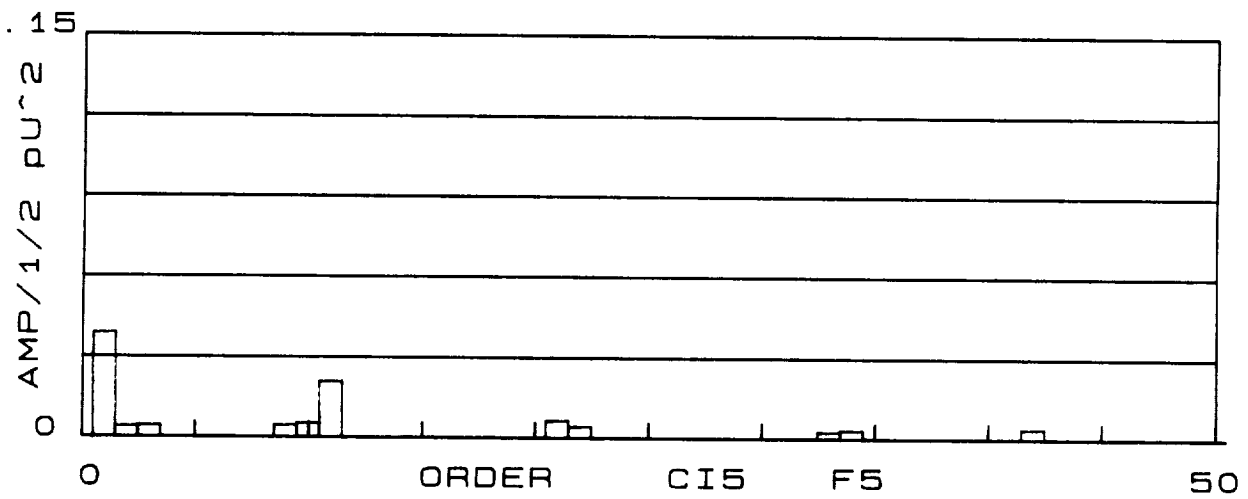
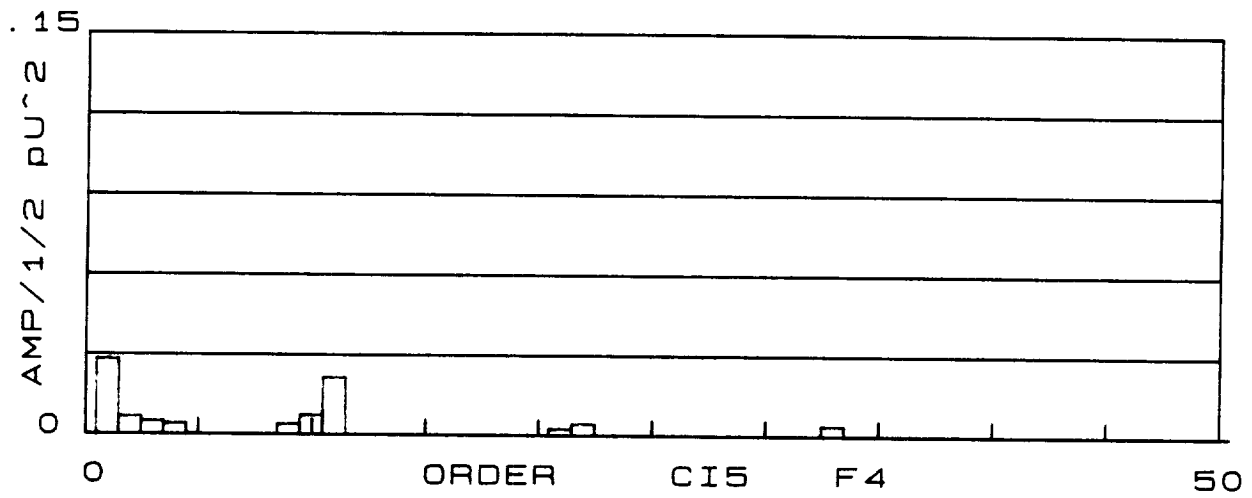
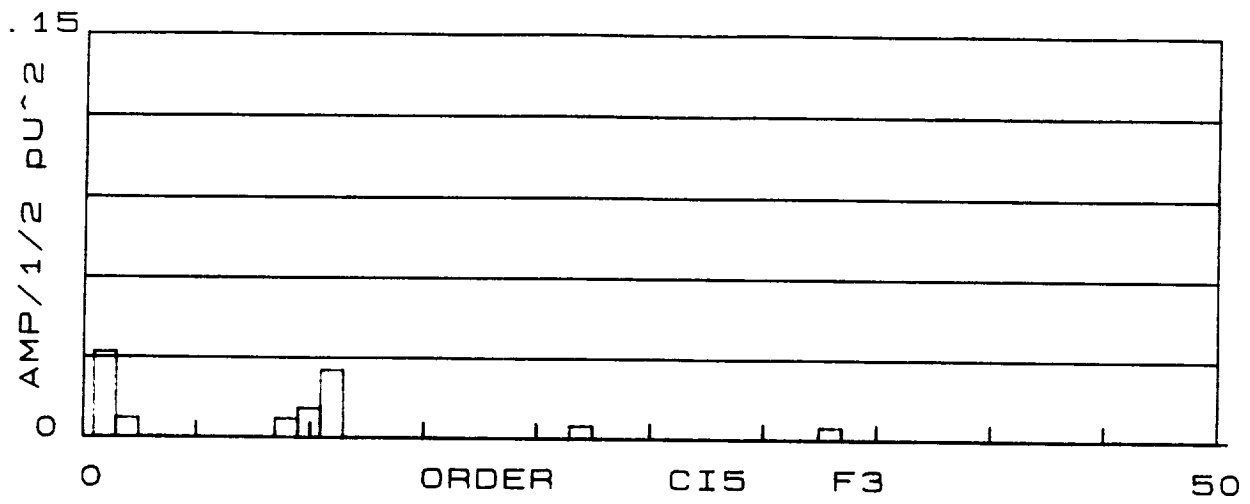










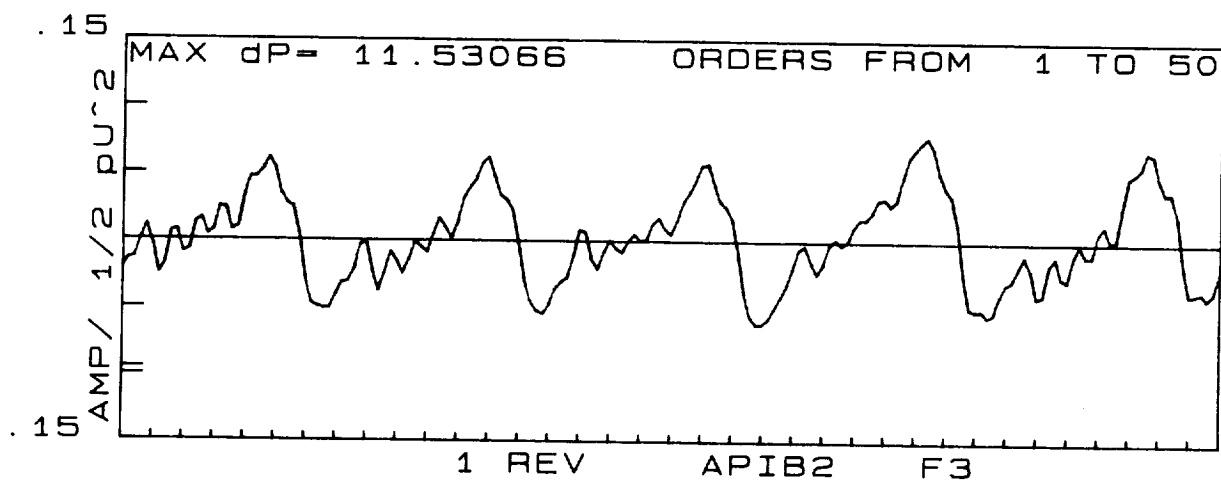
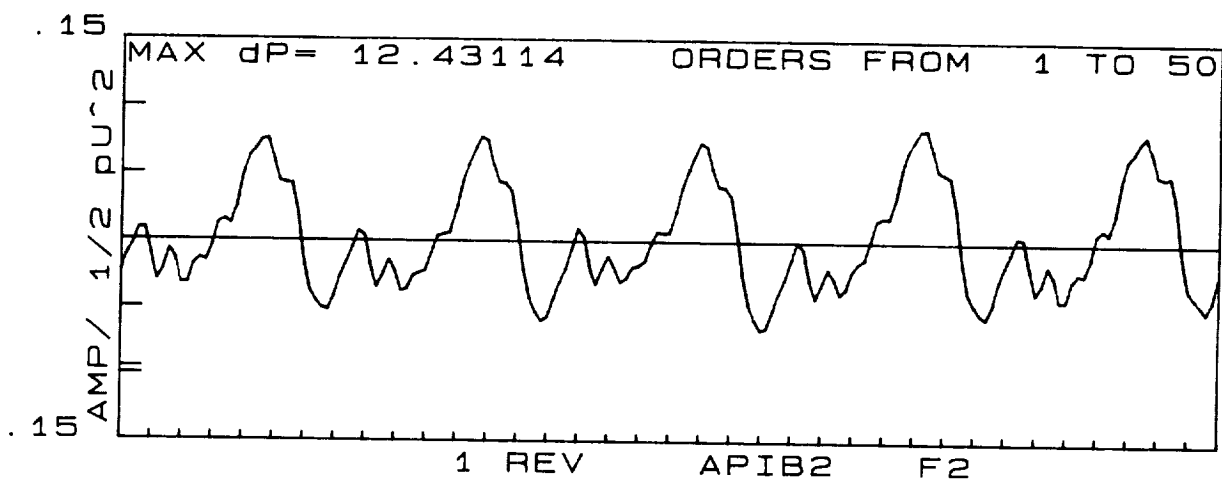
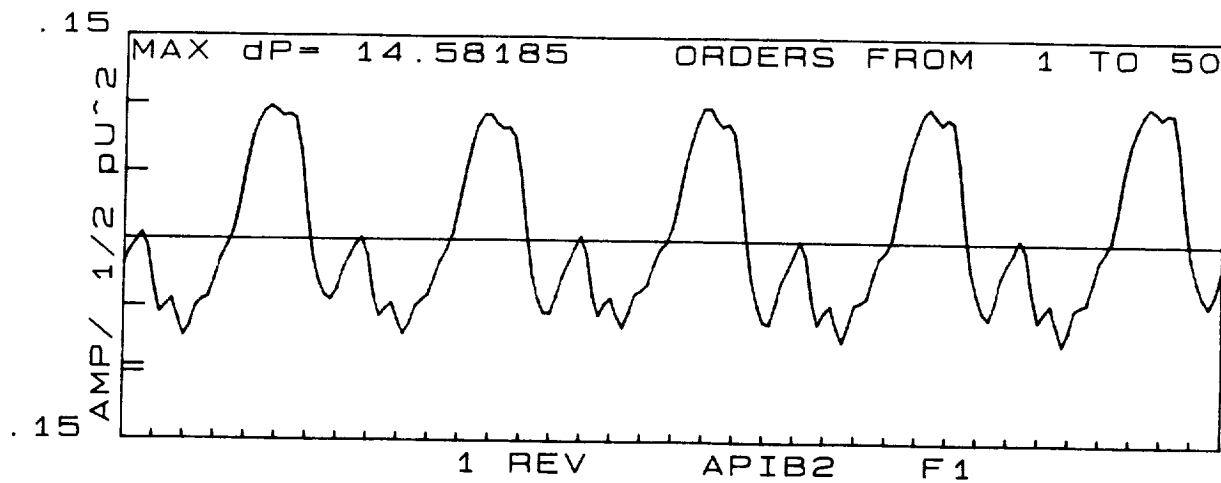


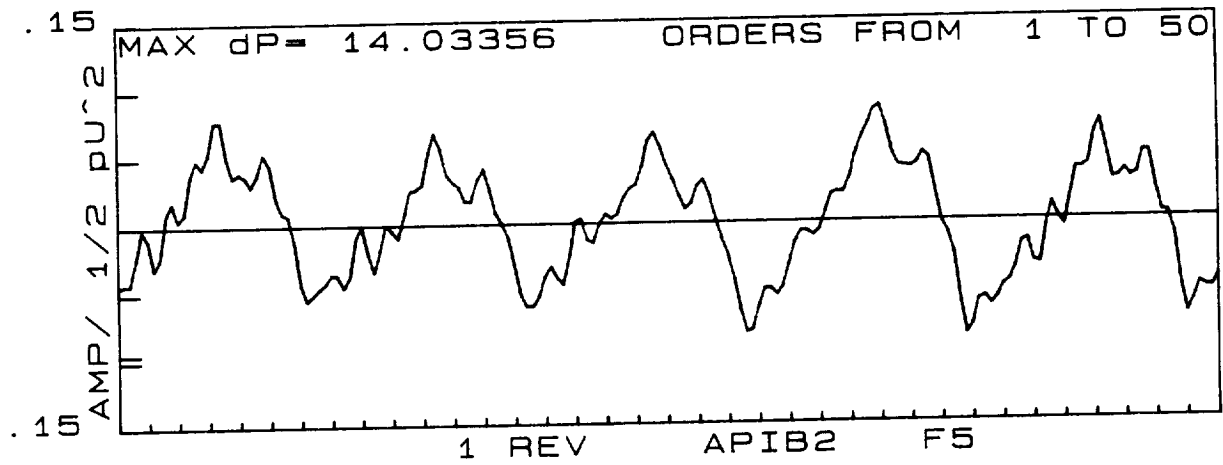
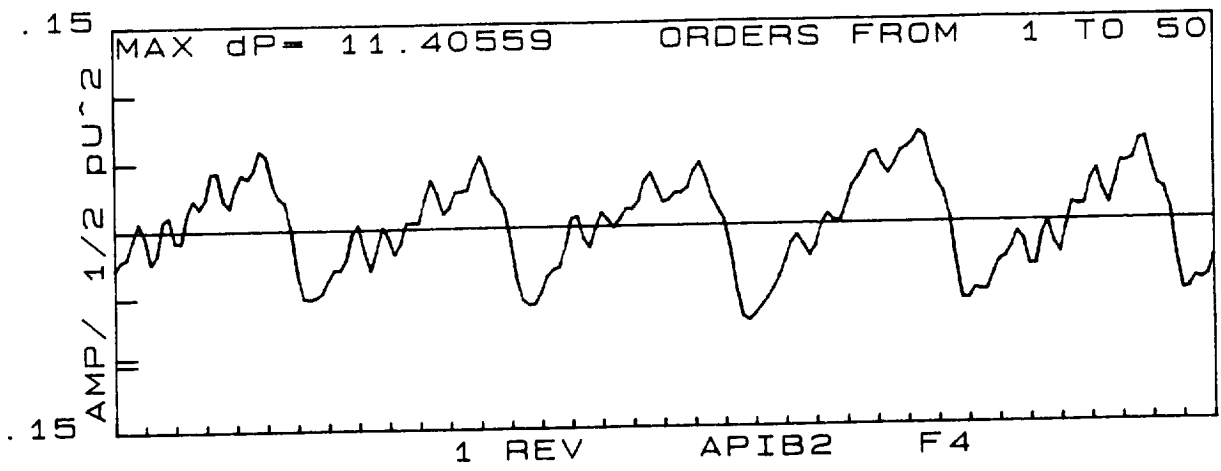
Effect of Impeller/Diffuser Clearance on Diffuser Inlet Sensors

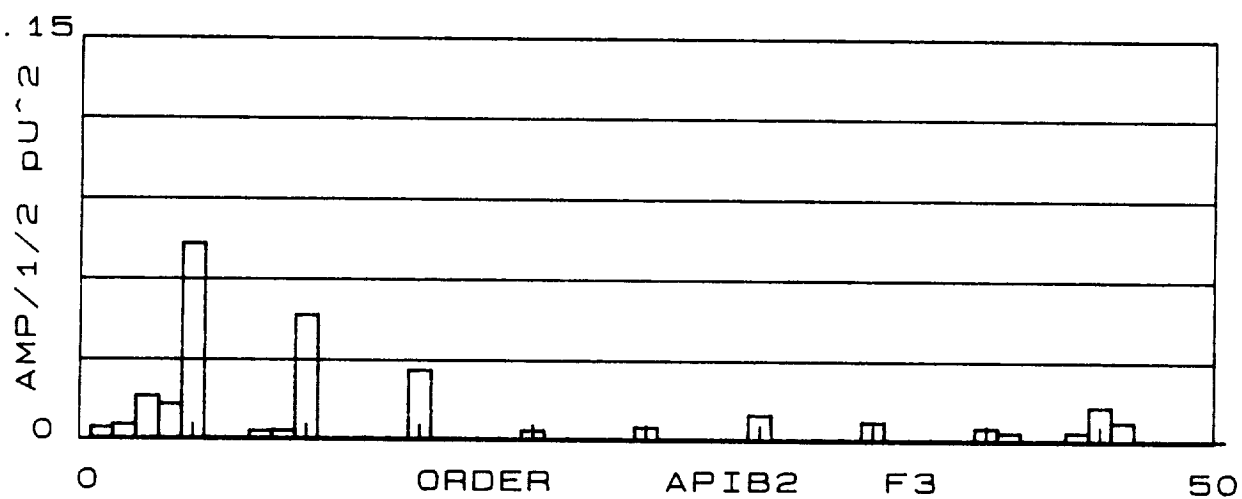
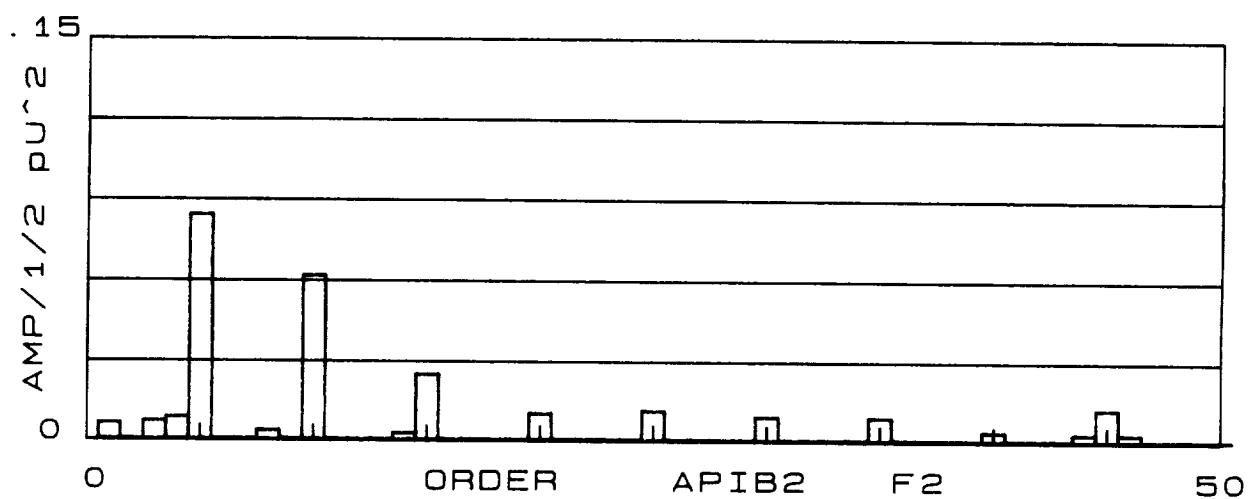
Locations: APIB2,BPIB2

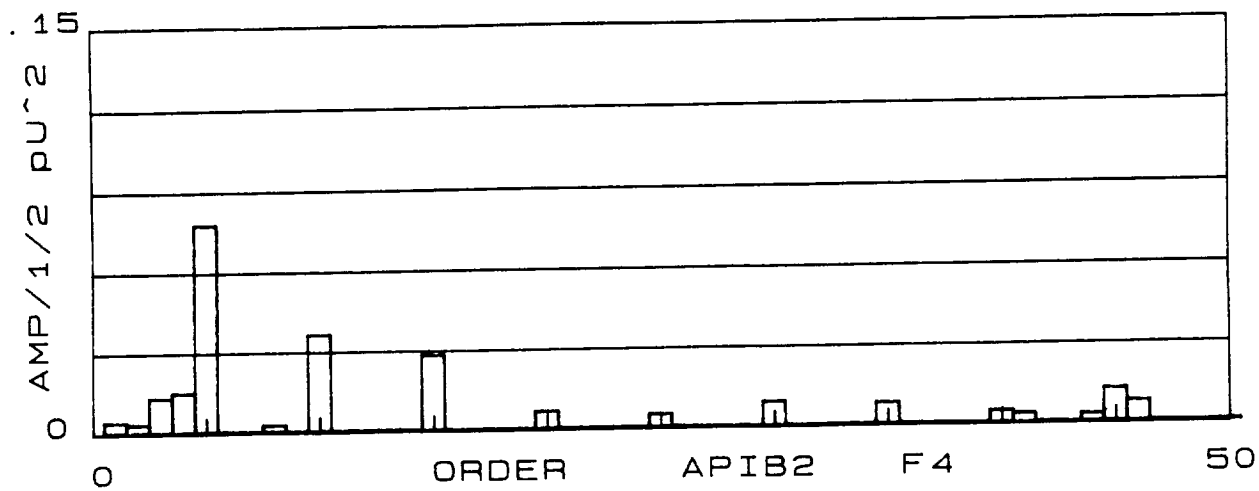
Conditions: F1,F2,F3,F4,F5

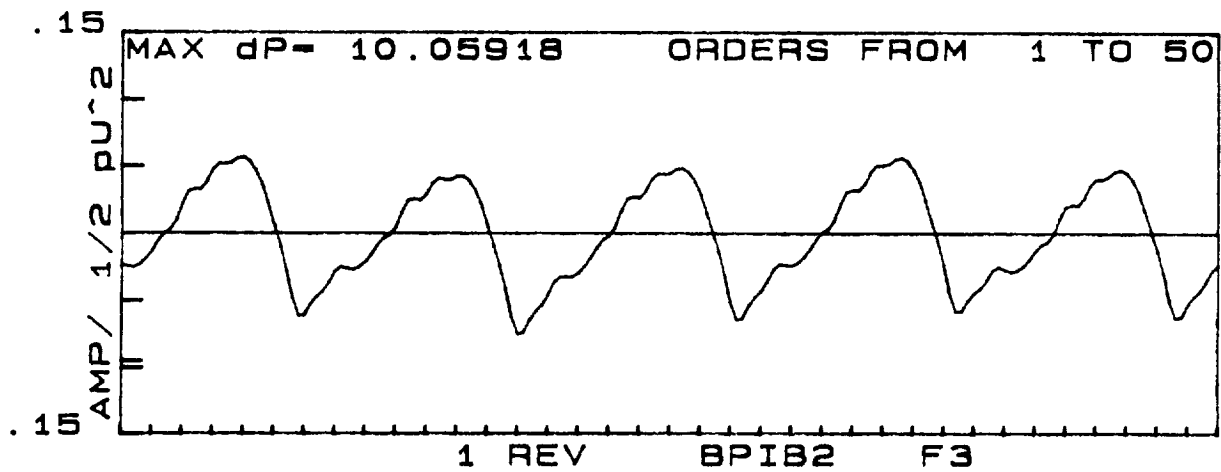
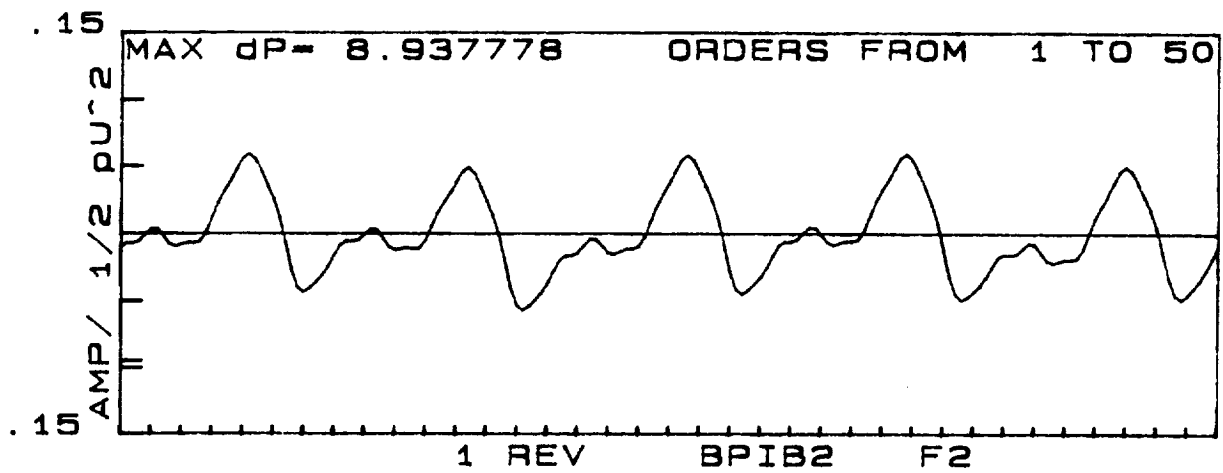
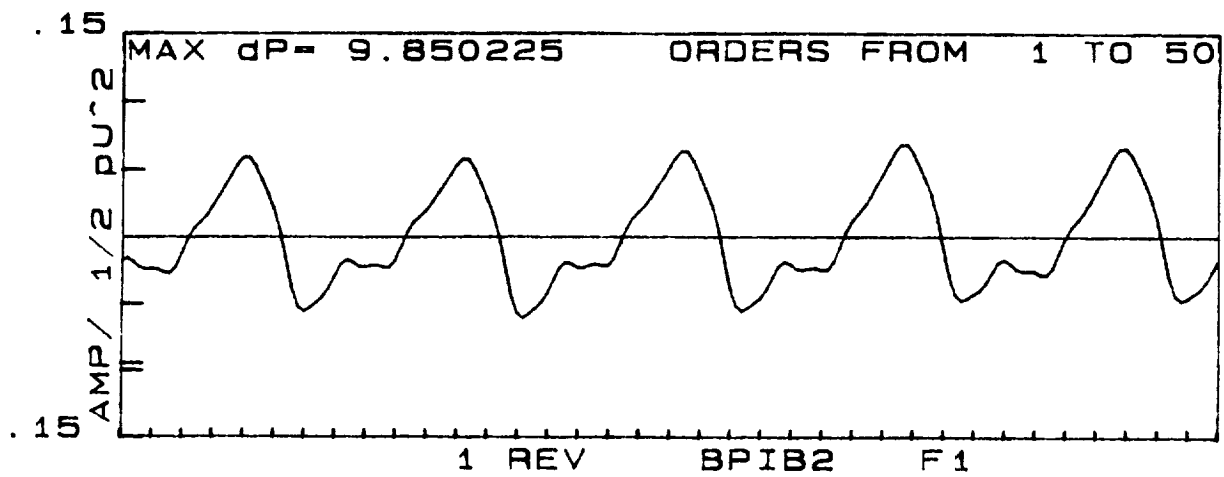
The effect of impeller/diffuser clearance on pulsation amplitudes at a location midway between the diffuser blade leading edges is shown in this group of plots. Data is shown for configurations A and B (clearance ratios of 1.021 and 1.059 respectively). Pulsation amplitudes decrease with increasing clearance.

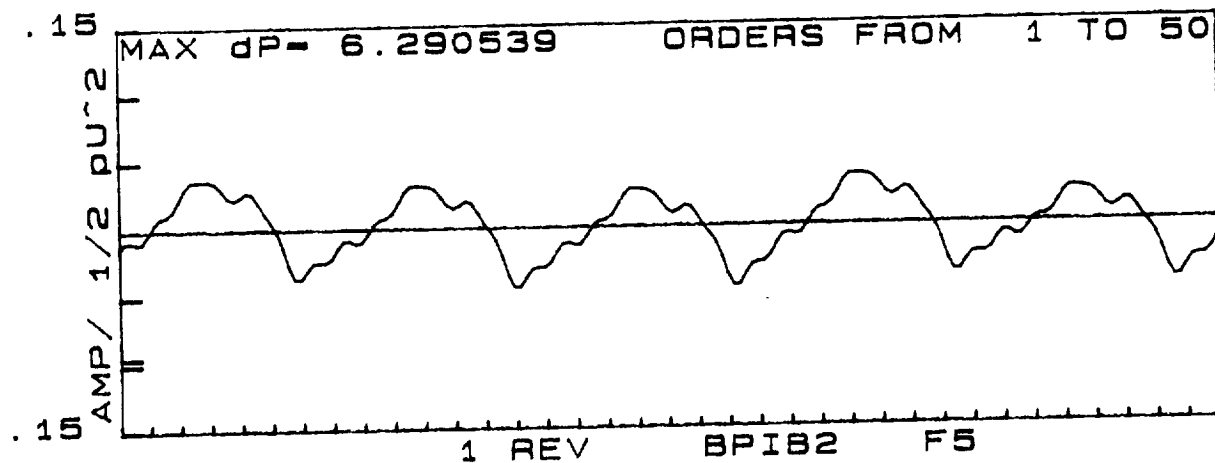
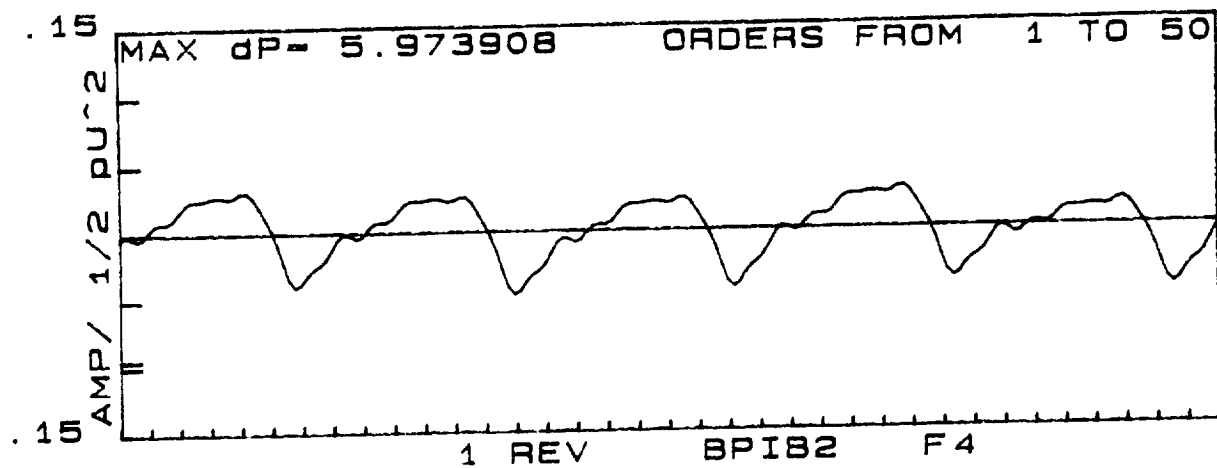


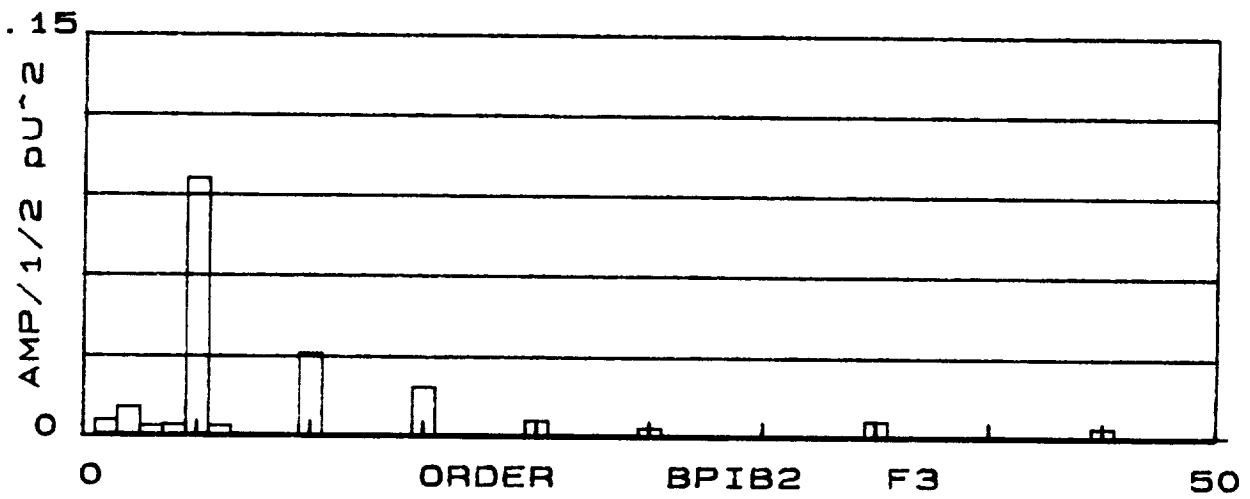
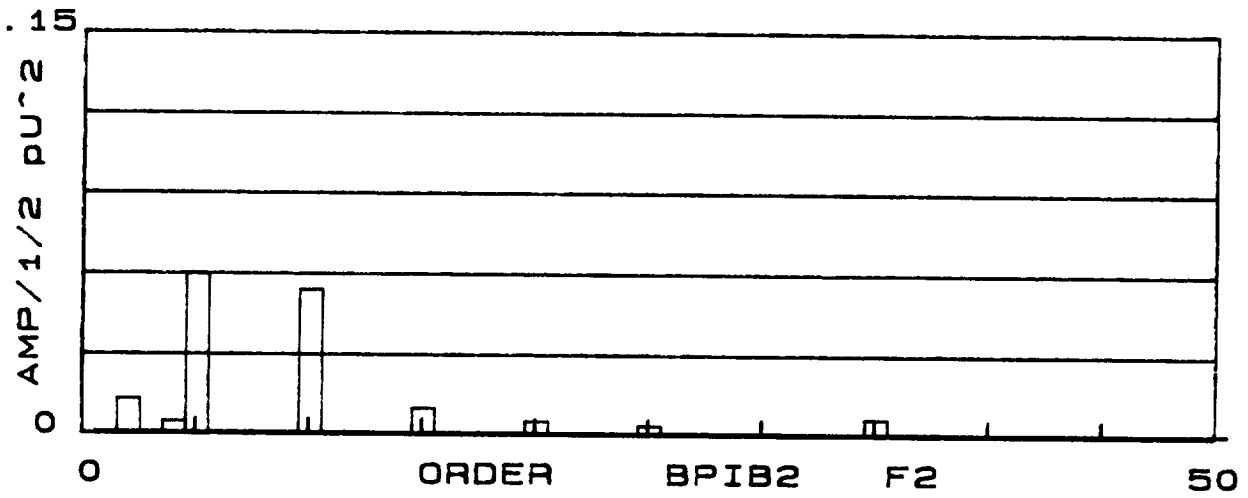
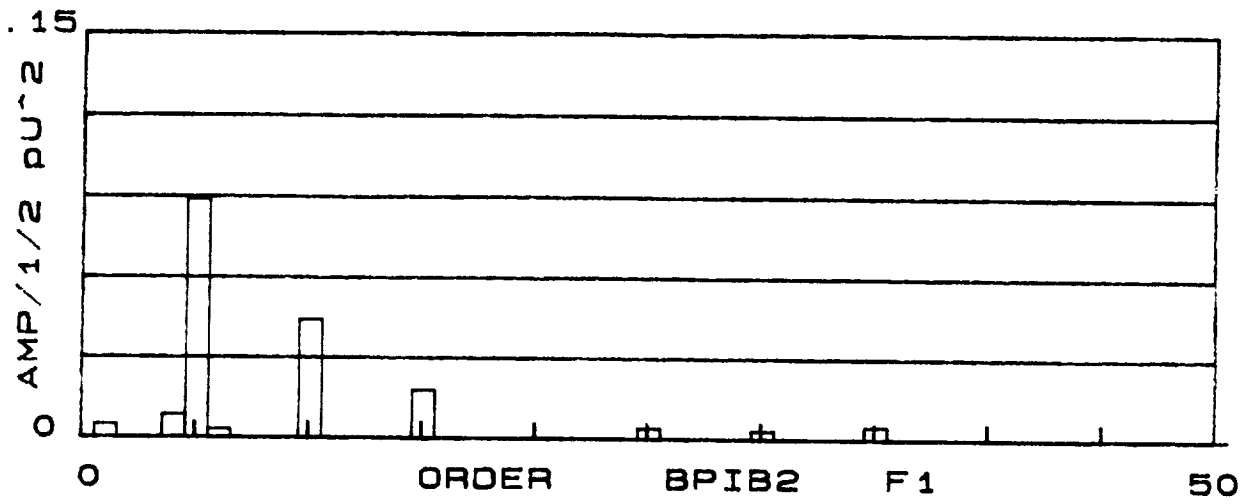


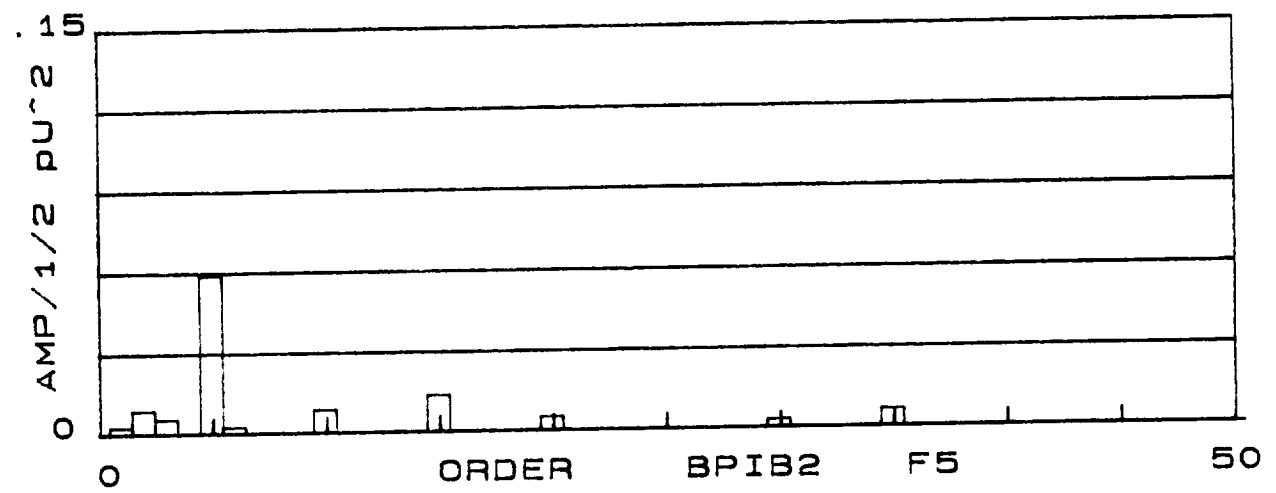
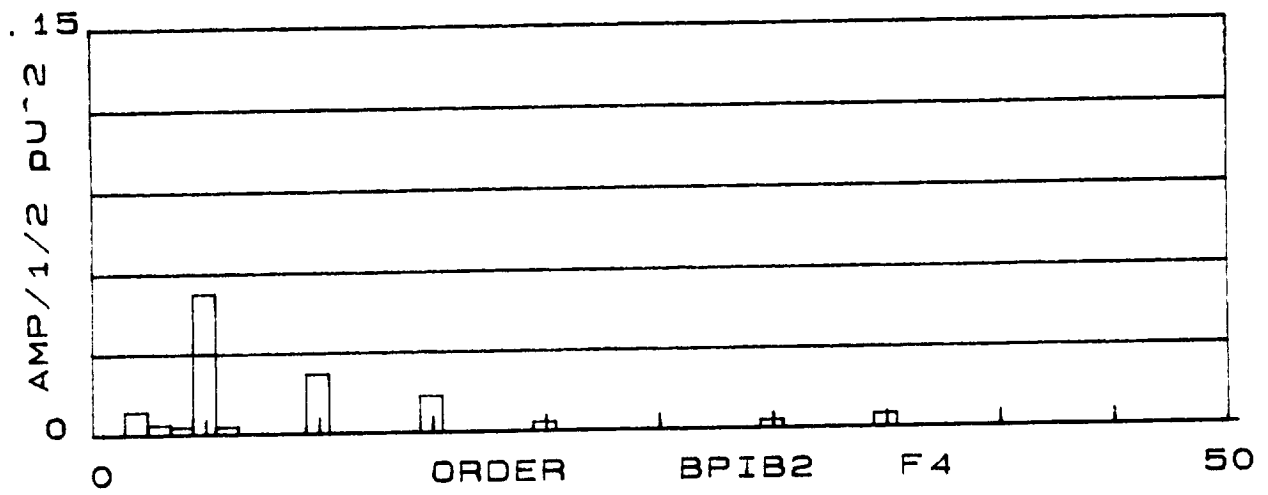












Effect of Impeller/Diffuser Clearance on Scroll Sensors

Locations: AS7,BS7,CS7

Conditions: F1,F3,F5

The effect of impeller/diffuser clearance on pulsation amplitudes in the scroll (specifically the outer wall, upstream of the throat) is displayed in this group of plots. Pulsations are reduced with increased clearance (configuration A vs B) or by increasing diffuser vane number (A vs C). The dominant frequency (or order of rotation) is 10 X rotation or twice the impeller vane passing frequency. This is expected for this combination of impeller and diffuser vanes. A method for identifying the orders of pulsation activity due to interaction of impeller and diffuser vane passing frequencies is found in Table 5.

CONFIGURATIONS "A" & "B"

		P2 = # Imp vanes x order of rotation									
		5	10	15	20	25	30	35	40	45	50
P3	9	4	<u>1</u>	6							
#	18		8	3	<u>2</u>						
Diff	27				7	<u>2</u>	3				
Vanes	36						6	<u>1</u>	4		
	45								5	<u>0</u>	5
		P2 - P3									

CONFIGURATION "C"

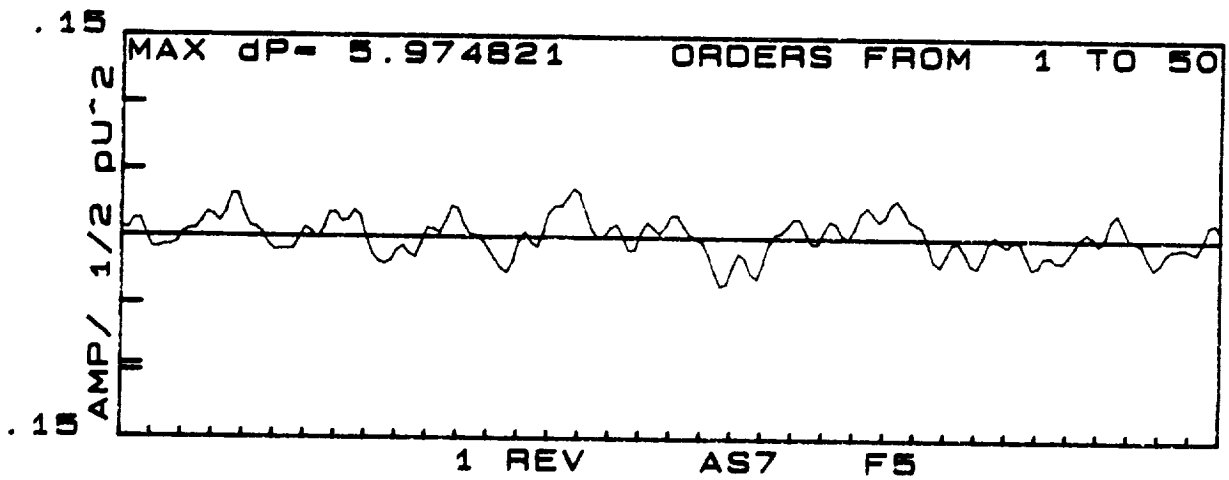
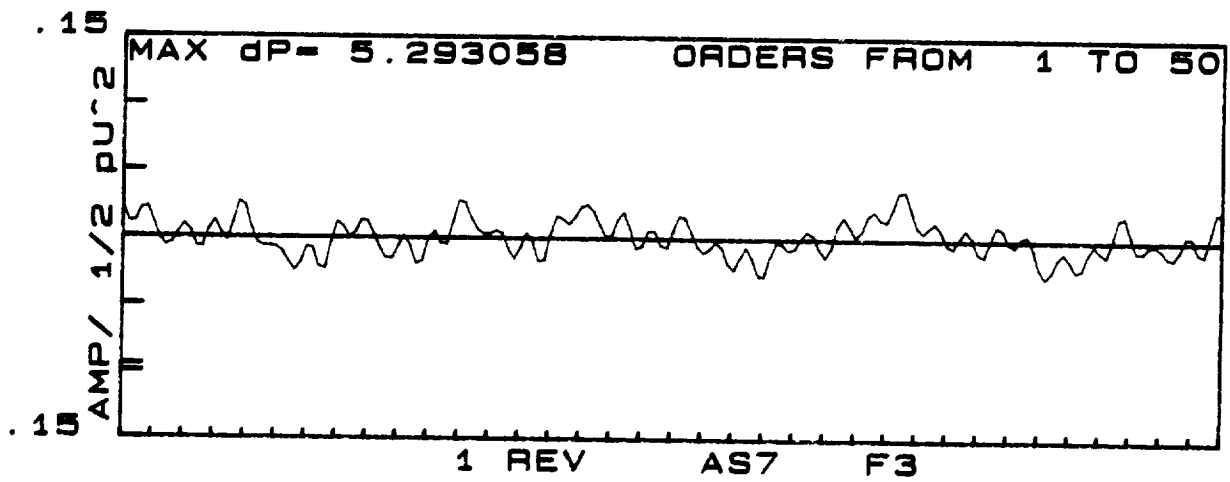
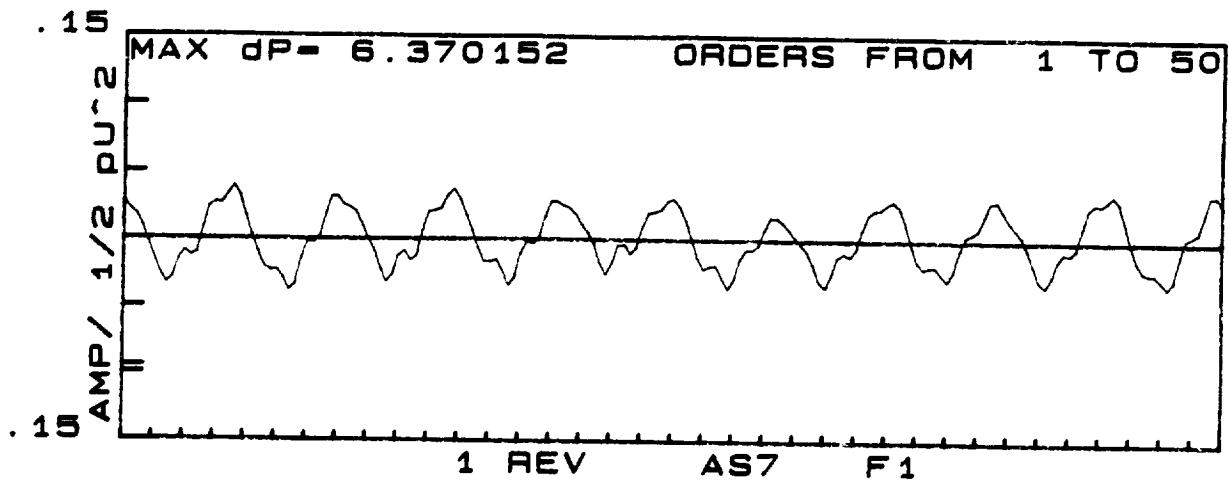
		P2 = # Imp vanes x order of rotation									
		5	10	15	20	25	30	35	40	45	50
P3	11	6	<u>1</u>	4							
#	22			7	<u>2</u>	3					
Diff	33						3	<u>2</u>	7		
Vanes	44								4	<u>1</u>	6
		P2 - P3									

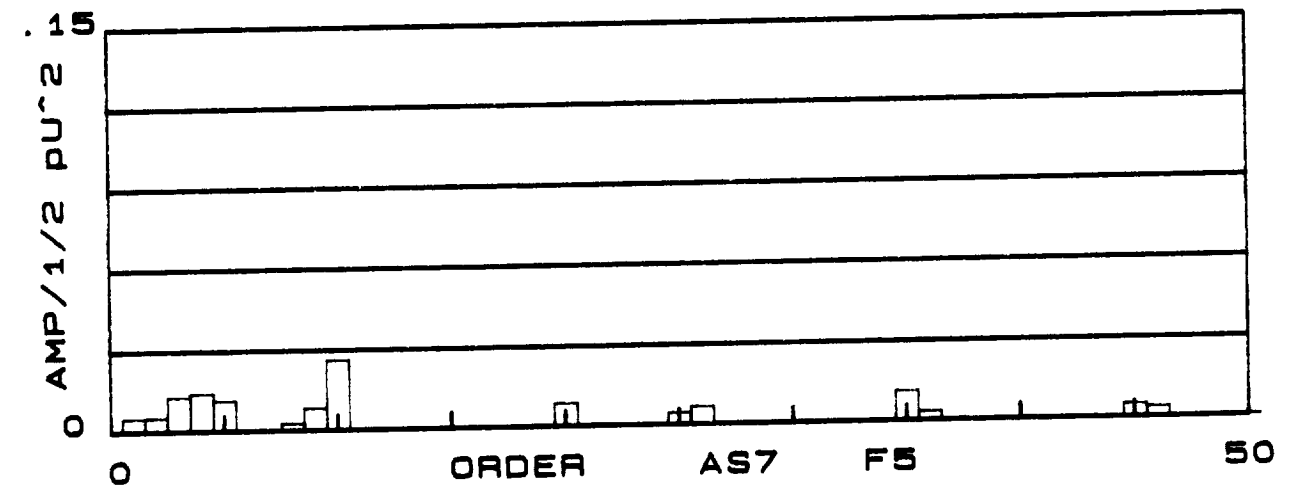
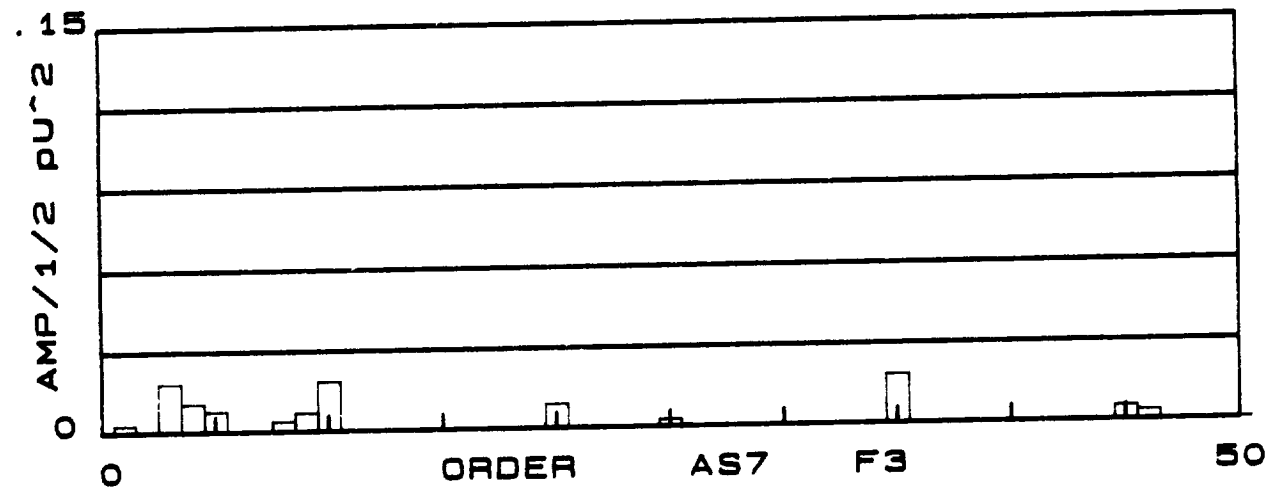
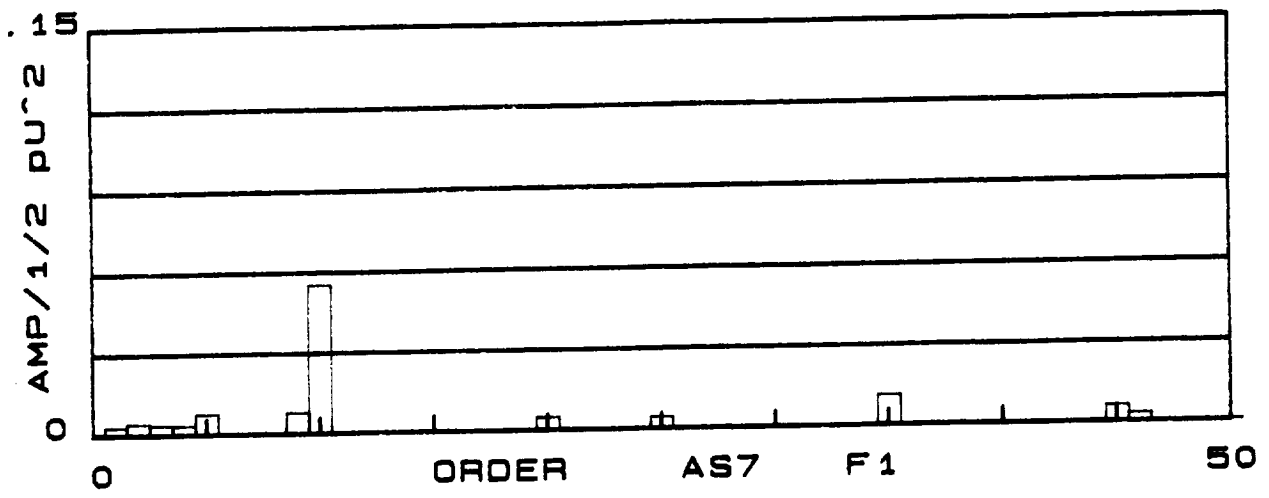
If $|P2-P3| = -0, 1$ or 2 Pressure pulsations will be present
Pulsations most severe if the difference is 0 .

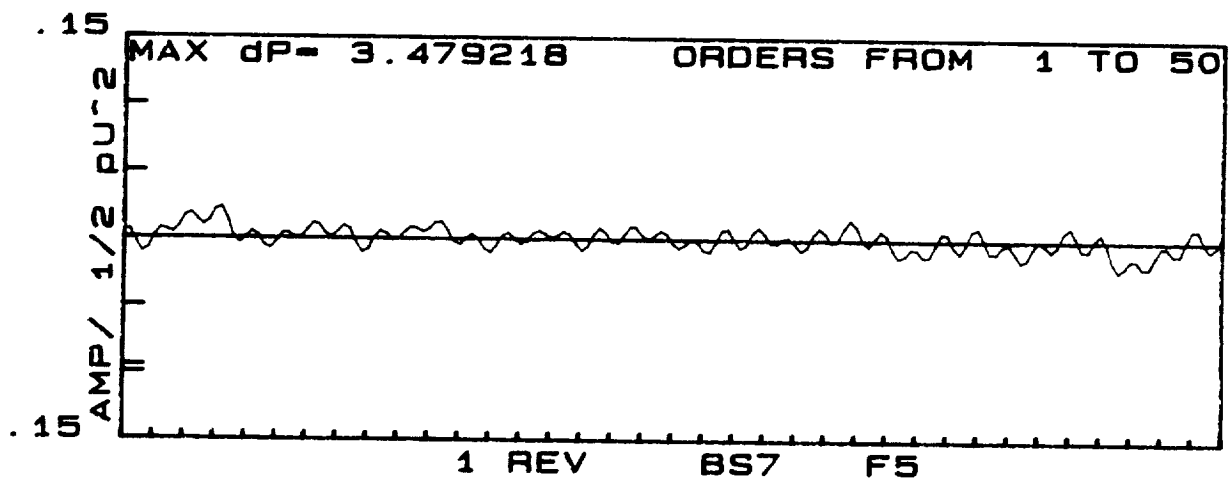
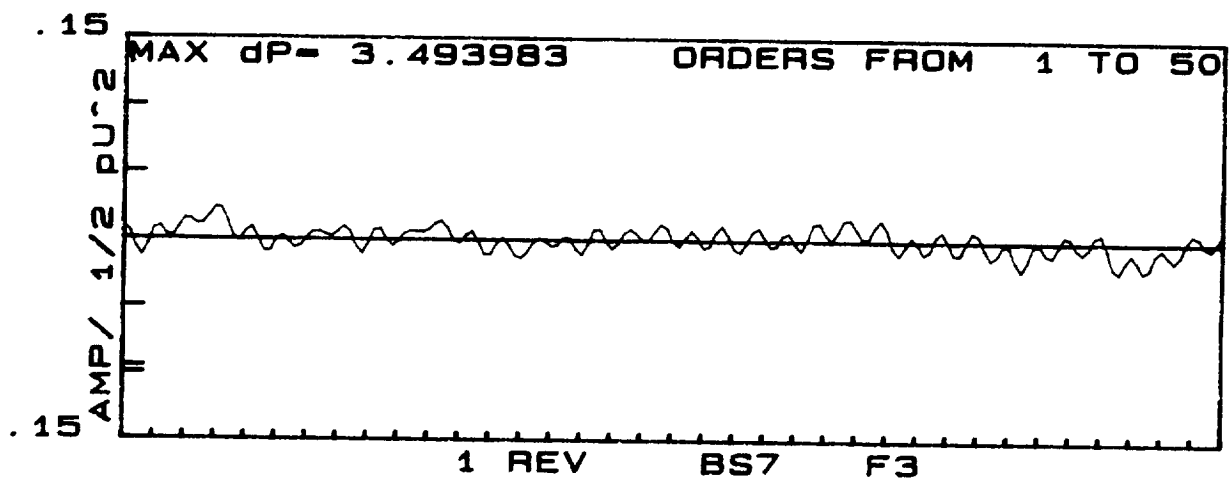
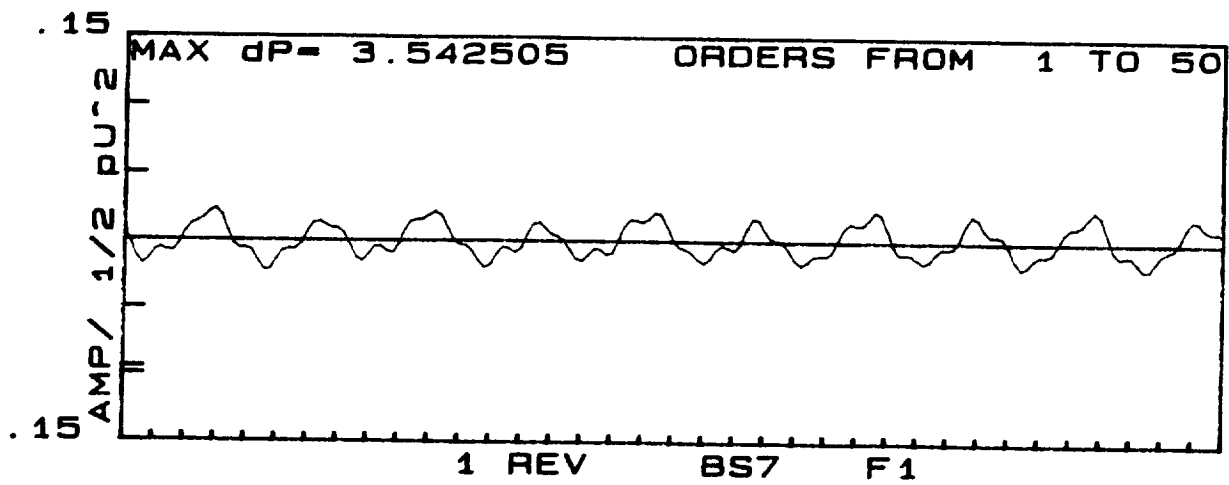
Reference: Bolleter, U., "Blade Passage Tones for Centrifugal Pumps",
Vibrations, Vol. 4, No. 3, September 1988..

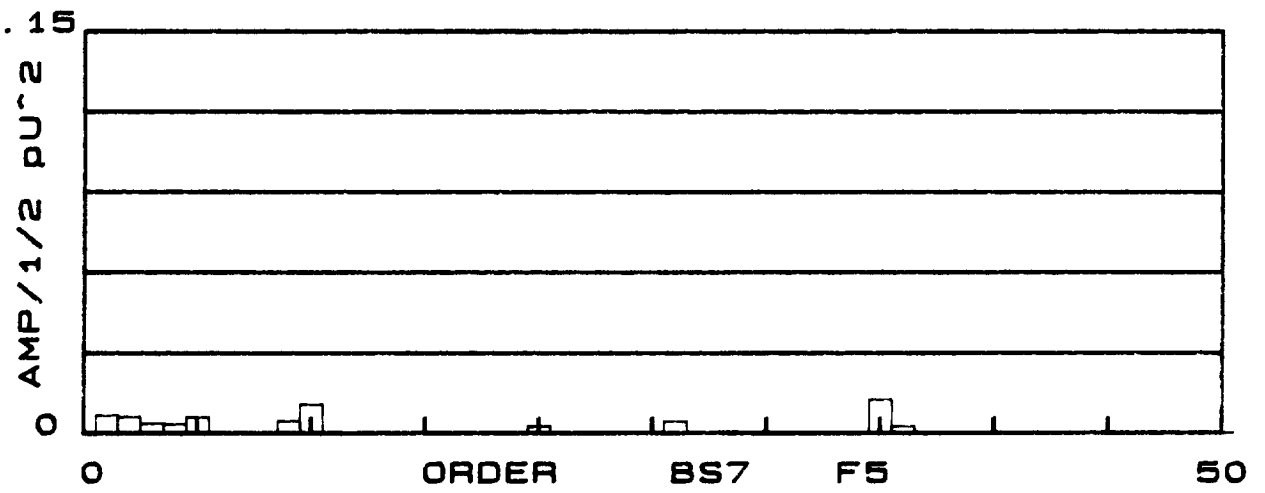
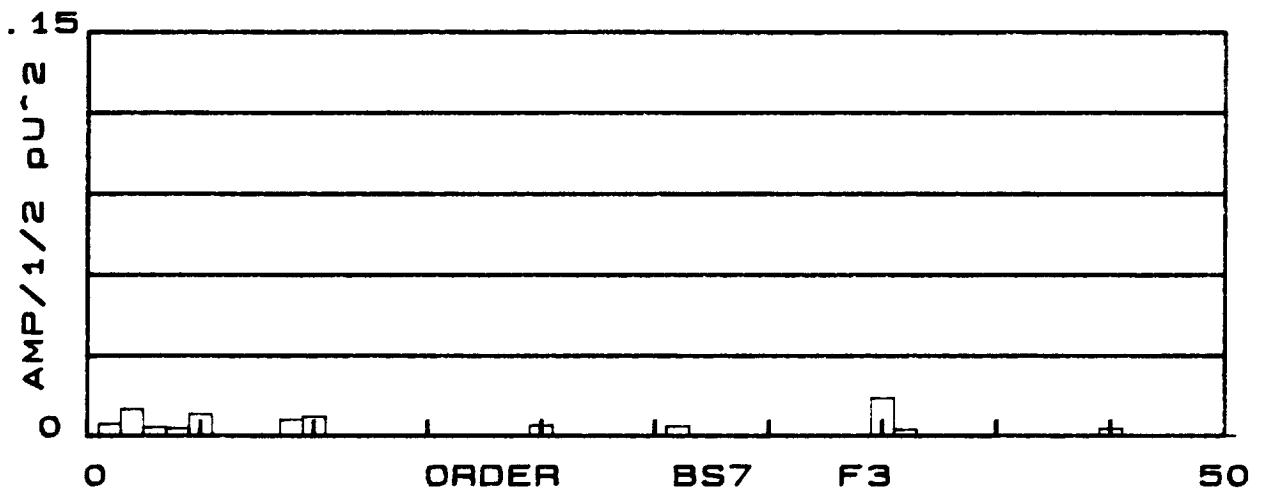
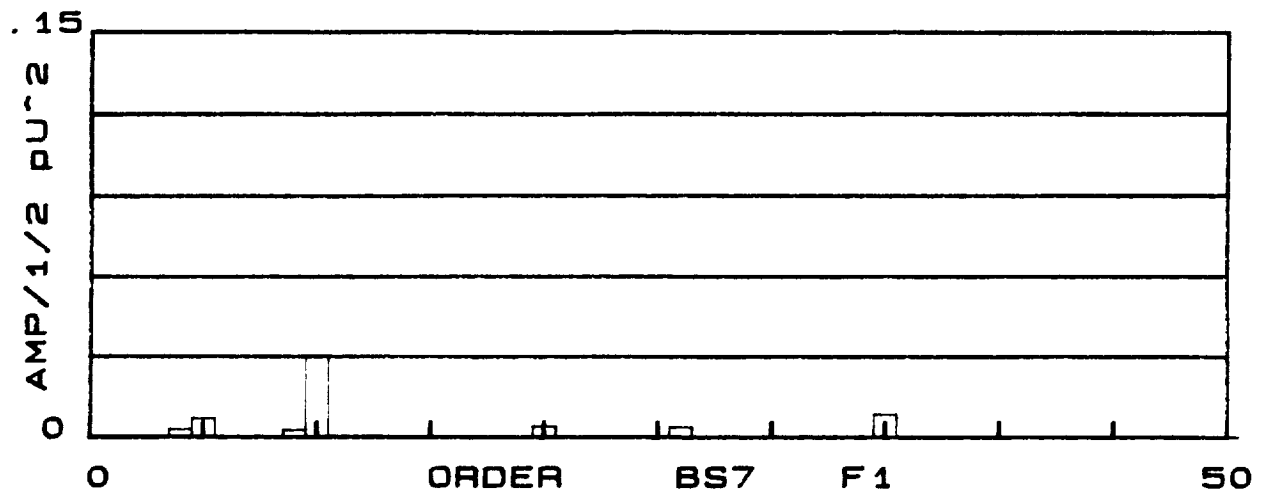
Table of Impeller/Diffuser Interactions

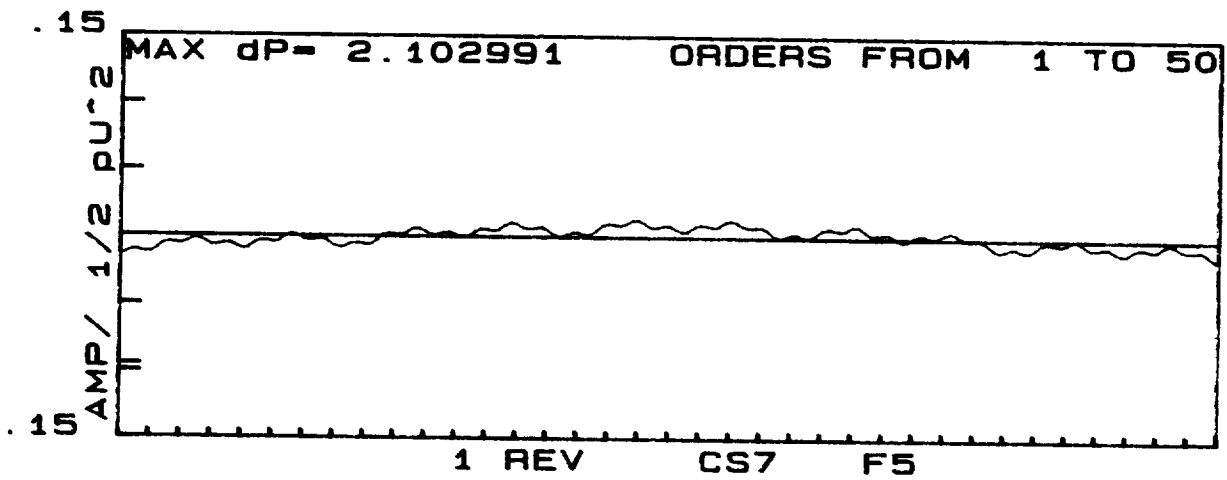
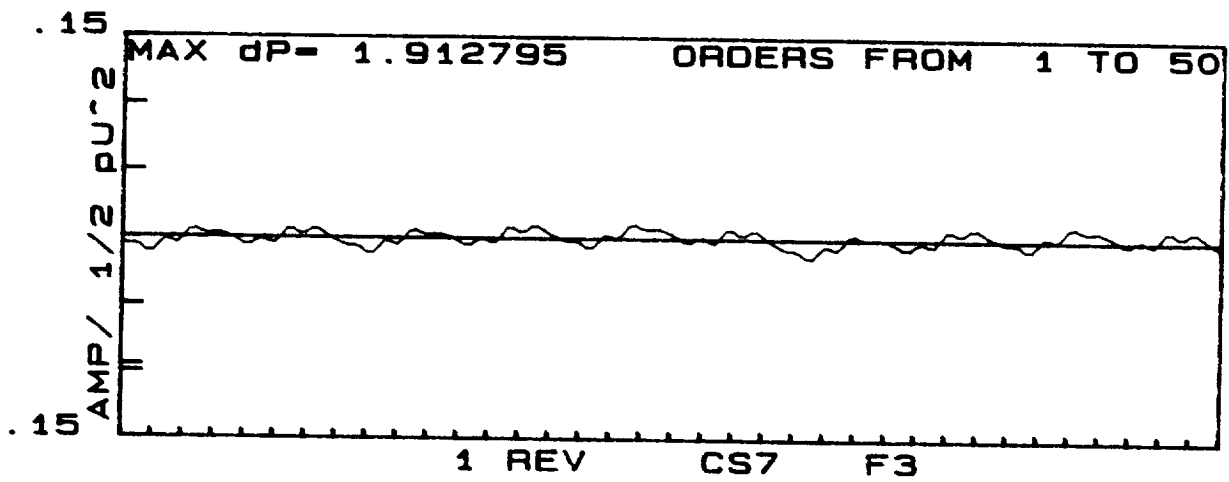
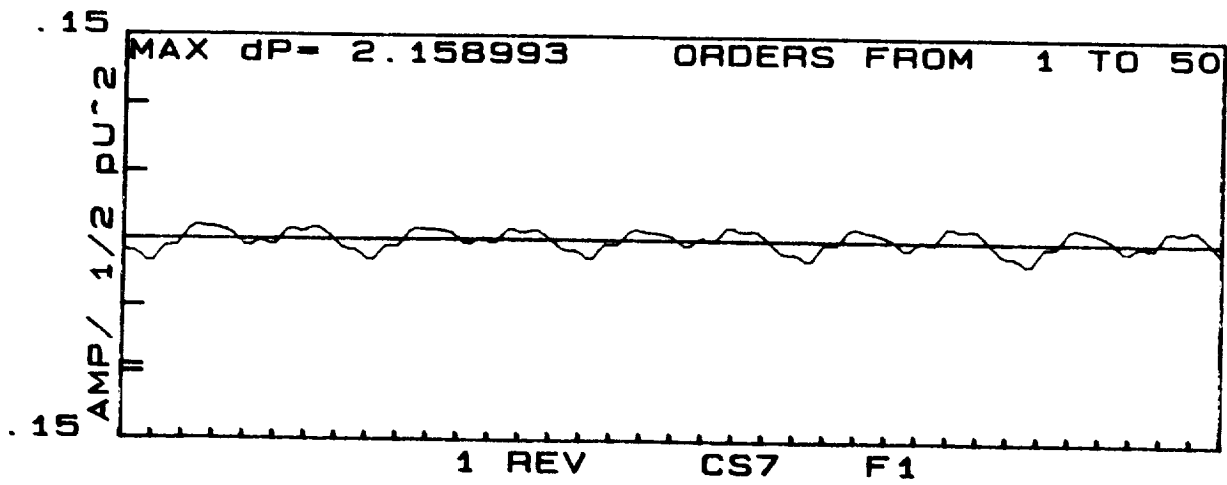
Table A-3

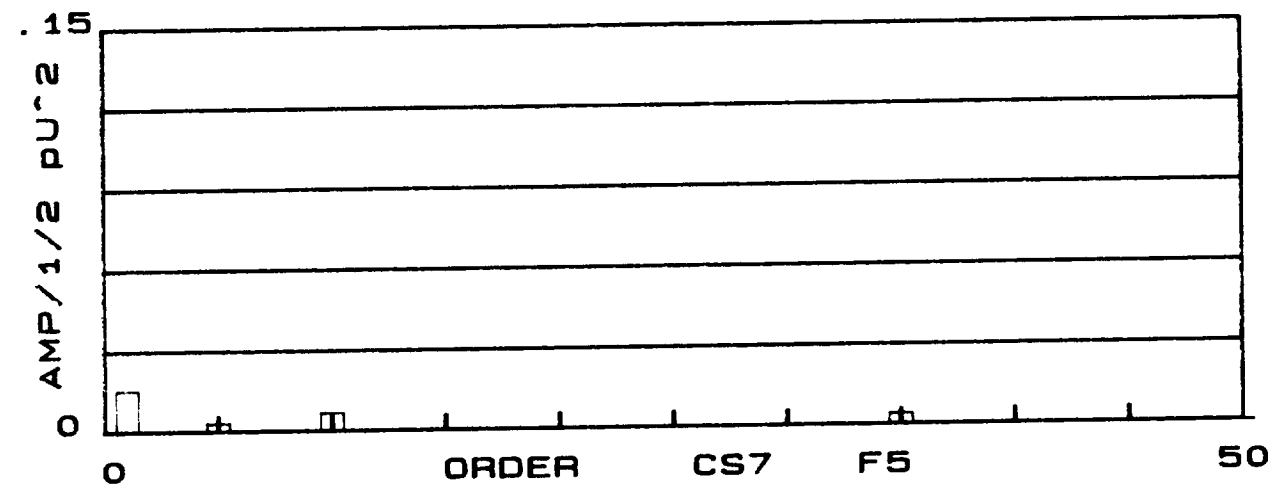
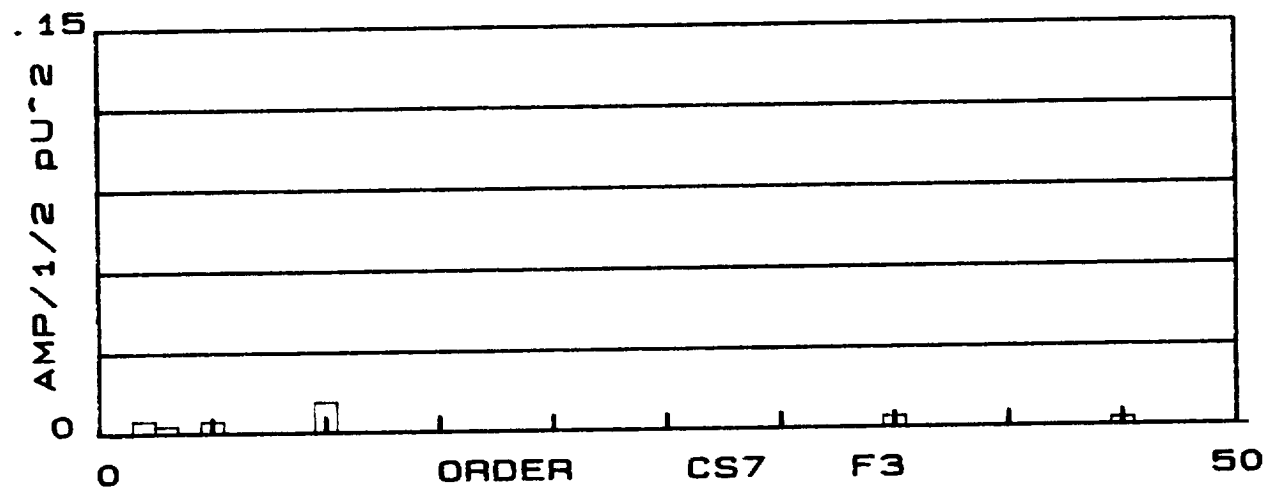
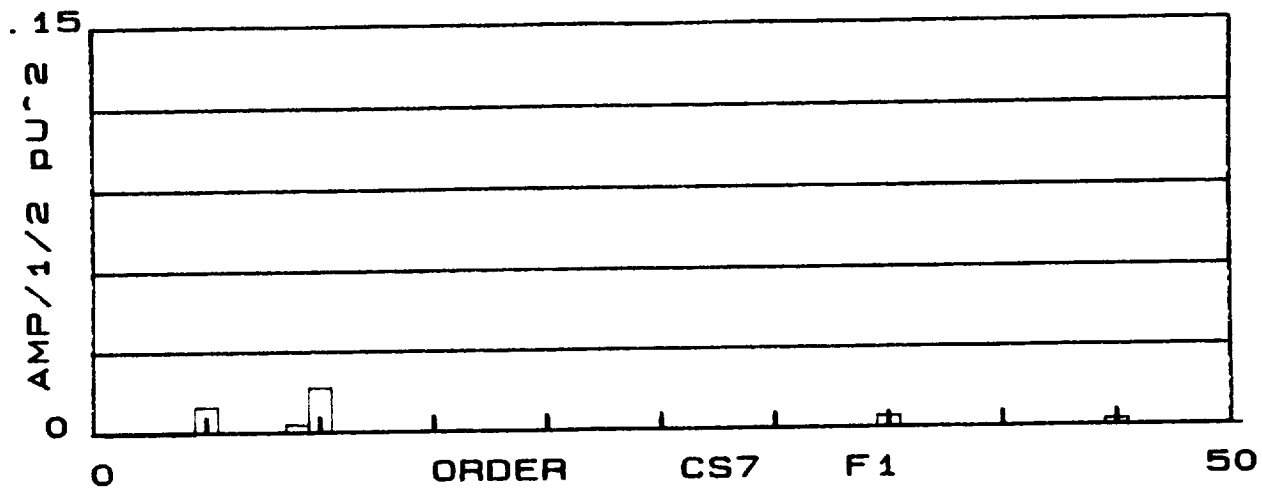












5th Order Pulsation Component at Diffuser Throat Sensors

Locations: AD1,...,AD17

BD1,...,BD17

CD1,...,CD21

Conditions: F1,F2,F3,F4,F5

The variation of the 5th order component of the pressure pulsations occurring in the inlet throats of all 3 configurations is shown on this plot. The values represent averages of all circumferential sensors. Configuration C deviates from the variation in fluctuations due to increased impeller/diffuser clearance due to its higher vane number (11 vs 9). This higher vane number leads to lower blade loading. Configurations A and B are identical diffusers in design but show the effect of increased clearance ratio (from 1.021 to 1.059).

DIFFUSER THROAT PRESSURE PULSATIONS

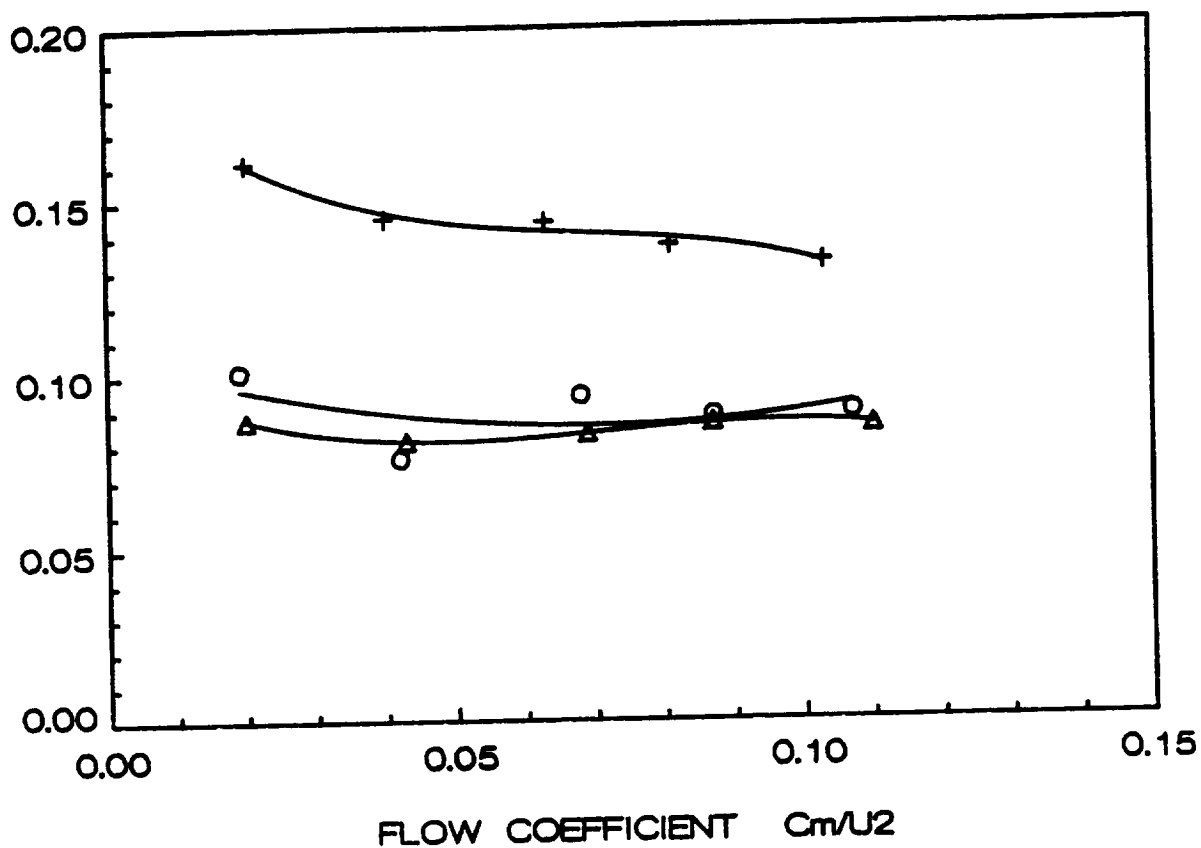
"A"&"B"-9 VANE "C"-11 VANE

+ CONFIG "A"
D3/D2=1.021

Δ CONFIG "B"
D3/D2=1.059

○ CONFIG "C"
D3/D2=1.047

5th Order Component $dP/1/2 \rho U^2$



Attenuation of Pulsation Components for Diffuser and Scroll Sensors

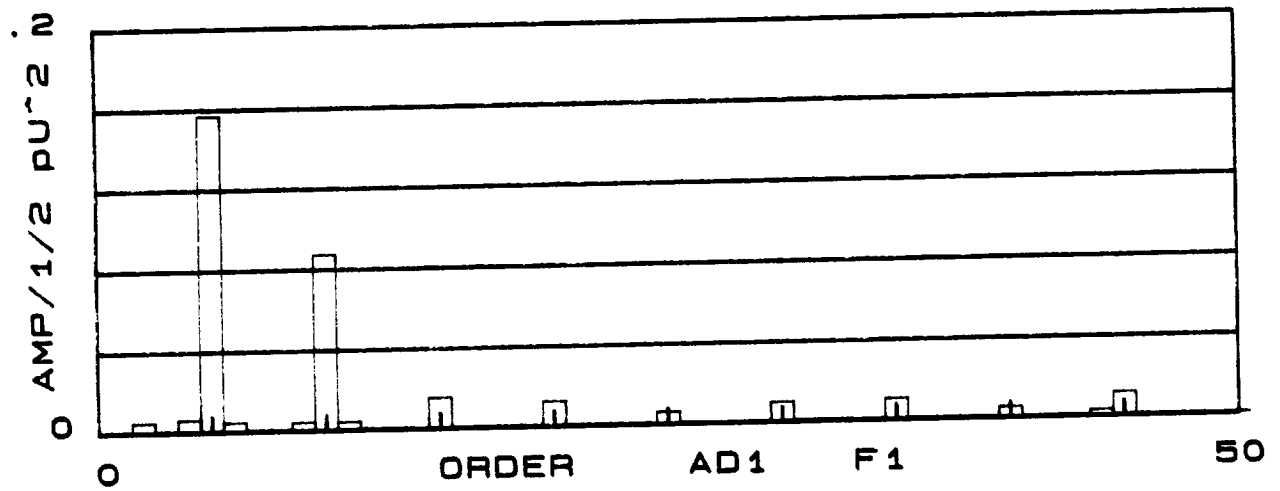
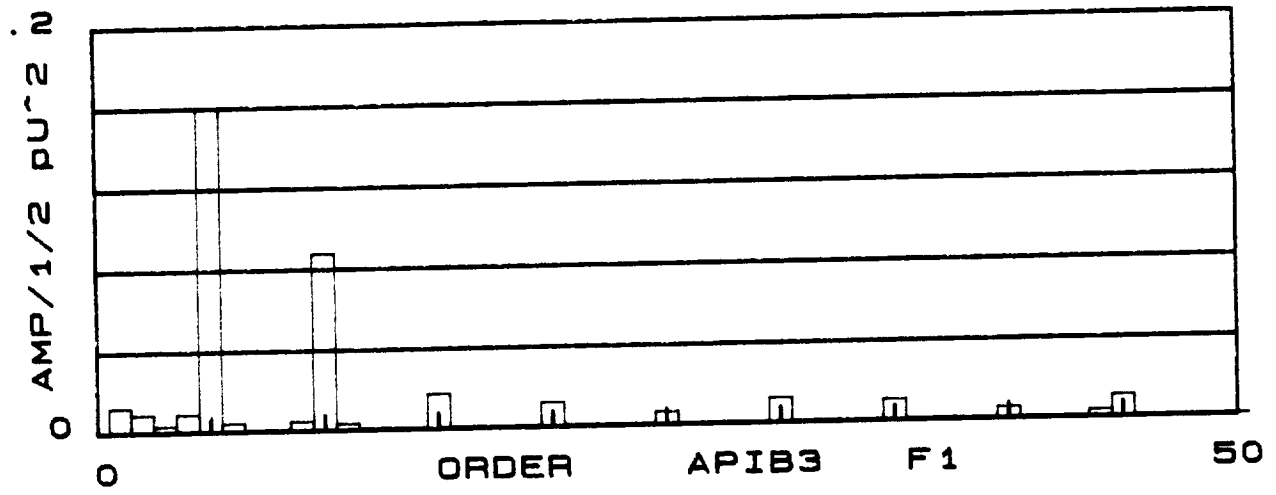
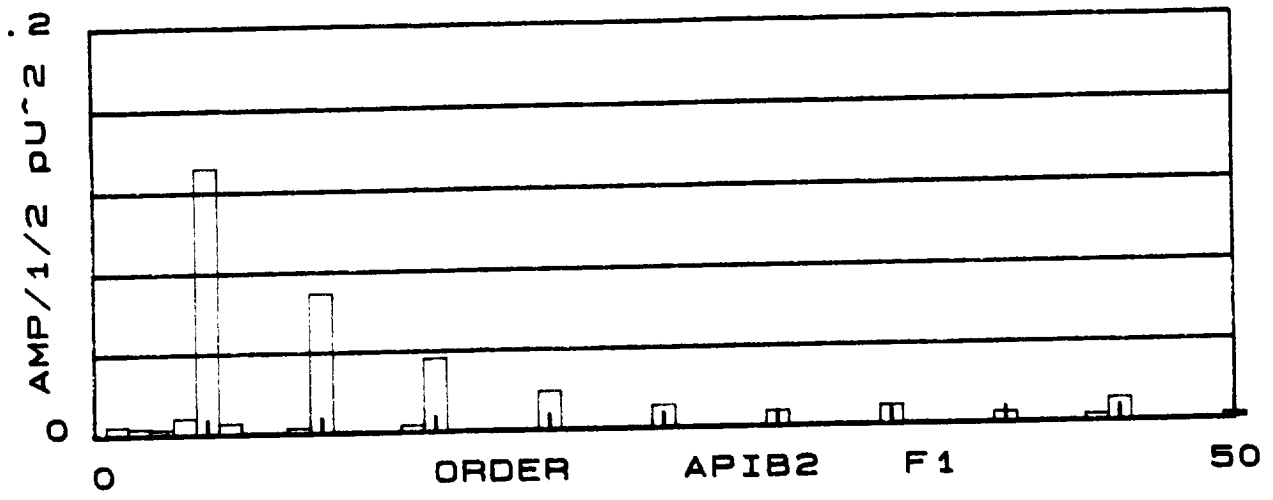
Locations: APIB2,APIB3,AD1,AD2,AS7,AS6

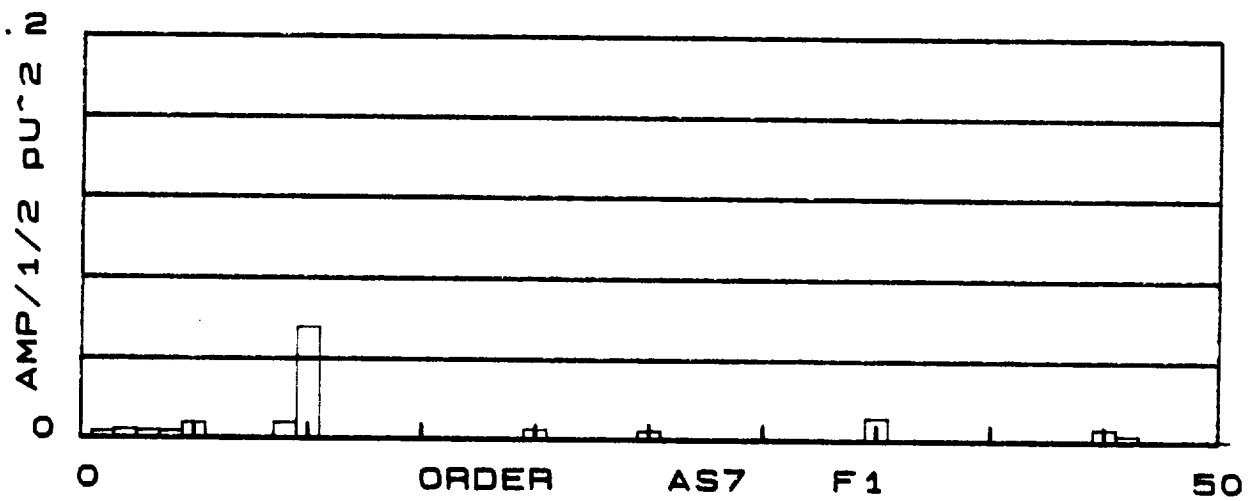
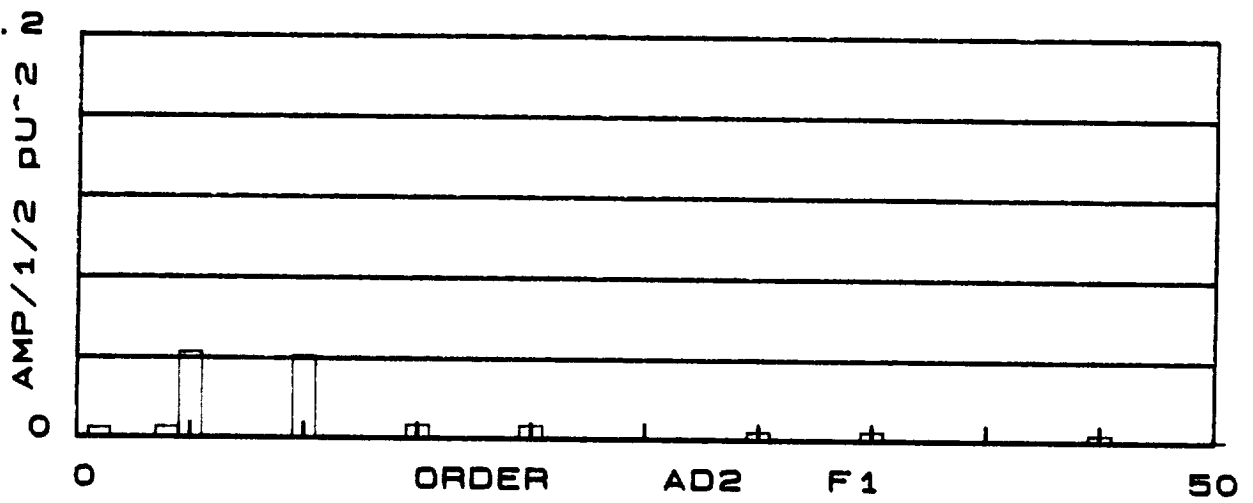
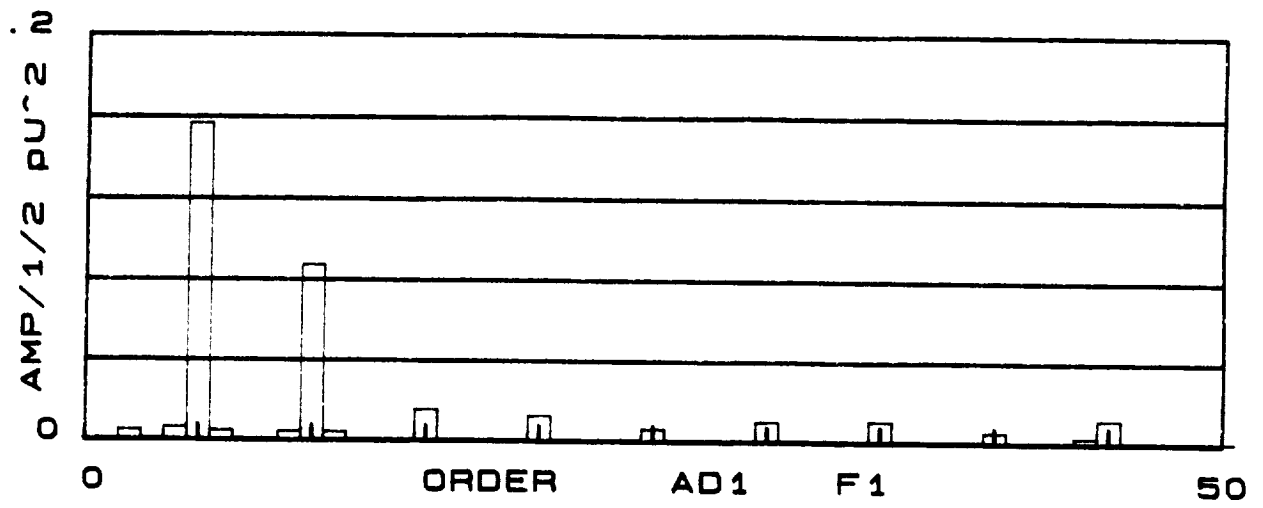
BPIB2,BPIB3,BD1,BD2,BS7,BS6

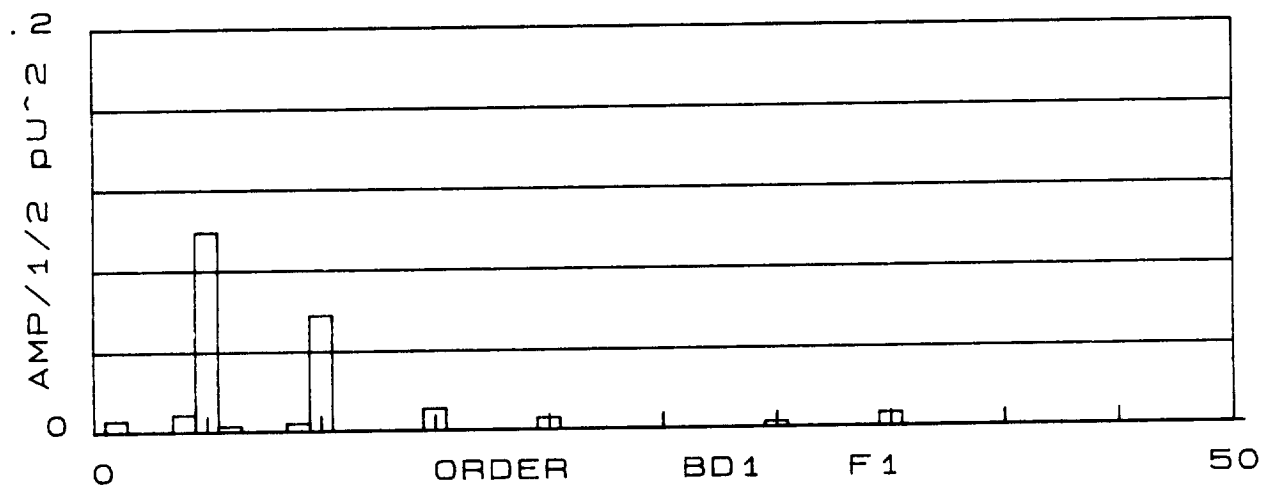
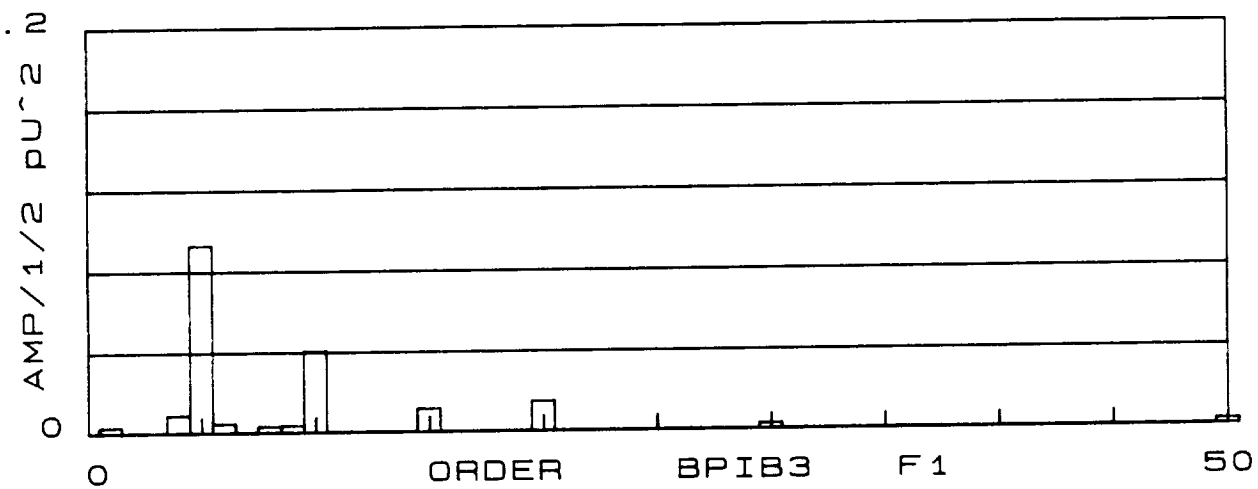
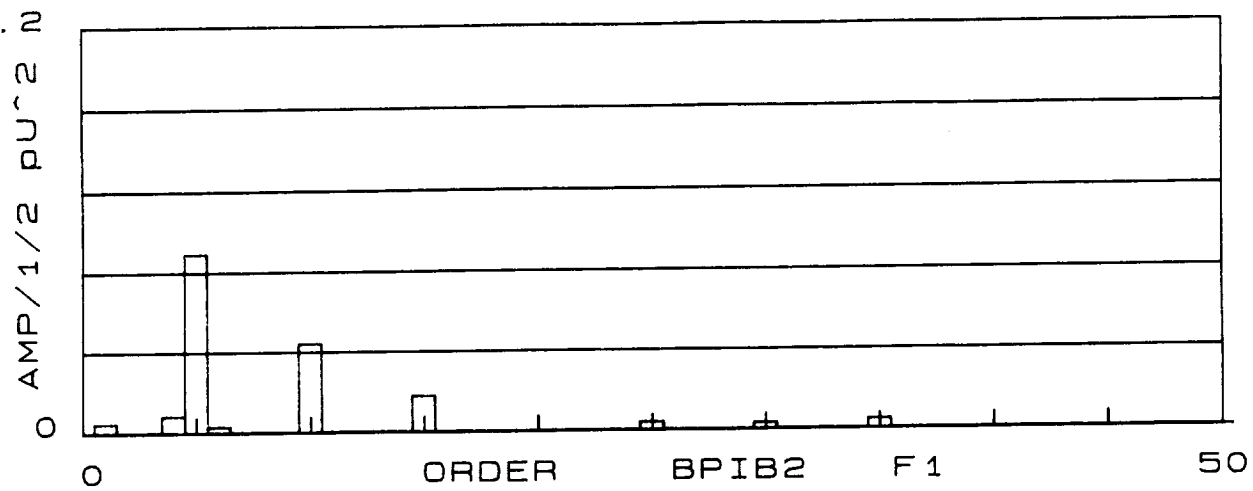
CD1,CD2,CS7,CS6

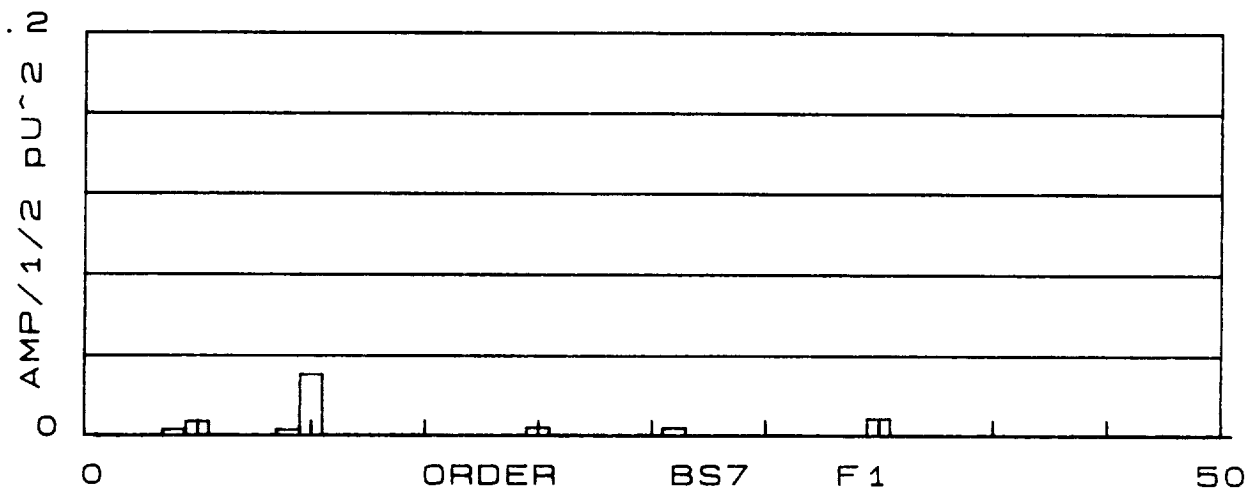
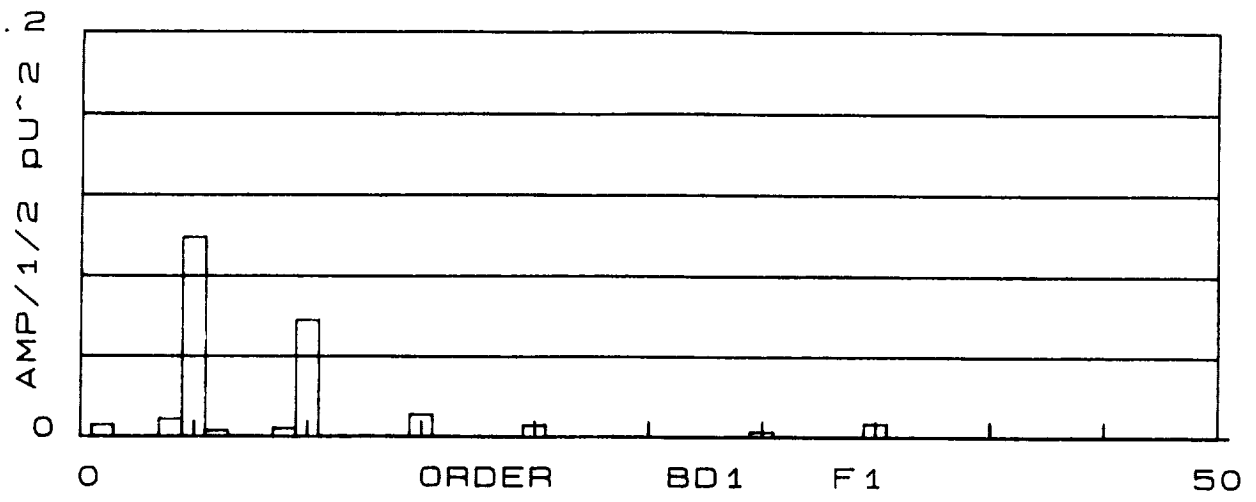
Condition: F1

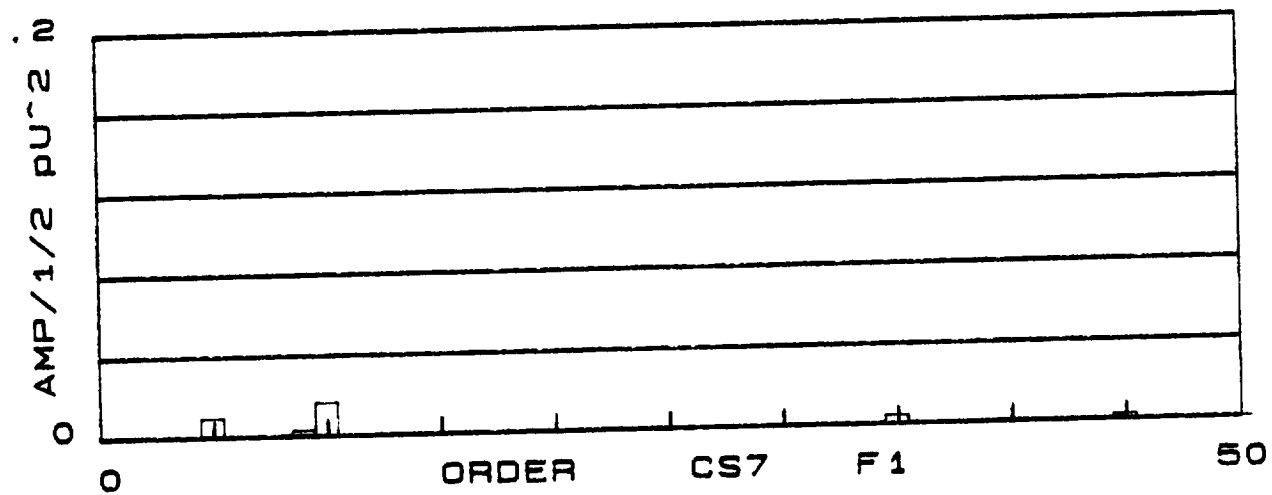
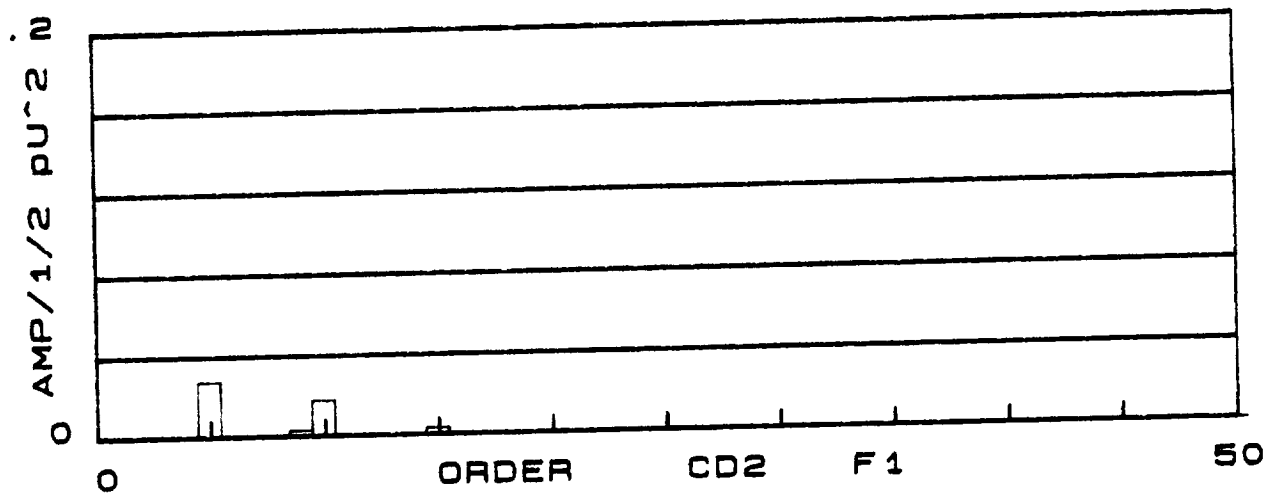
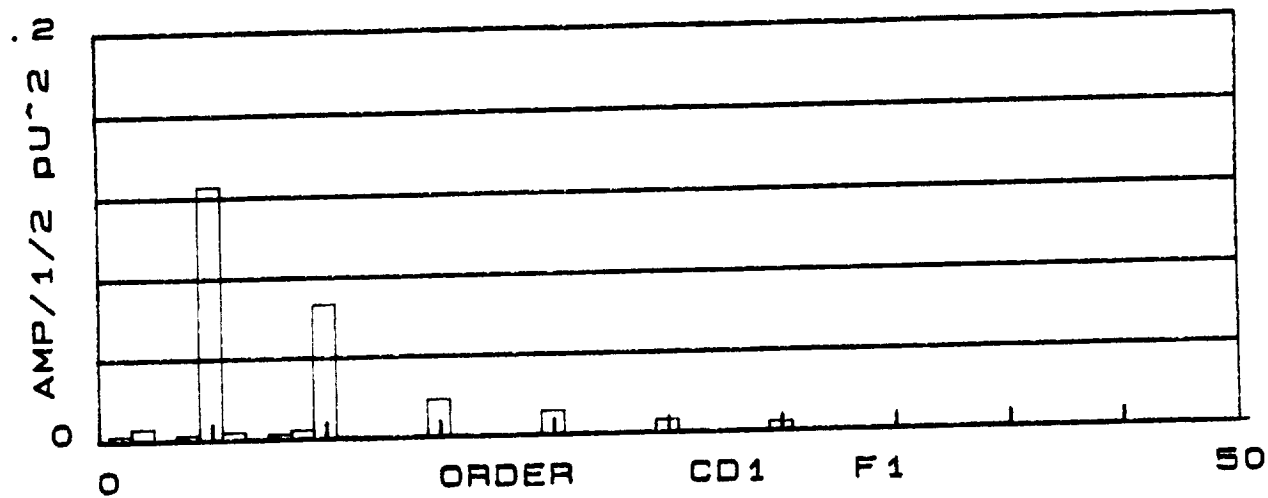
The attenuation of the components of the synchronous pressure waveforms from the diffuser inlet to the scroll locations is shown in this group of plots. A check of the potential interactions found on Table 5 shows the orders one expects to see due to the vane interaction. The 5th order dominates at locations close to the impeller but at locations farther from the impeller and closer to the discharge of the scroll the 10th order dominates. For configurations A and B, there is similarity in the pulsation characteristics for the three sensors located near the vane leading edge (PIB2, PBI3 and D1). The attenuation of the pulsations appear largest with configuration C.

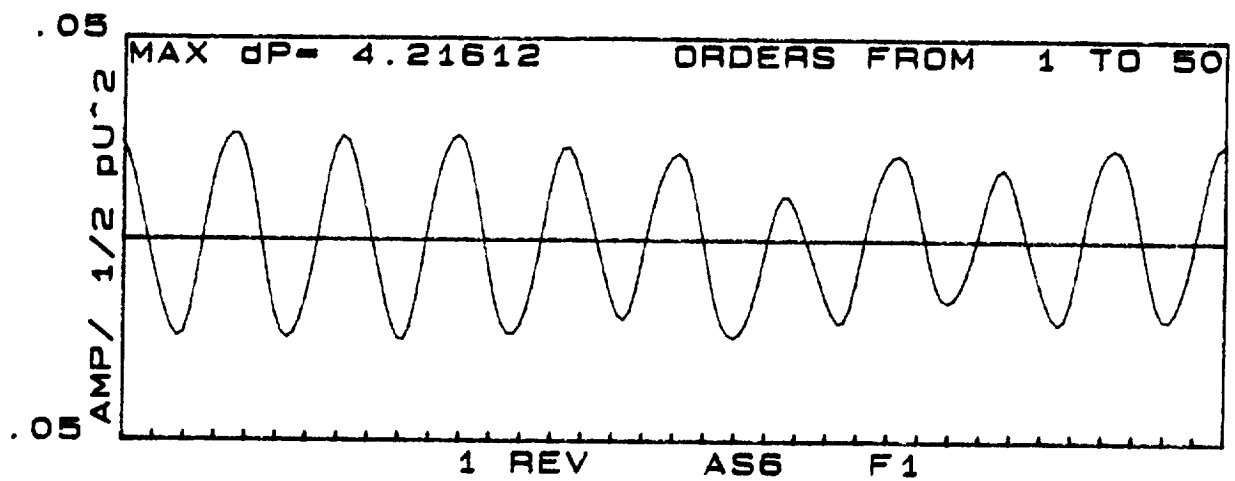
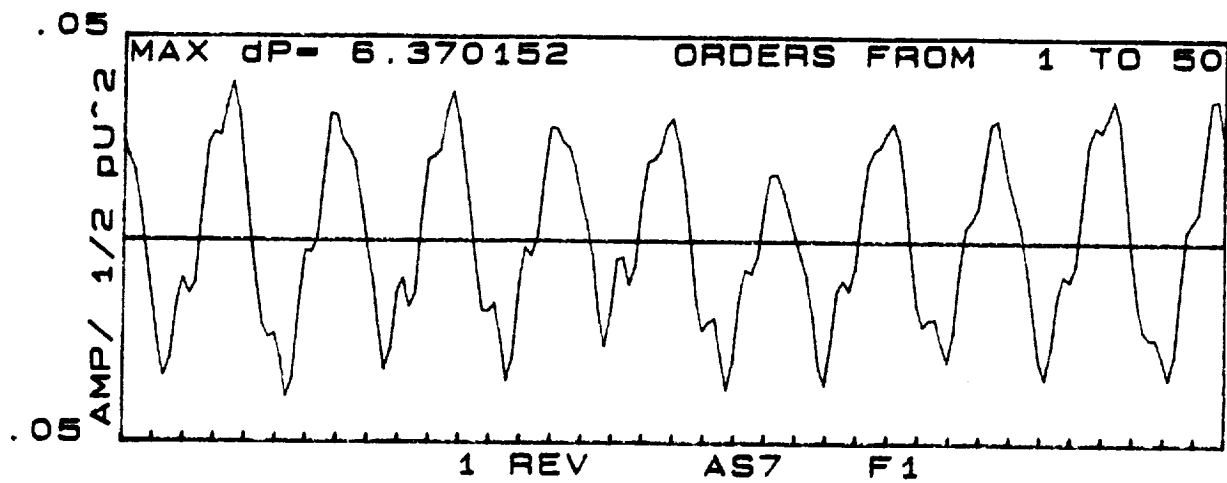


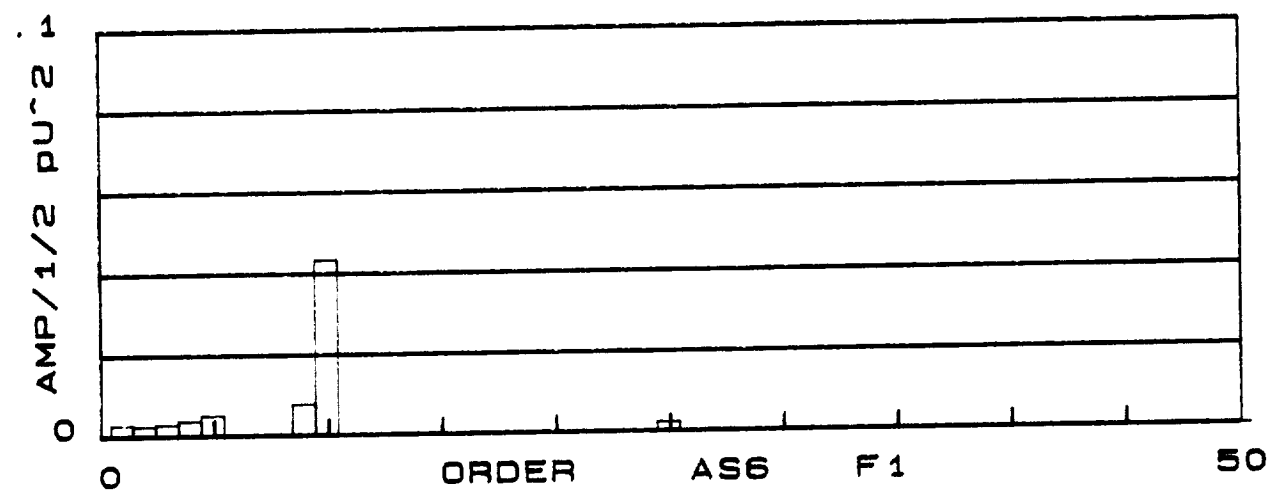
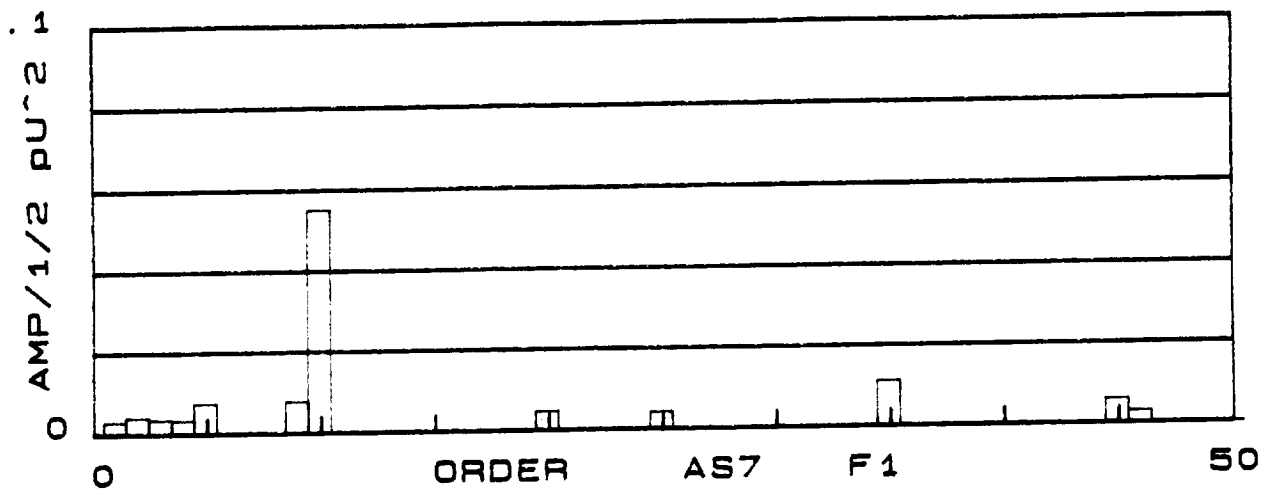


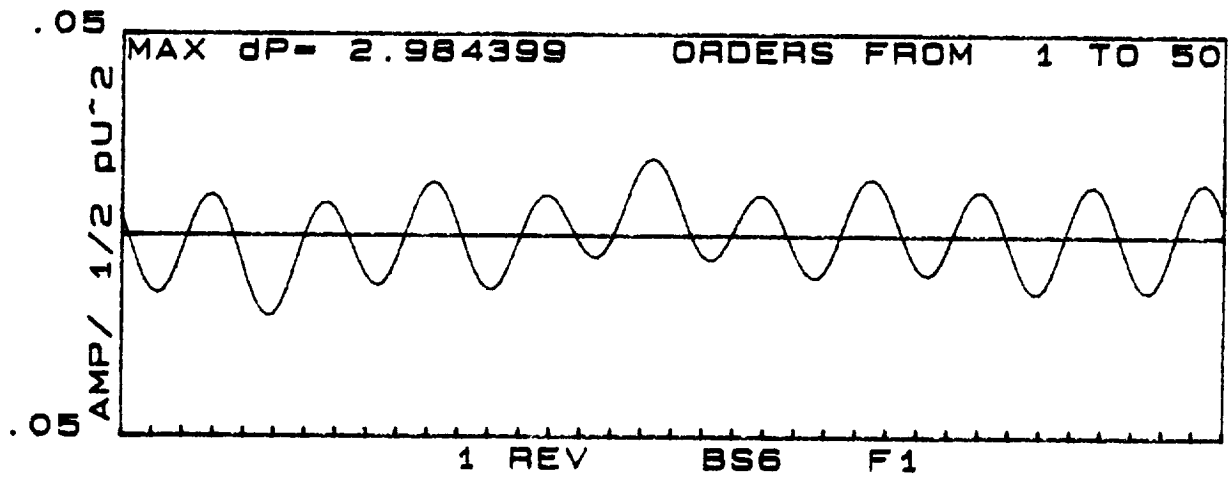
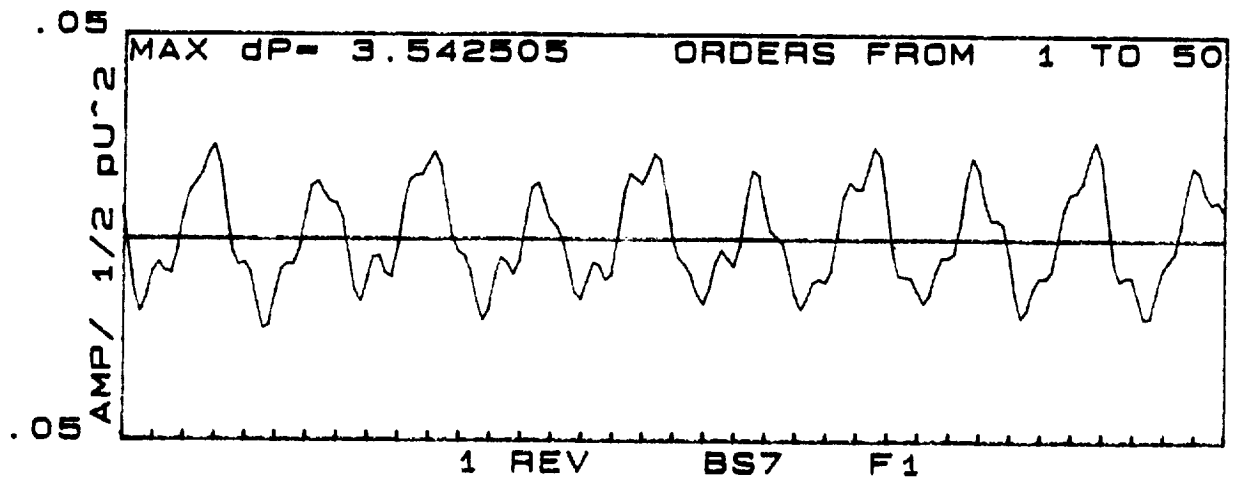


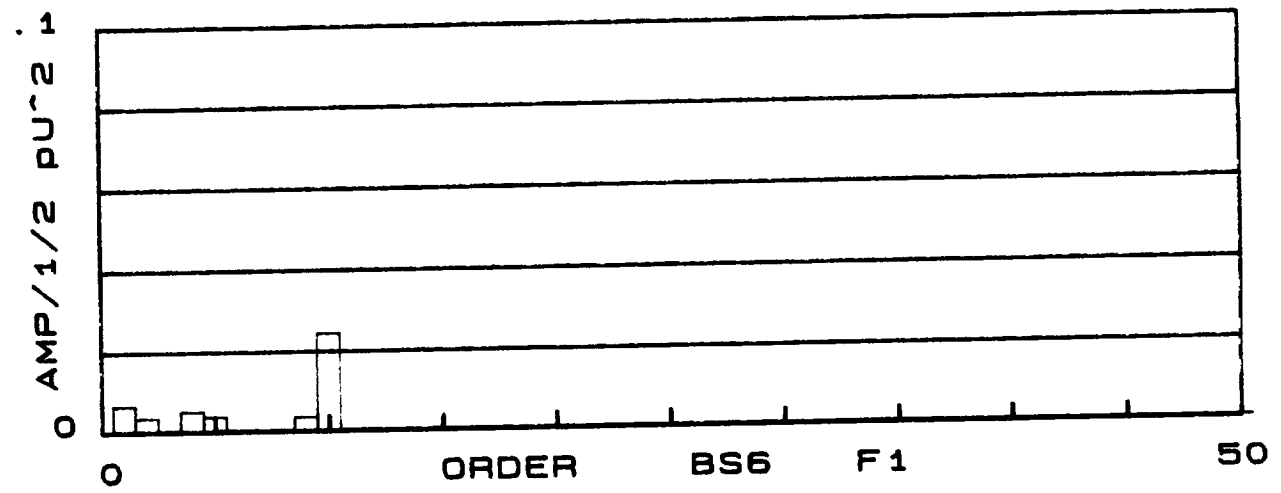
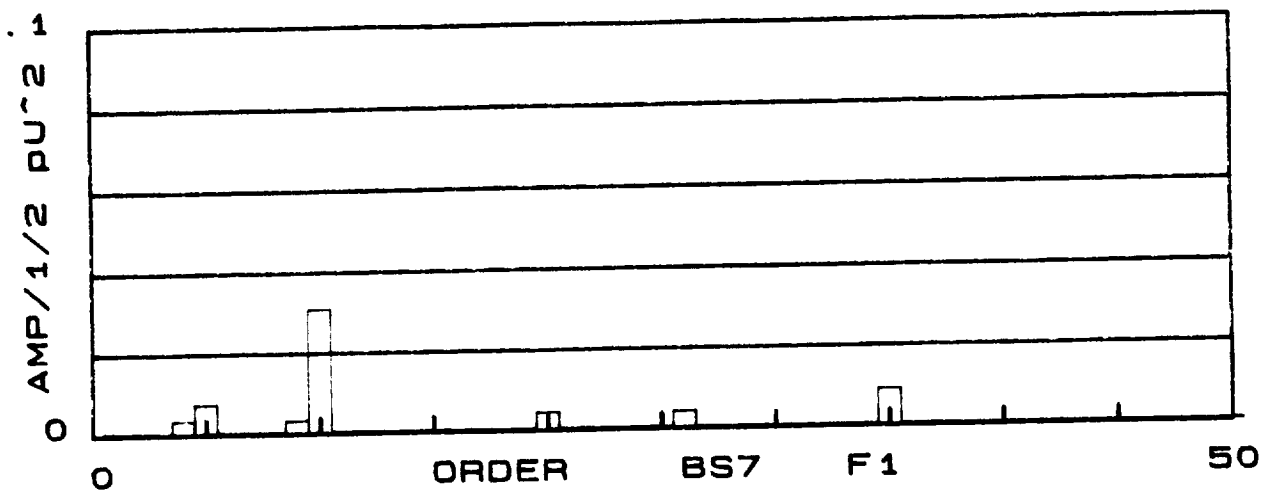


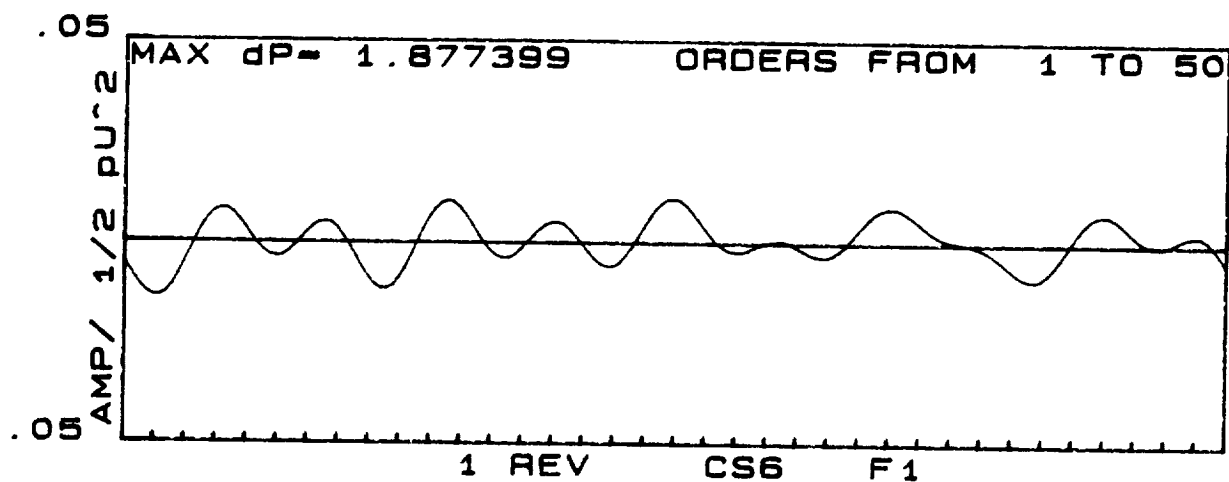
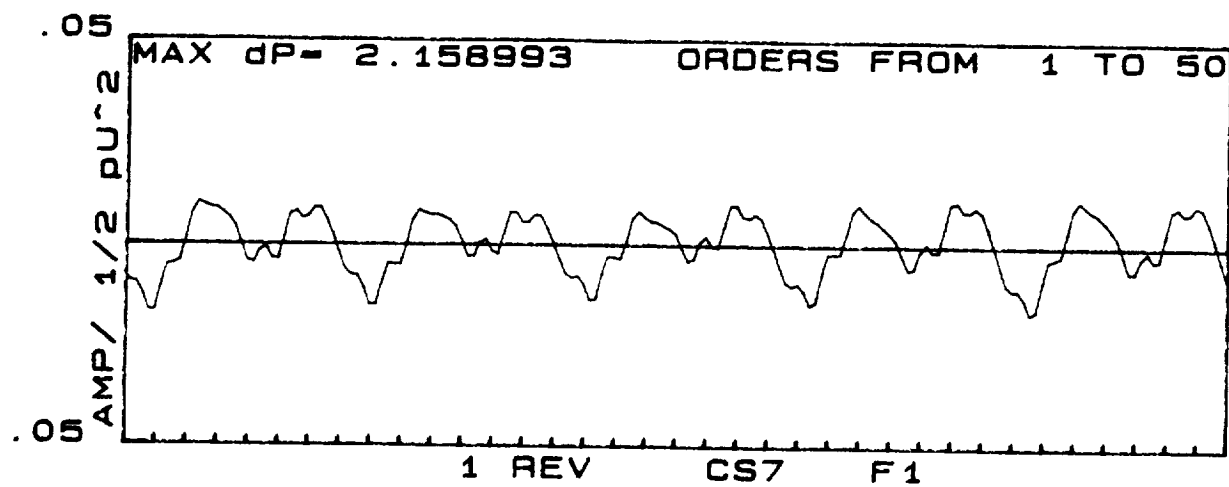


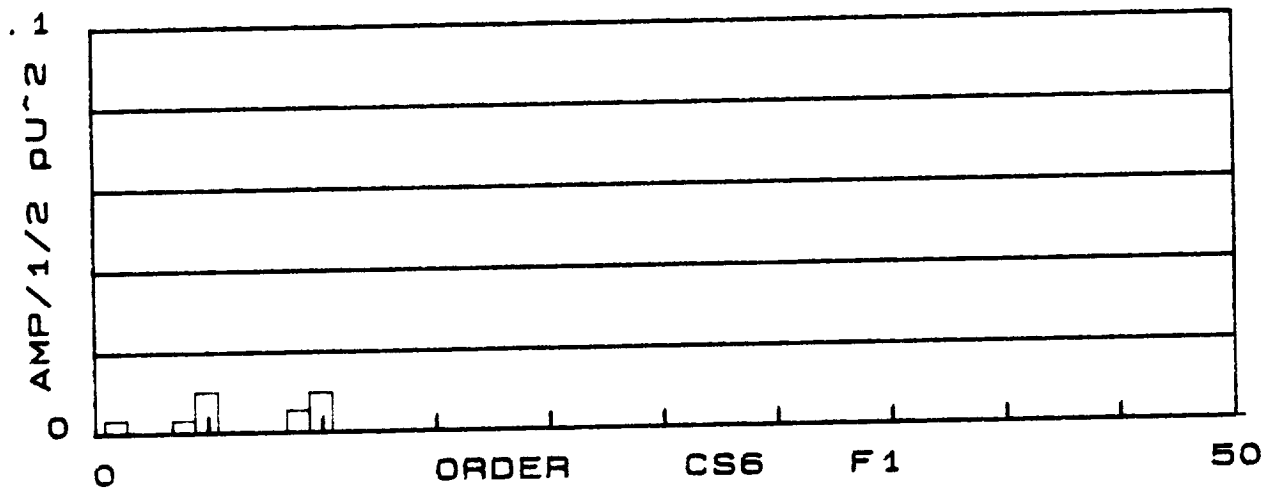
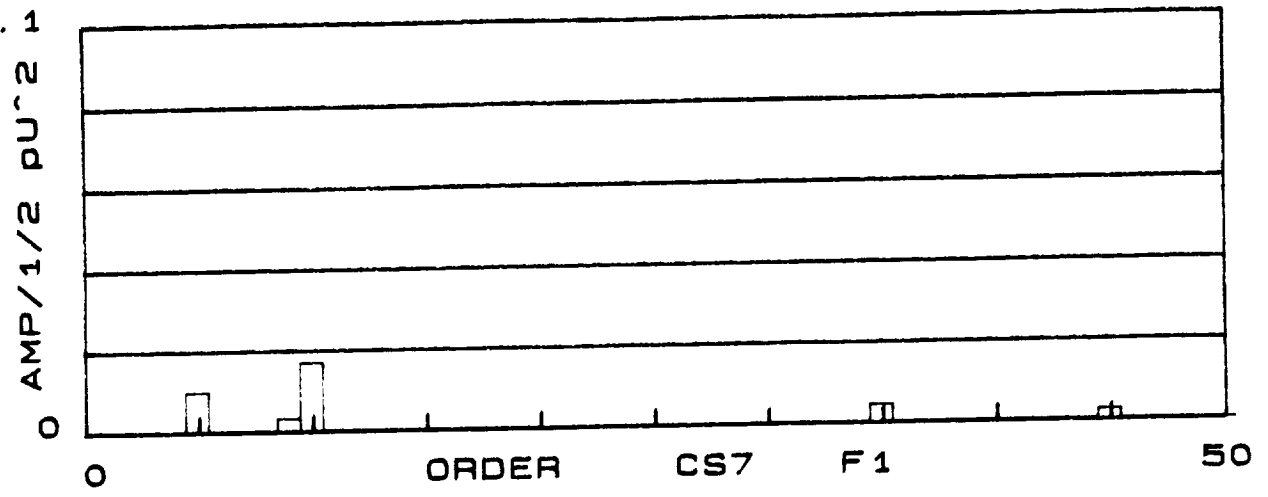










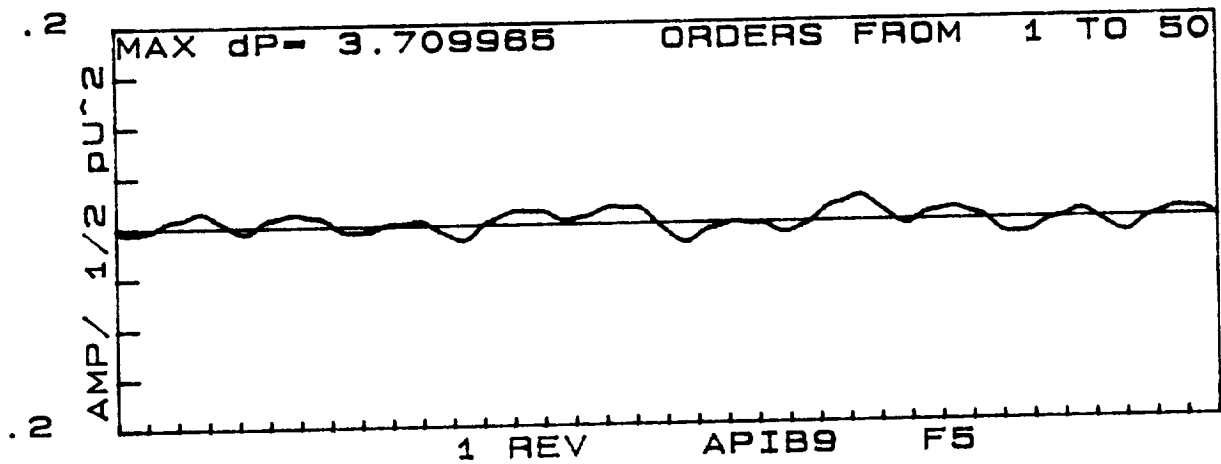
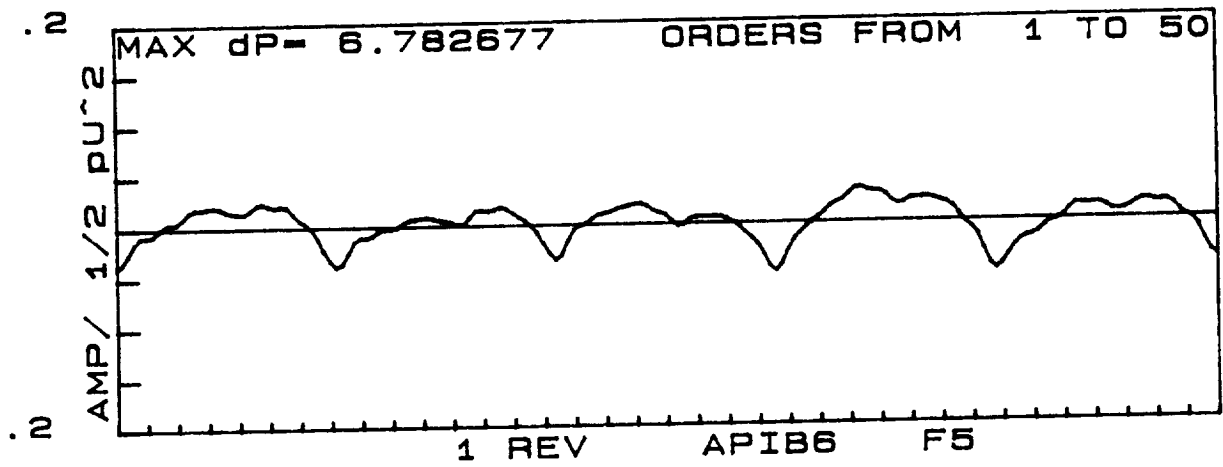
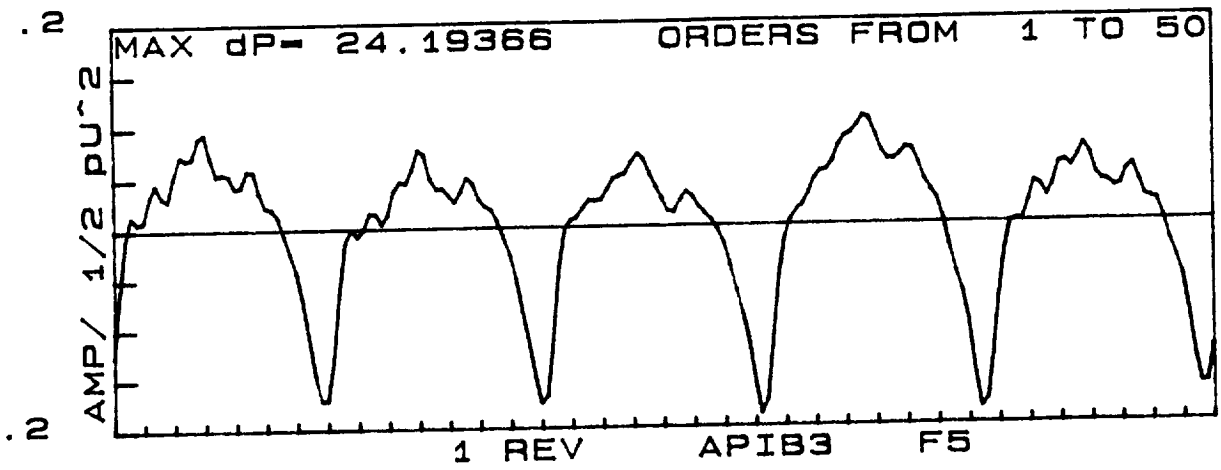


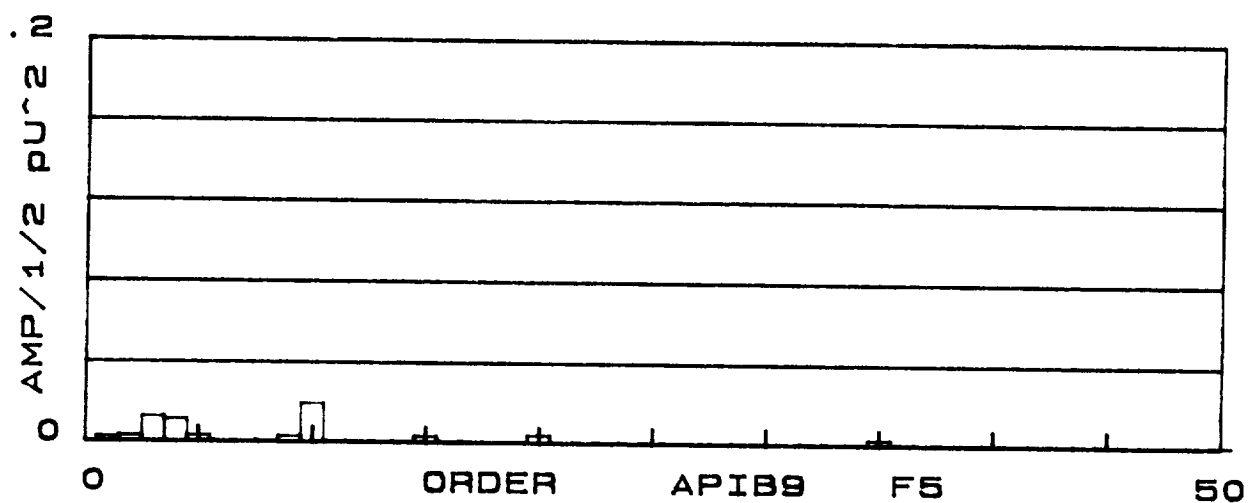
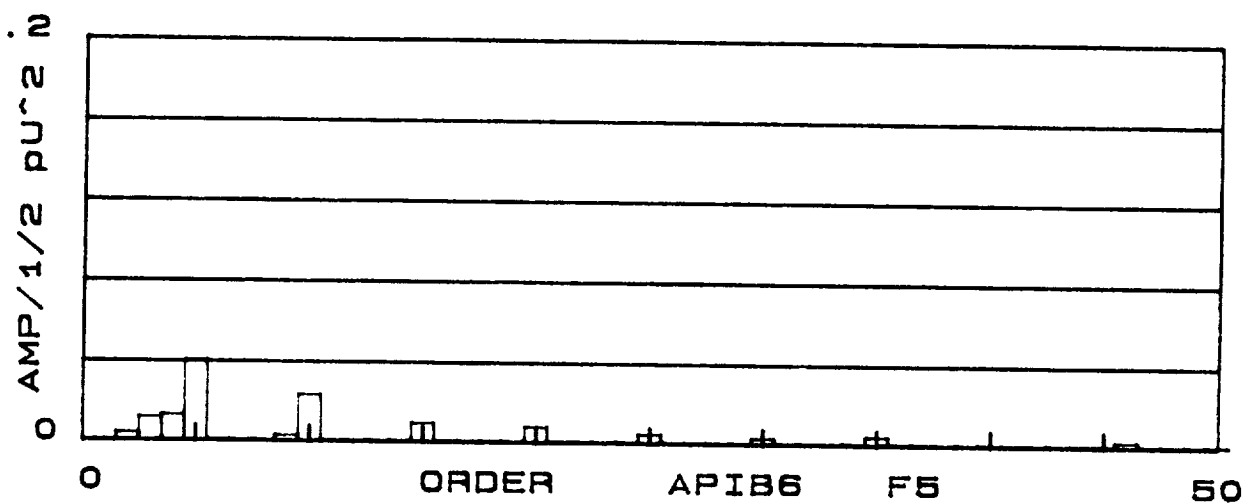
Attenuation of Pulsations, Pressure Side of Diffuser Passage

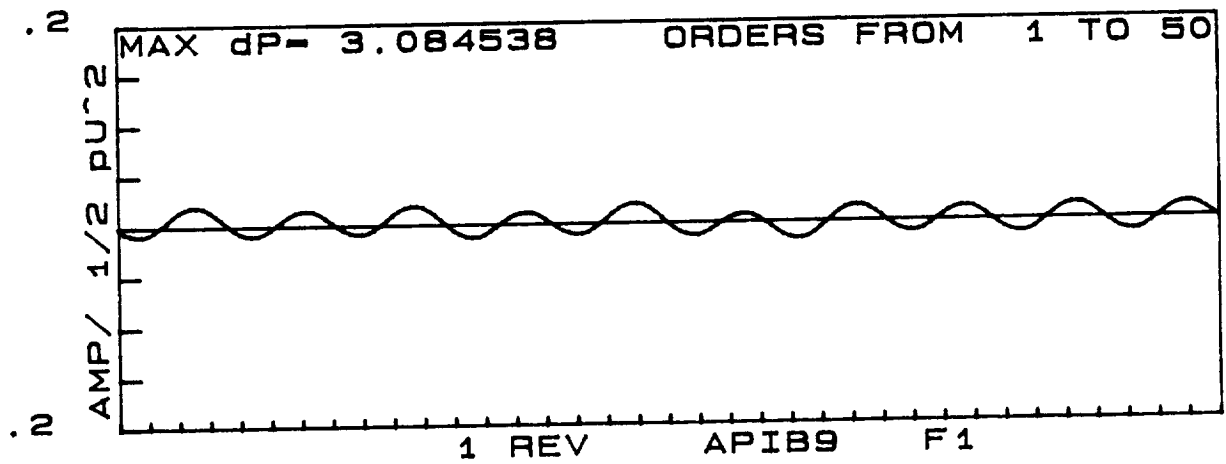
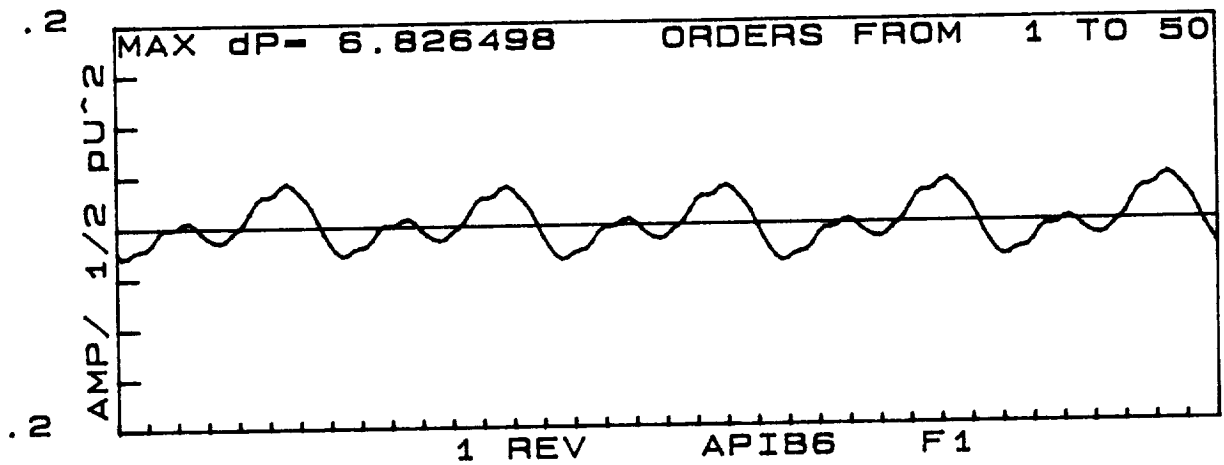
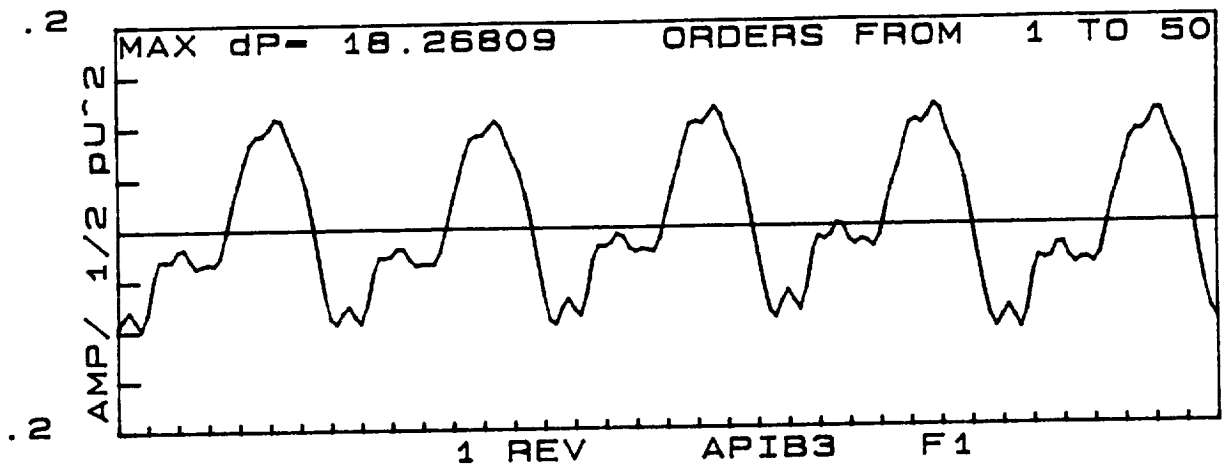
Locations: APIB3, APIB6, APIB9

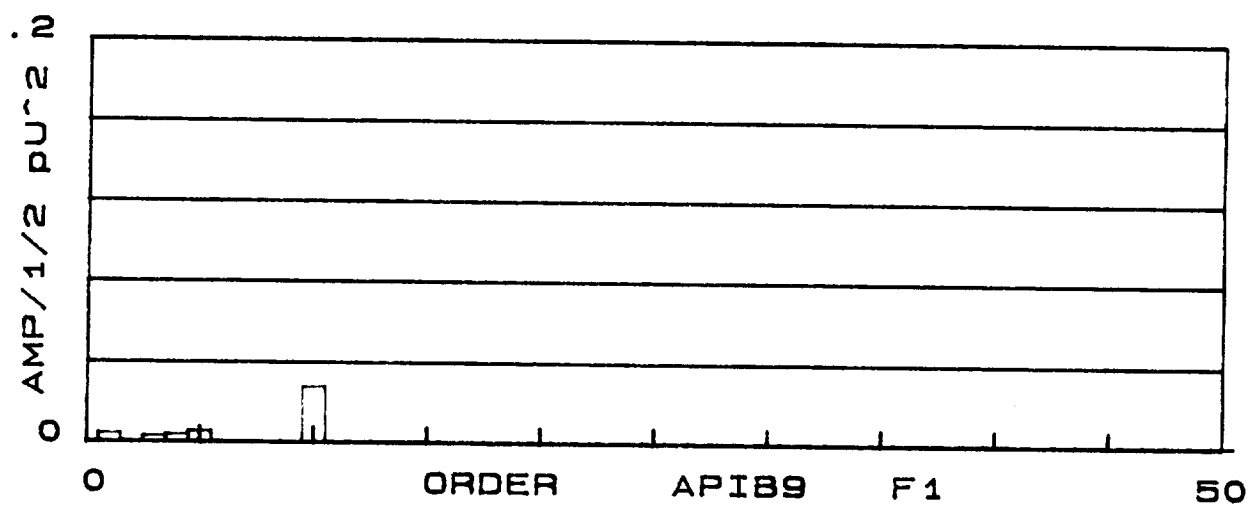
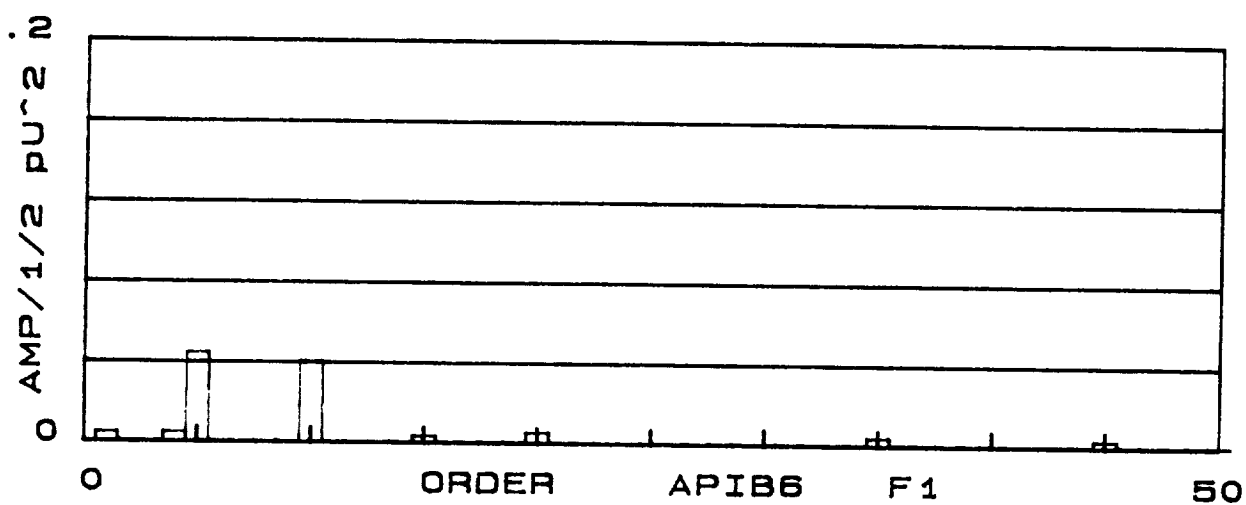
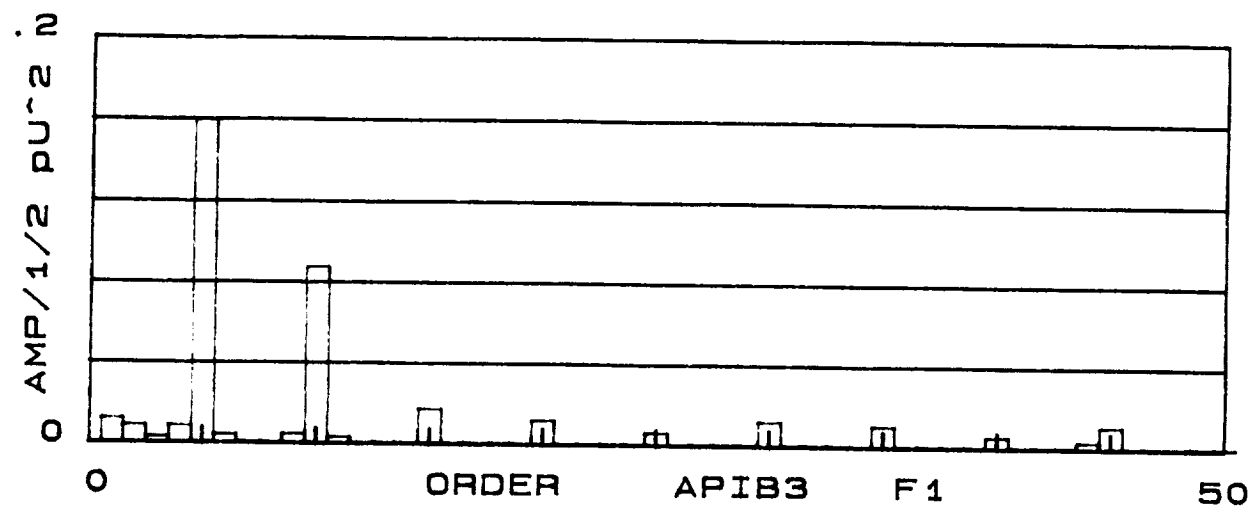
Conditions: F1, F5

The attenuation of pulsation activity along the pressure side of the diffuser vane is shown in these plots. The large 5th order component which dominates at the leading edge, is reduced at the trailing edge of the vane (APIB9) and the 10th order (which is a result of the interaction of all impeller and diffuser vanes) becomes dominant.







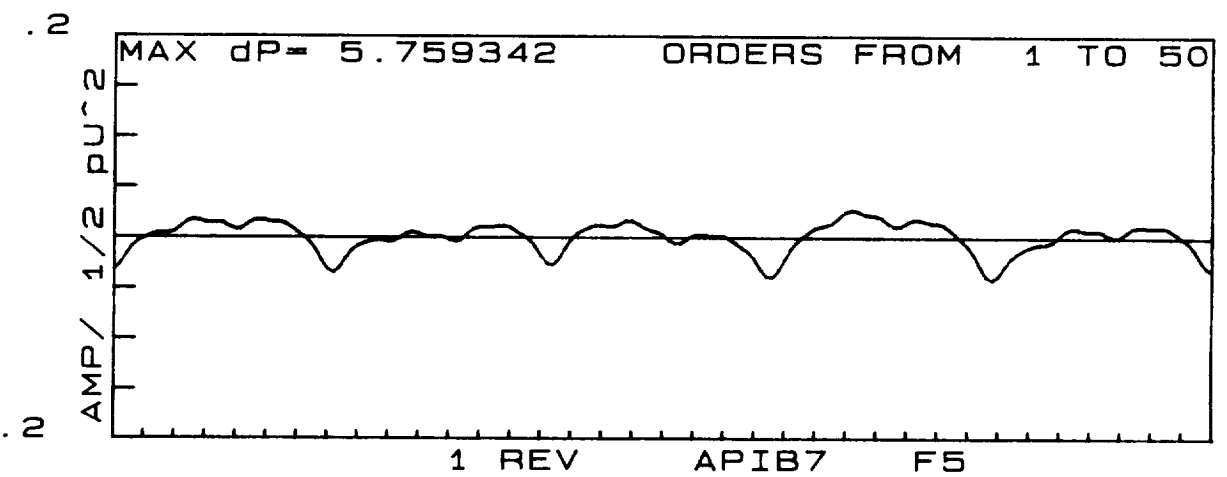
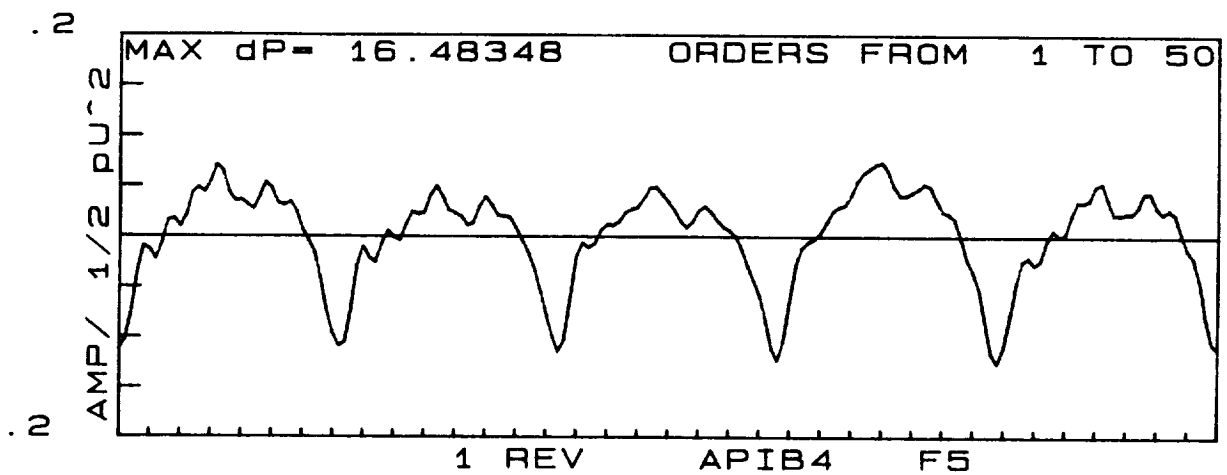
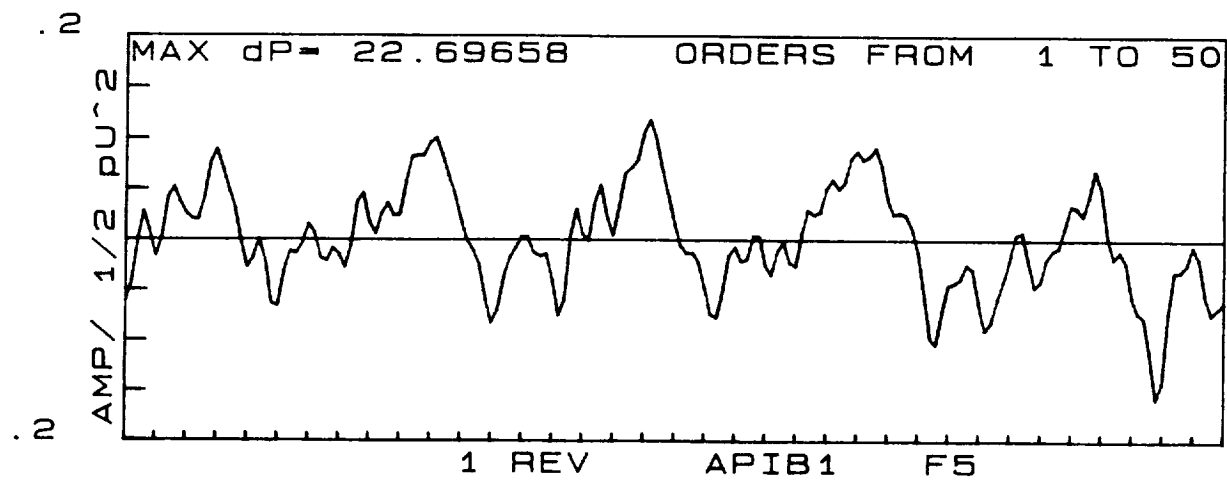


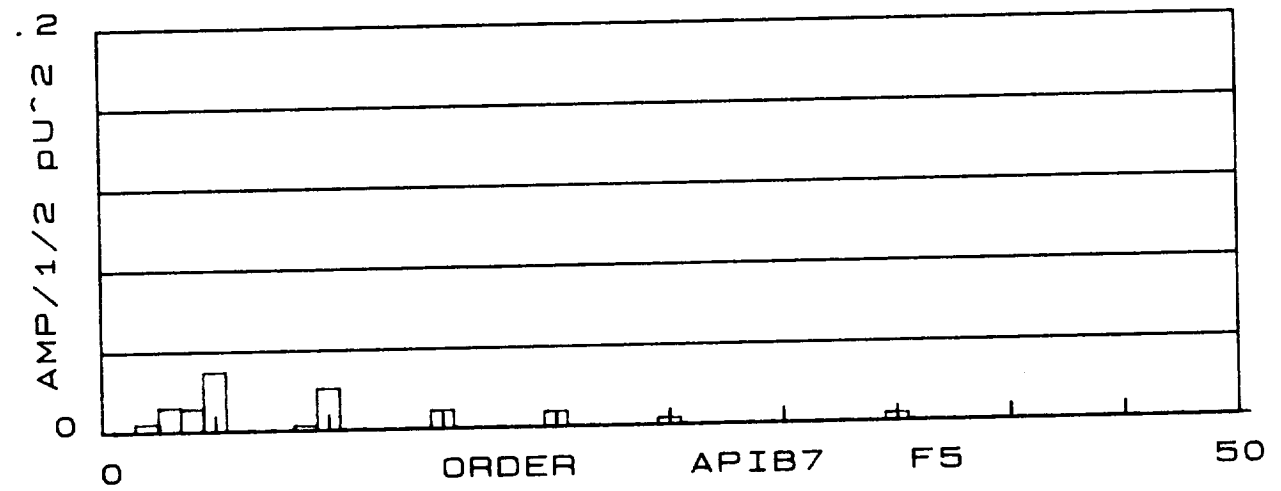
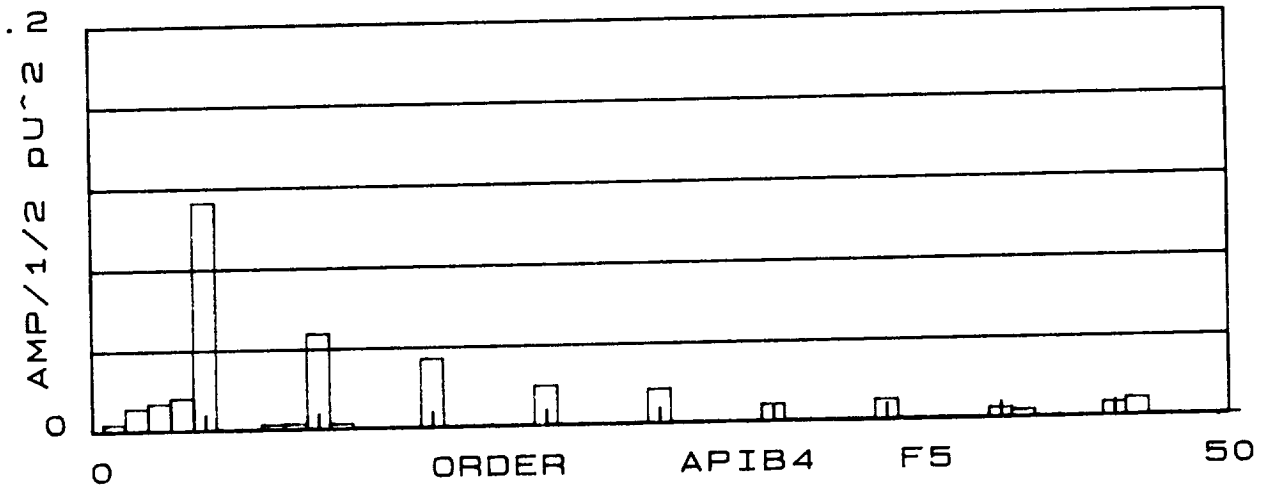
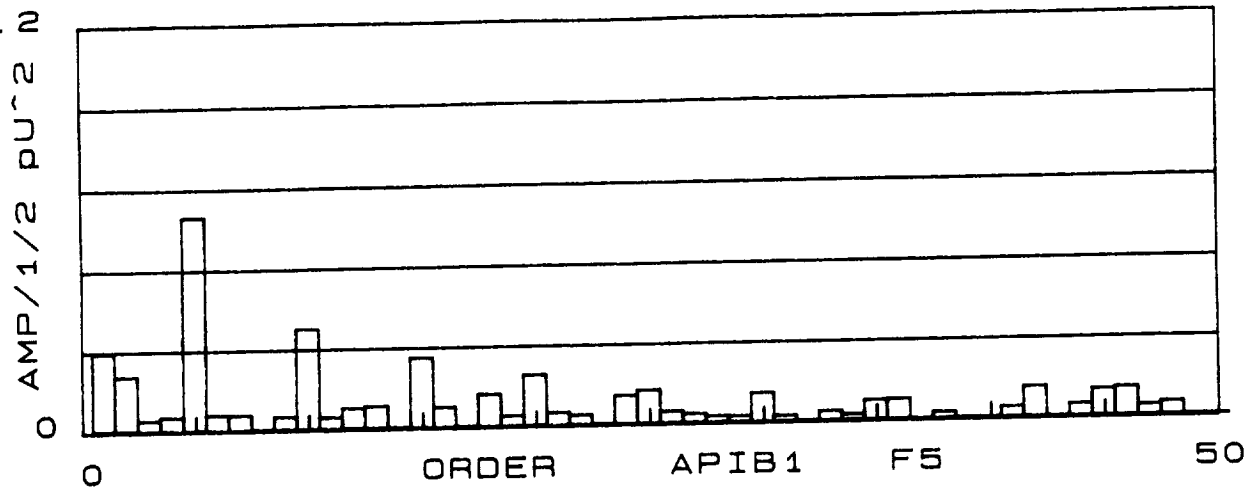
Attenuation of Pulsations, Suction Side of Diffuser Passage

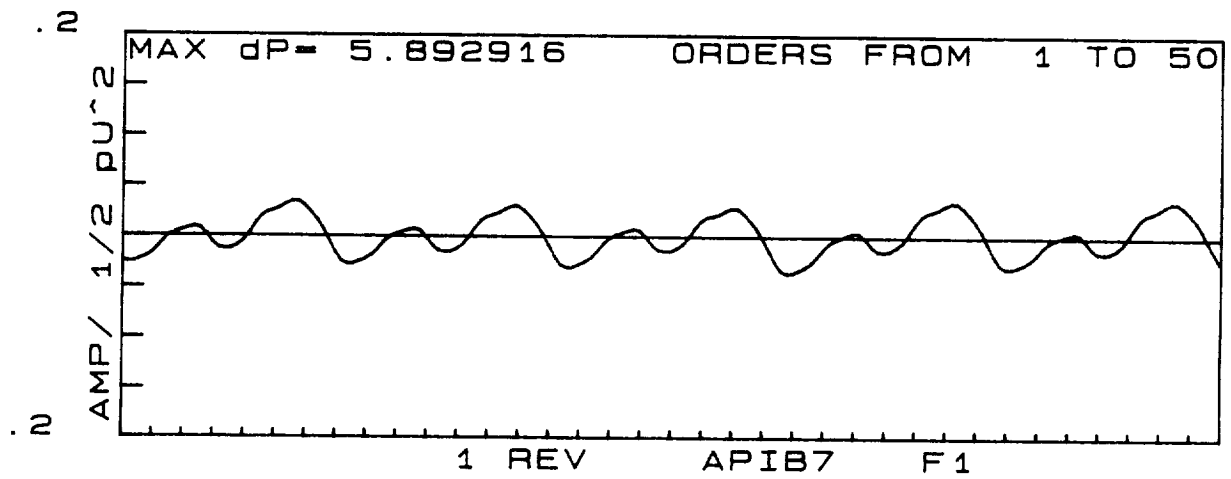
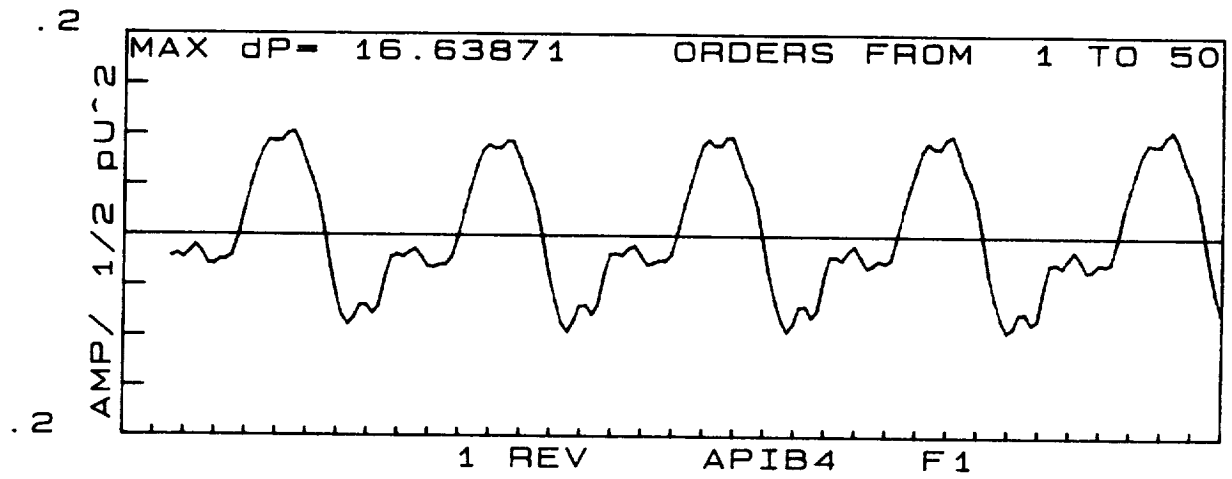
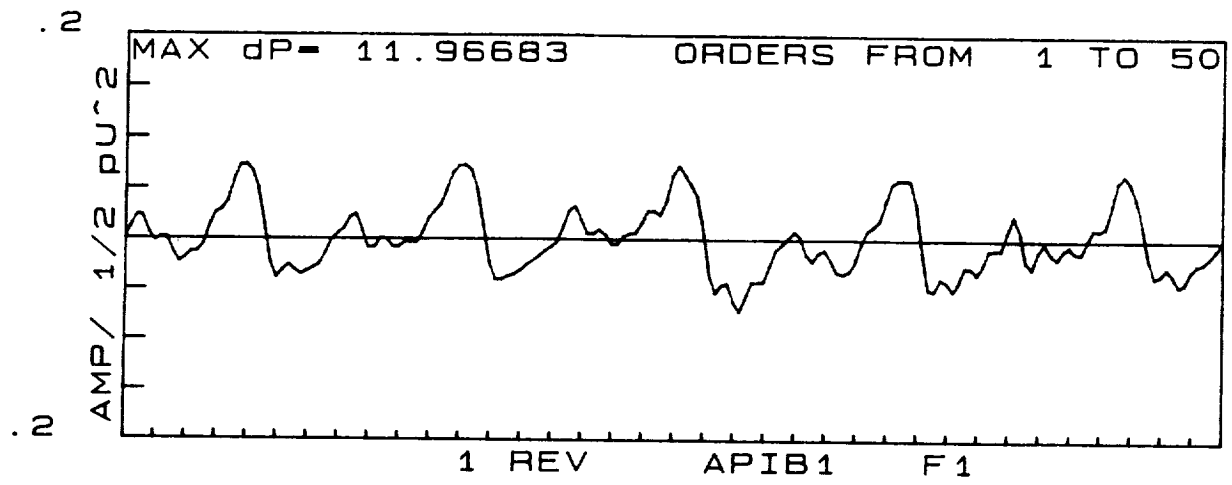
Locations: APIB1, APIB4, APIB7

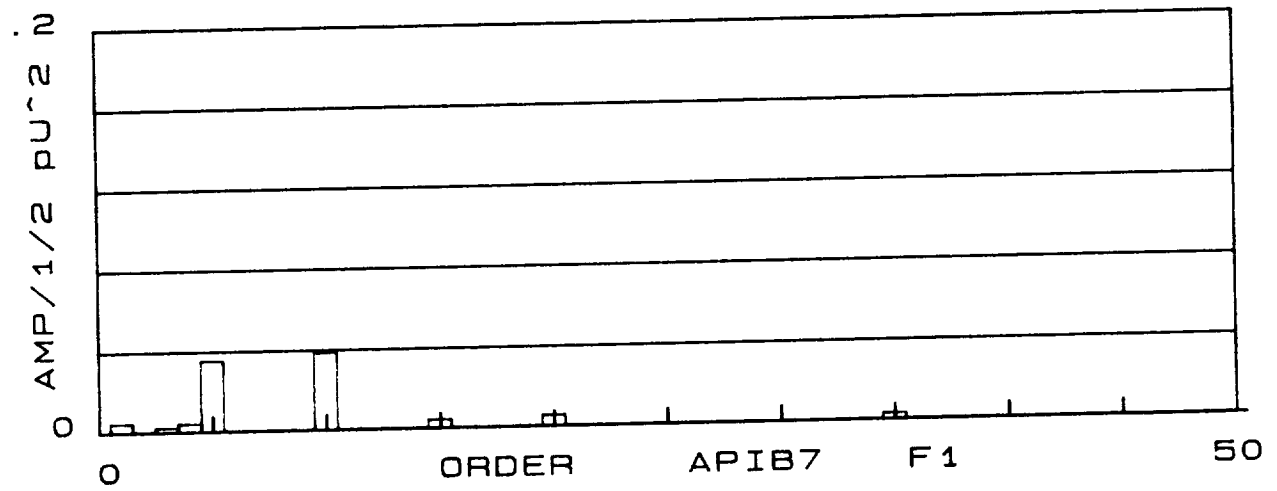
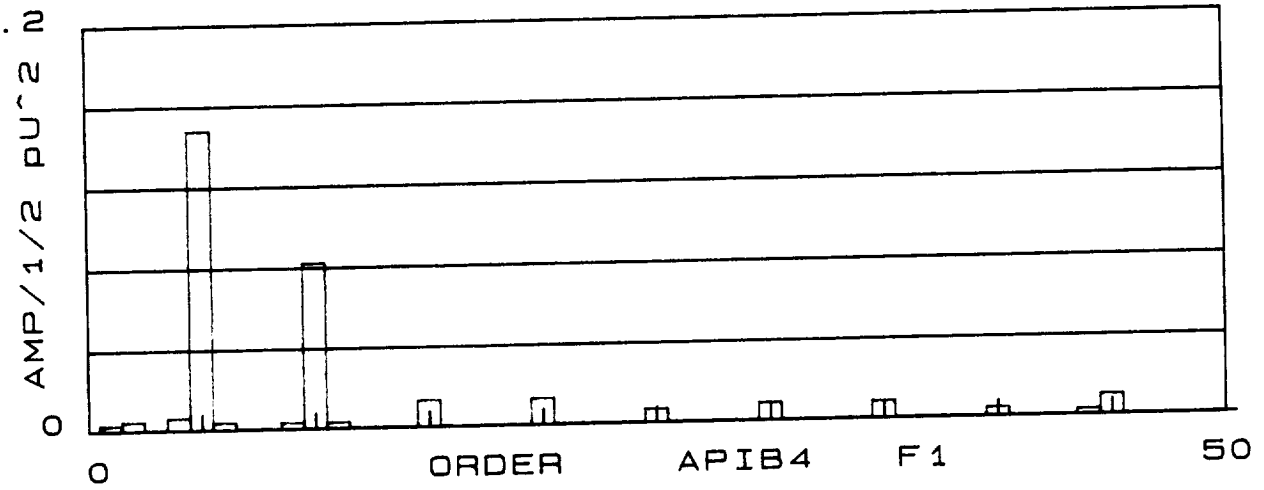
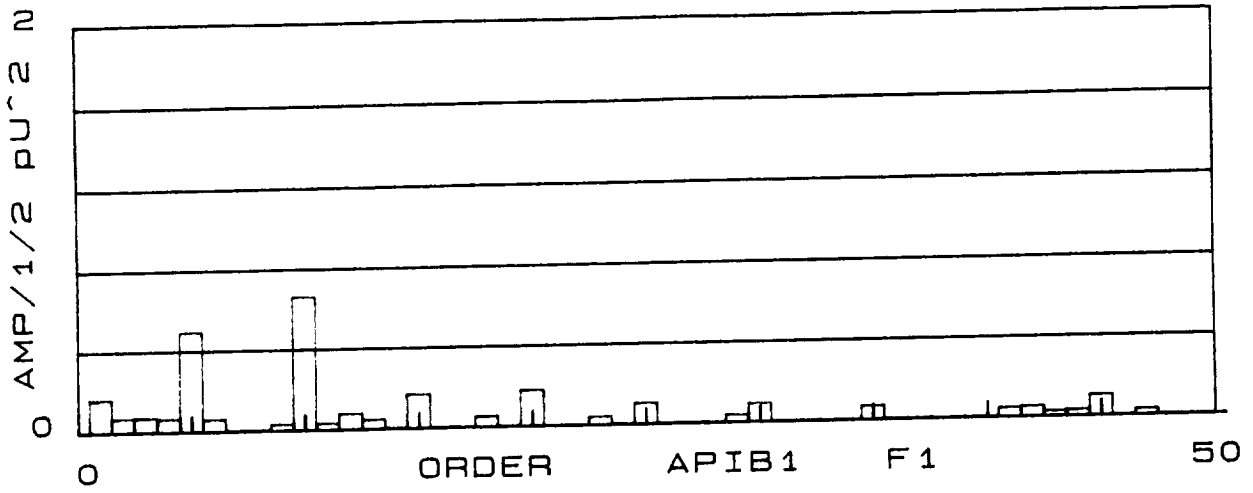
Conditions: F1, F5

The attenuation of pressure pulsation activity along the suction side of the diffuser vane is shown in these plots. The 5th order component of the pulsation is much reduced at the trailing edge location (APIB7). The sensor located at the leading edge (APIB1) displays different characteristics as compared with the other locations. A multitude of synchronous orders of measurable magnitude are present. It cannot be determined whether this phenomenon is a function of the behavior on the suction surface of the vane or is a problem with the sensor itself, the sensor installation, or the data acquisition process. The behavior occurs at both extremes of flow rate (F1 & F5), so does not appear to be seriously affected by changes of flow angle approaching the vane leading edge.







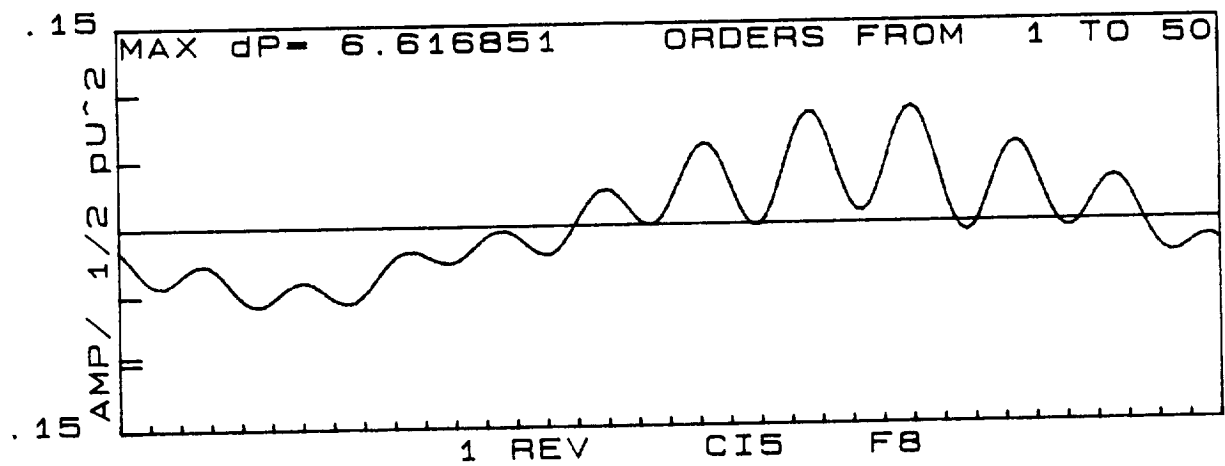
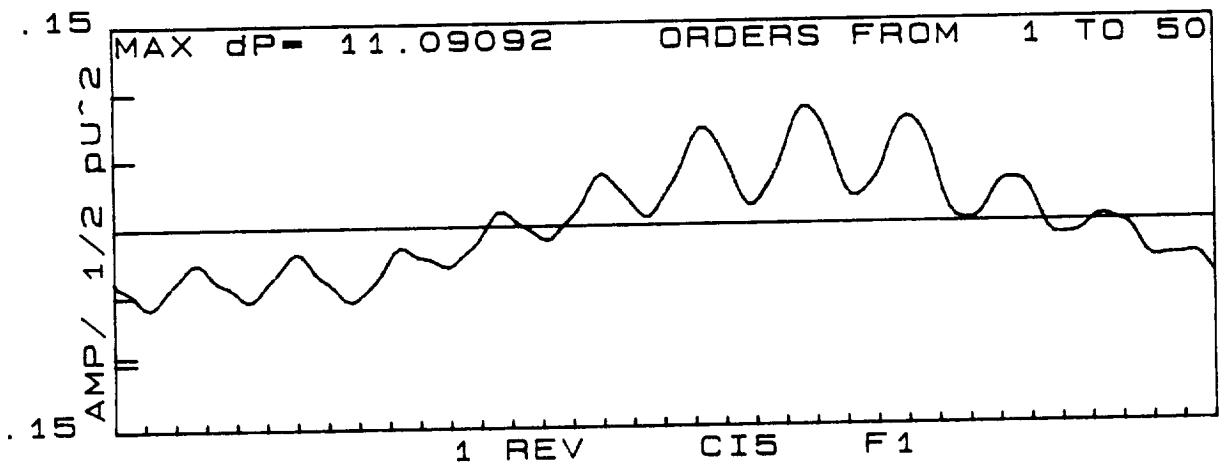
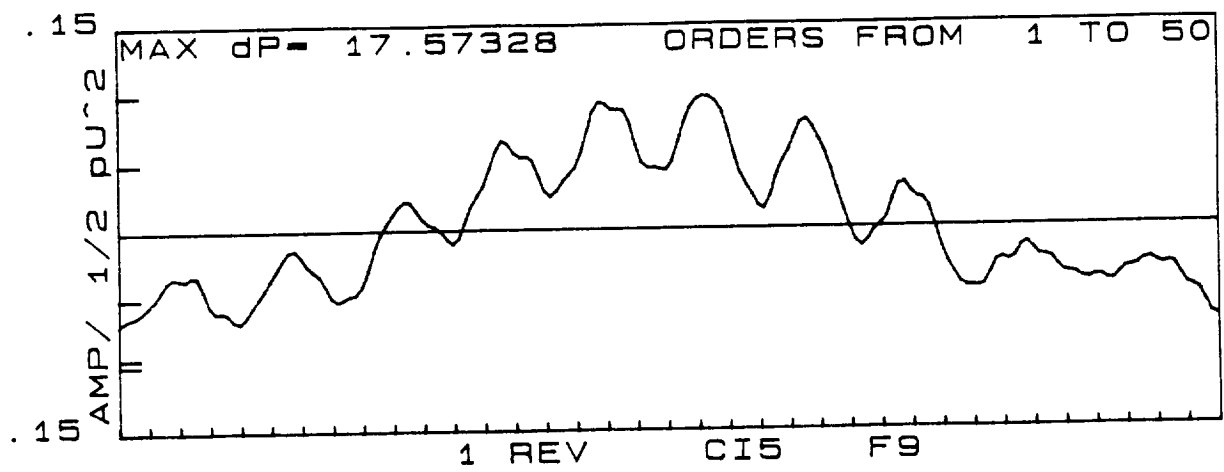


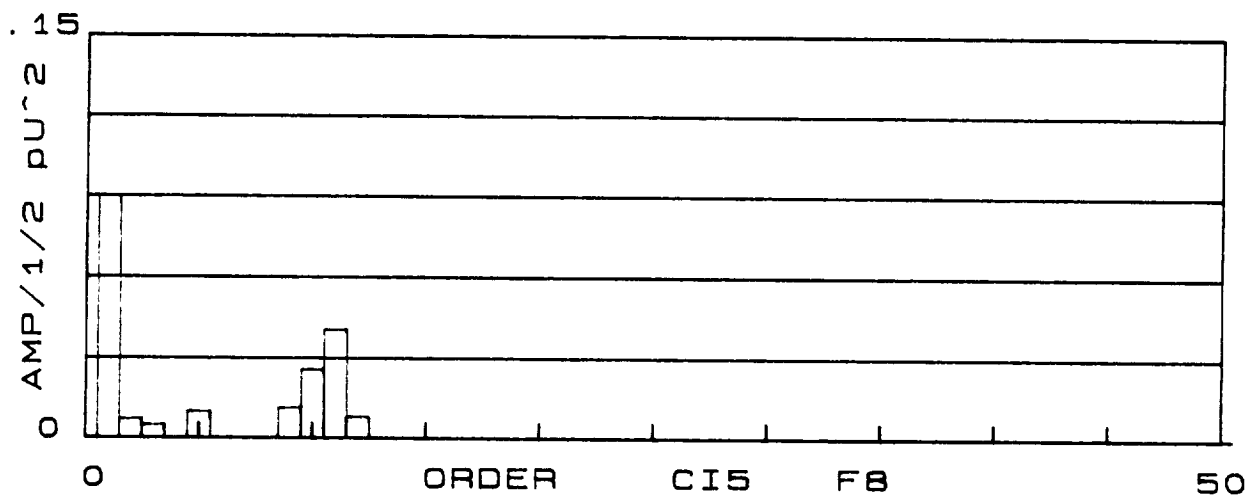
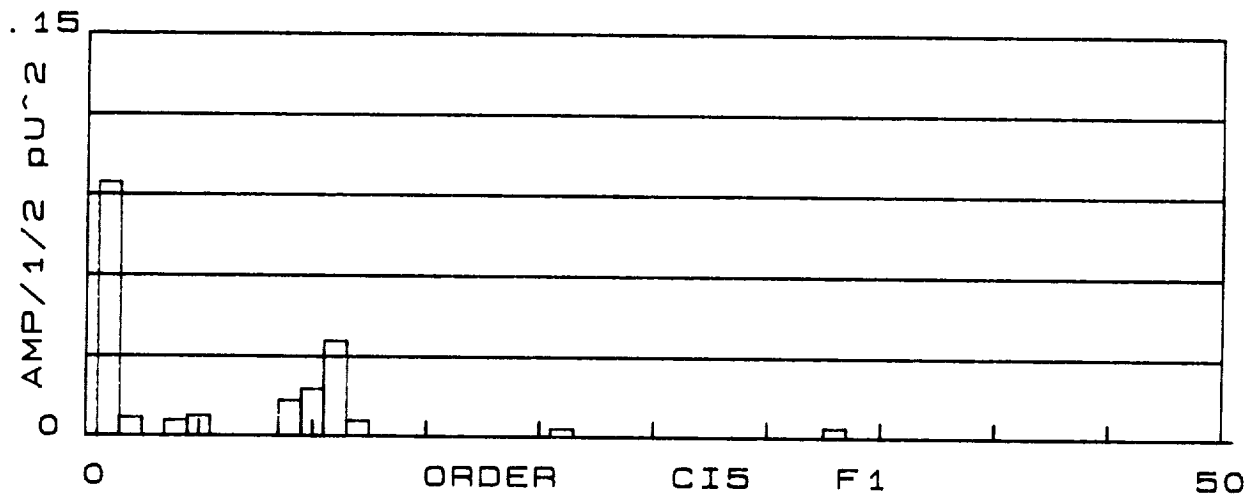
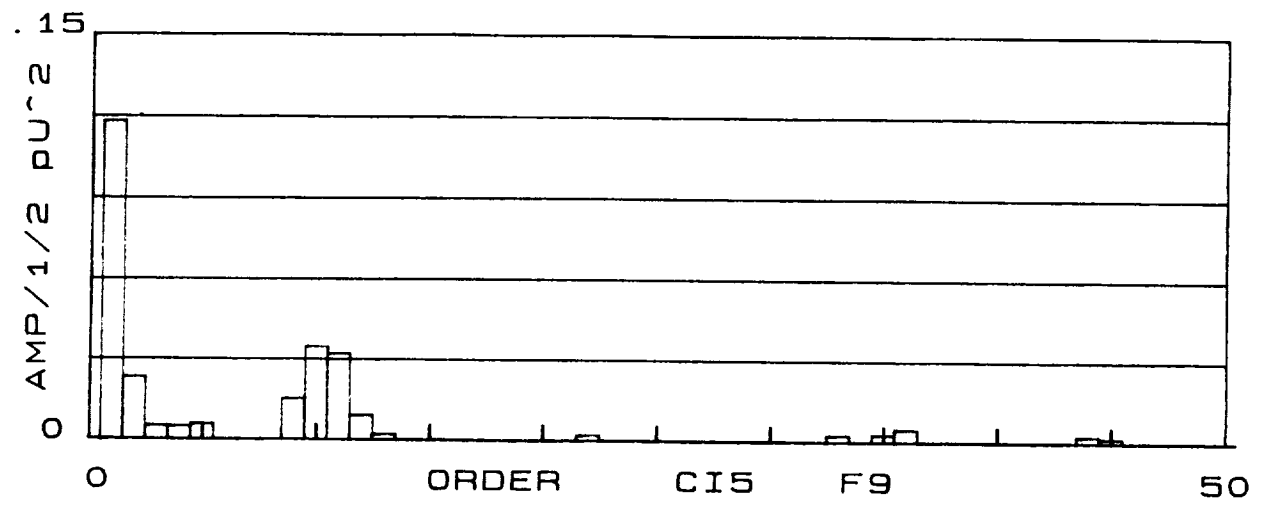
Scalability of Pulsation Activity, Impeller, Diffuser, Scroll Sensors

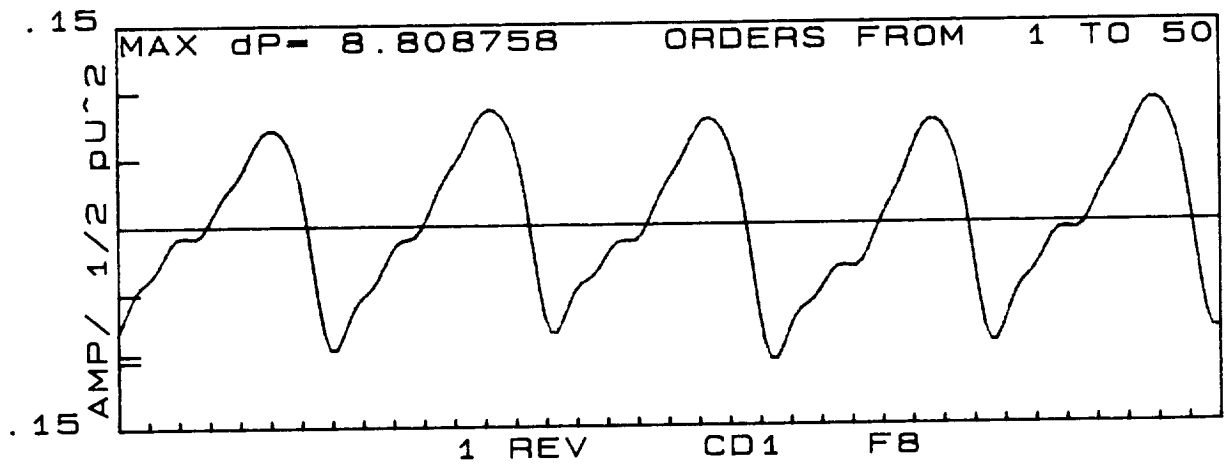
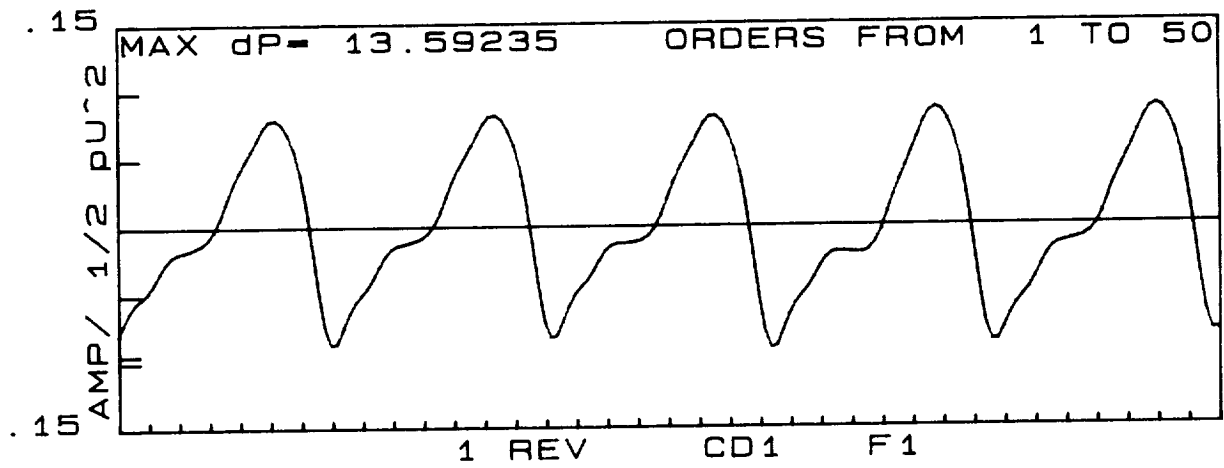
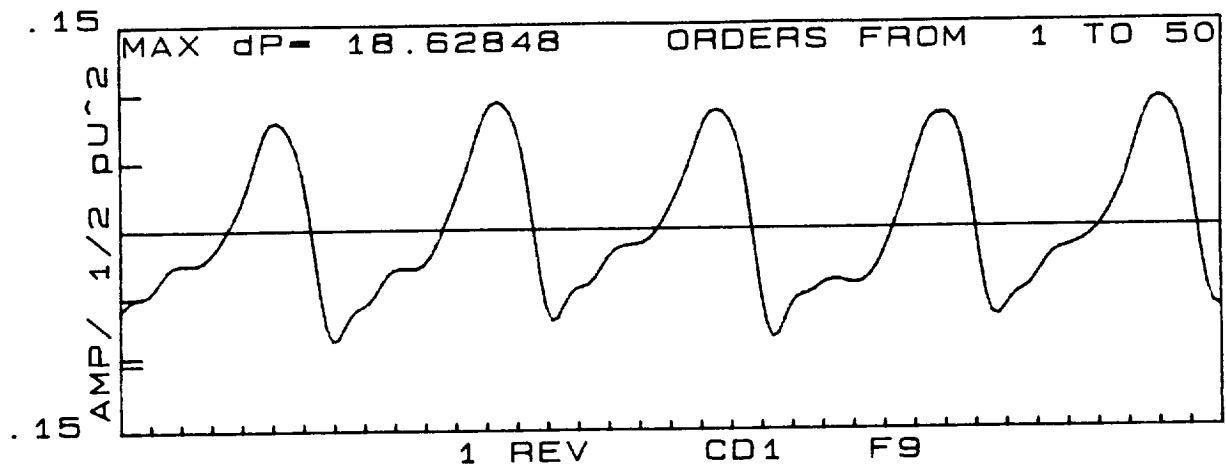
Locations: CI5, CD1, CS7

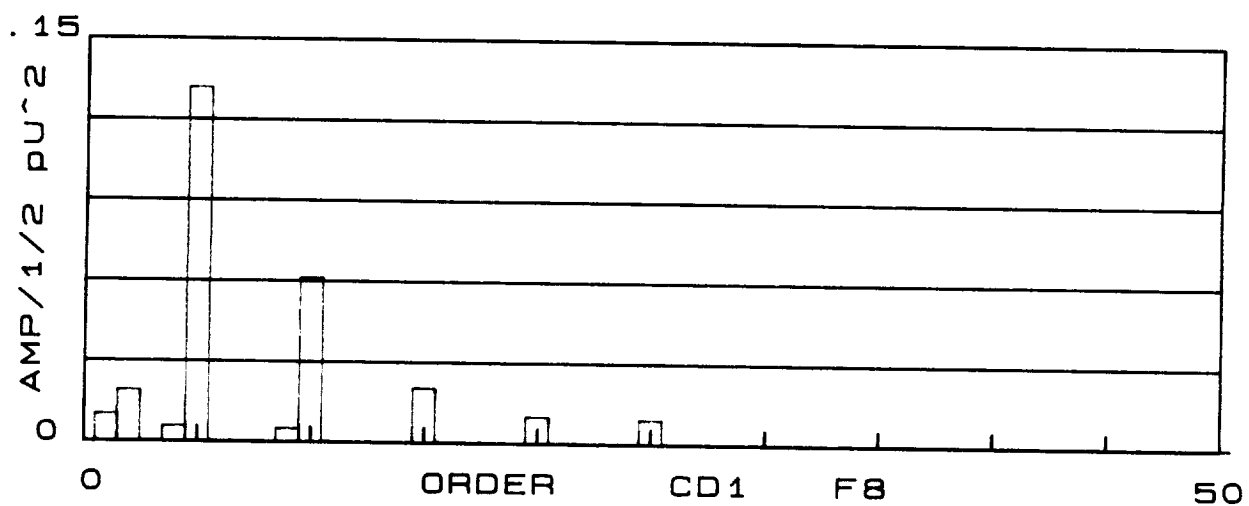
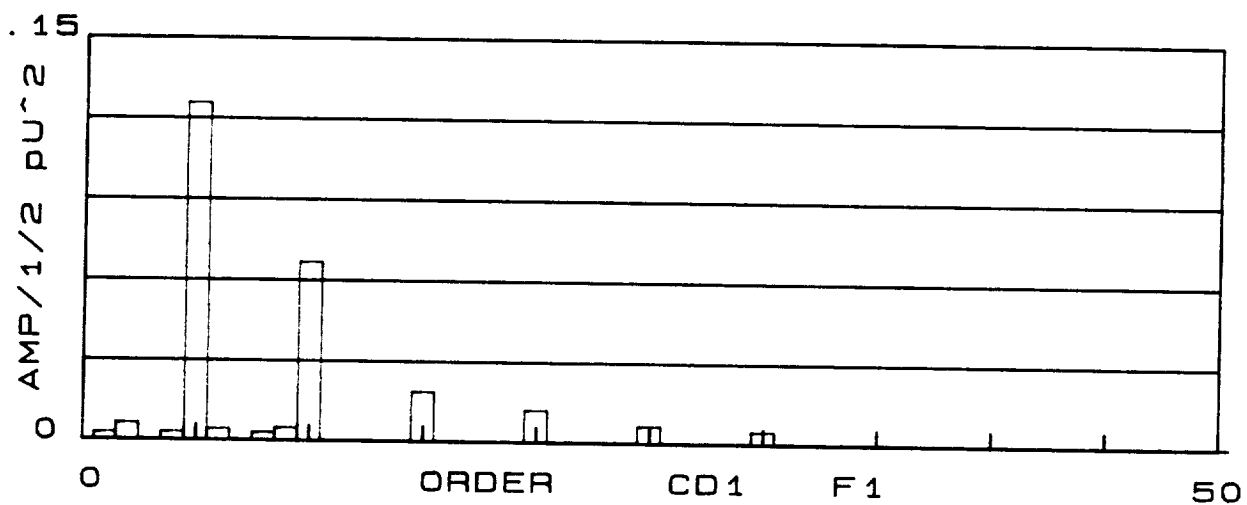
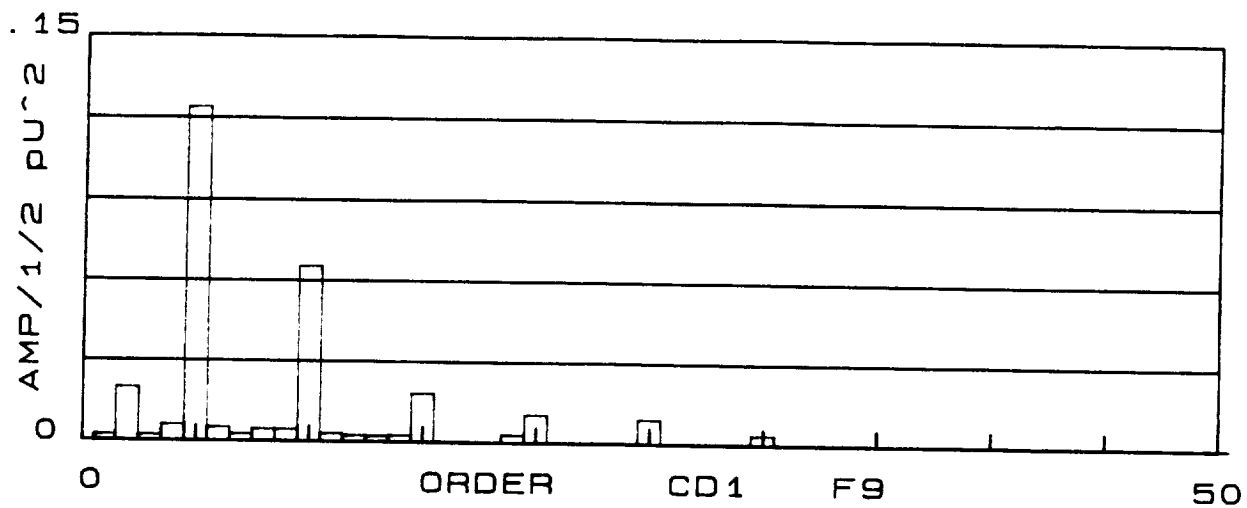
Conditions: F9, F1, F8

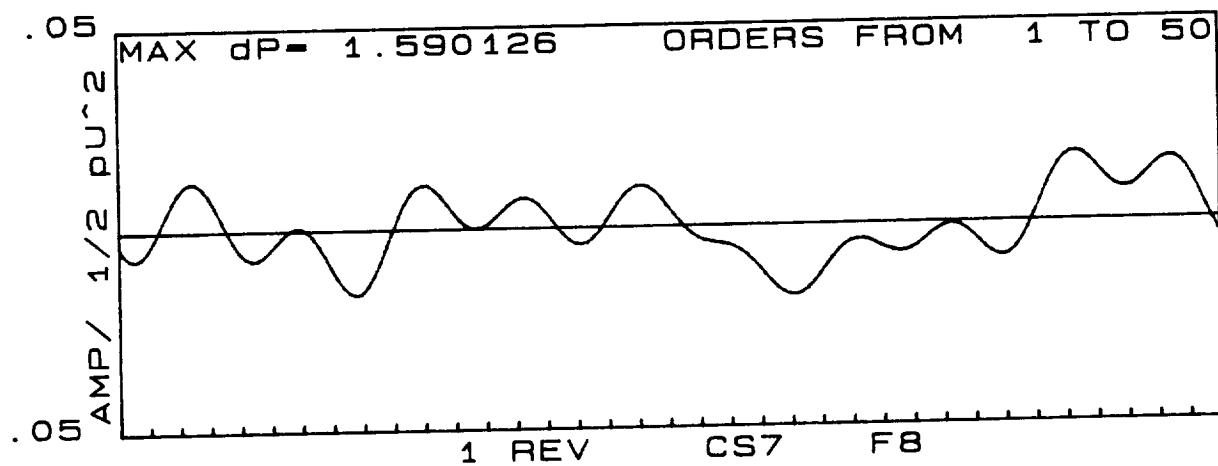
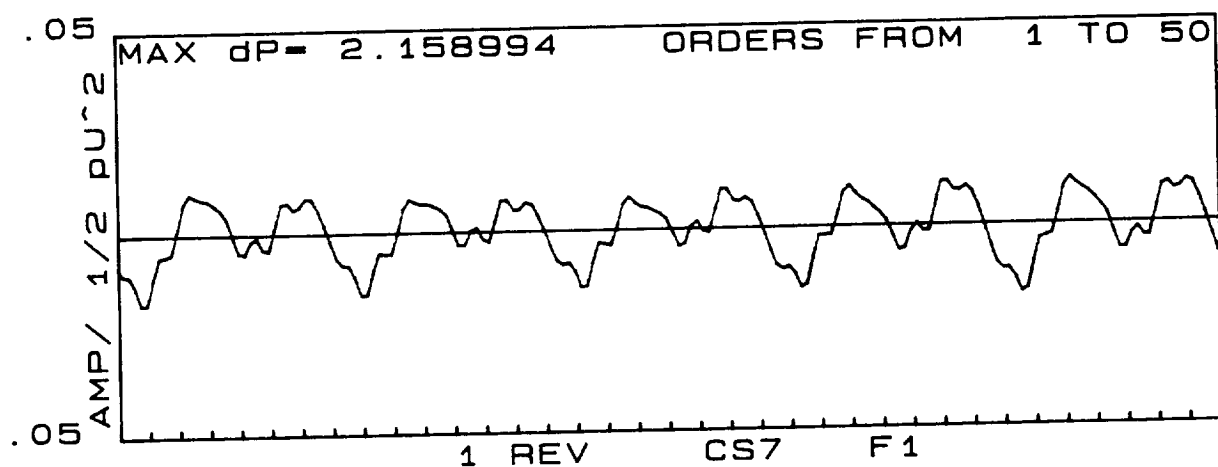
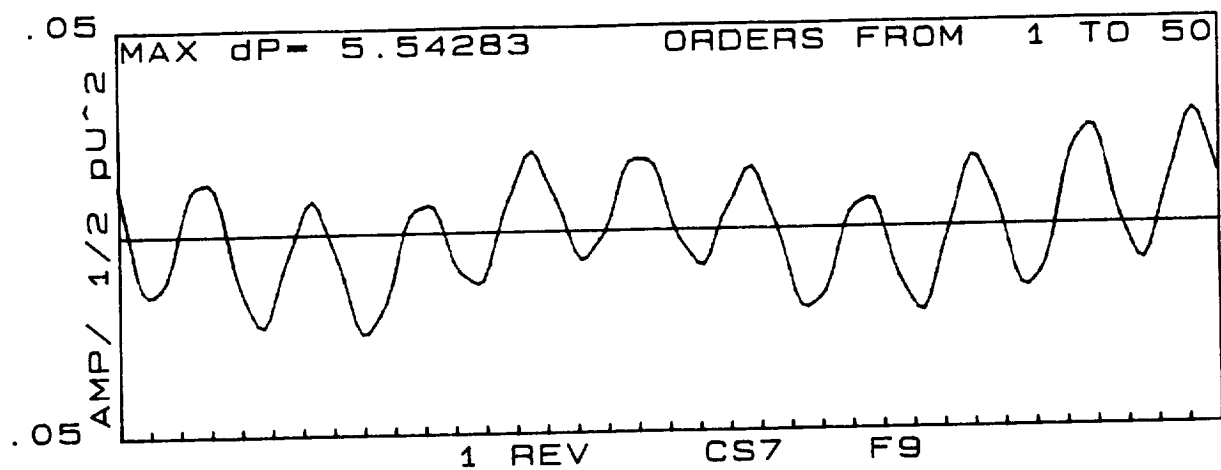
The variation of pressure pulsation for 3 speeds, at a constant fraction of flow rate (25% of design, flow coefficient of .019) is displayed in this series of plots. The 3 speeds displayed are 1780, 2300 and 2700 rpm. The order plots for each waveform are included and can be used to compare the scalability of the pulsations since the orders are plotted in non-dimensional form (normalized to impeller exit tip velocity head). The impeller (CI5) shows reasonable consistency in pulsation activity with some variation in the first order. The diffuser sensor (CD1) shows excellent scalability of the orders of pulsation activity. Poor scalability is observed in the scroll sensor (CS7) as evidenced by the 3 to 1 variation in the dominant 10th order. The high speed condition (F9, 2700 rpm) is 3 times that of the low speed condition (F8, 1780 rpm).

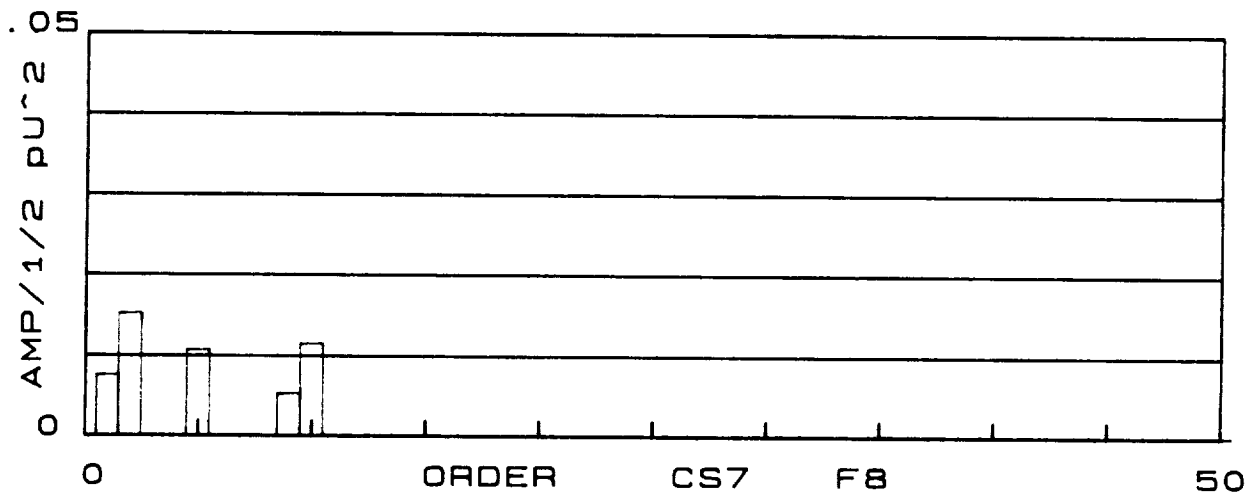
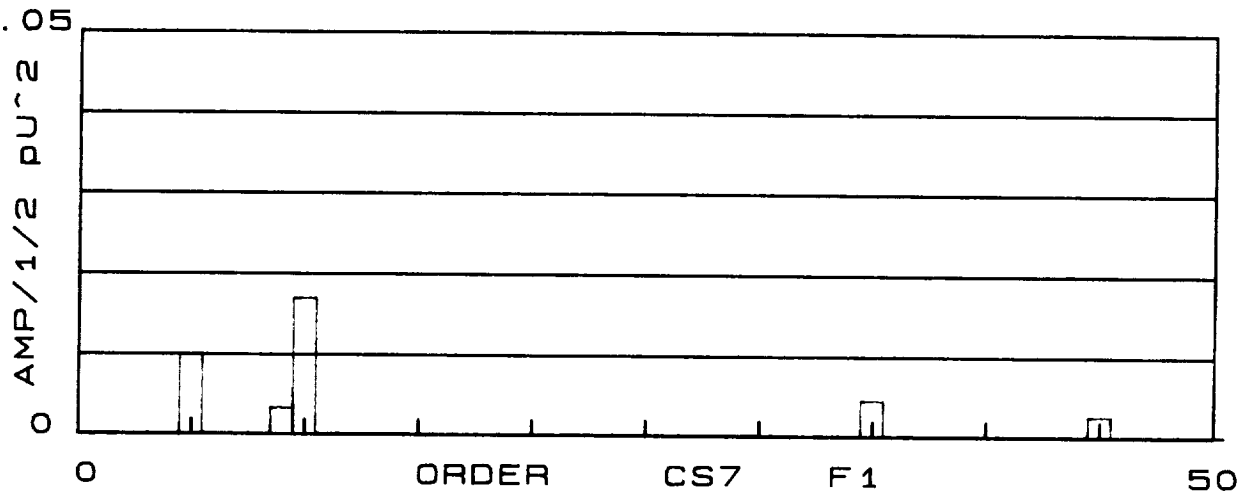
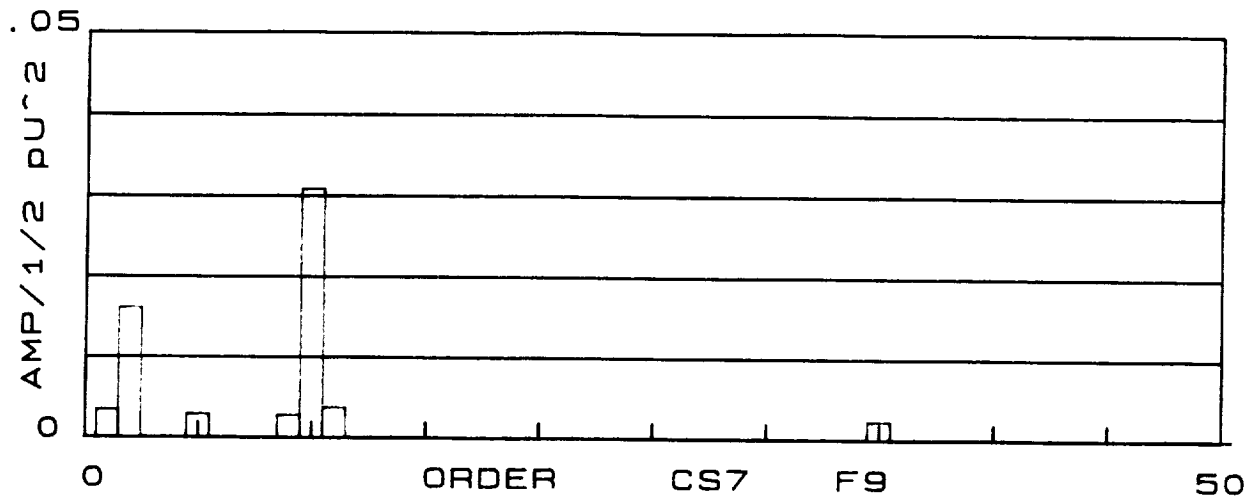










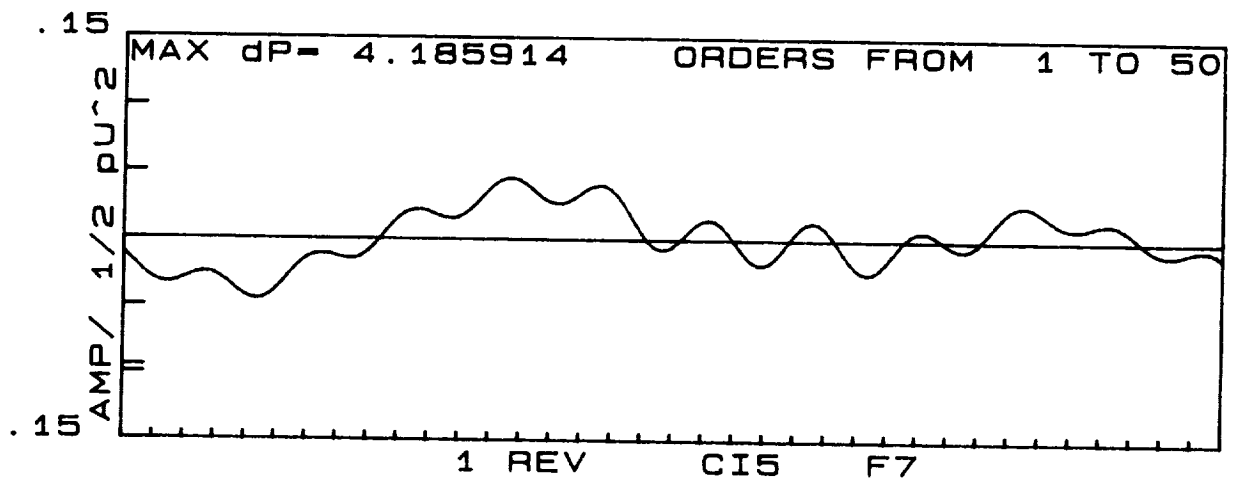
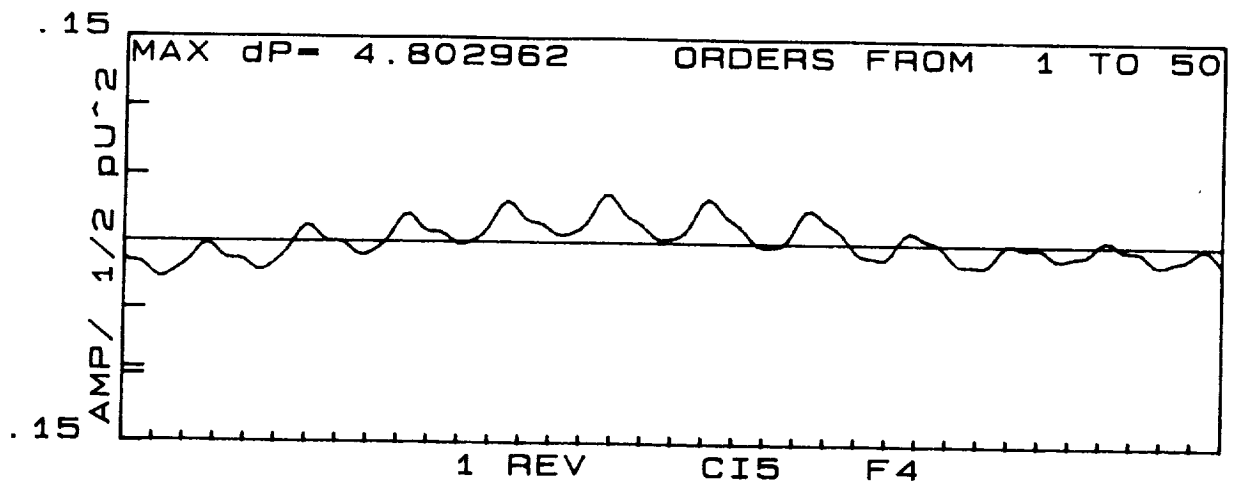


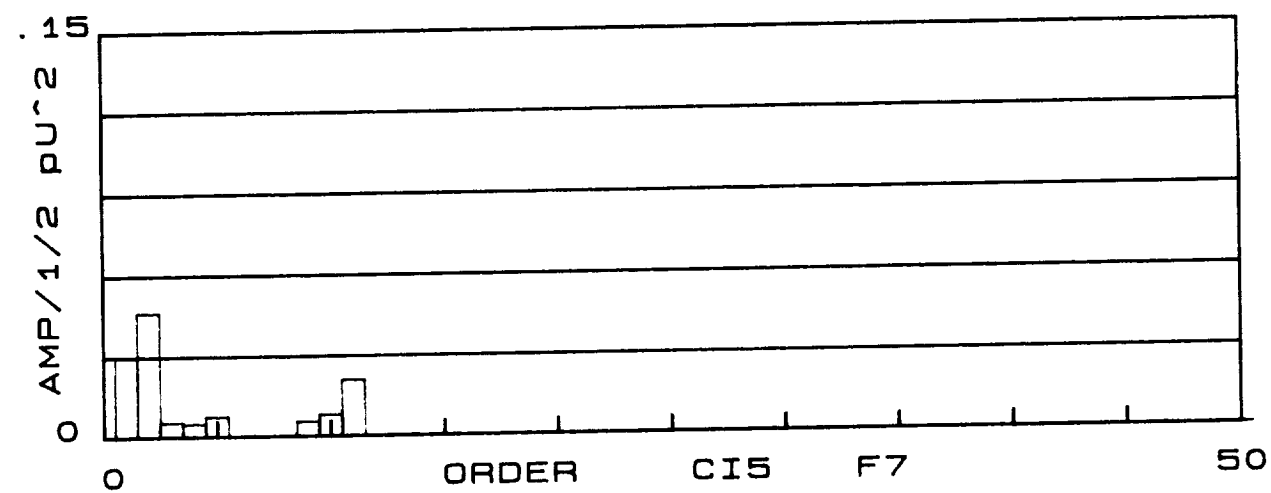
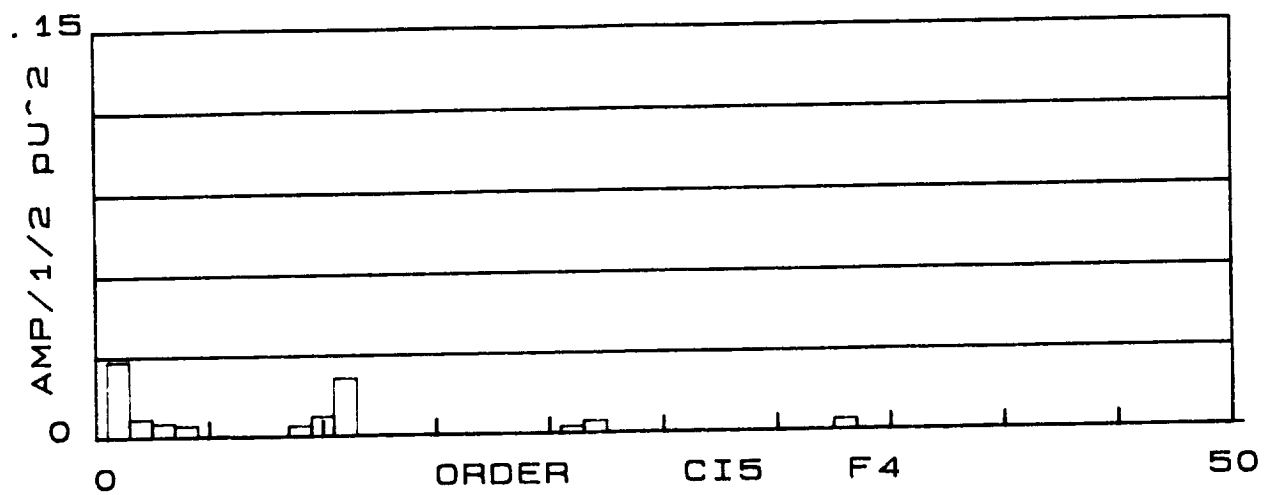
Scalability of Pulsation Activity, Impeller, Diffuser, Scroll Sensors

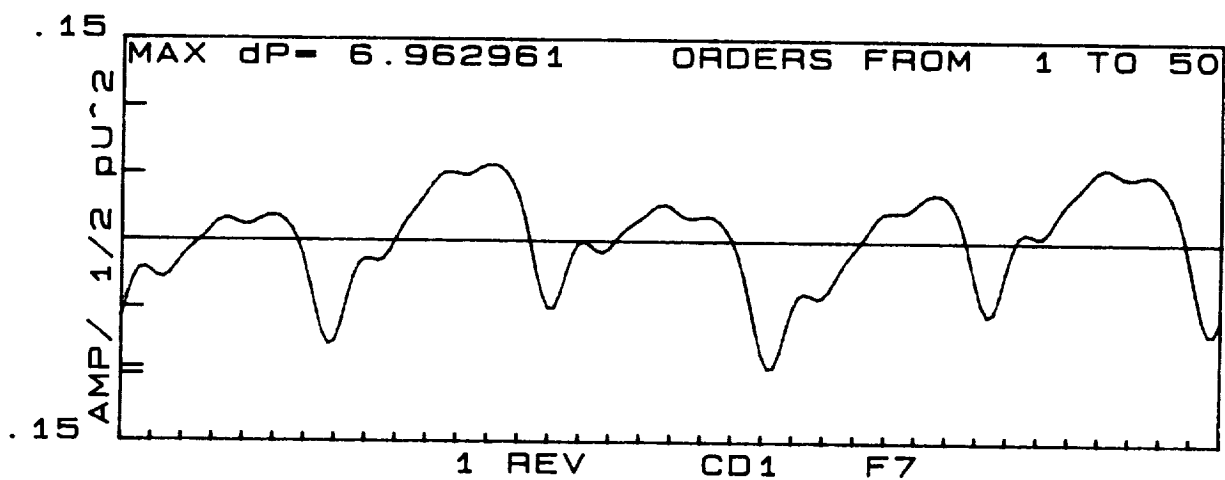
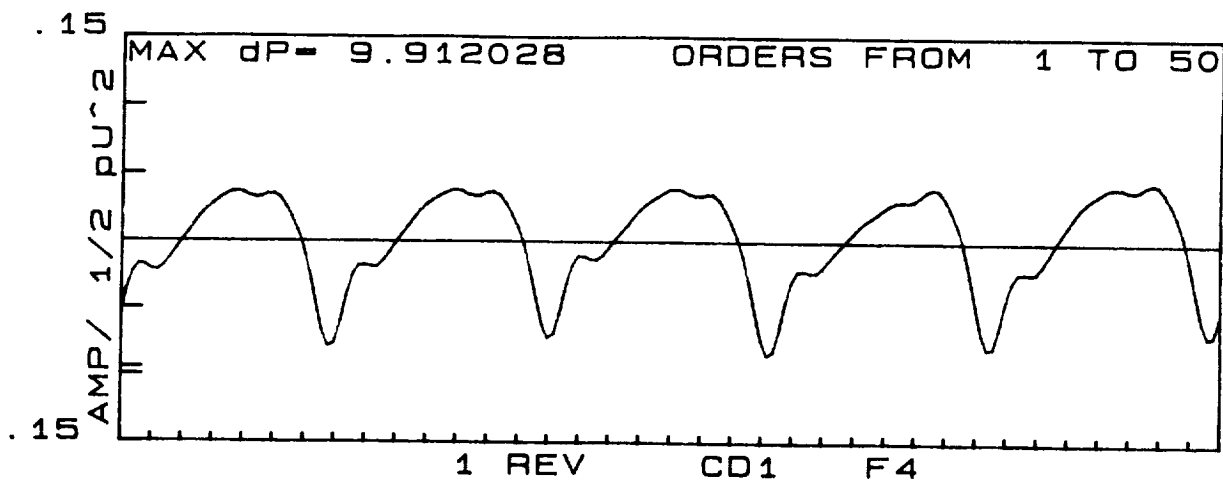
Locations: CI5, CD1, CS7, CS6

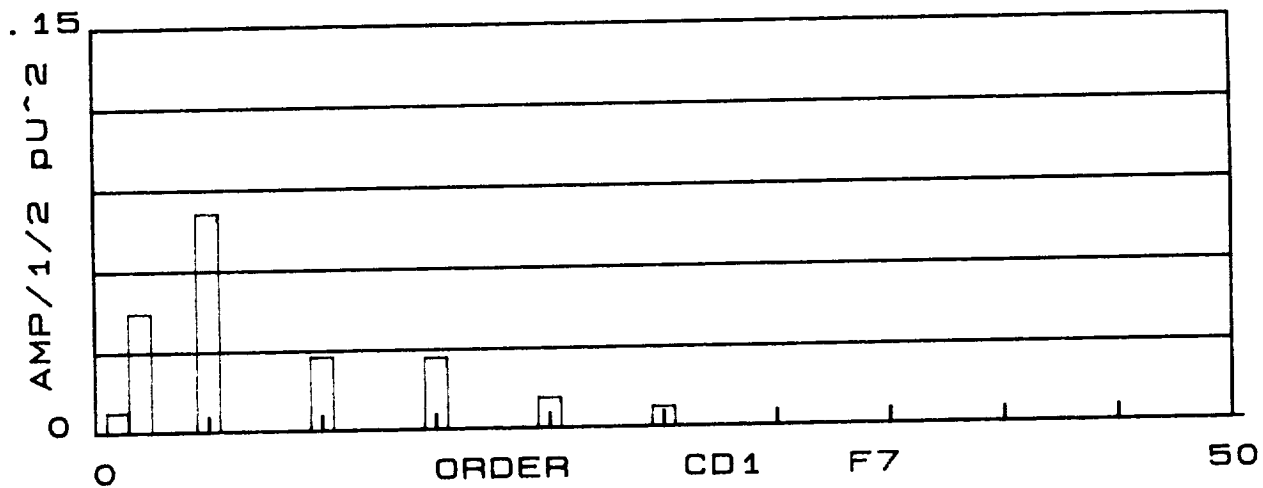
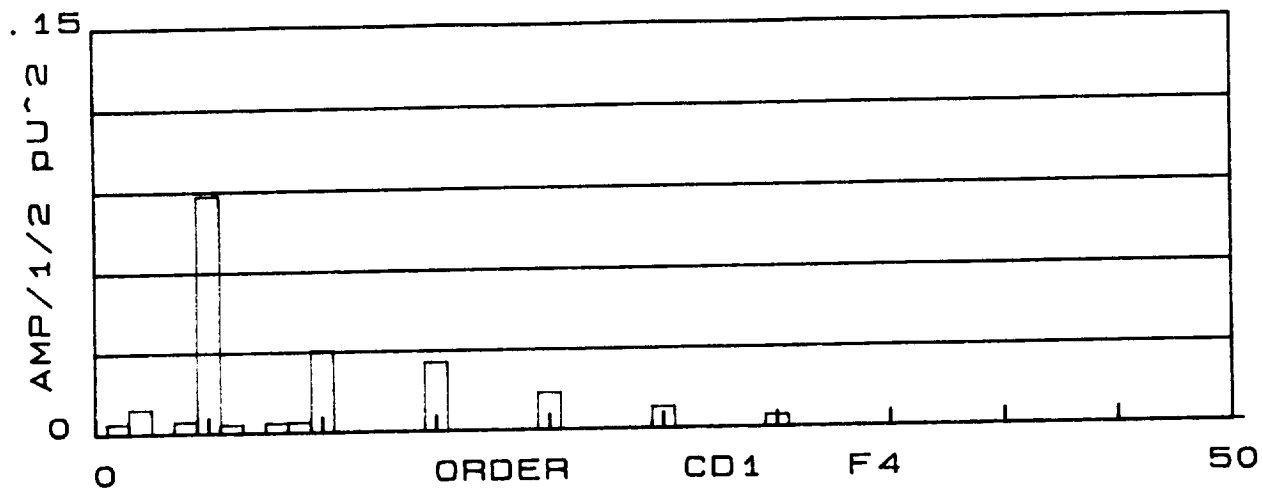
Conditions: F4, F7

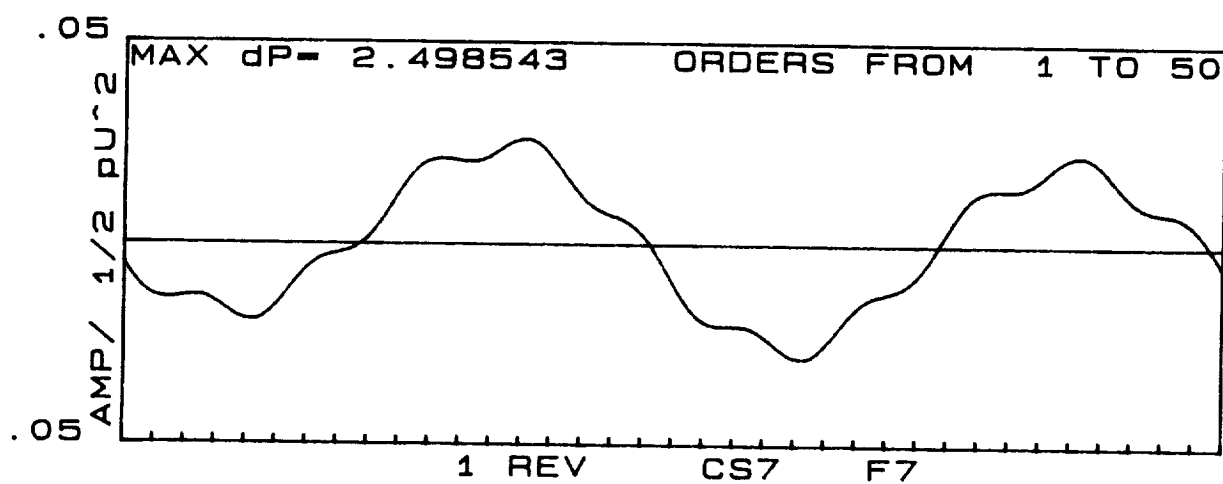
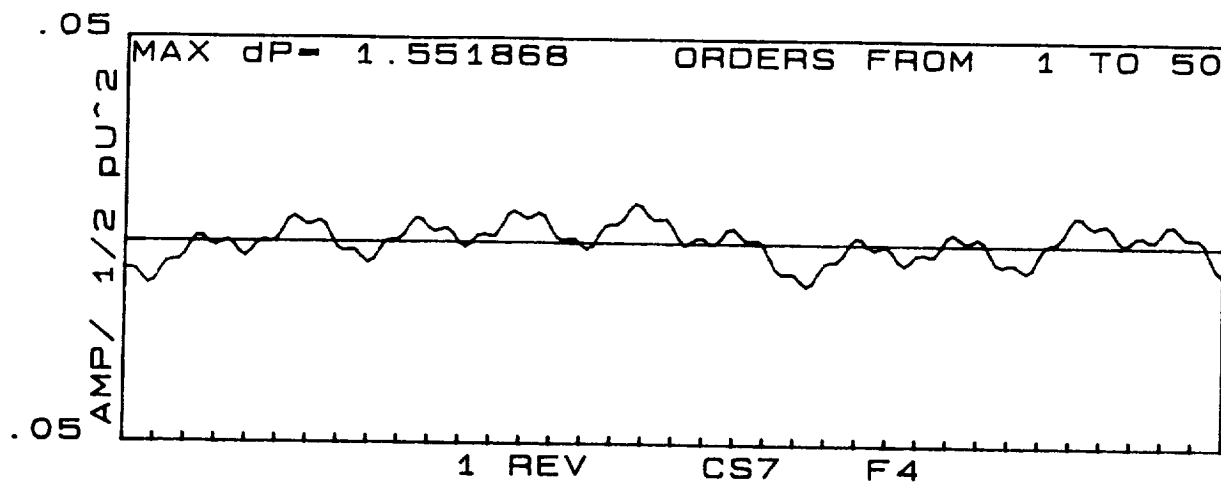
The scalability of pulsation amplitudes at the design flow of the test pump (100% flow, flow coefficient=.087) is shown in this series of plots. The plots of the orders of the pulsations can be used for direct comparison of scalability since they are plotted non-dimensionally (normalized to impeller exit tip speed). The impeller data indicates reasonable scalability, with an unexplained 2nd order amplitude present at the reduced speed (F7). The diffuser sensor produces good scalability at all orders, with a second order amplitude again present at reduced speed. The scroll sensors (CS6, CS7) produce good scalability of the dominant 10th order. The second order amplitude evident on all the low speed conditions may be a result of a shaft (rotordynamic) instability causing variations in impeller/diffuser clearance. This second order amplitude appears on all configurations (A, B, C) at the low speed conditions (F6, F7, F8)

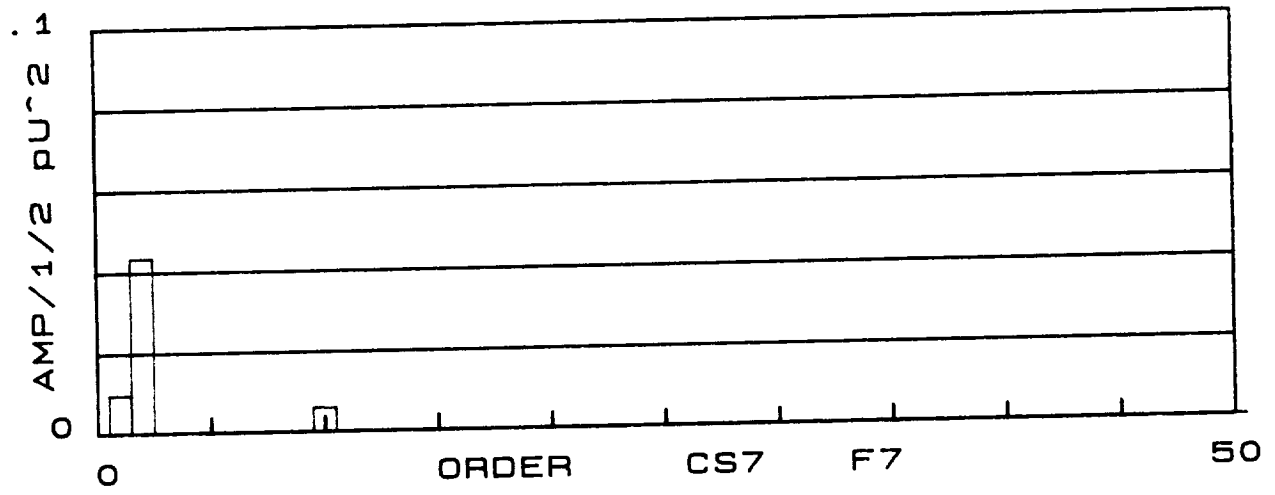
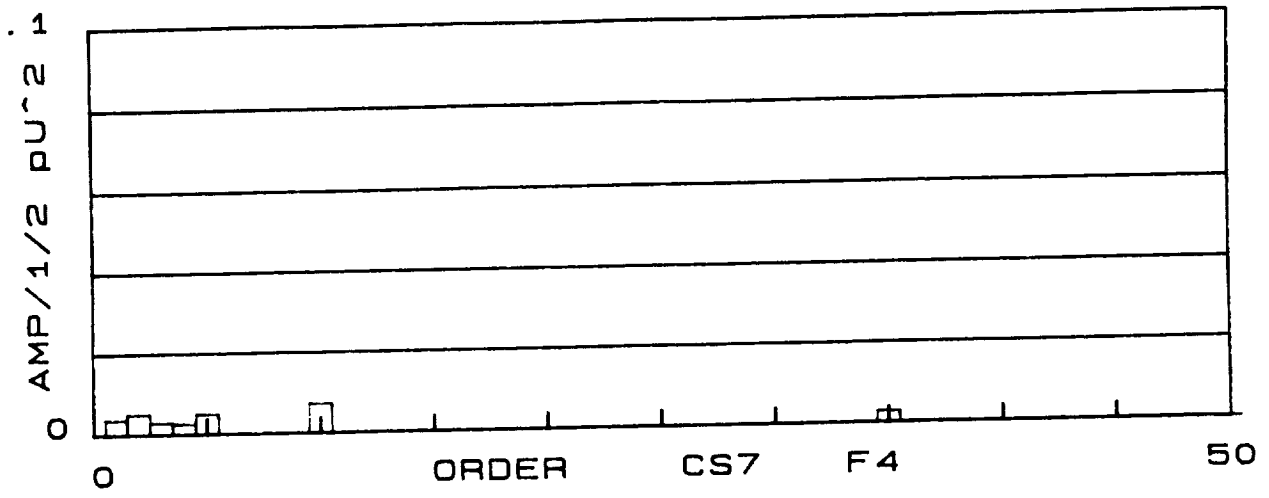


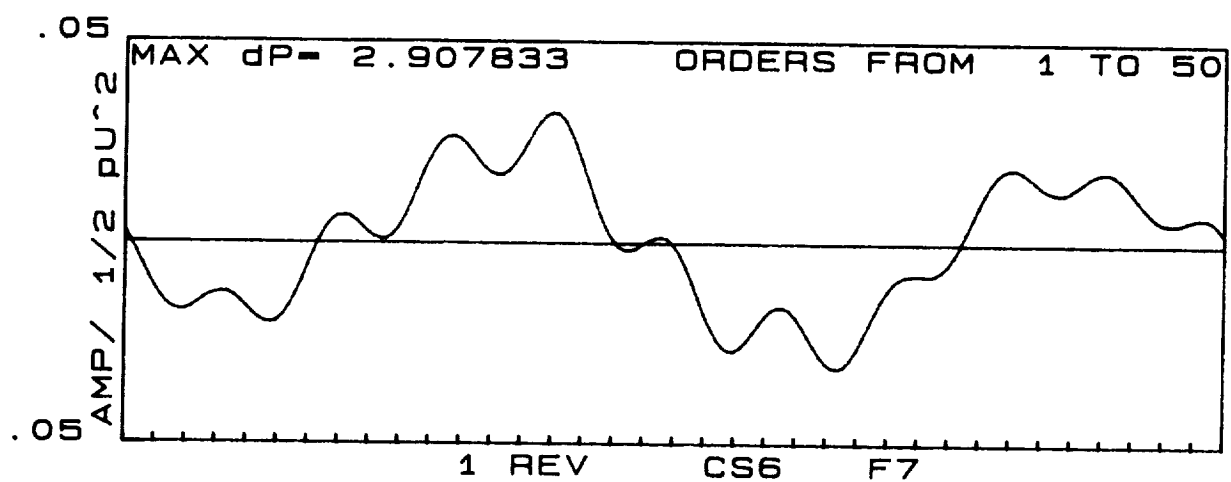
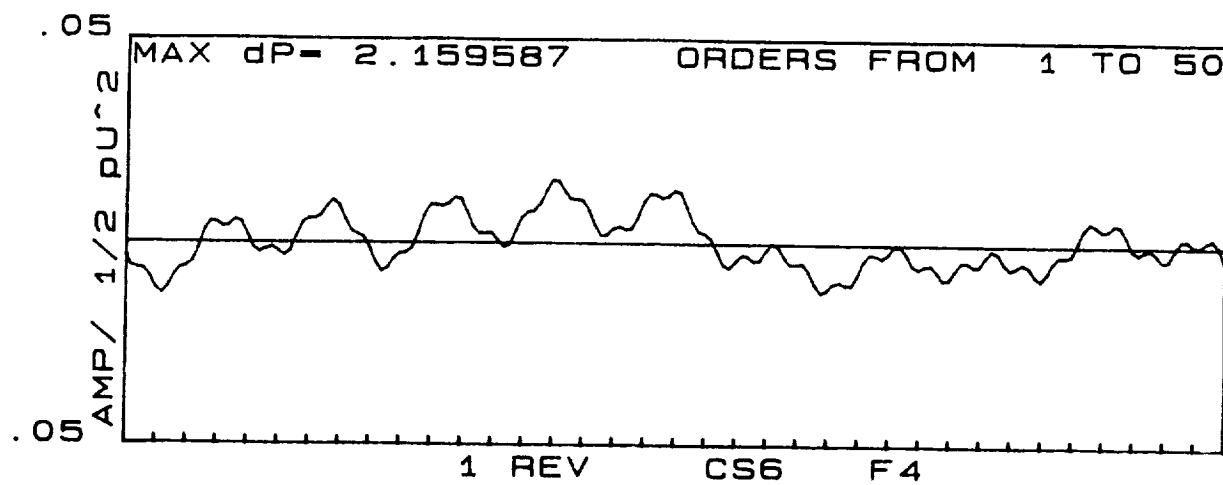


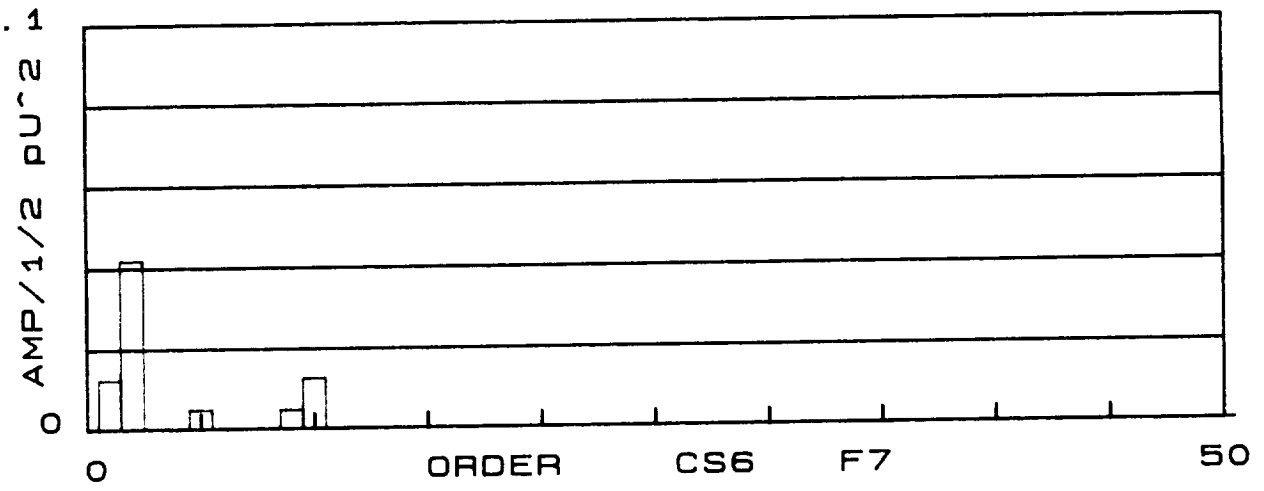
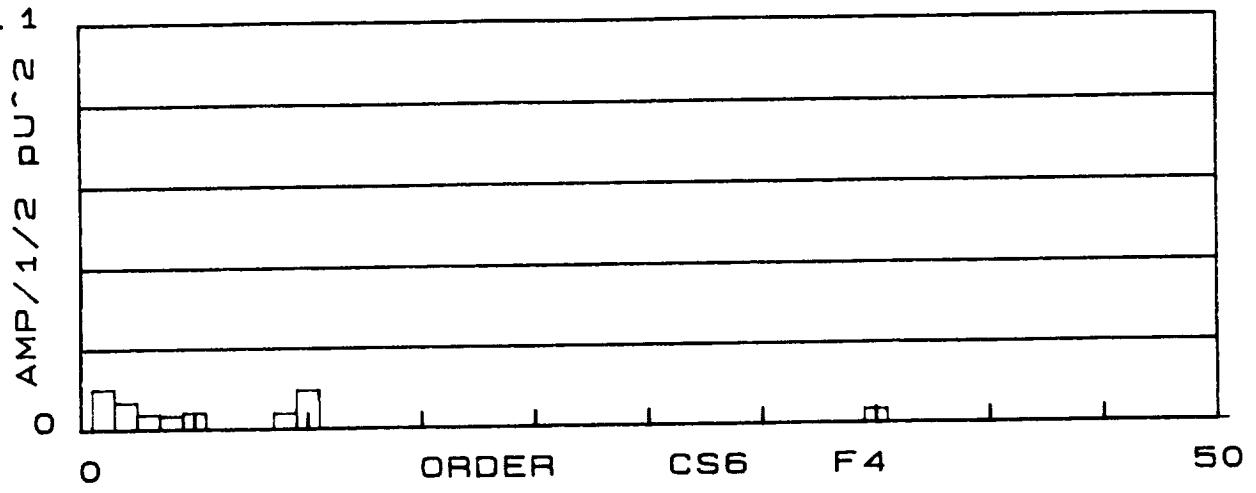










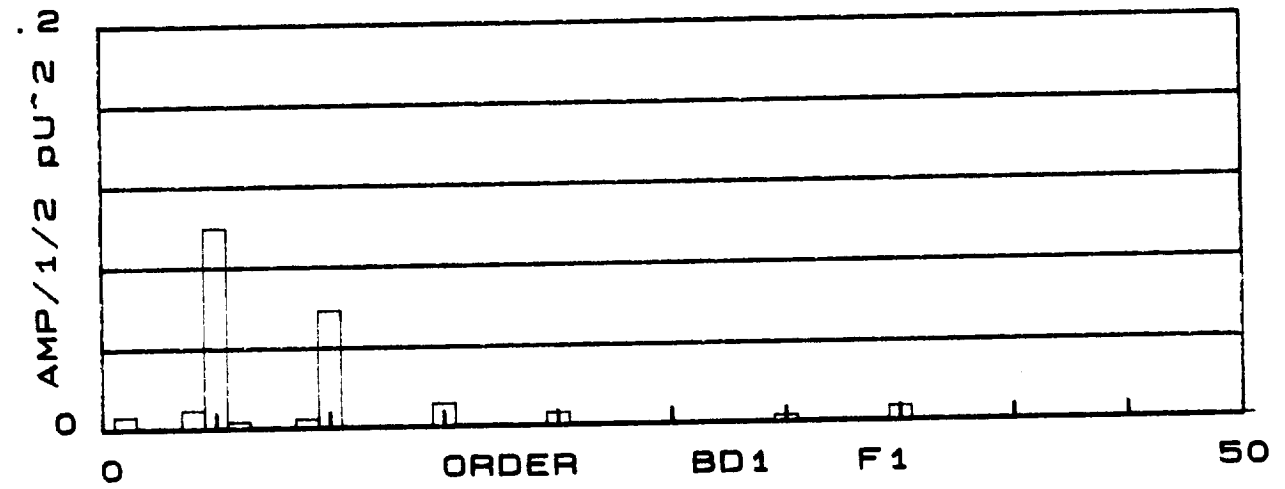
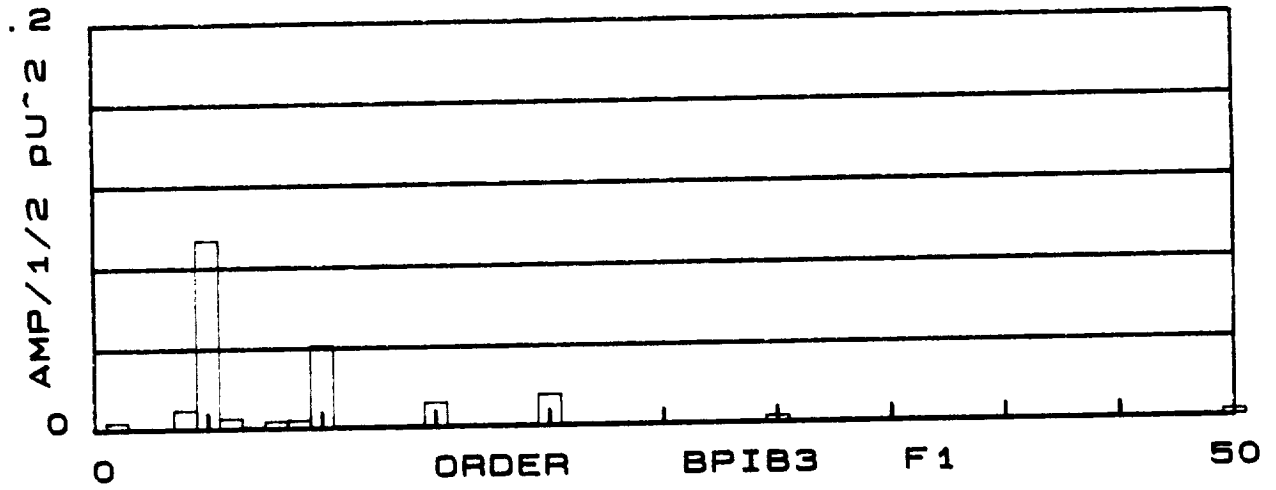
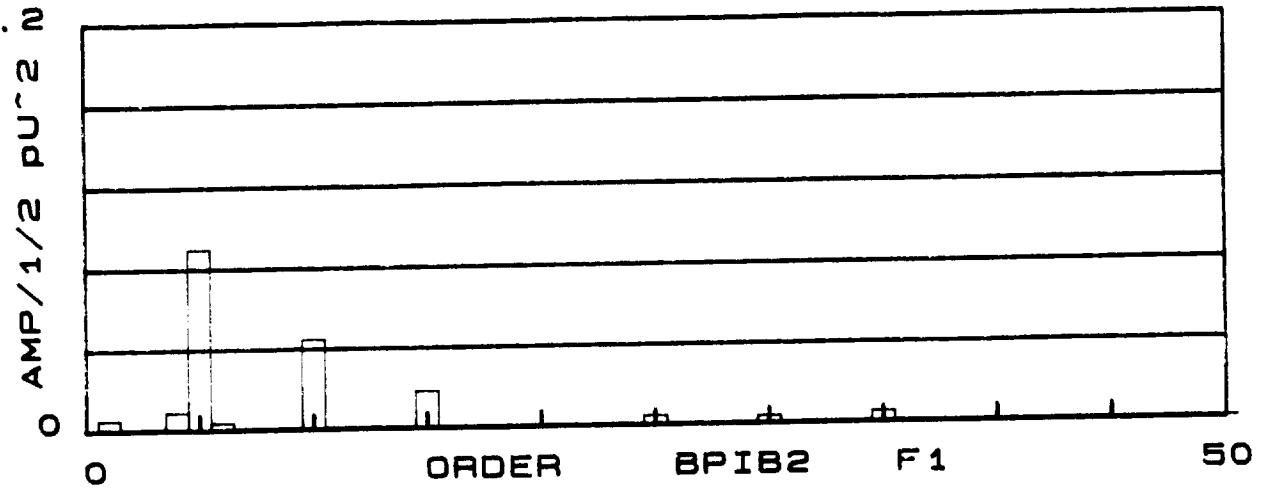


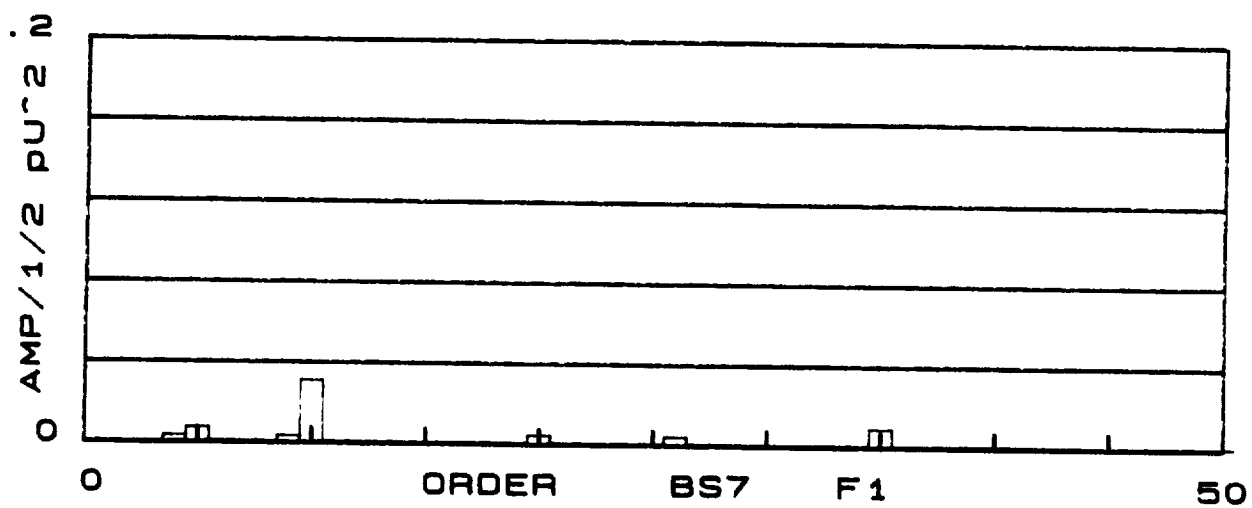
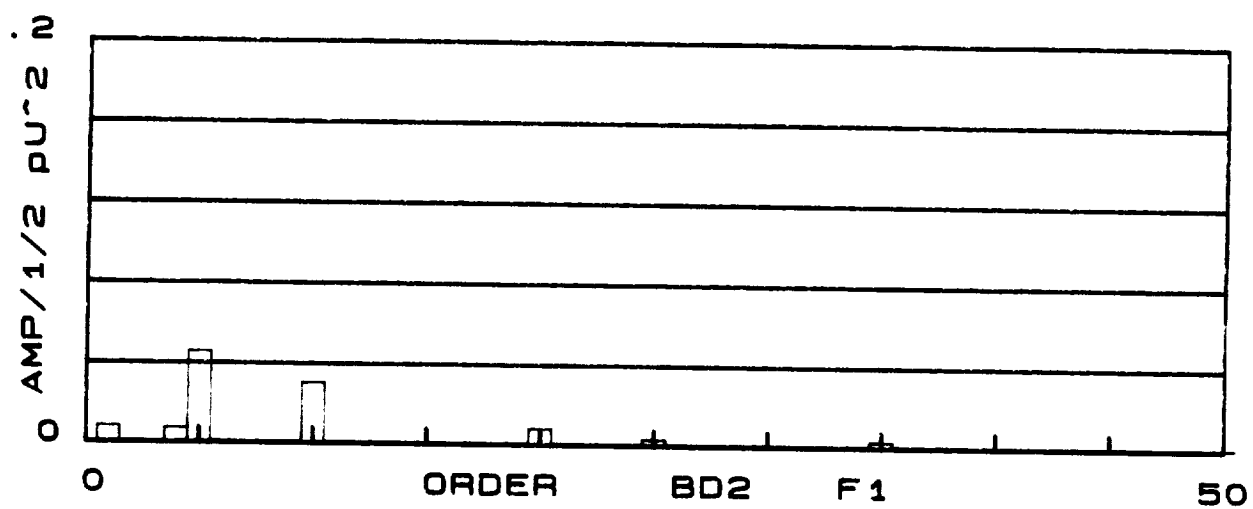
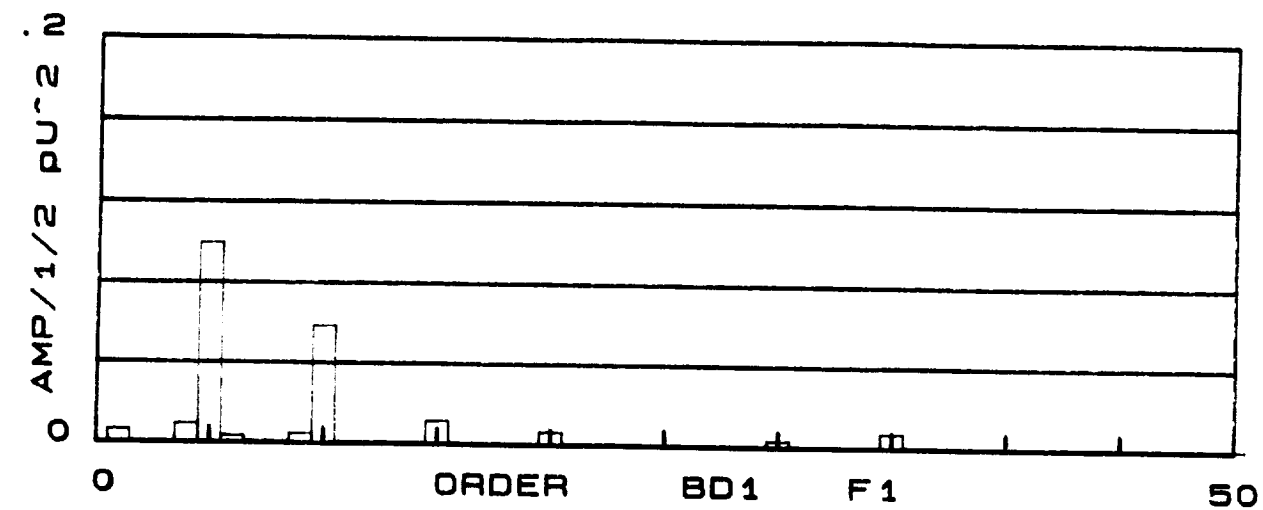
Pulsation Activity vs Flow Condition

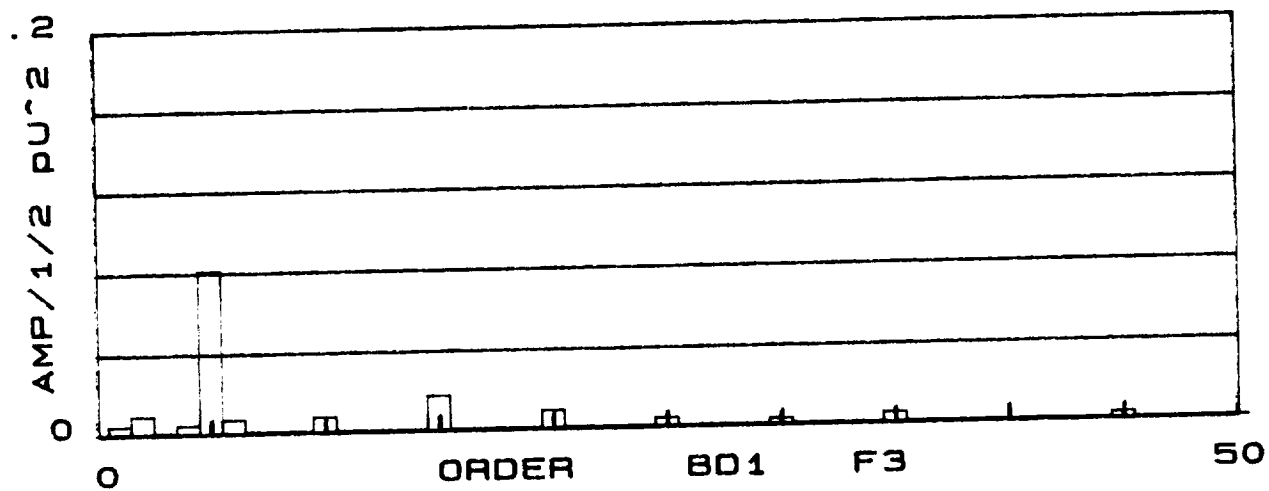
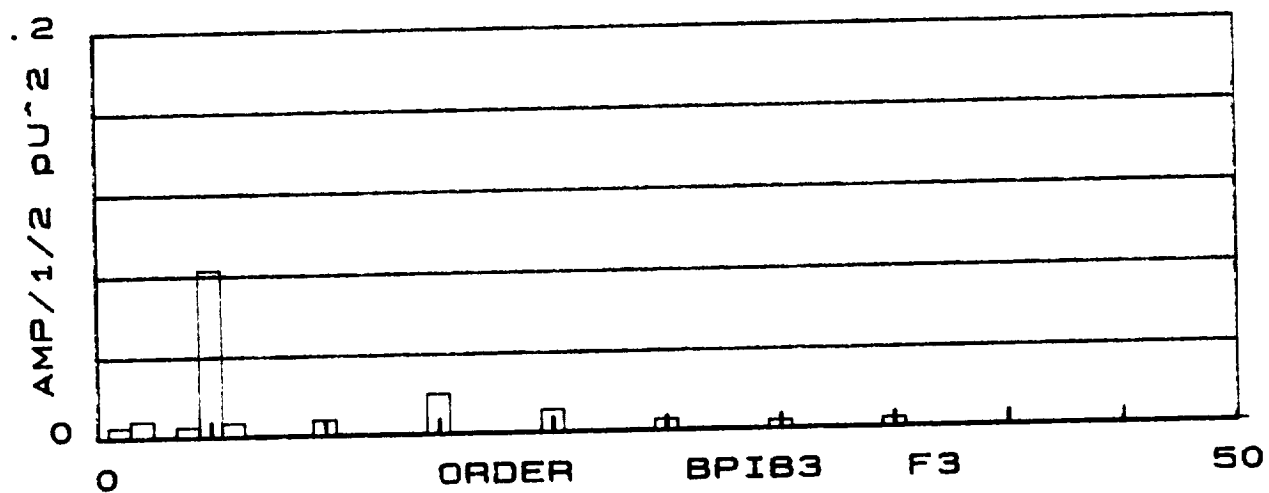
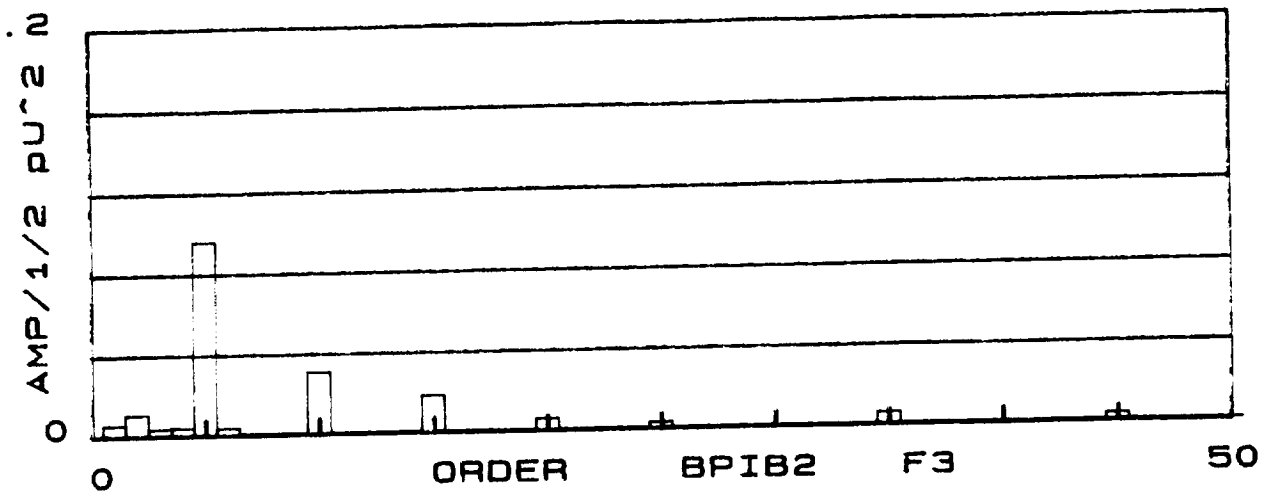
Locations: BPIB2, BPIB3, BD1, BD2, BS7

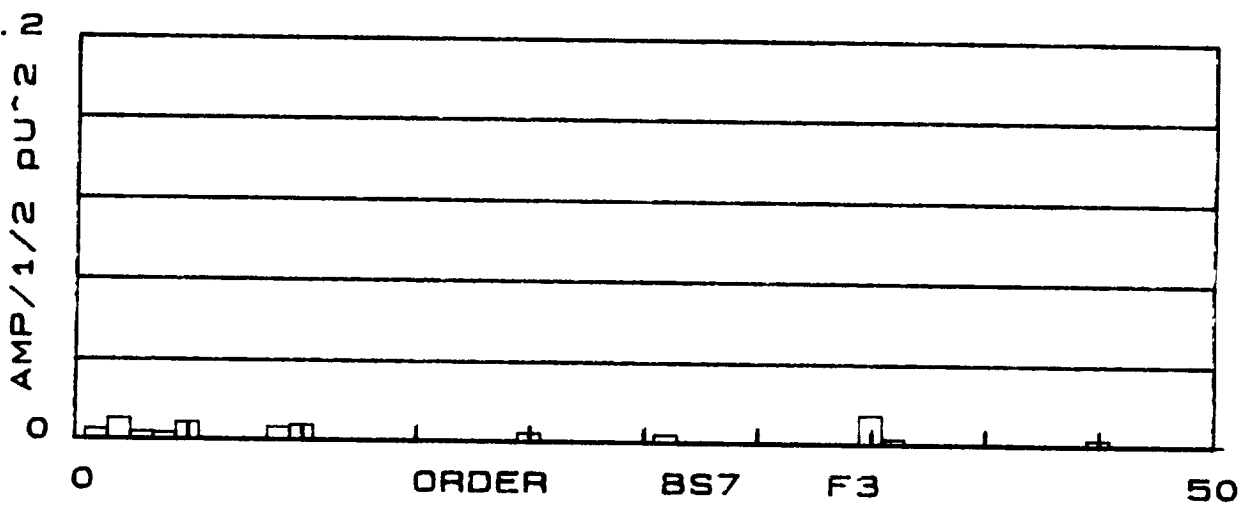
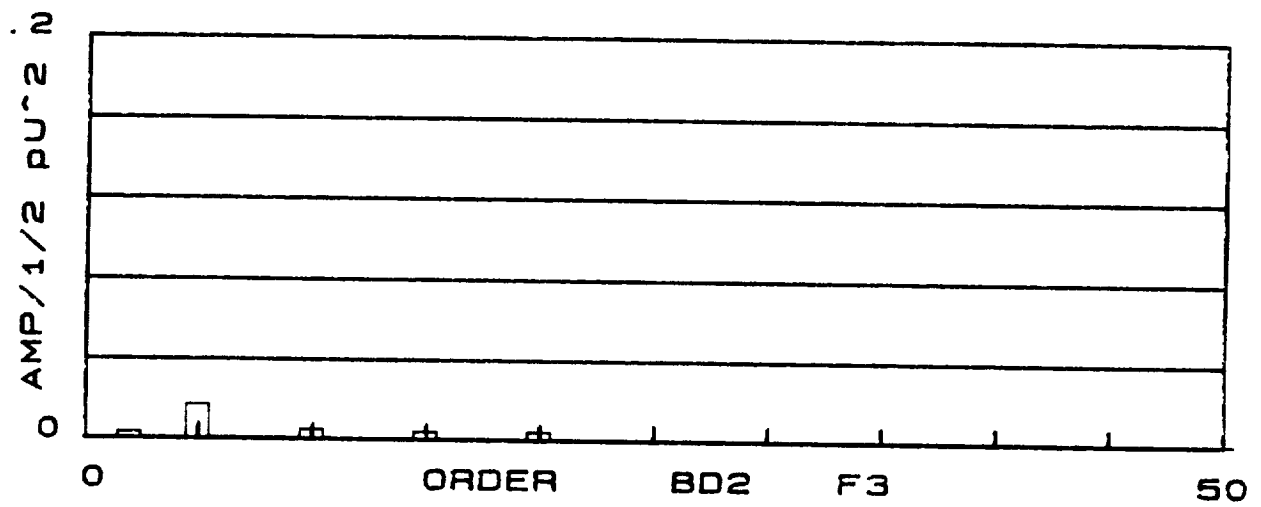
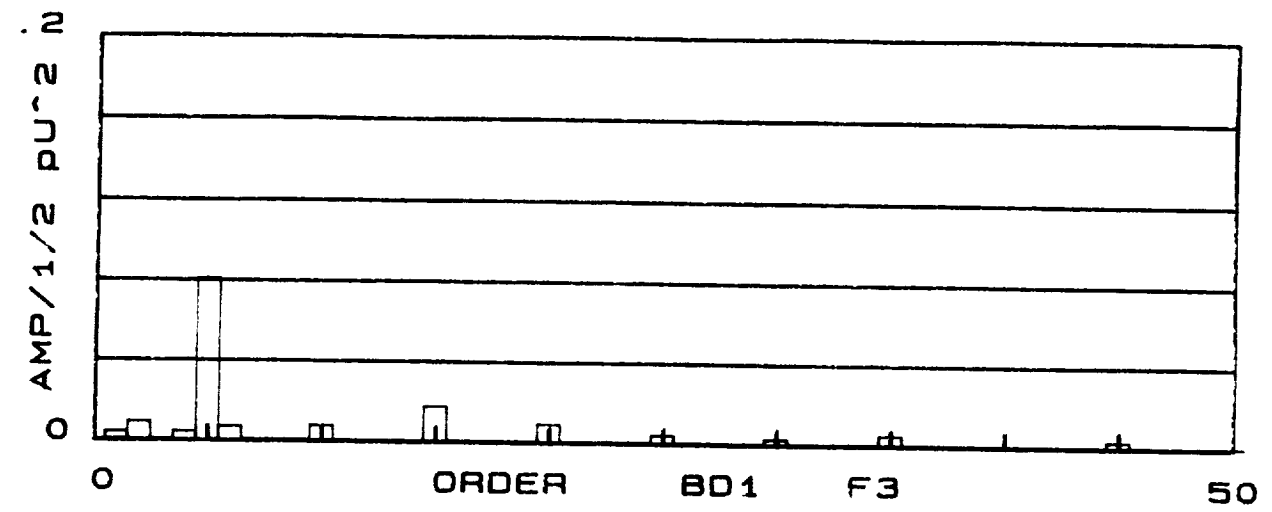
Conditions: F1, F3, F4, F5

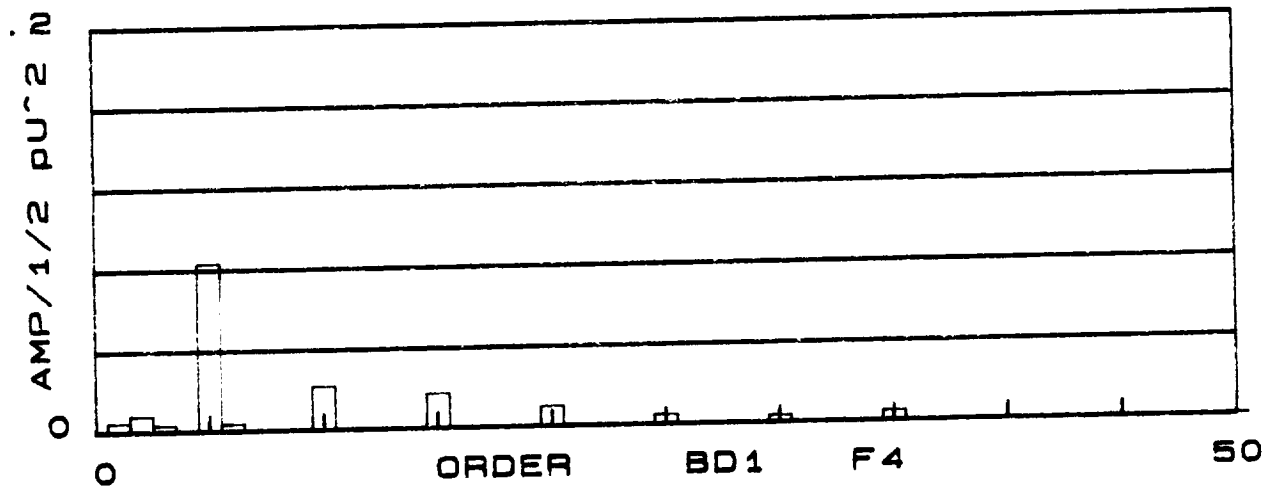
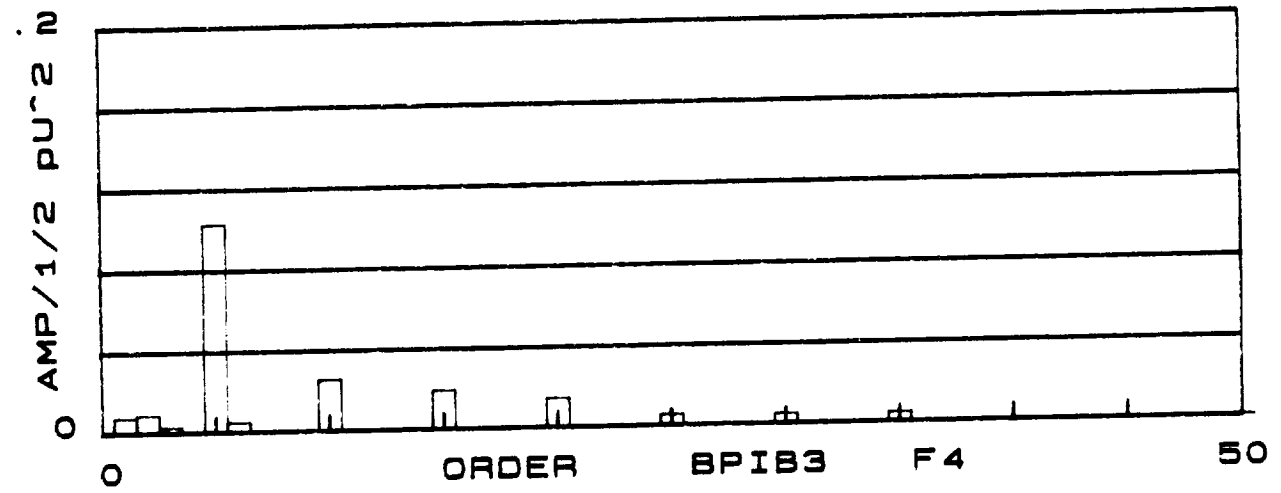
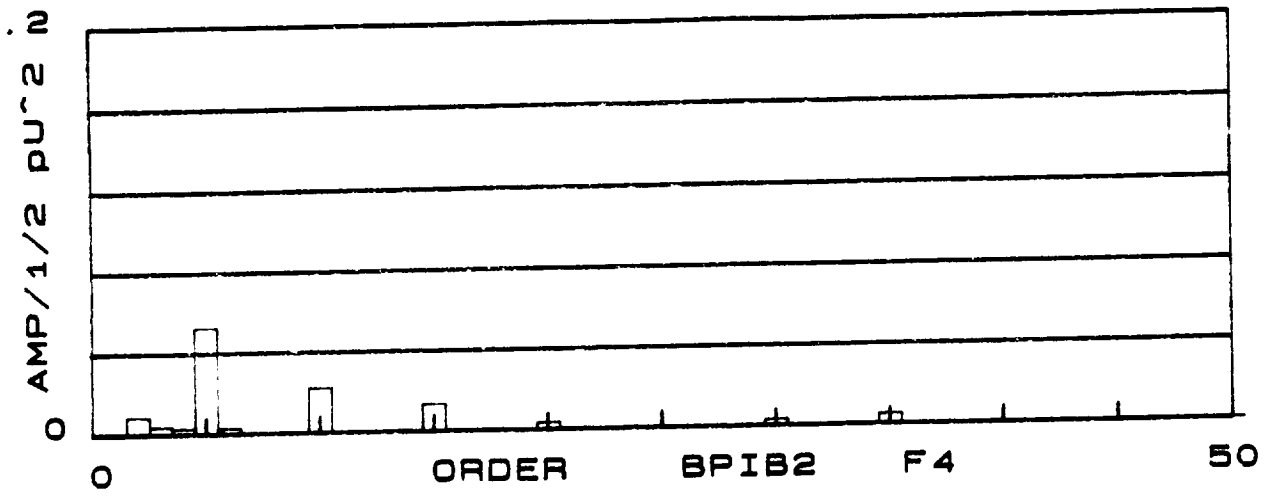
The attenuation of the synchronous components of pressure pulsations in the stationary elements of 'B' configuration for 4 flow conditions is shown in these plots. BPIB2, BPIB3, and BD1 are locations in the diffuser inlet area, BD2 is in the diffuser exit and BS7 is located in the scroll outer wall. The dominant order is the 5th, which corresponds with impeller blade passage frequency. The minimum of 5th order activity appears to occur at the F3 and F4 conditions (for the 3 sensors located near the impeller; BPIB2, BPIB3, and BD1). This is to be expected since the design point for this diffuser is F4 (100% Q). Synchronous pulsation levels in the scroll (BS7) are very low, with the largest amplitude occurring at the minimum flow condition, F1 and at the 10th order of rotation frequency.

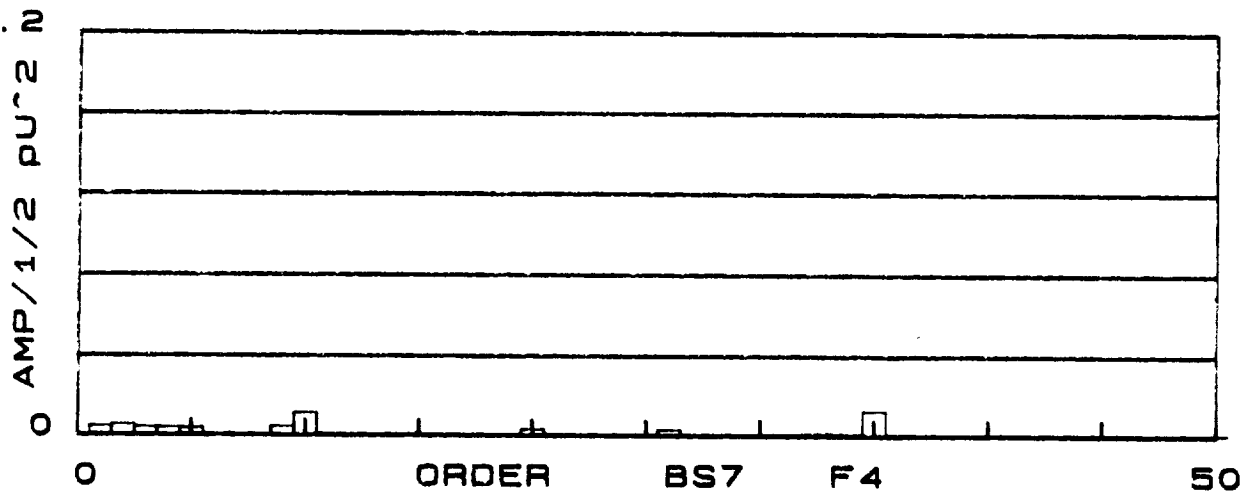
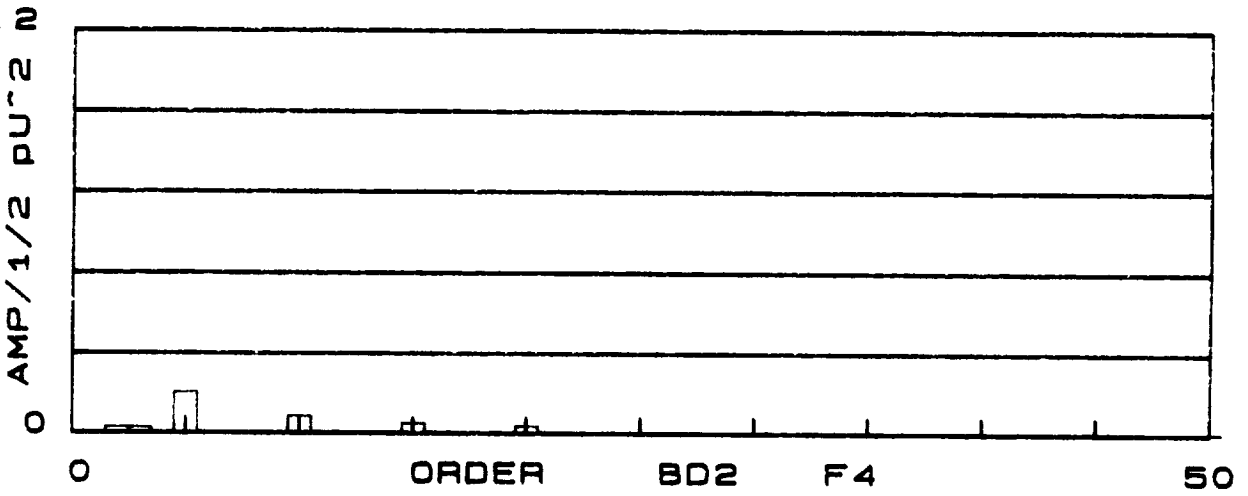
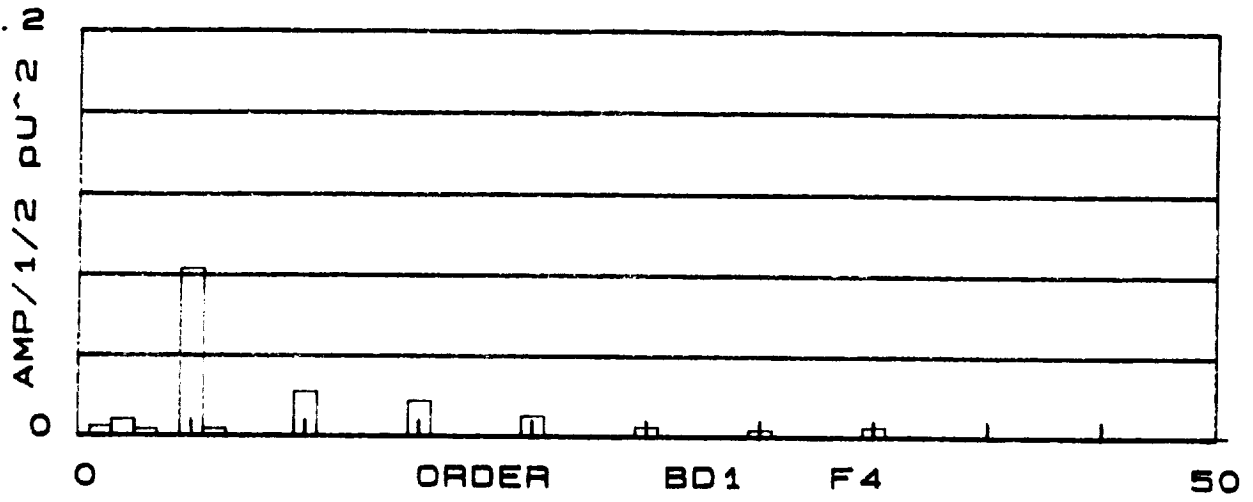


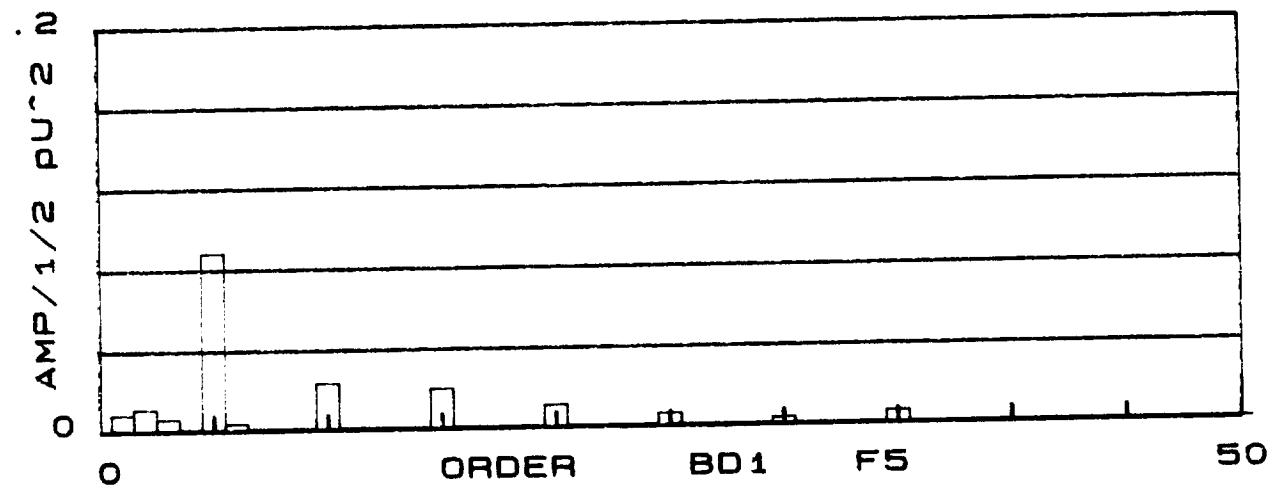
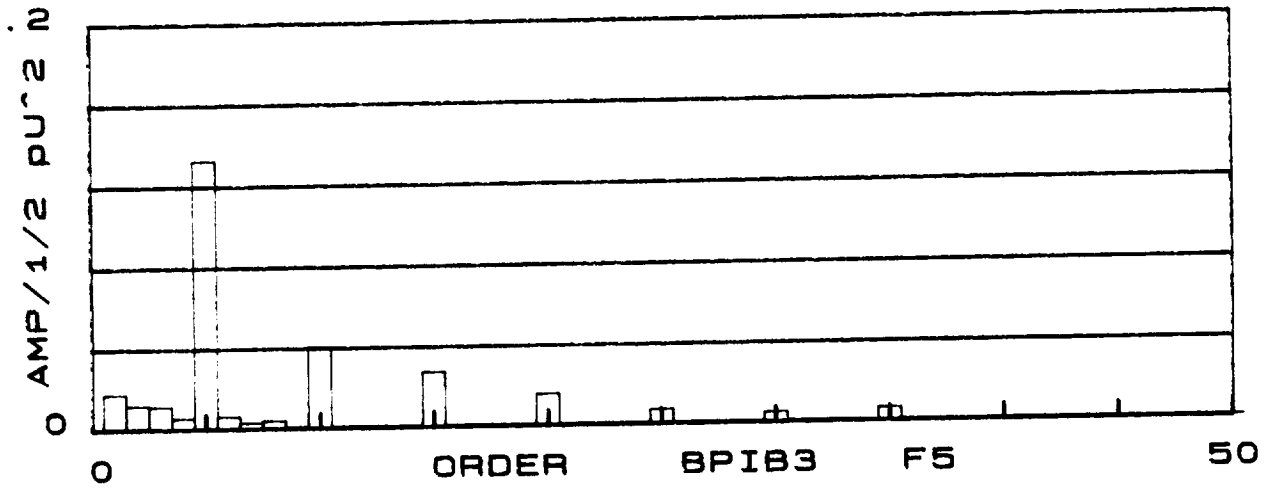
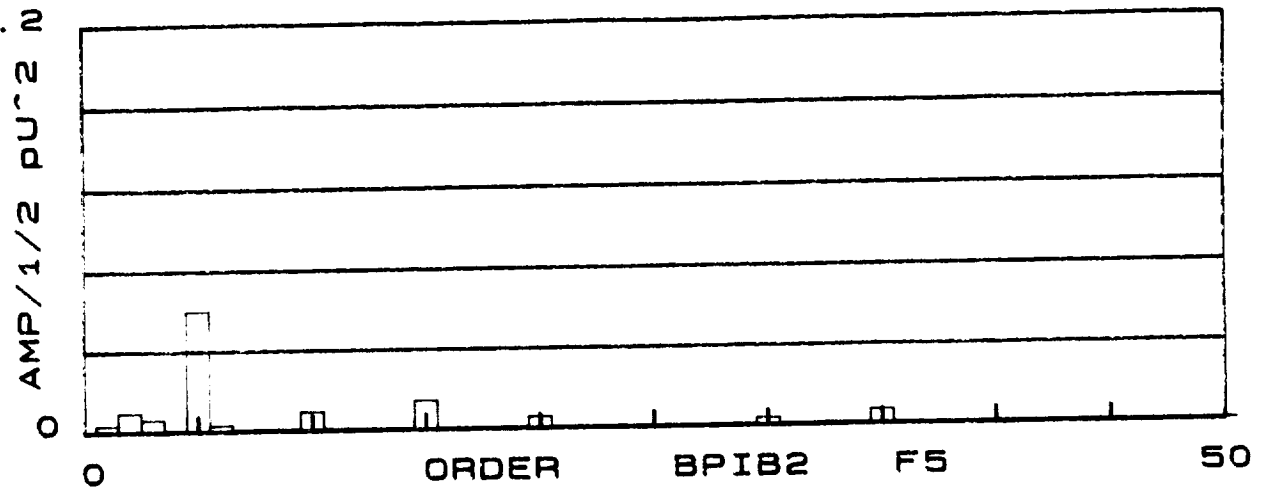


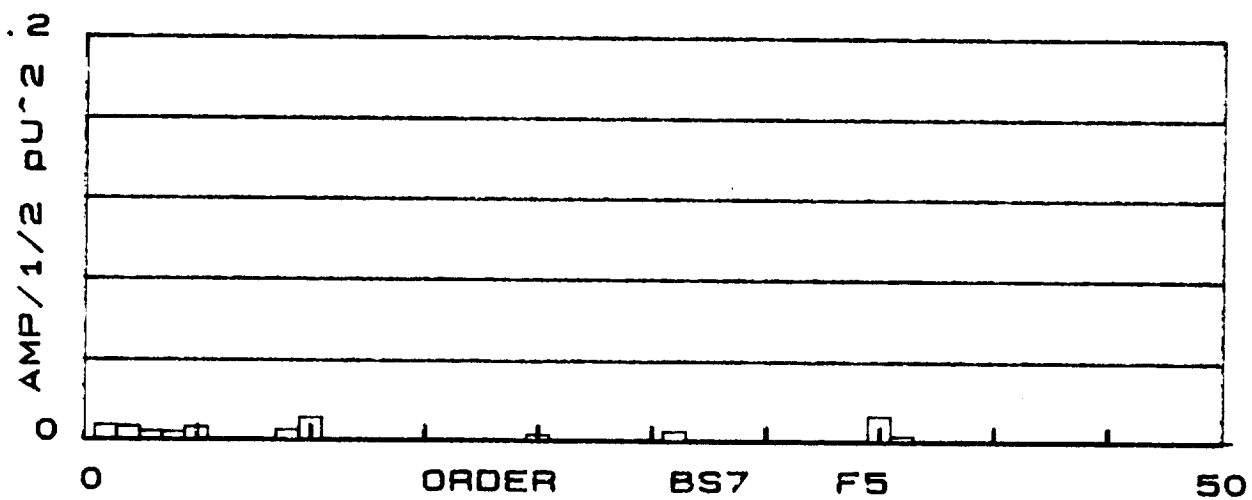
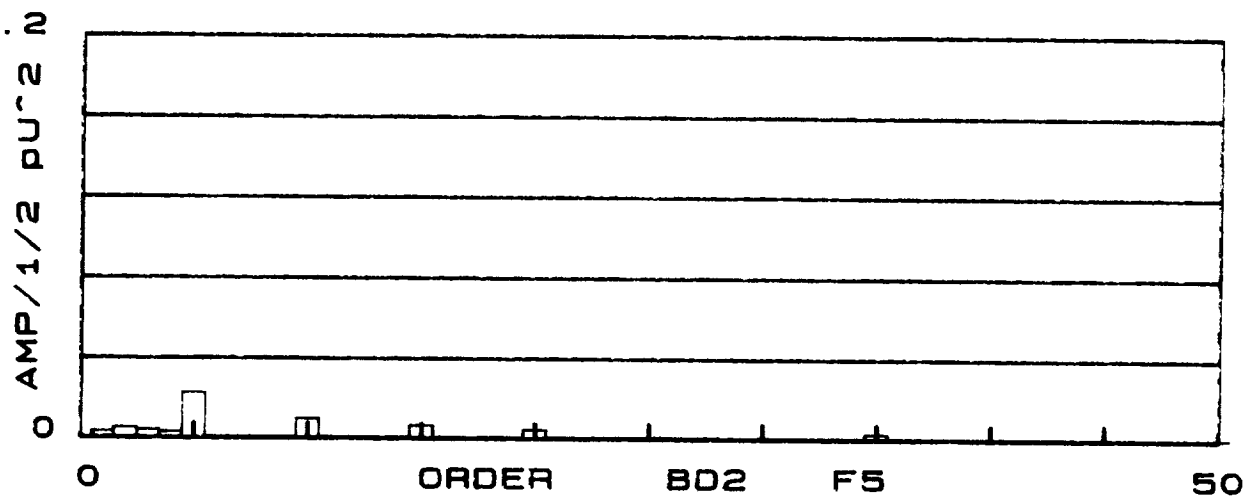
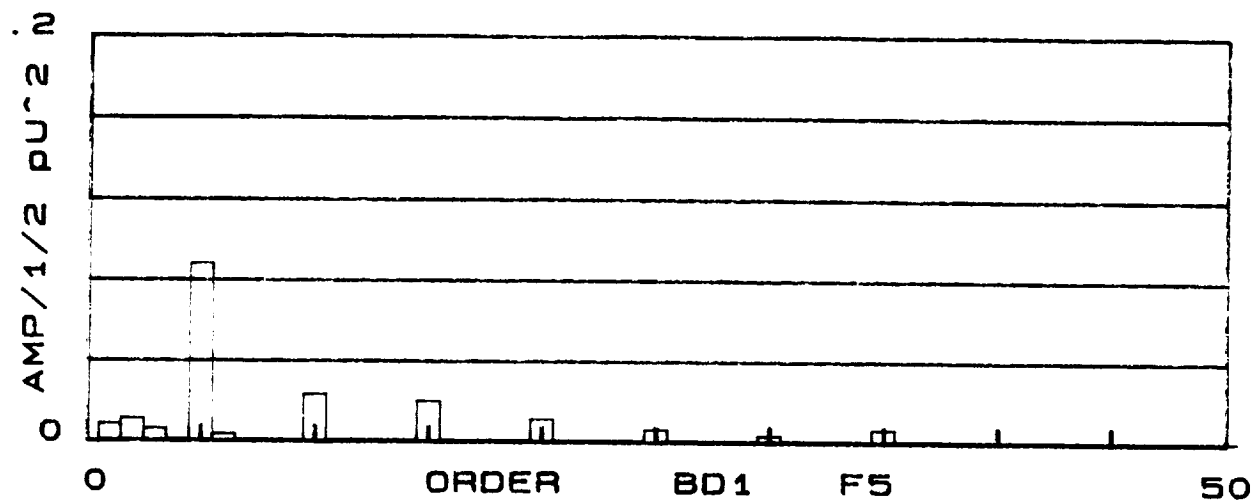










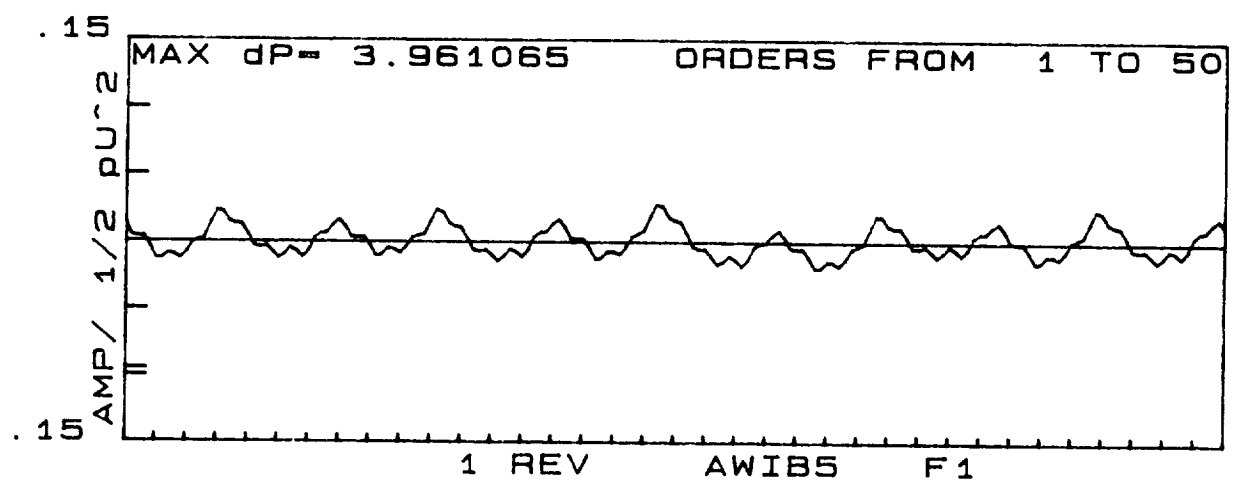
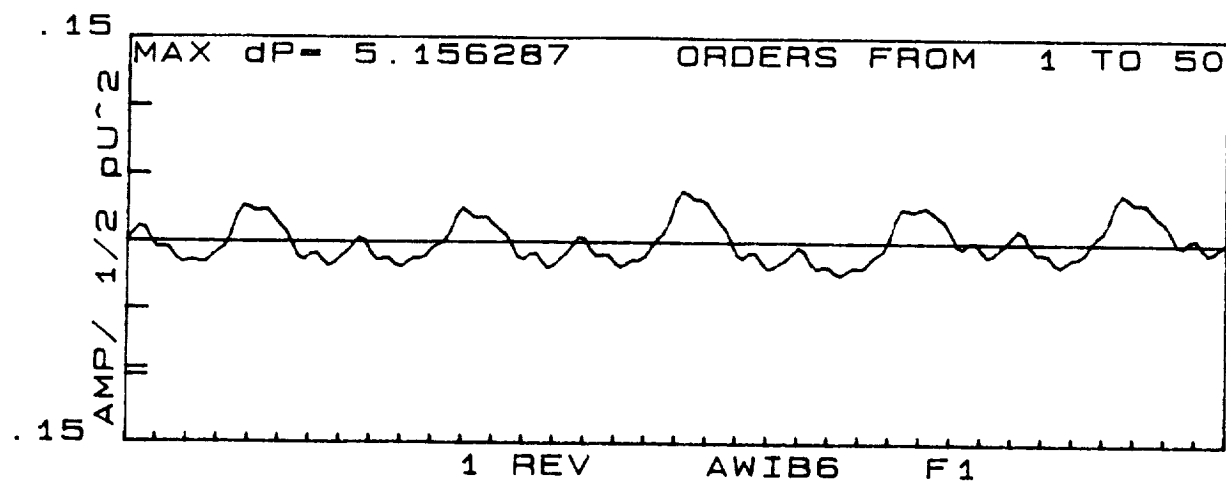


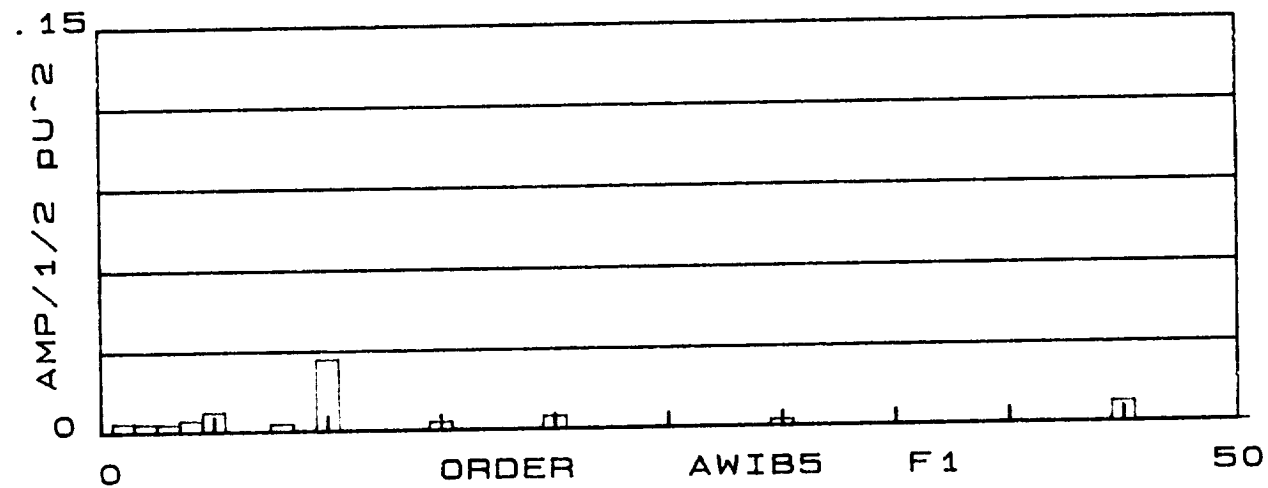
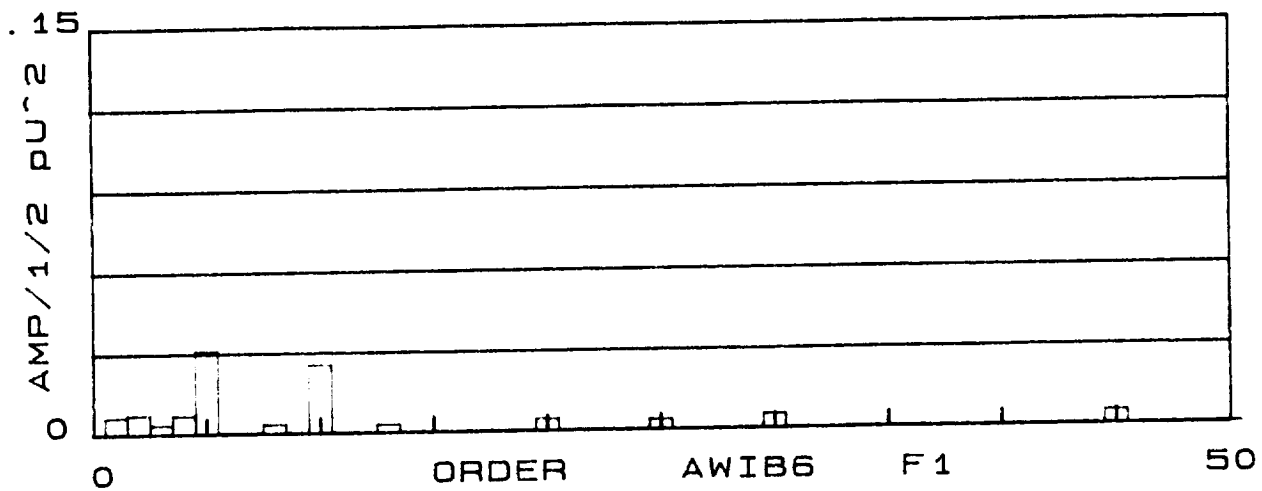
Stationary Sidewall Sensors

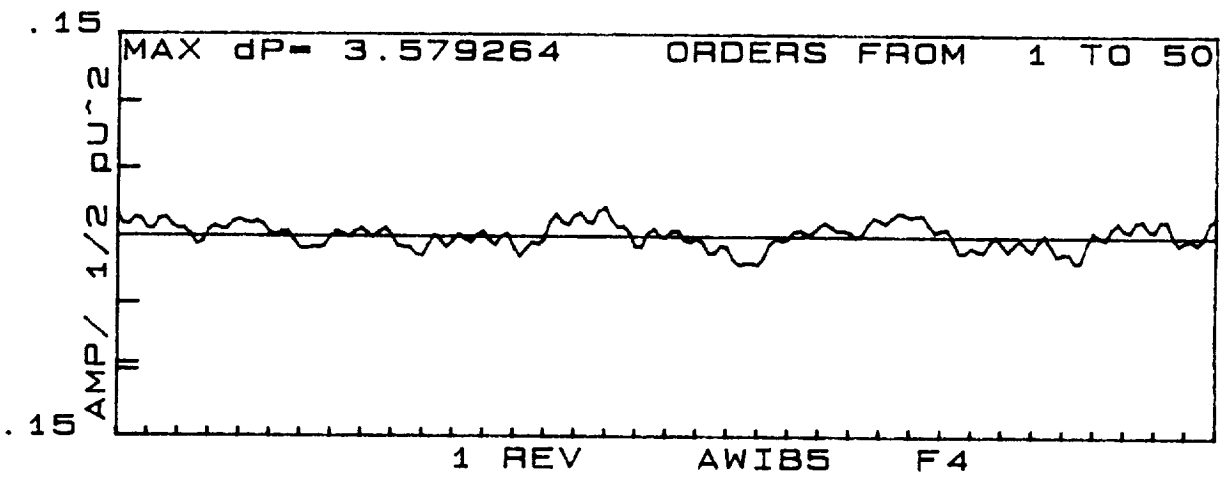
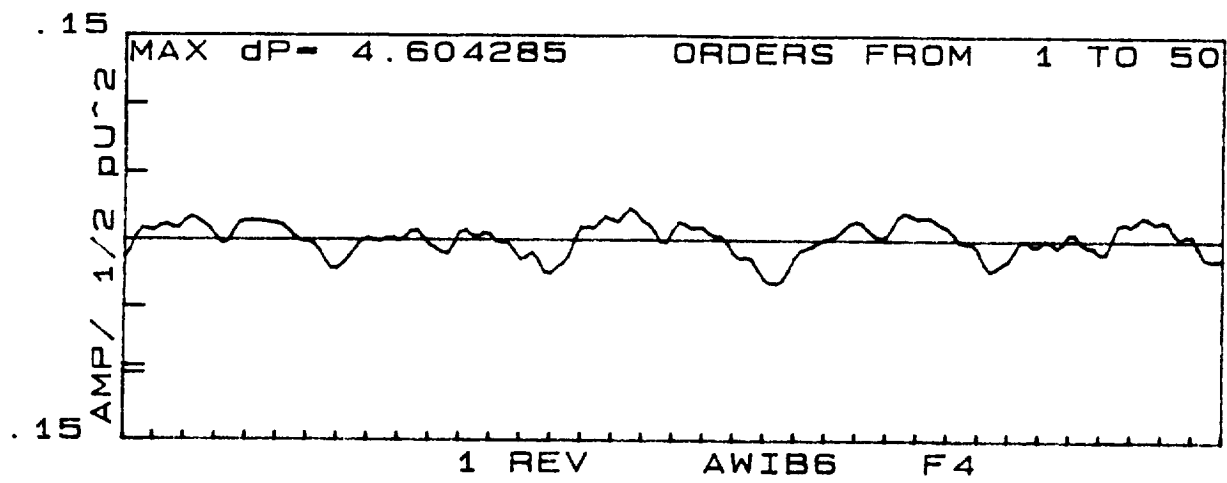
Locations: AWIB6, AWIB5

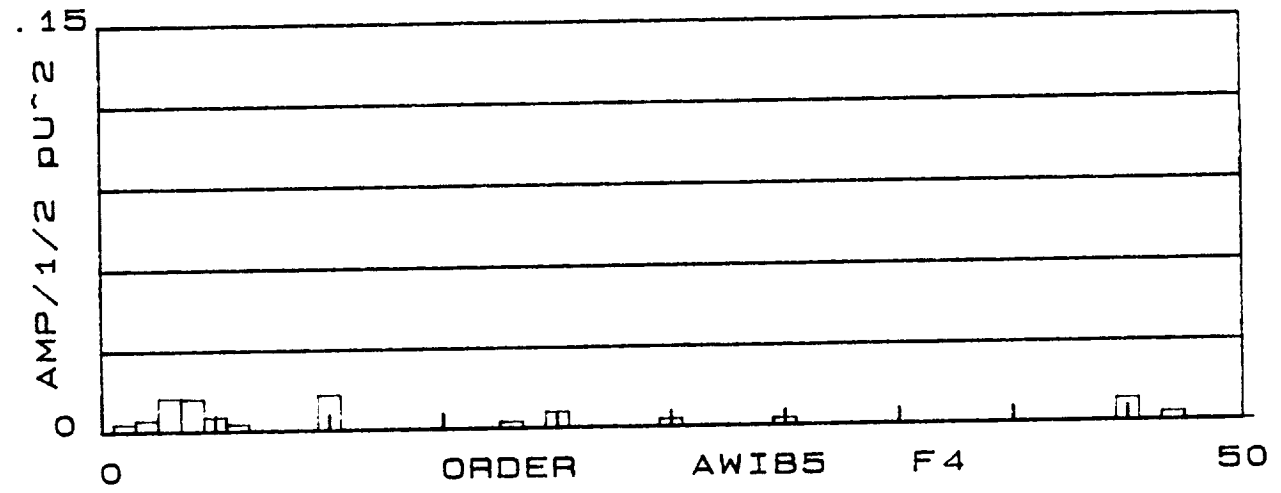
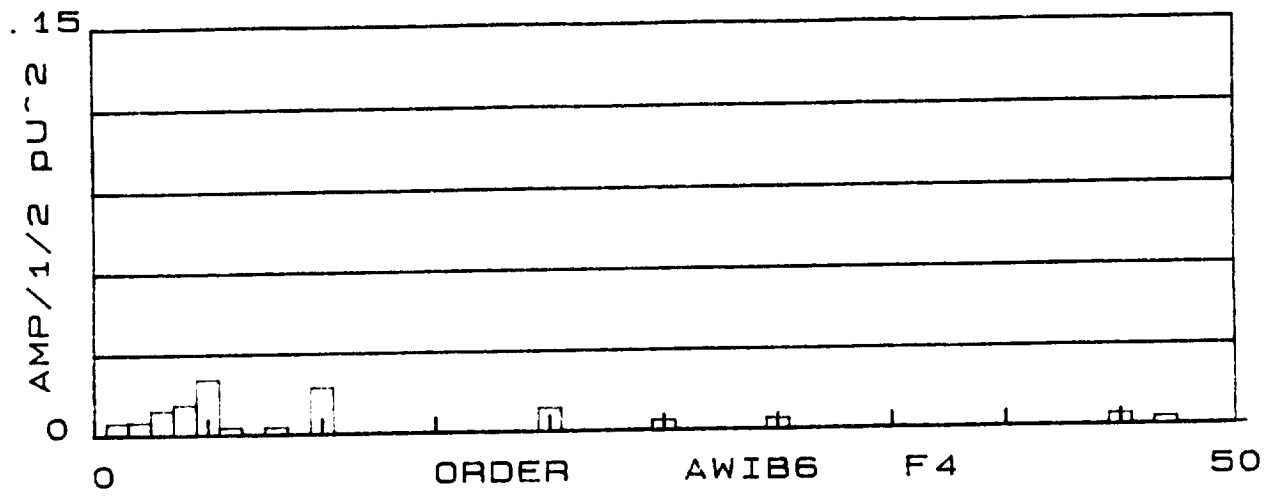
Conditions: F1, F4, F5

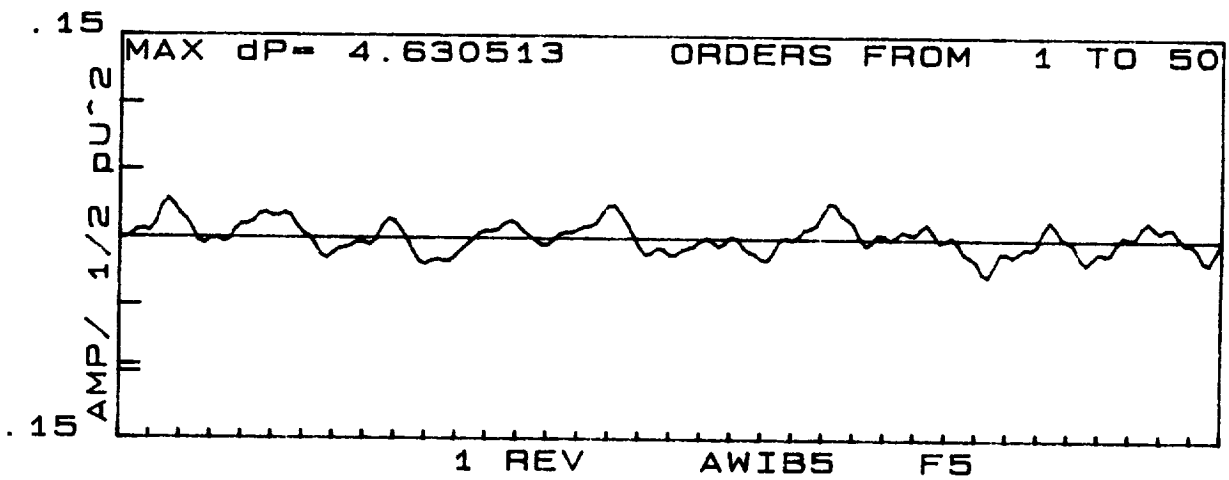
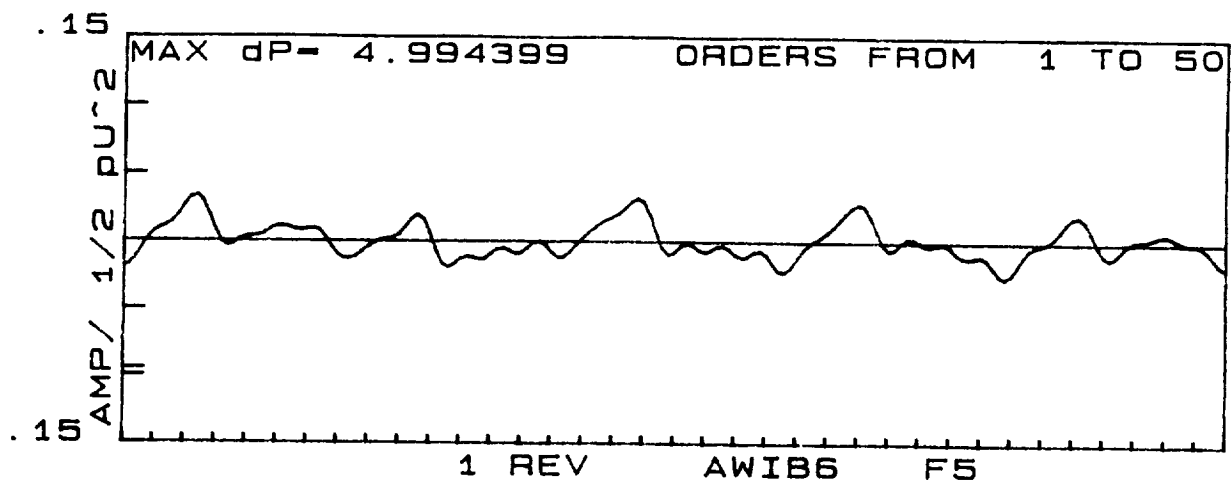
The effects of impeller/diffuser interaction in the clearance between the impeller and sidewall can be found in this series of plots at 3 different flow conditions. The variation in pulsation activity with flow follows the same pattern as do the diffuser sensors. The minimum of the activity occurs at the design flow condition (F4). The 10th order pulsation activity becomes dominant at the locations farther away from the interaction locations (WIB5) as is the case with sensors in the discharge.

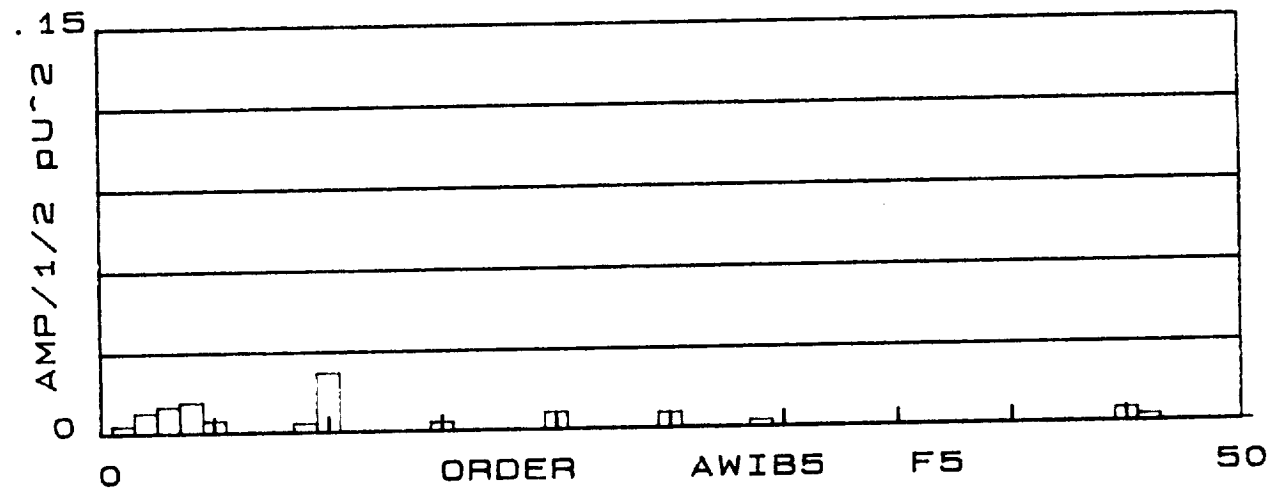
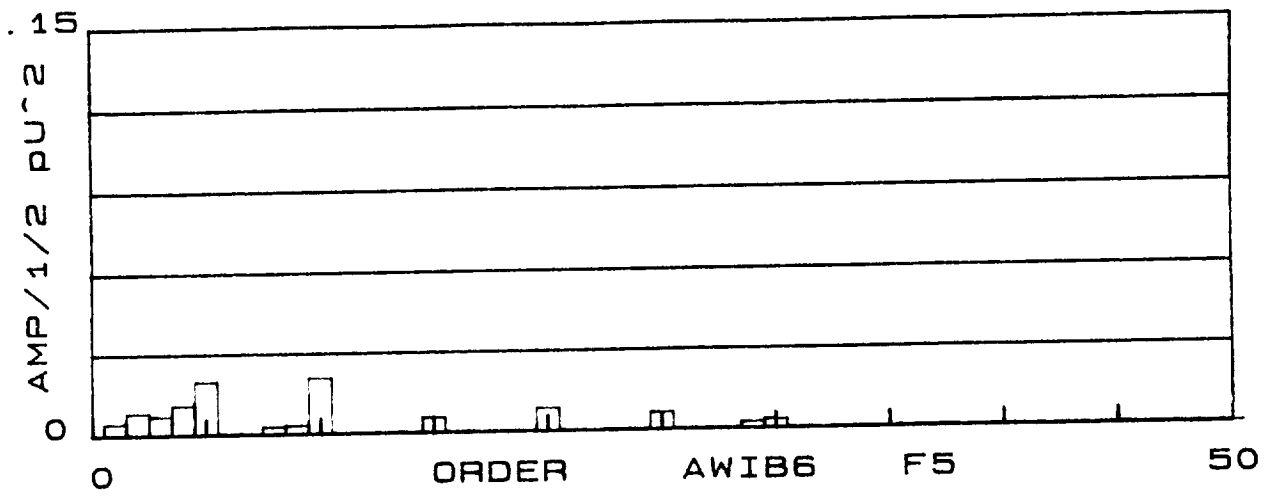










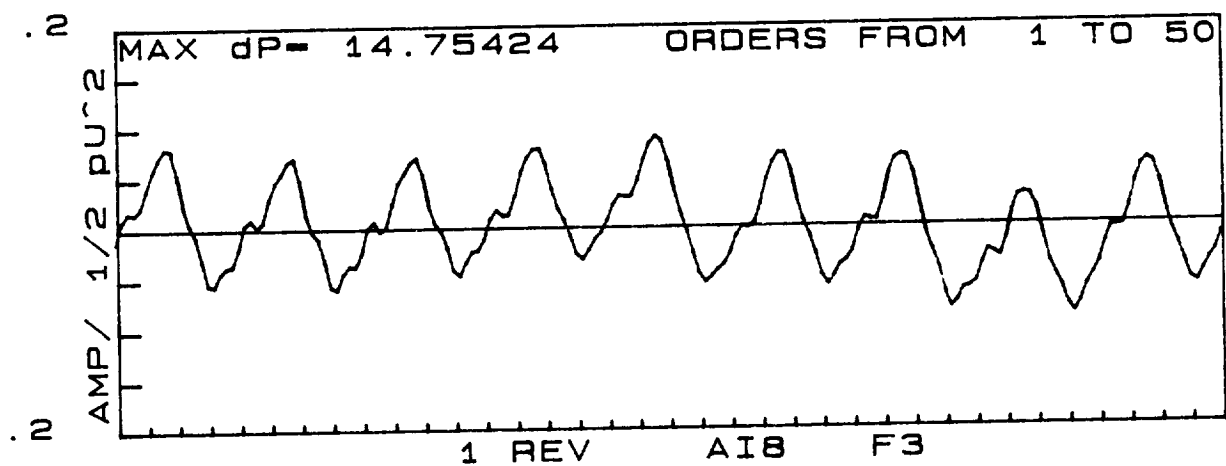
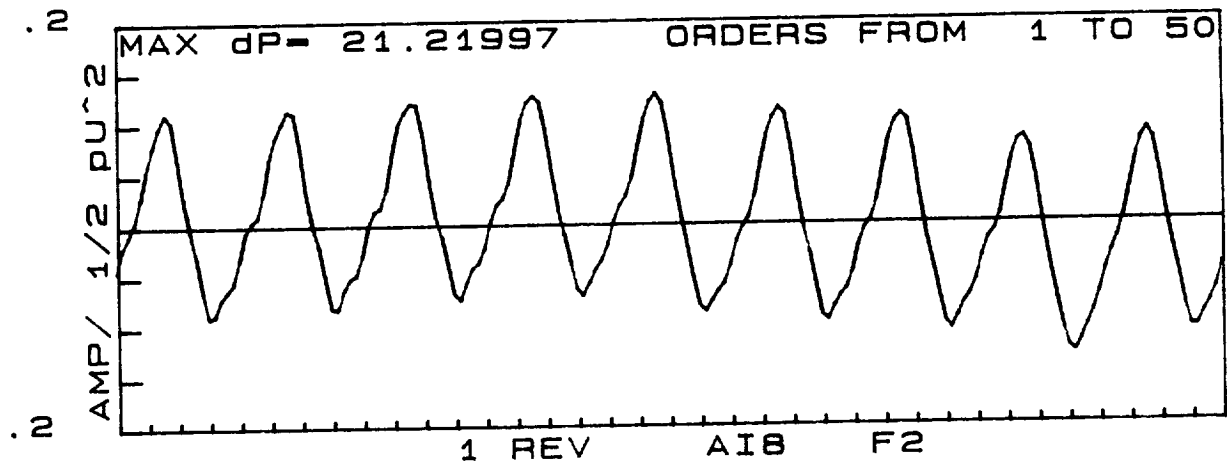
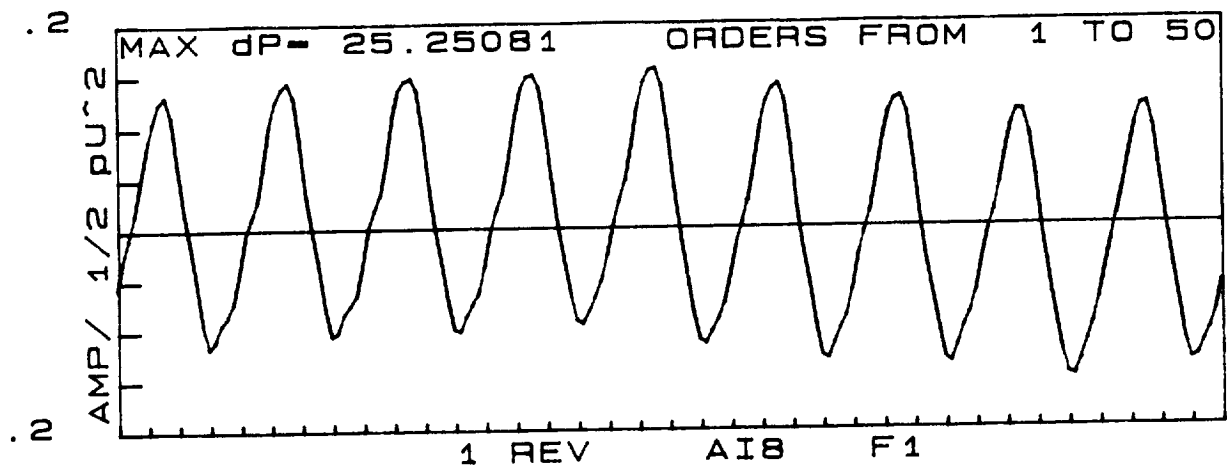


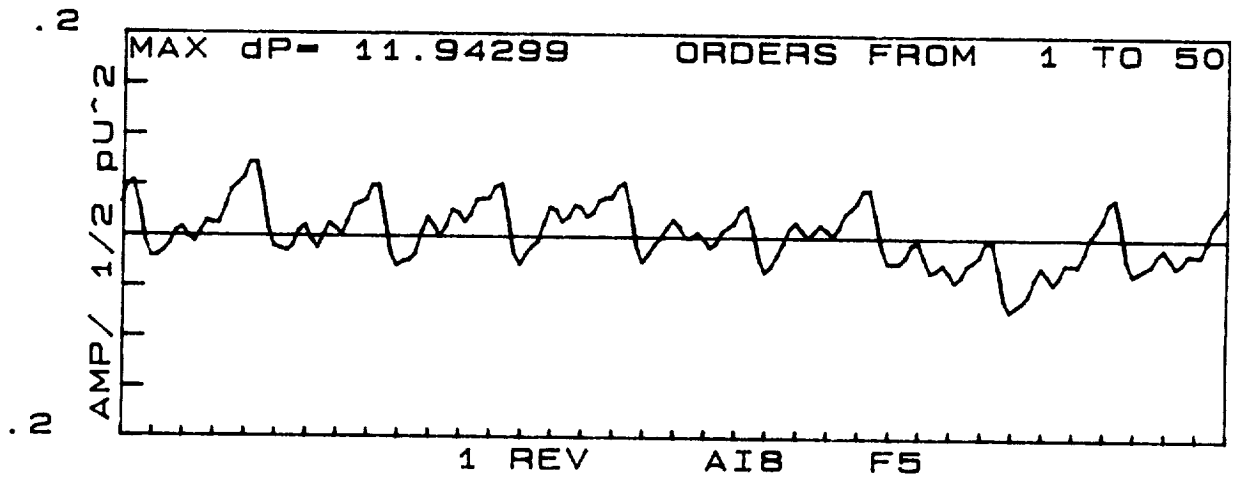
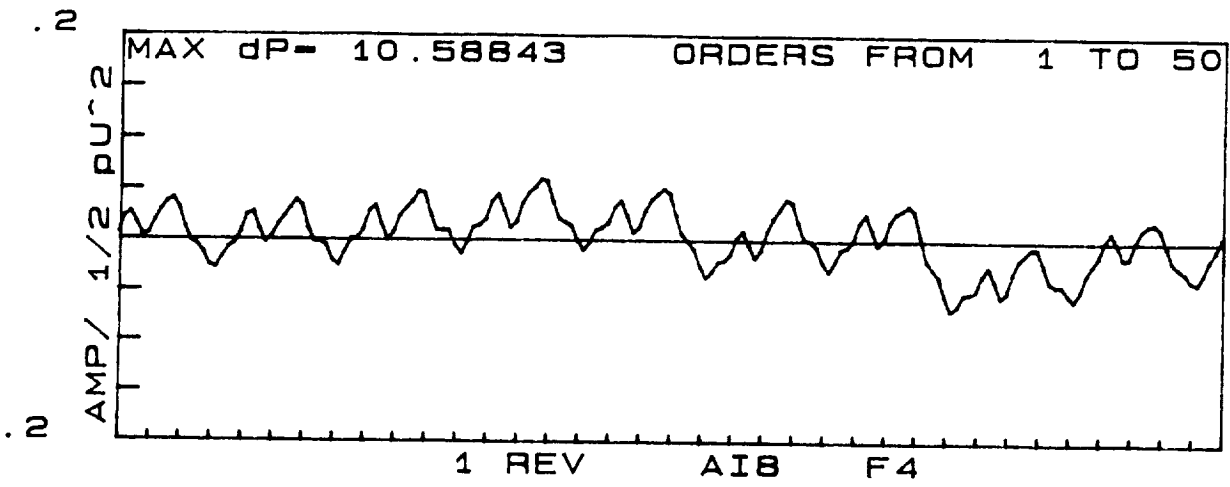
Maximum Amplitude Pulsations, Impeller Vane, Pressure Surface

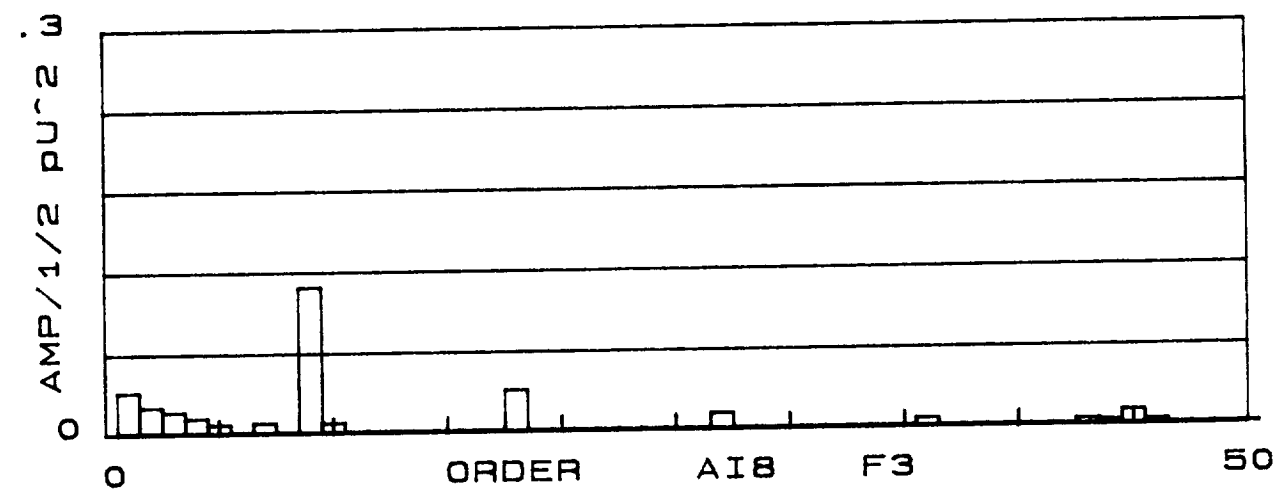
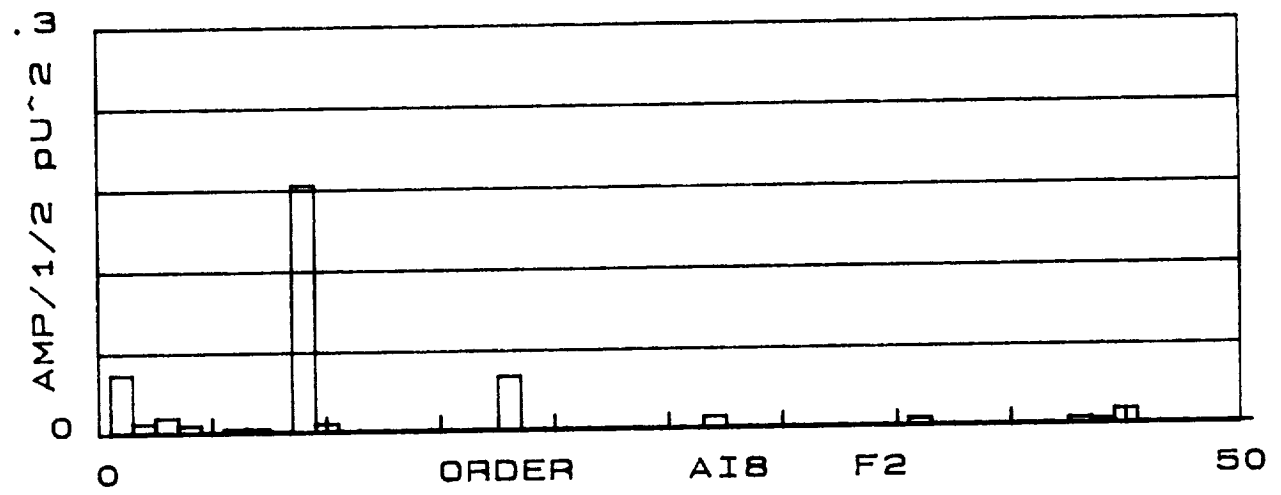
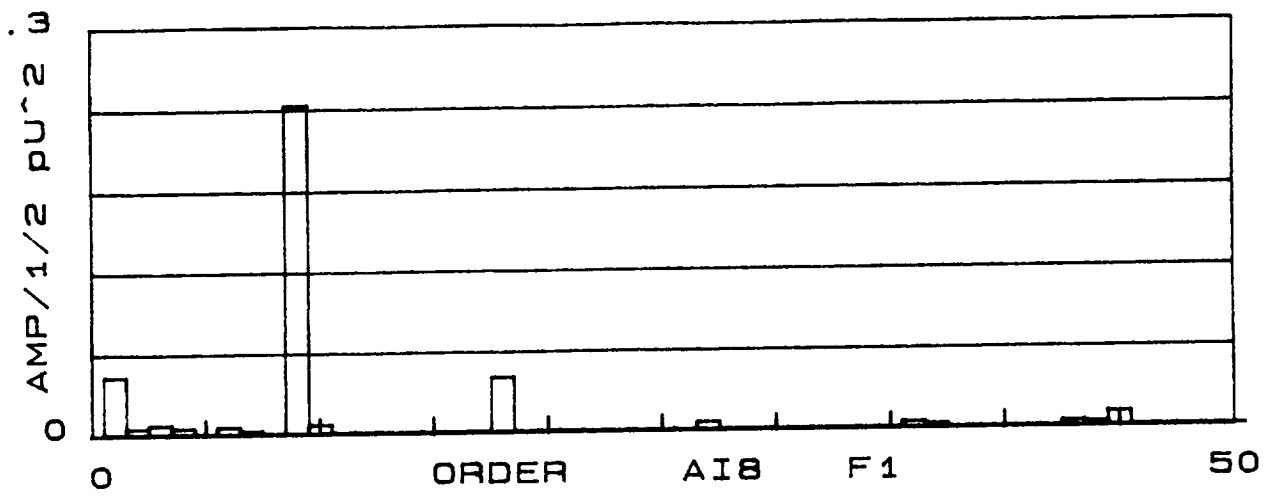
Locations: AI8, BI8, CI8

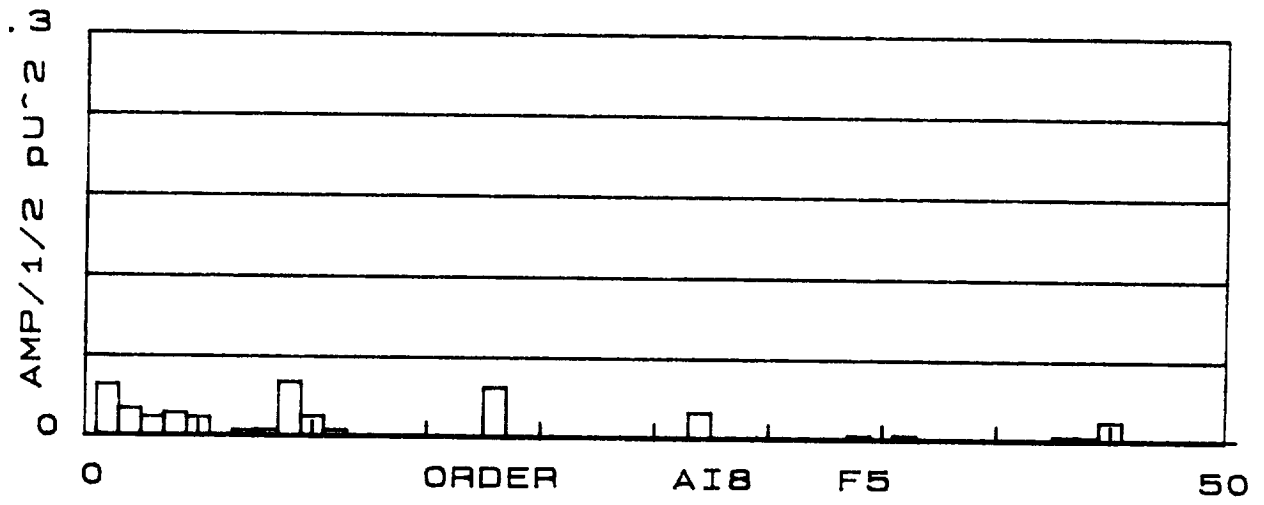
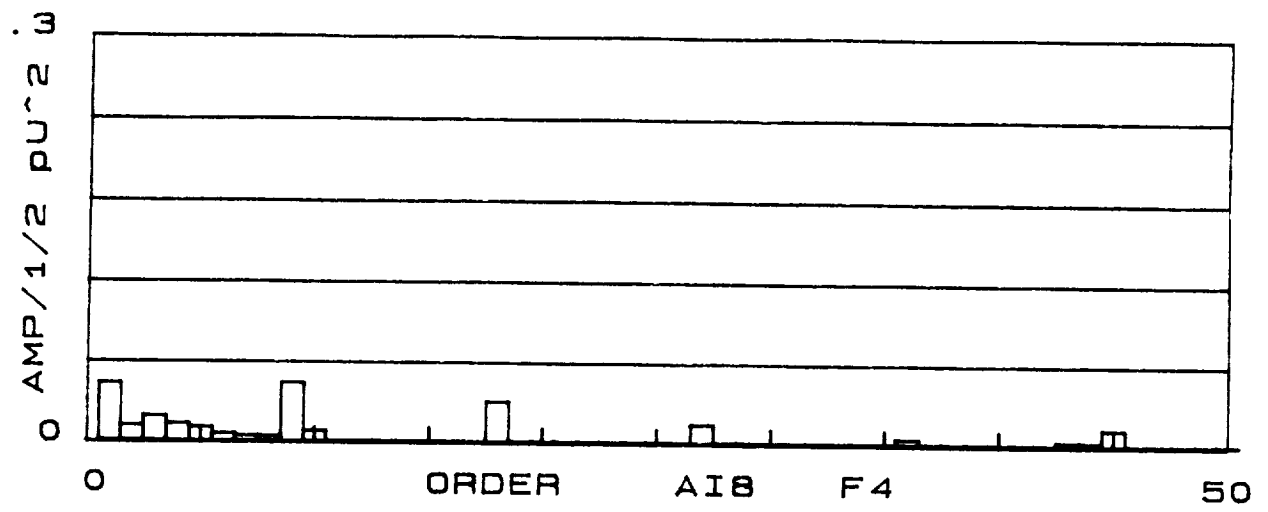
Conditions: F1, F2, F3, F4, F5

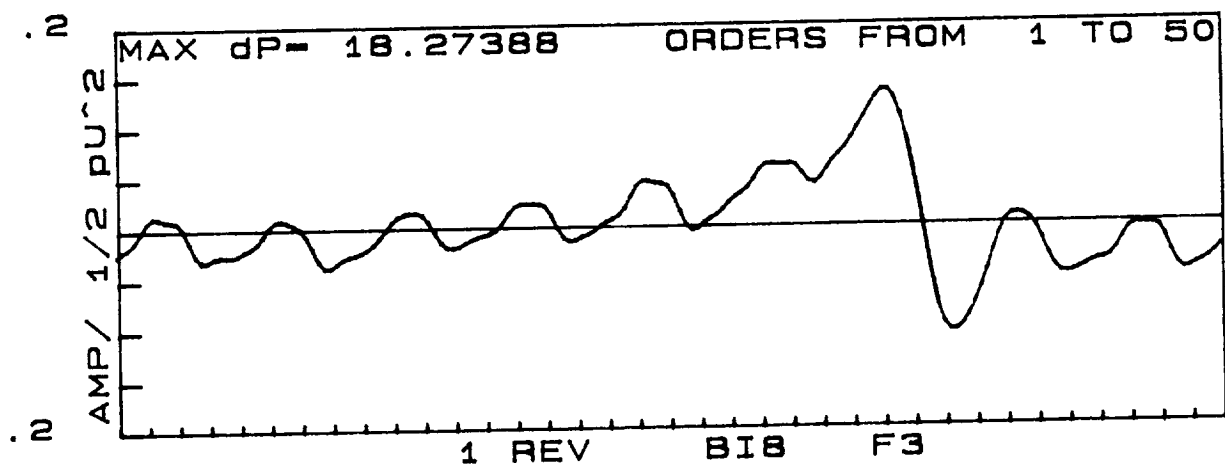
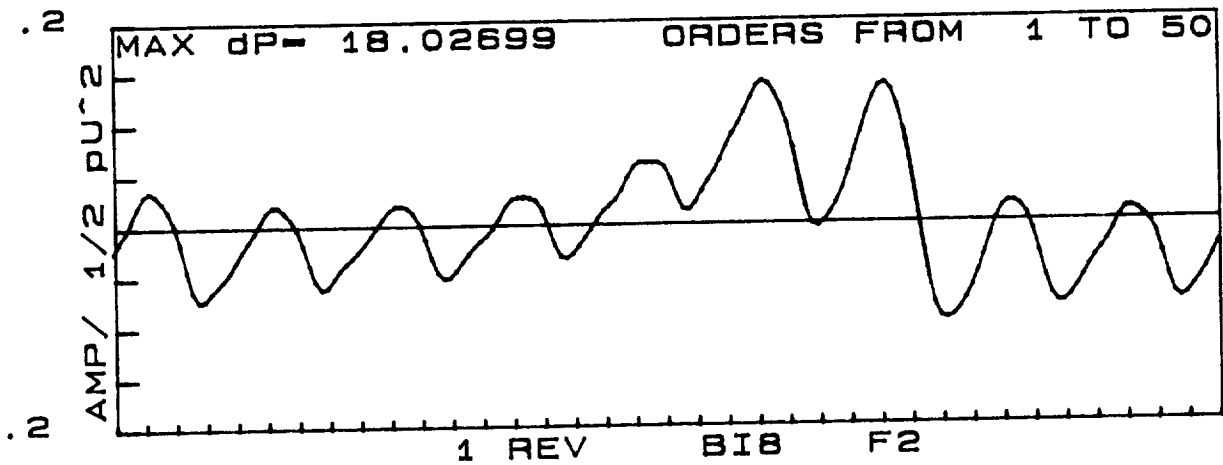
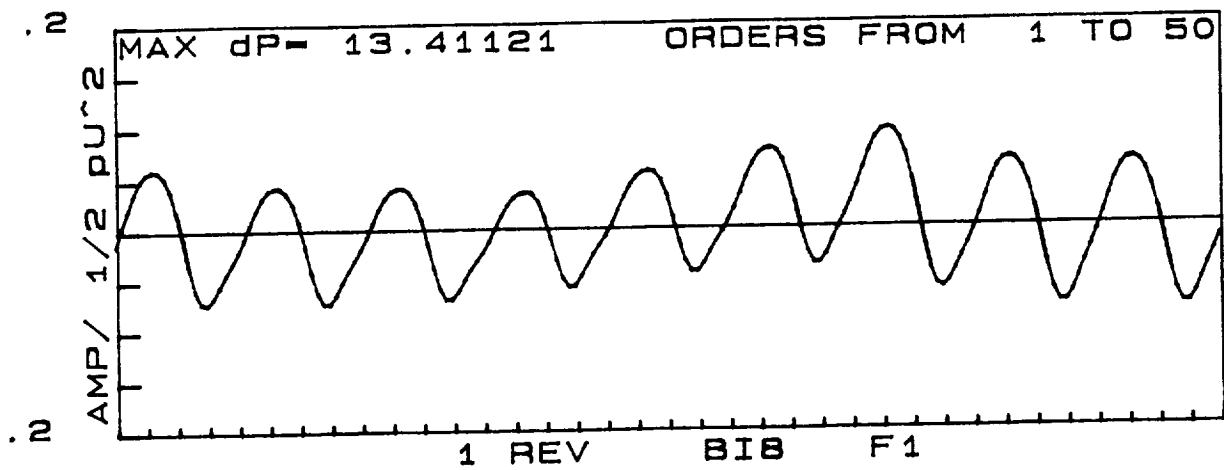
The largest pressure pulsations observed throughout the course of testing occurred on the pressure surface of the impeller (I8). The amplitudes of the pulsations at this location for all three configurations are shown in this series of plots. The maximum amplitude occurs at the low flow condition F1. Minimum activity is found at the design point condition of F4. The effect of impeller to diffuser clearance ratio is quite noticable (compare configuration A, 1.02 ratio with B, 1.06 ratio). Attenuation of the dominant 9th order (for configurations A & B) is on the order of 50% when the clearance is increased. The alternate diffuser design (Configuration C, with 11 vanes) produces much reduced pulsation activity in the impeller, due to its lower blade loading and reduced pressure difference from suction to pressure surface.

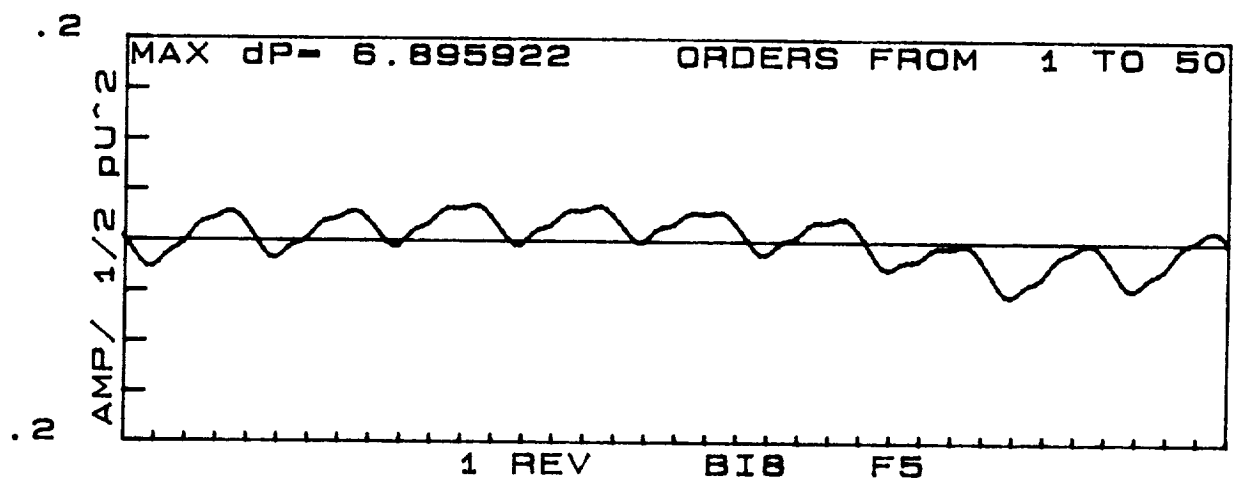
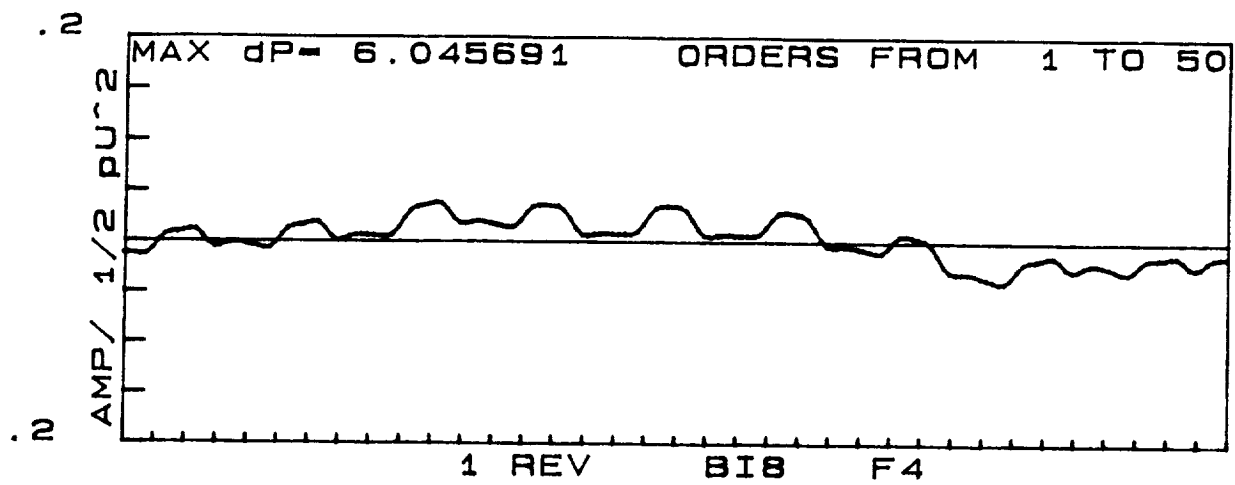


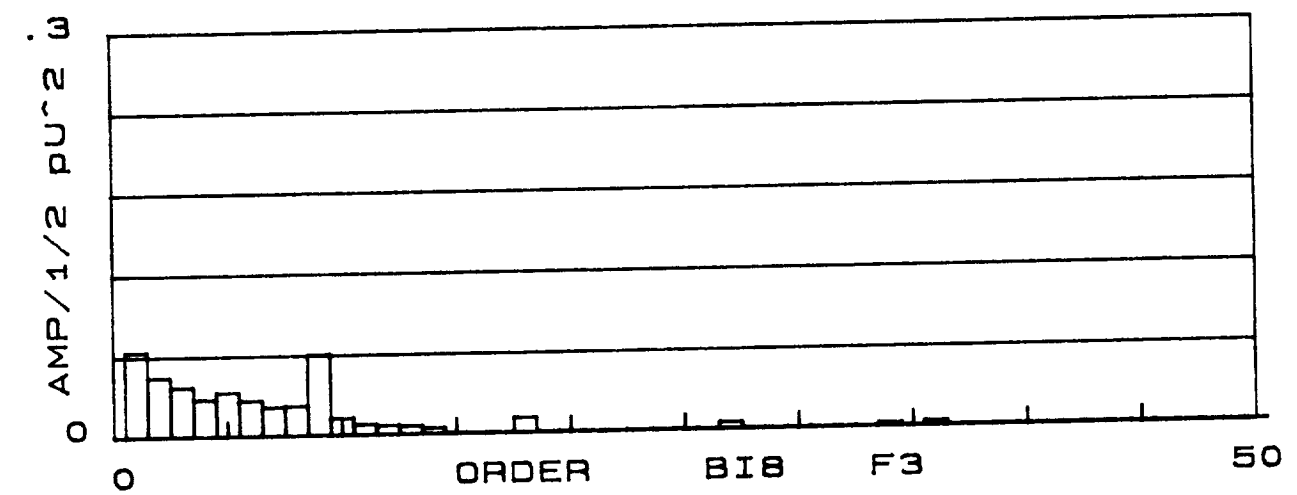
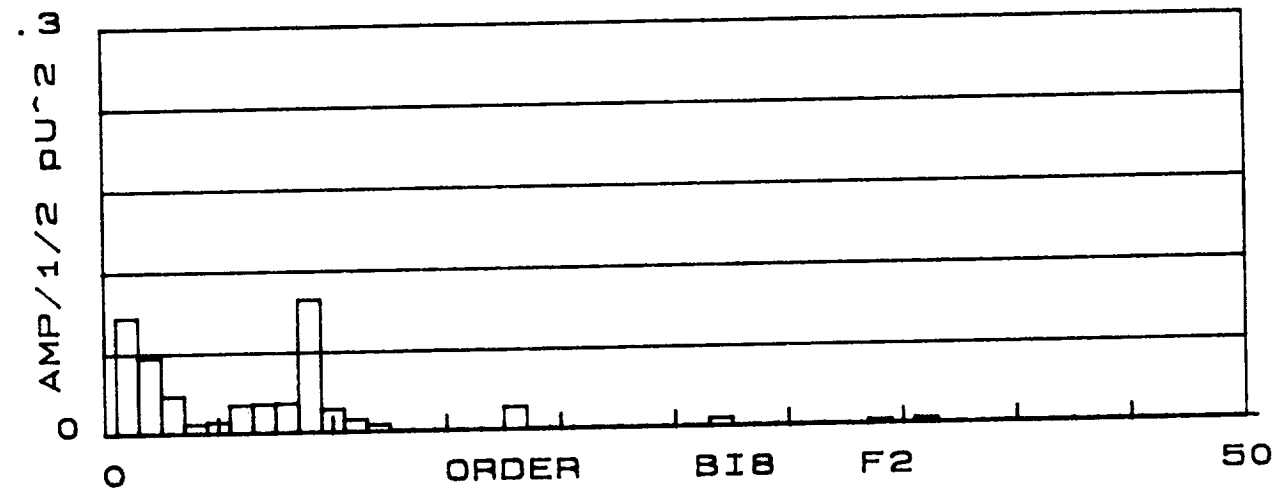
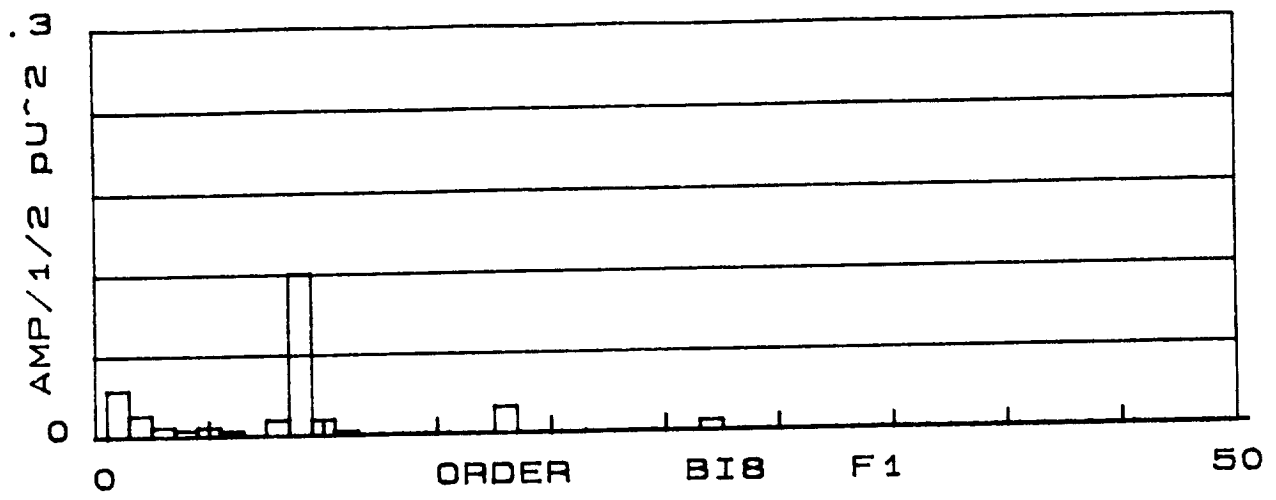


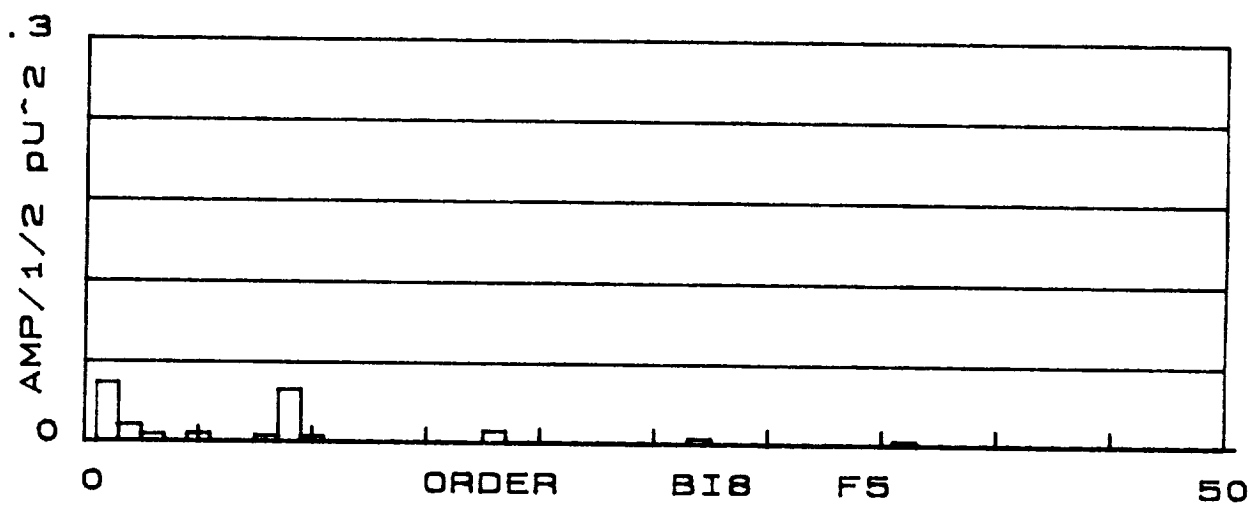
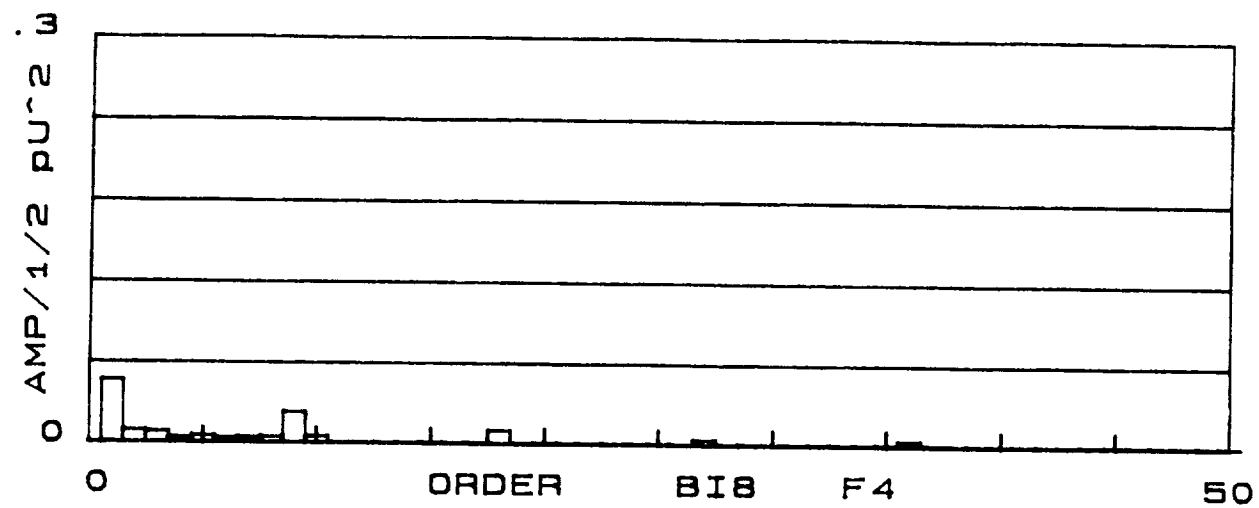


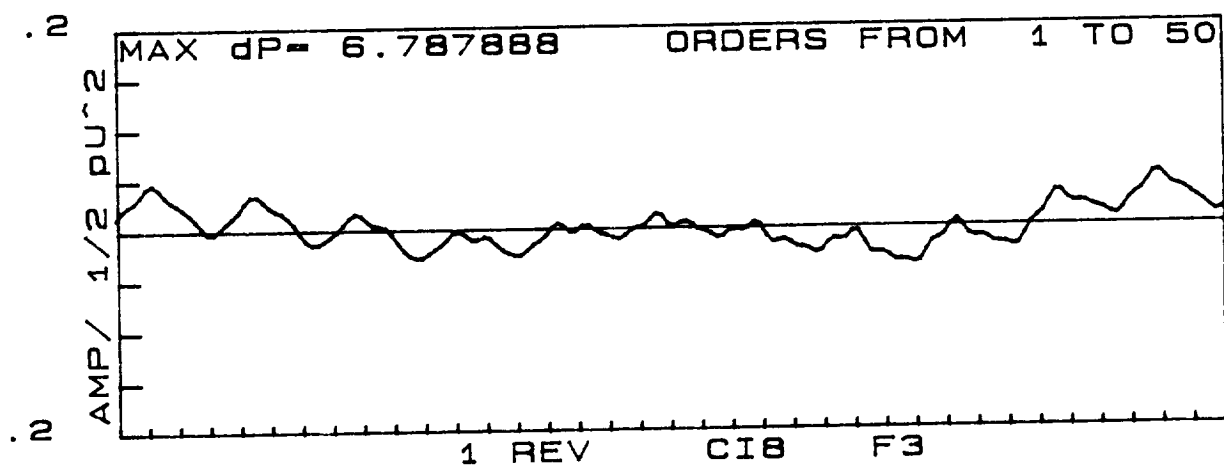
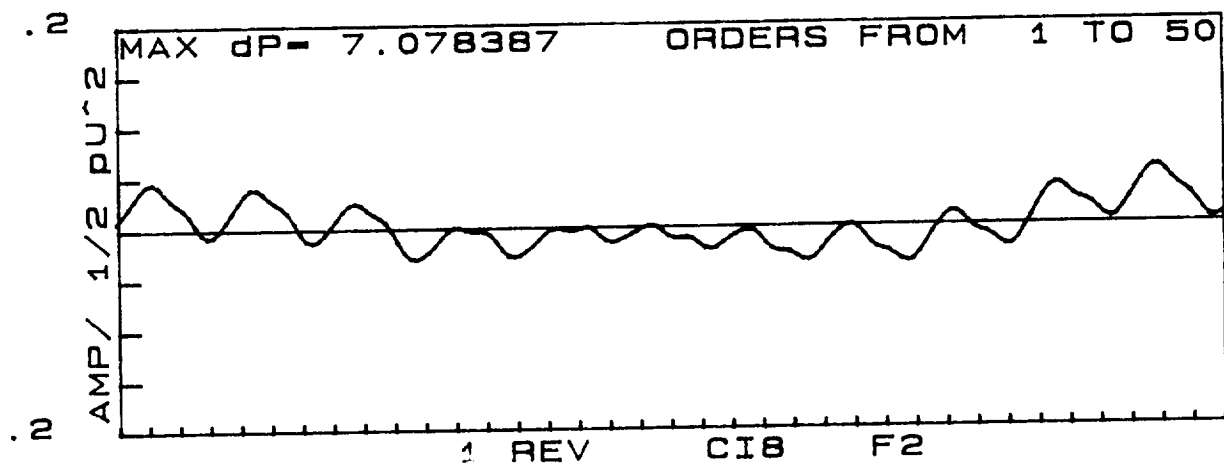
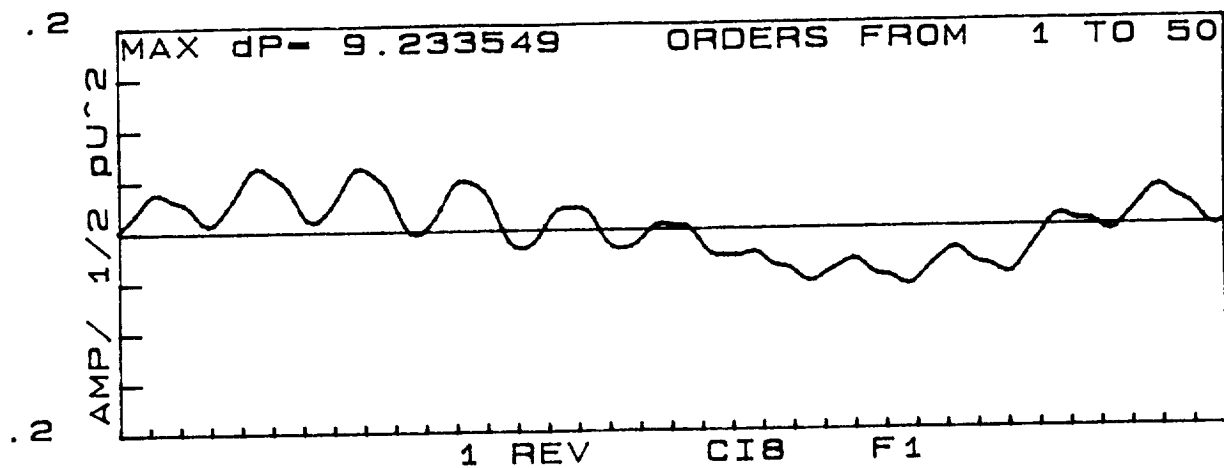


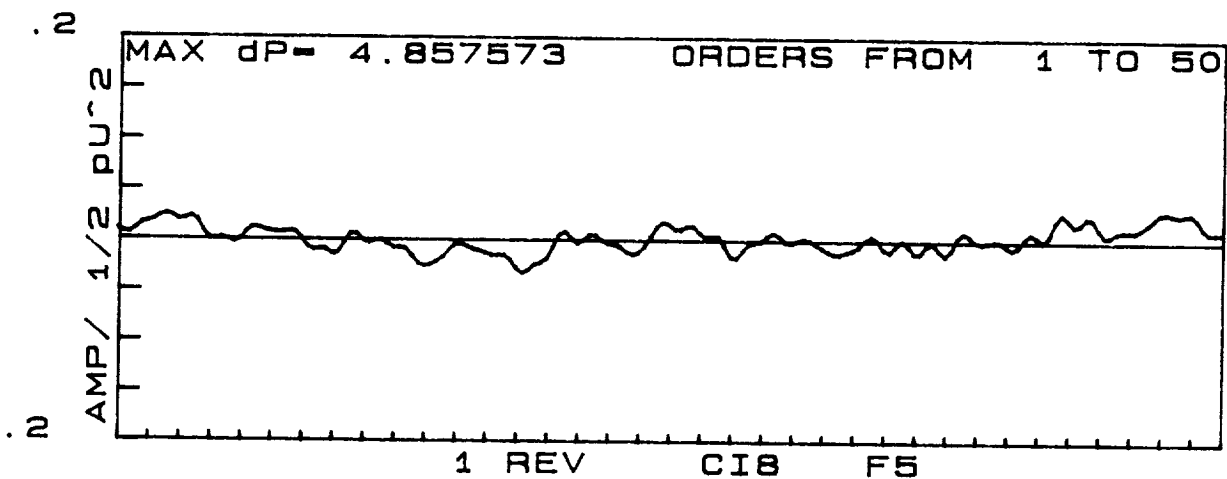
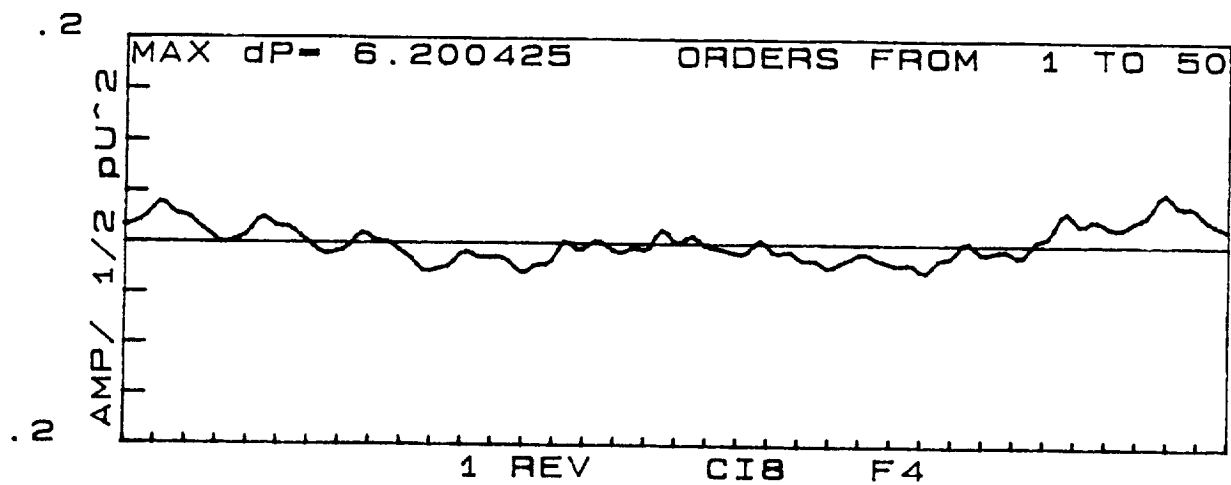


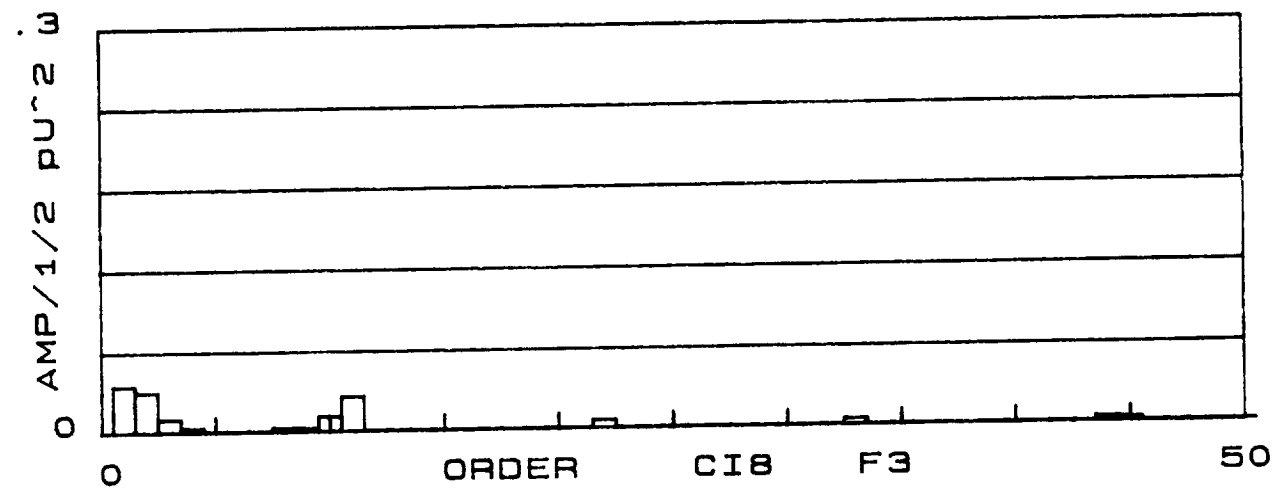
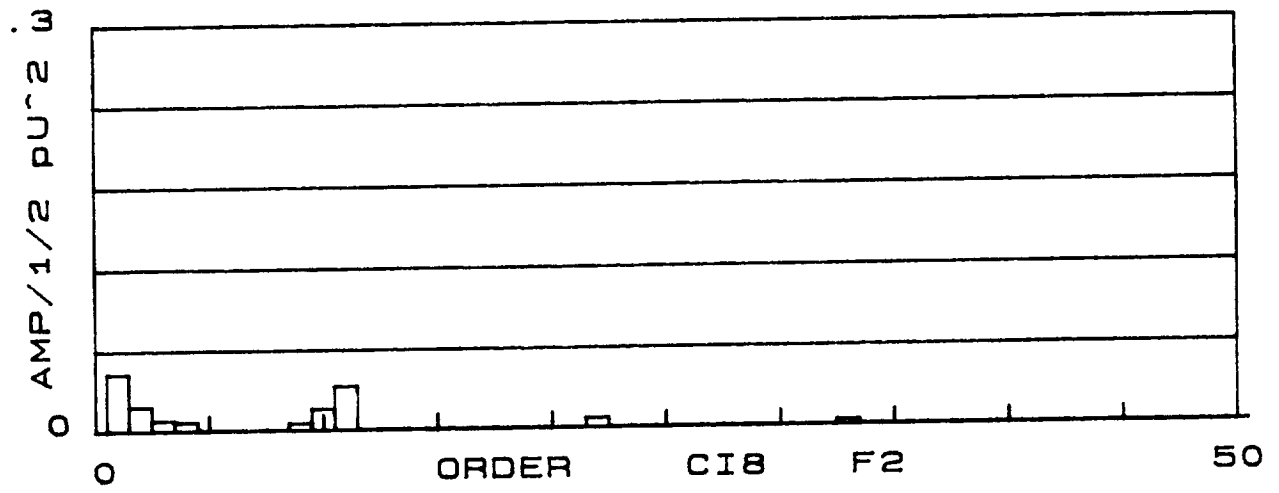
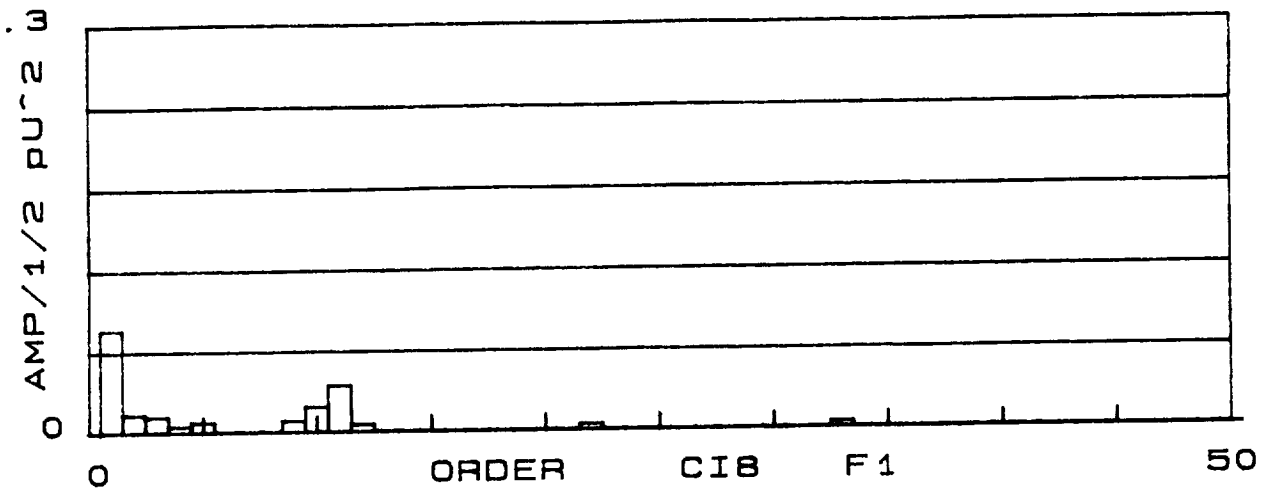


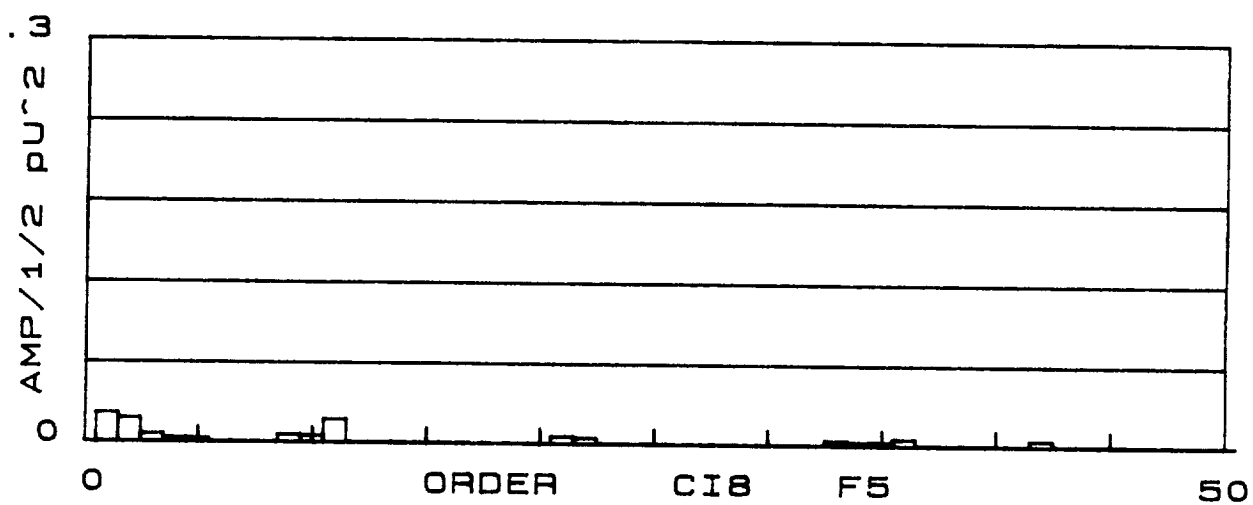
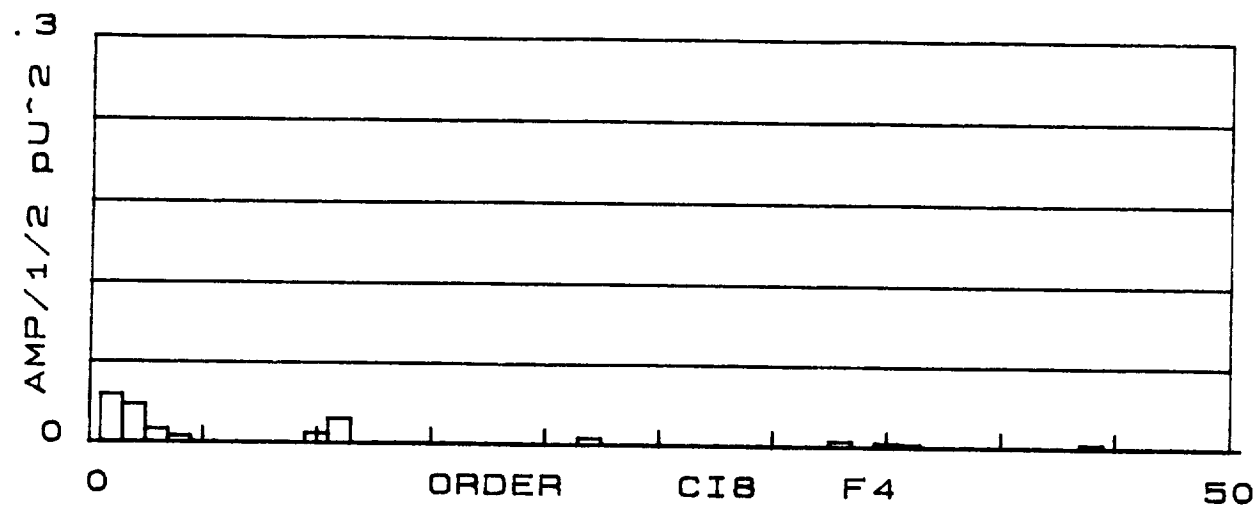












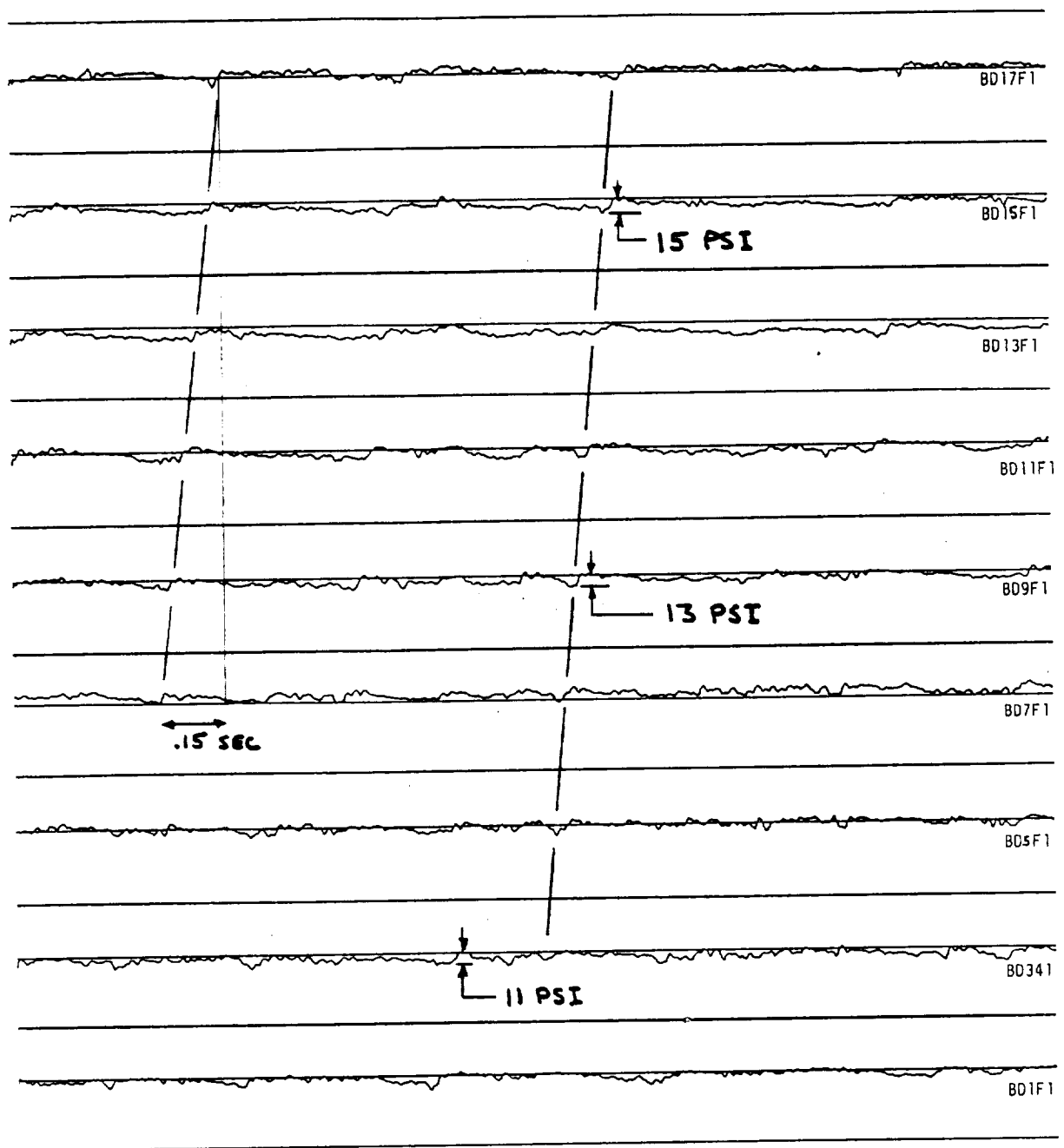
UNSTEADY
NON-SYNCHRONOUS
DATA

Diffuser Quasi-Rotating Stall

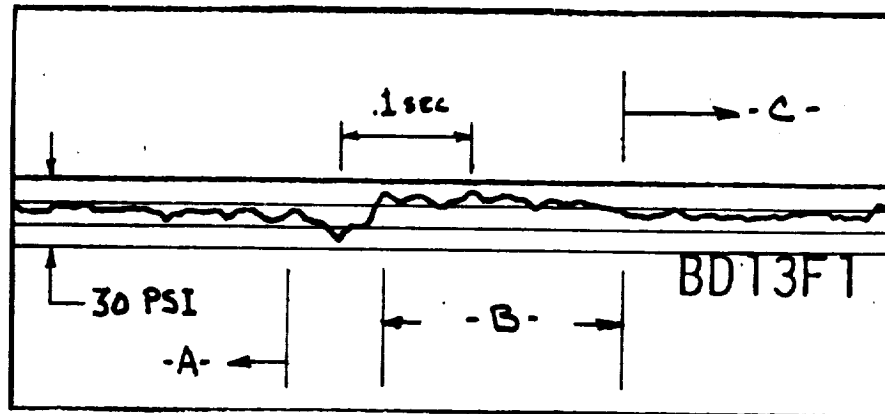
Locations: BD1, BD3, ... , BD17

Condition: F1

A family of plots containing the steady and alternating components of the pressure signal of diffuser inlet sensors operating at 25% of design flow is shown here. Evident in these plots is a trend showing a pressure fluctuation occurring at uniformly staggered time intervals in adjacent passages (indicated by dashed lines). This pattern is not fully developed and is not repetitive in a periodic fashion. An assumed frequency of rotation of the diffuser stall can be estimated and appears to be typically between 4 and 6 hz (for tests at the 38 hz rotation frequency). This phenomenon will be termed a quasi-rotating stall, since it is not fully developed in terms of rotation and periodicity. An enlarged portion of a small segment of a pressure waveform is shown on the next page and describes the conditions in the diffuser passage during the stall event. This phenomenon occurred on the 'B' and 'C' configurations. The close impeller/diffuser clearance of configuration 'A' apparently discouraged this behavior from occurring. Apparently the interaction of the impeller jet/wake exit flow condition influences the boundary layer development on the diffuser vanes. It is the boundary layer growth and separation which causes the passage to stall. This unsteady behavior is found only at low flows and was not found at any flow greater than 25% of design.



Time waveforms for 2.5 seconds of diffuser inlet pressure transducers. Waveform alignment is consistent with time = 0 on the left hand side. All data at 25% of design flow.



- A- Diffuser passage is operating with about a 5-6 psi pressure rise.
- B- Diffuser passage is stalled and discharge pressure is now seen at the diffuser inlet throat.
- C- Diffuser is 'unstalled' and is once again passing flow with a pressure rise similar to -A-.

Unsteady pressure behavior. Time waveform for pressure transducer located at diffuser throat inlet. Pump is operating at flow condition F1. 25% of design flow and 2300 rpm.

Scroll, Diffuser and Sidewall Sensors during Quasi-Rotating Stall Event

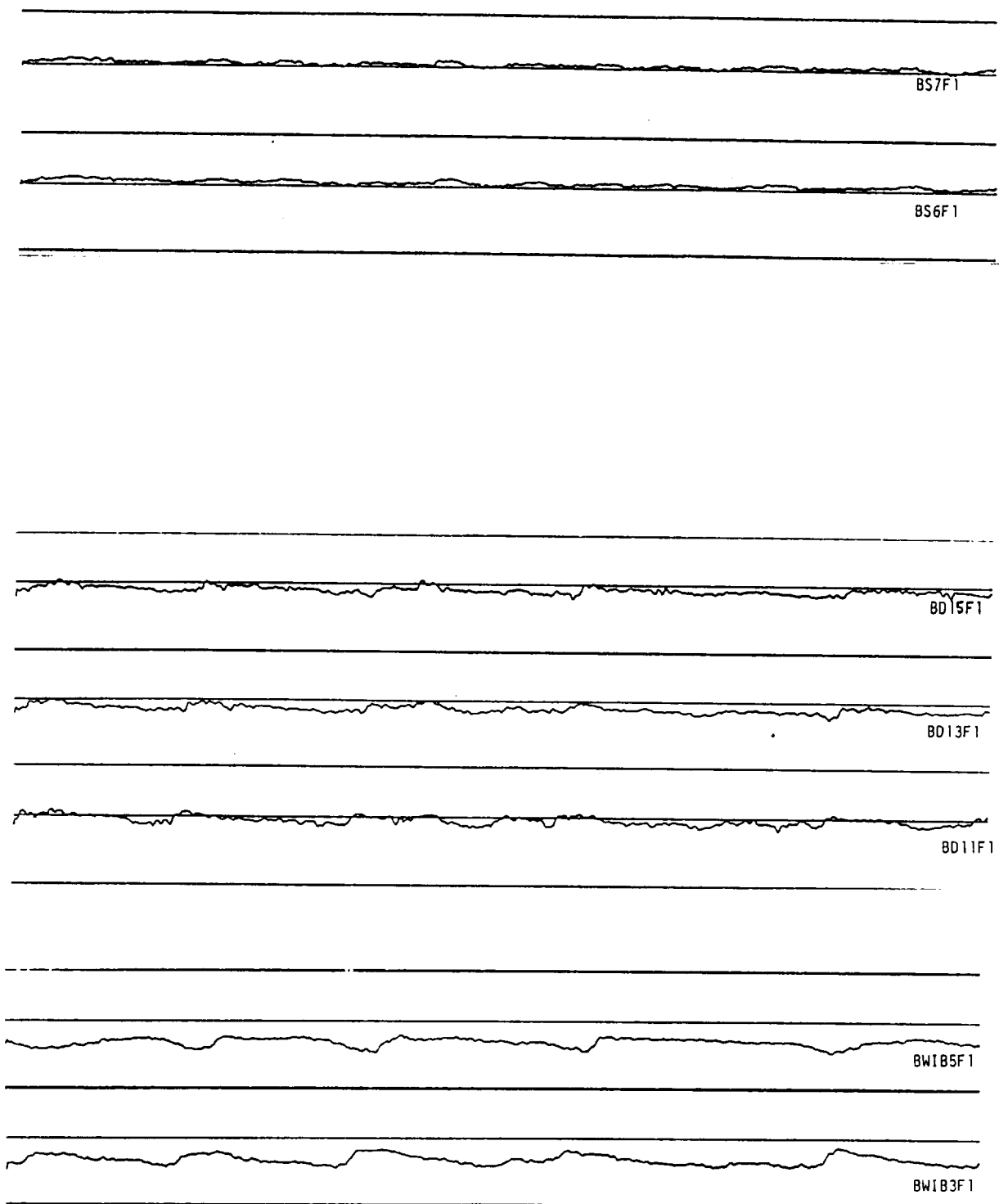
Locations: BS7,BS6

BD15, BD13, BD11

BWIB5, BWIB3

Condition: F1

The relationships between sensors in various areas of the pump stage during the quasi-rotating stall event (at 25% Q) is shown on this plot. The scroll sensors do show some response to the unsteady flow behavior occurring in the diffusers. Also noticable is the response in the clearance between the impeller and stationary sidewall. Pressure fluctuations here (WIB3, WIB5) relate to the events occurring at the diffuser and are of similar or larger magnitude. This behavior, so near the ring seal area can influence the rotordynamic characteristics of the shaft since the circumferential variation in pressure will affect the leakage rate and hence the stiffness and damping capability of the ring.



Time waveforms for 2.5 seconds for sensors located on the outer wall of the scroll (BS7 + BS6) and diffuser inlet (BD11 + BD13 + BD15). Waveform alignment in time is consistent with time = 0 on left hand side. All data at 25% of design flow.

Occurrence of Quasi-Rotating Stall in Configurations A & C

Locations: AD1, AD3, ... , AD17

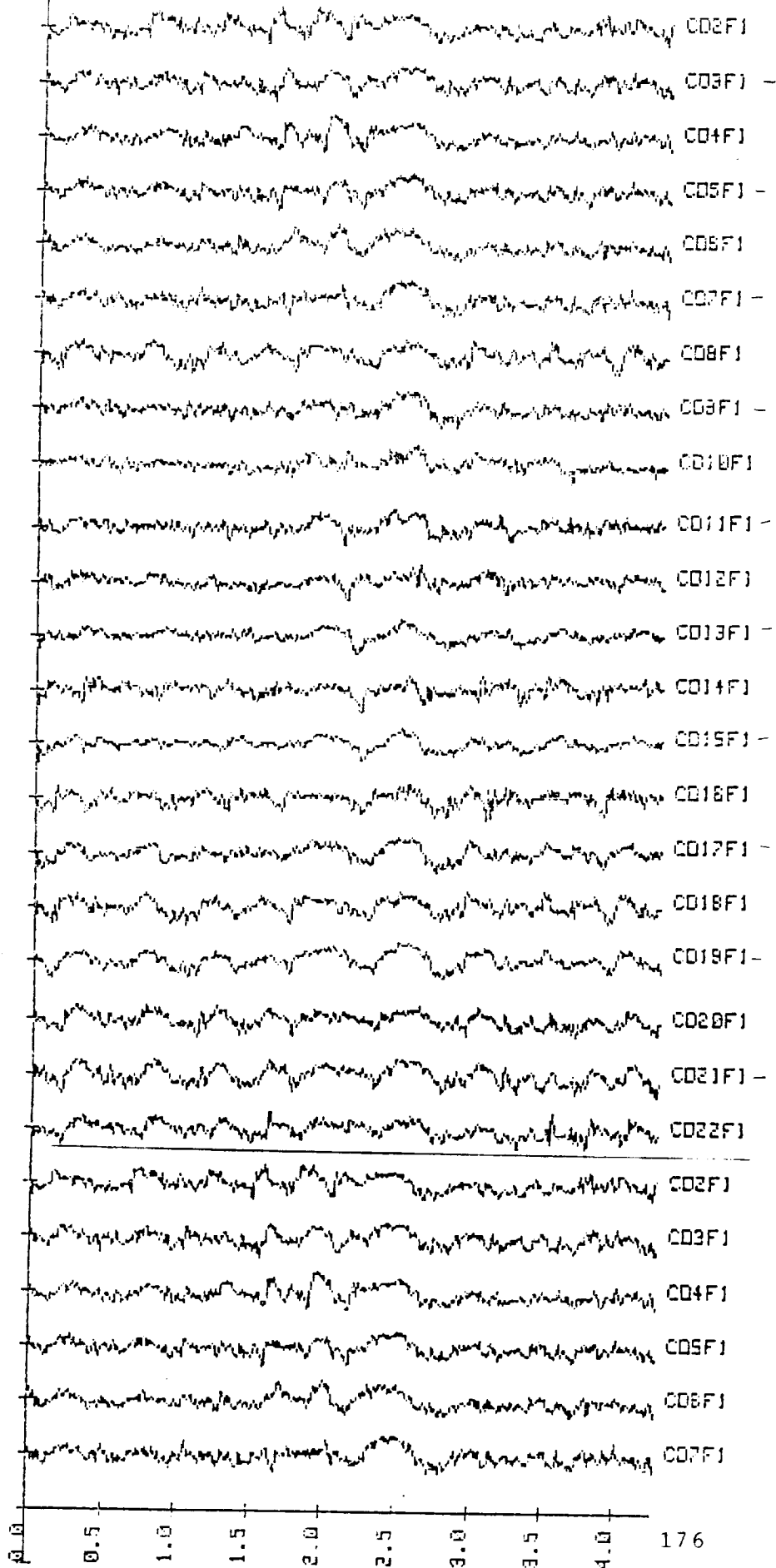
CD1, CD3, ... , CD21

Condition: F1

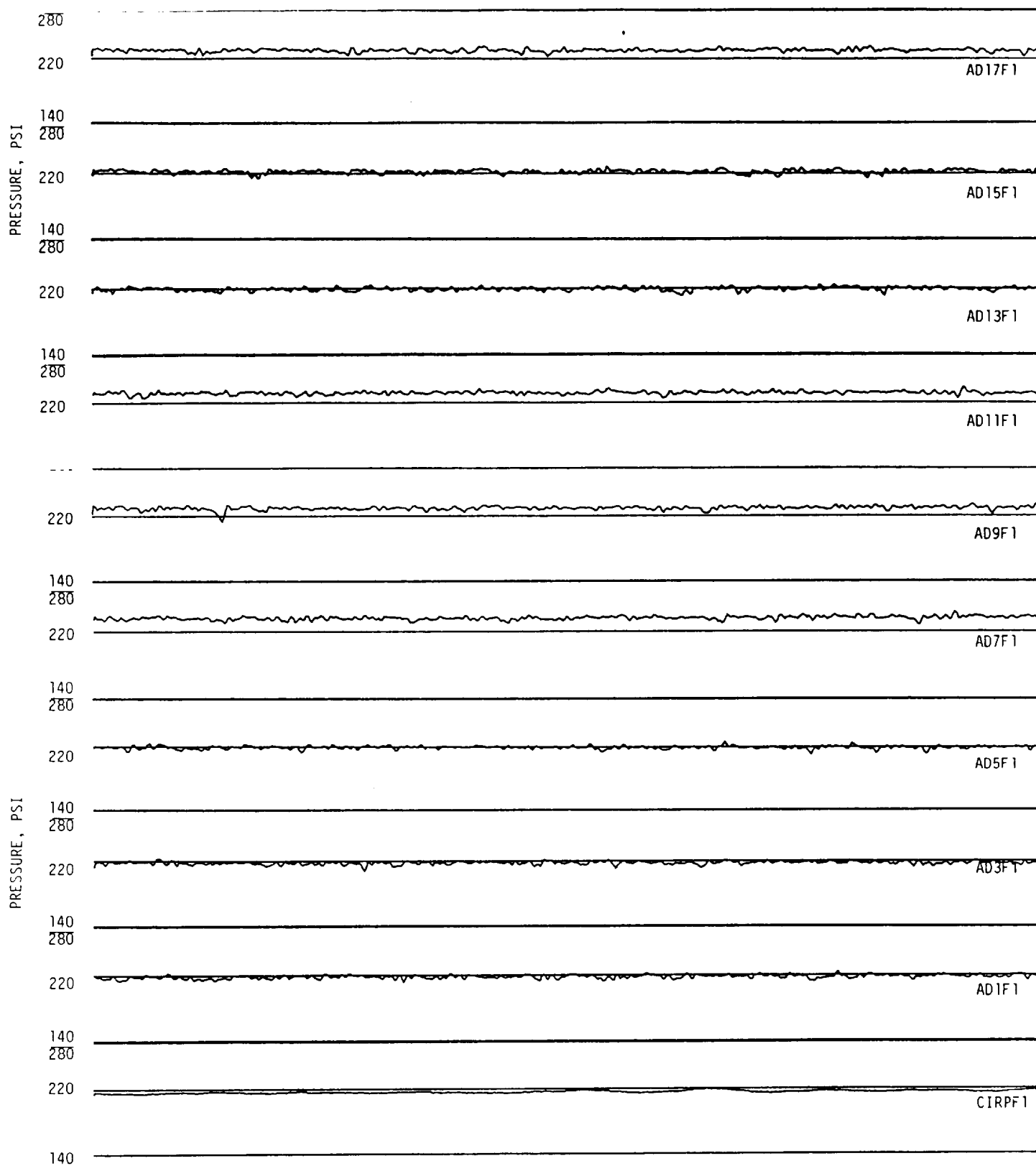
The quasi-rotating stall event (at low flow condition) occurs in configuration C but not in configuration A. The pressure waveforms for configurations A and C are shown in these two plots. Each plot contains about 95 shaft revolutions, or about 2.5 seconds of data. The boundary layer growth and separation characteristics which promote the passage stall are dependent on the strength of the jet/wake activity (ie. large variation in impeller exit relative velocities). This activity is most prevalent at low flow conditions. Configuration A, which has a 1.02 ratio of impeller OD. to diffuser ID., exhibits no quasi-rotating stall. The close proximity of the jet/wake activity exiting the impeller to the diffuser passage must discourage the growth of a thick boundary layer, which is a necessary ingredient for diffuser stall to occur. The increased clearance of configuration C (and for B shown earlier) provides the necessary distance for the attenuation of the jet/wake activity. This attenuated variation in exit velocity is not strong enough to upset the development of the boundary layer on the vane and side wall surfaces. The boundary layer, allowed to thicken, becomes susceptible to separation and hence leads to the switching of the stall from one diffuser passage to the next, and so on.

a

INGERSOLL RAND CONFIGURATION C 2.5 SEC



NOT SCALED FOR
PRESSURE LEVELS



Impeller Passage Stall at Low Flow

Locations: BI1, ..., BI5

Conditions: F1

These 5 impeller pressure transducers are located midway in the passage, between the suction and pressure surfaces of the blades at a 9.54 in. diameter, on the hub side wall (sensing element normal to the flow passage). The plot of BI1 thru BI5 is of pressure data taken over 2.5 seconds, or about 95 shaft revolutions. The large once-per-rev amplitudes are evident on the plot (if counted they number 95-96). The data is correctly phased in time, with $T=0$ on the left hand side. It is believed that the large once-per-rev amplitude is due to the eccentric operation of the impeller inside the vaned diffuser. In this condition, the individual sensors, as they are rotating, see a varying clearance to the diffuser. The physical eccentricity can be small and still create this effect. Superimposed on this periodic signal is a phenomenon which apparently interrupts the reaction of the sensor to this mechanically induced effect. The disruption occurs in all 5 passages, but not simultaneously or periodically. It is clear that the eccentricity is still present, since the unaffected passages retain the once-per-rev behavior. One explanation could be that the affected passage has stalled, and is no longer passing flow in an outward direction (in fact reverse flow may be occurring). With no positive flow, the passage is no longer reacting to the varying clearance in the manner that a fully flowing passage would. It appears that this behavior is completely random. This effect was only looked for at the F1 and F4 conditions. It does not occur at the design point flow, F4. No correlation can be found with the diffuser rotating stall event

described earlier and occurs in all configurations. This severe impeller stall is related to the well known inlet recirculation phenomenon encountered on pumps operating at flows below the design point.

280

220

140
280

220

140
280

220

140
280

220

140
280

220

140

B15F1

B14F1

B13F1

B12F1

B11F1

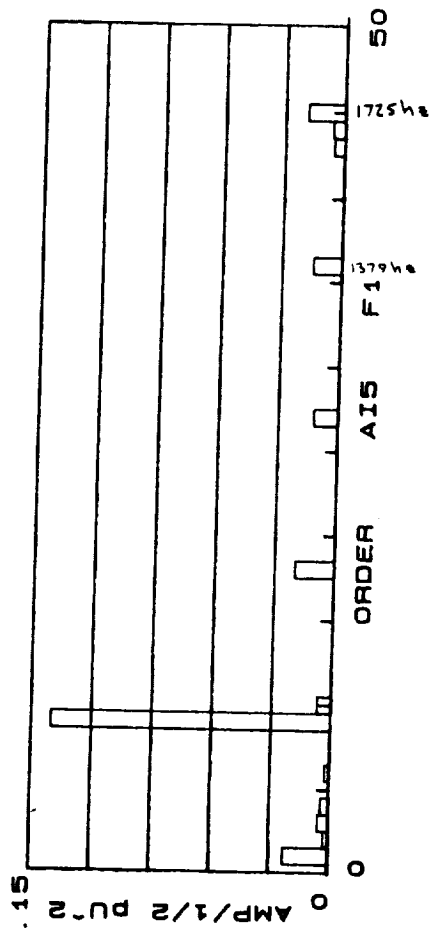
Impeller Shroud Resonance & Resulting Pulsation Activity

Locations: AI5, BI5

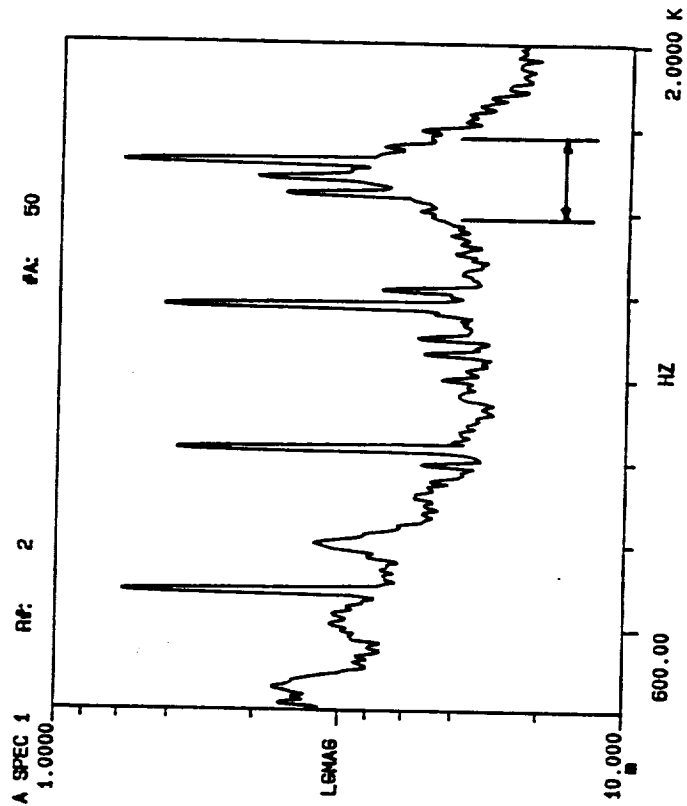
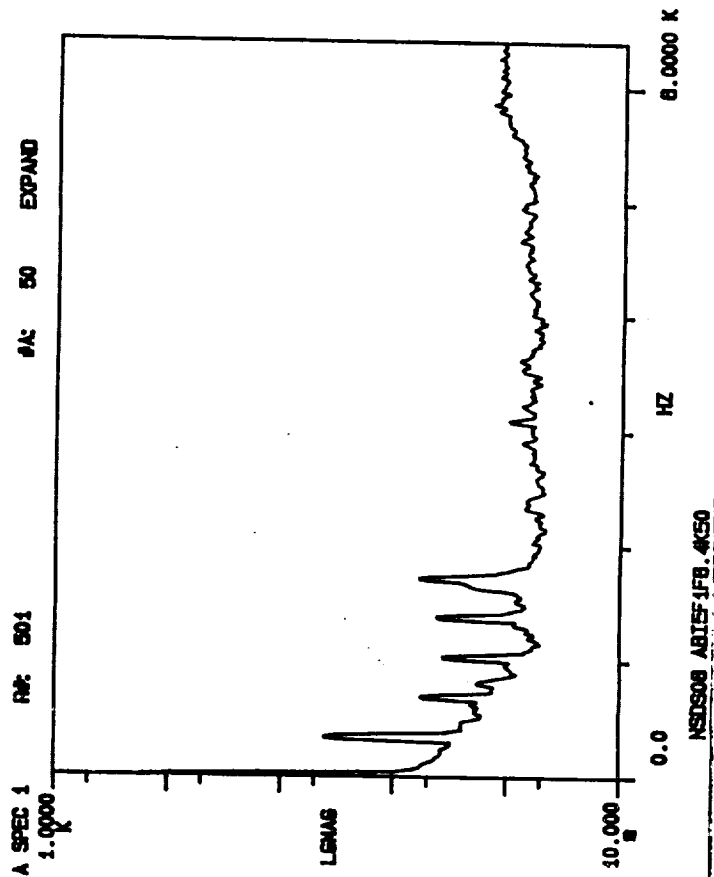
Conditions: F1, F4

The I5 sensor is located on the impeller hub side wall, facing the flow passage. The difference between configuration AI5 and BI5 consists of a reduced impeller diameter. The two bottom plots on the next four pages show the spectra of the pressure waveforms at two flows (25% - F1, and 100%, - F4) for 2 frequency ranges, using an RMS, half-amplitude psi scale. The orders of the synchronous pulsation activity are shown on the top plot. What appears on the power spectrum are pulsations which are not order (ie. rotation) related, as well as pulsations which are synchronous in nature (which are also shown in the top right plot). In the region between 1600 and 1800 hz (for AI5), we find amplitudes at the 43,44 and 45th order of rotation (rotation frequency is 38 hz) with a large amount of "sideband" activity. This indicates a resonance of the impeller side wall which contains the pressure transducer. This vibration causes the transducer to 'see' a pressure amplitude caused by the motion of the wall itself. This behavior occurs only with the "A" configuration. The cutting of the impeller diameter (to the "B" configuration) either reduced the excitation forces (the impeller/diffuser interaction phenomenon) or changes the resonant frequency of the impeller wall. The "B" configuration does not show this resonant behavior in the region of 1600-1800 hz. In fact it does show an amplitude at around 2200 hz which does not appear on the "A" configuration and could be explained as a higher impeller sidewall resonance frequency.

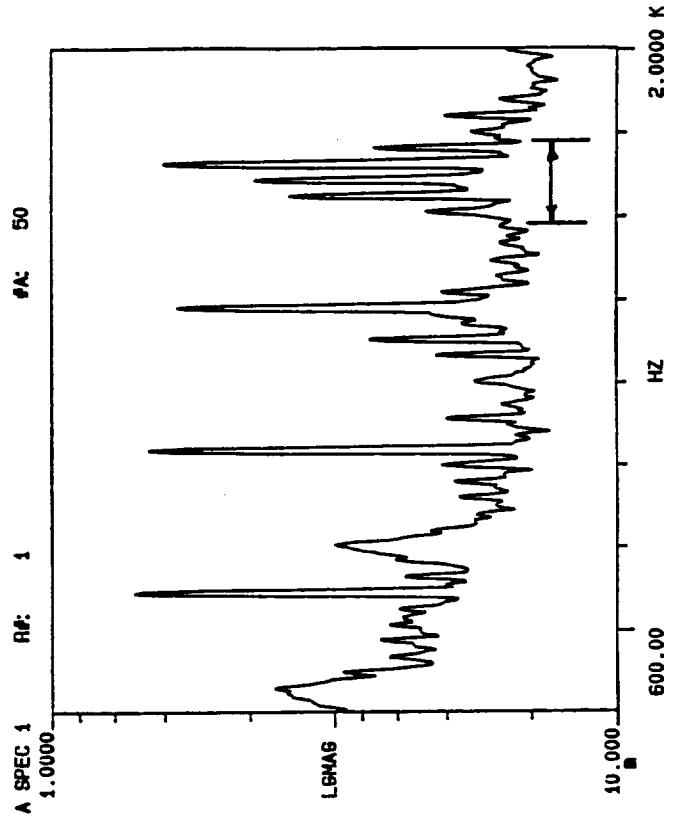
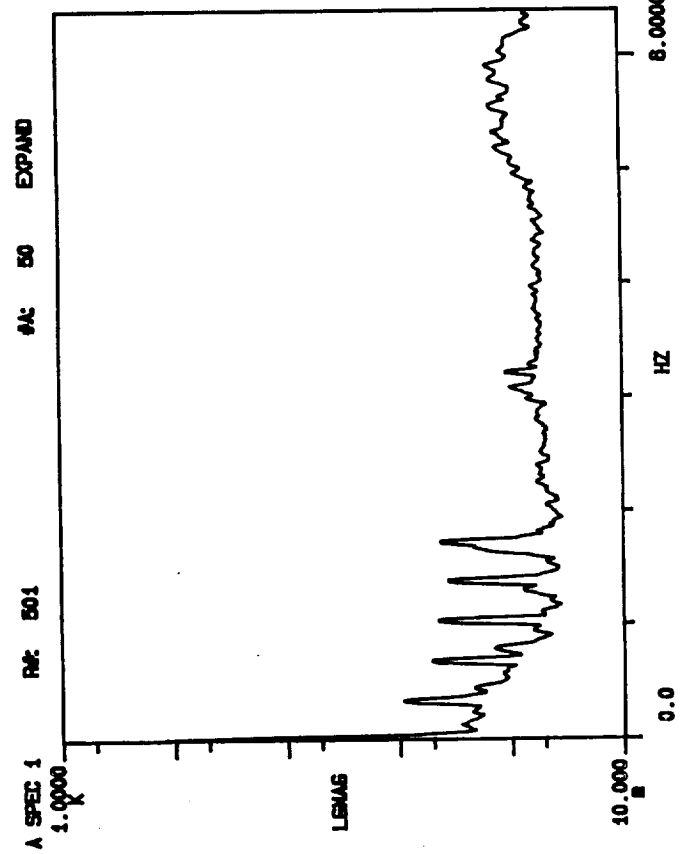
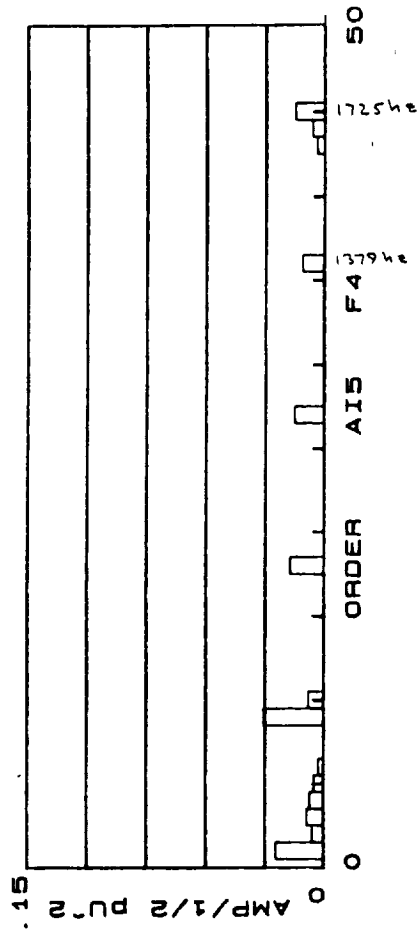
INGERSOLL-RAND 312801
 NON-SYNCHRONOUS SPECTRA
 CONFIGURATION A
 IMPELLER #5 FOLW #1
 TAPE FOOT 184 TO 197



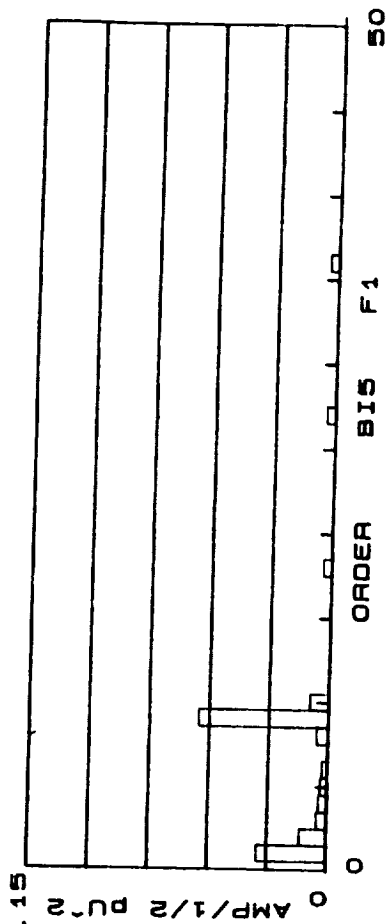
182



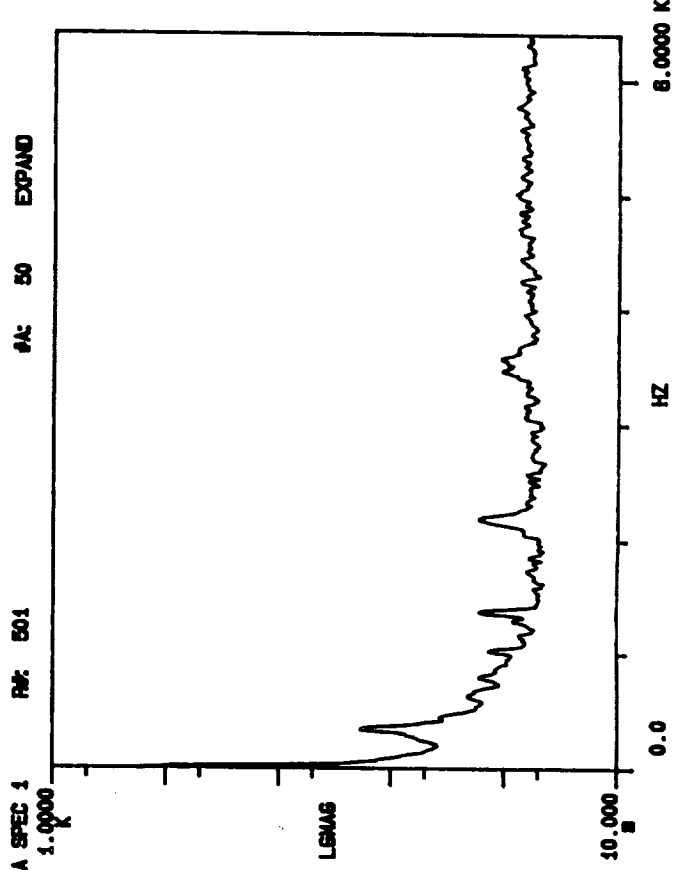
INGERSOLL-RAND 312801
 NON-ASYCHRONOUS SPECTRA
 CONFIGURATION A
 IMPELLER #5 FOLW #4
 TAPE FOOT 855 TO 880



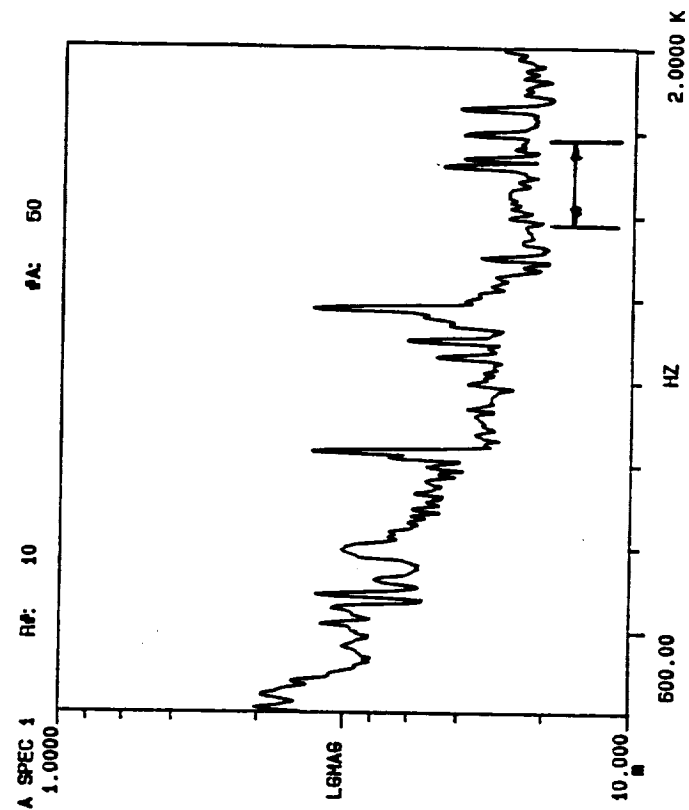
INGERSOLL-RAND 312801
 NON-SYNCHRONOUS SPECTRA
 CONFIGURATION B
 IMPELLER #5 FLOW #1
 TAPE FOOT 215 TO 230



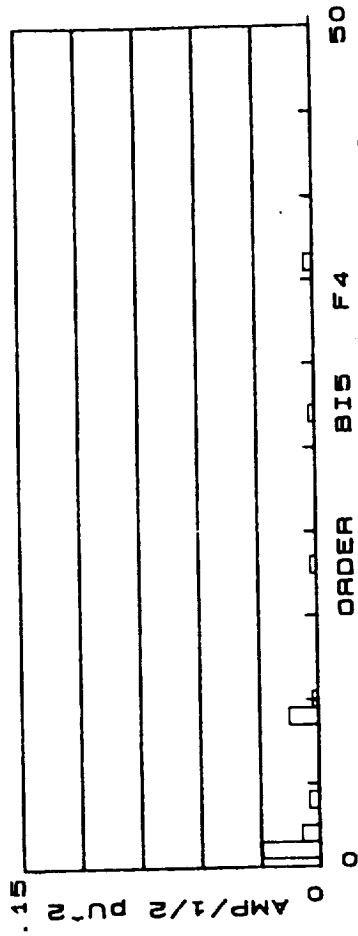
183



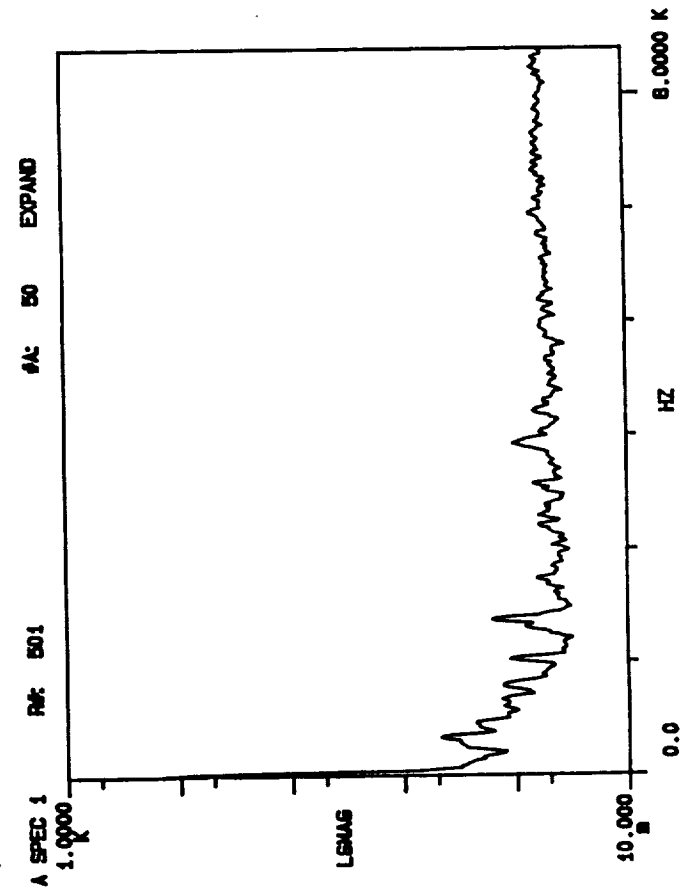
NSDS4088415F-1F8.4K30



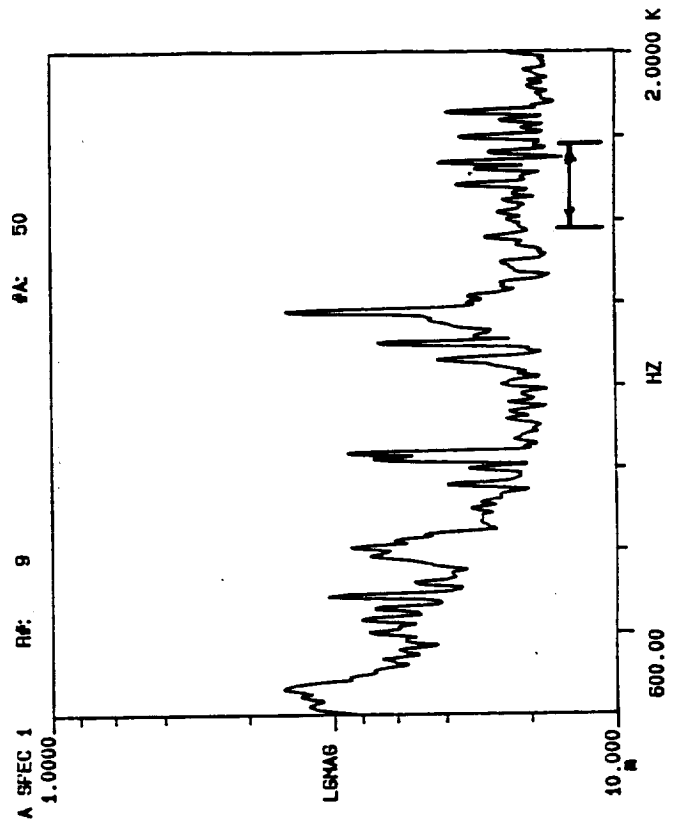
INGERSOLL-RAND 312801
 NON-SYNCHRONOUS SPECTRA
 CONFIGURATION B
 IMPELLER #5 FLOW #4
 TAPE FOOT 887 TO 904



184



NETS388B/F412F8.4K50



Pulsations Resulting From System Piping Resonance

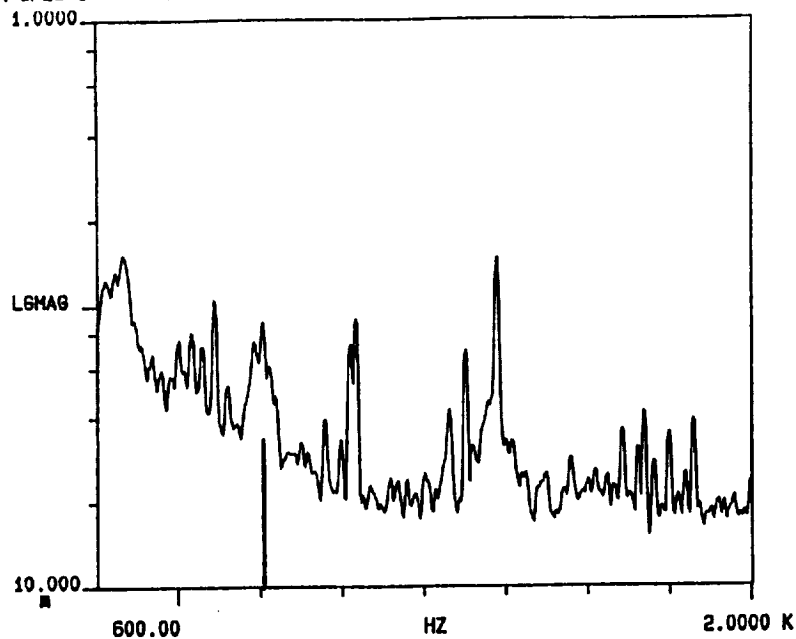
Locations: All Locations

Conditions: All Conditions

There appears around 800 hz on the spectra, a pulsation amplitude which is not related to rotation, impeller/diffuser interaction, sensor location or flow condition. This frequency may correspond to a piping resonance. A pipe length of 3 feet, undergoing a half-wave resonance would show pressure pulsation activity at 800 hz. This 800 hz resonance appears on all the plots shown. Pipes of 3 and 4 feet are mounted at the inlet and discharge of the pump, with ninety degree elbows attached to the end opposite the pump attachment.

A SPEC 1 R#: 9

#A: 50



INGERSOLL-RAND 312501

NON-SYNCHRONOUS SPECTRA

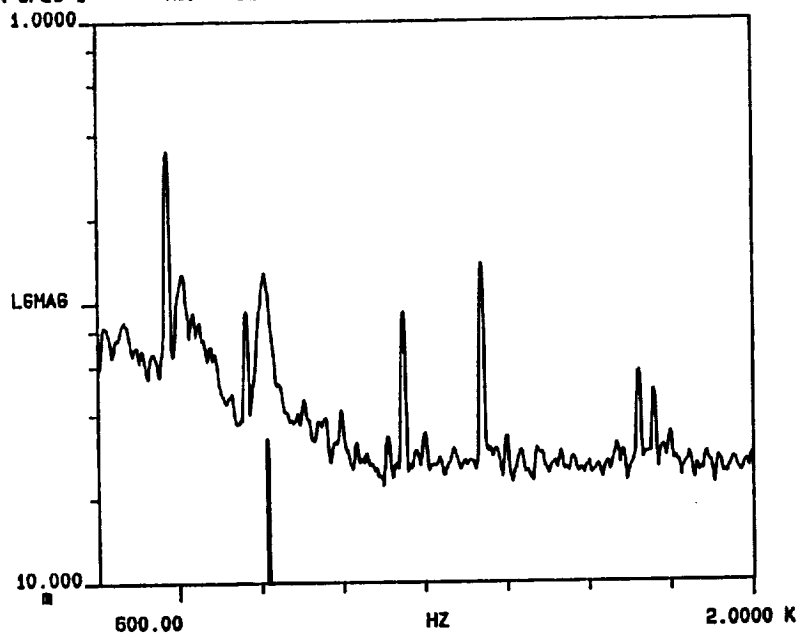
CONFIGURATION B

IMPELLER #5 FLOW #4

TAPE FOOT 887 TO 904

A SPEC 1 R#: 12

#A: 50



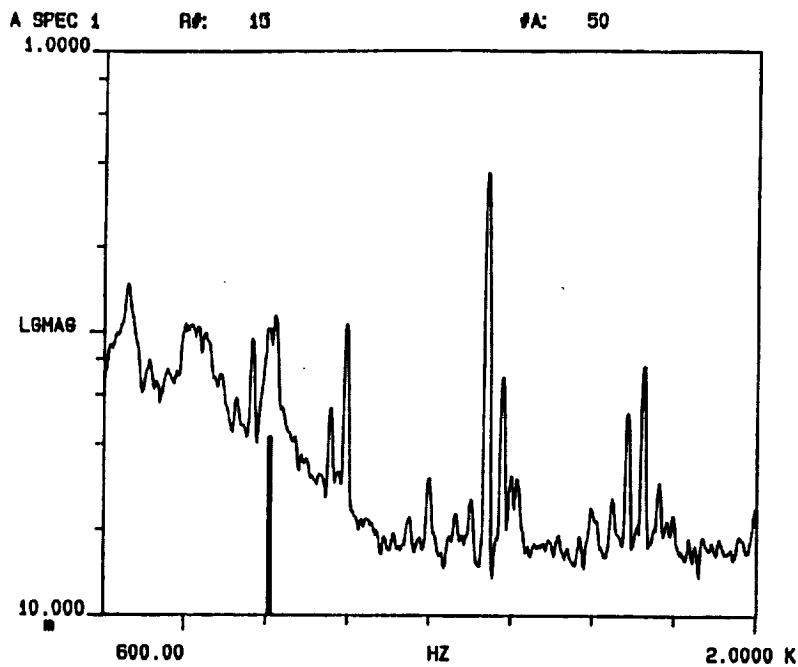
INGERSOLL-RAND 312501

NON-SYNCHRONOUS SPECTRA

CONFIGURATION B

INSD.PASSAGE #2 FLOW #4

TAPE FOOT 882 TO 896



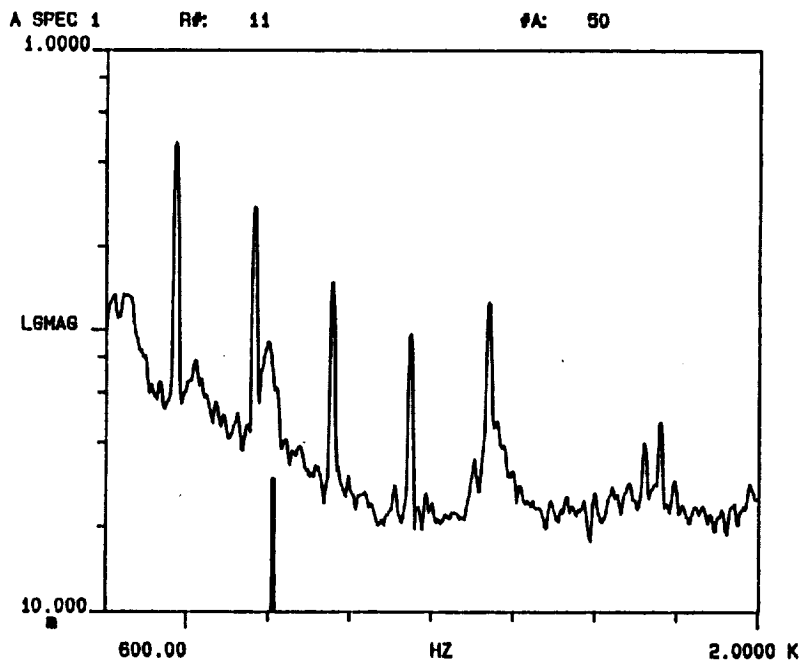
INGERSOLL-RAND 312801

NON-SYNCHRONOUS SPECTRA

CONFIGURATION B

SCROLL #7 FLOW #4

TAPE FOOT 886 TO 900



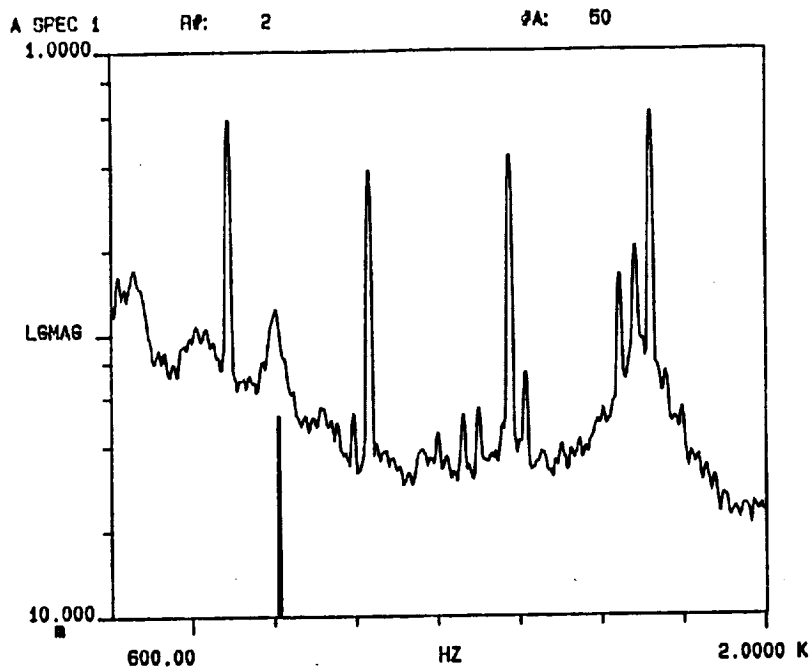
INGERSOLL-RAND 312801

NON-SYNCHRONOUS SPECTRA

CONFIGURATION B

DIFFUSER #1 FLOW #4

TAPE FOOT 882 TO 886



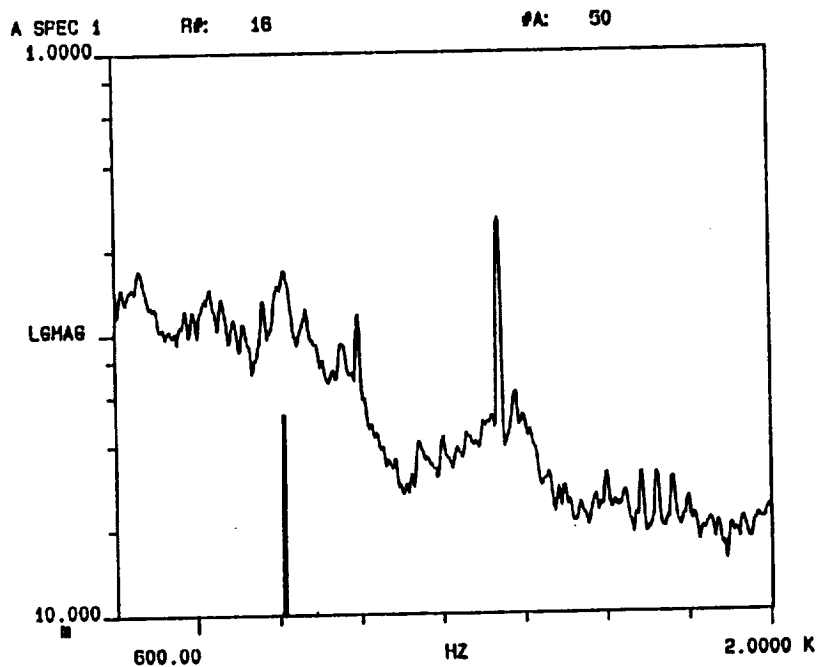
INGERSOLL-RAND 312801

NON-SYNCHRONOUS SPECTRA

CONFIGURATION A

IMPELLER #5 FLOW 1

TAPE FOOT 184 TO 187



INGERSOLL-RAND 312801

NON-SYNCHRONOUS SPECTRA

CONFIGURATION B

SCROLL #7 FLOW #1

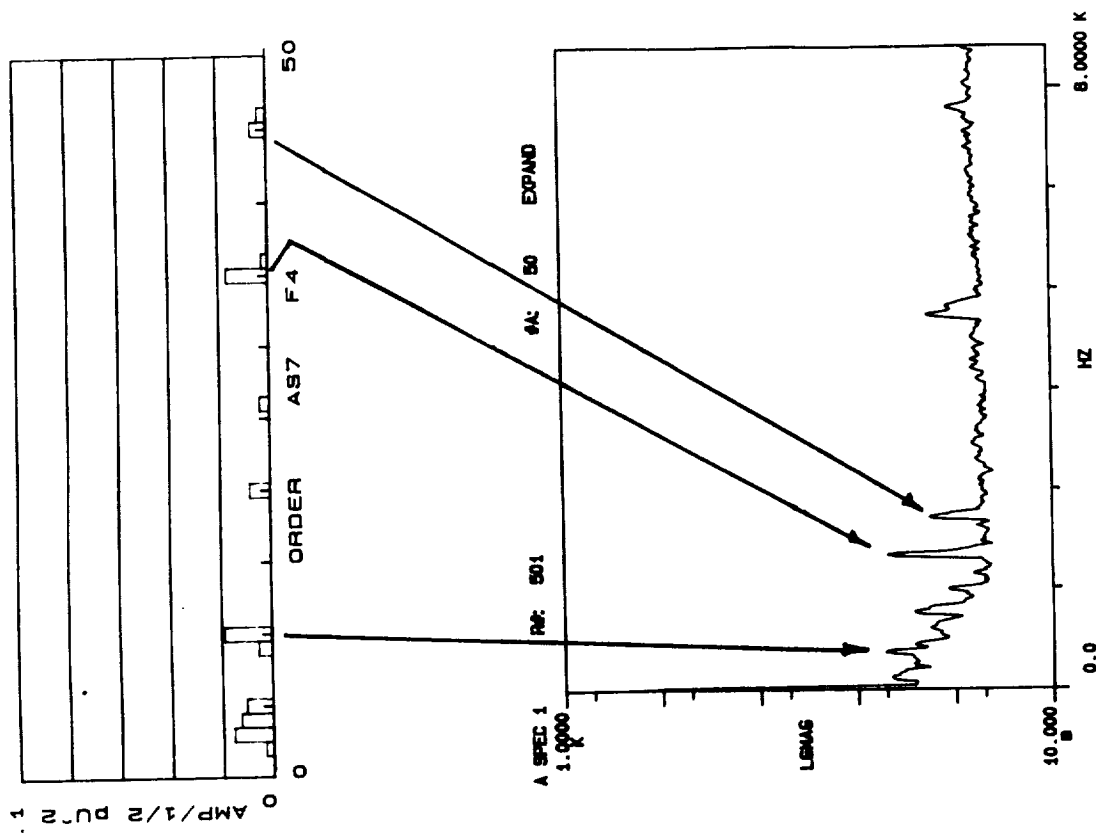
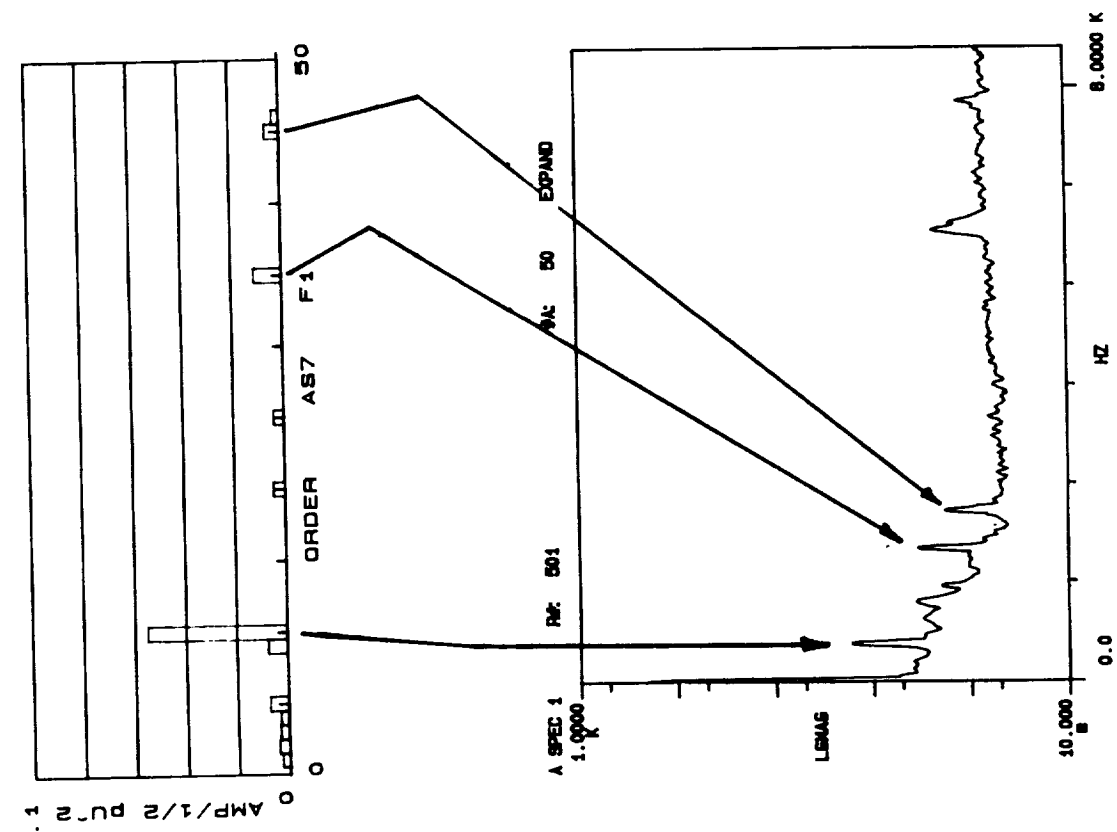
TAPE FOOT 215 TO 230

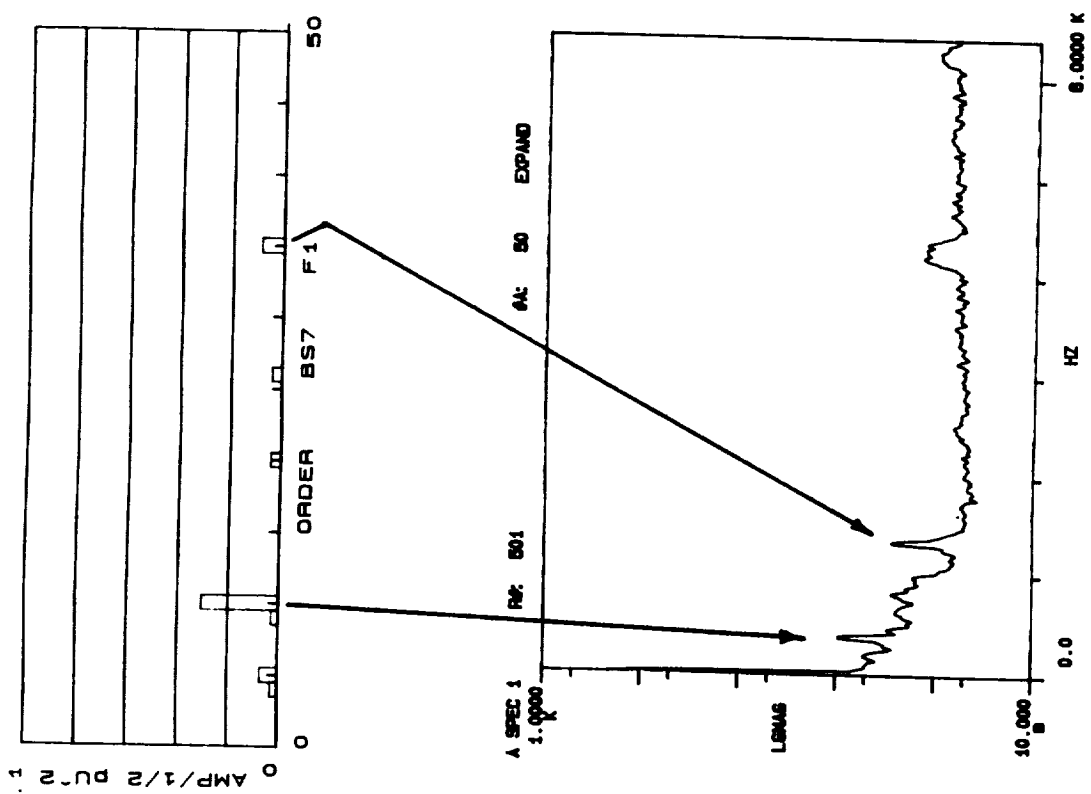
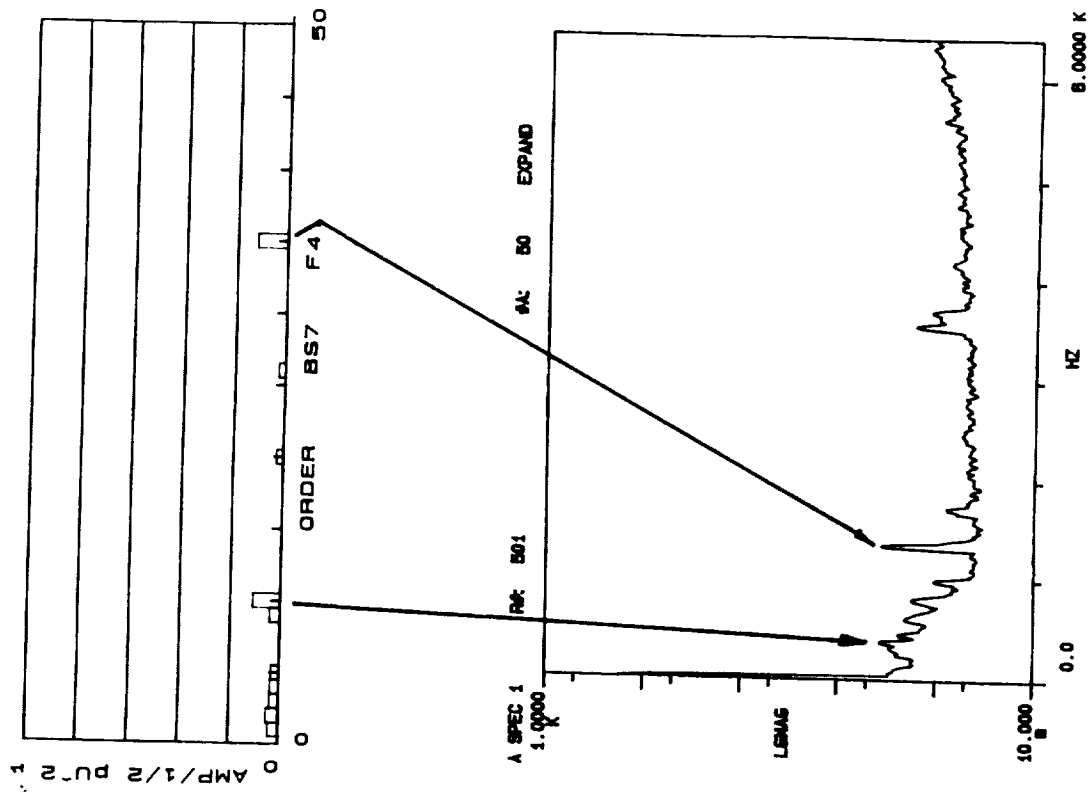
High Frequency Pulsation Activity in the Scroll

Locations: AS7, BS7

Conditions: F1, F4

Order related pulsation activity appears to be attenuated to levels not measurable with the test instrumentation. The following plots contain data for a scroll sensor operating at two flow rates and at two impeller to diffuser clearances. The top plot contains only order related information, and is a product of synchronous time averaging. All non-order related information is removed from this plot. The bottom plot is obtained from a free-running FFT spectrum analysis. It contains pulsation data (in a logarithmic, RMS psi amplitude scale) for both synchronous and non-synchronous phenomena. The scale for the bottom plot is logarithmic, and ranges from .01 to 1000 psi. It displays the data in half-amplitude, RMS values. To convert to peak-to-peak values in psi units, the value from the plotted scale must be multiplied by 2 and 1.414 (eg. 10th order from AS7, F1 1.6 psi x 1.414 x 2 = 4.52 psi peak-to-peak). The only activity observed on these bottom plots is a low level region of activity, less than .2 psi RMS and occurring between 3.6 and 4.5 KHz. It is believed that this pulsation is not related to the pump geometry, of any manner of fluid activity in the machine. After studying the behavior of sensors in the diffuser and impeller the conclusion was reached that this activity is due to the resonance of an air bubble trapped between the screen mesh and diaphragm of the transducer. The frequency is directly proportional to the change in local static pressure (for the same sensor, but observed at different flow rates).





CONCLUSIONS

The purpose of this test program has been to gain insight into the occurrence of pressure pulsations in a multistage centrifugal pump and identify areas of improvement for reducing the pulsation levels in the HPFTP. Detailed mapping of pressure pulsation activity in the elements of a diffuser pump stage of similar configuration to the SSME HPFTP was conducted. A total of three configurations were tested. The effects of geometrical changes on pressure pulsations within these three configurations, was documented. Conclusions based on this testing are split into two parts. First, the observations relating to the generic hardware tested will be described. Second, how these observations relate to the case of the HPFTP experience will be discussed.

Generic Configurations

1. The dominant pulsation activity is related to the interaction of impeller to diffuser vane passing. This leads to frequency components which are integer multiples of rotation frequency (also referred to as orders of running speed).
2. Maximum pulsation amplitudes occur at blade passing rate (which is true for stationary or rotating frame of reference) and at locations nearest the vane-to-vane interaction.

3. At locations farther away from the interaction (eg. the outer wall of the volute scroll), the dominant order of pulsation is the result of the summation of all the interactions which occur in the pump. This order is not necessarily the direct vane passing frequency.
4. A simple technique may be used to determine the synchronous pulsation frequency components which result from the impeller to diffuser interaction (Ref 2.)
5. The peak-to-peak pulsation levels in the scroll were never found to exceed 7% of the impeller exit velocity head (ie. $\Delta P / (\rho U_2^2 / 2g)$).
6. Increasing the impeller to diffuser vane clearance (from 1.021 to 1.059) reduces the pulsation level to a maximum of 5% of the impeller exit velocity head. Increase of the number of diffuser vanes (resulting in less diffusion and decreased vane loading) drops the scroll pulsation levels to a still lower level of 2%.
7. The maximum pulsation levels in the scroll were found to occur as the minimum flow condition of 25% of design point. Increasing the flow causes a reduction in peak-to-peak amplitudes in the scroll.
8. Pulsations dominated by the vane passing frequency (and measured near the area of the vane to vane interaction) are at a minimum when the flow is at or near the design flow condition. Pulsation levels increase as flow is either increased or decreased from the design point.

9. Highest peak-to-peak pressure pulsations were measured on the pressure surface of the impeller vane, at 25% flow and were 28% of the impeller exit velocity head. This occurred in the configuration with the closest clearance ratio. By increasing the clearance ratio from 1.021 to 1.059, this amplitude was reduced to 15% of the exit velocity head. Increased diffuser vane number also reduced the pulsation amplitudes.

10. Pressure pulsations measured in the impeller and diffuser, at different speeds (but at similar flow conditions) follow the affinity laws ($\Delta P \propto U_2^2$). Some pulsation levels measured in the scroll appear to deviate from the affinity laws. This is most likely due to resolution in the data collection and reduction process of the low level amplitudes in the scroll.

11. An impeller shroud resonance is responsible for a low level pulsation amplitude measured on the impeller side shroud. This structural resonance is excited by the synchronous pulsation activity generated by the impeller/diffuser vane interactions. The resonance changes from 1700 Hz to 2100 Hz when the impeller diameter is reduced.

12. A piping resonance of about 800 Hz is excited by the pulsations in the pump. The amplitude as measured in the pump is only about 2% of the impeller exit velocity head.

13. A rotating stall was observed in the vaned diffuser. The stall (with variations of pressure levels in the diffuser of 20% of the impeller exit velocity head) does not completely rotate from each passage to the next.

The stall moves between 5 or 6 adjacent passages. These were not the same 5 or 6 passages. For this reason, it is termed a quasi-rotating stall. The effective frequency of rotation (assuming a complete rotation) would be between 4 - 6 Hz. This phenomenon occurred only on the configurations with the largest clearance ratios (1.059 and 1.047). The close clearance configuration (A), did not exhibit this behavior. This quasi-rotating stall is observed only at the 25% flow condition.

14. Impeller passage stall occurs at the 25% flow condition. The passages stall randomly, and for a duration of 2 to 4 shaft revolutions before positive flow is resumed. This event signifies fully developed backflow (also known as suction recirculation) in that particular passage. The condition is not uniform for all passages.

15. Significant non-order and/or order related pulsation activity was not found above the 50th order of rotation.

SSME HPFTP Configuration

1. The HPFTP uses 13 diffuser vanes in its final stage, and a total of 24 exit impeller vanes (half of which are quarter blade length splitters). The following interaction table (generated in the same manner as Table 5) indicates that this is a favorable combination of vane numbers for avoiding synchronous pulsation problems (Ref 2.).

		Impeller Vane # Multiple		
		24	48	72
Diffuser	13	11	35	59
Vane #	26	<u>2</u>	22	46
Multiple	39	15	9	33

This conclusion is based on the premise that the 12 impeller exit splitter vanes are effective at sharing the blade loading with the longer impeller vanes. If separation has occurred in the impeller passage upstream of the splitters, the splitters will not be effective. An impeller operating with 12 effective blades would have an interaction table as follows.

		Impeller Vane # Multiple		
		12	24	36
Diffuser	13	<u>1</u>	11	23
Vane #	26	14	<u>2</u>	10
Multiple	39	27	15	3

This condition is more severe than that encountered in the generic testing (since a 1 value in the first column indicates pulsation activity at the 12th order of rotation).

2. The scroll mismatch to the diffuser exit causes the flow in the scroll to decelerate in front of the throat causing a circumferential variation of pressure around the OD. of the diffuser. This fact, along with the scroll cutwater extension to a diffuser vane which "seals" one possible pressure relief path, could lead to unsteady flow in the scroll. This

situation was not completely simulated in this test program (the generic hardware was never intended to accurately simulate the HPFTP case). Radial holes drilled in the HPFTP scroll liner and communicating to a common pressure chamber surrounding the liner may help to alleviate any pressure imbalance caused by any mismatch. The effectiveness of these holes is unknown.

3. The resonance of mechanical structures, excited from forces caused by pressure pulsations, introduces alternating mechanical stresses in the component. Large amplitudes and number of cycles can cause fatigue of the material and failure of the component. The possibility exists that pulsations, possibly of low amplitude, occur at frequencies close enough to a structural natural frequency of the HPFTP scroll liner, to cause significant alternating stresses and eventual material fatigue (especially in the locations where the liner fabrication has resulted in a weld seam). The excitation forces on the liner may be the result of low level pulsations acting in both interior and exterior surfaces of the liner. The circumferential balance holes can act as filters to the pulsations in the interior flow passage. Pulsations reaching the other side of these holes may be out of phase. Out of phase pulsations, acting on both surfaces of the liner, will deliver larger fluctuation of forces than would be encountered if pulsation activity occurs only on the through-flow side.

4. The operating conditions of the HPFTP require it to cover a wide flow range. Being a variable speed, turbine driven pump, the range of flow covered ($Q_{\max}/Q_{\min}=1.5$) is accomplished over a 1.33:1 speed ratio.

This means that at minimum flow, the pump is at only 85% of its design point, and at maximum flow (109% Thrust), the pump is at 101% of its design flow (refer to Figure 3.) The change in flow as a percent of design point flowrate is small. This means that the changes in impeller and diffuser blade loading, and incidence effects (all important in the generation of pressure pulsations) are also small. The testing conducted on the generic hardware covers a wide ratio of Q_{\min}/Q_{\max} , but at a constant speed. Large variations in pulsation activity were encountered in this testing due the changing flow conditions. The HPFTP will not encounter this type of flow variation, but it will encounter a 6.1% increase in speed when moving from the 100% thrust to the 109% thrust condition. Based on the test results of the generic hardware, the pulsation amplitudes and scalability of those pulsations encountered at the 100% thrust condition will increase by a factor of 1.125. Some synchronous activity will be present in the HPFTP at its design point. The severity of these pulsations is dependent on which of the two interaction tables, shown above in Item 1 of this conclusions list, is correct. Any pulsations present at 100% thrust, will be scaled up by a factor of 1.125 when the pump is required to operated at 109% thrust. Further increases in thrust, and hence operating speed and flow rate, will increase the pulsation amplitude even more.

REFERENCES

1. Kanki, H., Kawata, Y., Kawatani, T., "Experimental Research in the Hydraulic Excitation Force on the Pump Shaft." Presented at Design Engineering Technical Conference, September 20-23, 1981, Hartford, Conn., ASME (81-DET-71).
2. Bolleter, U., "Blade Passage Tones of Centrifugal Pumps." Vibrations, Vol 4, No. 8, September, 1988.
3. Sano, M., "Reduction of Pressure Pulsations in Pumps and Piping Systems."
4. Iino, T., "Potential Interaction Between a Centrifugal Impeller and a Vaned Diffuser." In Fluid/Structure Interactions in Turbomachinery, ASME, 1981, pp. 63-69.
5. Brennen, C.E., Franz, R., Arndt, N., "Rotor/Stator Unsteady Pressure Interactions." Proceedings of Advanced Earth-to-Orbit Propulsion Technology Conference, 1988, NASA Conference Publication 3012.
6. Sloteman, D.P., Cooper, P., Leon, R., "Fluctuating Pressures in Pump Diffusers and Collector Scrolls." Proceedings of Advanced Earth-to-Orbit Propulsion Technology Conference, 1988, NASA Conference Publication 3012.
7. McFarland, E.R., "Solution of Plane Cascade Flow Using Surface Singularity Methods." For The Twenty-sixth Annual International Gas Turbine Conference, Houston, Texas, March 8-12, 1981, Sponsored by ASME, Paper No. 81-GT-169.

Fluctuating Pressures
in
Pump Diffuser
and
Collector Scrolls

Part II
Appendices

Final Report

NASA Contract Number
NAS8-36223

By

Donald P. Sloteman

Ingersoll-Rand Company
Research & Development Department
Pump Group
942 Memorial Parkway
Phillipsburg, New Jersey 08865

Prepared for George C. Marshall Space Flight Center
Marshall Spaceflight Center, Alabama 35812

June 1989

APPENDIX A

LITERATURE SEARCH

Furst, R.: "Experimental Evaluation of Diffusing Crossover Systems for a High-Pressure Liquid Hydrogen Pump." In Return Passages of Multi-Stage Turbomachinery; ASME, 1983, pp. 45-52.

Rothe, K.: "Turbopump Configuration Selection for the Space Shuttle Main Engine." ASME Paper No. 74-FE-23, 1974.

Childs, D.W.: "The Space Shuttle Main Engine High-Pressure Fuel Turbopump Rotodynamic Instability Problem." Transactions of the ASME, Journal of Engineering for Power, Vol. 100, pp. 48-57, Jan. 1978.

Ek, M.C.: "Solution of the Sybsynchronous Whirl Problem in the High Pressure Hydrogen Turbomachinery of the Space Shuttle Main Engine." AIAA/SAE 14th Joint Propulsion Conference, Las Vegas, July 1978, Paper No. 78-1002 (AIAA.)

Chamieh, D. S.: "Forces on a Whirling Centrifugal Pump Impeller." Ph.D. thesis, Division of Engineering and Applied Science, California Institute of Technology, Pasadena, California, 1983.

Fischer, K., and Thoma, D.: "Investigation of the Flow Conditions in a Centrifugal Pump." Transactions of the ASME, Vol. 54, 1932, pp. 141-155.

Lorett, J.A., and Gopalakrishnan, S.: "Interaction Between Imepller and Volute of Pumps at off-Design Conditions." Transactions of the ASME, Journal of Fluids Engineering, Vol. 108, March 1986, pp. 12-18.

Iino, T.: Sato, H.: and Miyashiro, H.: "Hydraulic Axial Thrust in Multistage Centrifugal Pumps." ASME Paper 78-WA/FE-12, 1978.

Dussourd, J.L.: "An Investigation of Pulsations in the Boiler Feed System of a Central Power Station." Transactions of the ASME, Journal of Engineering for Power, December 1968, pp. 607-619.

Iino, T.: "Potential Interaction Between a Centrifugal Impeller and a Vaned Diffuser." In Fluid/Structure Interactions in Turbomachinery, ASME, 1981, pp. 63-69.

Cooper, P., and Kraft, D. W.: "Hydraulic Design of High Speed Inducer Pumps." Presented at the 60th Annual Conference of the Pacific Energy Association, Anaheim, California, October 16, 1985.

Rothe, P.J. and Runstadler, P.W., Jr.: "First Order Pump Surge Behavior." ASME Paper 77-WA/FE-12, 1977.

Cooper, P.; Dussourd, J. L., and Sloteman, D. P.: "Stabilization of the off-Design Behavior of Centrifugal Pumps and Inducers." Proceedings of the Second European Congress on Fluid Machinery for the Oil, Petrochemical and Related Industries, I. Mech. E., The Hague, March 1984.

Brennen, C., and Acosta, A.J.: "The Dynamic Transfer Function for a Cavitating Inducer." Transactions of the ASME, Journal of Fluids Engineering, Vol. 98, 1976, pp. 182-191.

Murakami, M.; Kikuyama, K.; and Asakura, E.: "Velocity and Pressure Distributions in the Impeller Passages of Centrifugal Pumps." In Measurement Methods in Rotating Components of Turbomachinery, ASME, 1980, pp. 81-89.

Jackson, E.D.: "Final Report, Study of Pump Discharge Pressure Oscillations." Rocketdyne Report R-6693-2, NASA Contract NAS8-20143, October 1966.

Blom, C.: "Development of the Hydraulic Design for the Grand Coulee Pumps." Transactions of the ASME, January 1950, pp. 53-70.

Kovats, A.: "Effect of Non-Rotating Passages on Performance of Centrifugal Pumps and Subsonic Compressors." In Flow in Primary Non-Rotating Passages in Turbomachines, ASME, 1979, pp. 1-14.

Kasztejna, P.J., and Cooper, P.: "Experimental Study of the Influence of Backflow Control on Pump Hydraulic-Mechanical Interaction." Proceedings of the Second International Pump Symposium, Houston, Texas, Texas A&M University, Sponsor, April 1985, pp. 33-40.

Fritsch, T.J.: "World's Largest Boiler Feed Pump." Presented at the 36th Annual Meeting of the American Power Conference, May 1, 1974.

Makay, E., and Szamody, O.: "Survey of Feed Pump Outages." EPRI FP-754, April 1978.

Cooper, P.; and Antunes, F.: "Cavitation Damage in Boiler Feed Pumps." Proceedings of EPRI Symposium on Power Plant Feed Pumps, held at Cherry Hill, New Jersey on June 2-4, 1982.

- Sloteman, D.P.; Cooper, P., and Dussourd, J. L.: "Control of Backflow at the Inlets of Centrifugal Pumps and Inducers." Proceedings of the First International Pump Symposium, Houston, Texas, Texas A&M University, Sponsor, May 1984, pp. 9-22.
- "Variable Capacity Centrifugal Pump Developed." Navy Fact Sheet, Vol. 11, No. 2, February 1986.
- Yang, T.T., et al: "An Improved Design Method and Experimental Performance of Two-Dimensional Curved Wall Diffusers." NASA CR 121024, Nov. 1972.
- Yoshinaga, Y., et al: "Aerodynamic Performance of a Centrifugal Compressor with Vaned Diffusers." In Flow in Primary, Non-Rotating Passages in Turbomachines, ASME, 1979, pp. 33-40.
- Makay, E., and Barrett, J.A.: "Changes in Hydraulic Component Geometries Greatly Increased Power Plant Availability and Reduced Maintenance Cost: Case Histories." Proceedings of the First International Pump Symposium, Houston, Texas, Texas A&M University, Sponsor, May 1984, pp. 85-97.
- Abdelhamid, A.N.: "Analysis of Rotating Stall in Vaneless Diffusers of Centrifugal Compressors." ASME Paper No. 80-GT-184.
- Nelik, L., and Cooper, P.: "Performance of Multi-Stage Radial-Inflow Hydraulic Power Recovery Turbines." ASME Paper No. 84-WA/FM-4.
- Phelan, J.J.; Russell, S.H. and Zeluff, W.C.: "A Study of the Influence of Reynolds Number on the Performance of Centrifugal Fans." ASME Paper 78-WA/PTC-3, 1978
- Stepanoff, A.J.: Centrifugal and Axial Flow Pumps. Second Edition, Wiley, 1957, p. 315.
- Eyen, J.J.: "The Application of Centrifugal Pumps for CO₂ Pipeline and Injection Services." Presented at the 1986 American Petroleum Institute Pipeline Conference, Houston, Texas, April 14-15, 1986.

4/5/1

187786 PA

Experimental research of the radial force on the centrifugal pumps. (1st report, influence of the impeller vane number and the casing type).

Kawata, Y.; Kanki, H.; Kawakami, T.

Mitsubishi Heavy Ind. Ltd.

Trans. Japan Soc. Mech. Engrs. Ser. C, vol.49, no.437, Jan. 1983, p.31-38. , ISSN 0387-5024

Languages: Japanese

Experimental test results to clarify hydraulic radial thrust on the pump impeller are described about a rotor dynamic analysis of the pump design stage. The tests were carried out on typical centrifugal pumps by applying highly advanced measuring techniques. The test pumps were end suction single stage type. Their impellers have 6 vanes and 7 vanes with double volute and vaned diffuser casings. The test results showed a fairly small static radial force and a large dynamic force at low flow rate. The dynamic force was mainly composed of low cycle component and vane passing frequency component. This experimental study gave a clear quantitative idea of the static and dynamic radial forces of the pump impeller. (from English abstract)

Section Heading Codes: P17

4/5/34

016008 PA (Pumps And Other Fluids Machinery Abstracts)

LH/SUB 2/ PUMP COMPONENT DEVELOPMENT TESTING IN THE ELECTRIC PUMP ROOM AT TEST CELL 'C' INDUCER NO. 1.

ANDREWS, F.X.; BRUNNER, J.J.; KIRK, K.G.; MATHEWS, J.P.; NISHIOKA, T.

AEROJET - GENERAL CORP.

NASA CR-132 232, 400 PP. %MAY, 1972<.,

Languages: English

THE NERVA ENGINE DICTATES THE TURBOPUMPS WITHIN THE SYSTEM SHALL HAVE CERTAIN CHARACTERISTICS.

TO ASCERTAIN THE PERFORMANCE OF THE PUMP CHARACTERISTICS AND TO IDENTIFY ANY PROBLEMS ASSOCIATED WITH ITS PERFORMANCE, EARLY COMPONENT TESTING OF VARIOUS PUMP CONFIGURATIONS WAS DESIRABLE AND WAS ACCOMPLISHED TO SUPPORT THE DESIGN SELECTION OF THE PUMP FOR THE NERVA TURBOPUMP.

THE NERVA PUMP IS A TWO STAGE CENTRIFUGAL PUMP WITH BOTH STAGES HAVING BACKSWEEP IMPELLERS AND AN INDUCER UPSTREAM OF THE FIRST STAGE IMPELLER. THE COMPONENT TESTS CONDUCTED AT TEST CELL 'C' INVESTIGATED THE PERFORMANCE OF THE FIRST STAGE COMPONENTS.

THE FIRST STAGE CONFIGURATION TESTED CONSISTED OF AN INDUCER, IMPELLER AND A VANED DIFFUSER FOLLOWED BY A PUMP VOLUTE. THE TEST PROGRAM PROVIDED DEMONSTRATION OF THE ABILITY OF THE DESIGN SELECTED FOR THE NERVA TURBOPUMP TO MEET THE REQUIREMENT IMPOSED BY THE NERVA ENGINE.

%FROM AUTHORS' INTRODUCTION<.

P875F)

Descriptors: PUMPS-CENTRIFUGAL, FIRST STAGE INDUCER/IMPELLER/DIFFUSER/VOLUTE TESTING; TEST RIGS; INSTRUMENTATION; MEASUREMENT TECHNIQUES; FUEL SYSTEMS; LIQUID HYDROGEN; CRYOGENICS; ROCKET ENGINES; PUMPS-TURBINE; INDUCERS; DIFFUSERS; CASINGS-VOLUTE

Section Heading Codes: P17

?

ORIGINAL PAGE IS
OF POOR QUALITY

4/5/81
047942 PA

How to avoid field problems with boiler feed pumps
Makay, E.

Energy Res. & Consult. Corp.

Hydrocarbon Process., vol.55, no.10, Dec. 1976, pp.79-84. ,

Languages: English

Hydraulically induced forces are sizeable and can influence rotor and bearing design requirements, can change rotor stability and the appearance of the pump rotor critical speeds (from jnl.). Sections of the article consider: radial or axial rotor response; hydraulic instability; pump efficiency; diffuser versus volute type pumps; seals; balancing devices; bearings, rotor dynamics, oil whip, friction induced whirl; radial hydraulic forces; standards; vibration; pressure pulsation; safe operating ranges; what can factory test tell about future problems?

Descriptors: centrifugal; pumps; impellers; forces; loads; testing; labyrinth; seals; off-design; secondary; flow; stall

4/5/6

0618970 E.I. Monthly No: EI7704023896 E.I. Yearly No: EI77031060

HOW TO AVOID FIELD PROBLEMS WITH. . . BOILER FEED PUMPS.

Makay, Elemer

Energy Res & Consult Corp, Morrisville, Pa

Hydrocarbon Processing v 55 n 12 Dec 1976 p 79-84

CODEN: HYPRAX ISSN: 0018-8190

Language: ENGLISH

As sizes of power generating facilities grow, the unexpected and unexplained number of large pump failures or pump-caused system operating difficulties also grows. As one begins to pay closer attention to these problems, it becomes clear that a large percentage of failures can be traced to rotor instability, occurring especially in the low percent flow regimes; in particular, in the minimum flow mode. Pump problems, as well as pump-caused feed water system problems in petroleum refineries are discussed in this paper. The discussion is done under headings -- radial or axial rotor response; hydraulic instability; pump stage geometry; pump efficiency; diffuser vs. volute type pumps; seals; balancing devices; bearings, rotor dynamics, oil whip, friction induced whirl; radial hydraulic forces; standards; vibration; pressure pulsation; safe operating ranges; factory tests and future problems.

Descriptors: *FEEDWATER PUMPS--*Failure; PETROLEUM REFINERIES--Equipment

Classification Codes: 513 (Petroleum Refining); 618 (Compressors & Pumps)

51 (PETROLEUM ENGINEERING); 61 (PLANT & POWER ENGINEERING)

4/5/7

0561292 E.I. Monthly No: EI7608055290 E.I. Yearly No: EI76062104

VOLUTES AND VANED DIFFUSERS FOR CENTRIFUGAL PUMPS.

Metwally, G. Maged; Gahin, S.

Paisley Coll of Technol, Scotl

Conf on Fluid Mach, 5th, Proc, Budapest, Hung, 1975 v 2 p 649-660. Publ by Akad Kiado, Budapest, Hung, 1975

Language: ENGLISH

A simple systematic design of pump volute is formulated. Vaned diffusers with negative deflection are considered. The performance of variable combinations of volute with vaned and vaneless diffusers is illustrated. 2 refs.

Descriptors: *PUMPS, CENTRIFUGAL--*Diffusers

Classification Codes: 618 (Compressors & Pumps)

61 (PLANT & POWER ENGINEERING)

ORIGINAL PAGE IS
OF POOR QUALITY

4/5/14

113701 PA

Experimental research on the hydraulic excitation forces on the shaft.

Kanki, H. ; Kawata, Y. ; Kawatani, T.

Mitsubishi Heavy Ind.Ltd.

Am. Soc. Mech. Engrs.

New York, U.S.A., Am. Soc. Mech. Engrs., Sep. 20-23, 1981, 9p. (ASME Paper No. 81-DET-71) , Coden: ASMSA4 ISSN 0402-1215

Languages: English

Results of experiments on the hydraulic exciting forces on centrifugal pump impellers are reported. The model pumps used in the tests were end suction single stage types with six or seven vaned impellers and double volute or vaned diffuser casings. Static and dynamic radial forces and pressure measurements were obtained. (N.G.G.)

Descriptors: rotodynamic pump

Section Heading Codes: P17

4/5/3

173576 PA

Dynamic interactions in pumps and turbines.

Schneck, R.J.

Virginia Univ.

Virginia Univ.

In: Vibrations in Pumps & Hydraulic Turbines, (Charlottesville, U.S.A.: Aug. 20-22, 1984), Charlottesville, U.S.A., Virginia Univ., 1984, Session D, 33p. ,

Languages: English

Dynamic interactions within the turbomachine are considered for two particular cases. Firstly between the rotor and its high pressure component for example the diffuser, volute or spiral casing etc. and secondly between the rotor and its low pressure component such as the inlet duct, draft tube, tailrace etc. The nature of such interactions and visible consequences are described and it is shown that the first situation is more difficult for pumps whilst the second is so for turbines. (P.J.8.)

Section Heading Codes: P3

4/5/4

146287 PA

Effect of the downstream environment geometry of the impeller on the characteristics of partial flow volume pumps.

Caignaert, G.

Soc. Hydrotech. France

In: Fonctionnement des Turbomachines a Debit Partiel, (Partial Flow Volume Turbomachines Operation), (Paris, France: Nov. 18-19, 1981), vol. 1, Paris, France, Soc. Hydrotech. France, 1981, 12p. (Comite Tech. Session No. 119) ,

Languages: French

Tests on single-volute and bladed-diffuser centrifugal machines reveal the effects of various geometric parameters of the kinetic energy recuperator on the partial flow volume characteristics, although the parameters concerned hardly vary from each other. The importance of relative radial gap DELTA , the volute end or the diffuser profile radius r, the nose section S SUB g or A SUB dz SUB 3b SUB 3 and the inlet angle, are supplemented by the effect of the diffuser casing (radial gap, lateral spaces, alignment or otherwise of the diffuser and the impeller). Further tests are being analysed by the S.H.F. No. 1 Working Party, in particular various results for a single impeller with widely differing downstream configurations (volute and diffuser, etc.), as a contribution to the study of the various physical phenomena, especially at the coupling between the impeller and the downstream components. (R.H.)

Section Heading Codes: P17

ORIGINAL PAGE IS
OF POOR QUALITY

4/5/1

1529210 E.I. Monthly No: EI8509082422 E.I. Yearly No: EI85092541
CENTRIFUGAL PUMPS - HYDRAULIC DESIGN.

Anon

Inst of Mechanical Engineers, Power Industries Div, London, Engl
I Mech E Conf Publ 1982-11, Centrifugal Pumps - Hydraul Des, London,
Engl, Nov 16 1982. Publ by Mechanical Engineering Publ Ltd, Bury St.
Edmunds, Engl for Inst of Mechanical Engineers, London, Engl, 1982 88p

CODEN: IMEPD4 ISSN: 0144-0799 ISBN: 0-85298-493-6

For individual papers see E.I. Conference No.: 03397 in file 165

Language: ENGLISH

Document Type: CP; (Conference Proceedings) Treatment: T; (Theoretical)
; X; (Experimental)

The seven papers in this conference present the opinions of a number of engineers on hydraulic design techniques for centrifugal pumps of three different types: radial diffuser, end section volute pump, and mixed flow bowl pump. The designers give their detailed opinions on the design of the pumps and their predictions of expected performance. Technical and professional papers from this conference are indexed and abstracted with the conference code no. 03397 in the Ei Engineering Meetings (TM) database produced by Engineering Information, Inc.

Descriptors: *PUMPS, CENTRIFUGAL--*Design; HYDRAULIC MACHINERY--Design;
TURBOMACHINERY; FLOW OF FLUIDS; FLUID DYNAMICS; CAVITATION

Identifiers: IMPELLER INLET DESIGN; FREE VORTEX APPROACH; AREA RATIO
METHOD; PERFORMANCE PREDICTION; EIREV

Classification Codes: 618 (Compressors & Pumps); 632 (Hydraulics & Pneumatics)

61 (PLANT & POWER ENGINEERING); 63 (FLUID DYNAMICS & VACUUM TECHNOLOGY)

ORIGINAL PAGE IS
OF POOR QUALITY

4/5/18

107921 PA

Enlarged radial gap in feed pumps: a remedy with minimal side effects.

Makay, E.

Energy Res. & Consult. Corp.

Power, vol.125, no.3, Mar. 1981, p.76-77. , Coden: POWEAD ISSN
0032-5929

Languages: English

The advantages of increasing impeller/diffuser or impeller/volute distance to reduce internal damage to feed pumps are described. (C.W.)

Descriptors: cavitation; impeller; volute; diffuser; centrifugal pump

Section Heading Codes: P10

4/5/19

106000 PA

Flow visualisation studies and the effect of tongue area on the performance of volute casings of centrifugal machines.

Yadav, R. ; Yahya, S.M.

M.N.R. Engng. Coll. Indian Inst. Technol., New Delhi

Int. J. Mech. Sci., vol.22, no.10, 1980, p.651-660. , Coden: IMSCAW
ISSN 0020-7403

Languages: English

The present paper deals with flow visualization studies and the effect of tongue area on the performance of the volute casings of centrifugal machines with a swirling flow free from jets and wakes at their inlet. The flow visualization studies by wool tuft movements were conducted in the volute channel as well as in the exit diffuser and interpreted according to Moore and Kline. Flow separation was observed at high inlet swirl angles near the volute tongue as well as in the exit diffuser. It was found that the volute performance was strongly dependent on the tongue area at low and high inlet swirl angles. (A)

Descriptors: centrifugal pump

Section Heading Codes: P17

4/5/20

098859 PA

Centrifugal pump hydraulic instability. Final report.

Makay, E.

Energy Res. & Consult. Corp.

Morrisville, U.S.A., Energy Res. & Consult. Corp., Jun. 1980, 72p.
(EPRI-CS-1445) ,

Languages: English

The principal objective was to define the causes of hydraulic instability in boiler feed pumps ; explain their origins, and relate them to the geometries of a pump stage (e.g. inlet, impeller, diffuser or volute). The approach is to examine the influence of each component of pump geometry on the flow path and flow mechanisms and thus estimate the magnitudes and directions of hydraulically-induced forces on a pump rotor which influence dynamic response, pump performance, and critical speeds. The techniques and results of experiments on pump hydraulic forces are described and assessed to explain common frequency ranges. A method is developed for calculating radial hydraulic forces in a pump. The hydraulic mechanisms at work are listed, described, and related in turn to specific elements of pump stage geometry. Forces for the case in which the impeller is replaced with a solid mass are estimated. Recommendations are given for future work to measure and characterize the forces in various types of pump geometry. Two important findings are: (1) feedwater pumps must be designed for stable operation over the full range of possible flow rates, even at the cost of some reduction of efficiency at best operating point; and (2) the complexities of flow within a pump stage are such that every new design must be tested to determine its dynamic and performance characteristics over the full flow range. (A)

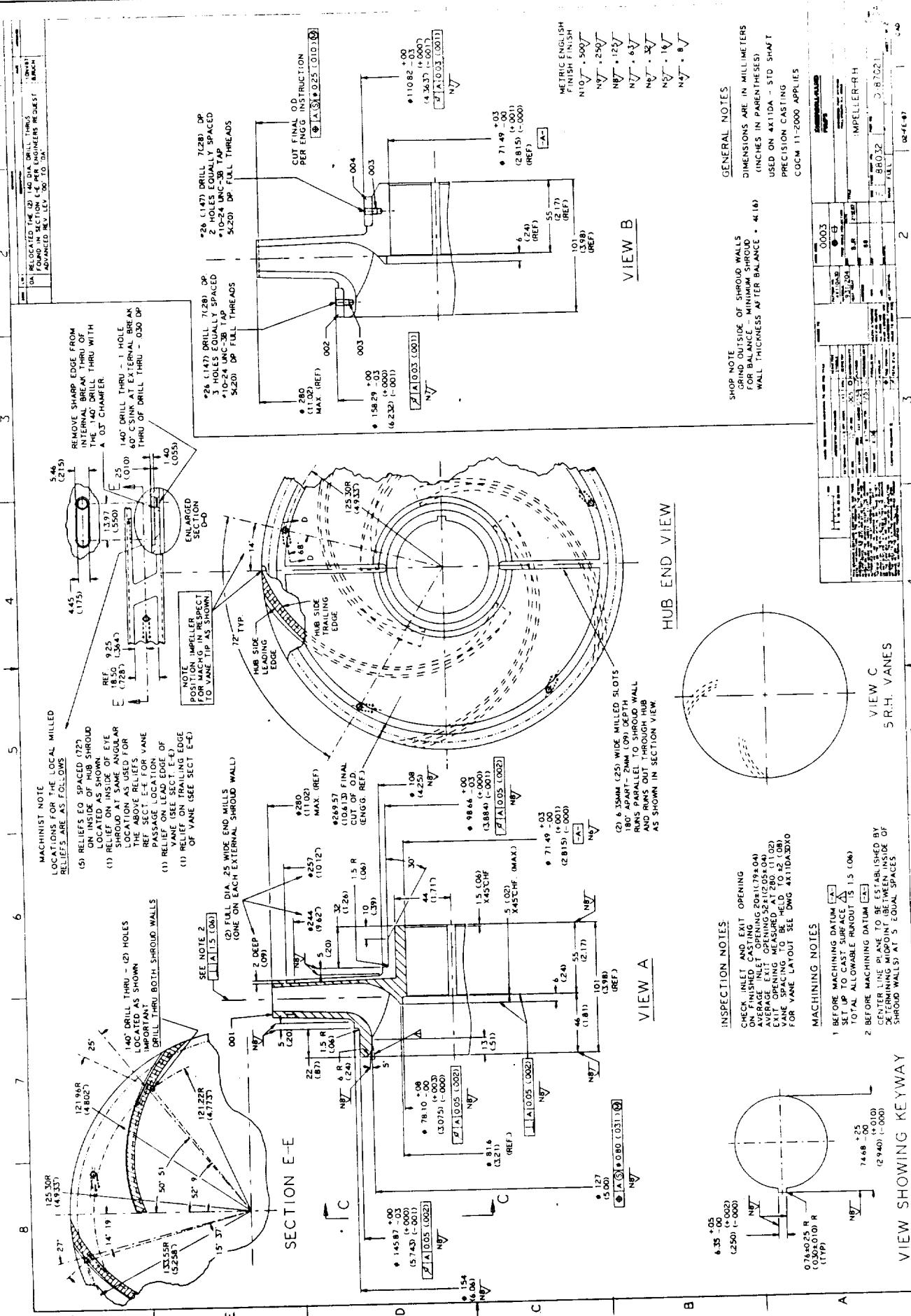
Section Heading Codes: P17

4/5/21

ORIGINAL PAGE IS
OF POOR QUALITY

APPENDIX B

TEST HARDWARE DESIGN DETAILS



ON RELOCATED THE (2) 140 DIA DRILL THRU'S
FOUND IN SECTION E-E PER ENGINEERS REQUEST - BENCH
ADVANCED MEV LVL. DO TO DA.

MACHINIST NOTE
LOCATIONS FOR THE LOCAL MILLED RELIEFS ARE AS FOLLOWS

(1) RELIEFS ED SPACED (7/2) ON INSIDE OF HUB SHROUD LOCATED AT SAME ANGULAR LOCATION AS USED FOR THE ABOVE RELIEFS

(2) 140" DRILL THRU - (2) HOLES LOCATED AS SHOWN

(3) 140" DRILL THRU - (2) HOLES LOCATED AT SAME ANGULAR LOCATION AS USED FOR THE ABOVE RELIEFS

(4) RELIEF ON LEAD EDGE OF VANE (SEE SECT. E-E)

(5) RELIEF ON TRAILING EDGE OF VANE (SEE SECT. E-E)

NOTE
POSITION IMPELLER TO VANE TIP AS SHOWN

ENLARGED SECTION D-D

REMOVE SHARP EDGE FROM INTERNAL BREAK THRU OF THE 140" DRILL THRU WITH A .03" CHAMFER

140" DRILL THRU - 1 HOLE LOCATED AT SAME ANGULAR LOCATION AS USED FOR THE ABOVE RELIEFS

140" DRILL THRU - 1 HOLE LOCATED AT SAME ANGULAR LOCATION AS USED FOR THE ABOVE RELIEFS

SECTION E-E

26 (1.47) DRILL 7/28 DP
2 HOLES EQUALLY SPACED
10-24 UNC-3B TAP
5/20 DP FULL THREADS

26 (1.47) DRILL 7/28 DP
2 HOLES EQUALLY SPACED
10-24 UNC-3B TAP
5/20 DP FULL THREADS

CUT FINAL OD PER ENG. INSTRUCTION

110.82 ± .00
(4.363) ± (.0017)
N7

71.49 ± .03
(2.815) ± (.000)
(REF.)

55.71 (REF.)

101 (13.98) (REF.)

6 (2.4) (REF.)

158.29 ± .03
(6.230) ± (.001)
N7

127 (5.00)
154 (6.06)
N7

145.87 ± .03
(5.743) ± (.001)
N7

78.10 ± .00
(3.075) ± (.000)
N7

81.6 (3.21)
(REF.)

127 (5.00)
154 (6.06)
N7

145.87 ± .03
(5.743) ± (.001)
N7

78.10 ± .00
(3.075) ± (.000)
N7

81.6 (3.21)
(REF.)

127 (5.00)
154 (6.06)
N7

VIEW A

26 (1.47) DRILL 7/28 DP
2 HOLES EQUALLY SPACED
10-24 UNC-3B TAP
5/20 DP FULL THREADS

26 (1.47) DRILL 7/28 DP
2 HOLES EQUALLY SPACED
10-24 UNC-3B TAP
5/20 DP FULL THREADS

CUT FINAL OD PER ENG. INSTRUCTION

110.82 ± .00
(4.363) ± (.0017)
N7

71.49 ± .03
(2.815) ± (.000)
(REF.)

55.71 (REF.)

101 (13.98) (REF.)

6 (2.4) (REF.)

158.29 ± .03
(6.230) ± (.001)
N7

127 (5.00)
154 (6.06)
N7

145.87 ± .03
(5.743) ± (.001)
N7

78.10 ± .00
(3.075) ± (.000)
N7

81.6 (3.21)
(REF.)

127 (5.00)
154 (6.06)
N7

145.87 ± .03
(5.743) ± (.001)
N7

78.10 ± .00
(3.075) ± (.000)
N7

81.6 (3.21)
(REF.)

127 (5.00)
154 (6.06)
N7

VIEW B

26 (1.47) DRILL 7/28 DP
2 HOLES EQUALLY SPACED
10-24 UNC-3B TAP
5/20 DP FULL THREADS

26 (1.47) DRILL 7/28 DP
2 HOLES EQUALLY SPACED
10-24 UNC-3B TAP
5/20 DP FULL THREADS

CUT FINAL OD PER ENG. INSTRUCTION

110.82 ± .00
(4.363) ± (.0017)
N7

71.49 ± .03
(2.815) ± (.000)
(REF.)

55.71 (REF.)

101 (13.98) (REF.)

6 (2.4) (REF.)

158.29 ± .03
(6.230) ± (.001)
N7

127 (5.00)
154 (6.06)
N7

145.87 ± .03
(5.743) ± (.001)
N7

78.10 ± .00
(3.075) ± (.000)
N7

81.6 (3.21)
(REF.)

127 (5.00)
154 (6.06)
N7

145.87 ± .03
(5.743) ± (.001)
N7

78.10 ± .00
(3.075) ± (.000)
N7

81.6 (3.21)
(REF.)

127 (5.00)
154 (6.06)
N7

HUB END VIEW

26 (1.47) DRILL 7/28 DP
2 HOLES EQUALLY SPACED
10-24 UNC-3B TAP
5/20 DP FULL THREADS

26 (1.47) DRILL 7/28 DP
2 HOLES EQUALLY SPACED
10-24 UNC-3B TAP
5/20 DP FULL THREADS

CUT FINAL OD PER ENG. INSTRUCTION

110.82 ± .00
(4.363) ± (.0017)
N7

71.49 ± .03
(2.815) ± (.000)
(REF.)

55.71 (REF.)

101 (13.98) (REF.)

6 (2.4) (REF.)

158.29 ± .03
(6.230) ± (.001)
N7

127 (5.00)
154 (6.06)
N7

145.87 ± .03
(5.743) ± (.001)
N7

78.10 ± .00
(3.075) ± (.000)
N7

81.6 (3.21)
(REF.)

127 (5.00)
154 (6.06)
N7

145.87 ± .03
(5.743) ± (.001)
N7

78.10 ± .00
(3.075) ± (.000)
N7

81.6 (3.21)
(REF.)

127 (5.00)
154 (6.06)
N7

VIEW C
S.R.H. VANES

26 (1.47) DRILL 7/28 DP
2 HOLES EQUALLY SPACED
10-24 UNC-3B TAP
5/20 DP FULL THREADS

26 (1.47) DRILL 7/28 DP
2 HOLES EQUALLY SPACED
10-24 UNC-3B TAP
5/20 DP FULL THREADS

CUT FINAL OD PER ENG. INSTRUCTION

110.82 ± .00
(4.363) ± (.0017)
N7

71.49 ± .03
(2.815) ± (.000)
(REF.)

55.71 (REF.)

101 (13.98) (REF.)

6 (2.4) (REF.)

158.29 ± .03
(6.230) ± (.001)
N7

127 (5.00)
154 (6.06)
N7

145.87 ± .03
(5.743) ± (.001)
N7

78.10 ± .00
(3.075) ± (.000)
N7

81.6 (3.21)
(REF.)

127 (5.00)
154 (6.06)
N7

145.87 ± .03
(5.743) ± (.001)
N7

78.10 ± .00
(3.075) ± (.000)
N7

81.6 (3.21)
(REF.)

127 (5.00)
154 (6.06)
N7

VIEW SHOWING KEYWAY

26 (1.47) DRILL 7/28 DP
2 HOLES EQUALLY SPACED
10-24 UNC-3B TAP
5/20 DP FULL THREADS

26 (1.47) DRILL 7/28 DP
2 HOLES EQUALLY SPACED
10-24 UNC-3B TAP
5/20 DP FULL THREADS

CUT FINAL OD PER ENG. INSTRUCTION

110.82 ± .00
(4.363) ± (.0017)
N7

71.49 ± .03
(2.815) ± (.000)
(REF.)

55.71 (REF.)

101 (13.98) (REF.)

6 (2.4) (REF.)

158.29 ± .03
(6.230) ± (.001)
N7

127 (5.00)
154 (6.06)
N7

145.87 ± .03
(5.743) ± (.001)
N7

78.10 ± .00
(3.075) ± (.000)
N7

81.6 (3.21)
(REF.)

127 (5.00)
154 (6.06)
N7

145.87 ± .03
(5.743) ± (.001)
N7

78.10 ± .00
(3.075) ± (.000)
N7

81.6 (3.21)
(REF.)

127 (5.00)
154 (6.06)
N7

GENERAL NOTES

SHOP NOTE

GRIND OUTSIDE OF SHROUD WALLS FOR BALANCE - MINIMUM SHROUD WALL THICKNESS AFTER BALANCE - .41 (16)

DIMENSIONS ARE IN MILLIMETERS (INCHES IN PARENTHESES)

USED ON AX10DA - STD SHAFT

PRECISION CASTING

COCM 11-2000 APPLIES

INSPECTION NOTES

CHECK INLET AND EXIT OPENING ON FINISHED CASTING 20H1179A-04

AVERAGE INLET OPENING 32.81 (1.291)

EXIT OPENING MEASURED AT 280 (11.02)

VANE SPACING TO BE MEASURED FOR VANE LAYOUT SEE ENG. AX10A20X0

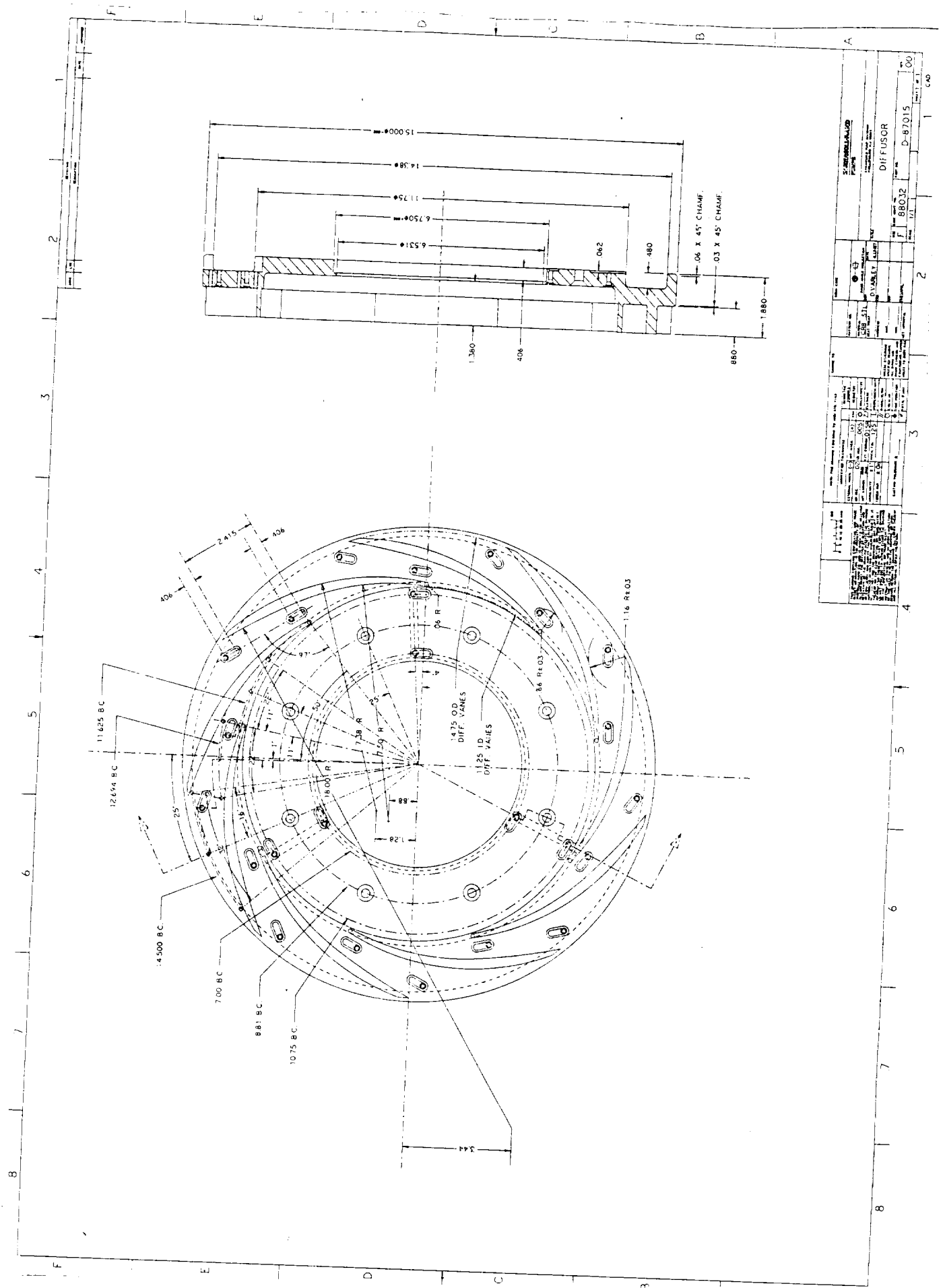
MACHINING NOTES

1 BEFORE MACHINING DATUM SET UP TO CAST SURFACE

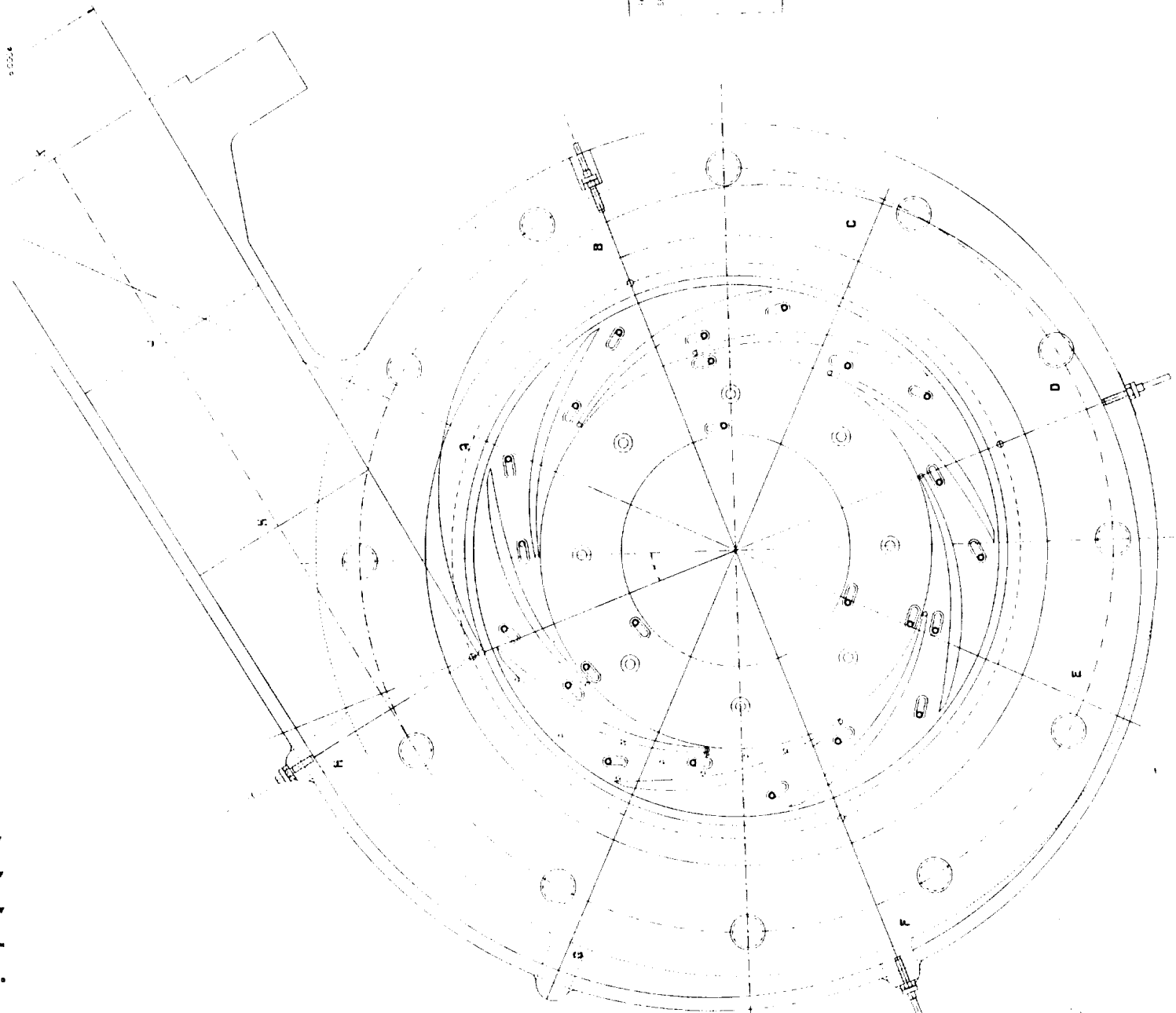
TOTAL ALLOWABLE RUNOUT IS 1.5 (0.06)

2 BEFORE MACHINING DATUM CENTER LINE PLANE TO BE ESTABLISHED BY DETERMINING MIDPOINT BETWEEN INSIDE OF SHROUD WALLS AT 5 EQUAL SPACES

ORIGINAL PAGE IS OF POOR QUALITY

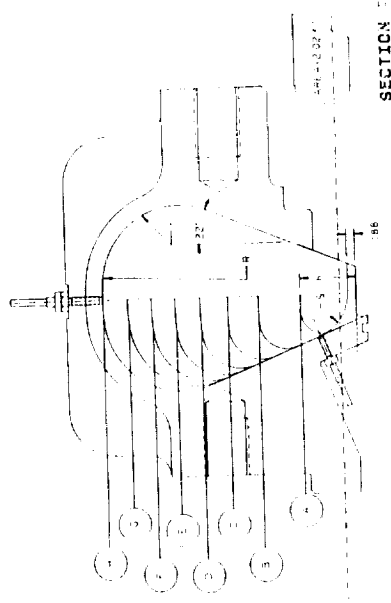


2. APPROVALS DESIGNED BY: [Signature] CHECKED BY: [Signature] DATE: 1/1		3. PART IDENTIFICATION PART NAME: DIFFUSOR PART NUMBER: 88012 DRAWING NUMBER: D-87015	
4. MATERIALS MATERIAL: [Blank] QUANTITY: [Blank]		5. OTHER INFORMATION [Blank]	



B-3

ORIGINAL FACE IS
OF POOR QUALITY



SECTION 1

TABLE 1 - COOLING TOWER WITH 22' DIA. AND 17'4" DIA. TO 17'4" DIA.

SECTION	NO. OF RIBS	AREA	PERIMETER	DIAMETER
1	12	2.356	2.818	2.00
2	12	2.194	2.618	1.88
3	12	2.032	2.418	1.76
4	12	1.870	2.218	1.64
5	12	1.708	2.018	1.52
6	12	1.546	1.818	1.40
7	12	1.384	1.618	1.28
8	12	1.222	1.418	1.16
9	12	1.060	1.218	1.04
10	12	0.898	1.018	0.92
11	12	0.736	0.818	0.80
12	12	0.574	0.618	0.68
13	12	0.412	0.418	0.56
14	12	0.250	0.218	0.44
15	12	0.088	0.018	0.32
16	12	0.000	0.000	0.20



ORIGINAL PAGE
BLACK AND WHITE PHOTOGRAPH

Photos showing volute scroll and configuration A & B
diffuser installed in the scroll.

ORIGINAL PAGE
BLACK AND WHITE PHOTOGRAPH

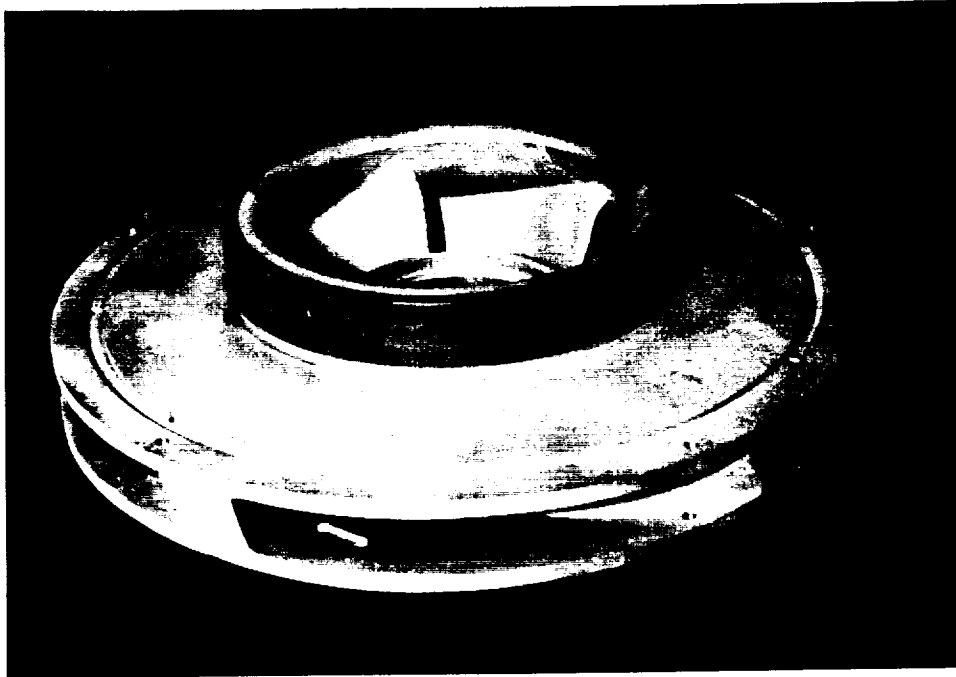
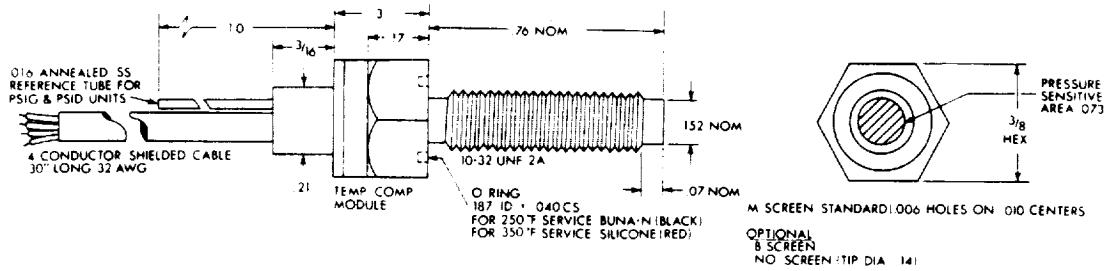
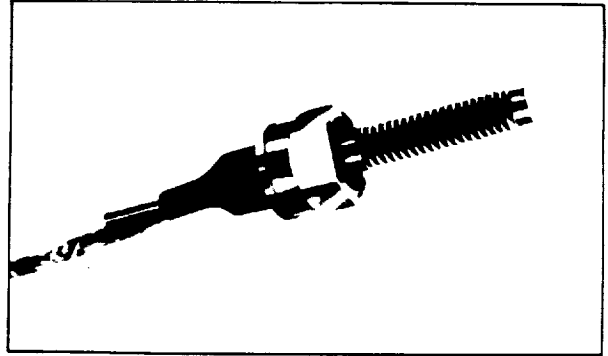


Photo showing test impeller with a mounting recess
for sensor installation shown in passage.

XT-190 SER EE

- 3 Integrated Sensor (IS)*
- 3 Easy Installation
- 4 High Natural Frequencies
- 10-32 UNF Thread

ORIGINAL FACTORY
OF POOR QUALITY



INPUT											
Pressure Range		5	10	25	50	100	200	300	500	1000	2000 PSI
Operational Mode		Absolute, Gage, Sealed Gage, Differential									
Over Pressure		20	20	100	100	200	400	600	1000	2000	3000 PSI
Burst Pressure		3 Times Rated Pressure									
Pressure Media		All Nonconductive, Noncorrosive Liquids or Gases									
Rated Electrical Excitation		10 VDC/AC									
Maximum Electrical Excitation		15 VDC/AC									
Input Impedance		500 Ohms (Min.)									
OUTPUT											
Output Impedance		500 Ohms (Nom.)									
Full Scale Output (FSO)		100 mV (Nom.)									
Residual Unbalance		±5% FSO									
Combined Non-Linearity and Hysteresis		±0.3% FS BFSL *See Note 1									
Hysteresis		Less Than 0.1%									
Repeatability		0.5%									
Resolution		Infinite									
Natural Frequency (KHz)		70	70	100	130	160	200	270	350	500	650
Acceleration Sensitivity % FS/g											
Perpendicular		.002	.001	.0005	.0004	.0002	.00013	.00012	.00009	.00006	.00005
Transverse		.0004	.0002	.0001	.00008	.00004	.000026	.000024	.000018	.000012	.00001
Insulation Resistance		50 Megohm Min. at 100 VDC									
ENVIRONMENTAL											
Operating Temperature Range		-65°F to 250°F (-55°C to 120°C) Temperatures to 350°F (175°C) Available on Special Order									
Compensated Temperature Range		80°F to 180°F (25°C to 80°C) Any 100°F Range Within The Operating Range on Request									
Thermal Zero Shift		±1% FS/100°F (Max.)									
Thermal Sensitivity Shift		±1%/100°F (Max.)									
Steady Acceleration and Linear Vibration		1000g, Sine									
PHYSICAL											
Electrical Connection		4 Conductor 32 AWG Shielded Cable 24" Long									
Weight		5 Grams (Nom.) Excluding Module and Leads									
Sensing Principle		Fully Active Four Arm Wheatstone Bridge									
Mounting Torque		15 Inch-Pounds (Max.)									

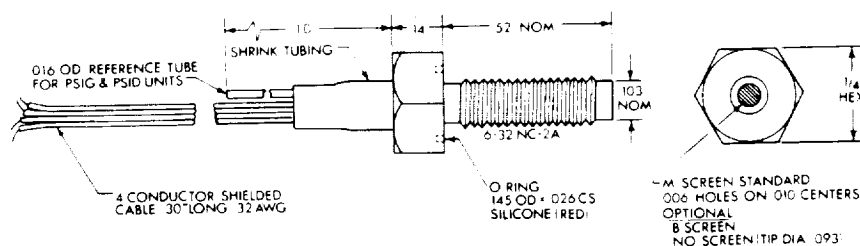
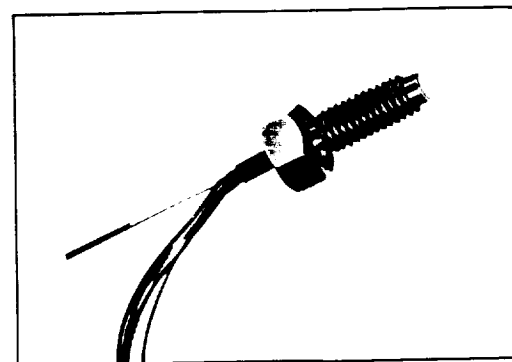
Note 1: .15% available on special order.

These units are available with metric size threads. Std. Metric Thread M5 x .8 XT-67M-190 On special order M5 x .5 XT-1M-190

KULITE SEMICONDUCTOR PRODUCTS, INC. • 1039 Hwy. Avenue • Ridgewood, New Jersey 07067 • Tel. 201-945-3000 • Cable: Kultung • Telex: 685 3296 • Fax: 943-3294

Easy Installation
Smallest Threaded Device Available
High Natural Frequencies
6-32 UNF Thread

**ORIGINAL PAGE IS
OF POOR QUALITY**

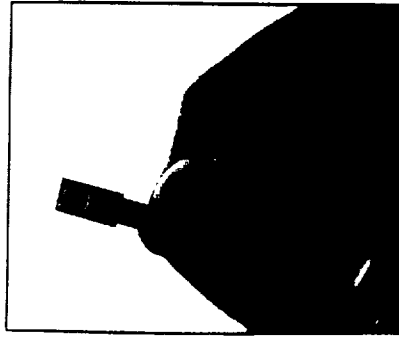


INPUT	25	50	100	200	500 PSI
Pressure Range	Absolute, Gage, Sealed Gage, Differential				
Operational Mode					
Over Pressure	50	100	200	400	1000 PSI
Burst Pressure	3 Times Rated Pressure				
Pressure Media	All Nonconductive, Noncorrosive Liquids or Gases				
Rated Electrical Excitation	10 VDC/AC				
Maximum Electrical Excitation	15 VDC/AC				
Input Impedance	500 Ohms (Min.)				
OUTPUT					
Output Impedance	500 Ohms (Nom.)				
Full Scale Output (FSO)	100 mV (Nom.)				
Residual Unbalance	±5% FSO				
Combined Non-Linearity and Hysteresis	±0.5% FS BFSL				
Hysteresis	Less Than 0.1%				
Repeatability	0.1%				
Resolution	Infinite				
Natural Frequency (KHz)	125	150	210	280	420
Acceleration Sensitivity % FS/g					
Perpendicular	.0003	.0002	.0001	.00009	.00005
Transverse	.00006	.00004	.00002	.000018	.00001
Insulation Resistance	50 Megohm Min. at 100 VDC				
ENVIRONMENTAL					
Operating Temperature Range	-65°F to 250°F (-55°C to 120°C) Temperatures to 350°F (175°C) Available On Special Order				
Compensated Temperature Range	80°F to 180°F (25°C to 80°C) Any 100°F Range Within The Operating Range on Request				
Thermal Zero Shift	± 1% FS/100°F (Max.)				
Thermal Sensitivity Shift	± 1%/100°F (Max.)				
Steady Acceleration and Linear Vibration	1000g, Sine				
PHYSICAL					
Electrical Connection	4 Conductor 30 AWG Teflon Cable 24" Long				
Weight	6 Grams Approx. (Without Cable)				
Sensing Principle	Fully Active Four Arm Wheatstone Bridge				
Mounting Torque	15 Inch-Pounds (Max.)				

Note 1. Can be supplied for 5V excitation special order.

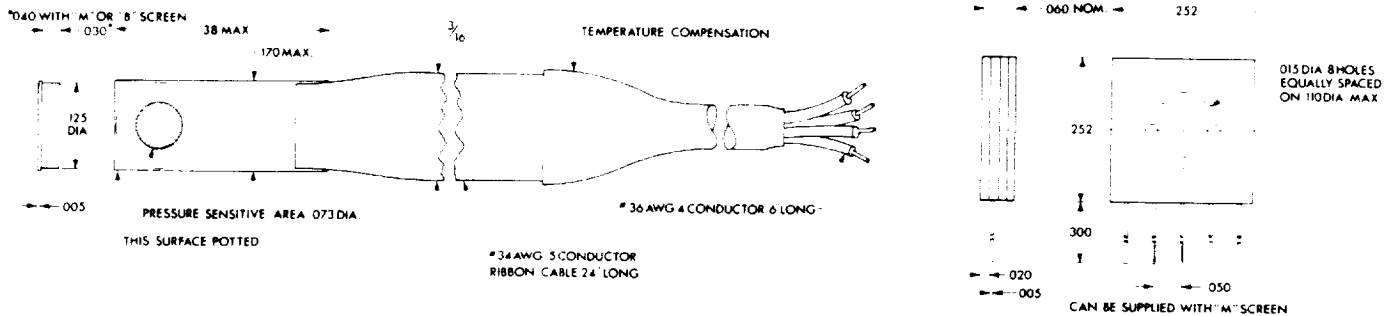
High Natural Frequency
Large Output
Excellent Stability
Flight Qualified

ORIGINAL PAGE IS
OF POOR QUALITY



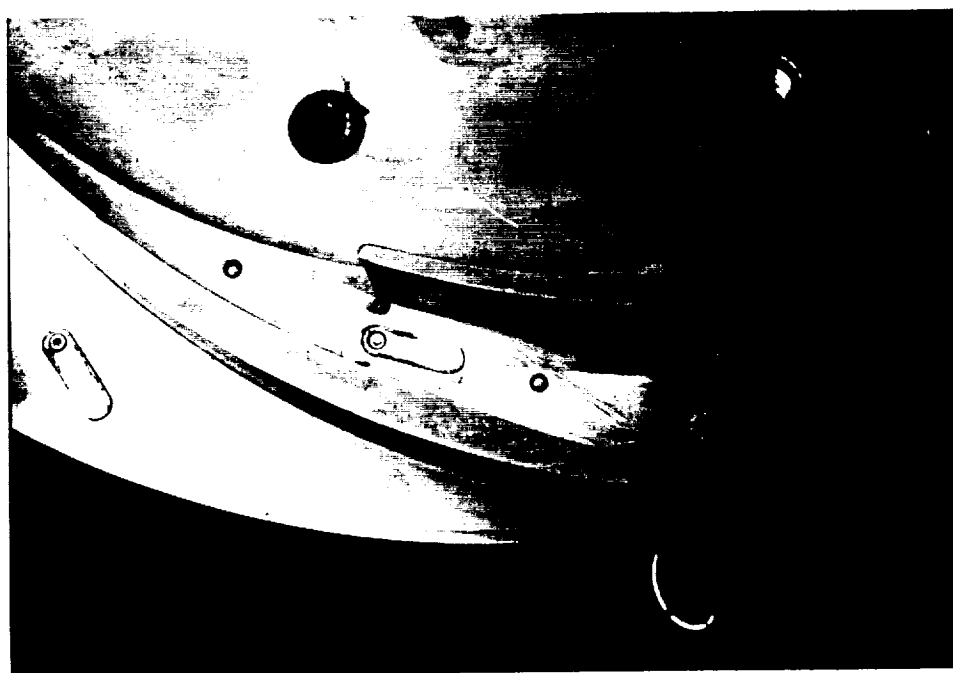
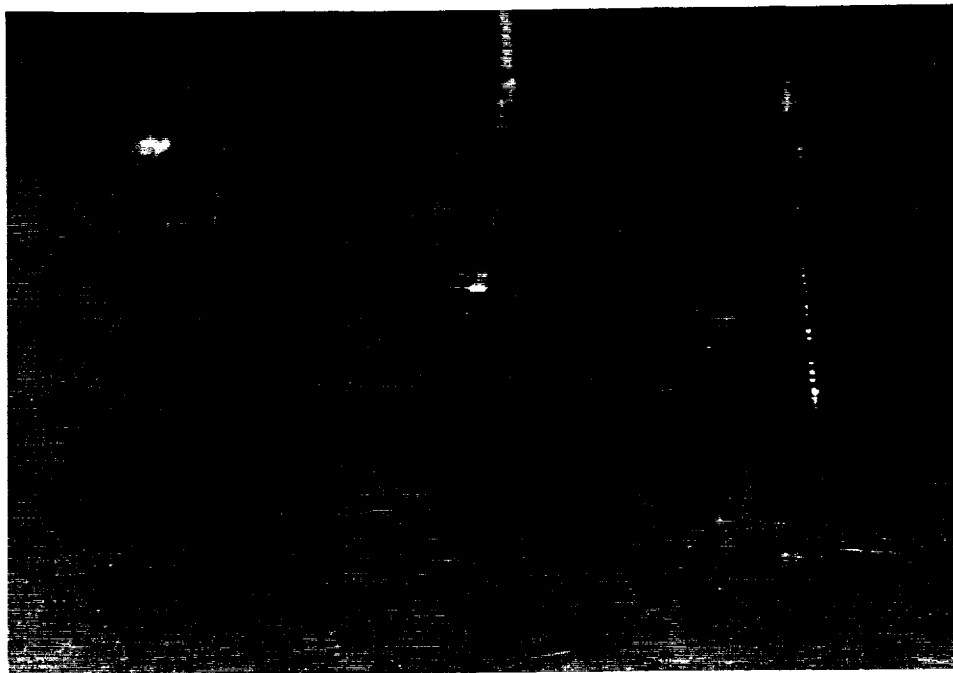
LQ-125

LQ-30-125



INPUT							
Pressure Range	5	10	25	50	100	200	500 PSI
Operational Mode	Absolute, Gage, Sealed Gage, Differential						
Over Pressure	20	20	100	100	200	400	1000 PSI
Burst Pressure	3 Times Rated Pressure						
Pressure Media	All Nonconductive, Noncorrosive Liquids or Gases						
Rated Electrical Excitation	10 VDC/AC						
Maximum Electrical Excitation	15 VDC/AC						
Input Impedance	400 Ohms (Min.)						
OUTPUT							
Output Impedance	500 Ohms (Max.)						
Full Scale Output (FSO)	100 mV (Nom.)						
Residual Unbalance	±5% FSO						
Combined Non-Linearity and Hysteresis	±0.5% FS BFS						
Hysteresis	Less Than 0.1%						
Repeatability	±.25%						
Resolution	Infinite						
Natural Frequency (KHz)	70	70	100	130	160	200	350
Acceleration Sensitivity % FS/g	.002	.001	.0005	.0004	.0002	.0002	.00008
Perpendicularity	.0004	.0002	.0001	.00008	.00004	.00004	.000016
Transverse							
Insulation Resistance	50 Megohm Min. at 100 VDC						
ENVIRONMENTAL							
Operating Temperature Range	0°F to 250°F (-20°C to 120°C) Temperatures to 350°F (175°C) Available on Special Order						
Compensated Temperature Range	80°F to 180°F (25°C to 80°C) Any 100°F Range Within The Operating Range on Request						
Thermal Zero Shift	±2% FS/100°F						
Thermal Sensitivity Shift	±2%/100°F						
Steady Acceleration and Linear Vibration	1000g, Sine						
PHYSICAL							
Electrical Connection	4 Leads 30" Long						
Weight	.6 Gram (Nom.) Excluding Module and Leads						
Sensing Principle	Fully Active Four Arm Wheatstone Bridge Diffused into Silicon Diaphragm						

Note: LQ30-125 is normally supplied uncompensated but can be supplied compensated on special order.



ORIGINAL PAGE
BLACK AND WHITE PHOTOGRAPH

Photos showing 3 different types of transducer sensors
and
typical sensor installation in a diffuser passage.

APPENDIX C

FLUCTUATING PRESSURES

IN

PUMP DIFFUSERS

AND

COLLECTOR SCROLLS

FLUCTUATING PRESSURES
IN
PUMP DIFFUSERS & COLLECTOR SCROLLS

Donald P. Sloteman
Paul Cooper
Ingersoll-Rand Company
Pump Group R&D
Phillipsburg, NJ 08865

Robert Leon
Liberty Technology
Conshohocken, PA 19428

ABSTRACT

Pressure pulsation activity associated with impeller, diffuser, and scroll interaction has been identified with cracking of the volute liner on the SSME HPTFP. A major source of pulsation activity is related to the matching of flow conditions between diffuser exit and the throat of the volute collector. This program involves extensive internal measurement of the pressure pulsation activity associated with this match condition, as well as that associated with other flow phenomena, on a typical commercially designed centrifugal pump. These results will be related to the operational experience of the present HPTFP design.

INTRODUCTION

Fluctuating pressures generated by the interaction of unsteady diffuser discharge flow and the surrounding volute scroll flow field are believed to be the source of adverse mechanical response, namely, cracking of the volute type scroll liner that surrounds the diffuser of the last (third) stage, of the Space Shuttle Main Engine (SSME) High Pressure Fuel Turbopump (HPFTP). The difficulty of analytically understanding the complex unsteady flow phenomena involved in this and essentially any other high head or high energy centrifugal pump with surrounding vaned diffuser and scroll requires that detailed static pressure measurements be obtained experimentally at strategic locations both upstream and downstream of the assumed interaction region, namely, within and outside of the rotating impeller of a model pump that is sufficiently similar to the SSME HPFTP to produce the flow phenomena and associated fluctuations of interest.

A program is being conducted which will utilize a two-stage centrifugal pump of configuration similar to the HPFTP to obtain detailed pressure vs time history at 66 locations in the final stage. Experience tells us that the pressure signal is composed of various components. The static pressure level is the most obvious component, various synchronous components are present (due to impeller blades passing diffuser vanes and or scroll cutwaters), and the somewhat more obscure non-synchronous pressure components (arising from unsteady flow behavior in hydraulic passages, which is not necessarily related to rotation speed). By using sophisticated signal processing techniques, the waveforms associated with various hydraulic phenomena can be obtained. By analyzing these waveforms, an understanding of the nature and intensity of different pressure pulsation types can be achieved, and possible design changes suggested to reduce or eliminate destructive behavior.

The test hardware used in this program is of typical, commercial design. These designs have evolved over the years and produce good efficiency with a minimum of instability at or around the design point. Off design operation of today's commercial designs sometimes lead to unstable pump behavior in the form of pressure pulsation activity which leads to mechanical distress and ultimately component failure. A cursory analysis of the current HPFTP design, suggests that a mismatch exists between the third stage vaned diffuser and the surrounding scroll. This mismatch would result in off-design type behavior at the design point. To study the effects of this suspected mismatch, a second diffuser design will be tested which is intentionally designed to simulate the area ratios present in the HPFTP diffuser and scroll. Analyzing the pressure data from both configurations will allow us to compare the effects which the two design approaches have on pressure pulsation behavior.

HIGH-ENERGY PUMPS AND PRESSURE PULSATIONS

Pressure pulsations arise in centrifugal pumps from a) the unsteady interaction of the pressure fields of the diffuser vanes (or volute tongues) and the impeller blades (Ref 1), b) the fluctuation of flow rate in any given hydraulic passage as it is subjected to an unsteady pressure difference (such as in a rotating impeller passage subjected to the peripherally non-uniform volute pressure described in Ref 2 and Ref 3) and c) the separated flows that produce rotating stall, backflow and other unsteady flow behavior that generally occur when the pump is operated at flow rates that are below the design point value - but which can also occur at the design point if separation or stall exists there (Ref 4). These phenomena are related to single-phase flow, which can fairly be assumed to be the case in the SSME HPFTP.

[Introduction of vapor and the capacitance of the resulting two-phase flow has been demonstrated to alter the character of these unsteady flows and to amplify substantially the resulting pressure pulsations - as described in Ref 5 and 6].

Incompressible, single-phase flow fields and accompanying pressure pulsations that occur in pumps are subject to the familiar "affinity laws" - velocity magnitudes are proportional to pump speed and size and pressure differences are in turn proportional to the square of velocity or the product of pump rotative speed and size - so long as Reynolds number effects are small. Such effects are indeed of little significance for typical centrifugal pumps handling water or other fluids of lesser viscosity (Ref 7). Thus, a small, rather conventional, slow speed pump developing, say 40 psi pressure rise, might experience discharge pressure fluctuations of 2% or 0.8 psi (Ref 8). For the structures of such a pump, this amount of pressure fluctuation in the fluid is harmless and in fact nearly unnoticeable and inaudible. However, when the same design is sped up to produce 2000 psi (as in each stage of the SSME HPFTP) 2% of this or 40 psi can be of concern structurally.

This concern about structural integrity in the presence of pressure pulsations is probably the best way to quantify the term "High Energy Pump". In fact, closer examination of certain points within the pump, usually reveals pressure pulsations amounting to considerably more than the 2% figure typically perceived in the fluid at the discharge port. For example, Iino (Ref 1) predicts a double amplitude of about 75% of the pump pressure rise at the impeller OD due to interaction of the diffuser and impeller pressure fields - if the ID of the diffuser blade is 3% greater than the impeller OD and the pump flow rate is 70% of the design flow rate. Obviously, significant fluctuating loads can be deduced to occur on impeller

blades, shrouds, diffuser vanes and adjacent scroll walls as a consequence of such activity. For example, the stress S at the juncture of a diffuser vane and the adjacent sidewall would be (Ref 6)

$$S = (\delta p/2) \times b^2/t^2 \quad (1)$$

where δp is the instantaneous pressure difference applied to the vane, b is the axial width or span of the vane and t is the vane thickness at the vane leading edge. For $t = 0.1$ in. (at the vane leading edge) and $\delta p = 1000$ psi (half the SSME HPFTP stage pressure rise) and $b = 0.75$ in., (Equation 1) gives $S = 28,125$ psi - more than enough to raise concern about the mechanical integrity of this "High Energy Pump."

Introduction into Equation (1) of geometrical relationships arising from this optimization of centrifugal pump hydraulic design vs specific speed (N_s) together with typical commercial experience, has led to the curve of Figure 1 (Ref 6). Pump stages having pressure rise greater than that shown by the curve can generally be considered as "high energy." Certainly the SSME HPFTP, which has $N_s = 1000$ and pressure rise of 2000 psi in each stage, is very definitely a high energy pump by this rather crude commercial standard.

Thus, it behooves the designer and researcher of such a pump to assess rather thoroughly the zones of the machine that could conceivably be exposed to pressure fluctuations arising from the various unsteady flow phenomena that are possible in a centrifugal pump but which can go unnoticed for a pump in the "low energy" category. Corrective action is often possible and ranges from making thicker vanes and shrouds, to increasing the impeller-diffuser radial clearance, etc. (Ref 6). In the case of the SSME HPFTP, improvement may be possible through hydraulic design modification as suggested by

the following analysis as well as that of the planned test measurements.

DIFFUSER AND COLLECTOR SCROLL DESIGN ANALYSIS

The matching of the collector scroll around the final diffuser stage is critical to the smooth operation of a centrifugal pump. The matching of the diffuser to scroll follows the same principles used in matching an impeller to a volute type scroll. The usual approach used, typically follows the technique described by Worster (Ref 2). Simply put, Worster says that the angular momentum present at the impeller discharge will equal the angular momentum at the volute throat plus the angular momentum lost due to wall friction and mixing losses. The flow rate where this match occurs is usually the best efficiency flow of the pump (providing the impeller inlet blading is at or near its minimum loss at this flow). The same approach can be used for matching a diffuser to a volute scroll. The diffuser to volute match is more critical, since the proportions of the exit velocity triangle from the diffuser change little (i.e., absolute flow angle is maintained) as the flow rate changes. On the other hand, the impeller velocity diagram undergoes large variations with changes in flow rate. This means that an impeller will match a volute at some flow rate. For typical pump applications, the losses in angular momentum from impeller to diffuser are small. Usually 95% or more of the angular momentum at the impeller (or diffuser) exit is available at the volute throat.

A simple equation will help illustrate the matching of impeller or diffuser to scroll throat. If we assume no losses, the angular momentum at the impeller (or diffuser) exit can be represented by the left hand portion of this equation:

$$r V_{\theta} = r_{th} V_{th} \quad (2)$$

The right hand part of Equation (2) represents the integrated angular momentum at the volute throat (where r_{th} is the mean radius to the throat and V_{th} is the throat velocity found from continuity). With viscous effects there are losses due to wall friction and boundary layer blockage of the scroll throat area. For typical pumps, taking these factors into account, experience gives us the following relationship for matching collector elements:

$$\Gamma = (r_{th} V_{th}) / (r V_{\theta}) \quad (3)$$

where Γ is typically .95.

This relationship gives us a means for judging the degree of mismatch between discharge and collector elements. When the operating flow rate produces $\Gamma < .95$, the mean throat velocity is lower than that of the match condition. This causes a deceleration of the flow approaching the throat and hence a local static pressure rise in the flow as it approaches the throat. This rise is above that expected from the radial diffusion resulting from the change in radius at the match flow condition. Conversely, for $\Gamma > .95$ the mean throat velocity is higher than the match condition and the resulting acceleration of the approach flow causes a static pressure drop in the scroll in the vicinity upstream of the throat. For the case of an impeller discharging into a volute collector, these conditions can cause variations in impeller passage flows due to varying static pressure around the impeller periphery and radial loading of the rotor due to this uneven pressure distribution. In the case of a diffuser discharging into a volute, this mismatch will exist at all flows, and be about of the same degree. The variation in pressure around the diffuser will cause variation in exit pressures for each diffuser passage. This will be felt all the way back to the diffuser ID

and probably into the impeller itself. The introduction of unsteady flow phenomena at any of these elements could cause local variations in flow rate which would manifest itself as pressure pulsations.

This program was initiated by NASA to investigate and understand the fluid behavior associated with pressure pulsations due to flow interactions of impeller, diffuser and volute scroll. This was prompted by observed pressure pulsations and some scroll cracking (on test firings) in the SSME HPFTP. The program initially involved testing a pump design which could be termed "generic". Our generic hydraulics are based on a standard Ingersoll-Rand multi-stage diffuser type pump. A 5-vaned impeller of 1200 specific speed ($\text{rpm} \times \text{gpm}^{1/2}/\text{ft}^{3/4}$) with a 9-vaned diffuser discharges into a volute scroll. The area of the volute throat was determined using the Worster method just described. The volute sections and shape were laid out on the basis of our internal hydraulic guidelines. These include linear distribution of scroll area and scroll section shape. The dimensions critical to the matching of diffuser to volute are found in Figure 2. Due to a slight casting problem, the area of the throat was cast too small. By using Equation (3) we have determined that $\Gamma=1.00$. This implies that at any operating condition, the throat velocity will be slightly higher than the free vortex (as modified by losses) condition. The absolute velocity shown at location 'D' was computed via one-dimensional calculations with assumptions for boundary layer blockage based on past experience. The $\Gamma=1.00$ results in a small mismatch, the impact of which on scroll operation will be determined through testing.

We have compared this "generic" design with the SSME HPFTP third stage. The exit conditions for the third stage diffuser were determined using PANEL (a 2-dimensional, inviscid code). The effect of no boundary layer blockage in the calculation is not serious since

the cascade is actually accelerating the flow from inlet to discharge. Even without the blockage, a Γ of .80 is indicated using Equation (2); (with blockage, an even lower Γ would be indicated). This would indicate that the scroll throat is oversized, and a circumferential pressure gradient will exist around the diffuser OD. From the scroll detail drawings, it is seen that a series of holes are present around the scroll which communicate with the outer chamber (defined by the pressure containment structure of the pump itself). We did not determine the effectiveness of these holes to balance the pressures around the scroll. Assuming that the balance holes do not pass sufficient flow to balance the scroll, we look for what effect a scroll mismatch and resulting circumferential pressure gradient have on the dynamic behavior of each of the other hydraulic components. The dynamic behavior of the flow may be further complicated by the lack of diffusion in the third stage diffuser vanes and the unusual practice of extending one of the diffuser vanes to blend into the inner wall of the discharge trumpet. The existence of all these features in this very high energy machine may create unsteady flow phenomena like those described earlier in this paper, only more severe.

In order to pursue the effects of such a drastic mismatch as is indicated in the SSME HPFTP, we will design an alternate diffuser to our "generic" design. Since we are committed to use the existing scroll hardware, our throat area is fixed. In order to achieve $\Gamma = .80$, the diffuser will be designed to provide less diffusion of the absolute flow with the result being a higher tangential velocity component at diffuser exit than exists with our "generic" design. Preliminary design data for this diffuser is shown in Figure 2. An attempt at modeling the flow that exists in the HPFTP would create very large velocities at the diffuser exit, which would in turn lead

to very low r values (on the order of .5 or less). We feel that this represents too great a mismatch. The compromise of achieving reasonable diffusion while presenting the scroll with a large mismatch will provide results of interest regarding the diffuser/scroll interaction that we believe exists in the SSME HPFTP.

TEST PROGRAM

The test program for both diffuser designs (generic and alternate) will be conducted in the Ingersoll-Rand Pump Group R&D Laboratory. Installation of instrumentation, data collection and reduction will be done by Liberty Technology Center. Analysis of the data will involve both IR and Liberty. A special 2-stage pump is being adapted to a configuration similar to that found in the SSME HPFTP, differing in that the intermediate stage is being left out. This test pump will be run at 2500 rpm through a variable speed 120 hp DC motor. We will use water as the pumped fluid in order to produce measurable levels of pressure pulsations from which scaling statements can be made to apply the experimental results to the SSME experience as well as other diffuser type pumps. This pump, operating at 2500 rpm with an 11-inch diameter impeller generates a stage pressure rise of 100 psi at a flow rate of about 800 gpm. Water is believed to be a suitable fluid since the Mach number on the SSME hydrogen pump (based on impeller exit conditions) is about .4 and the stage density ratio is about 1.04. If we assume that the pulsations and resulting scroll cracking on the HPFTP are produced by the same phenomena as seen on high energy commercial pumps, we can say they are not compressibility-related as long as the Mach number is kept at least this far below unity. The Reynolds number based on wheel radius and tip speed for the water test is two orders of magnitude less than the HPFTP (5 million vs 500 million). Literature indicates that the pressure pulsations as a fraction of stage

pressure rise will remain the same regardless of Reynolds No. (Ref 9). Also Stepanoff indicates that Reynolds No. effects become significant in pumps run at Reynolds No. below 5 million (Ref 7). A photo to the two-stage test pump can be found in Figure 3.

A cross-section of the second stage of the test pump can be found in Figure 4. In designing the components, we kept two features in mind. First, the installation of pressure sensors in key locations of the hydraulic passages and the modularity of the pieces (providing the potential of easily incorporating alternate designs). Provisions for a total of 58 stationary pressure transducers are in the hardware design. These sensors are located in the scroll, diffuser passages (one passage is fully instrumented with 11 sensors on both sidewalls) and along the sidewalls adjacent to the impeller. A view of the diffuser and scroll showing positions of sensors is shown in Figure 5. The impeller is instrumented with 8 sensors with signals extracted via a slip ring assembly positioned between the motor and pump coupling hubs. The impeller (5 vane) has a sensor in each passage located at mid-passage on the hub wall near the impeller OD. One impeller passage also has sensors on the opposite wall and a sensor on the suction and pressure surfaces of adjacent blades.

In order to measure and locate the sources of the various pressure pulsations phenomena described earlier in this paper, a large amount of signal processing of the data will be required. This will be done for three hardware configurations. It is anticipated that data from all transducers will not be needed in all test series. As specific relevant phenomena emerge, it is likely that these phenomena can be described by considerably fewer transducers than the full complement needed initially to cover all possible locations and spatial and temporal relationships. Therefore, Liberty will reduce data on 100% of the transducers for the first test series. We will then determine

which transducers are yielding relevant data and will restrict the data reduction to 75% of the transducer for the second test series. Similarly, we will reduce this percentage to approximately 50% for the last test series. The following information will be provided for each test configuration:

- a) Order-related waveforms for each sensor in the above schedule.
- b) Non order-related waveforms for each sensor in the above schedule. (The non order-related waveforms will be obtained by subtracting the order-related waveforms from each raw waveform)
- c) Spectra, transfer function phase, and other plots as warranted. (Note that phasing information will be built into the basic waveforms because all are referenced by the same once per rev trigger).

Written summaries will be provided with plots so that their meaning and significance will be made clear.

Use of the four common channels on all eight (8) recorders provides for synchronization allowing transfer functions to be determined between any two pressure channels. Additionally, simultaneous broadband noise recorded on all channels of each tape recorder will enable corrective transfer functions to be determined to correct for interchannel time delays. This will be utilized if found to be necessary.

The data collection and reduction just described will be applicable to three hardware configurations. The first two configurations will use the generic volute and diffuser designs. However, the impeller O.D. will be cut down following the first test. This will allow the comparison between two different diffuser to impeller clearance ratios. This ratio is important in regard to blade passing

frequency-related pressure pulsations. The first diffuser to impeller diameter ratio will be 1.02. The second ratio will be a more typical 1.06. Effects due to diffuser to scroll mismatch should be similar on both these configurations. The third configuration tested will use the generic volute scroll and the alternate diffuser design. The diffuser ID to impeller OD ratio will remain at 1.06. This test will show differences in the flow behavior due to a large mismatch of diffuser to scroll area. This behavior may produce unsteady flow in one or more diffuser passages which cause pressure pulsation activity in the scroll itself. The detailed pressure pulsation history for each sensor location will provide us with a means of identifying the locations of origin for these pulsations and where their intensity is of greatest concern.

Testing of the hardware just described will begin in early May, 1988. The test program should be completed in late June. The final report will follow by the end of August 1988.

CONCLUSIONS

High-Energy multi-stage centrifugal pumps of commercial design are known to be sensitive to pressure pulsation behavior. These pulsations can be order related, such as impeller vanes passing diffuser leading edges; or random, such as rotating diffuser stall encountered at off design flow conditions. The pulsation activity may be non-synchronous in nature, caused by unsteady flow behavior in diffuser passages or in a discharge collector (volute/scroll). In robust commercial designs this variety of pulsation behavior can cause impeller, shaft or diffuser breakages and severe piping system instabilities. The comparatively fragile structure of the SSME HPFTP, which is a true high-energy machine with a lamp power density ratio is probably more sensitive to pressure pulsation behavior

than are its commercial brothers. Our efforts to understand the mechanics of these pressure pulsations include the testing, at low speed of typical pump hydraulics in various configurations. These configurations cover two key areas of concern; impeller to diffuser inlet clearance and diffuser to volute/scroll matching. Some information regarding diffuser blade loading effects may also be gained. The test program will collect data from a multiplicity of pressure sensors located in the scroll, diffuser, sidewalls and in the rotating impeller. Advanced data reduction techniques will be applied to uncover the pressure pulsation history at each sensor location in an effort to understand the fluid behavior behind the pulsation activity. By understanding this behavior, pump designers should be able to make more enlightened decisions regarding high-energy pump design in terms of minimizing mechanical damage resulting from discharge related pressure pulsation activity.

References:

1. Iino, T.: "Potential Interactions Between a Centrifugal Pump Impeller and a Vaned Diffuser." In Fluid/Structure Interactions in Turbomachinery, ASME, 1981, pg. 63-69
2. Worster, R. C.: "The Flow in Volute and Its Effect on Centrifugal Pump Performance." Proceedings of the Institution of Mechanical Engineers, Hydraulic Plant and Machinery Group, Vol. 177, No. 31, 1963, pg. 843-876.
3. Lorett, J. A., and Gopalakrishnan, S.: "Interaction Between Impeller and Volute of Pumps at Off-Design Conditions." Transactions of the ASME, Journal of Fluids Engineering, Vol. 108, March 1986, pg. 12-18.
4. Fischer, K., and Thoma, D.: "Investigation of the Flow Conditions In a Centrifugal Pump." Transactions of the ASME, Vol. 54, 1932, pg. 141-155.
5. Brennen, C., and Acosta, A. J.: "The Dynamic Transfer Function For a Cavitating Inducer." Transactions of the ASME, Journal of Fluids Engineering, Vol. 98, 1976, pg. 182-191.
6. Cooper, P.; Wotring, T. L.; Makay, E.; and Corsi, L.: "Minimum Continuous Stable Flow In Feed Pumps." EPRI Power Plant Pumps Symposium, New Orleans, March 1987.
7. Stepanoff, A. J.: Centrifugal and Axial Flow Pumps. Second Edition, Wiley, 1957, pg. 315

References: (Continued)

8. Warring, R. H. : Pumping Manual, Seventh Edition, Trade & Technical Press Limited, 1984, pg. 273
9. Phelan, J. J. ; Russell, S. H. and Zeluff, W. C.: "A Study of the Influence of Reynolds Number on the Performance of Centrifugal Fans." ASME Paper 78-WA/PTC-3, 1978

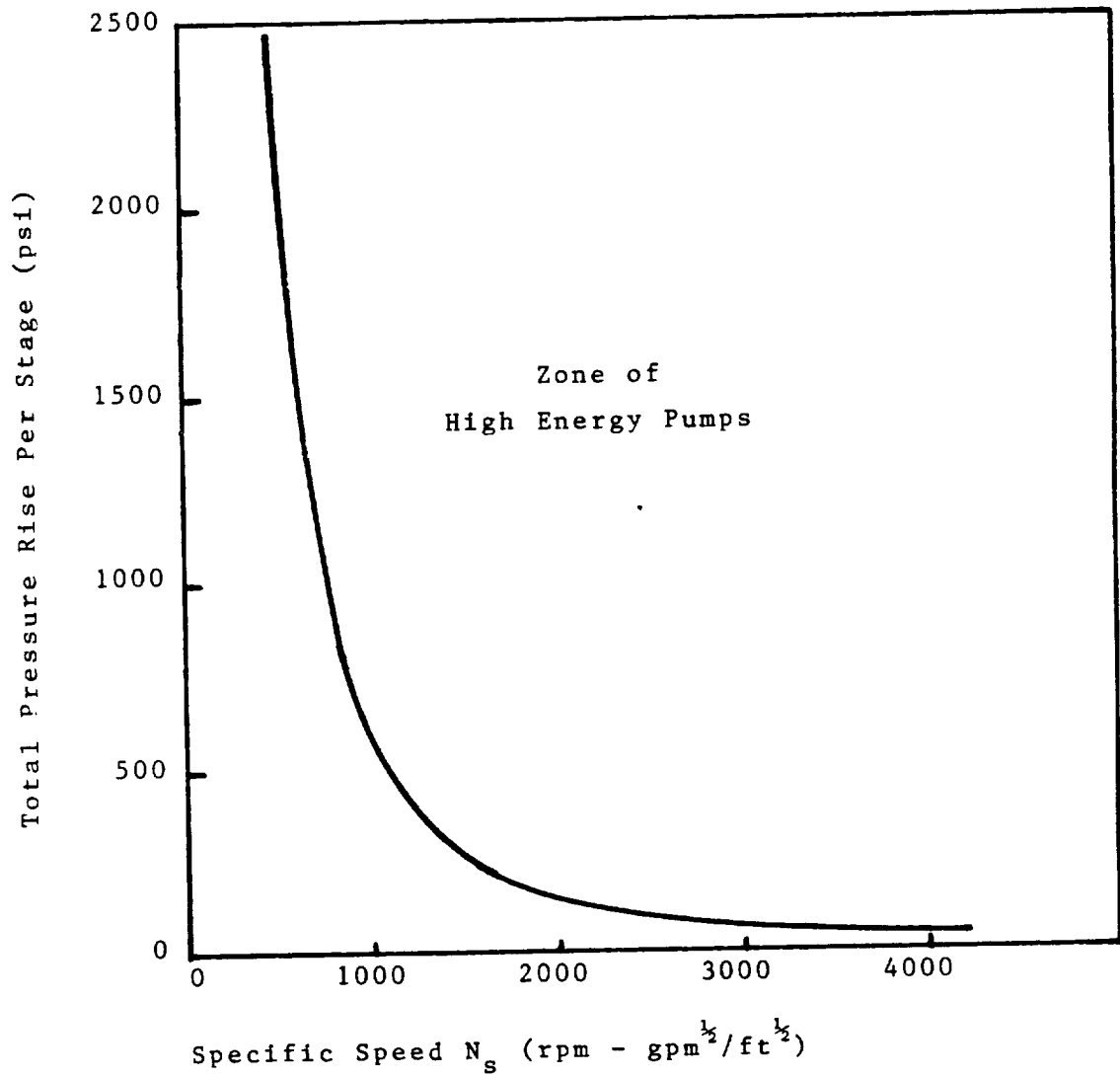


FIGURE 1. High Energy Pump Concept. Results of simplified analysis for typical constant thickness/diameter ratio and constant limiting stresses.

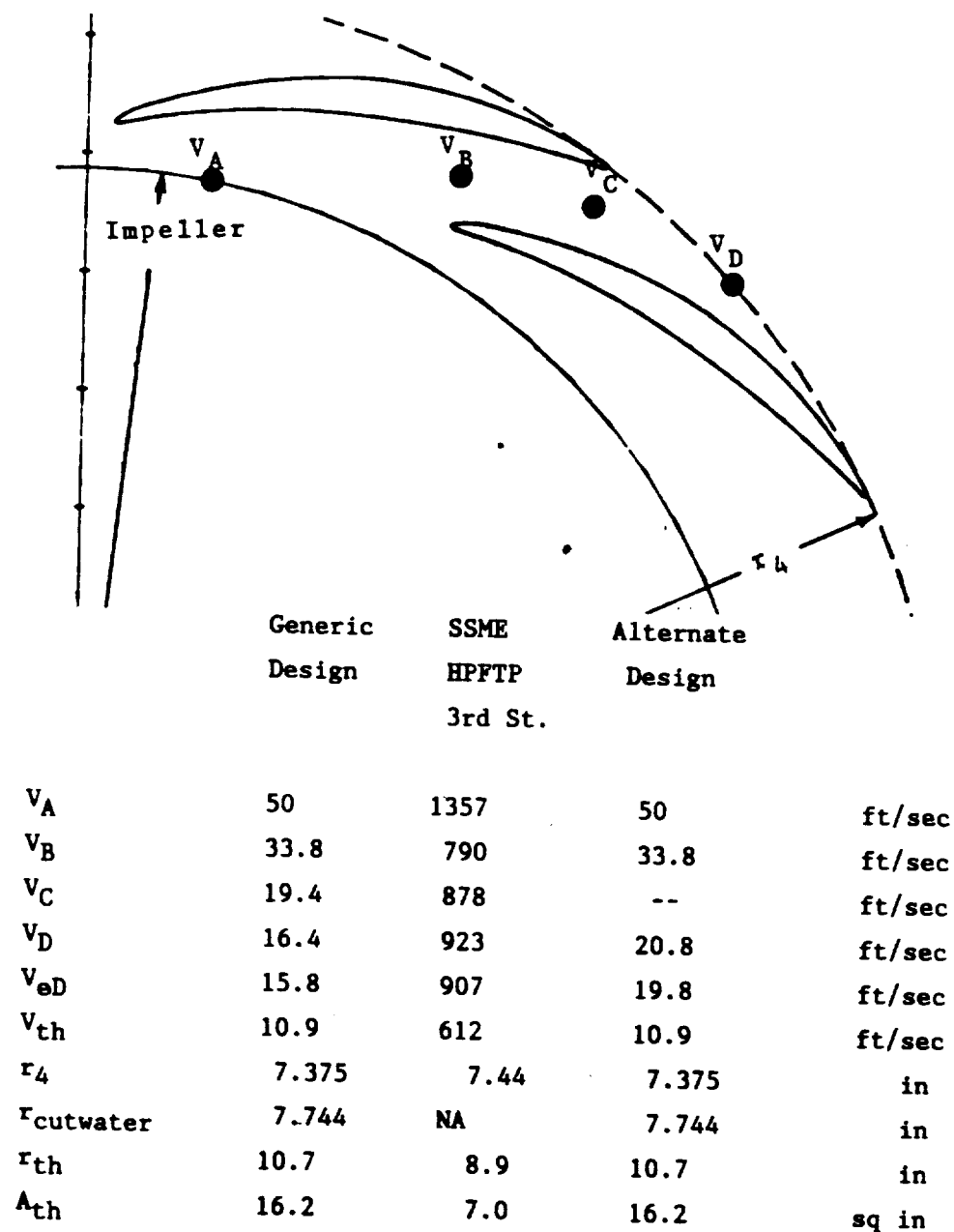
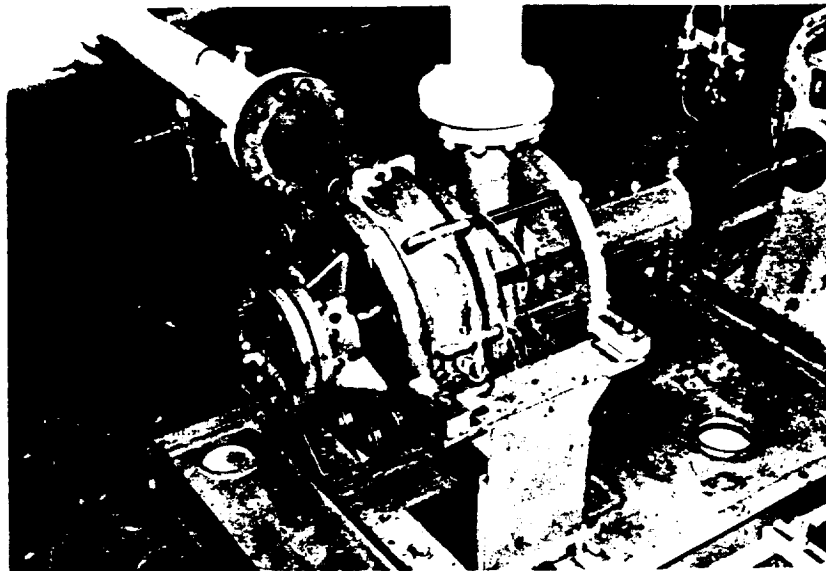


Figure 2. Summary of diffuser and volute geometries and velocities at nominal design flow (550 gpm @ 1780 rpm for generic design), at various locations in the diffuser (photos) and volute scroll.



ORIGINAL PAGE IS
OF POOR QUALITY

Figure 3. Photograph of two-stage test
pump on Test Stand.

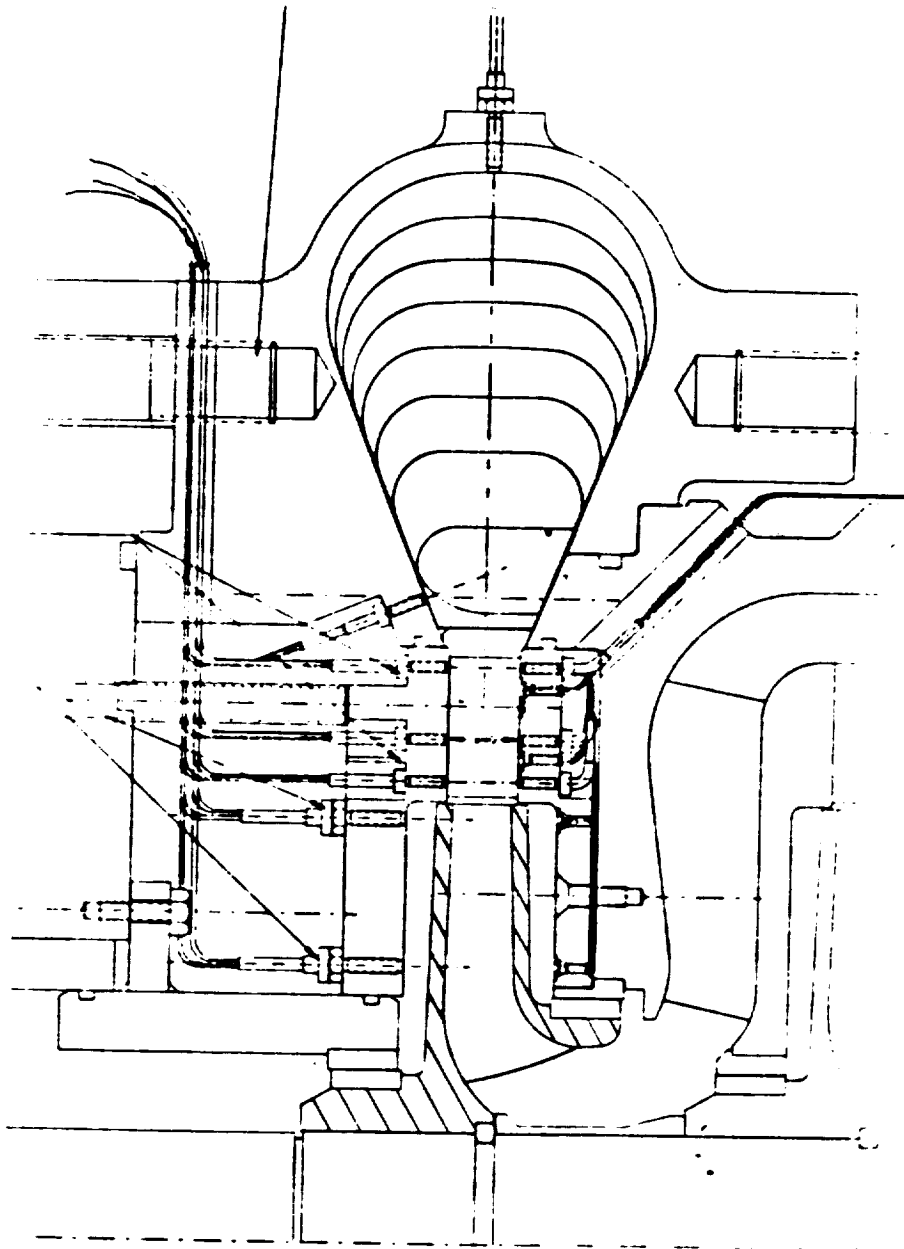


Figure 4. Cross-section of last stage of test pump, showing circumferential development of volute scroll sections.

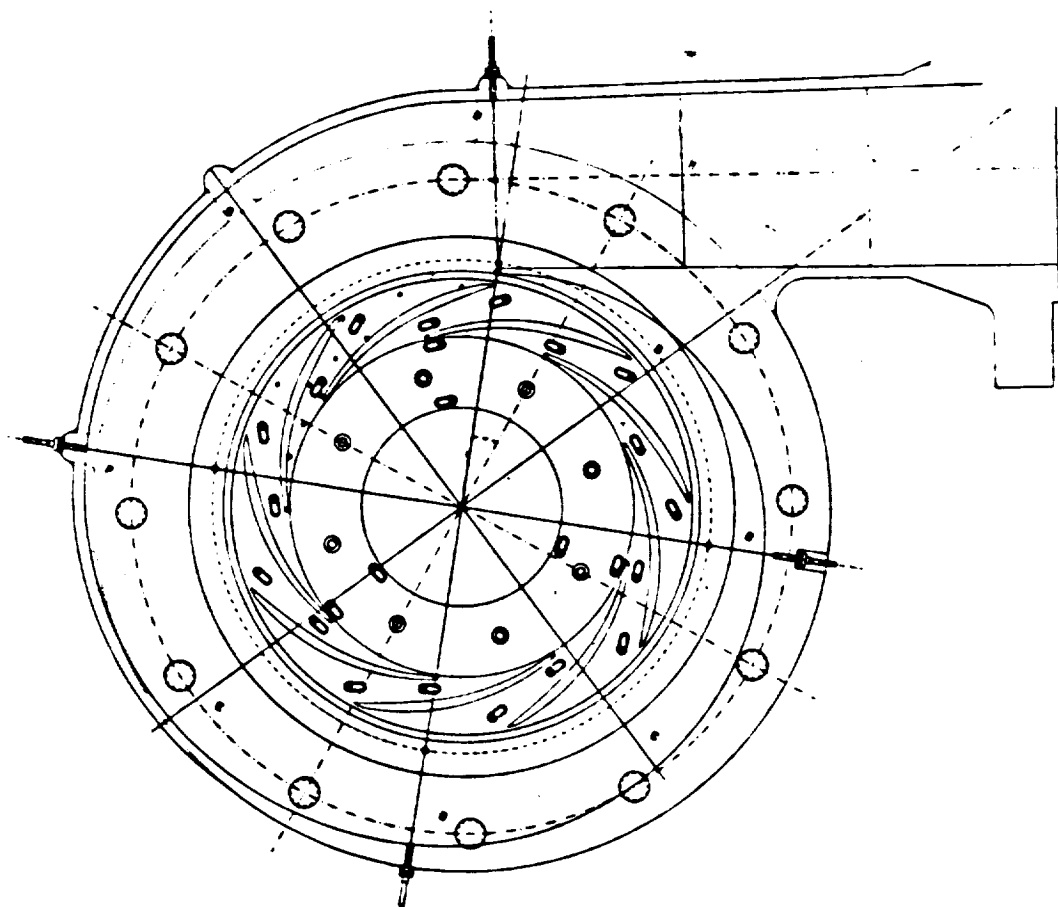


Figure 5. View of volute scroll and vaned diffuser showing transducer locations.

APPENDIX D

SUMMARY

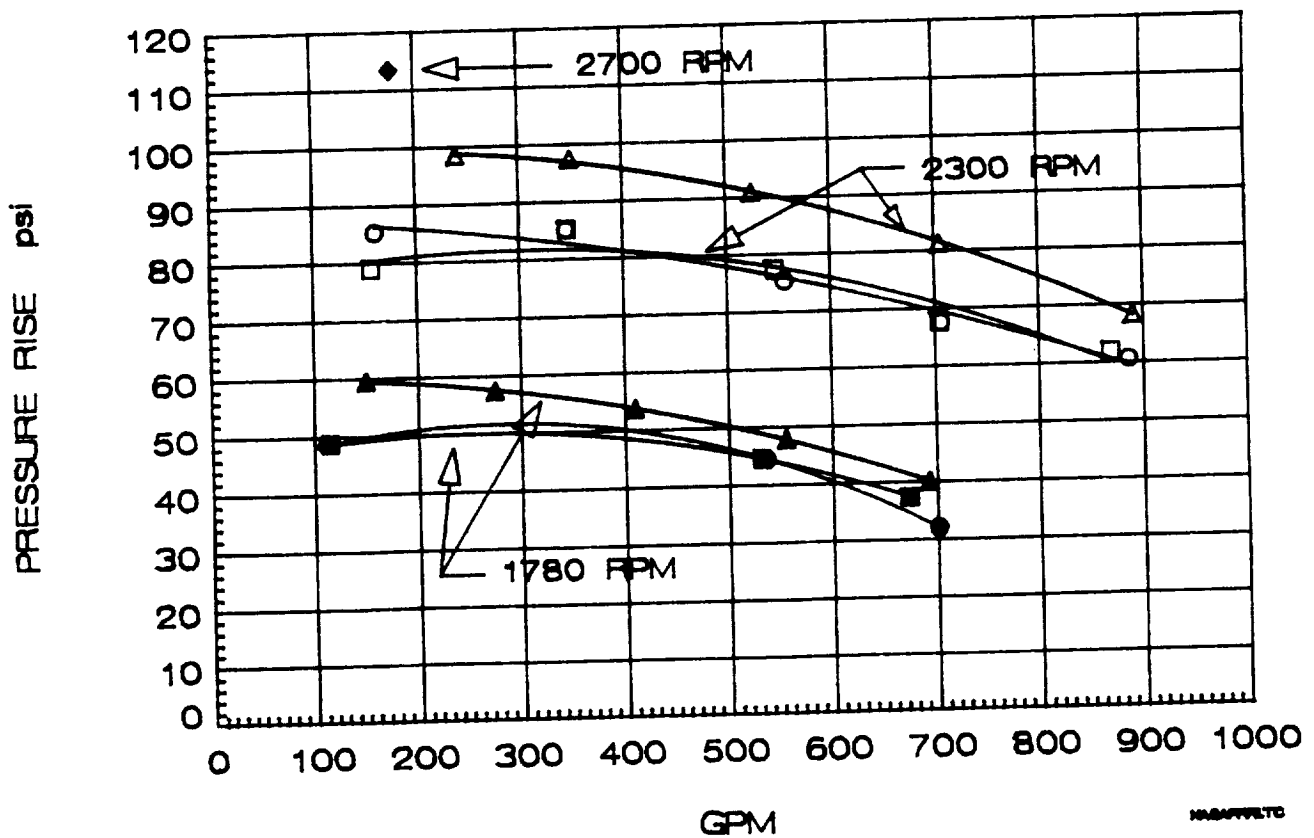
OF

STEADY STATE TEST DATA

4x11 CB/V STAGE PRES. RISE

DESIGN FLOW = 550 gpm

Δ 'A' ○ 'B' □ 'C' ▲ 'A' ● 'B' ■ 'C' ◆ 'C'



STATIC PRESSURE LEVELS (PSIA)

	F1	F2	F3	FLOW CONDITION		F6	F7	F8	F9
				F4	F5				
AI1	183.56	181.85	171.41	158.14	139.85	98.80	109.92	124.85	
AI2	173.30	171.20	160.72	147.87	129.34	86.82	98.01	112.80	
AI3	179.98	178.29	167.64	154.18	135.81	92.47	104.71	118.50	
AI4	173.84	170.85	159.98	146.69	127.84	85.60	97.45	112.13	
AI5	174.84	172.77	162.23	149.46	130.71	88.57	99.86	114.93	
AI7	172.72	171.12	160.39	147.66	129.44	87.43	99.12	114.40	
AI8	191.04	187.17	177.56	165.38	147.98	101.11	114.50	127.36	
AD1	212.80	207.72	193.36	172.94	142.93	96.49	115.56	139.95	
AD2	230.44	226.66	210.44	191.06	163.18	110.19	128.71	151.87	
AD3	217.46	210.81	192.70	168.96	137.23	92.45	112.97	141.07	
AD4	226.59	220.82	203.56	181.46	152.53	104.94	122.25	147.44	
AD5	221.62	215.25	198.05	175.53	143.38	97.58	118.70	145.86	
AD6	227.88	221.49	203.32	181.01	152.52	105.02	123.08	147.26	
AD7	238.35	232.55	216.24	193.49	160.29	113.43	133.74	160.62	
AD8	247.80	234.85	220.74	202.16	175.24	124.12	142.75	166.76	
AD9	229.36	222.93	206.68	184.09	152.56	103.20	123.27	149.58	
AD10	229.23	225.35	209.39	189.56	162.12	110.08	128.12	151.92	
AD11	226.62	220.13	203.88	180.48	147.52	100.99	121.18	148.63	
AD12	225.27	220.96	204.09	185.03	157.58	105.77	123.65	147.09	
AD13	215.38	209.09	192.49	171.76	139.05	92.56	112.92	138.03	
AD14	224.01	219.18	202.42	183.80	156.60	105.13	122.53	146.18	
AD15	221.49	215.36	199.02	176.61	144.37	96.22	117.18	142.86	
AD16	204.07	202.24	188.46	172.31	147.12	97.85	116.08	139.86	
AD17	232.48	226.40	210.46	187.44	155.65	106.54	127.62	154.15	
AD18	213.63	212.25	198.39	180.62	154.55	105.21	122.71	144.76	
AS1	225.28	220.08	205.37	189.25	164.85	114.40	129.96	150.24	
AS2	225.70	220.28	203.50	185.66	158.67	104.68	121.65	144.26	
AS3	228.17	223.03	207.95	189.69	163.71	109.23	125.58	147.66	
AS4	221.38	216.41	200.42	182.12	155.70	102.46	119.31	142.12	
AS6	226.25	221.13	207.15	189.04	162.88	110.37	126.98	149.06	
AS7	222.71	218.40	202.67	185.29	159.96	106.55	122.71	144.68	

STATIC PRESSURE LEVELS (PSIA)

	F1	F2	F3	FLOW CONDITION		F6	F7	F8	F9
				F4	F5				
AD19	224.22	219.61	202.16	180.92	149.15	100.89	121.58	147.21	
AD20	215.43	210.94	196.10	177.29	151.09	100.22	117.50	140.13	
AWIB2	196.14	189.93	176.81	162.57	142.29	97.28	110.01	129.15	
AWIB3	187.45	183.16	170.65	158.43	139.20	99.99	112.40	133.82	
AWIB4	193.02	185.20	172.33	157.99	138.22	93.59	106.39	124.32	
AWIB5	190.54	182.25	167.57	153.00	132.75	91.65	104.62	126.56	
AWIB6	196.61	190.71	178.38	164.62	144.94	99.54	112.52	131.18	
APIB1	200.58	194.37	178.34	161.72	139.88	98.51	111.61	131.52	
APIB2	208.92	203.06	187.36	171.42	148.94	102.60	117.14	139.48	
APIB3	224.79	220.33	205.43	182.75	147.11	102.24	124.75	150.11	
APIB4	222.89	217.82	202.01	182.33	153.67	105.30	123.31	147.40	
APIB6	224.82	220.80	205.58	186.40	158.54	106.64	124.10	147.20	
APIB7	236.68	233.34	218.05	199.07	171.66	119.47	137.41	159.48	
APIB8	226.86	221.51	203.13	181.70	153.18	107.30	124.53	147.83	
APIB9	229.89	226.04	210.20	190.96	164.12	111.70	128.75	151.82	
APOB1	197.48	191.24	178.10	163.41	143.21	97.04	109.78	129.95	
APOB2	207.98	199.54	183.75	167.47	144.01	95.71	134.24		
APOB5	221.32	217.08	201.32	181.52	152.26	102.12	120.44	144.87	
APOB6	218.07	214.00	198.51	179.34	151.82	100.90	117.84	141.12	
APOB7	234.06	230.68	214.29	194.15	167.22	114.13	131.32	154.27	
APOB9	225.58	221.34	204.97	185.66	158.82	104.61	122.16	145.39	

STATIC PRESSURE LEVELS (PSIA)

	FLOW CONDITION								
	F1	F2	F3	F4	F5	F6	F7	F8	F9
BI1	192.63	191.93	178.09	165.15	145.35	100.76	113.88	132.30	
BI2	181.25	180.18	166.64	154.33	134.88	89.49	102.14	119.92	
BI3	187.10	185.24	172.48	159.99	141.29	95.72	108.51	124.40	
BI4	185.87	184.48	170.04	157.55	138.96	93.39	106.32	123.77	
BI5	186.60	184.90	171.32	158.32	138.90	93.51	106.55	124.83	
BI6	183.75	180.43	163.55	149.36	129.07	86.89	101.19	123.53	
BI7	183.95	182.14	168.52	155.82	136.72	92.13	105.35	124.37	
BI8	197.84	192.30	178.90	166.39	147.95	100.19	112.57	134.48	
BD1	218.14	218.13	201.04	177.42	147.38	104.15	119.87	144.04	
BD2	222.77	222.86	204.71	187.58	160.75	107.75	126.58	147.91	
BD3	213.41	212.46	193.62	169.20	137.43	92.12	113.34	140.38	
BD4	223.29	224.27	204.45	186.26	158.75	107.88	126.82	149.10	
BD5	220.78	219.05	195.54	178.37	146.25	99.88	121.76	148.04	
BD6	220.46	219.79	199.08	182.90	155.30	104.01	123.14	145.96	
BD8	235.42	235.48	215.60	200.46	172.92	120.69	139.74	161.40	
BD9	218.20	215.53	194.35	177.99	147.91	99.27	120.39	144.05	
BD10	221.31	220.40	201.57	185.77	159.09	107.40	125.79	146.81	
BD11	221.92	216.48	194.87	178.51	147.13	99.63	121.50	145.21	
BD12	220.71	220.29	201.48	185.73	158.56	106.30	124.85	145.88	
BD13	215.03	211.51	190.60	173.87	141.75	93.60	115.97	139.09	
BD14	222.23	221.77	203.09	187.29	159.91	107.68	126.19	147.34	
BD15	213.93	209.49	190.11	171.63	139.60	92.19	114.15	136.75	
BD16	212.35	212.70	197.49	182.89	157.78	107.92	126.44	147.86	
BD17	221.51	221.65	200.27	182.36	151.04	103.50	124.35	148.77	
BD18	216.37	215.94	197.70	181.98	155.08	100.27	119.85	142.80	
BS1	217.50	218.14	201.09	185.70	159.57	106.56	123.39	143.38	
BS2	219.86	221.42	212.34	183.71	157.48	102.58	120.36	141.78	
BS3	223.85	225.48	205.27	188.63	163.10	107.75	125.03	145.79	
BS4	222.40	229.59	200.01	183.11	156.30	101.55	119.72	141.82	
BS6	221.03	226.18	207.39	190.52	165.24	110.92	128.07	149.43	
BS7	222.71	225.62	205.16	189.17	163.35	107.66	125.38	145.76	

STATIC PRESSURE LEVELS (PSIA)

	FLOW CONDITION								
	F1	F2	F3	F4	F5	F6	F7	F8	F9
BD19	221.64	222.80	204.91	181.70	149.68	100.37	122.22	146.68	
BD20	107.21	107.57	98.45	90.26	76.13	49.50	58.49	69.64	
BWIB2	205.33	200.70	185.66	171.81	151.82	103.59	117.14	138.56	
BWIB3	197.01	192.75	177.60	167.36	147.66	104.03	117.65	138.33	
BWIB4	200.30	195.83	181.34	168.32	148.52	100.18	113.85	134.05	
BWIB5	194.73	193.65	176.14	158.02	138.54	95.21	108.57	132.10	
BWIB6	202.28	199.38	183.87	170.57	150.52	102.18	115.41	135.55	
BPIB1	201.22	199.05	184.68	164.23	142.77	95.26	109.21	131.87	
BPIB2	213.92	214.86	198.08	174.13	152.67	102.22	117.39	140.29	
BPIB3	220.09	221.15	206.39	181.65	144.68	98.56	120.94	147.44	
BPIB4	218.55	218.52	202.63	180.33	151.50	96.27	122.89	144.40	
BPIB6	222.45	222.42	203.45	185.74	158.75	105.79	124.59	146.32	
BPIB7	231.63	232.13	215.01	198.94	172.77	118.90	136.90	156.90	
BPIB8	220.29	218.42	199.78	182.55	154.37	103.20	121.84	144.14	
BPIB9	227.84	227.31	209.57	192.63	166.40	113.11	131.37	152.90	
BPOB1	206.54	206.06	192.04	171.60	150.75	101.49	116.12	137.96	
BPOB5	220.54	434.52	396.44	357.30	298.99	195.45	235.48	281.25	
BPOB6	228.13	221.84	202.85	185.05	156.81	104.08	123.09	145.65	
BPOB7	223.52	224.33	207.16	190.57	163.88	110.70	128.39	149.37	

STATIC PRESSURE LEVELS (PSIA)

	FLOW CONDITION								
	F1	F2	F3	F4	F5	F6	F7	F8	F9
CI1	169.58	176.71	167.36	154.31	139.90	94.72	105.57	119.19	240.79
CI2	177.96	176.31	164.72	150.80	135.33	91.77	103.12	117.77	-417.58
CI3	168.74	164.09	149.90	134.80	118.87	79.97	91.72	108.88	225.74
CI4	173.16	166.93	153.39	138.47	122.77	81.05	92.73	108.31	228.77
CI5	173.14	172.88	160.85	147.80	132.76	85.39	99.87	114.74	236.20
CI6	171.71	166.06	155.24	143.30	129.52	86.56	95.63	112.92	234.42
CI7	173.77	172.19	160.18	146.57	131.44	87.57	98.39	112.50	233.08
CI8	173.54	171.04	159.13	145.28	129.81	86.44	97.61	111.63	231.89
CD1	204.53	208.46	192.66	172.61	149.77	100.69	115.62	135.00	278.71
CD2	203.74	209.01	195.01	176.13	154.93	103.48	116.83	134.40	276.93
CD3	202.57	206.10	190.56	168.59	144.99	98.15	112.82	133.55	273.45
CD4	205.41	211.62	195.67	176.16	154.70	103.86	118.13	135.78	278.27
CD5	203.39	207.21	191.06	168.81	144.85	98.41	114.39	135.08	273.49
CD7	200.88	202.99	187.10	166.65	143.63	96.13	112.30	130.70	269.19
CD8	202.93	206.71	192.11	173.74	151.33	101.57	115.63	132.51	236.80
CD9	199.53	203.04	187.93	168.86	145.93	97.71	113.08	131.30	268.09
CD10	200.21	204.49	190.05	171.55	146.33	100.28	113.72	130.93	234.64
CD11	197.15	199.95	186.30	166.97	143.02	96.17	110.21	127.93	227.86
CD13	198.41	202.11	187.36	169.56	146.78	98.97	113.51	130.71	268.01
CD14	196.70	200.82	186.16	169.09	148.20	99.54	112.92	128.47	264.91
CD15	197.51	201.06	185.97	167.89	144.63	96.99	111.65	127.97	267.42
CD16	203.28	207.40	192.51	175.31	153.76	102.64	116.43	133.24	275.16
CD17	202.11	205.46	189.92	172.50	148.30	99.76	115.11	132.48	274.88
CD18	200.60	205.24	191.11	172.84	152.41	101.15	115.56	132.50	273.10
CD19	272.64	274.48	225.14	169.90	148.86	96.56	109.01	123.51	232.99
CD20	196.57	201.52	186.71	167.87	145.75	96.56	110.14	126.85	267.29
CD21	199.15	203.10	187.13	167.38	144.65	96.58	111.03	129.43	270.03
CD22	202.53	208.18	192.81	172.89	145.86	103.86	117.93	136.16	278.90
CS1	202.83	208.52	194.35	176.34	156.22	104.38	118.68	135.40	281.68
CS2	192.84	196.81	182.39	165.15	146.16	97.37	110.36	126.51	261.86
CS3	201.02	203.98	190.19	172.02	151.98	99.87	113.48	130.88	274.33
CS4	197.72	199.54	184.12	166.52	145.91	94.01	107.82	124.74	267.58
CS5	203.27	207.73	193.10	175.52	155.71	103.23	116.92	133.35	276.52
CS6	205.22	209.78	195.73	178.07	158.41	105.54	119.26	135.99	279.50
CS7	202.56	216.26	192.63	174.77	154.88	101.74	115.50	132.87	276.49
CS8	202.96	206.18	191.83	174.98	154.65	101.53	115.57	133.13	277.08

ORIGINAL PAGE IS
OF POOR QUALITY

PUMP PERFORMANCE

DURING TEST

D₁ = 11.25
D₂ = 11.25
1.021

CONFIGURATION 'A'

NASA PRESSURE PULSE DATA (MOD 1)
06/14/88 10:43:15

BAROMETER (IN. HG.) - 30.09				OXYGEN (PPH) - 4				TAU				OMEGA			
PT	RPM	GPM FLOW	MPSH	TIN	TORQUE	BMP	EFF	P INLET	P DISCH	T INLET	T DISCH	T HEX	T DISCH	T INLET	T DISCH
1	2300	170.9	65.8	456.5	0	0.0	0.0	28.92	226.21	76.5	76.5	79.0	76.5	76.5	1.682
2	2300	170.8	65.7	456.6	1	0.0	0.0	28.90	226.21	76.6	76.6	79.2	76.6	76.6	1.681
3	2300	170.8	65.8	457.4	0	0.0	0.0	28.93	226.57	76.8	76.8	79.1	76.8	76.8	1.683
4	2300	170.8	66.1	457.2	0	0.0	0.0	29.07	226.62	76.9	76.9	79.2	76.9	76.9	1.691
5	2300	349.5	65.7	449.7	0	0.0	0.0	28.83	223.12	77.1	77.1	79.3	77.1	77.1	1.681
6	2300	348.4	66.0	448.2	0	0.0	0.0	28.93	222.58	77.1	77.1	79.2	77.1	77.1	1.687
7	2300	348.0	65.8	447.4	0	0.0	0.0	28.87	222.16	77.1	77.1	79.2	77.1	77.1	1.684
8	2300	349.4	66.0	448.4	0	0.0	0.0	28.93	222.67	77.2	77.2	79.2	77.2	77.2	1.687
9	2300	349.3	65.9	448.8	0	0.0	0.0	28.88	222.80	77.3	77.3	79.3	77.3	77.3	1.684
10	2300	500.2	65.1	424.1	0	0.0	0.0	28.43	211.65	77.6	77.6	79.3	77.6	77.6	1.664
11	2300	521.8	64.6	417.9	0	0.0	0.0	28.20	208.77	77.5	77.5	79.3	77.5	77.5	1.651
12	2300	542.5	64.0	409.4	0	0.0	0.0	27.95	204.83	77.7	77.7	79.4	77.7	77.7	1.637
13	2300	543.6	67.2	413.1	0	0.0	0.0	29.31	207.77	78.1	78.1	79.6	78.1	78.1	1.718
14	2300	545.1	68.5	413.8	0	0.0	0.0	29.90	208.67	78.2	78.2	79.6	78.2	78.2	1.752
15	2300	544.8	66.2	412.4	0	0.0	0.0	28.87	207.01	78.3	78.3	79.4	78.3	78.3	1.691
16	2300	543.9	66.1	412.2	0	0.0	0.0	28.83	206.92	78.3	78.3	79.7	78.3	78.3	1.689
17	2300	683.5	65.6	376.0	0	0.0	0.0	28.48	190.90	78.6	78.6	79.5	78.6	78.6	1.677
18	2300	704.4	66.4	372.0	0	0.0	0.0	28.82	189.51	78.5	78.5	79.5	78.5	78.5	1.699
19	2300	703.6	66.5	372.5	0	0.0	0.0	28.87	189.78	78.8	78.8	79.5	78.8	78.8	1.701
20	2300	701.3	66.6	371.0	0	0.0	0.0	28.90	189.17	78.9	78.9	79.5	78.9	78.9	1.697
21	2300	701.3	66.4	370.3	0	0.0	0.0	28.80	188.76	79.1	79.1	79.5	79.1	79.1	1.697
22	2300	701.3	66.2	367.8	0	0.0	0.0	28.74	187.60	79.3	79.3	79.7	79.3	79.3	1.693
23	2300	875.7	66.0	318.6	0	0.0	0.0	28.41	166.03	79.4	79.4	79.7	79.4	79.4	1.687
24	2300	895.7	68.2	311.9	0	0.0	0.0	29.34	164.07	79.6	79.6	79.7	79.6	79.6	1.744
25	2300	897.6	66.8	311.4	0	0.0	0.0	28.74	163.23	79.9	79.9	79.8	79.9	79.9	1.708
26	2300	896.4	65.8	311.2	0	0.0	0.0	28.31	162.75	80.2	80.2	79.9	80.2	80.2	1.683
27	2300	895.1	67.2	310.5	0	0.0	0.0	28.91	163.01	80.2	80.2	79.9	80.2	80.2	1.718
28	2300	893.5	67.1	310.6	0	0.0	0.0	28.88	163.04	80.5	80.5	79.7	80.5	80.5	1.715
29	1780	702.4	65.9	184.0	0	0.0	0.0	28.64	108.10	80.7	80.7	79.7	80.7	80.7	2.815
30	1780	702.0	66.4	183.6	0	0.0	0.0	28.86	108.15	80.8	80.8	79.9	80.8	80.8	2.836
31	1780	702.9	66.6	184.0	0	0.0	0.0	28.92	108.39	80.7	80.7	79.8	80.7	80.7	2.843
32	1780	704.4	66.5	184.1	0	0.0	0.0	28.89	108.39	80.8	80.8	79.9	80.8	80.8	2.839
33	1780	704.2	66.5	183.5	0	0.0	0.0	28.87	108.13	81.0	81.0	79.9	81.0	81.0	2.838
34	1780	703.1	66.6	183.9	0	0.0	0.0	28.91	108.36	80.8	80.8	79.9	80.8	80.8	2.842
35	1780	703.2	66.5	183.5	0	0.0	0.0	28.87	108.15	80.8	80.8	79.7	80.8	80.8	2.838
36	1780	704.0	66.3	183.7	0	0.0	0.0	28.78	108.13	80.9	80.9	79.8	80.9	80.9	2.829
37	1780	702.1	66.4	183.2	0	0.0	0.0	28.84	107.95	80.9	80.9	79.8	80.9	80.9	2.834
38	1780	702.9	66.4	183.1	0	0.0	0.0	28.83	107.91	80.9	80.9	79.8	80.9	80.9	2.833
39	1780	700.2	66.2	184.2	0	0.0	0.0	28.78	108.35	80.9	80.9	79.7	80.9	80.9	2.828
40	1780	703.0	66.2	183.3	0	0.0	0.0	28.88	107.97	80.9	80.9	79.9	80.9	80.9	2.838
41	1780	704.0	66.5	183.0	0	0.0	0.0	28.93	108.15	81.0	81.0	79.9	81.0	81.0	2.838
42	1780	704.2	66.6	183.4	0	0.0	0.0	28.90	108.06	80.9	80.9	79.7	80.9	80.9	2.840
43	1780	704.0	66.5	183.3	0	0.0	0.0	28.90	108.13	81.0	81.0	79.8	81.0	81.0	2.840
44	1780	704.2	66.5	183.4	0	0.0	0.0	28.90	108.13	81.0	81.0	79.8	81.0	81.0	2.840
45	1780	702.3	66.6	184.0	0	0.0	0.0	28.93	108.39	80.9	80.9	79.7	80.9	80.9	2.843
46	1780	523.3	67.3	229.2	0	0.0	0.0	29.45	128.46	81.0	81.0	79.8	81.0	81.0	2.875
47	1780	529.4	67.4	224.6	0	0.0	0.0	29.46	126.45	81.0	81.0	79.7	81.0	81.0	2.877
48	1780	561.4	67.3	217.4	0	0.0	0.0	29.37	123.29	81.1	81.1	79.8	81.1	81.1	2.871
49	1780	567.1	67.1	217.4	0	0.0	0.0	29.37	123.29	81.1	81.1	79.8	81.1	81.1	2.871

D-8

52	1780	341.4	87.3	422.8	0.0	0.0	0.0	125.56	81.1	81.1	79.8	2.	38.8
53	1780	341.8	67.0	222.2	0.0	0.0	0.0	125.24	81.1	81.1	79.8	2.	38.8
54	1780	342.5	66.3	222.3	0.0	0.0	0.0	125.00	81.1	81.1	79.9	2.851	38.8
55	1780	342.0	66.0	222.9	0.0	0.0	0.0	125.10	81.1	81.1	79.9	2.818	38.8
56	1780	340.7	65.8	222.2	0.0	0.0	0.0	124.74	81.2	81.2	79.9	2.808	38.8
57	1780	342.1	65.8	222.2	0.0	0.0	0.0	124.75	81.1	81.1	79.9	2.809	38.8
58	1780	341.6	66.1	222.6	0.0	0.0	0.0	125.00	81.3	81.3	80.0	2.820	38.8
59	1780	342.6	66.5	222.6	0.0	0.0	0.0	125.18	81.1	81.1	79.9	2.833	38.8
60	1780	342.0	66.3	222.8	0.0	0.0	0.0	125.21	81.2	81.2	79.9	2.839	38.8
61	1780	342.6	65.8	223.3	0.0	0.0	0.0	125.24	81.3	81.3	79.9	2.830	38.8
62	1780	340.2	65.7	223.0	0.0	0.0	0.0	125.03	81.2	81.2	79.8	2.811	38.8
63	1780	342.0	65.8	222.7	0.0	0.0	0.0	124.98	81.3	81.3	79.9	2.806	38.8
64	1780	341.7	66.0	222.0	0.0	0.0	0.0	124.75	81.2	81.2	80.0	2.811	38.8
65	1780	341.9	66.1	223.1	0.0	0.0	0.0	125.24	81.2	81.2	80.0	2.820	38.8
66	1780	341.4	66.1	222.6	0.0	0.0	0.0	125.00	81.3	81.3	80.0	2.820	38.8
67	1780	343.8	66.0	226.4	0.0	0.0	0.0	125.00	81.3	81.3	80.1	2.820	38.8
68	1780	442.8	66.2	247.1	0.0	0.0	0.0	117.92	81.2	81.2	79.8	2.817	38.8
69	1780	218.5	66.8	243.3	0.0	0.0	0.0	135.74	81.4	81.4	80.0	2.826	38.8
70	1780	217.0	66.7	243.4	0.0	0.0	0.0	134.47	81.3	81.3	80.0	2.851	38.8
71	1780	224.5	66.7	270.0	0.0	0.0	0.0	134.49	81.5	81.5	79.8	2.848	38.8
72	1780	210.1	66.8	274.5	0.0	0.0	0.0	145.98	81.5	81.5	80.0	2.847	38.8
73	1780	211.9	66.8	272.1	0.0	0.0	0.0	147.94	81.4	81.4	80.0	2.851	38.8
74	1780	177.6	66.8	273.9	0.0	0.0	0.0	146.92	81.4	81.4	79.9	2.852	38.8
75	1780	128.0	66.9	277.7	0.0	0.0	0.0	147.70	81.5	81.5	79.9	2.850	38.8
76	1780	126.6	66.9	274.6	0.0	0.0	0.0	149.42	81.4	81.4	80.0	2.856	38.8
77	1780	131.1	67.0	275.1	0.0	0.0	0.0	148.07	81.4	81.4	80.0	2.857	38.8
78	1780	109.9	66.9	275.7	0.0	0.0	0.0	148.33	81.5	81.5	80.0	2.859	38.8
79	1780	106.6	67.0	272.7	0.0	0.0	0.0	148.57	81.4	81.4	80.1	2.858	38.8
80	1780	106.8	66.6	275.1	0.0	0.0	0.0	147.30	81.5	81.5	80.1	2.860	38.8
81	1780	106.8	65.9	273.1	0.0	0.0	0.0	148.17	81.4	81.4	80.1	2.846	38.8
82	1780	106.6	65.2	272.6	0.0	0.0	0.0	147.00	81.5	81.5	80.0	2.815	38.8
83	1780	106.6	64.9	274.8	0.0	0.0	0.0	146.50	81.5	81.5	80.2	2.783	38.8
84	1780	106.6	64.9	274.6	0.0	0.0	0.0	147.33	81.6	81.6	80.1	2.772	38.8
85	1780	106.6	65.0	273.1	0.0	0.0	0.0	147.21	81.5	81.5	79.9	2.772	38.8
86	1780	106.8	64.9	275.7	0.0	0.0	0.0	146.62	81.4	81.4	80.0	2.774	38.8
87	1780	106.8	64.9	274.9	0.0	0.0	0.0	147.70	81.5	81.5	80.0	2.771	38.8
88	1780	106.6	64.8	273.5	0.0	0.0	0.0	147.33	81.5	81.5	80.2	2.771	38.8
89	1780	106.6	64.8	273.7	0.0	0.0	0.0	146.72	81.3	81.3	80.0	2.768	38.8
90	1780	103.8	64.7	275.5	0.0	0.0	0.0	146.79	81.3	81.3	79.8	2.769	38.8
91	1780	106.8	64.7	274.0	0.0	0.0	0.0	147.52	81.4	81.4	80.0	2.764	38.8
92	1780	106.1	64.9	274.1	0.0	0.0	0.0	146.86	81.4	81.4	80.0	2.762	38.8
93	1780	106.6	64.8	273.9	0.0	0.0	0.0	147.00	81.4	81.4	80.0	2.769	38.8
94	1780	104.2	64.9	274.6	0.0	0.0	0.0	146.89	81.4	81.4	79.8	2.767	38.8
95	1780	106.6	64.8	274.0	0.0	0.0	0.0	147.21	81.3	81.3	79.9	2.771	38.8
96	1780	106.6	64.9	274.1	0.0	0.0	0.0	146.94	81.4	81.4	80.0	2.767	38.8
97	1780	106.8	64.8	274.1	0.0	0.0	0.0	146.98	81.4	81.4	79.8	2.771	38.8
98	1780	261.3	64.8	260.1	0.0	0.0	0.0	140.38	81.4	81.4	80.0	2.767	38.8
99	1780	425.7	64.6	246.9	0.0	0.0	0.0	140.88	81.6	81.6	80.0	2.766	38.8
100	2080	488.7	64.4	337.0	0.0	0.0	0.0	134.99	81.5	81.5	80.0	2.757	38.8
101	2219	517.8	64.4	381.0	0.0	0.0	0.0	173.73	81.7	81.7	80.0	2.011	45.3
102	2318	537.0	64.3	415.9	0.0	0.0	0.0	192.70	81.8	81.8	80.0	1.768	48.4
103	2303	536.1	65.9	412.8	0.0	0.0	0.0	207.73	81.6	81.6	80.0	1.619	50.5
104	2339	538.7	66.4	414.5	0.0	0.0	0.0	207.50	81.6	81.6	79.9	1.681	50.5
105	2310	536.8	65.8	414.5	0.0	0.0	0.0	208.00	81.7	81.7	80.0	1.641	51.0
106	2241	538.2	64.8	414.8	0.0	0.0	0.0	207.74	81.9	81.9	80.0	1.667	50.4
107	2316	536.8	64.4	414.7	0.0	0.0	0.0	207.45	82.1	82.1	80.2	1.744	48.8
108	1405	352.1	64.8	163.6	0.0	0.0	0.0	207.27	82.0	82.0	80.2	1.624	50.5
109	392	124.3	65.0	11.6	0.0	0.0	0.0	99.18	82.0	82.0	80.1	4.442	30.6
110	0	0.0	64.9	0.0	0.0	0.0	0.0	33.73	82.1	82.1	80.3	57.040	8.5
				0.0	0.0	0.0	0.0	28.80	82.2	82.2	80.1	0.000	0.0
				0.0	0.0	0.0	0.0	150.98	80.5	80.5	79.8	2.936	41.7

CONFIDENTIAL

NASA PRESSURE PULSE D (MOD 2)

06/17/88 11:42:59

D₃ = 10.25
D₂ = 10.44

1.379

BAROMETER (IN.HG.) - 29.8

OXYGEN (PPM) - 4

POINT	TIMER	RPM	FLOW	NPSH	TDH	PSIA INLET	PSIA DISCH	T INLET	T DISCH	T HEX	TAU	SPSPD
1	928.31	2268	155.1	62.6	414.5	27.6	206.6	82.4	82.4	81.9	1.646	1268.9
2	936.16	2220	155.4	62.1	425.7	27.4	211.2	82.4	81.0	81.9	1.704	1250.2
3	950.66	2323	153.7	61.9	425.1	27.3	210.8	82.4	82.4	81.8	1.550	1305.1
4	965.68	2323	153.2	61.9	424.5	27.3	210.6	82.2	82.2	81.8	1.549	1303.5
5	980.68	2279	155.5	61.4	425.4	27.1	210.8	82.3	82.3	82.0	1.598	1295.7
6	995.66	2300	160.2	61.2	424.8	27.0	210.4	82.3	82.3	81.9	1.564	1330.0
7	1010.68	2300	160.1	61.3	429.5	27.0	212.5	82.5	82.5	82.0	1.568	1327.5
8	1026.23	2300	160.2	61.1	426.0	27.0	210.9	82.4	82.4	81.9	1.563	1331.1
9	1040.70	2300	161.7	60.9	422.5	26.8	209.3	82.4	82.4	81.9	1.556	1341.8
10	1016	2300	164.1	60.8	428.4	26.8	211.8	82.6	82.6	82.0	1.554	1352.7
11	25.16	2300	161.7	60.5	426.8	26.7	210.9	82.4	82.4	81.8	1.546	1348.3
12	40.70	2300	162.0	60.4	424.4	26.6	209.9	82.6	80.7	81.8	1.544	1350.9
13	55.15	2300	162.3	60.5	427.0	26.7	211.1	82.5	82.5	81.7	1.547	1350.2
14	70.11	2300	159.4	60.2	428.7	26.6	211.7	82.7	82.7	82.0	1.539	1342.7
15	85.15	2300	160.9	60.0	428.3	26.5	211.4	82.7	82.7	82.0	1.535	1352.1
16	100.70	2300	162.7	59.8	429.8	26.3	211.8	82.7	82.7	81.9	1.523	1367.9
17	115.15	2300	161.7	59.8	425.6	26.4	210.2	82.7	82.7	81.9	1.529	1359.3
18	130.11	2300	160.2	60.4	429.5	26.6	212.1	82.5	82.5	81.9	1.544	1343.5
19	145.16	2300	162.3	62.2	426.1	27.4	211.4	82.6	82.6	81.8	1.589	1323.0
20	160.65	2300	162.4	64.7	424.9	28.2	211.9	82.7	82.6	81.8	1.654	1284.3
21	175.15	2300	162.0	66.6	426.9	29.3	213.6	82.6	82.6	82.1	1.702	1255.6
22	190.16	2300	161.3	66.2	422.5	29.1	211.6	82.6	82.6	82.0	1.692	1258.3
23	205.16	2300	161.0	65.1	429.8	28.7	214.3	82.8	82.8	81.9	1.654	1283.7
24	220.73	2300	162.3	64.7	428.2	28.5	213.4	82.8	82.8	81.7	1.648	1287.3
25	235.15	2300	162.3	64.5	425.1	28.4	212.0	82.6	82.6	81.8	1.647	1288.8
26	250.13	2300	162.4	64.4	420.3	28.4	209.8	82.8	82.8	81.9	1.623	1857.7
27	265.13	2300	330.3	63.5	418.7	27.9	208.7	83.1	83.1	81.8	1.613	1975.9
28	280.71	2300	370.0	63.1	420.4	27.7	209.2	83.0	83.0	81.7	1.605	1972.3
29	295.15	2300	366.2	62.8	421.8	27.6	209.7	83.1	83.1	81.7	1.600	1924.7
30	310.11	2300	347.1	62.6	424.8	27.5	210.9	83.1	83.1	81.9	1.600	1927.6
31	325.16	2300	348.1	62.6	423.6	27.5	210.4	83.2	80.7	81.8	1.647	1886.6
32	340.08	2300	348.3	64.4	424.3	28.3	211.5	83.1	83.1	81.8	1.692	1851.4
33	355.16	2300	349.2	66.2	423.4	29.1	211.9	83.1	83.1	81.8	1.689	1855.6
34	370.16	2300	350.0	66.1	424.0	29.0	212.1	83.1	83.1	81.9	1.682	1859.9
35	385.16	2300	349.2	65.8	423.8	28.9	211.9	83.2	83.2	81.9	1.672	1870.5
36	400.16	2300	350.2	65.4	423.7	28.7	211.3	83.2	80.9	81.6	1.669	1871.5
37	415.16	2300	349.5	65.3	423.1	28.7	211.3	83.2	83.2	81.8	1.666	1875.7
38	430.16	2300	350.1	65.2	425.0	28.6	212.1	83.2	83.2	81.9	1.661	1879.9
39	445.16	2300	350.2	65.0	423.5	28.5	211.4	83.2	80.9	81.8	1.664	1877.7
40	460.16	2300	350.2	65.1	425.7	28.6	212.4	83.4	83.4	81.9	1.675	1866.2
41	475.16	2300	350.2	65.1	424.0	28.8	211.8	83.3	83.3	81.7	1.684	1861.1
42	490.16	2300	349.5	65.9	427.0	28.9	212.0	83.5	83.5	81.8	1.680	1867.0
43	505.16	2300	351.3	65.7	424.4	28.9	213.5	83.4	83.4	81.9	1.679	1866.6
44	520.16	2300	350.9	65.7	424.4	28.9	212.1	83.5	83.5	81.9	1.675	1869.0
45	535.16	2300	350.6	65.5	422.2	28.8	211.1	83.5	83.5	81.9	1.673	1870.1
46	550.16	2300	350.2	65.4	423.0	28.7	211.4	83.6	83.6	81.9	1.672	1873.8
47	565.16	2300	351.3	65.4	423.2	28.7	211.4	83.5	83.5	81.9	1.670	1874.8
48	580.16	2300	351.1	65.3	424.8	28.7	212.1	83.5	83.5	81.8	1.665	2133.2
49	595.16	2300	352.4	65.1	404.3	28.5	203.1	83.5	83.5	81.7	1.627	2498.6
50	610.16	2300	359.6	63.6	365.5	27.8	185.5	83.7	83.7	81.9	1.645	2587.0
51	625.16	2300	353.3	64.3	359.7	28.0	183.3	83.7	83.7	81.8	1.646	2436.7
52	640.16	2300	358.2	64.4	386.2	28.1	194.9	83.7	83.7	81.9	1.651	2301.3
53	655.16	2300	359.3	64.6	399.3	28.3	200.6	83.8	83.8	82.1	1.642	2429.9
54	670.16	2300	377.3	64.2	373.7	28.1	189.3	84.0	84.0	82.0	1.637	2513.1
55	685.16	2300	397.5	64.0	397.5	27.9	199.7	83.9	83.9	81.9	1.644	2340.5
56	700.16	2300	534.3	64.3	397.5	28.1	199.7	83.9	83.9	81.9	1.644	2340.5

CONFIDENTIAL
OF POOR QUALITY

58	7.76	2300	553.8	64.2	384.3	48.1
59	22.78	2300	554.8	64.1	384.5	28.0
60	38.25	2300	554.6	64.0	384.7	28.0
61	52.78	2300	553.2	64.6	385.3	28.2
62	67.73	2300	555.1	65.1	385.3	28.4
63	82.78	2300	555.0	65.8	384.6	28.9
64	98.31	2300	553.8	66.2	384.1	28.9
65	112.78	2300	554.5	66.5	385.6	29.1
66	127.75	2300	554.5	66.3	384.2	29.0
67	142.78	2300	554.5	66.2	384.4	28.9
68	158.31	2300	555.7	66.1	385.4	28.9
69	172.76	2300	556.4	66.1	385.4	28.9
70	187.76	2300	553.8	65.9	385.1	28.8
71	202.73	2300	554.0	65.6	385.3	28.7
72	218.26	2300	554.5	65.7	385.3	28.7
73	232.76	2300	554.5	65.7	385.0	28.7
74	247.76	2300	555.1	65.8	384.8	28.7
75	262.73	2300	554.5	65.6	384.7	28.7
76	278.28	2300	554.5	65.6	384.7	28.7
77	292.76	2300	553.8	64.9	385.5	28.2
78	307.76	2300	553.8	64.7	384.7	28.1
79	322.73	2300	553.8	64.7	384.7	28.1
80	337.73	2300	553.8	64.7	384.7	28.1
81	352.73	2300	553.8	64.7	384.7	28.1
82	367.73	2300	553.8	64.7	384.7	28.1
83	382.73	2300	553.8	64.7	384.7	28.1
84	397.73	2300	553.8	64.7	384.7	28.1
85	412.73	2300	553.8	64.7	384.7	28.1
86	427.73	2300	553.8	64.7	384.7	28.1
87	442.73	2300	553.8	64.7	384.7	28.1
88	457.73	2300	553.8	64.7	384.7	28.1
89	472.73	2300	553.8	64.7	384.7	28.1
90	487.73	2300	553.8	64.7	384.7	28.1
91	502.73	2300	553.8	64.7	384.7	28.1
92	517.73	2300	553.8	64.7	384.7	28.1
93	532.73	2300	553.8	64.7	384.7	28.1
94	547.73	2300	553.8	64.7	384.7	28.1
95	562.73	2300	553.8	64.7	384.7	28.1
96	577.73	2300	553.8	64.7	384.7	28.1
97	592.73	2300	553.8	64.7	384.7	28.1
98	607.73	2300	553.8	64.7	384.7	28.1
99	622.73	2300	553.8	64.7	384.7	28.1
100	637.73	2300	553.8	64.7	384.7	28.1
101	652.73	2300	553.8	64.7	384.7	28.1
102	667.73	2300	553.8	64.7	384.7	28.1
103	682.73	2300	553.8	64.7	384.7	28.1
104	697.73	2300	553.8	64.7	384.7	28.1
105	712.73	2300	553.8	64.7	384.7	28.1
106	727.73	2300	553.8	64.7	384.7	28.1
107	742.73	2300	553.8	64.7	384.7	28.1
108	757.73	2300	553.8	64.7	384.7	28.1
109	772.73	2300	553.8	64.7	384.7	28.1
110	787.73	2300	553.8	64.7	384.7	28.1
111	802.73	2300	553.8	64.7	384.7	28.1
112	817.73	2300	553.8	64.7	384.7	28.1
113	832.73	2300	553.8	64.7	384.7	28.1
114	847.73	2300	553.8	64.7	384.7	28.1
115	862.73	2300	553.8	64.7	384.7	28.1
116	877.73	2300	553.8	64.7	384.7	28.1
117	892.73	2300	553.8	64.7	384.7	28.1
118	907.73	2300	553.8	64.7	384.7	28.1
119	922.73	2300	553.8	64.7	384.7	28.1
120	937.73	2300	553.8	64.7	384.7	28.1
121	952.73	2300	553.8	64.7	384.7	28.1

ORIGINAL PAGE IS
OF POOR QUALITY

125	1780	703.7	67.2	169.1	29.2	81.6	2.938	191
126	1780	705.5	66.8	169.0	29.1	81.6	2.868	201.1
127	1780	703.1	66.2	170.7	28.8	81.6	2.853	202.1
128	1780	704.8	66.0	169.8	28.7	81.6	2.826	203.7
129	1780	704.2	65.7	170.1	28.6	81.6	2.817	204.3
130	1780	704.8	65.8	170.1	28.6	81.6	2.806	204.1
131	1780	705.5	65.6	169.6	28.5	81.6	2.810	204.9
132	1780	701.1	65.7	170.7	28.6	81.5	2.806	204.7
133	1780	703.1	65.5	170.2	28.5	81.6	2.797	204.8
134	1780	703.7	65.5	170.3	28.5	81.6	2.797	204.8
135	1780	704.1	65.7	170.5	28.6	81.6	2.807	204.6
136	1780	705.7	66.0	169.9	28.7	81.6	2.827	204.4
137	1780	703.9	66.2	170.1	28.8	81.6	2.827	204.4
138	1780	701.4	66.2	169.8	28.9	81.7	2.840	203.0
139	1780	700.1	66.2	170.9	28.9	81.6	2.840	203.0
140	1780	701.6	66.4	170.1	28.9	81.5	2.835	202.8
141	1780	701.9	66.3	170.6	28.8	81.5	2.830	202.8
142	1780	588.2	66.5	197.4	29.1	81.7	2.841	185.1
143	1780	523.3	66.5	213.5	29.1	81.7	2.841	1746.3
144	1780	539.5	66.4	208.2	29.1	81.6	2.836	1775.9
145	1780	541.9	66.4	209.2	29.0	81.6	2.833	1781.3
146	1780	542.2	66.1	210.0	28.9	81.5	2.823	1786.5
147	1780	542.2	65.8	209.1	28.8	81.6	2.813	1791.1
148	1780	540.9	65.8	209.2	28.8	81.5	2.809	1791.2
149	1780	540.5	65.6	209.7	28.7	81.6	2.802	1793.7
150	1780	541.5	65.4	209.2	28.6	81.5	2.794	1799.4
151	1780	542.1	65.2	209.7	28.5	81.4	2.785	1804.8
152	1780	542.2	65.2	209.7	28.5	81.5	2.783	1805.5
153	1780	540.9	65.1	209.8	28.5	81.5	2.779	1805.5
154	1780	541.5	65.0	209.9	28.5	81.5	2.777	1807.5
155	1780	540.2	65.0	209.4	28.5	81.5	2.775	1807.5
156	1780	540.2	65.2	210.4	28.5	81.6	2.784	1801.7
157	1780	541.5	65.3	209.7	28.6	81.7	2.788	1802.1
158	1780	542.8	65.5	209.5	28.7	81.6	2.795	1800.7
159	1780	540.9	65.7	209.3	28.7	81.5	2.803	1793.7
160	1780	541.7	65.8	208.9	28.8	81.7	2.808	1792.9
161	1780	541.5	65.9	209.6	28.8	81.6	2.813	1790.1
162	1780	401.1	66.3	216.3	29.1	81.8	2.831	1533.4
163	1780	225.0	66.6	251.3	29.4	81.7	2.845	1144.2
164	1780	128.8	67.0	261.2	29.5	81.7	2.860	852.3
165	1780	128.1	66.8	258.3	29.5	81.6	2.854	861.3
166	1780	119.4	67.0	255.0	29.6	81.7	2.862	830.0
167	1780	109.9	68.0	255.0	30.0	81.6	2.905	787.3
168	1780	92.2	67.4	255.1	29.7	81.7	2.877	726.7
169	1780	92.5	67.4	254.8	29.7	81.6	2.875	727.9
170	1780	158.0	67.7	253.1	29.8	81.6	2.890	947.6
171	1780	157.8	67.6	261.1	29.8	81.5	2.887	947.9
172	1780	144.3	67.5	261.6	29.8	81.5	2.883	907.3
173	1780	116.4	67.6	256.4	29.8	81.6	2.887	814.0
174	1780	113.3	64.8	255.7	28.6	81.7	2.765	829.6
175	1780	111.7	64.8	257.6	28.7	81.6	2.765	823.7
176	1780	113.3	65.1	256.7	28.7	81.6	2.780	826.3
177	1780	113.3	65.2	257.3	28.8	81.6	2.785	825.2
178	1780	113.3	64.9	255.4	28.7	81.6	2.773	827.7
179	1780	113.3	65.3	254.9	28.8	81.4	2.787	824.6
180	1780	113.1	64.9	254.9	28.6	81.4	2.770	827.7
181	1780	113.3	64.9	257.6	28.6	81.5	2.770	828.5
182	1780	113.3	64.9	256.8	28.6	81.4	2.779	825.7
183	1780	113.1	65.1	254.3	28.7	81.6	2.763	829.3
184	1780	113.1	64.7	255.0	28.6	81.3	2.765	828.9
185	1780	113.1	64.8	257.0	28.6	81.4	2.764	829.1
186	1780	113.1	64.7	256.7	28.6	81.4	2.770	827.6
187	1780	113.1	64.9	257.6	28.6	81.4	2.770	827.6

ORIGINAL PAGE IS
OF POOR QUALITY

191	243.00	80	110.3	64.8	253.9	28.6	1	85.5	80.7	81.5	2.756	1
192	258.03	80	130.6	64.6	374.2	28.6	1	85.4	85.4	81.4	2.766	3
193	272.96	2300	135.7	64.8	417.6	28.5	150.0	85.3	85.3	81.4	2.757	894.7
194	287.96	2300	136.0	64.5	427.9	28.5	208.9	85.4	85.4	81.4	1.657	1172.5
195	303.01	2306	136.8	64.6	427.4	28.5	213.2	85.4	85.4	81.4	1.649	1177.9
196	9.60	1270	84.4	65.0	135.1	28.7	212.9	85.4	85.4	81.3	1.642	1184.0
197	24.61	482	38.9	65.0	19.9	28.7	87.0	85.4	85.4	81.4	5.446	509.9
198	40.63	0	0.0	65.0	0.0	28.7	37.3	85.5	85.5	81.5	37.779	131.4
AVERAGE	2087		469.9	65.3	315.9	28.5	164.9	84.6	83.9	81.7	2.265	1895.3

ORIGINAL PAGE IS
OF POOR QUALITY

ORIGINAL PAGE IS
OF POOR QUALITY

DS 14
24256

CONF 'C'

NASA PRESSURE PULSE DATA (MOD 3)

09/29/88 14:09:19

OXYGEN (PPM) - 2.5

BAROMETER (IN.HG.)-30.2

POINT	TIMER	RPM	FLOW	NPSH	TDH	PSIA INLET	PSIA DISCH	T INLET	T DISCH	T HEX	TAU	SPOSD
1	0.01	2300	157.0	66.8	412.9	29.3	207.8	73.4	73.4	69.8	1.709	1232.5
2	0.87	2300	157.0	64.7	414.7	28.3	207.6	73.4	73.4	70.0	1.654	1263.1
3	1.70	2300	157.6	62.8	413.8	27.5	206.4	73.6	73.6	70.0	1.605	1294.2
4	1.97	2300	156.9	61.8	415.3	27.1	206.6	73.7	73.7	69.9	1.581	1305.8
5	2.21	2300	156.6	60.9	415.4	26.7	206.3	73.5	73.5	70.0	1.557	1319.6
6	2.45	2300	156.5	60.8	415.5	26.2	206.3	73.6	73.6	70.0	1.555	1320.4
7	2.71	2300	156.2	59.8	413.3	26.1	204.9	73.6	73.6	70.0	1.529	1336.2
8	2.95	2300	156.7	59.2	414.1	26.0	205.0	73.6	73.6	70.1	1.520	1339.2
9	3.22	2300	156.2	58.6	414.4	25.7	204.8	73.8	73.8	69.9	1.514	1348.3
10	3.45	2300	156.2	57.8	414.3	25.4	204.4	73.9	73.9	70.1	1.497	1370.8
11	3.70	2300	174.9	58.7	411.9	25.8	203.8	73.9	73.9	70.1	1.501	1433.7
12	3.96	2300	204.4	58.5	413.8	25.7	204.5	73.9	73.9	69.9	1.496	1533.9
13	4.20	2300	259.2	60.2	411.4	26.4	204.2	73.9	73.9	70.1	1.540	1711.6
14	4.47	2300	402.7	61.2	395.4	26.7	197.6	74.0	74.0	69.9	1.564	2109.2
15	4.70	2300	404.7	62.5	402.4	27.3	201.2	74.2	74.2	70.0	1.597	2081.4
16	4.97	2300	353.1	63.7	414.4	27.8	207.0	74.2	74.2	70.1	1.628	1916.4
17	5.21	2300	345.4	64.5	418.9	28.2	209.3	74.1	74.1	70.1	1.650	1876.5
18	5.45	2300	344.9	65.5	417.1	28.6	208.9	74.1	74.1	70.0	1.675	1853.6
19	5.71	2300	344.8	66.2	416.7	29.0	209.1	74.2	74.2	70.0	1.694	1838.3
20	5.95	2300	344.7	66.5	416.2	29.0	209.0	74.0	74.0	70.0	1.699	1833.7
21	6.22	2300	347.0	66.3	420.7	29.0	210.8	74.1	74.1	70.1	1.695	1843.4
22	6.45	2300	346.9	66.5	422.8	29.1	211.8	74.2	74.2	70.1	1.701	1837.8
23	6.70	2300	347.0	66.9	422.8	29.2	212.0	74.1	74.1	70.0	1.710	1831.2
24	6.96	2300	347.0	67.0	422.4	29.3	211.7	74.1	74.1	70.0	1.713	1830.5
25	7.20	2300	346.2	67.0	422.1	29.3	211.6	74.3	74.3	70.1	1.714	1828.0
26	7.46	2300	347.1	67.0	421.7	29.3	211.1	74.3	74.3	70.1	1.712	1829.5
27	7.70	2300	347.0	67.0	420.7	29.3	211.3	74.2	74.2	70.0	1.707	1831.4
28	7.97	2300	346.3	66.8	421.2	29.2	211.3	74.4	74.4	70.1	1.703	1836.0
29	8.21	2300	346.8	66.6	421.4	29.1	211.3	74.4	74.4	70.0	1.702	1835.3
30	8.45	2300	346.3	66.6	420.6	29.1	210.9	74.4	74.4	70.0	1.699	1838.3
31	8.71	2300	346.1	66.6	420.6	29.1	211.1	74.3	74.3	70.0	1.699	1838.3

38	10.	2300	422.7	65.9	411.9	204.5	74.4	69.9	1.691	1843.4
39	10.1	2300	553.6	65.4	375.8	206.8	74.5	69.9	1.686	2022.6
40	10.98	2300	552.6	65.6	384.8	190.9	74.5	70.0	1.685	2043.7
41	11.22	2300	547.3	66.0	386.8	194.9	74.6	70.0	1.672	2351.9
42	11.46	2300	546.1	66.4	388.3	195.9	74.5	70.0	1.678	2343.9
43	0.15	2300	545.3	66.7	388.1	196.7	74.6	70.0	1.689	2321.2
44	1.14	2300	546.3	67.8	388.5	196.7	74.6	69.8	1.698	2308.7
45	2.15	2300	546.4	67.6	388.3	197.4	74.7	70.0	1.698	2308.7
46	3.14	2300	544.9	67.5	388.3	197.2	74.8	70.0	1.705	2300.4
47	3.99	2300	545.1	67.2	386.9	196.5	75.0	69.8	1.735	2272.9
48	4.21	2300	544.9	67.2	386.9	196.5	75.0	69.8	1.729	2272.8
49	4.48	2300	563.4	67.2	387.5	196.5	75.3	70.0	1.726	2278.8
50	4.71	2300	697.8	66.7	383.5	196.7	75.3	70.0	1.719	2286.2
51	4.96	2300	707.2	66.7	337.5	195.0	75.4	70.0	1.719	2285.4
52	5.22	2300	701.0	66.5	348.6	174.7	75.4	69.9	1.718	2324.7
53	5.46	2300	706.0	67.1	346.1	178.5	75.4	70.0	1.705	2602.2
54	5.71	2300	703.0	67.5	347.3	179.1	75.4	70.0	1.699	2626.1
55	5.97	2300	699.0	67.7	347.2	179.3	75.5	69.9	1.710	2604.0
56	6.21	2300	701.9	68.0	347.7	179.5	75.5	69.9	1.717	2603.9
57	6.46	2300	704.3	68.0	346.7	179.5	75.5	69.9	1.727	2587.4
58	6.73	2300	703.3	67.9	346.9	179.3	75.7	70.0	1.730	2575.7
59	6.96	2300	703.3	68.0	347.1	179.3	75.7	69.9	1.739	2571.9
60	7.21	2300	704.1	67.9	346.1	179.4	75.8	69.9	1.738	2576.5
61	7.47	2300	703.8	67.9	346.9	179.0	75.7	70.0	1.737	2576.7
62	7.71	2300	705.8	67.9	347.6	179.3	75.8	70.1	1.739	2574.2
63	7.96	2300	702.7	67.9	347.3	179.6	75.9	70.1	1.737	2578.0
64	8.22	2300	703.6	68.0	347.3	179.5	75.9	70.0	1.737	2577.2
65	8.46	2300	703.4	68.0	348.1	179.5	75.9	70.1	1.737	2580.5
66	8.71	2300	703.8	68.1	347.6	179.8	75.9	70.1	1.737	2575.3
67	8.98	2300	703.5	68.1	347.6	179.6	76.0	70.0	1.738	2575.6
68	9.21	2300	704.8	68.1	347.6	179.7	76.1	70.0	1.739	2574.6
69	9.46	2300	704.6	68.1	347.8	179.7	76.1	70.0	1.740	2573.8
70	9.74	2300	704.6	68.1	348.2	179.7	76.1	70.0	1.740	2573.8
71	9.97	2300	4916.5	115.7	316.5	179.9	76.1	70.0	1.740	2575.3
72	10.21	2300	745.4	68.3	321.9	166.5	76.1	70.1	1.741	2574.7
73	10.48	2300	753.7	68.2	328.0	168.7	76.2	70.1	1.731	503.1
74	10.72	2300	854.9	67.7	329.7	171.3	76.2	70.0	1.731	4569.1
75	10.96	2300	864.2	67.8	307.4	171.9	76.2	70.1	1.745	2640.5
76	11.23	2300	1018.2	67.2	305.8	161.9	76.3	70.1	1.745	2658.3
77	11.46	2300	928.5	67.4	250.0	161.3	76.4	70.1	1.731	2847.2
78	11.73	2300	886.2	67.5	287.4	153.0	76.5	70.1	1.734	2859.6
79	11.97	2300	886.6	67.5	298.0	157.7	76.5	70.1	1.717	3126.1
80	12.21	2300	909.4	67.3	300.9	159.0	76.5	70.1	1.723	2977.6
81	12.47	2300	883.8	67.3	288.2	153.4	76.7	70.0	1.725	2906.7
82	12.71	2300	876.4	67.5	299.1	153.4	76.7	70.0	1.726	2906.2
83	12.98	2300	878.3	67.4	300.4	158.2	76.7	70.1	1.721	2950.0
84	13.22	2300	875.1	67.4	302.9	158.8	76.7	70.1	1.735	2903.1
85	13.46	2300	874.4	67.4	302.2	159.8	76.8	70.1	1.725	2890.8
86	13.73	2300	867.3	67.4	301.5	159.5	76.9	70.1	1.722	2897.5
87	13.96	2300	866.0	67.5	300.7	159.3	76.9	70.2	1.723	2891.2
88	14.23	2300	873.8	67.6	303.0	158.9	77.0	70.2	1.724	2888.6
89	14.47	2300	868.0	67.6	303.0	159.4	77.1	70.0	1.723	2877.9
90	14.71	2300	869.0	67.8	302.8	160.0	77.1	70.1	1.725	2873.1
91	14.98	2300	865.7	67.9	303.1	160.0	77.1	70.1	1.729	2873.1
92	15.21	2300	864.7	68.0	304.1	160.2	77.2	70.1	1.733	2867.0
93	15.48	2300	864.7	68.2	303.5	160.6	77.2	70.1	1.737	2863.4
94	15.72	2300	866.0	68.3	303.9	160.6	77.2	70.0	1.739	2855.7
95	15.96	2300	866.0	68.5	305.4	161.3	77.3	70.2	1.743	2848.8
96	16.23	2300	862.0	68.5	305.3	161.3	77.3	70.0	1.745	2847.1
97	16.46	2300	863.1	68.4	305.4	161.4	77.5	70.1	1.747	2847.0
98	16.74	1780	867.3	68.2	306.0	161.6	77.4	70.2	1.750	2842.2
99	16.97	1780	867.3	68.7	304.9	161.1	77.5	70.1	1.751	2835.6
100	17.21	1780	867.3	68.7	228.6	128.4	77.5	70.1	1.748	2840.7
101	17.45	1780	867.3	68.7	228.6	128.4	77.5	70.1	1.745	2851.3

102	17.73	1780	673.2	67.8	181.4	29.3	77.6	69.9	2.894	353.9
103	17.9	1780	675.1	67.6	181.4	29.3	77.6	69.9	2.888	360.0
104	18.2	1780	675.7	67.4	181.6	29.2	77.6	70.0	2.877	366.3
105	18.46	1780	671.5	67.2	181.5	29.1	77.6	70.0	2.861	368.3
106	18.73	1780	671.5	67.0	180.9	29.0	77.6	70.0	2.858	372.2
107	18.97	1780	673.2	66.9	180.9	29.0	77.7	70.0	2.848	377.5
108	19.21	1780	673.2	66.7	181.0	28.9	77.7	70.1	2.842	378.0
109	19.48	1780	671.5	66.6	180.8	28.9	77.6	70.0	2.833	382.7
110	19.71	1780	671.5	66.4	181.6	28.8	77.7	70.1	2.828	389.9
111	19.98	1780	674.4	66.2	181.7	28.7	77.8	70.0	2.824	391.4
112	20.22	1780	674.1	66.1	181.5	28.7	77.8	70.1	2.817	396.0
113	20.46	1780	674.7	66.0	181.2	28.6	77.7	70.0	2.812	399.6
114	20.73	1780	671.3	65.9	181.6	28.6	77.8	70.0	2.801	400.2
115	20.96	1780	673.3	65.8	181.5	28.4	77.8	69.9	2.798	400.1
116	21.23	1780	670.5	65.5	181.4	28.4	77.6	70.0	2.794	404.6
117	21.47	1780	670.5	65.4	181.5	28.4	77.6	70.0	2.837	409.4
118	21.71	1780	670.5	65.4	181.4	28.8	77.8	69.9	2.868	414.2
119	21.98	1780	671.3	65.3	181.0	29.1	77.8	70.0	2.904	430.7
120	22.21	1780	660.7	65.0	180.9	29.5	77.8	70.0	2.950	437.3
121	22.49	1780	535.3	63.1	215.8	30.1	77.8	69.9	2.979	465.8
122	22.71	1780	517.0	62.8	215.9	30.4	77.9	69.9	3.005	465.3
123	22.96	1780	510.0	60.4	217.8	30.7	77.8	69.9	3.016	475.3
124	23.23	1780	576.7	70.6	197.0	30.7	77.8	70.0	3.042	468.4
125	23.46	1780	541.1	71.3	209.4	31.0	77.9	70.0	3.062	4673.9
126	23.71	1780	537.8	71.7	210.4	31.2	78.0	70.1	3.079	4655.1
127	23.97	1780	530.0	72.1	210.1	31.4	78.0	69.9	3.094	4814.1
128	24.21	1780	532.1	72.5	209.5	31.5	78.0	69.9	2.916	4727.2
129	24.46	1780	532.0	68.3	210.1	29.8	78.0	69.9	2.912	4725.9
130	24.73	1780	530.1	68.2	210.2	29.7	78.1	69.9	2.909	4727.8
131	24.96	1780	530.4	68.1	210.2	29.7	77.9	70.0	2.904	4731.5
132	25.21	1780	531.4	68.0	210.1	29.6	77.9	70.0	2.899	4733.9
133	25.47	1780	531.5	67.9	211.0	29.6	78.1	69.9	2.889	4738.0
134	25.71	1780	531.3	67.7	210.7	29.5	78.1	69.9	2.879	4742.7
135	25.96	1780	531.3	67.4	210.7	29.4	78.1	69.9	2.867	4749.3
136	26.22	1780	532.0	67.1	211.6	29.3	78.1	69.9	2.857	4752.6
137	26.46	1780	531.4	66.9	210.6	29.2	78.1	69.9	2.847	4755.8
138	26.71	1780	530.5	66.7	210.6	29.1	78.1	69.9	2.840	4759.9
139	26.98	1780	531.0	66.5	210.7	29.0	78.2	70.0	2.829	4765.9
140	27.21	1780	531.9	66.3	210.3	28.9	78.1	69.9	2.820	4771.3
141	27.46	1780	532.3	66.1	210.7	28.8	78.1	69.9	2.814	4774.0
142	27.72	1780	532.1	65.9	211.0	28.7	78.3	69.9	2.806	4750.7
143	27.96	1780	516.1	65.7	212.7	28.7	78.2	70.0	2.827	493.5
144	28.21	1780	168.0	66.2	257.1	29.1	78.2	70.0	2.823	4971.0
145	28.48	1780	160.2	66.1	254.2	29.0	78.2	69.9	2.818	4988.8
146	28.71	1780	116.3	66.0	253.9	29.0	78.1	69.9	2.810	4930.5
147	28.96	1780	116.3	65.8	252.0	28.9	78.1	69.9	2.806	4930.8
148	29.23	1780	116.3	65.7	253.4	28.9	78.3	70.0	2.801	4931.9
149	29.46	1780	116.1	65.6	253.2	28.8	78.1	70.0	2.796	4930.1
150	29.71	1780	115.4	65.5	249.6	28.8	78.2	70.0	2.791	4932.6
151	29.97	1780	115.8	65.4	253.2	28.7	78.2	70.0	2.786	4935.2
152	30.21	1780	116.1	65.3	254.7	28.7	78.2	70.0	2.779	4935.4
153	30.46	1780	115.8	65.1	253.2	28.6	78.2	70.0	2.777	4937.2
154	30.73	1780	116.1	65.0	252.9	28.6	78.1	69.9	2.770	4934.0
155	30.96	1780	114.8	64.9	252.4	28.5	78.2	69.9	2.765	4937.9
156	31.21	1780	115.6	64.8	252.5	28.5	78.2	69.9	2.761	4936.0
157	31.48	1780	114.8	64.7	252.2	28.4	78.2	69.9	2.755	4938.9
158	31.71	1780	114.4	64.5	250.6	28.4	78.2	70.0	2.745	4937.4
159	31.96	1780	115.0	64.4	251.9	28.3	78.2	70.0	2.738	4941.1
160	32.22	1780	114.2	64.3	252.4	28.3	78.2	69.9	2.734	4940.1
161	32.46	1780	114.8	64.1	251.7	28.2	78.1	69.9	2.731	4942.9
162	32.71	1780	114.2	64.0	252.4	28.2	78.1	69.8	2.731	4941.9
163	32.98	1780	114.8	64.0	252.3	28.1	78.1	69.9	2.731	4941.9
164	33.21	1780	114.8	64.0	252.3	28.1	78.1	69.9	2.731	4941.9

ORIGINAL PAGE IS
OF POOR QUALITY

169	1.46	2291	136.1	63.7	413.3	28.0	206.6	78.2	78.2	69.8	1.1	1185.7
170	4.71	2263	141.4	63.6	414.2	28.0	207.0	78.2	78.2	69.9	1.1	1184.9
171	34.98	2328	144.1	63.6	422.4	28.0	206.9	78.2	78.2	69.9	1.678	1195.0
172	35.21	2413	148.5	63.6	457.6	27.9	210.4	78.2	78.2	69.8	1.587	1239.9
173	35.46	2534	153.3	63.6	507.6	27.9	225.6	78.3	78.3	69.9	1.477	1305.4
174	35.73	2631	157.9	63.5	547.8	27.9	247.2	78.2	78.2	69.9	1.338	1393.5
175	35.96	2646	159.3	63.5	561.8	27.9	264.6	78.3	78.3	69.8	1.241	1468.8
176	36.21	2668	158.5	63.8	567.4	28.1	270.6	78.4	78.4	69.9	1.227	1483.4
177	36.47	2673	158.8	63.9	563.4	28.1	271.5	78.4	78.4	69.9	1.213	1486.9
178	36.71	2655	159.0	64.1	565.2	28.2	272.3	78.5	78.5	69.8	1.210	1488.6
179	36.96	2680	158.6	64.2	568.1	28.2	273.6	78.6	78.6	69.8	1.230	1477.0
180	37.23	2485	152.8	64.4	514.9	28.2	250.7	78.5	78.5	69.9	1.410	1487.4
181	37.46	1920	124.8	64.3	295.1	28.3	155.8	78.5	78.5	69.9	2.360	944.0
182	37.71	1757	117.9	64.4	245.2	28.3	134.2	78.6	78.6	69.9	2.820	839.0
183	37.98	1773	118.2	64.4	245.4	28.3	134.3	78.6	78.6	69.9	2.769	848.1
184	38.21	1757	118.2	64.4	245.4	28.3	134.3	78.5	78.5	69.9	2.819	840.6
185	38.46	1780	118.6	64.4	246.1	28.3	134.6	78.6	78.6	69.8	2.748	852.6
186	38.73	1782	117.9	64.4	247.0	28.3	135.0	78.6	78.6	69.9	2.742	850.9
187	38.96	1760	119.0	64.5	246.0	28.3	134.6	78.6	78.6	69.9	2.813	843.9
188	39.21	1755	119.2	64.4	248.0	28.3	135.5	78.5	78.5	69.9	2.829	842.2
189	39.48	1788	119.0	64.4	248.8	28.3	135.8	78.7	78.7	69.9	2.722	858.2
190	39.71	1766	118.2	64.4	247.8	28.3	135.4	78.7	78.7	69.9	2.794	844.2
191	39.96	1765	119.0	64.5	247.1	28.3	135.1	78.7	78.7	69.9	2.799	846.0
192	40.23	1780	119.0	64.4	247.9	28.3	135.4	78.7	78.7	69.9	2.746	854.3
193	40.46	1784	119.0	64.4	246.8	28.3	135.0	78.6	78.6	69.8	2.739	855.3
194	40.71	1772	118.4	64.4	247.2	28.3	135.1	78.8	78.8	69.8	2.775	847.6
195	40.98	1558	109.8	64.5	194.6	28.4	112.4	78.8	78.8	69.9	3.590	717.7
196	41.21	1521	107.2	64.5	184.5	28.4	108.1	78.8	78.8	69.8	3.767	692.0
197	41.46	1554	107.6	64.4	183.9	28.3	107.8	78.8	78.8	70.0	3.607	708.8
198	41.73	1492	107.6	64.4	186.0	28.3	108.7	78.8	78.8	69.9	3.911	680.8
199	41.96	1535	107.2	64.4	184.5	28.3	108.1	78.9	78.9	69.8	3.697	698.7
200	42.21	1493	107.2	64.4	184.7	28.3	108.1	78.9	78.9	69.8	3.905	680.0
201	42.48	1521	107.8	64.5	184.4	28.3	108.0	78.9	78.9	69.9	3.766	694.2
202	42.71	1528	107.2	64.5	185.1	28.4	108.3	79.0	79.0	69.9	3.735	695.0
203	42.96	1529	107.0	64.5	184.0	28.4	107.8	78.9	78.9	69.9	3.726	695.2
204	0.44	1761	121.4	63.5	251.3	27.9	136.5	79.4	79.4	69.9	2.765	863.1
205	0.68	2164	140.9	63.5	357.5	27.9	182.4	79.5	79.5	69.9	1.834	1141.6
206	0.93	2493	157.1	63.4	477.4	27.9	234.1	79.5	79.5	70.0	1.380	1389.5
207	1.21	2713	168.4	63.3	568.4	27.8	273.4	79.5	79.5	70.0	1.163	1568.5
208	1.43	2944	176.5	63.3	591.6	27.9	283.4	79.5	79.5	69.9	0.988	1741.3
209	1.68	2692	176.6	63.3	580.2	27.8	278.5	79.5	79.5	70.1	1.180	1594.0
210	1.96	2706	176.8	64.3	580.4	28.3	279.0	79.5	79.5	70.0	1.187	1584.9
211	2.18	2696	176.1	65.2	578.0	28.7	278.3	79.5	79.5	70.0	1.213	1558.4
212	2.44	2791	177.5	66.0	580.0	29.0	279.6	79.6	79.6	70.1	1.145	1605.2
213	2.71	2732	176.6	66.1	582.1	29.1	280.5	79.6	79.6	70.1	1.198	1564.8
214	2.93	2669	177.6	66.3	582.1	29.1	280.7	79.6	79.6	70.1	1.258	1530.8
215	3.19	2808	177.0	66.6	582.3	29.3	282.6	79.6	79.6	70.1	1.142	1602.1
216	3.43	2714	177.1	66.5	582.8	29.2	280.9	79.6	79.6	70.0	1.220	1551.0
217	3.68	2773	177.1	66.5	584.7	29.2	280.9	79.6	79.6	70.0	1.161	1591.9
218	3.93	2738	176.8	66.0	584.7	29.0	281.5	79.8	79.8	70.0	1.182	1576.2
219	4.21	2702	176.1	65.6	578.5	28.8	278.7	79.7	79.7	70.0	1.205	1568.0
220	4.43	2678	175.8	65.1	582.2	28.6	280.1	79.7	79.7	70.2	1.220	1556.1
221	4.69	2718	175.7	64.5	579.7	28.5	278.8	79.7	79.7	70.0	1.179	1583.5
222	4.96	2669	176.2	64.1	581.2	28.3	279.4	79.7	79.7	70.0	1.216	1564.1
223	5.18	2701	176.5	64.1	579.9	28.2	278.7	79.7	79.7	70.2	1.183	1588.3
224	5.44	2737	176.7	63.8	584.6	28.1	280.6	80.1	80.1	70.0	1.148	1614.3
225	5.71	2667	175.6	63.6	582.8	28.0	279.7	79.8	79.8	70.0	1.206	1571.2
226	5.93	2696	175.6	63.5	578.2	27.9	277.7	79.9	79.9	70.1	1.176	1592.4
227	6.19	2694	175.4	63.2	580.5	27.8	278.5	80.1	80.1	70.2	1.177	1597.5
228	6.43	2676	176.7	63.2	585.4	27.7	280.6	80.0	80.0	70.1	1.189	1586.8
229	6.68	2286	156.5	63.0	581.5	27.7	278.9	79.9	79.9	70.1	1.630	1278.5
			441.3	63.0	441.3	27.7	218.3	79.9	79.9	70.1		

APPENDIX E

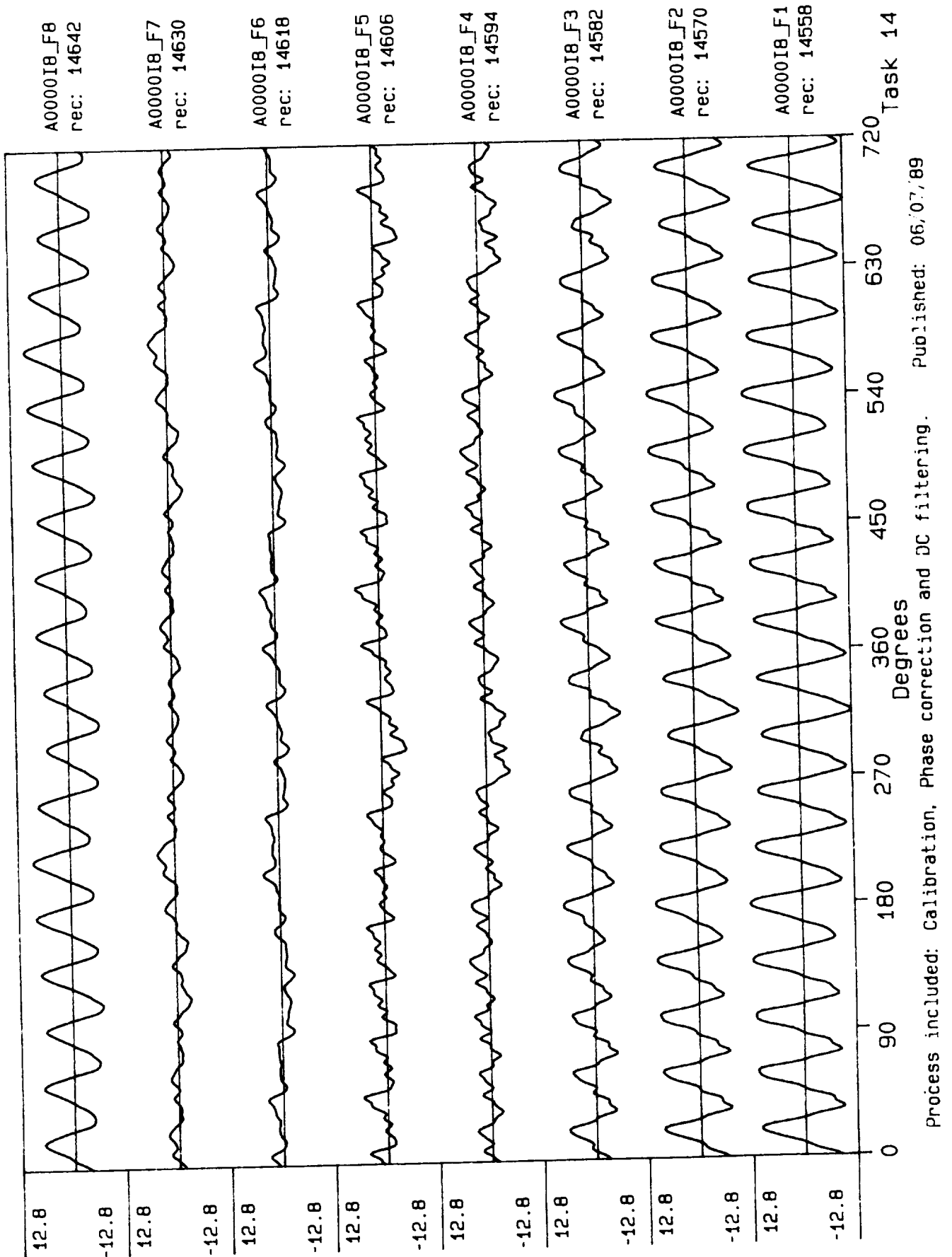
SUMMARY

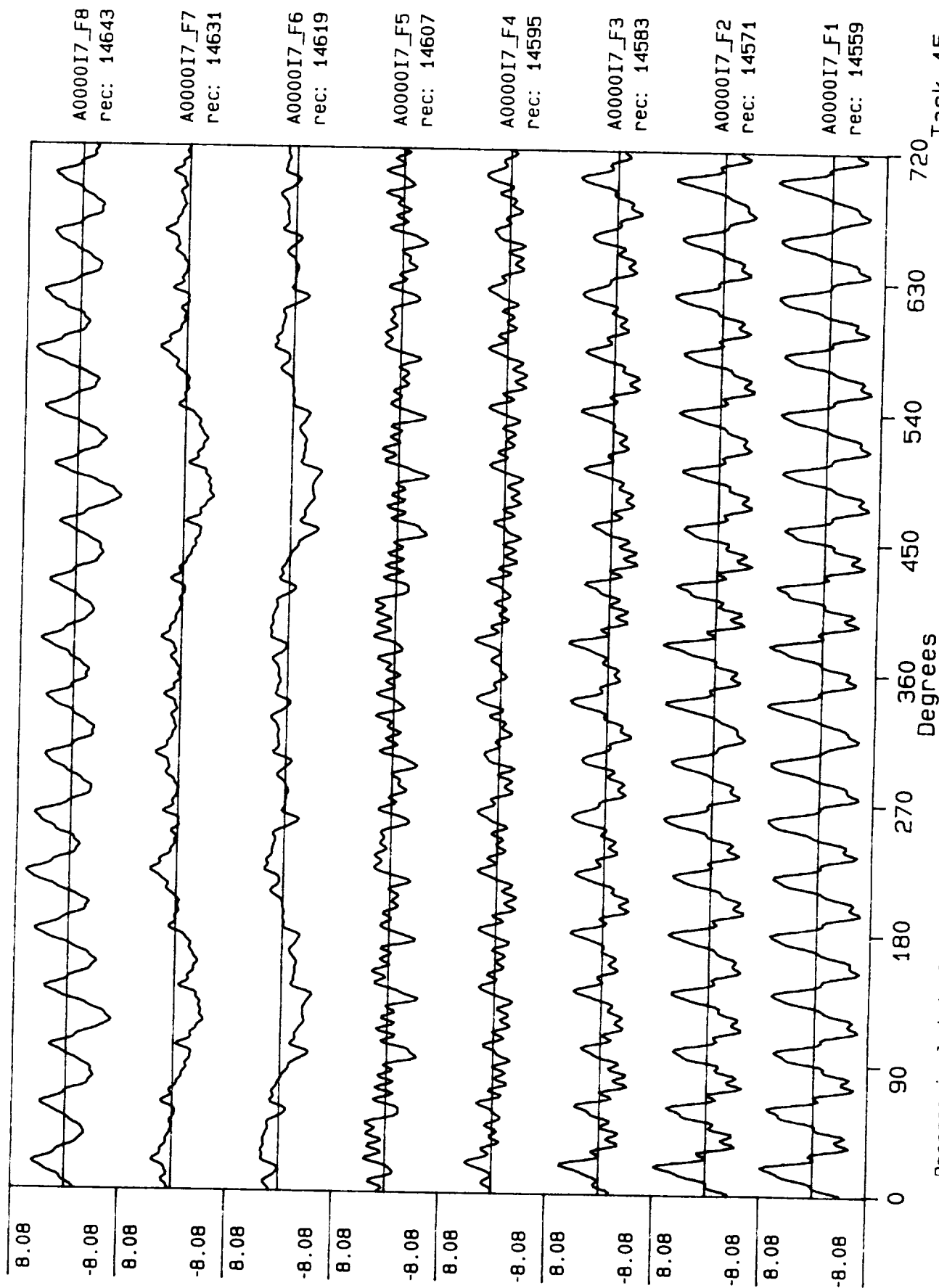
OF

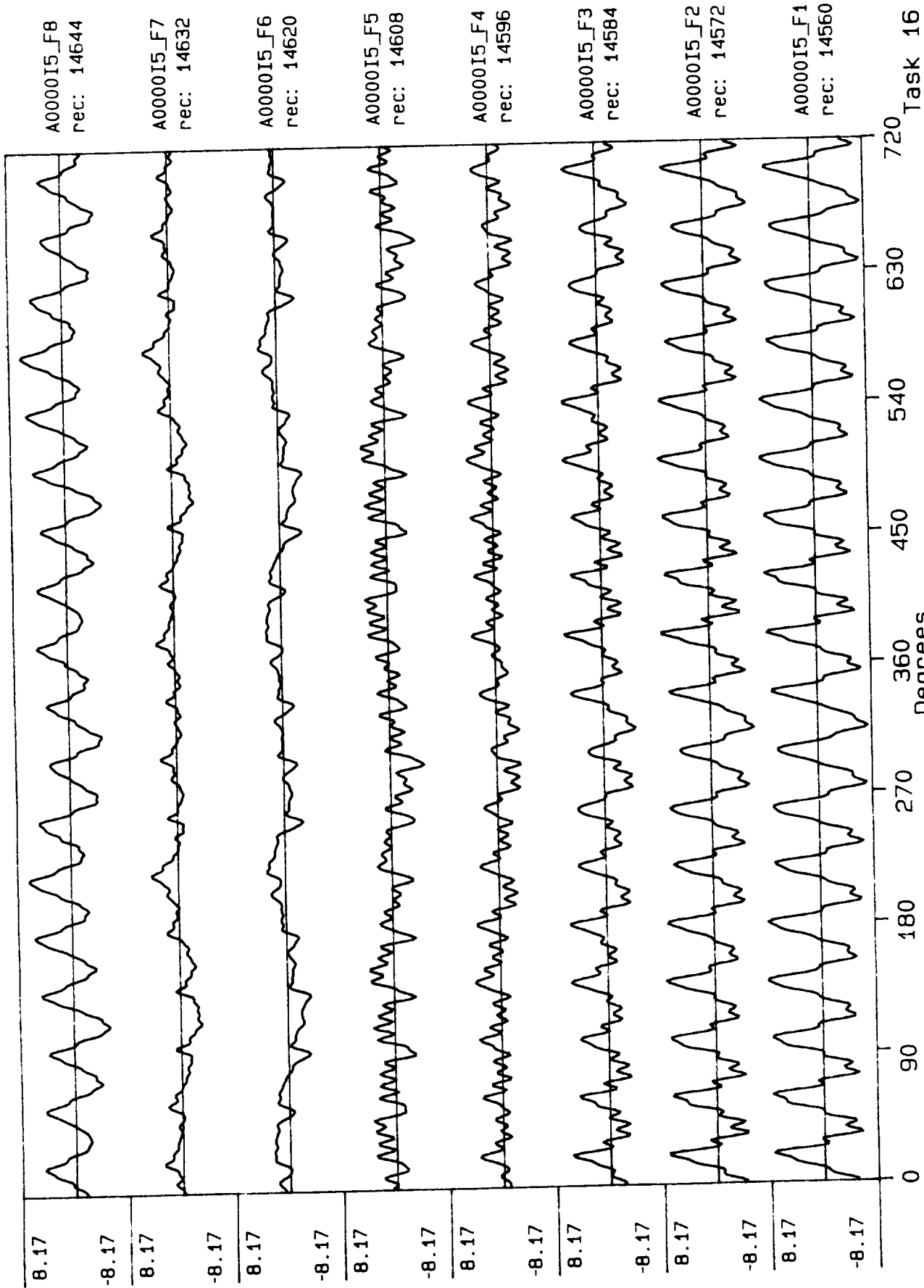
SYNCHRONOUS PULSATION TEST DATA

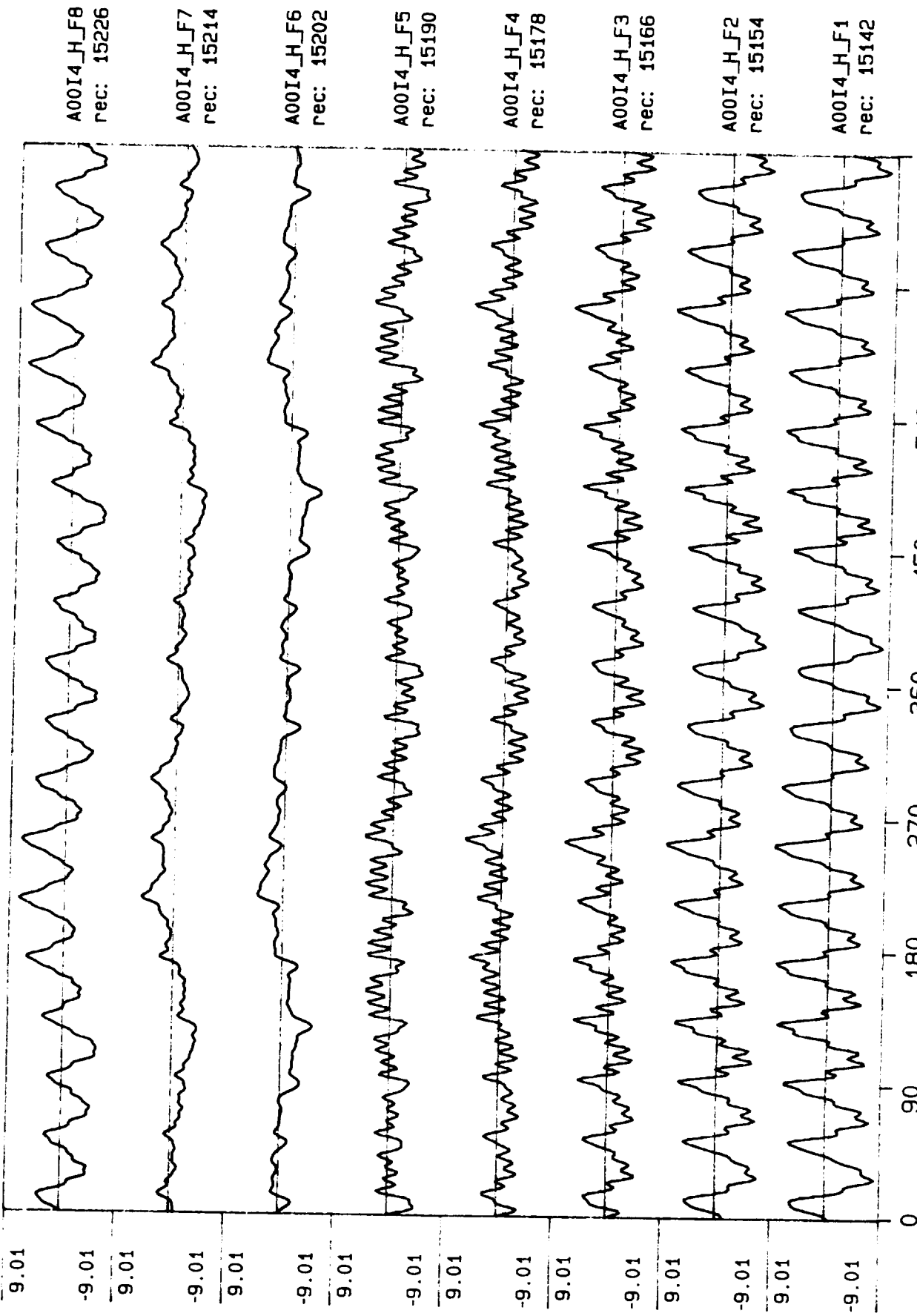
This appendix contains the complete history of synchronous (or order related) pressure pulsations for configurations A and C. The waveforms are filtered for DC component of pressure, so only the fluctuating, of AC component remains. The waveforms include two shaft revolutions. The 0 degree position on all plots refers to the "top-dead-center" position of the shaft key phasor. The TDC position occurs 10 degrees upstream of the position of the scroll cutwater leading edge.

The time waveforms for configuration B are in the process of being corrected for phase. Once completed, this set of data will be included in this appendix.

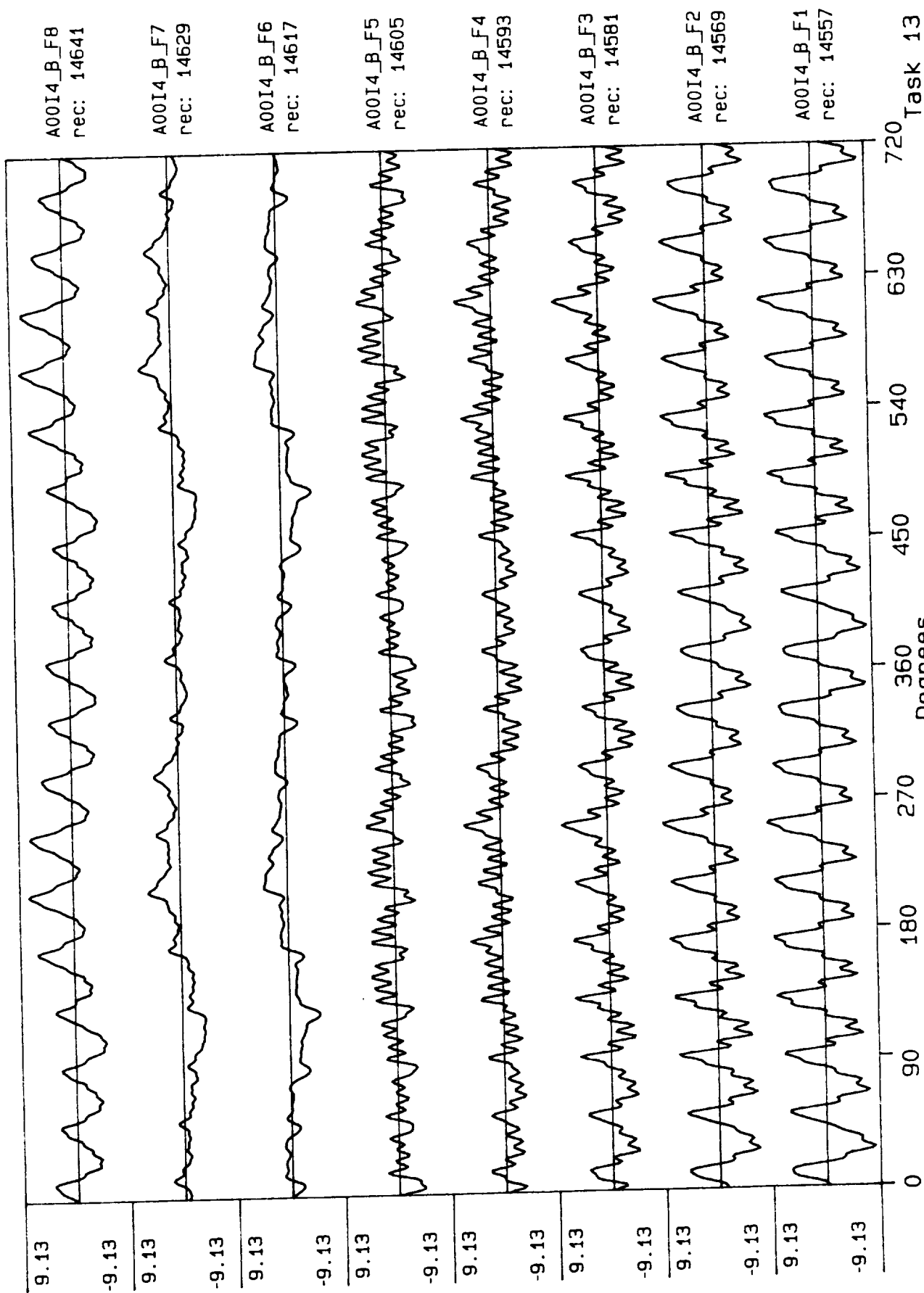


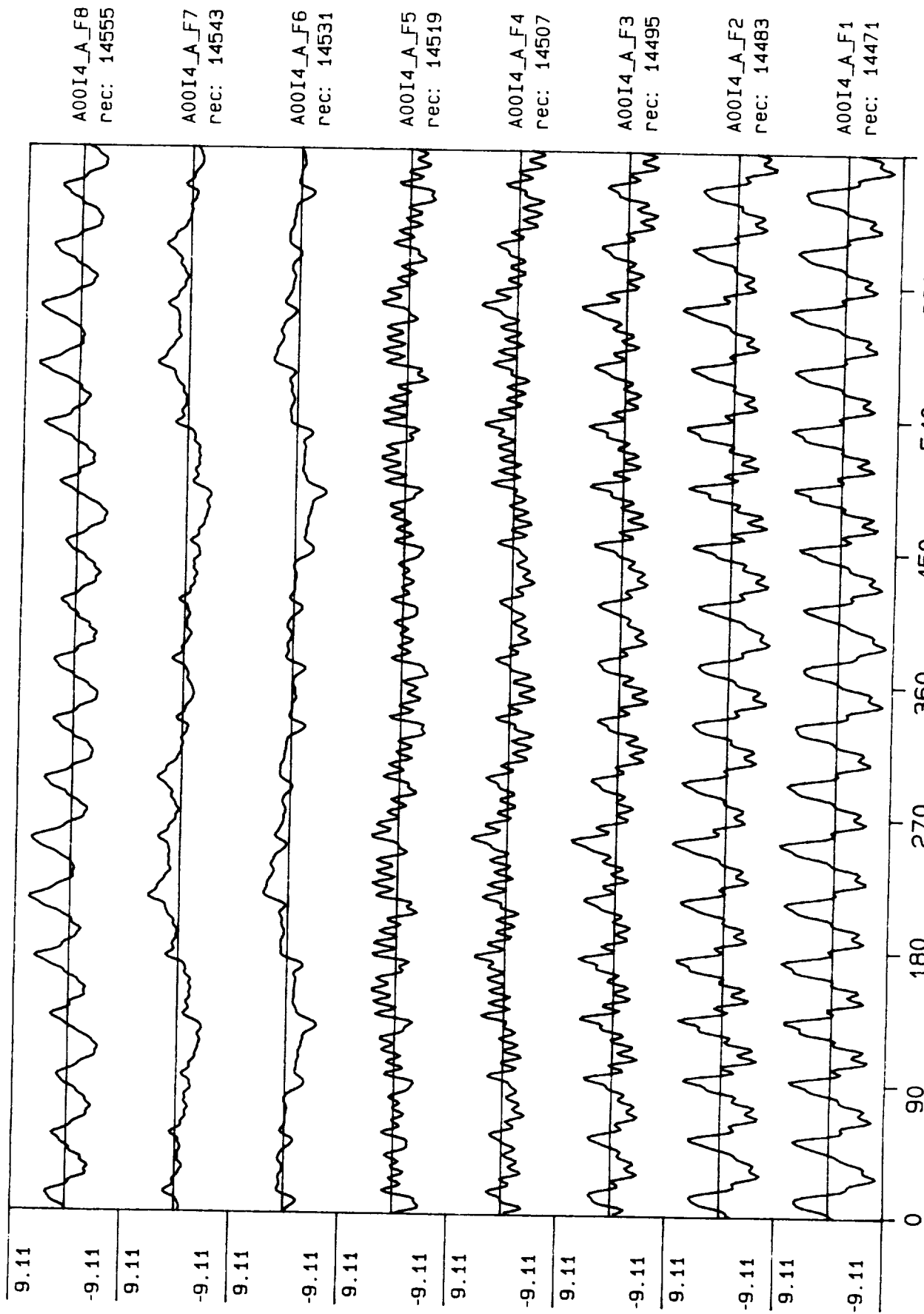


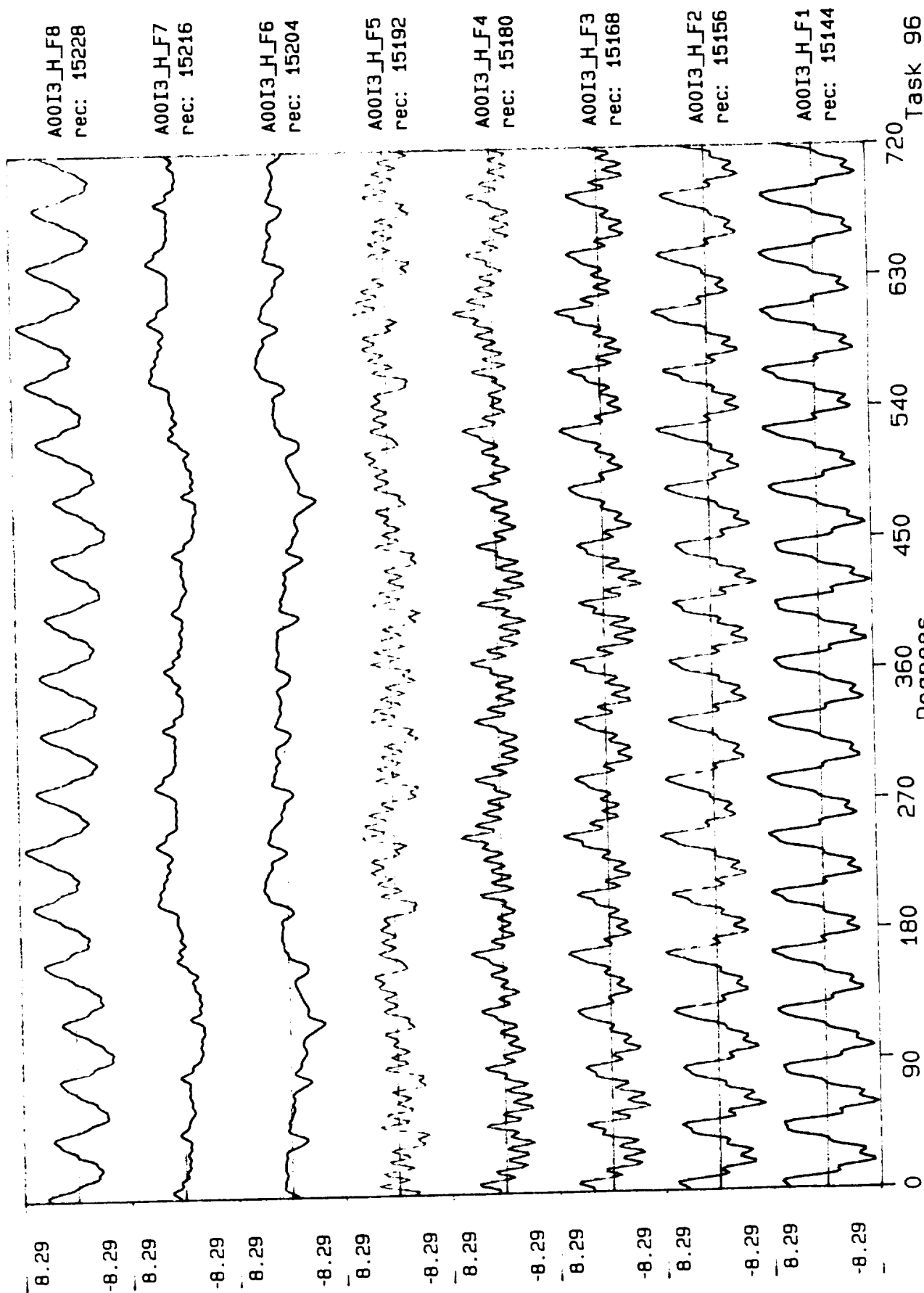




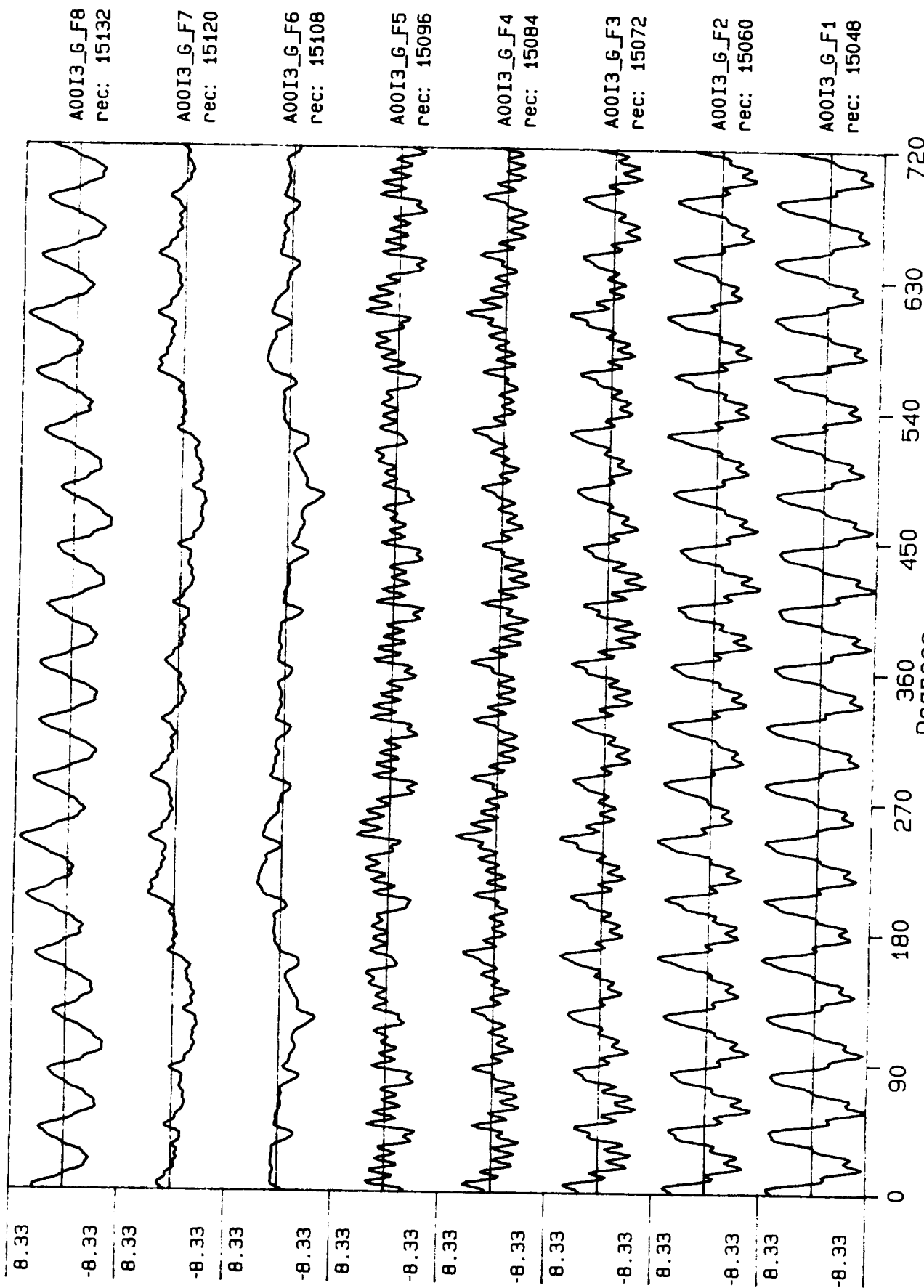
Process included: Calibration, Phase correction and DC filtering. Published: 06, 07, 89

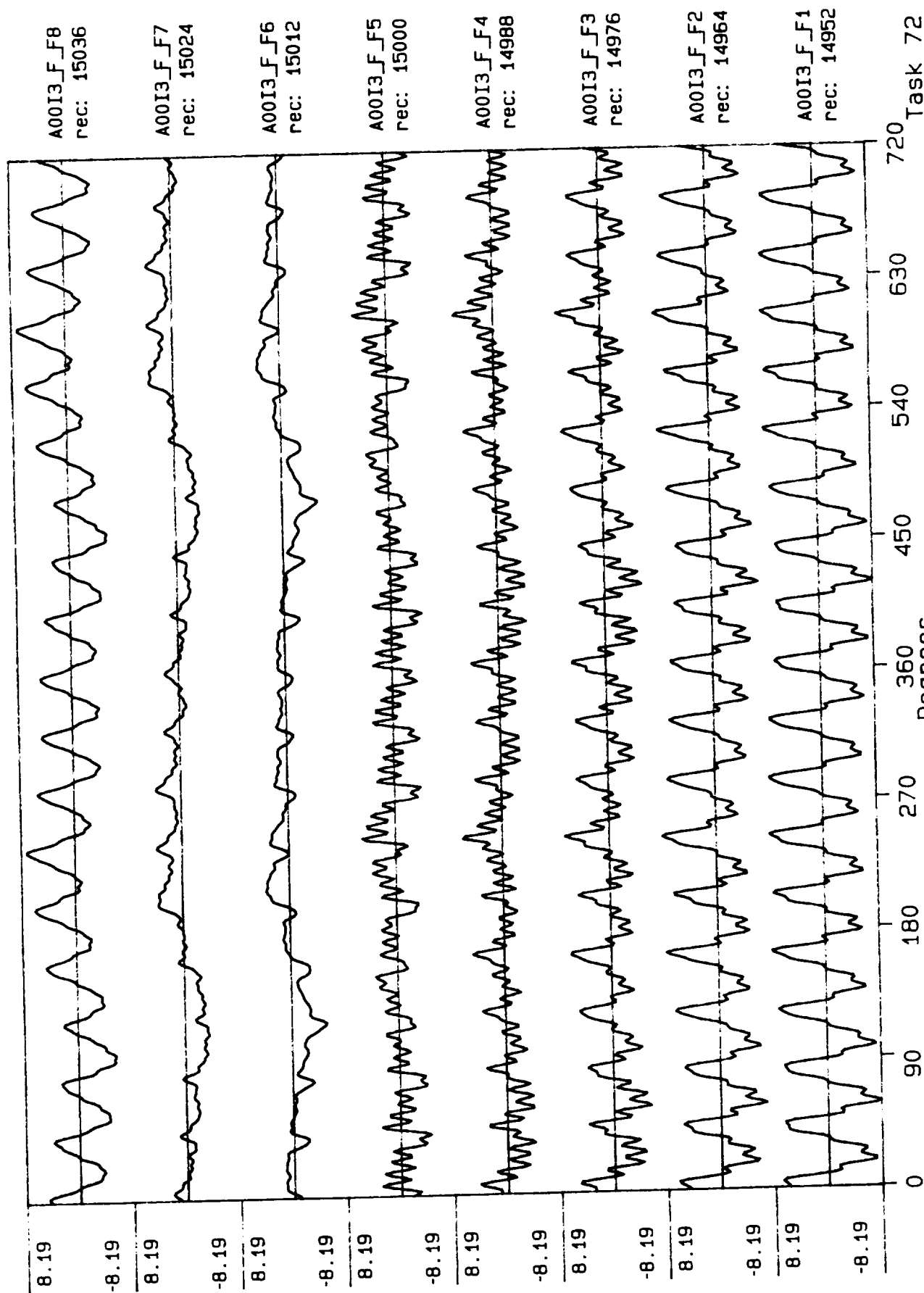




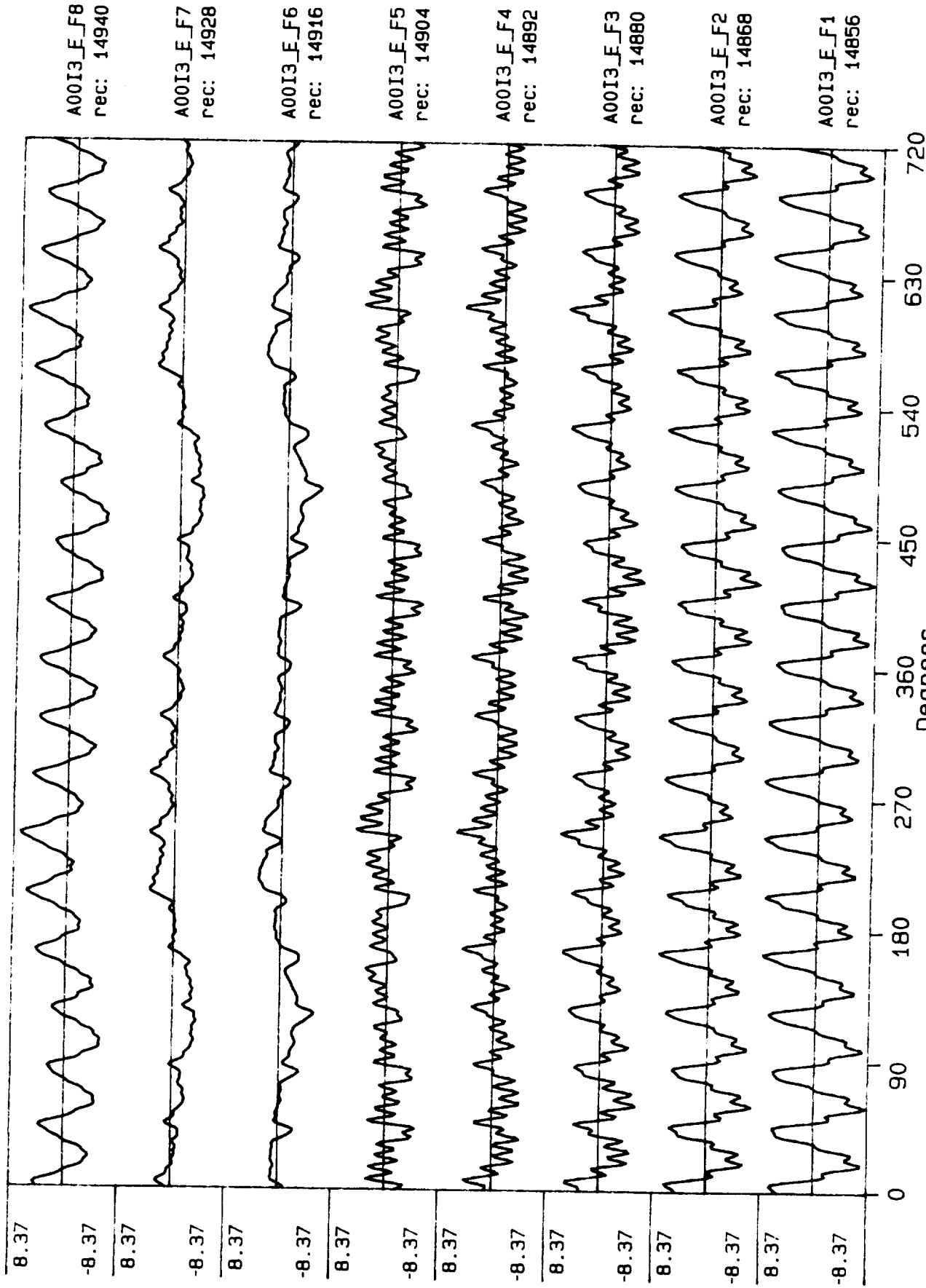


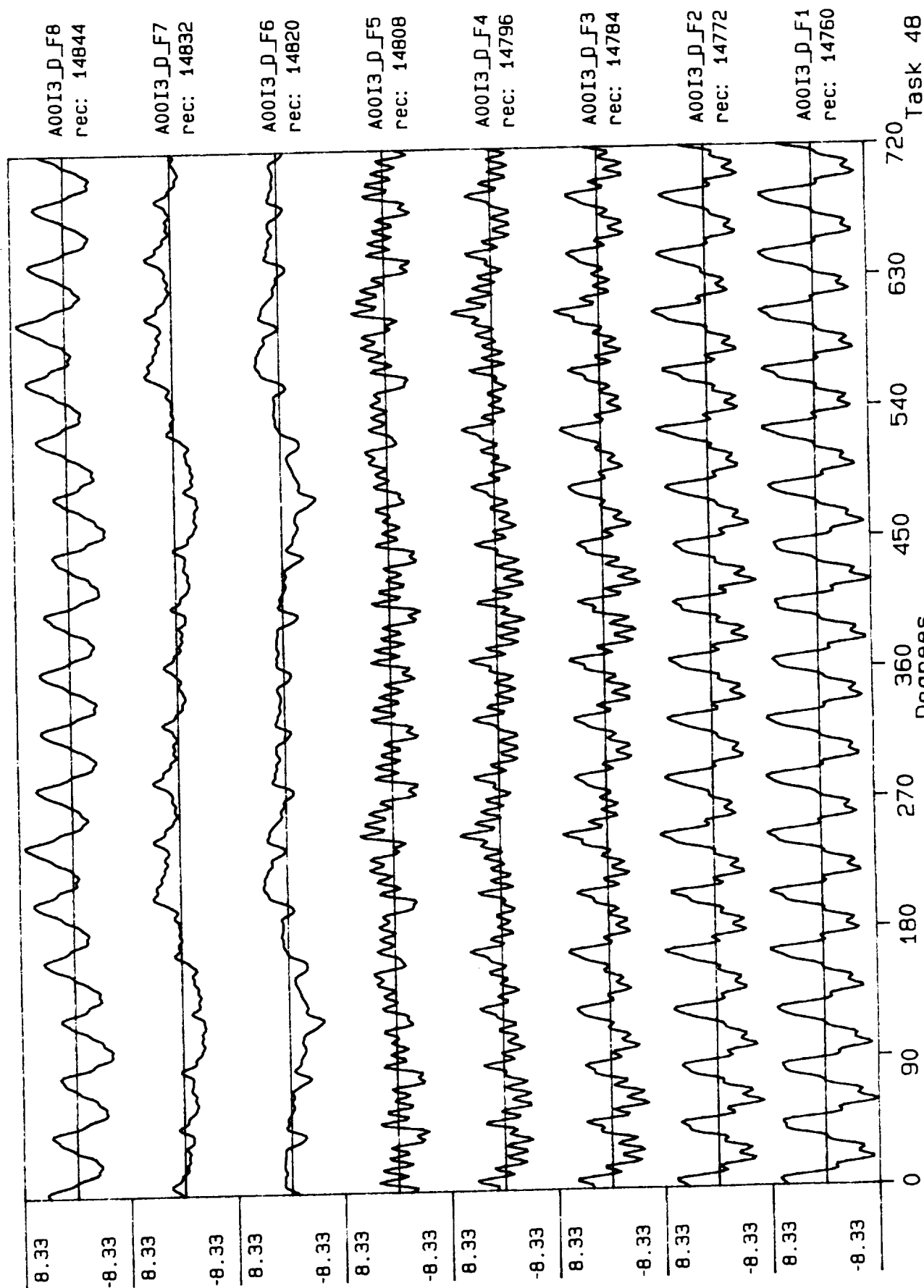
Process included: Calibration, Phase correction and DC filtering. Published: 06/07/89

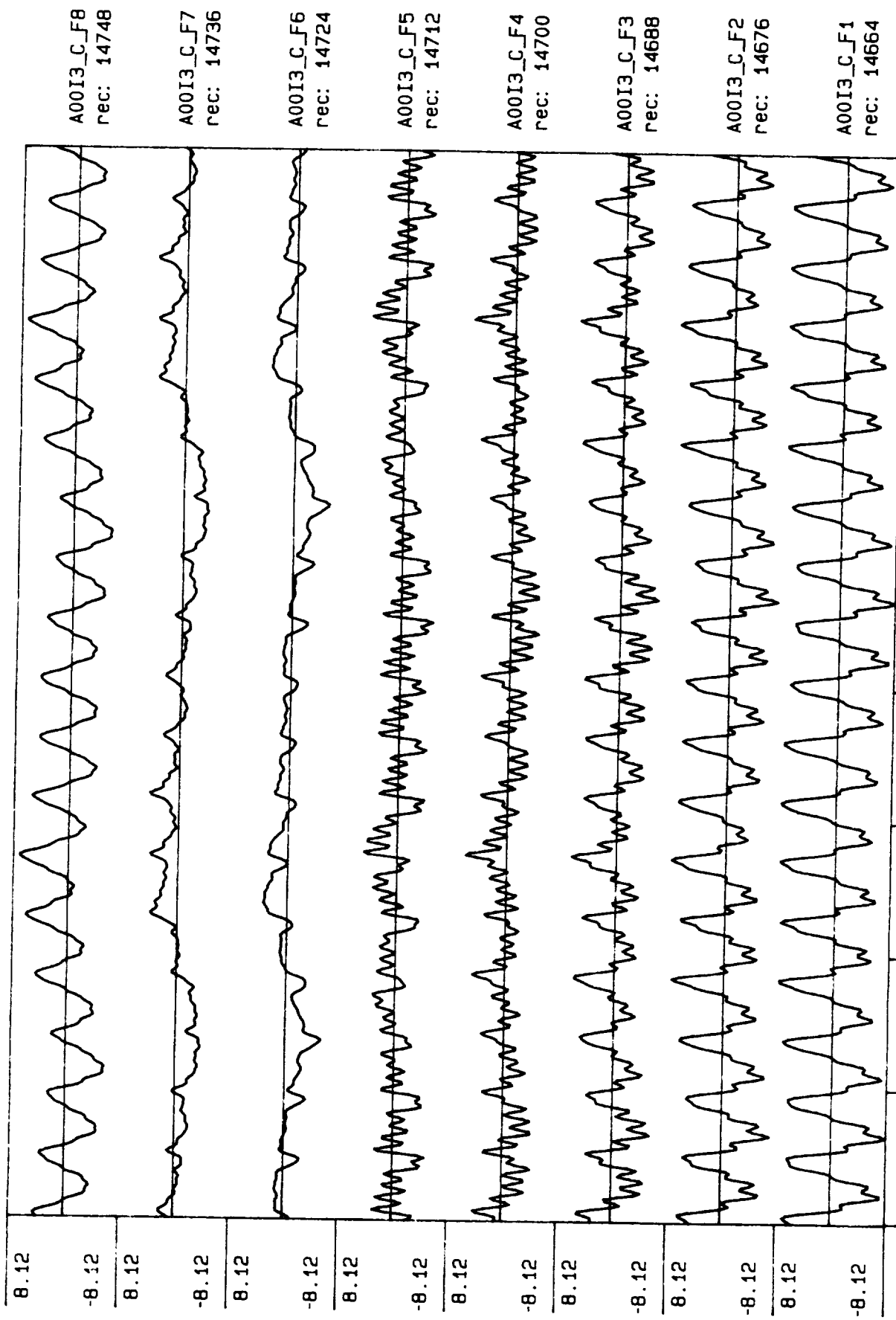


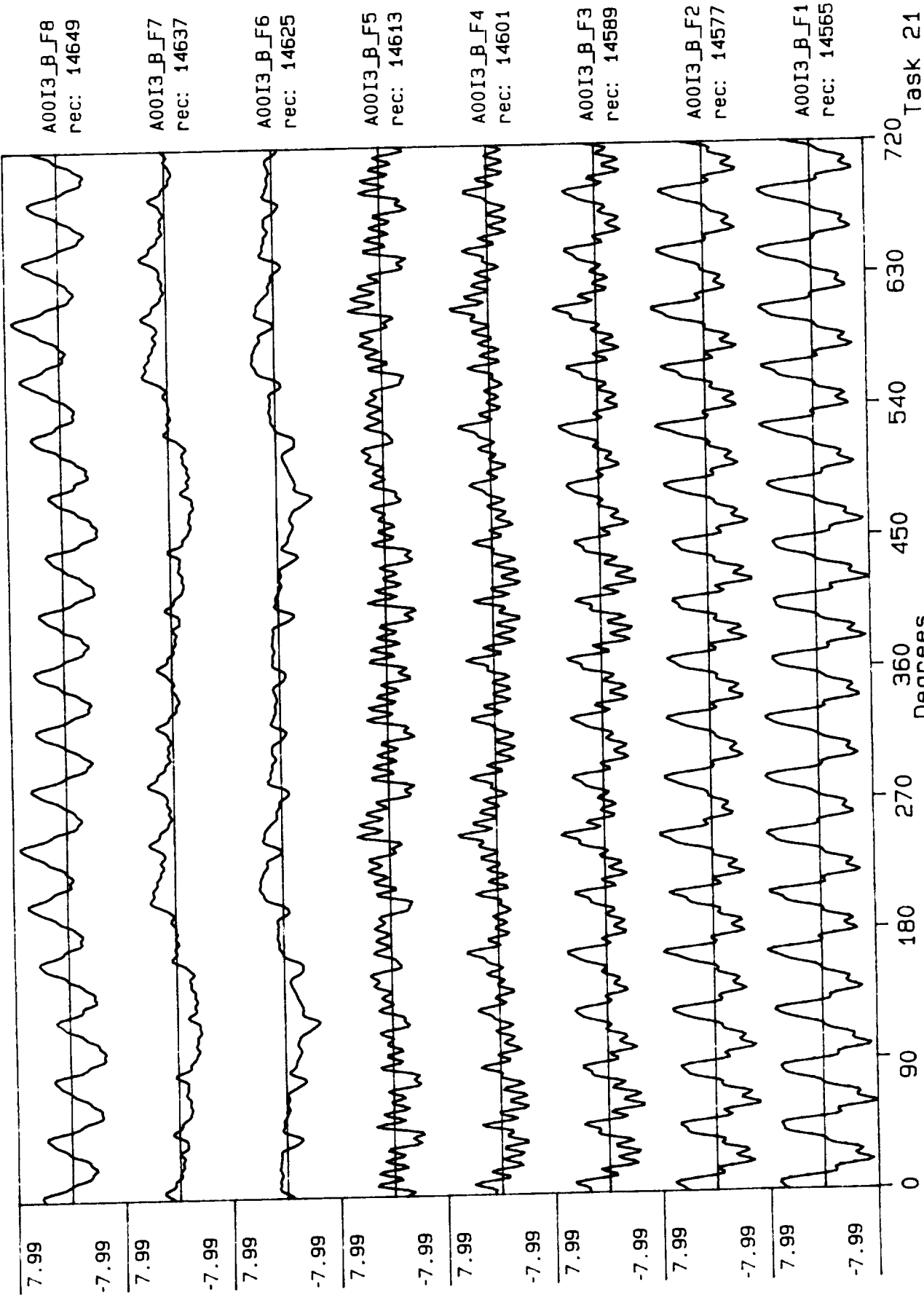


Process included: Calibration, Phase correction and DC filtering. Published: 05,07,89

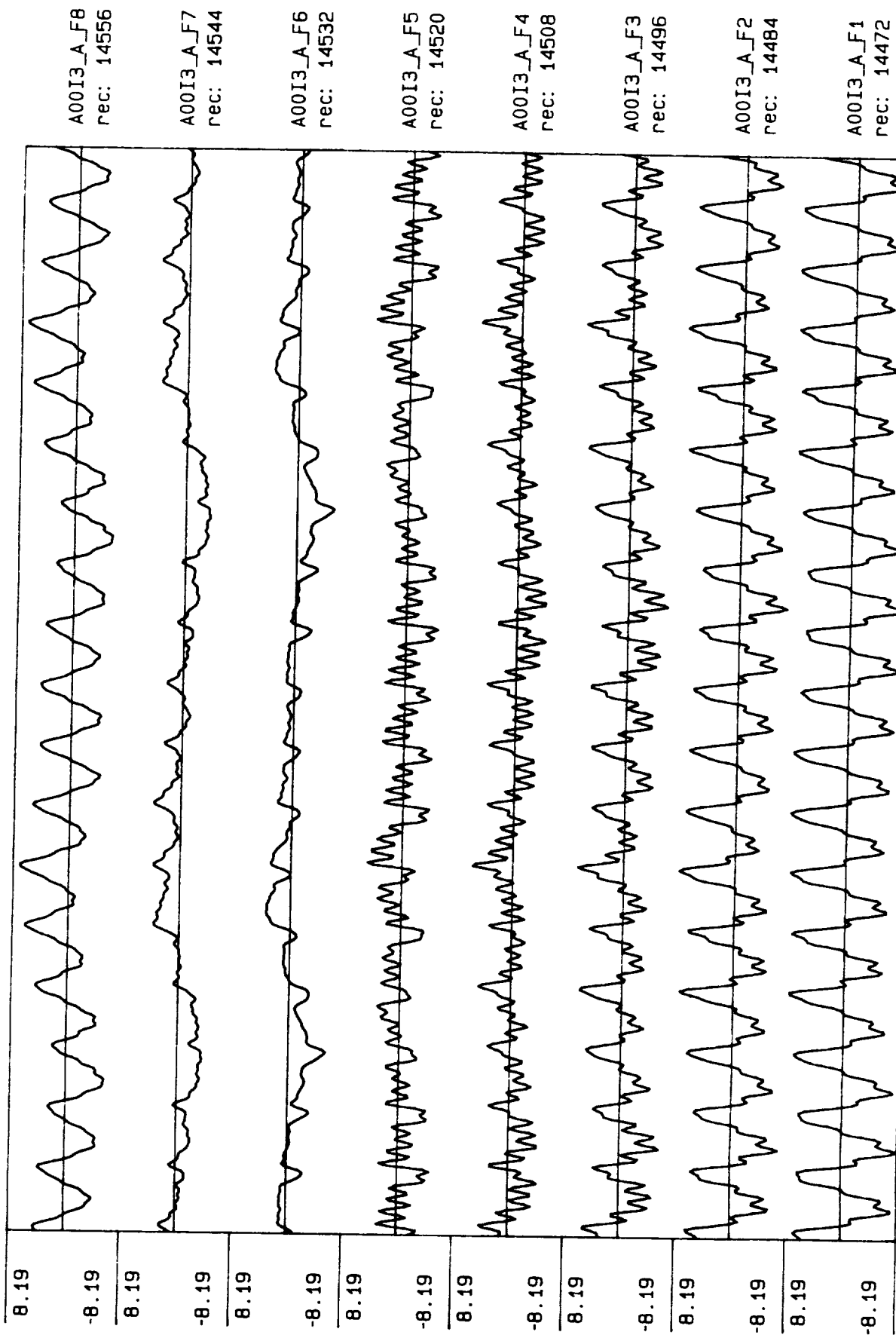


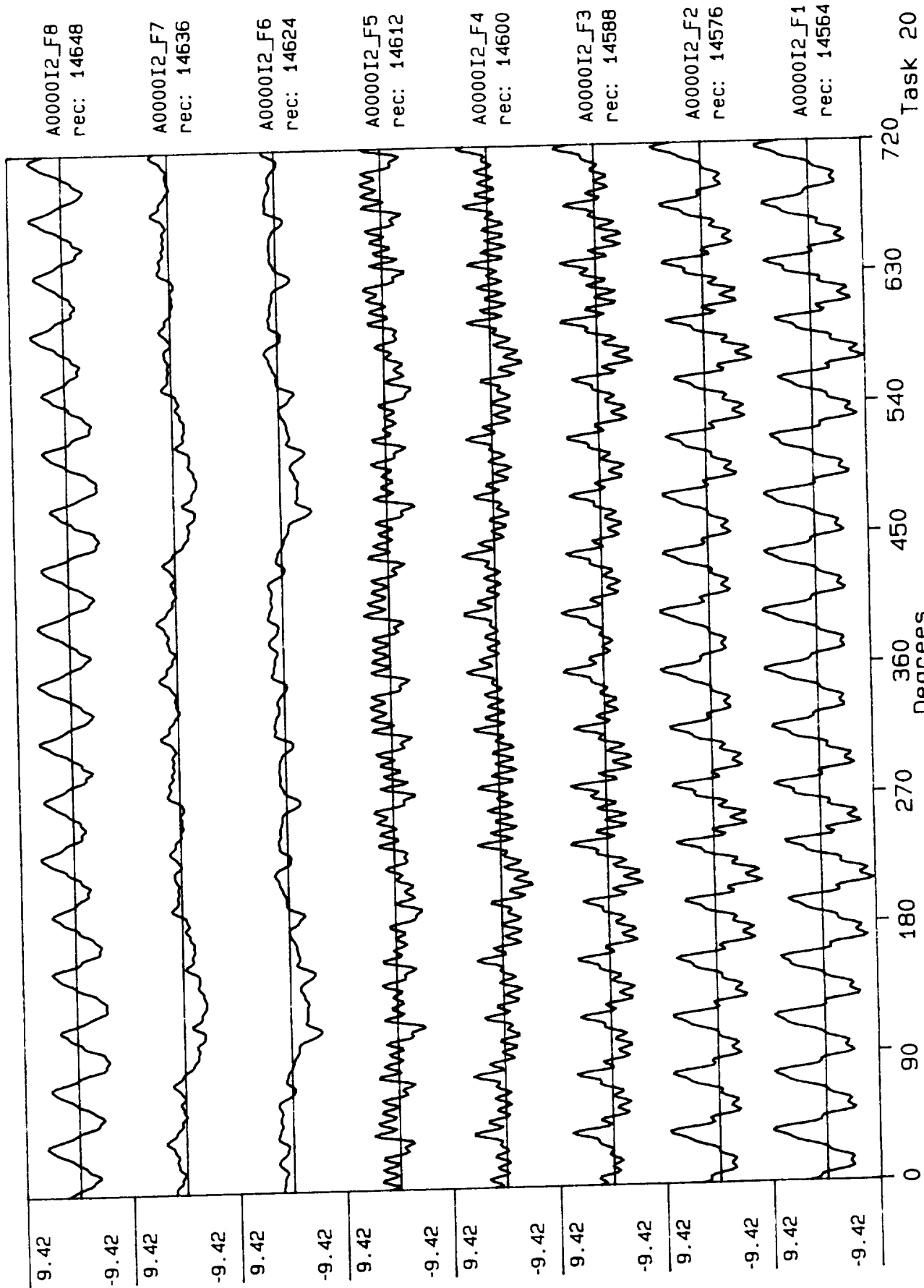




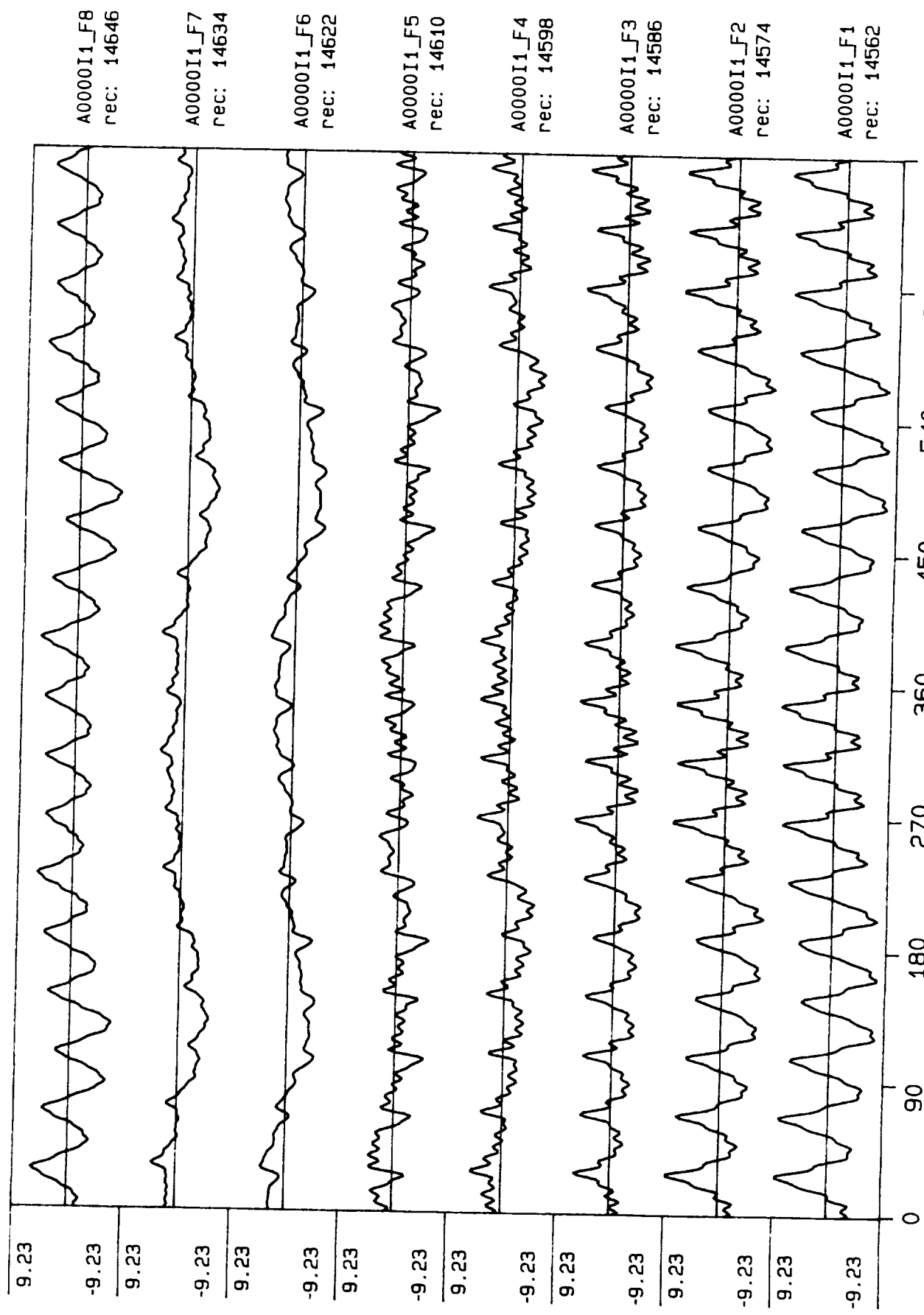


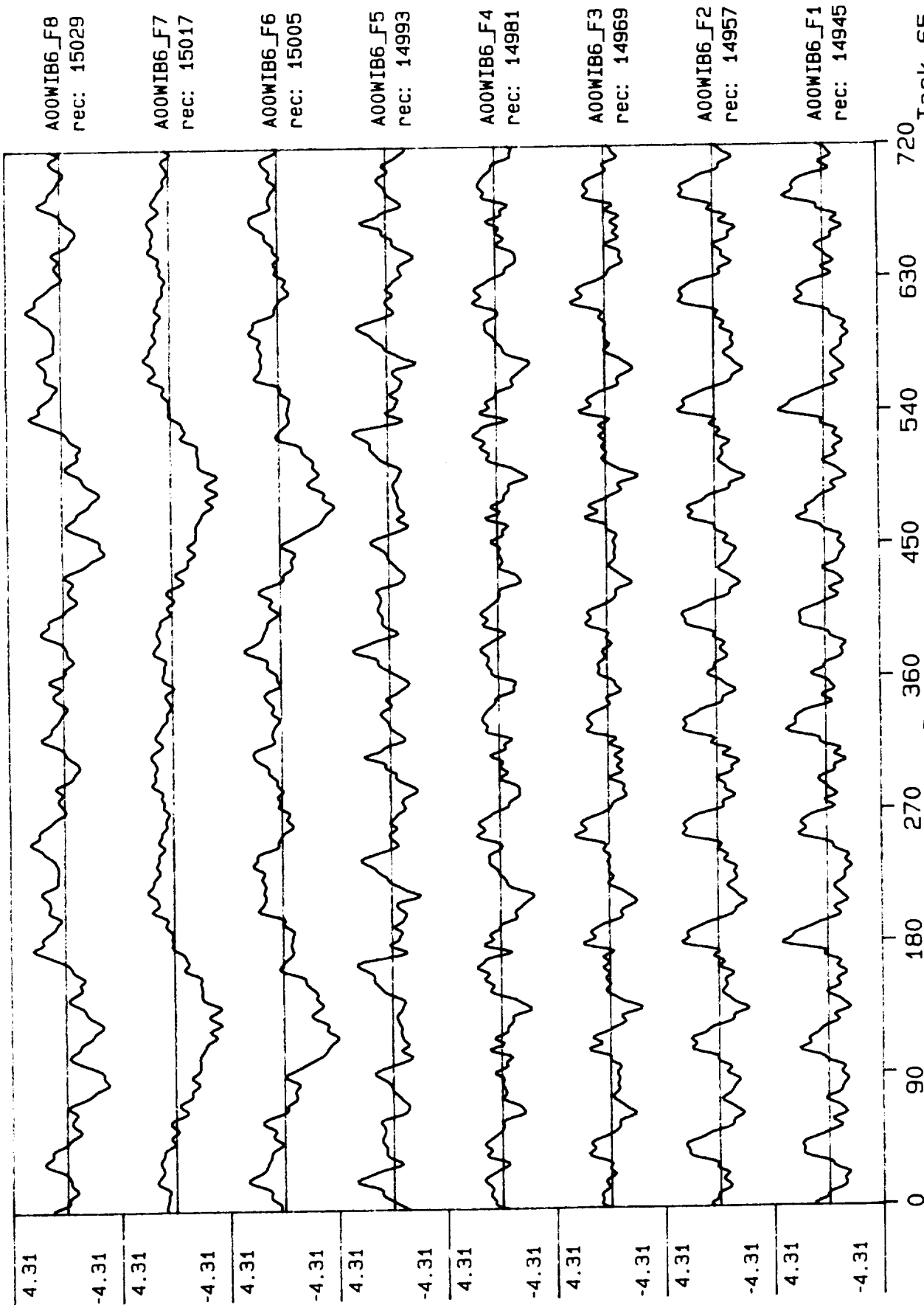
Process included: Calibration, Phase correction and DC filtering. Published: 06,07,89



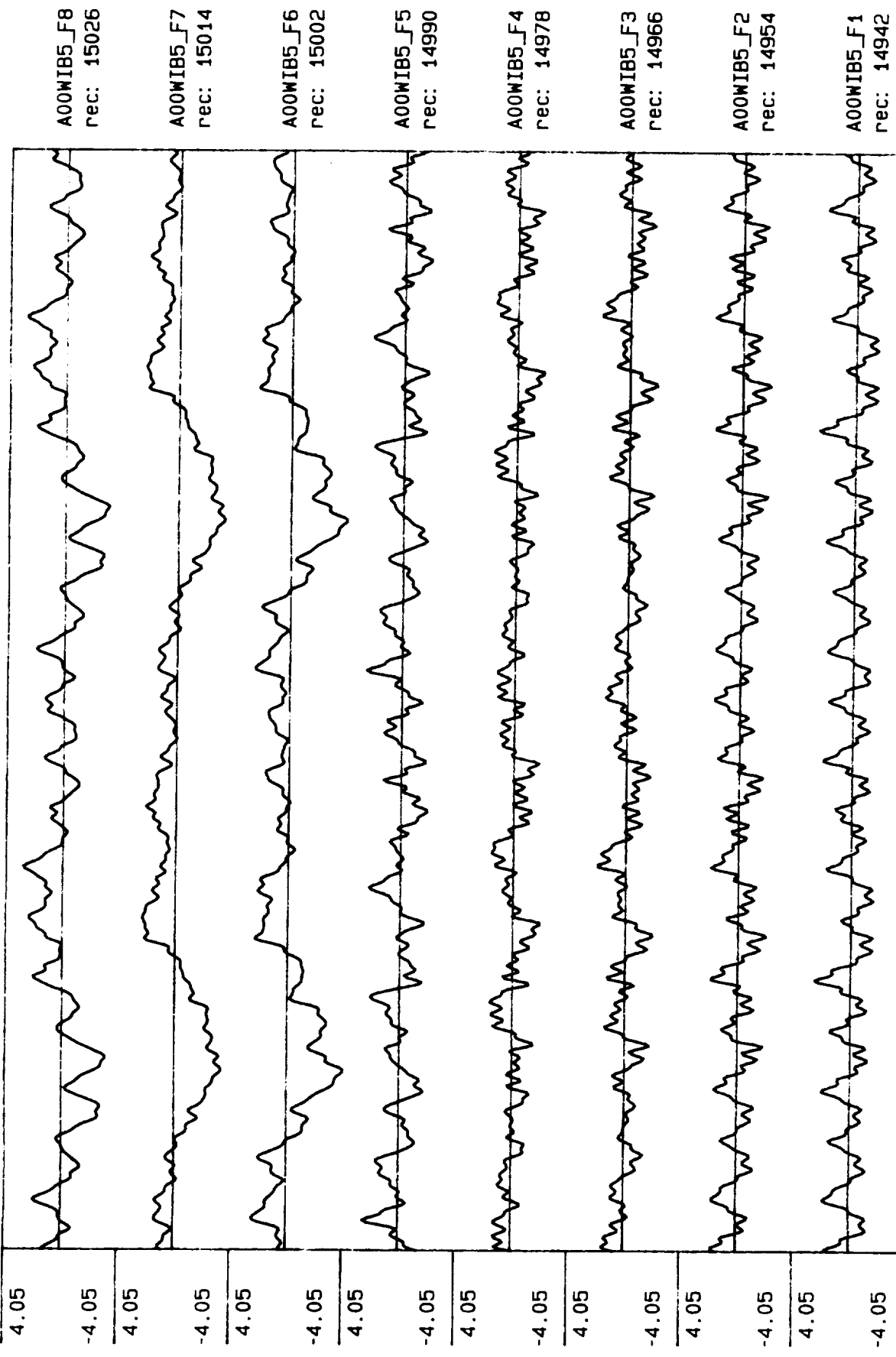


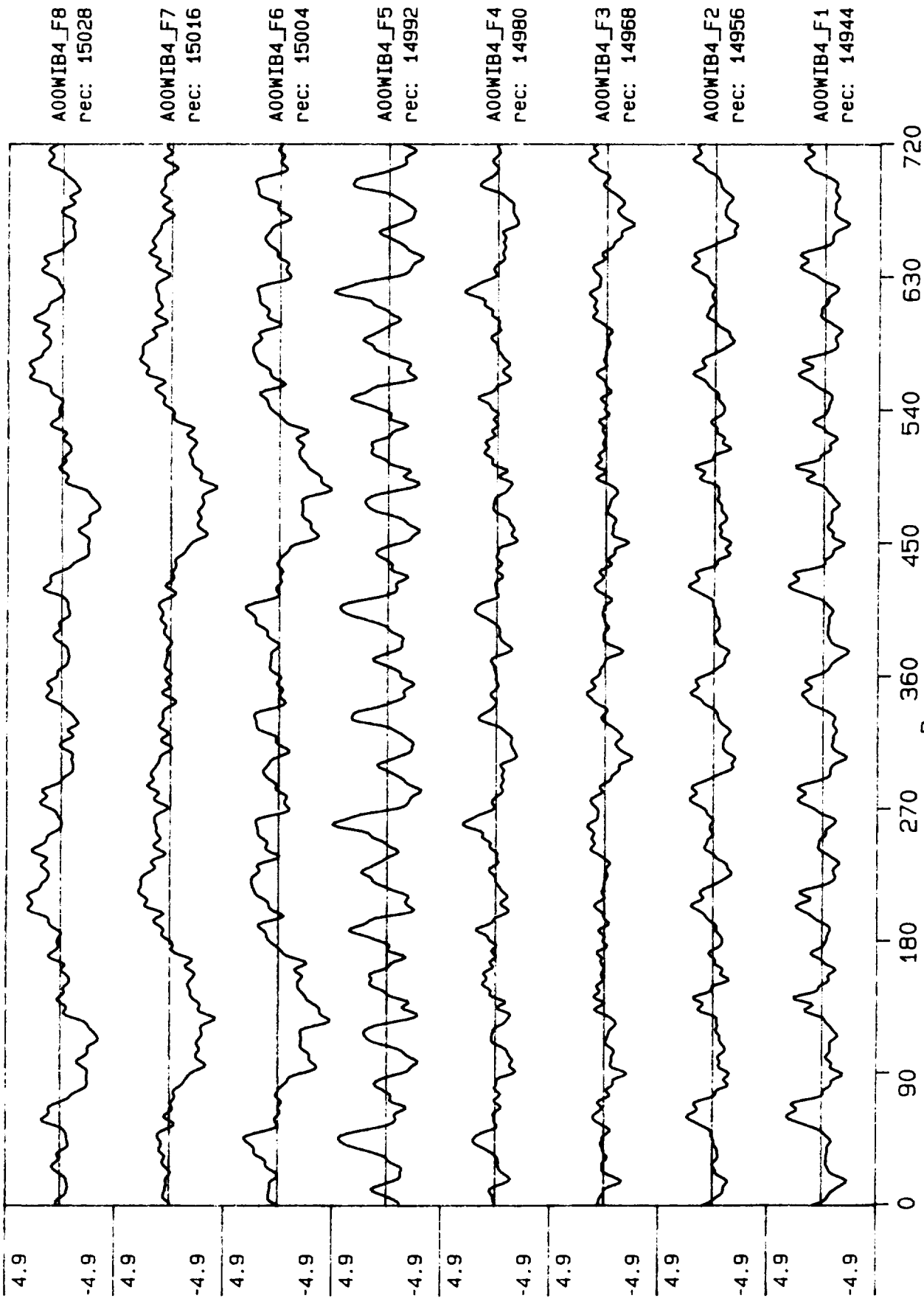
Process included: Calibration, Phase correction and DC filtering. Published: 06/07/89



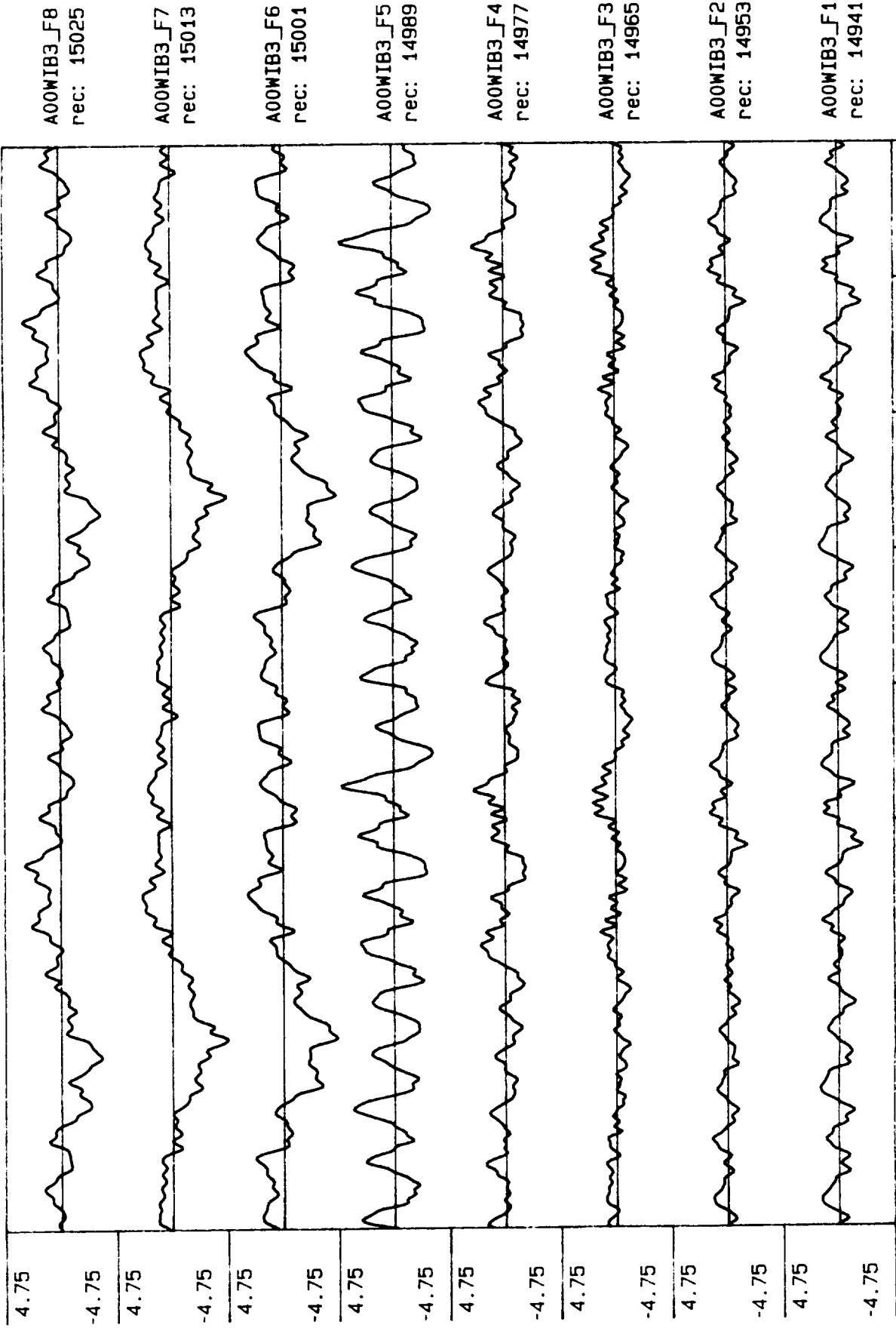


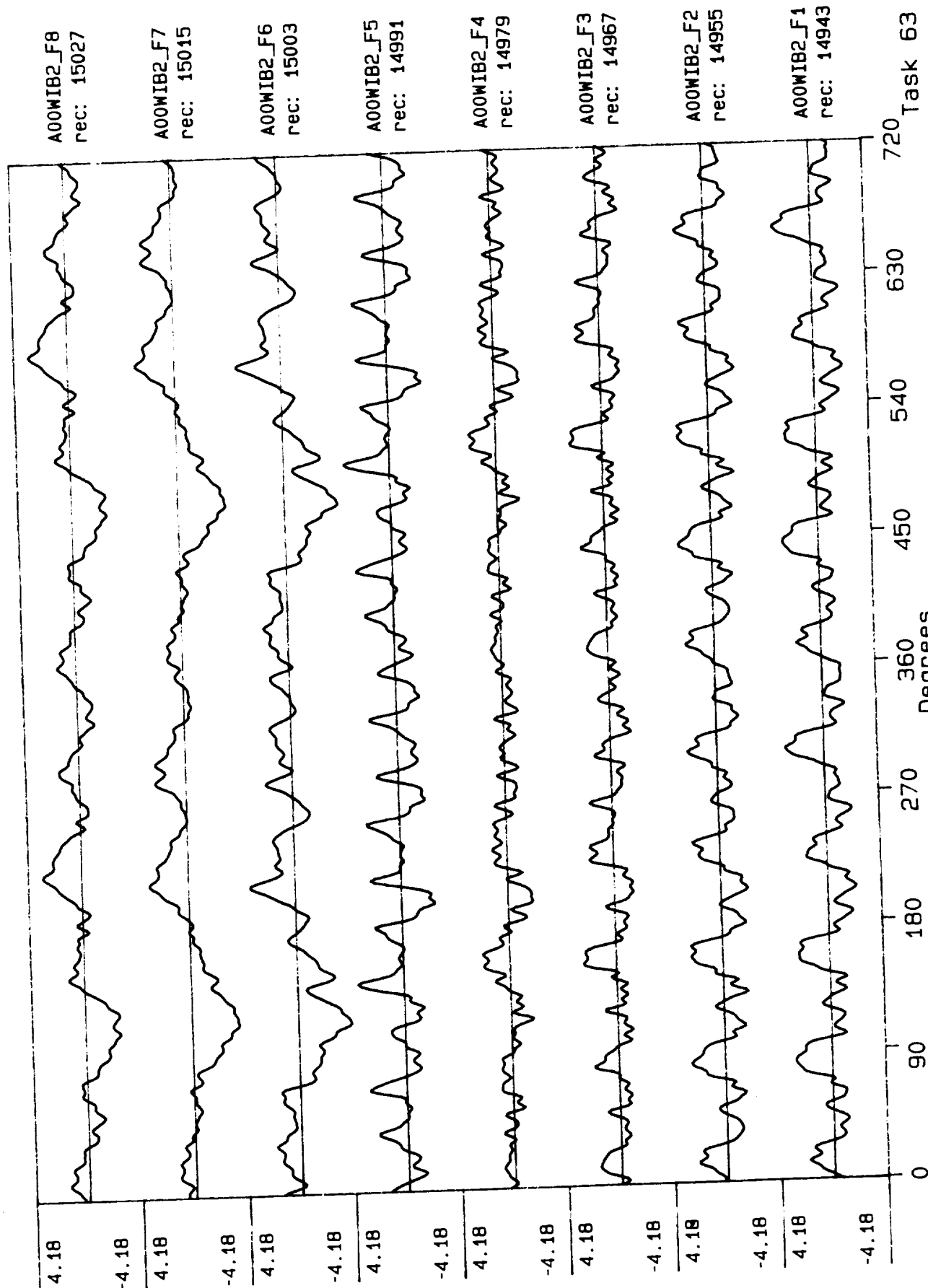
Process included: Calibration, Phase correction and DC filtering. Published: 06,07,89



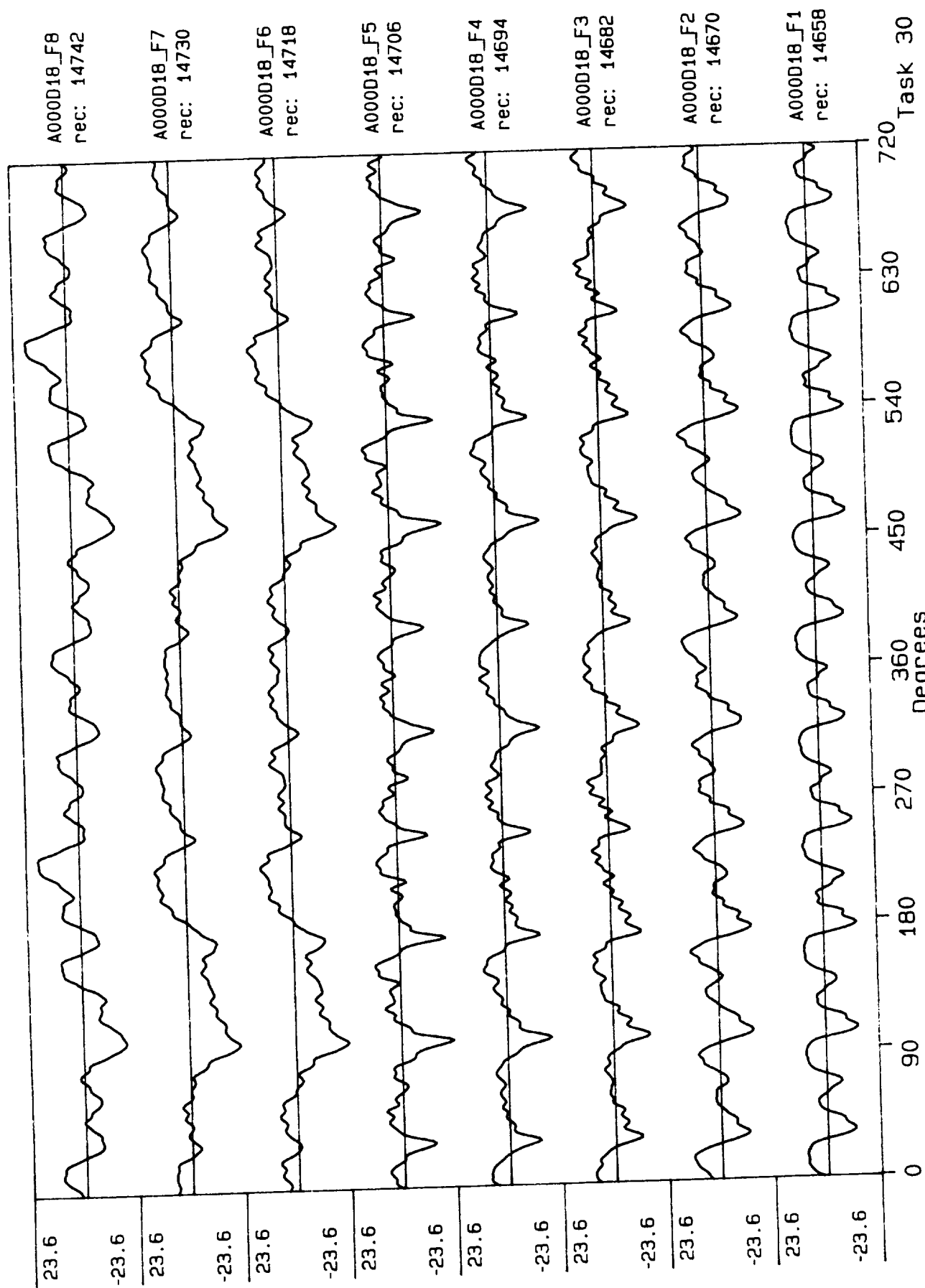


Process included: Calibration, Phase correction and DC filtering. Published: 06,0',89

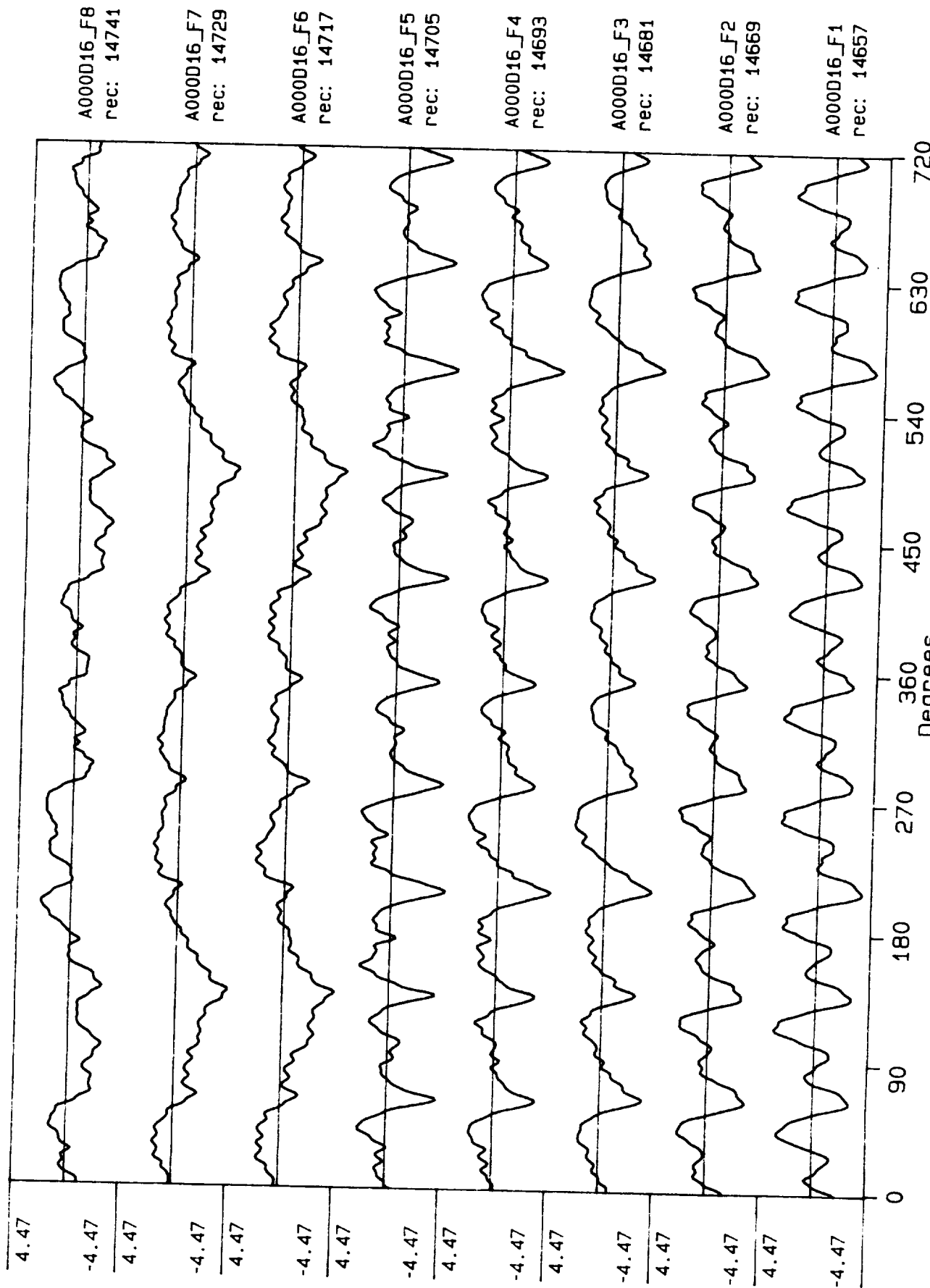


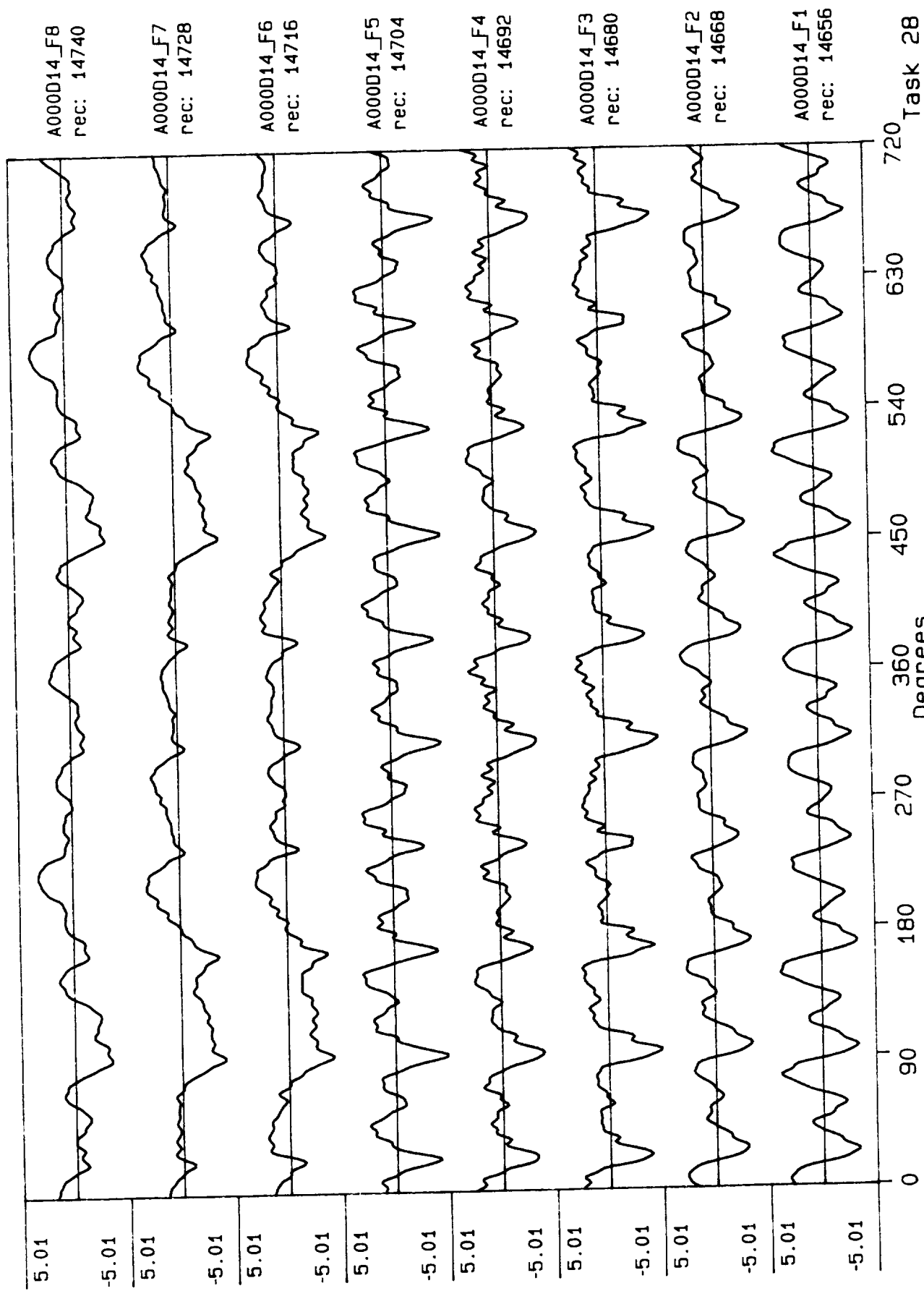


Process included: Calibration, Phase correction and DC filtering. Published: 06/07/89

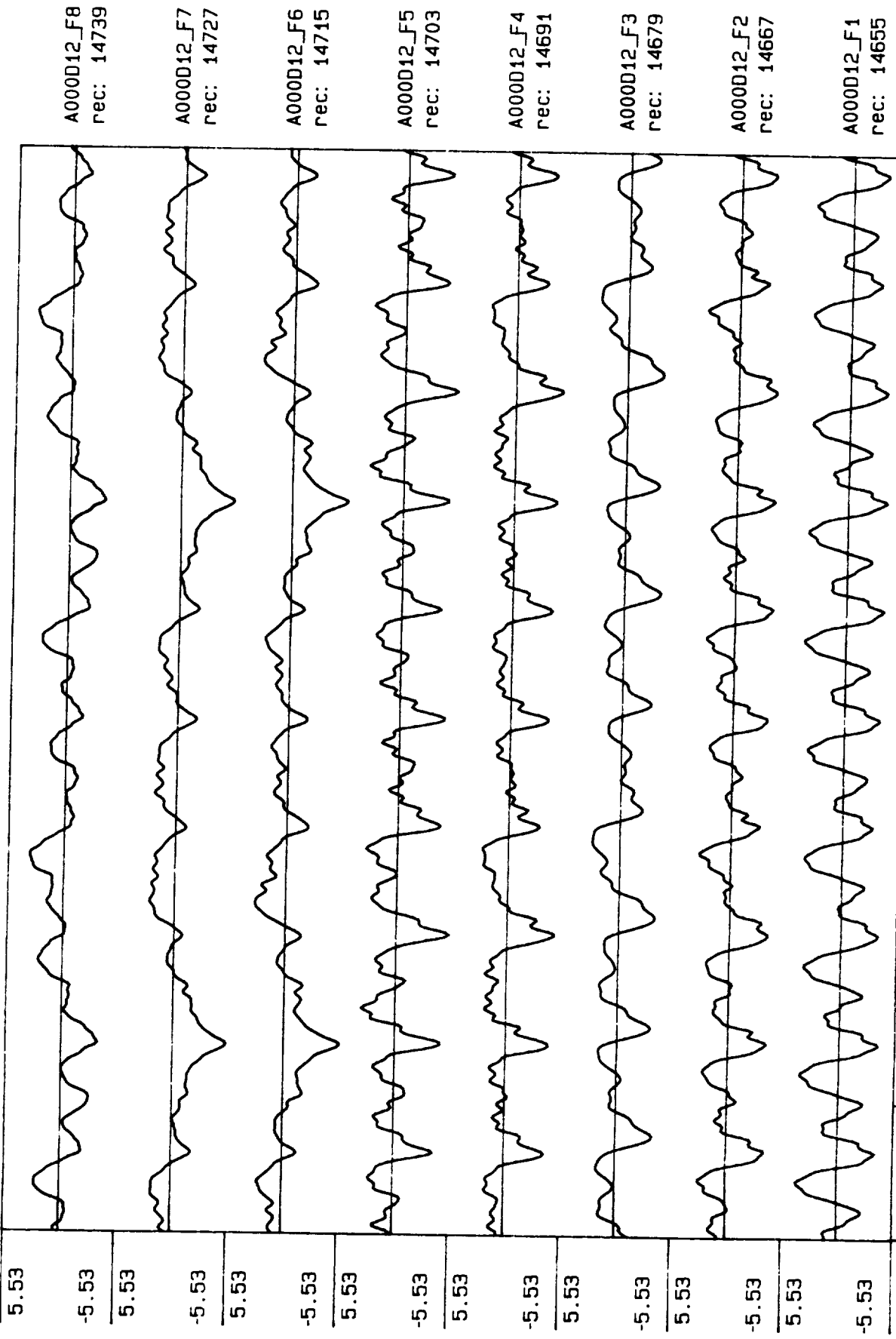


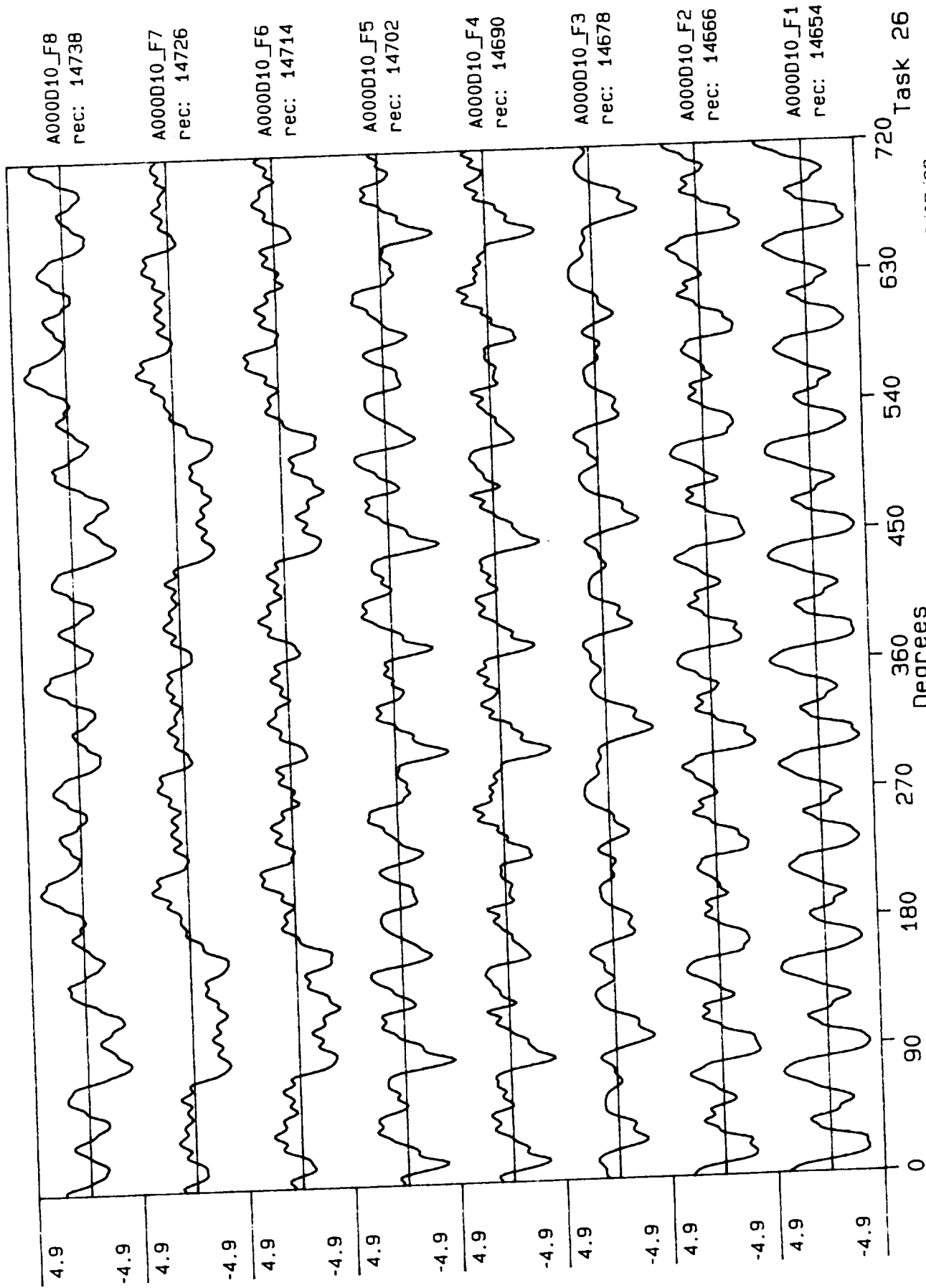
Process included: Calibration, Phase correction and DC filtering. Published: 06,07,89



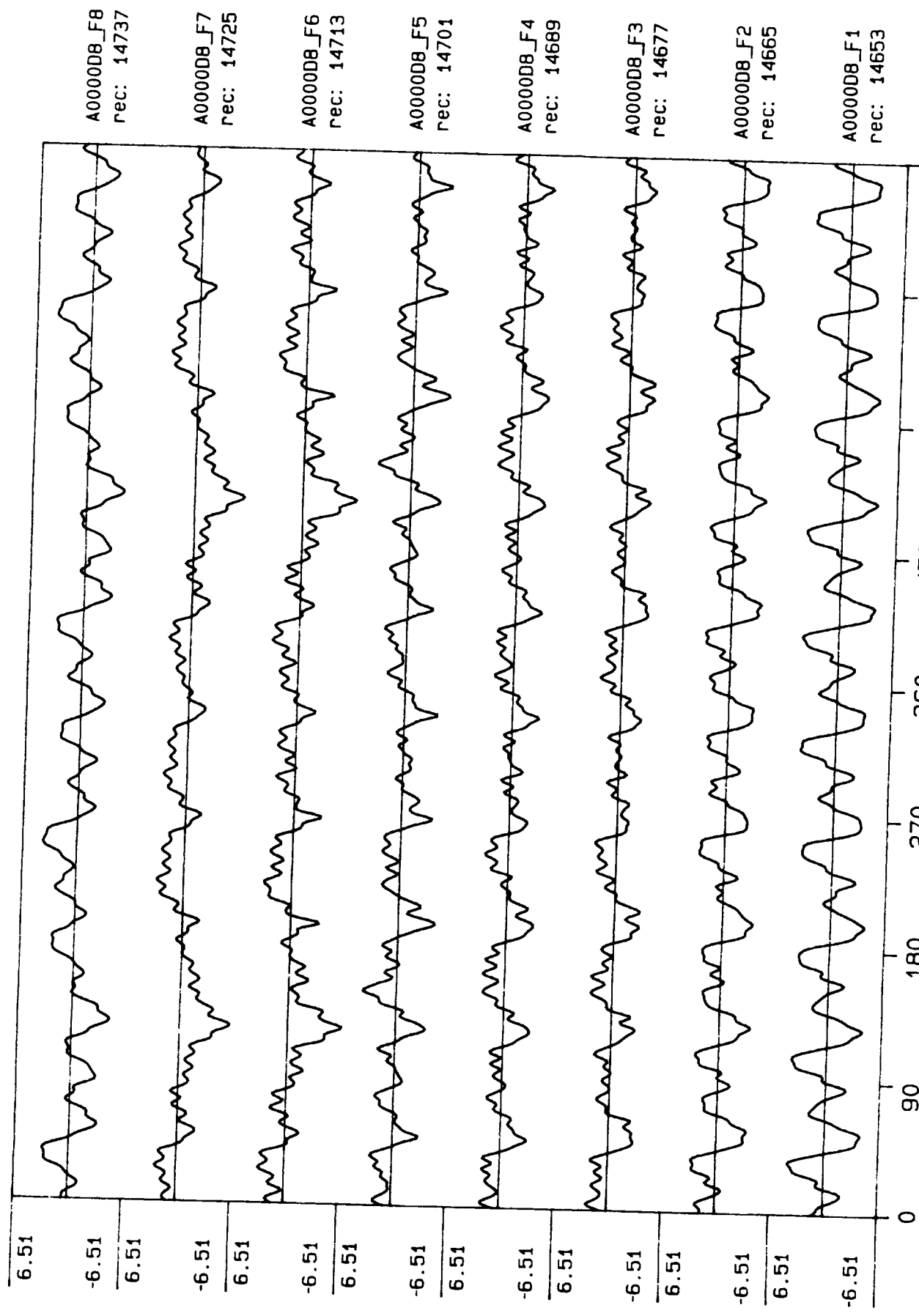


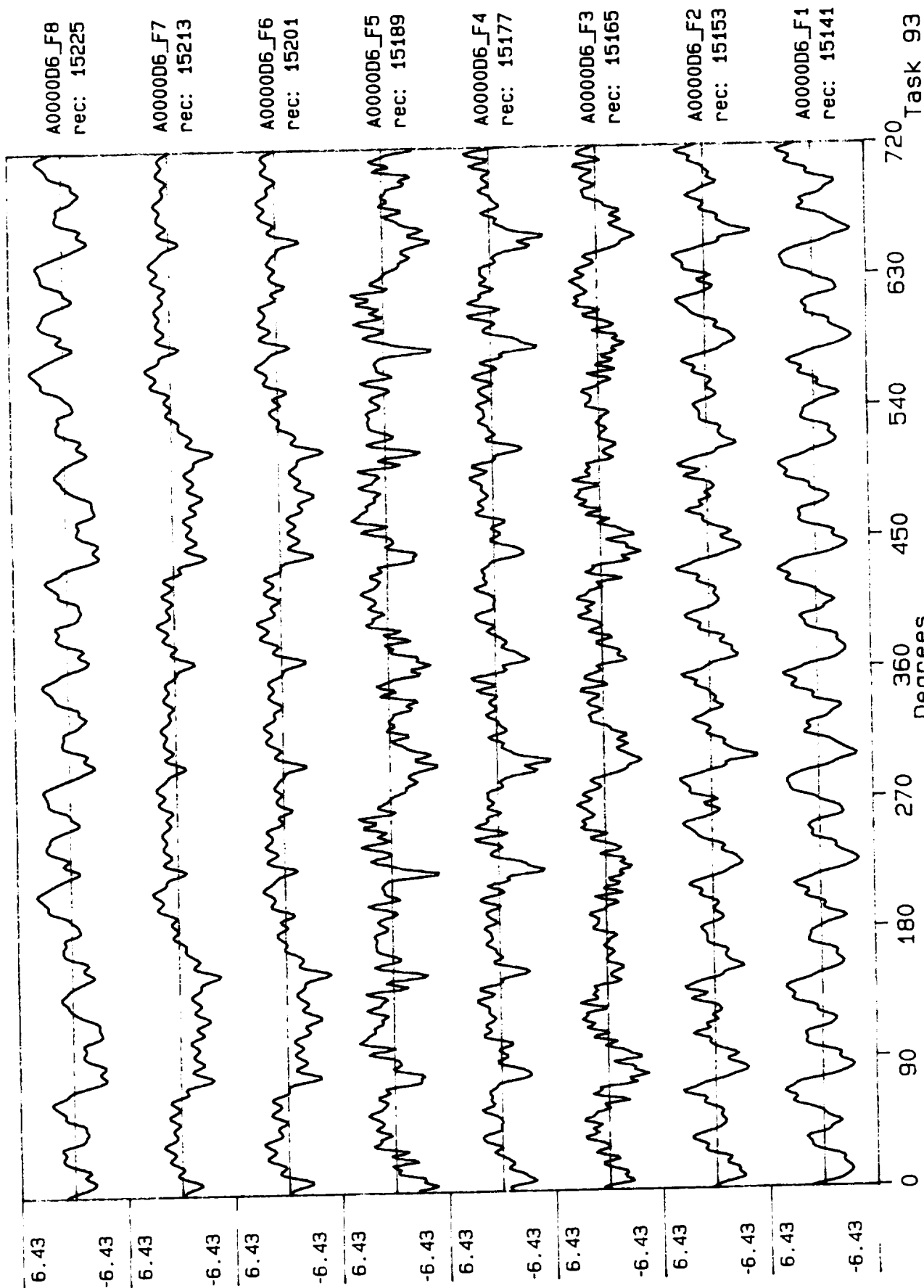
Process included: Calibration, Phase correction and DC filtering. Published: 06,07,89



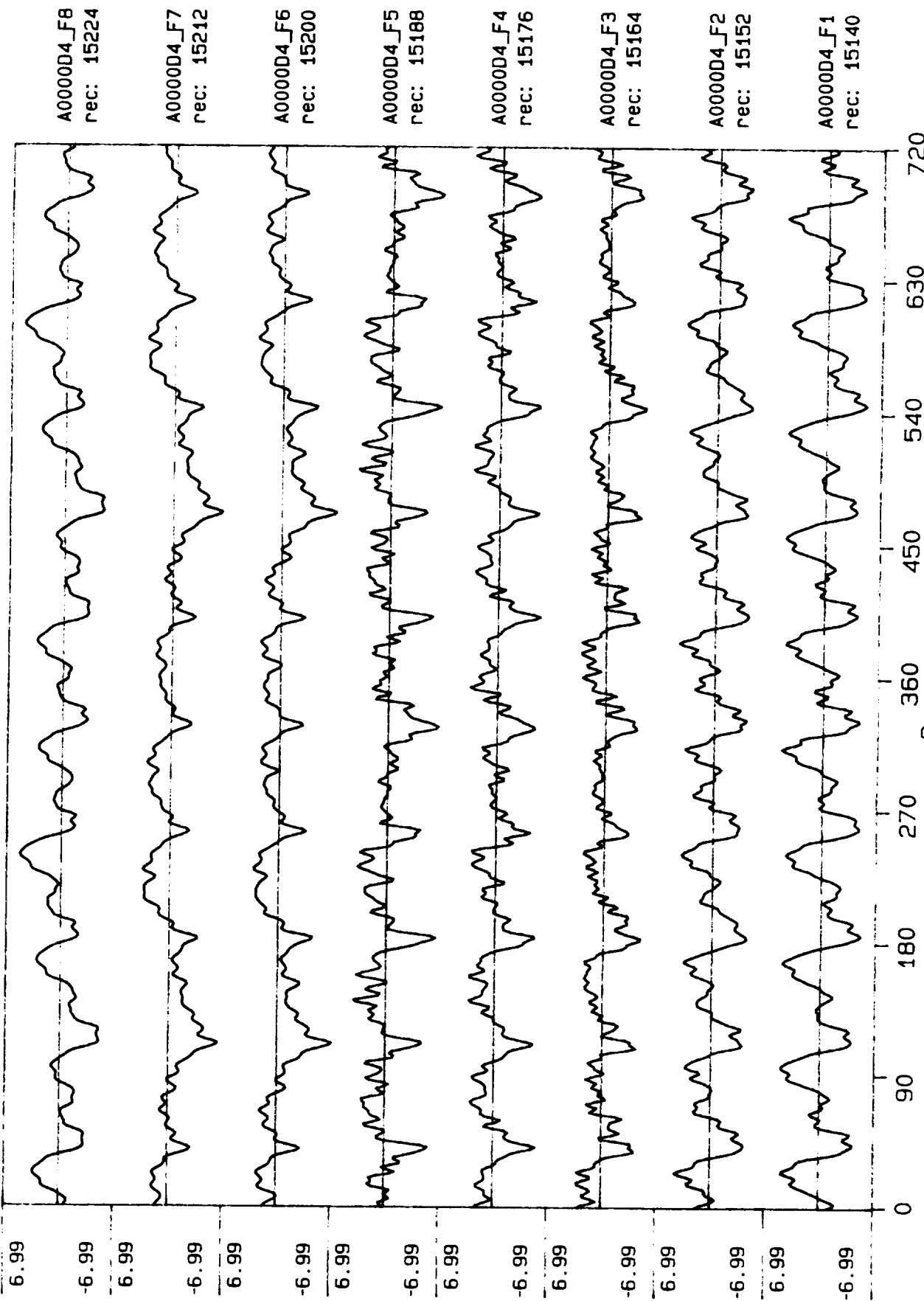


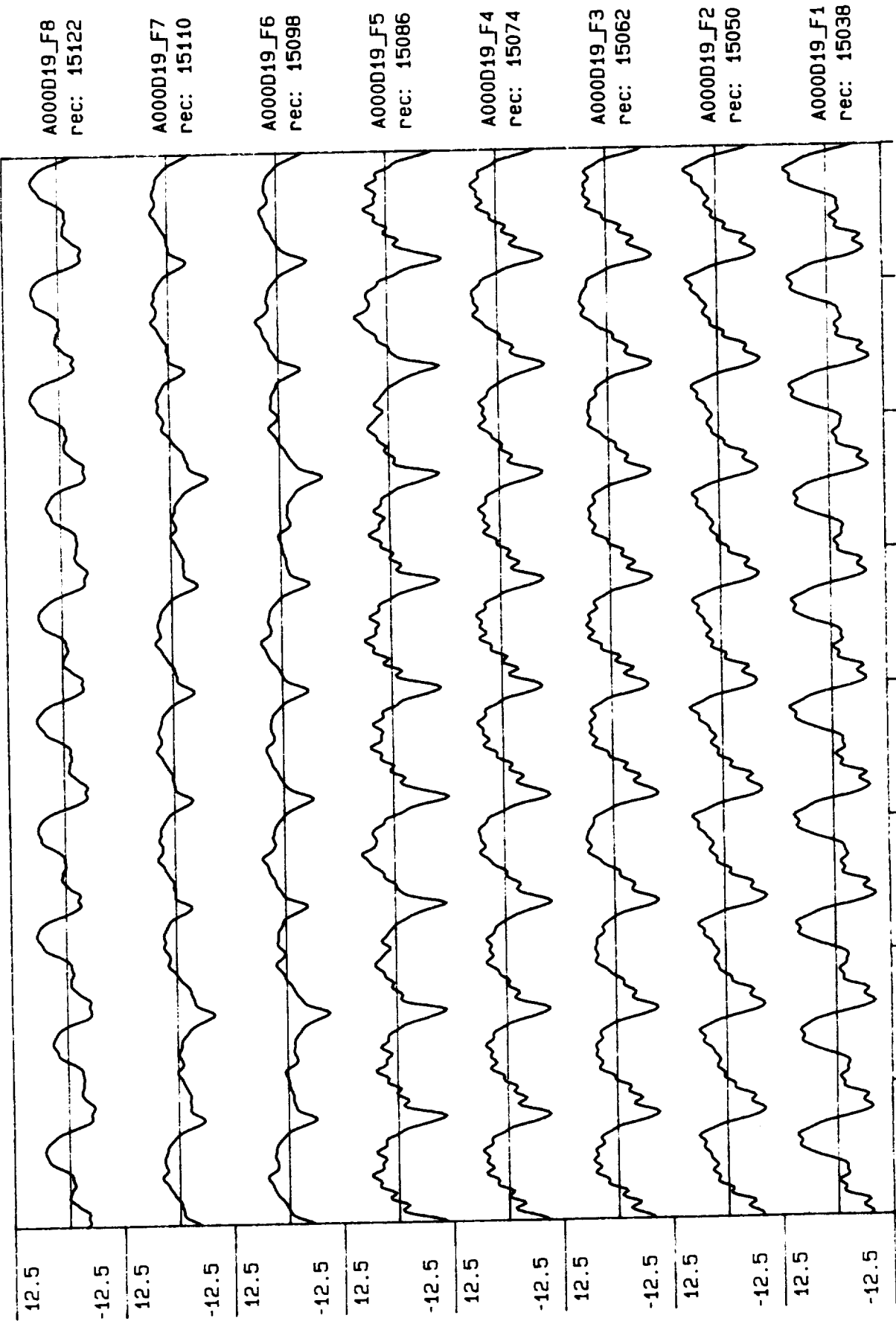
Process included: Calibration, Phase correction and DC filtering. Published: 06,07,89



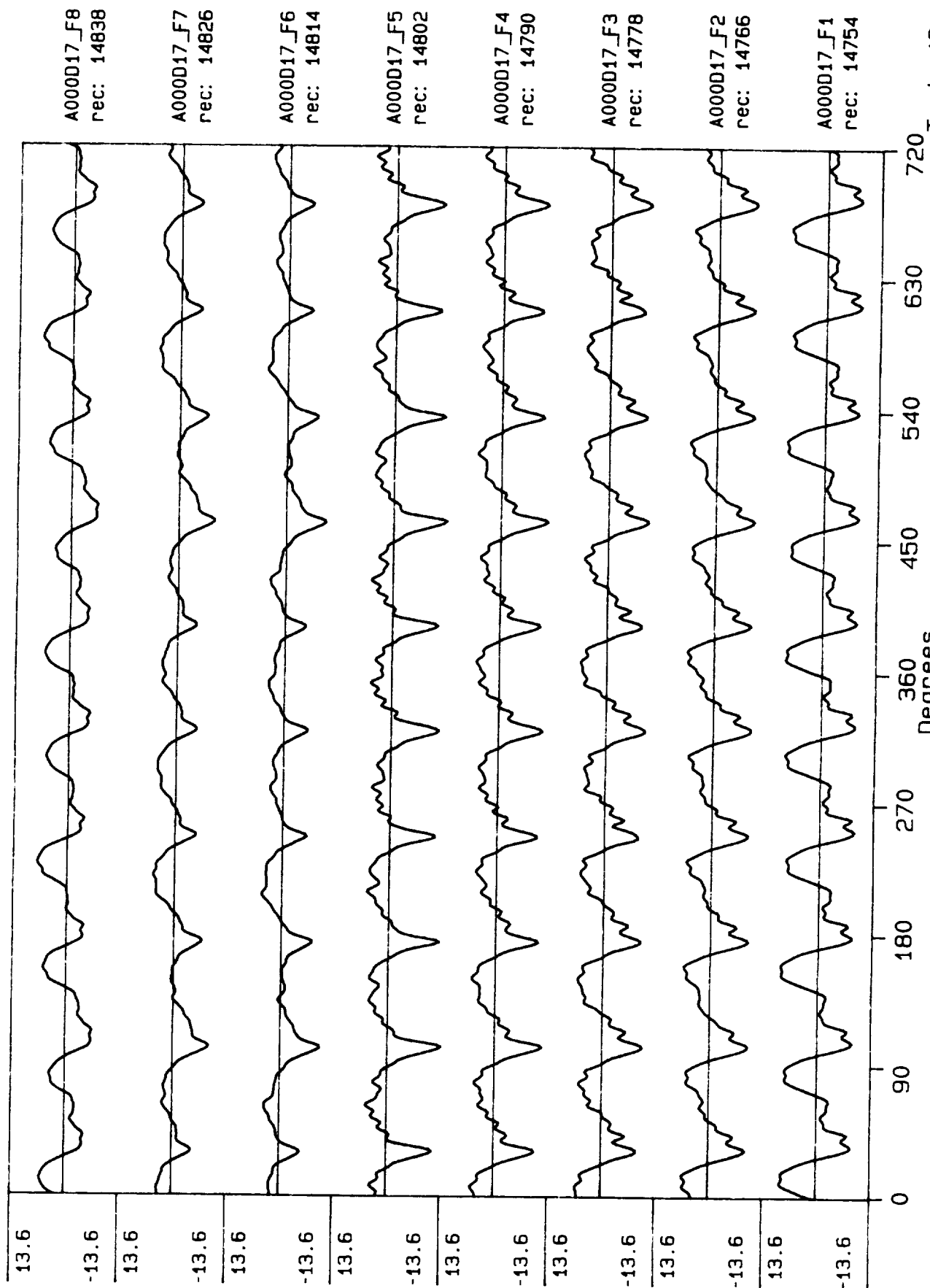


Process included: Calibration, phase correction and DC filtering. Published: 06.07.89

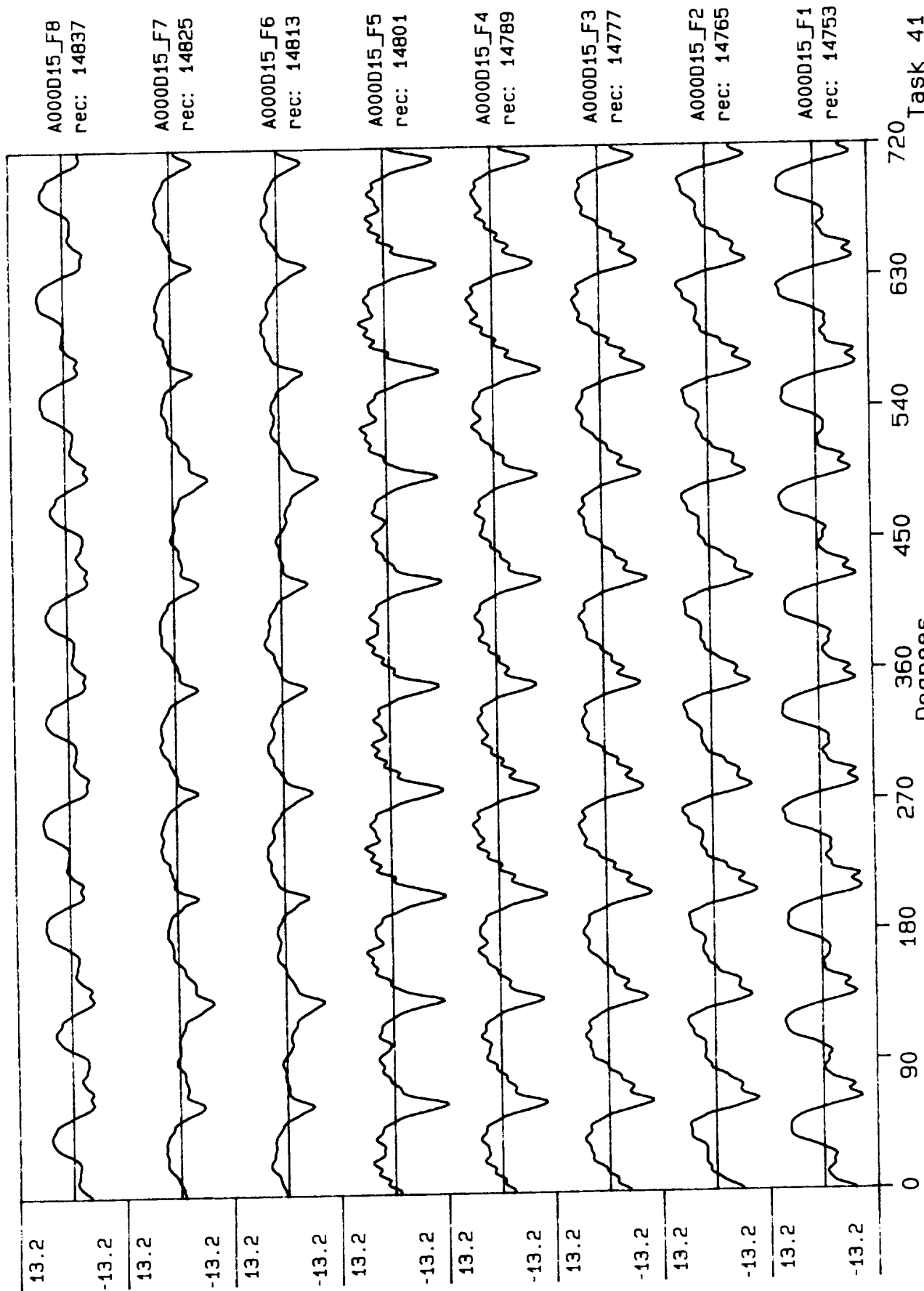




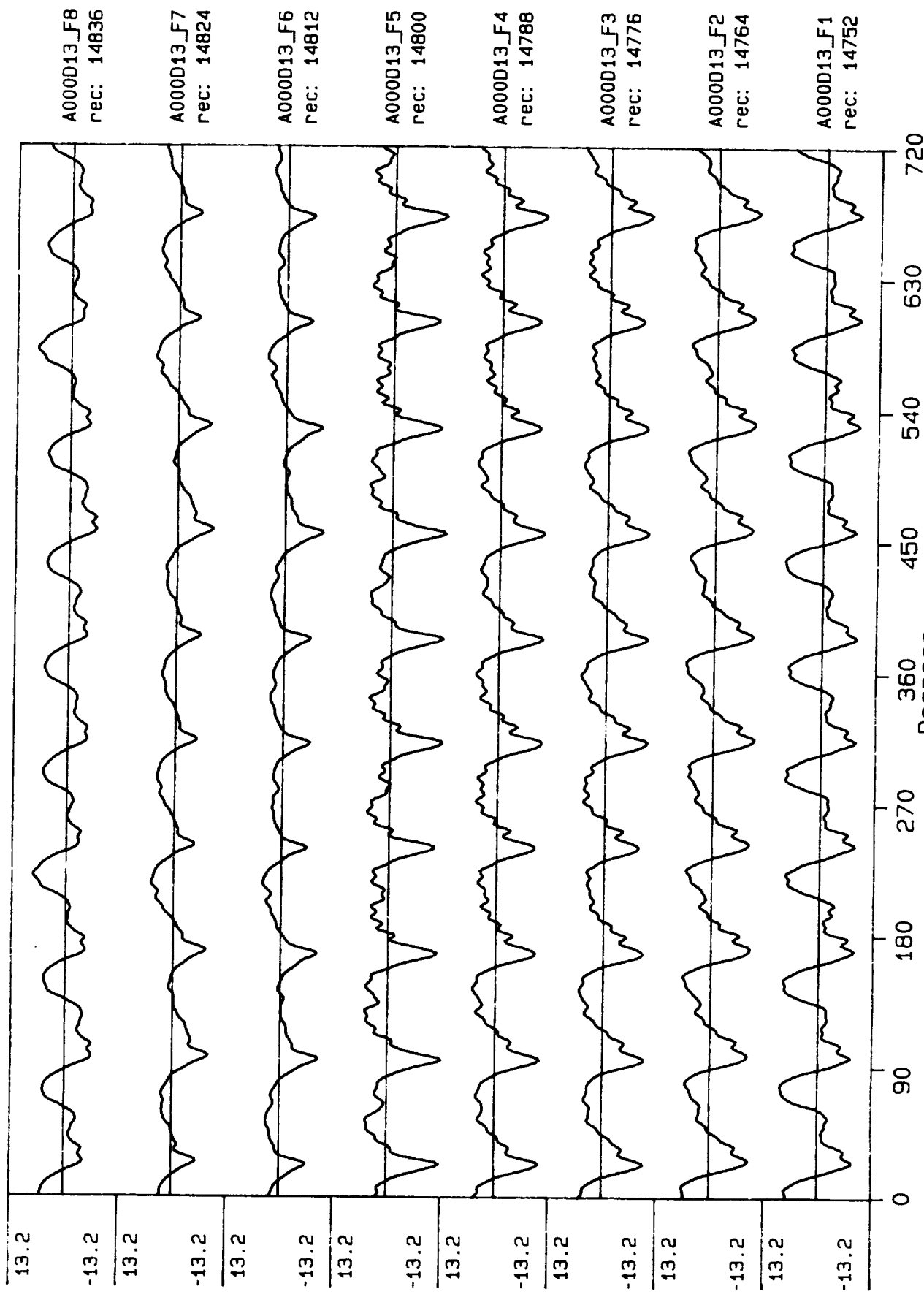
Task 74



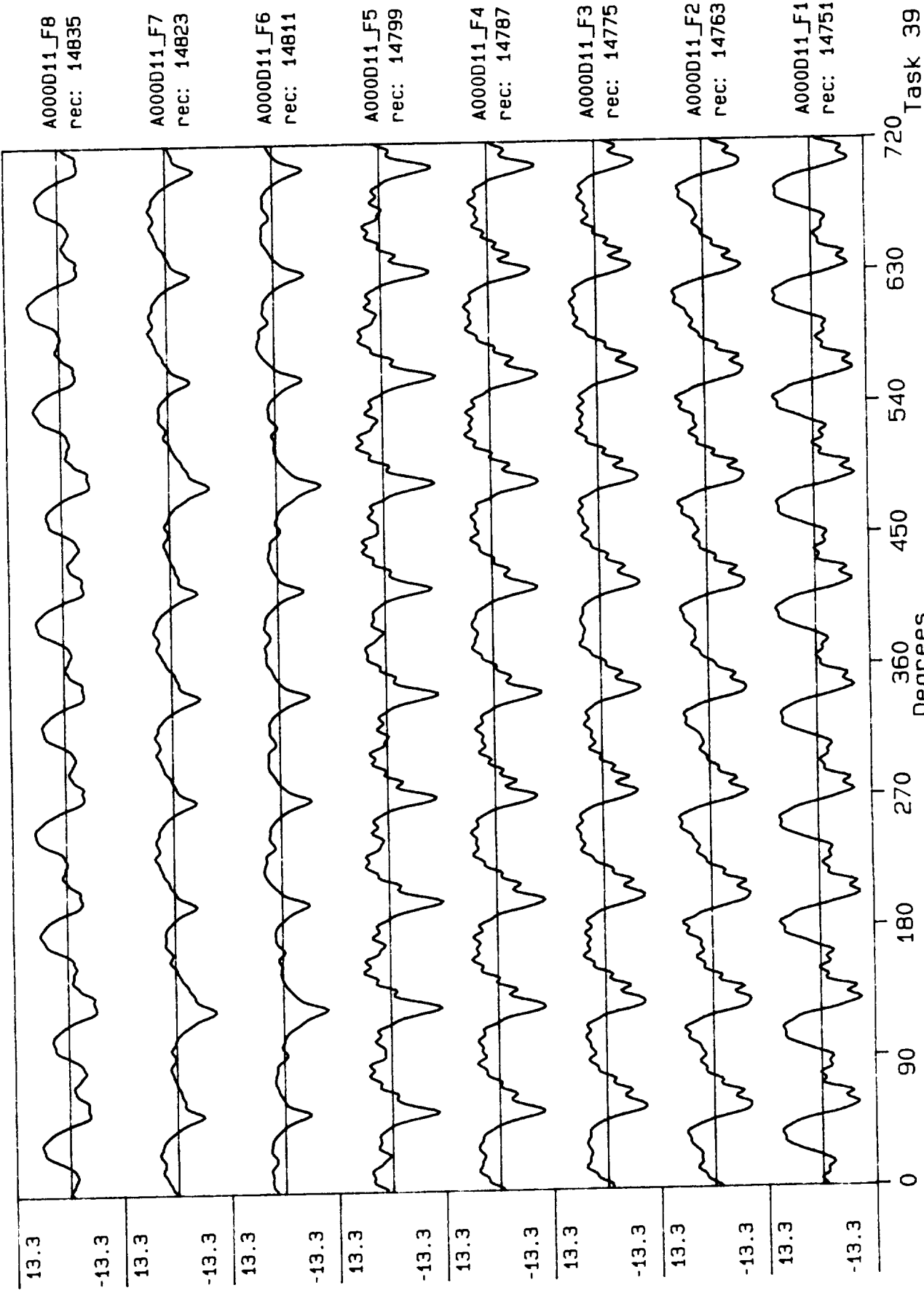
Process included: Calibration, Phase correction and DC filtering. Published: 06,07,89

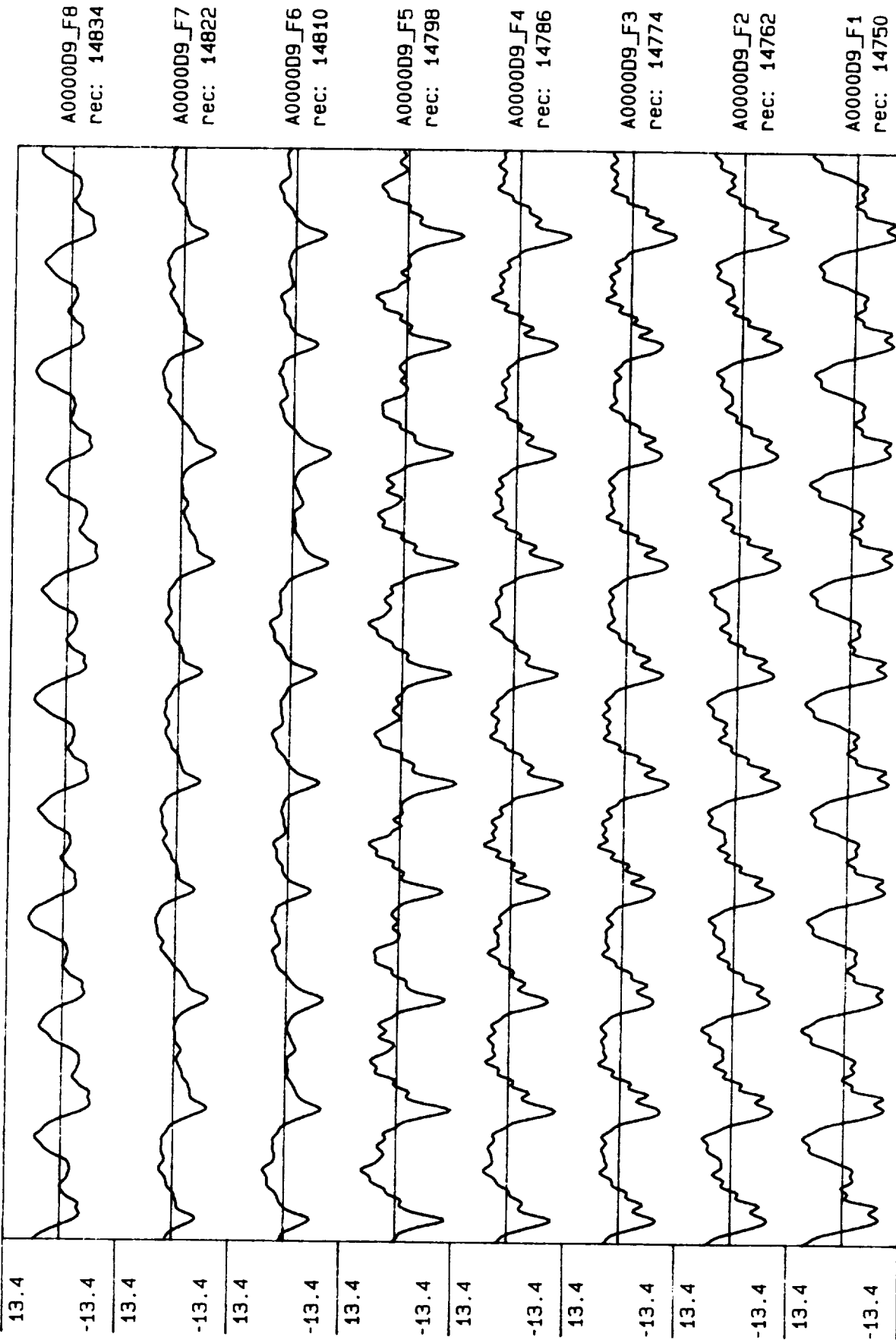


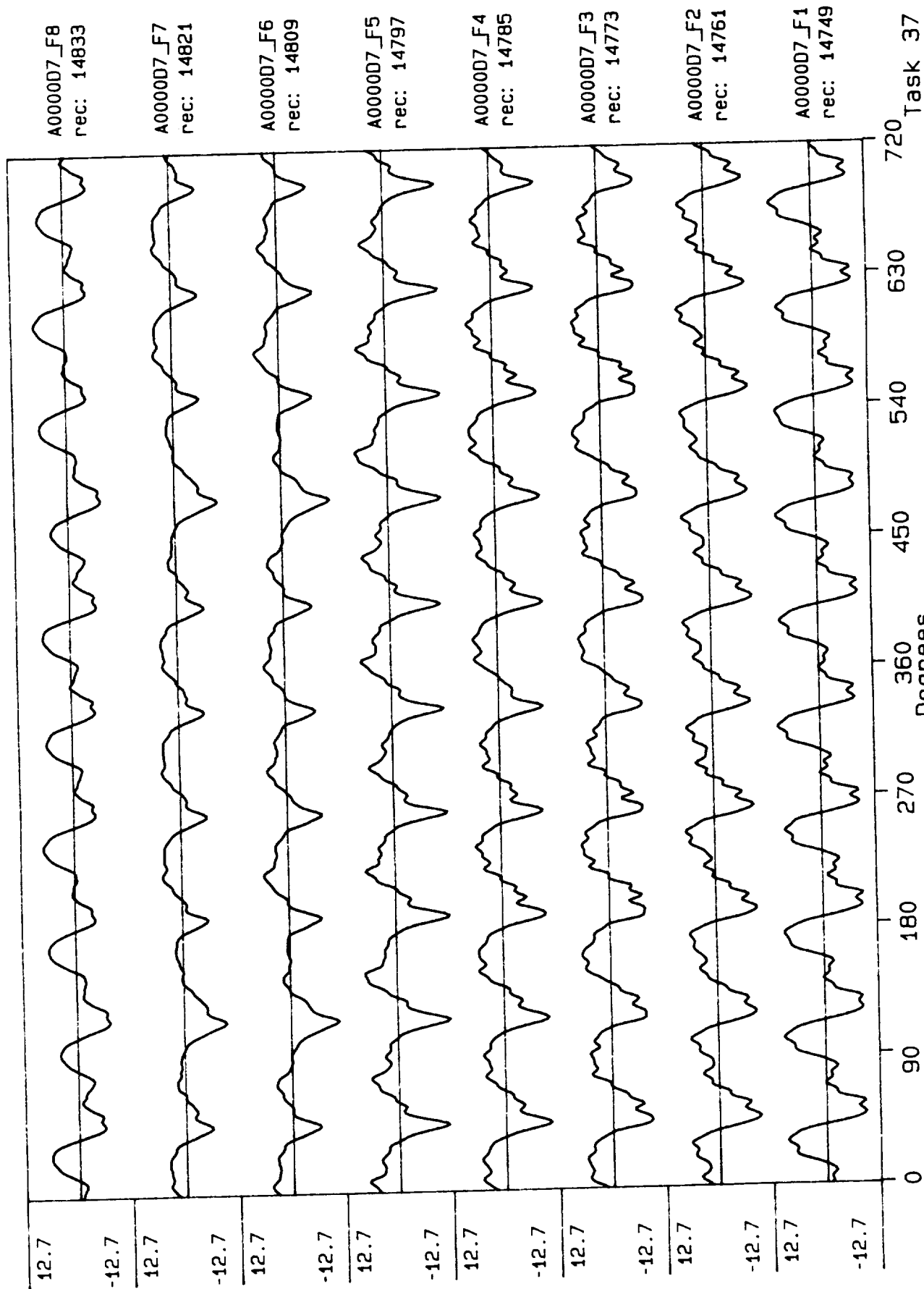
Process included: Calibration, Phase correction and DC filtering. Published: 06/07/89



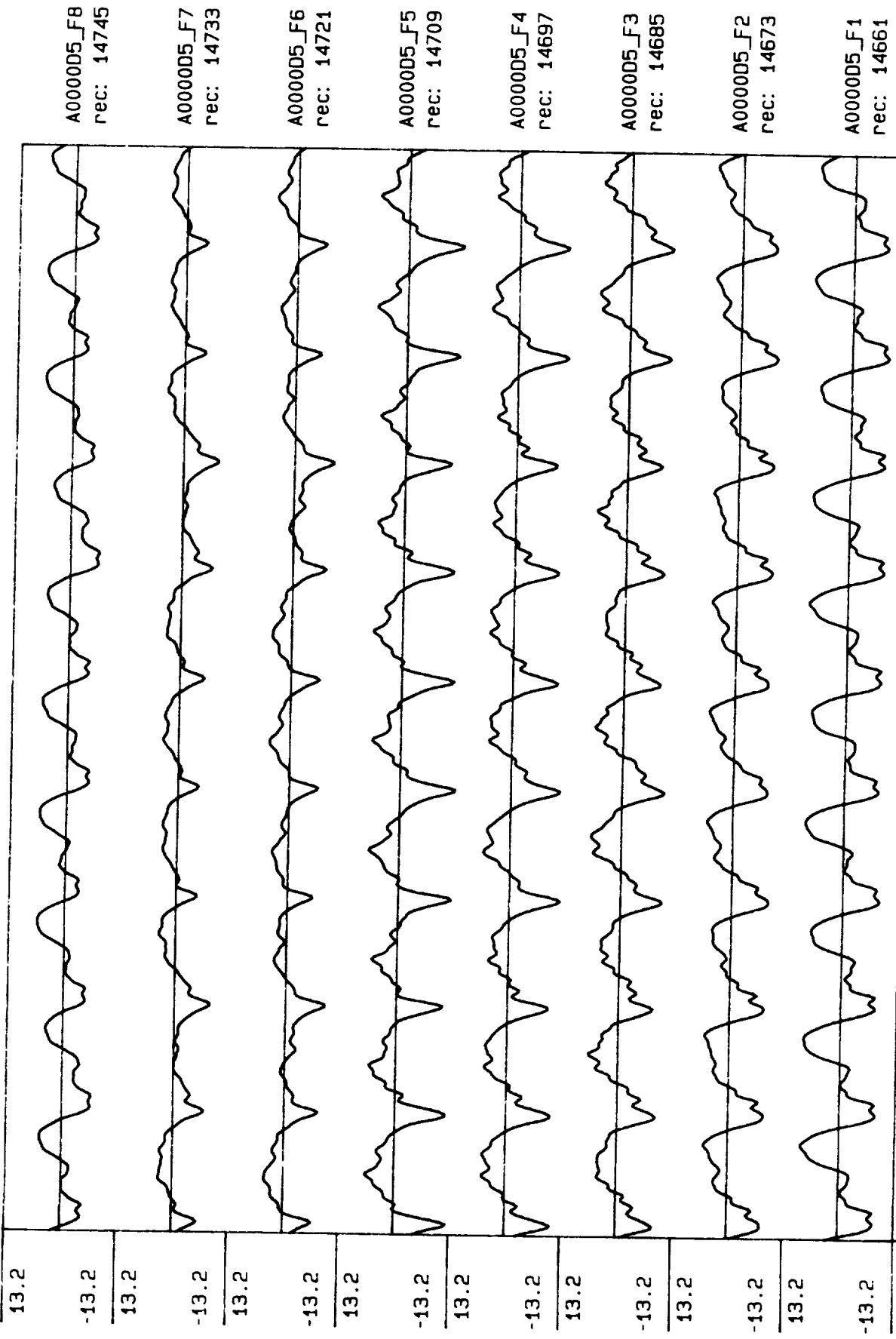
Process included: Calibration, Phase correction and DC filtering. Published: 06,07,89

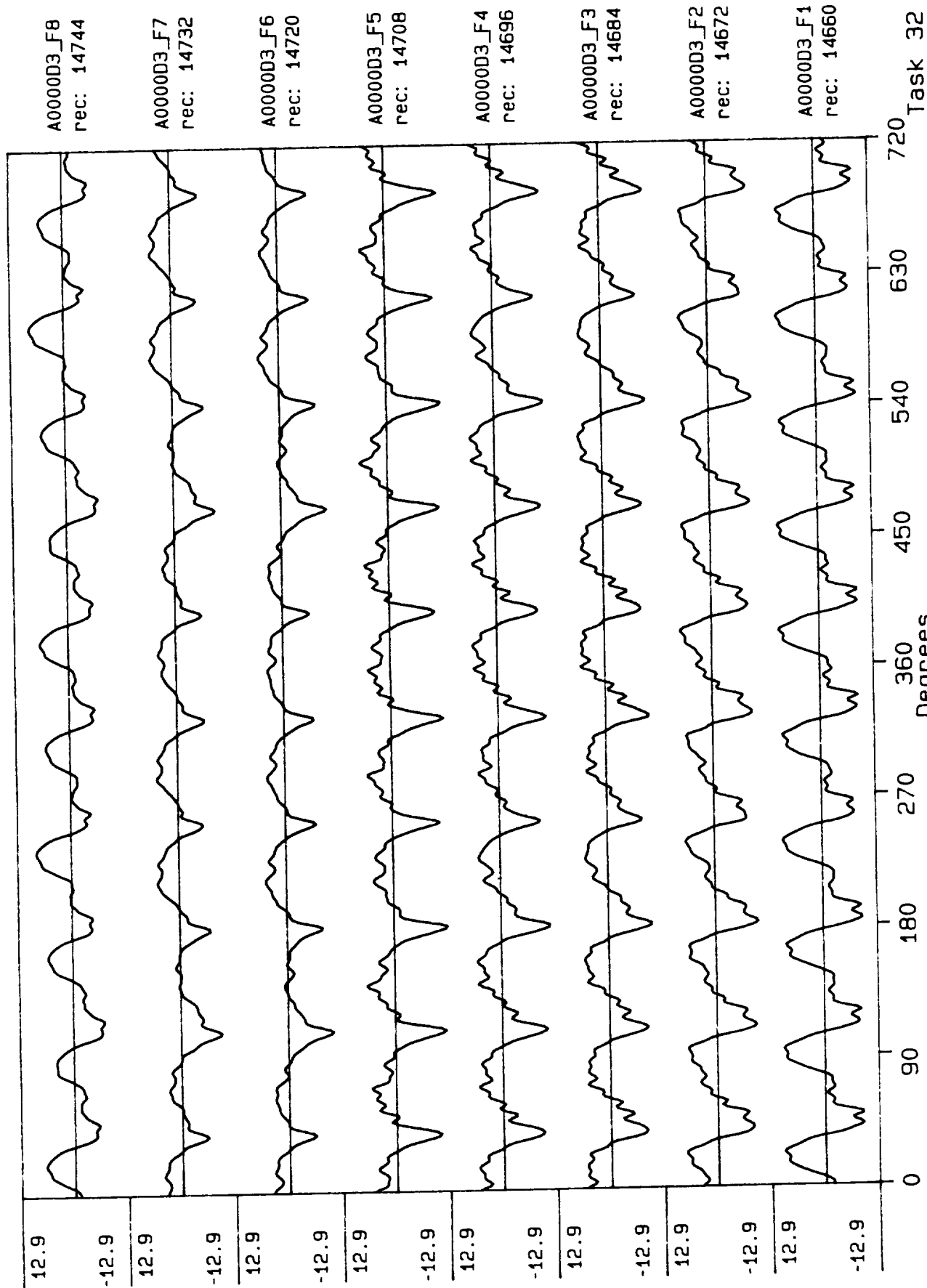




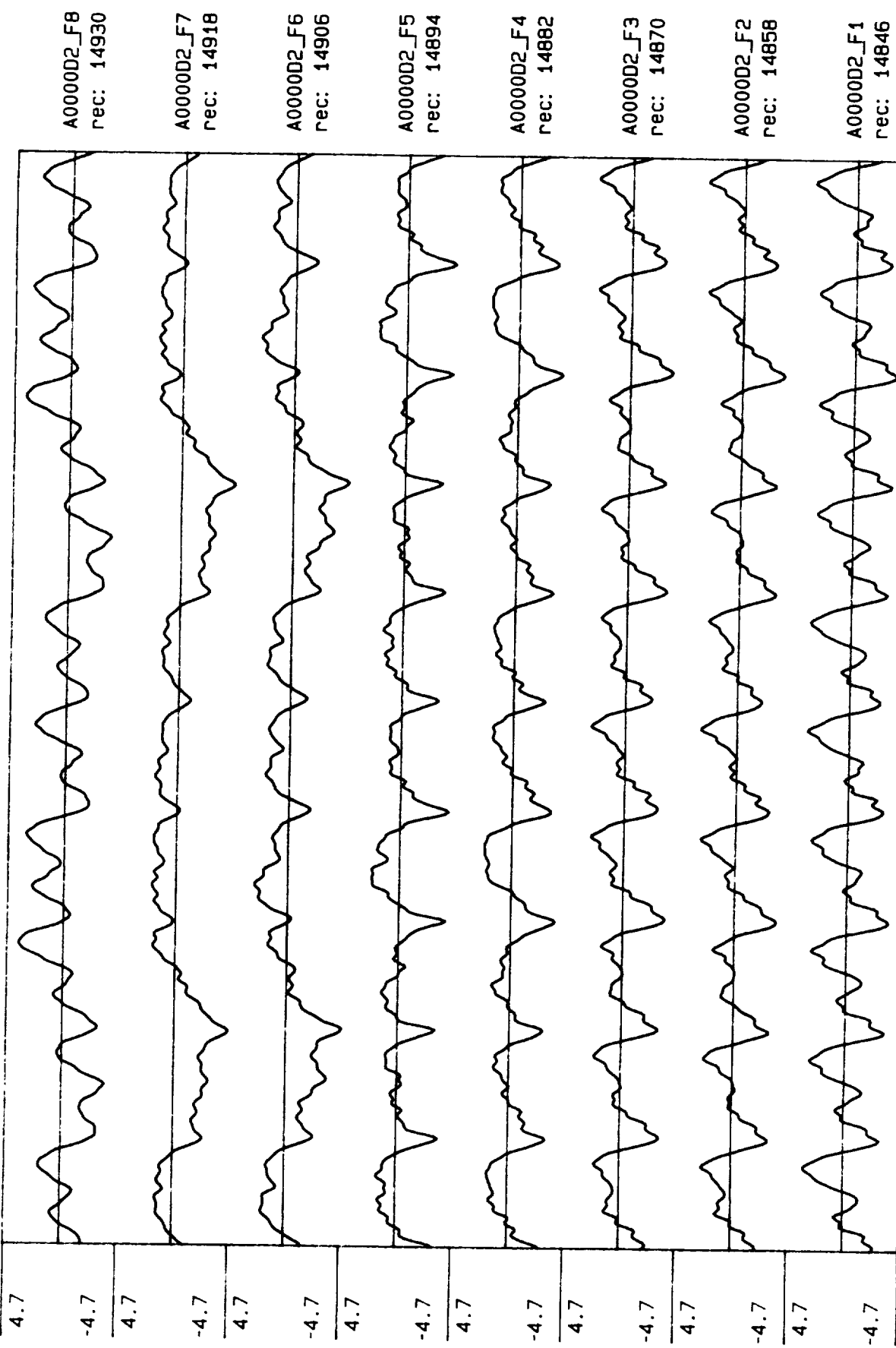


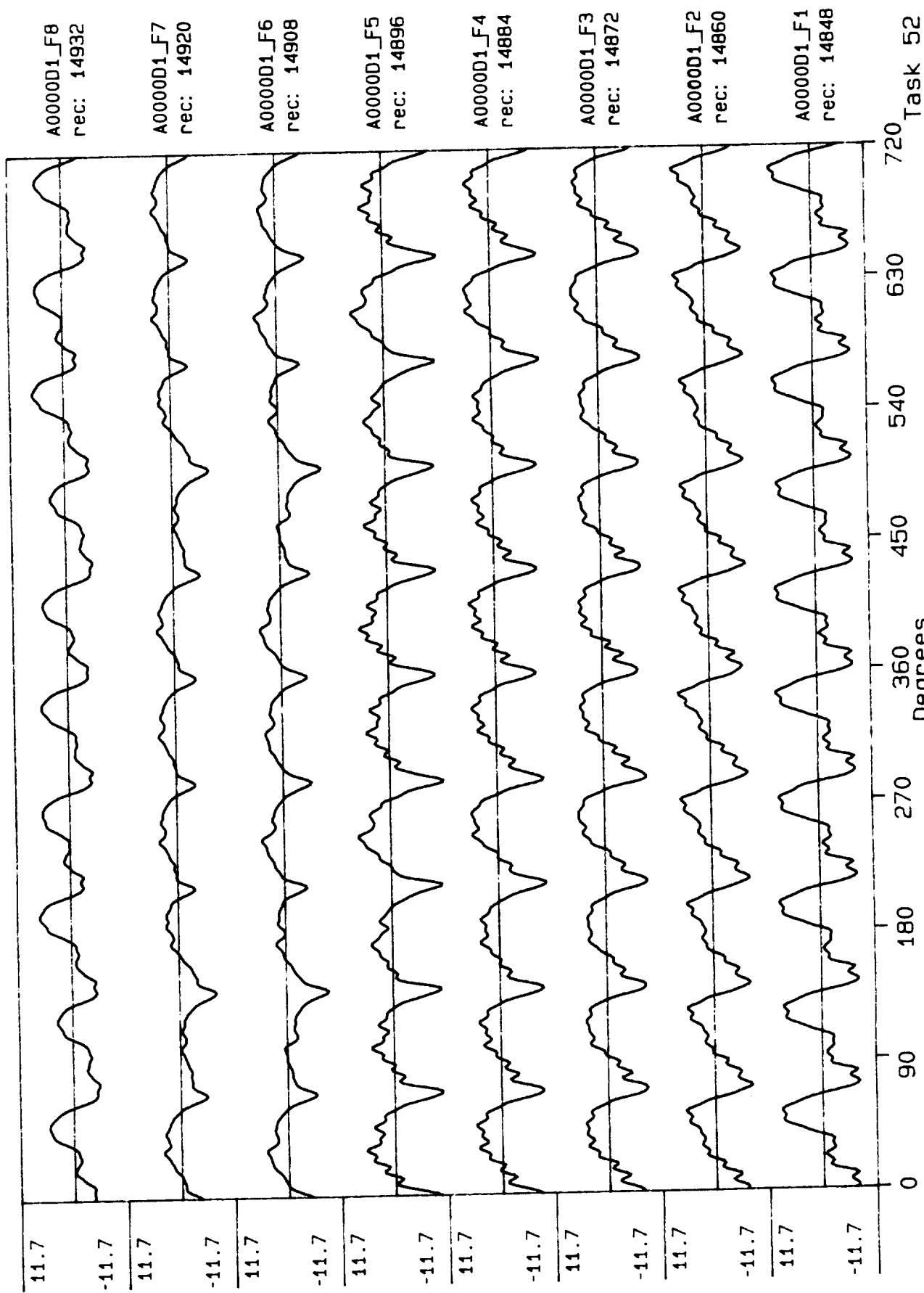
Process included: Calibration, Phase correction and DC filtering. Published: 06/07/89



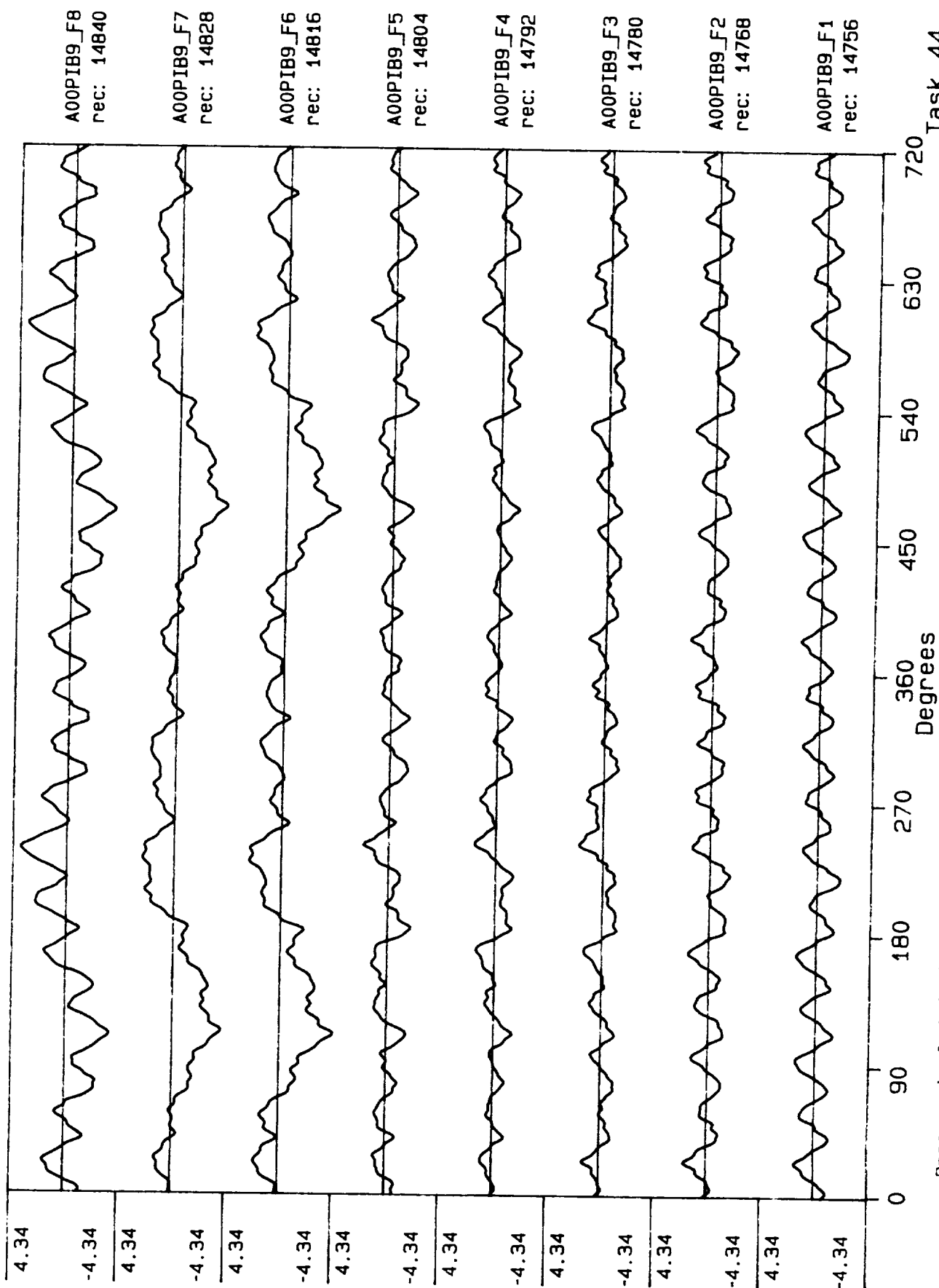


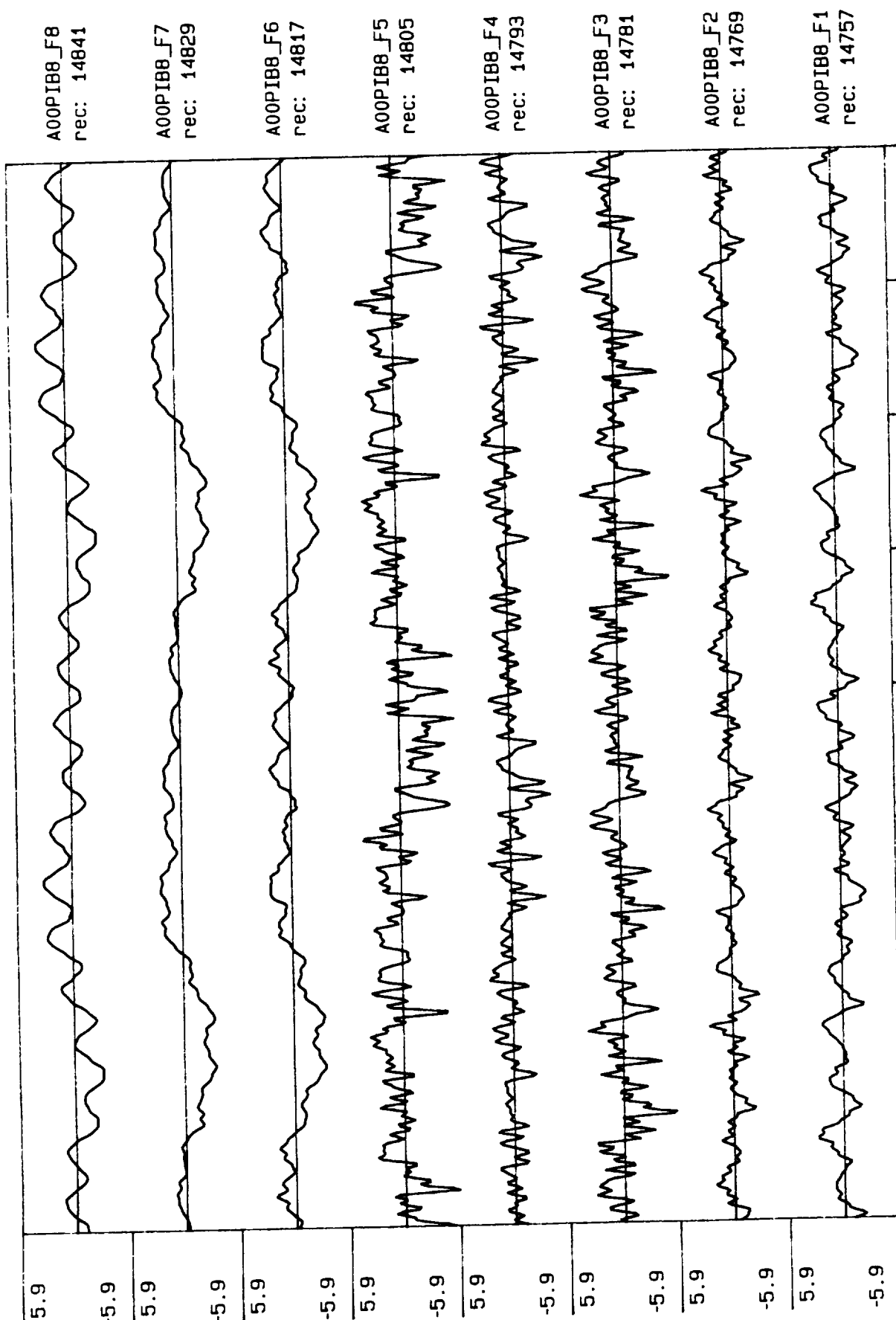
Process included: Calibration, Phase correction and DC filtering. Published: 06/07/89





Process included: Calibration, Phase correction and DC filtering. Published: 06,07,89





A00PIB8_F8
rec: 14841

A00PIB8_F7
rec: 14829

A00PIB8_F6
rec: 14817

A00PIB8_F5
rec: 14805

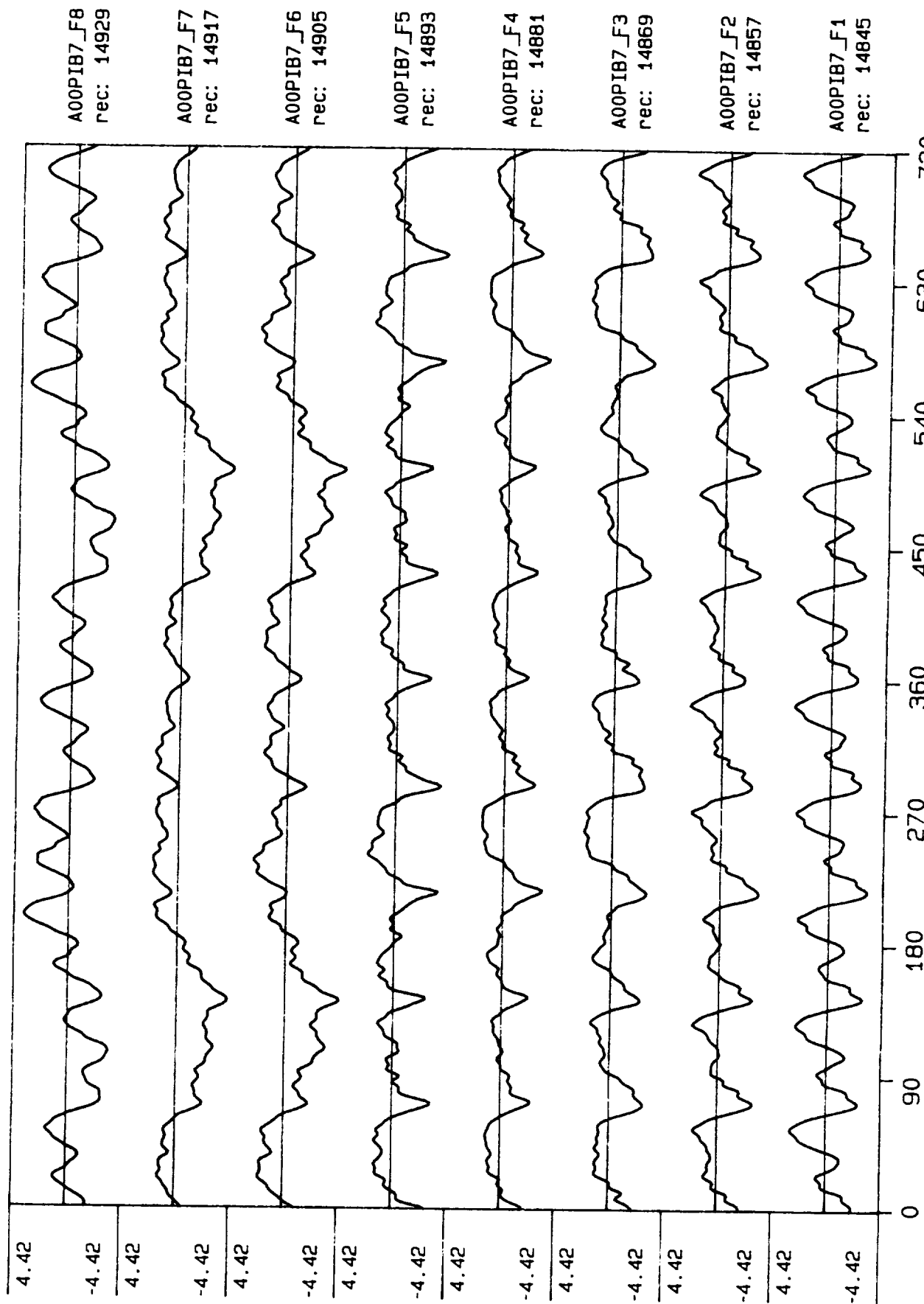
A00PIB8_F4
rec: 14793

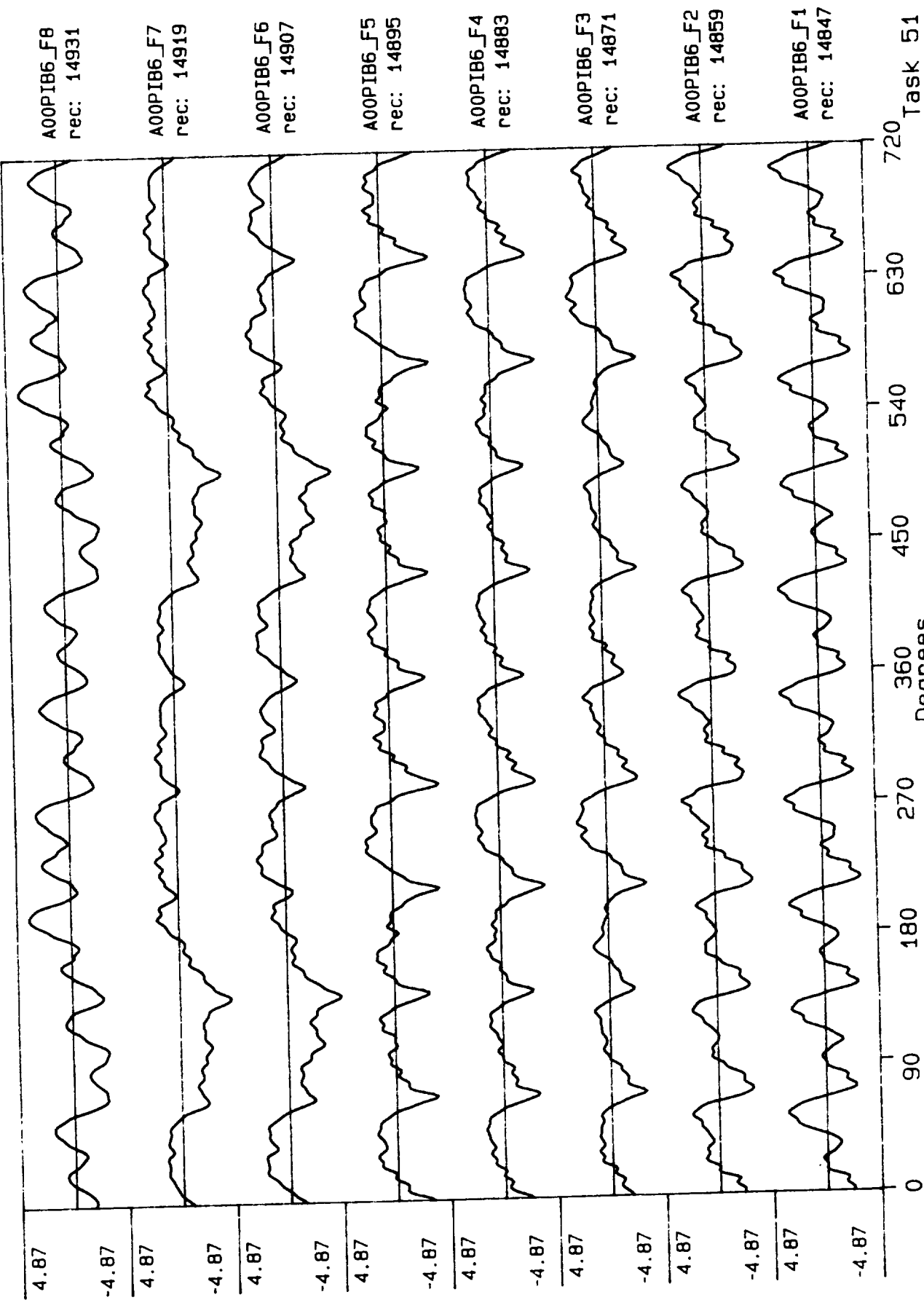
A00PIB8_F3
rec: 14781

A00PIB8_F2
rec: 14769

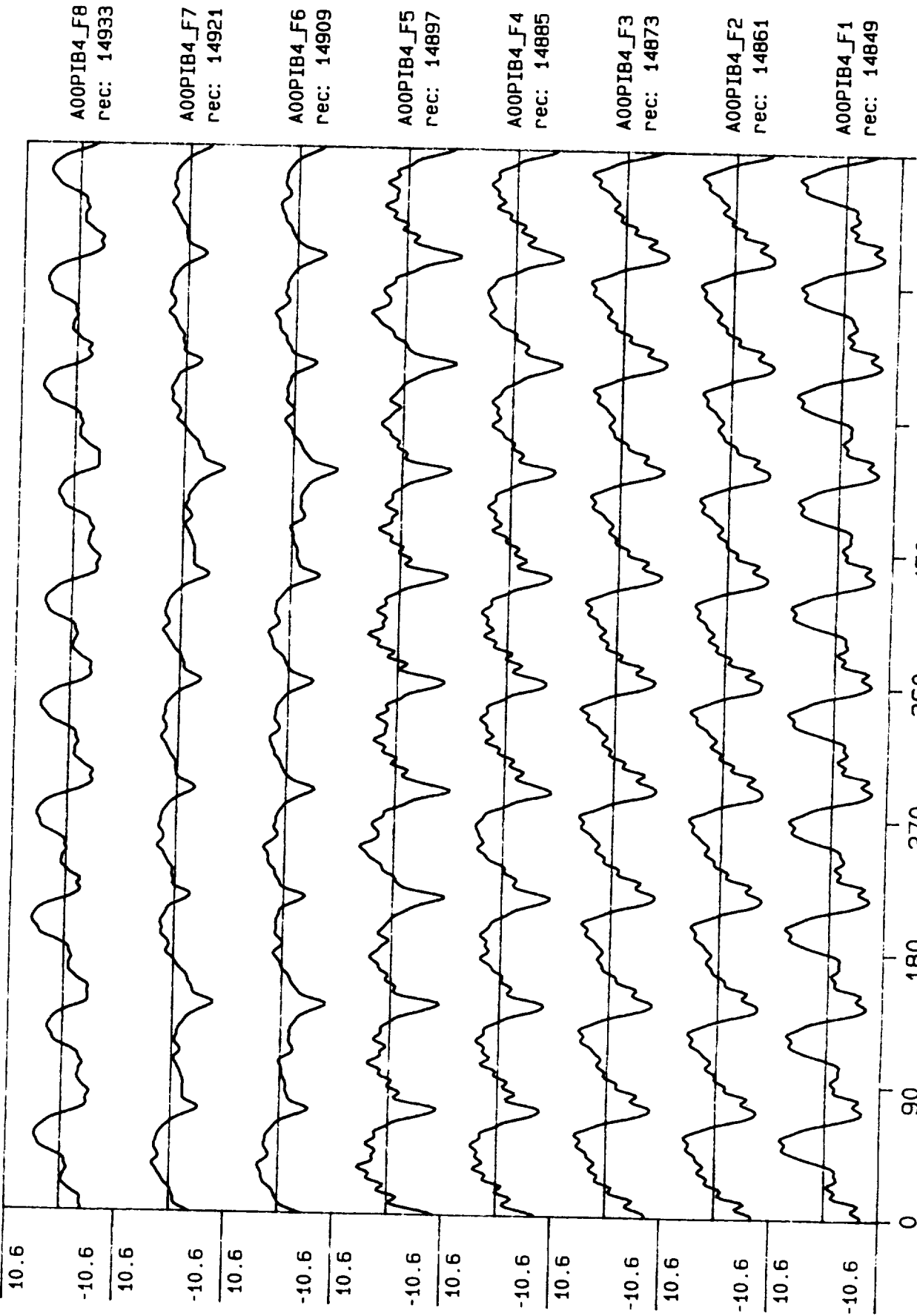
A00PIB8_F1
rec: 14757

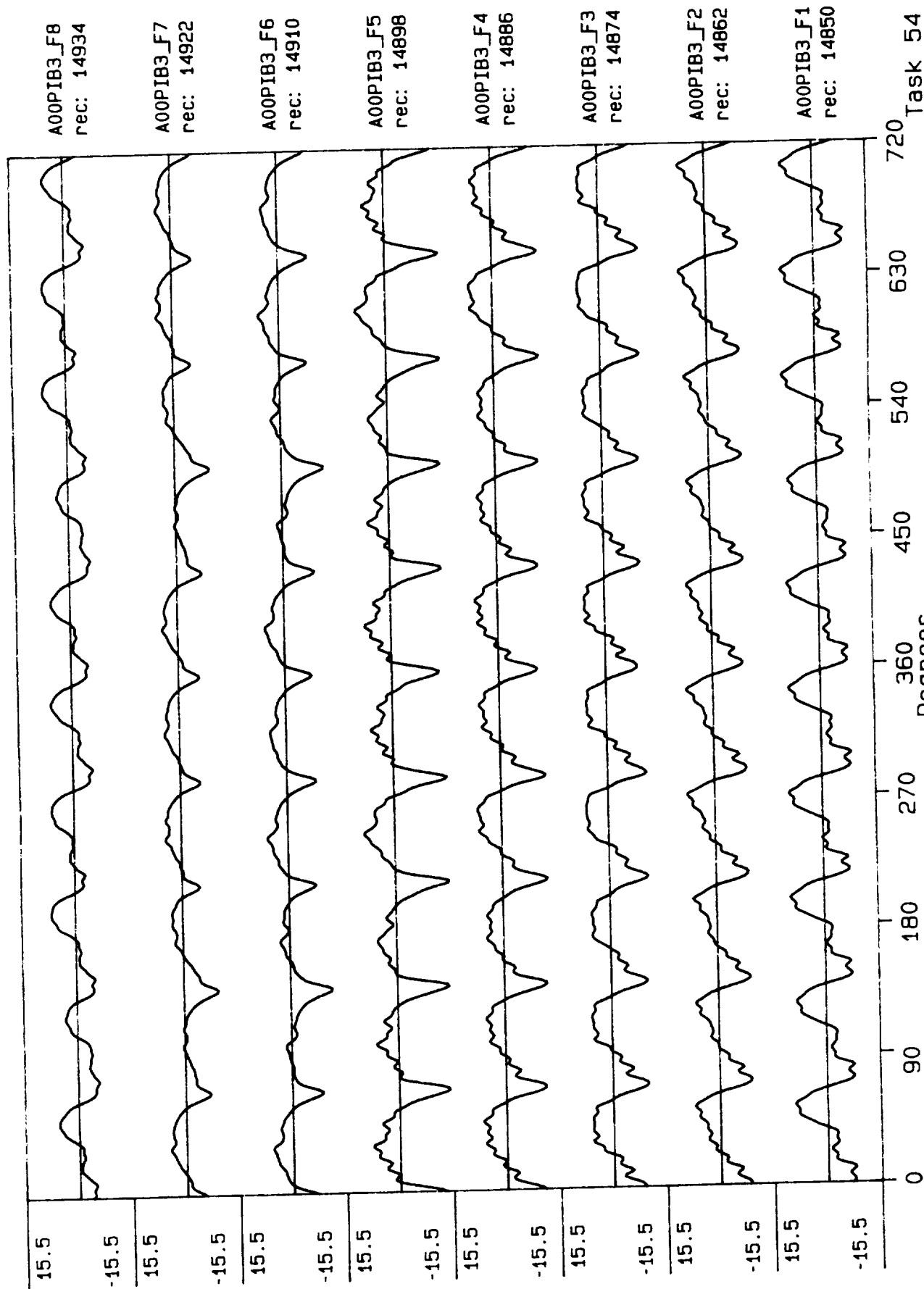
Task 45



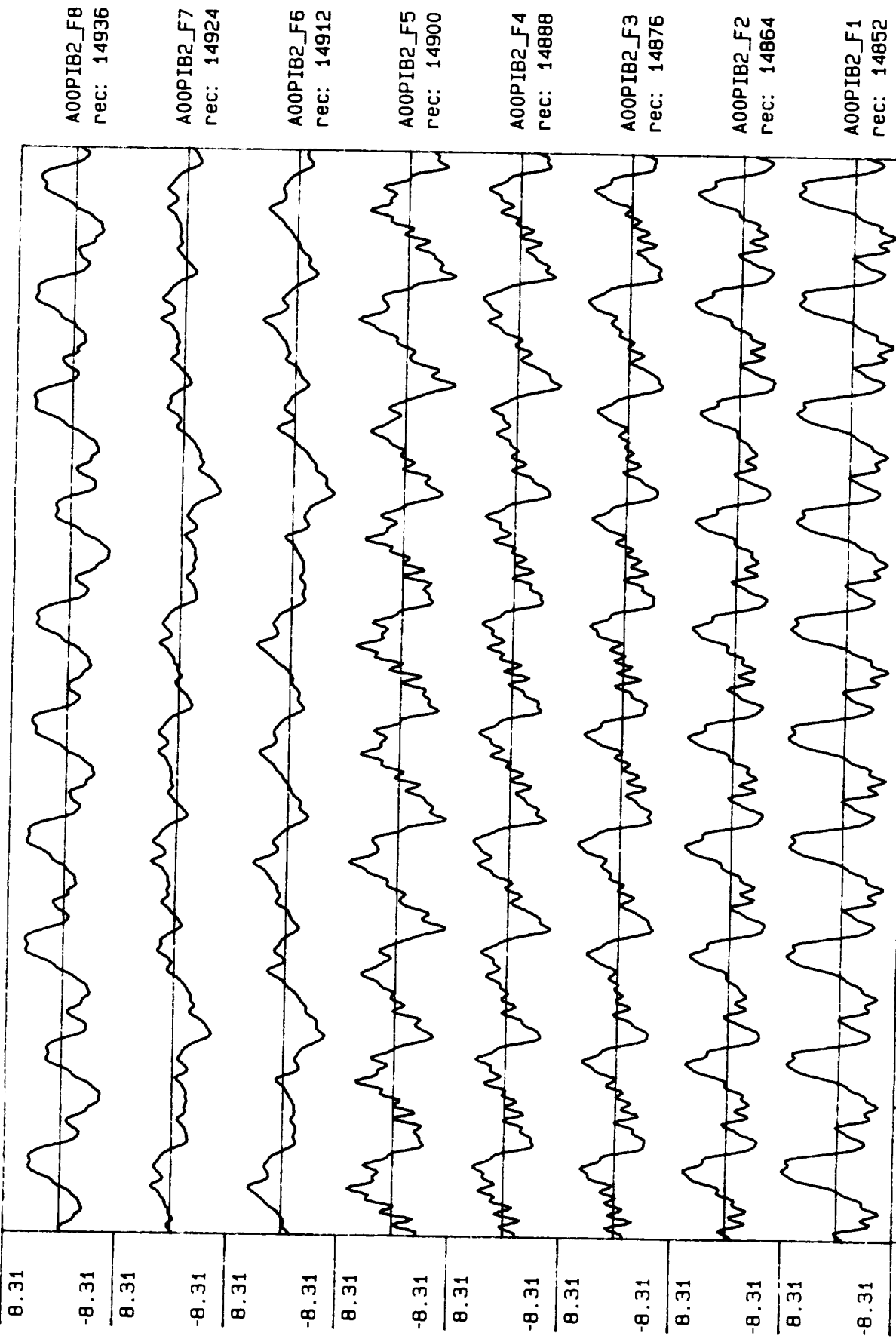


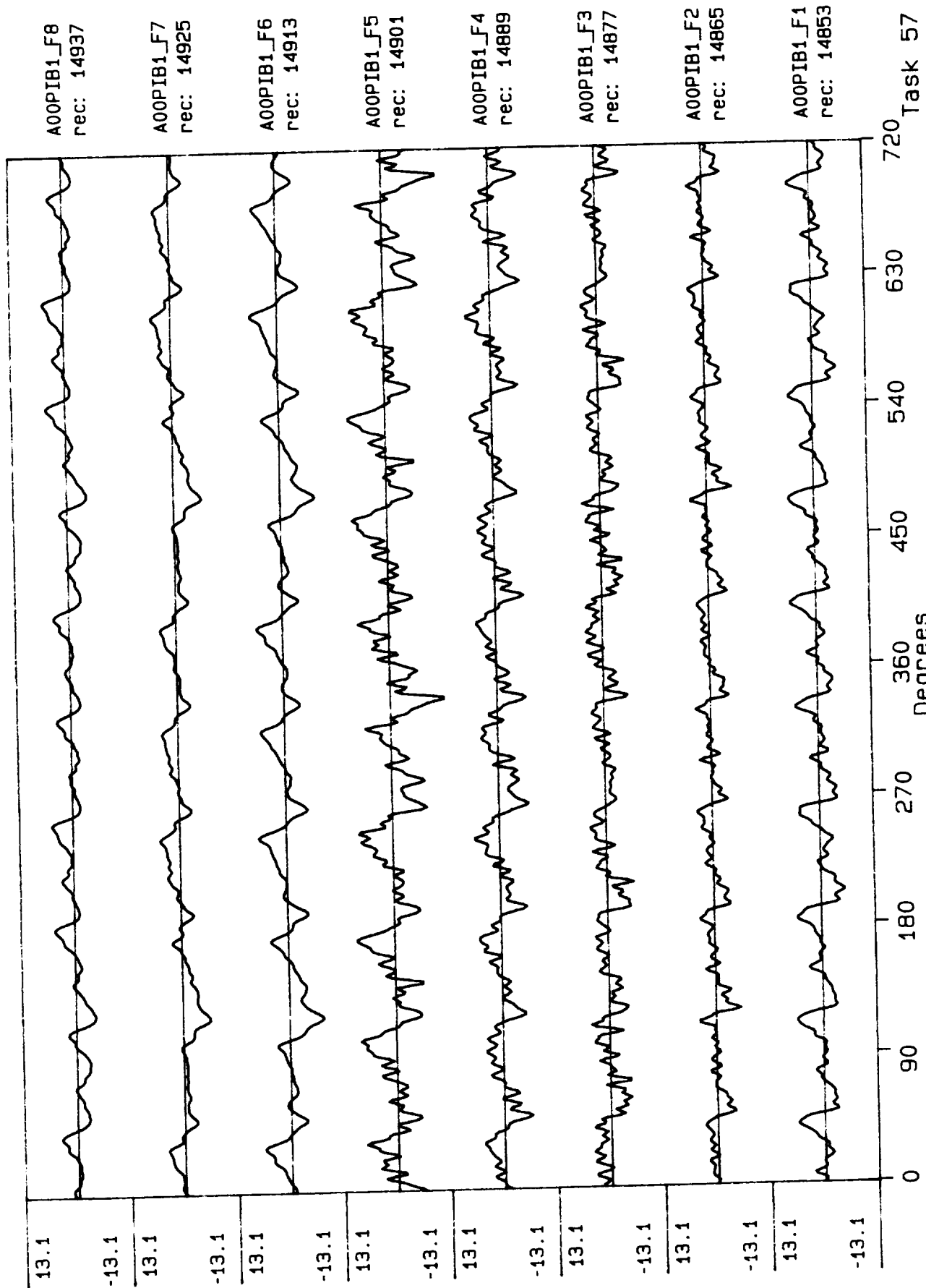
Process included: Calibration, Phase correction and DC filtering. Published: 06,07,89



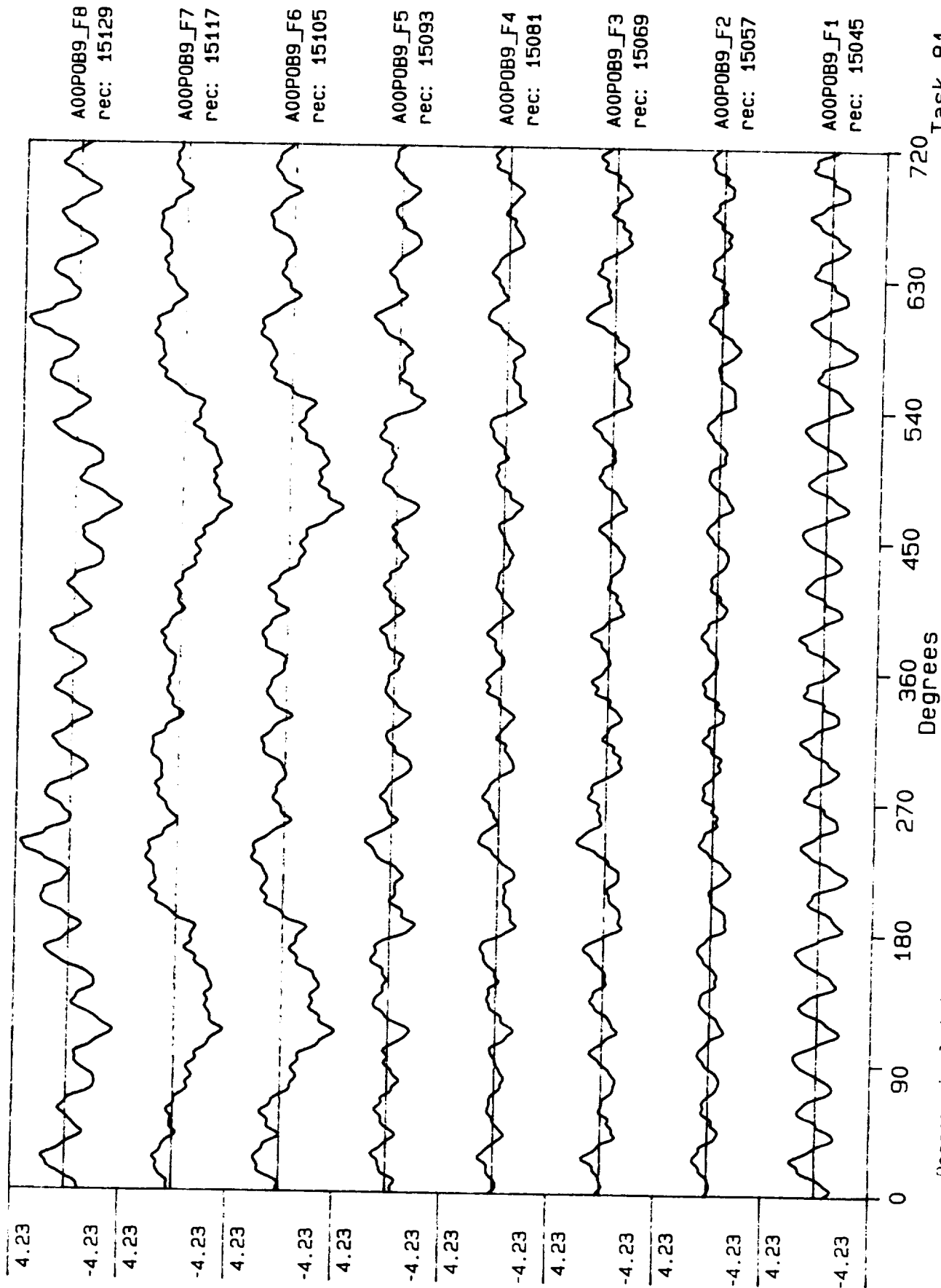


Process included: Calibration, Phase correction and DC filtering. Published: 06/07/89

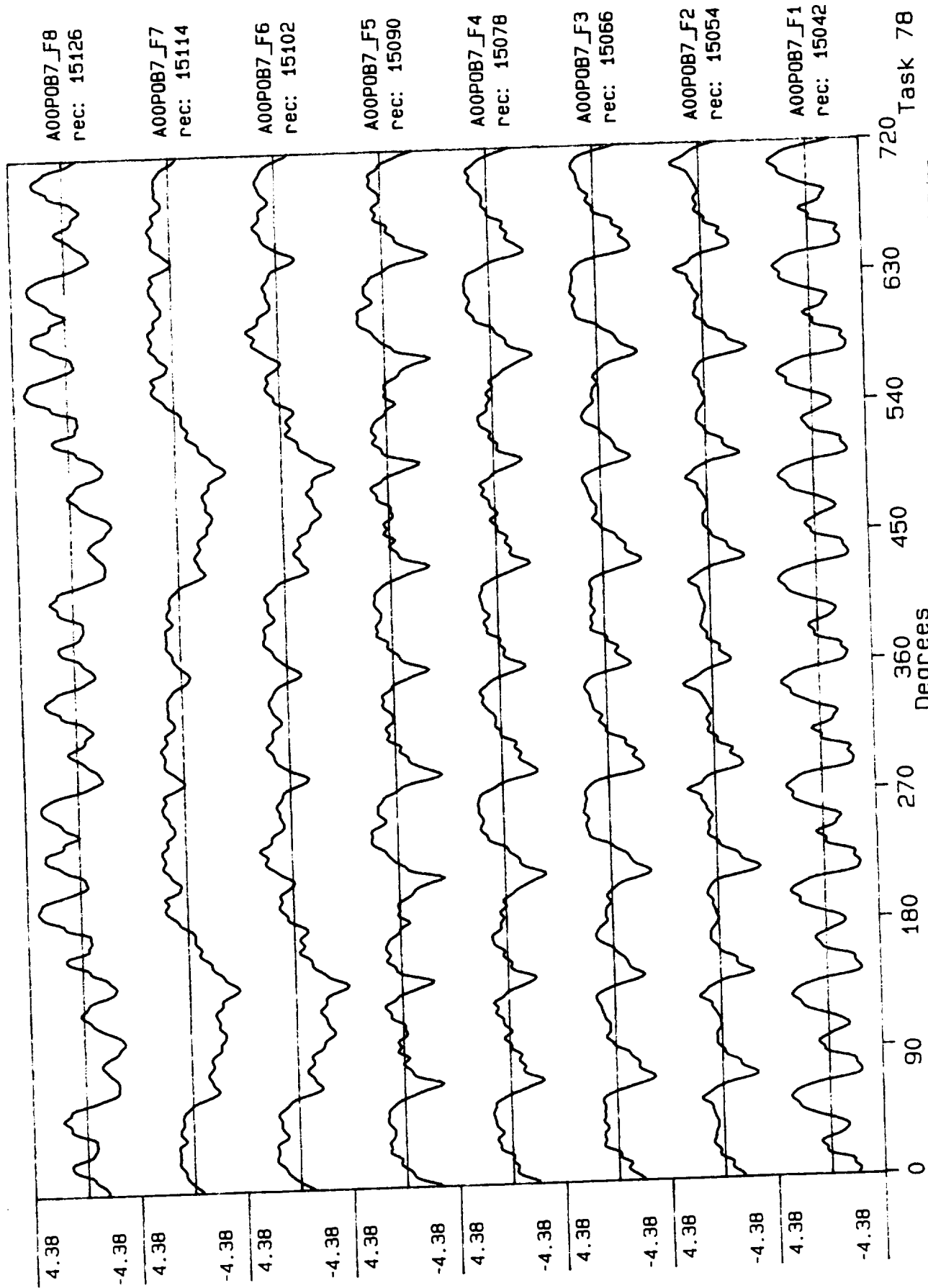




Process included: Calibration, Phase correction and DC filtering. Published: 06/07/89

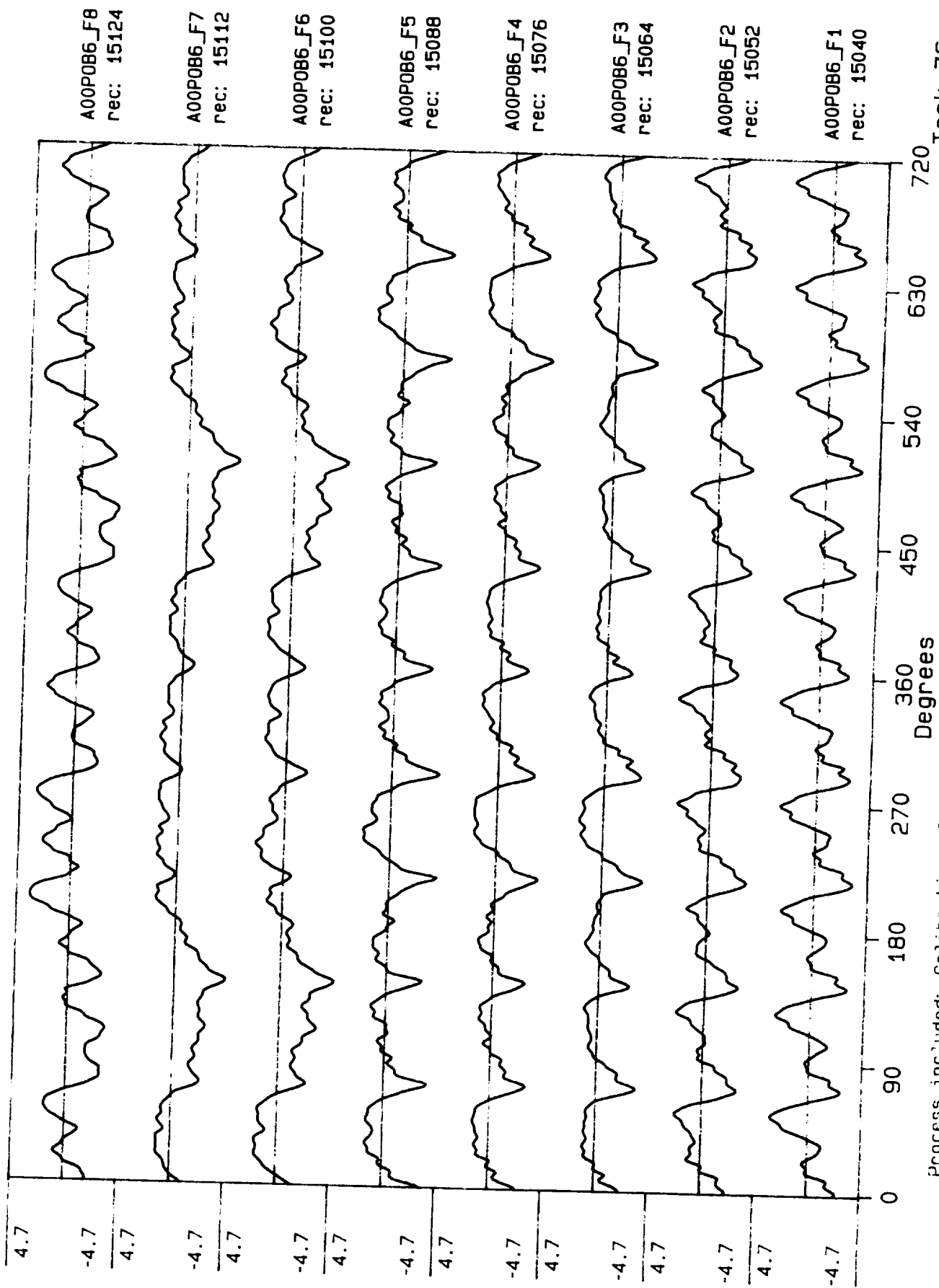


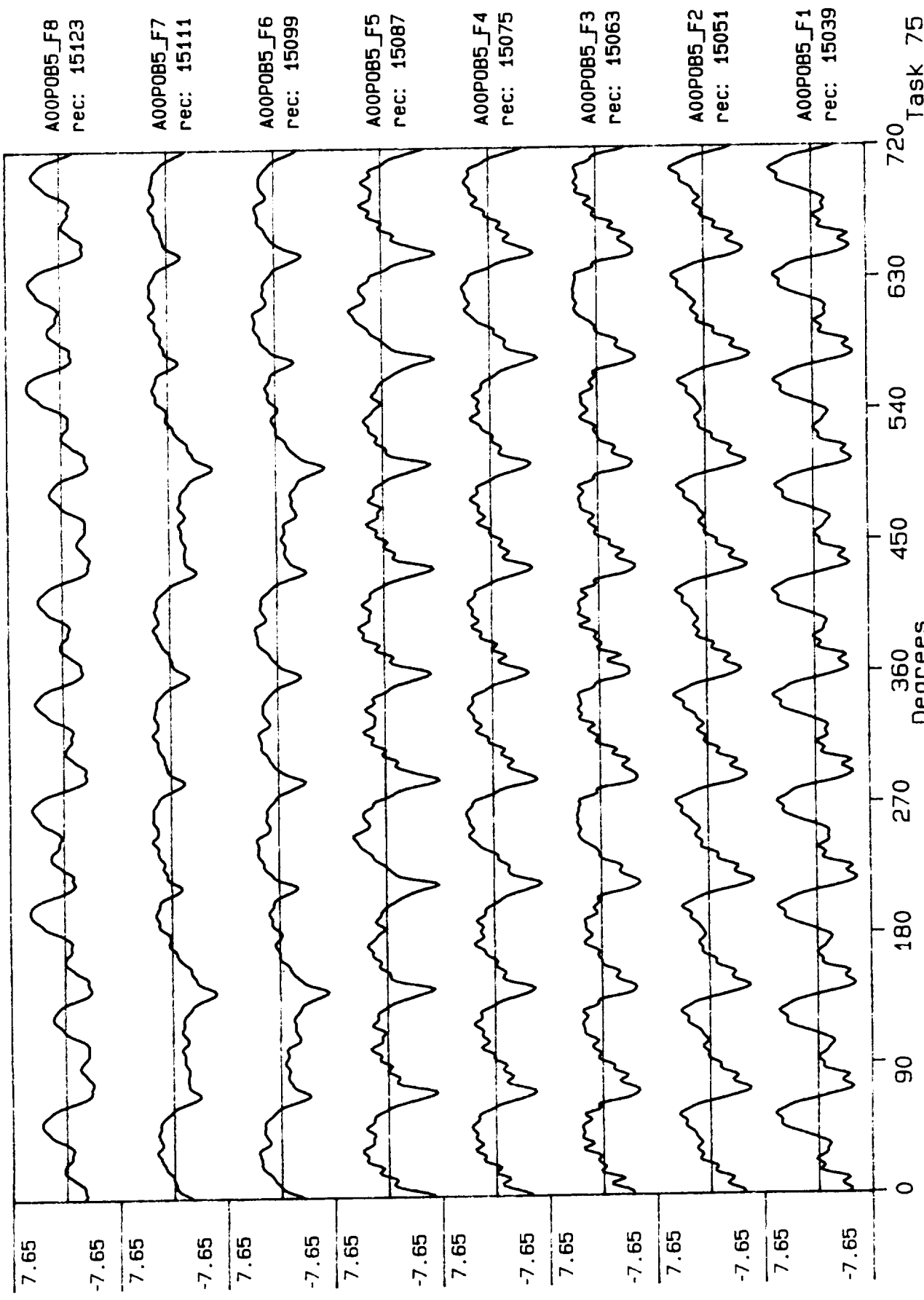
Process included: Calibration, Phase correction and DC filtering. Published: 06,07,89



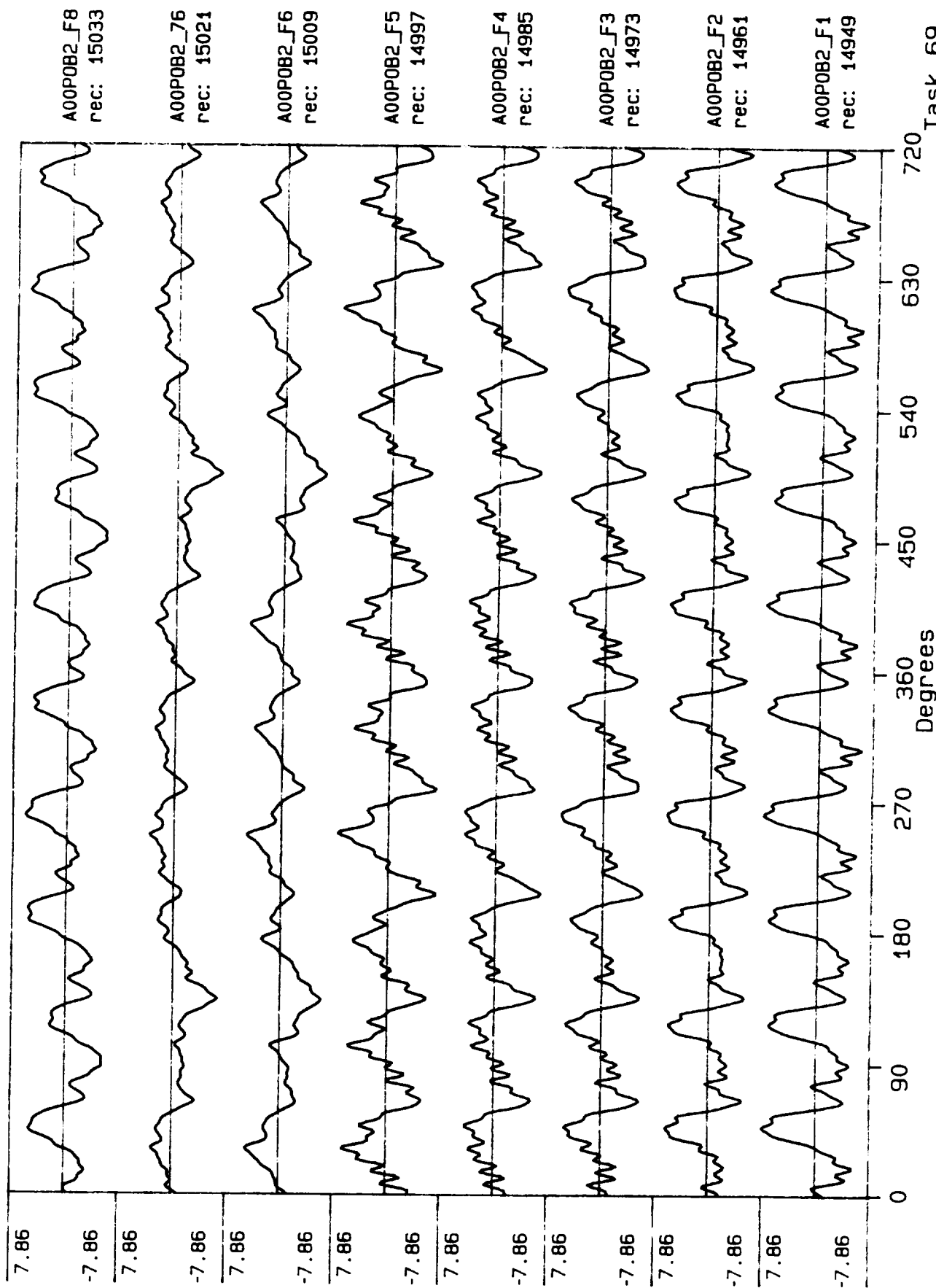
process included: Calibration, Phase correction and DC filtering. Published: 06/07/89

Task 78

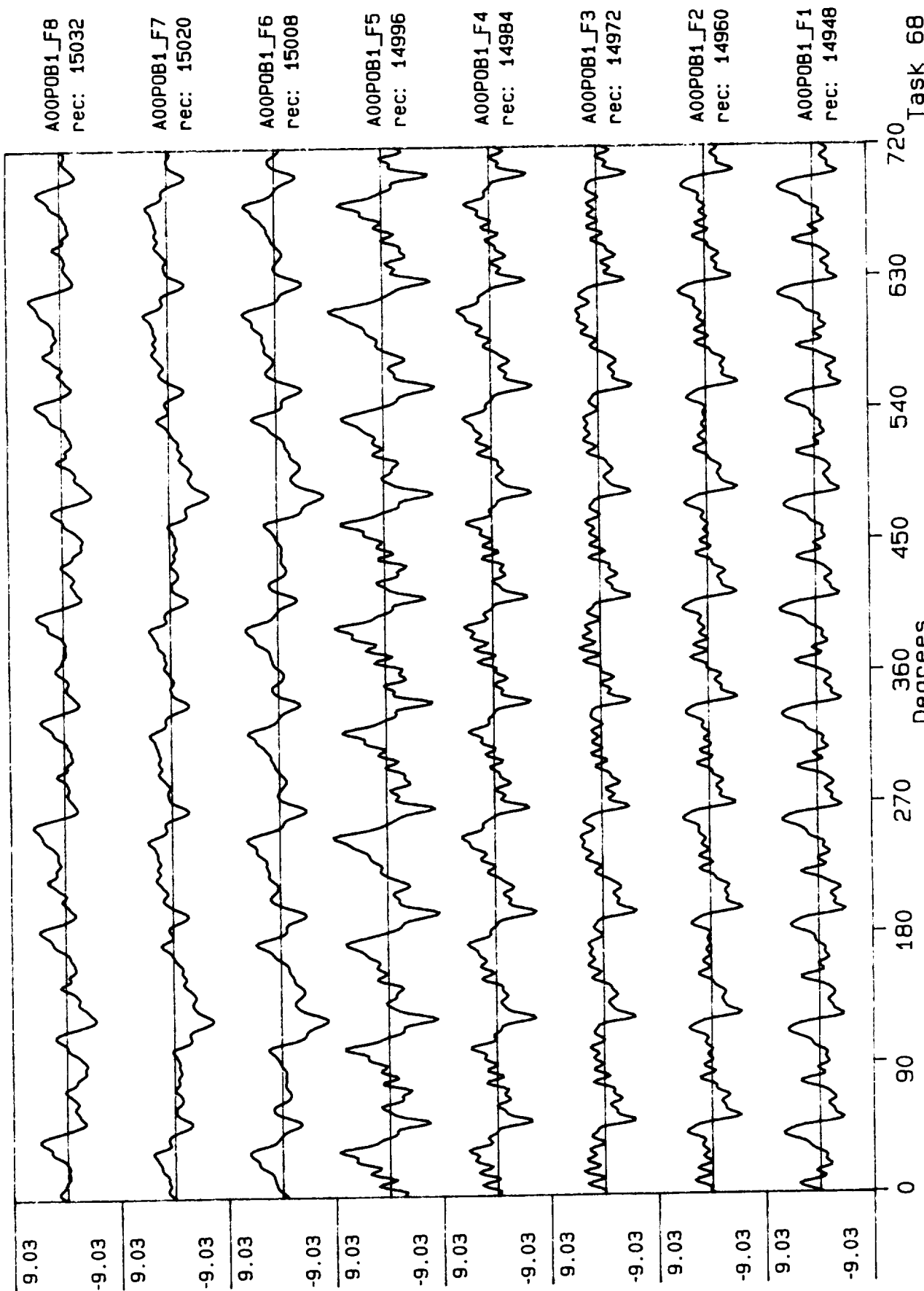




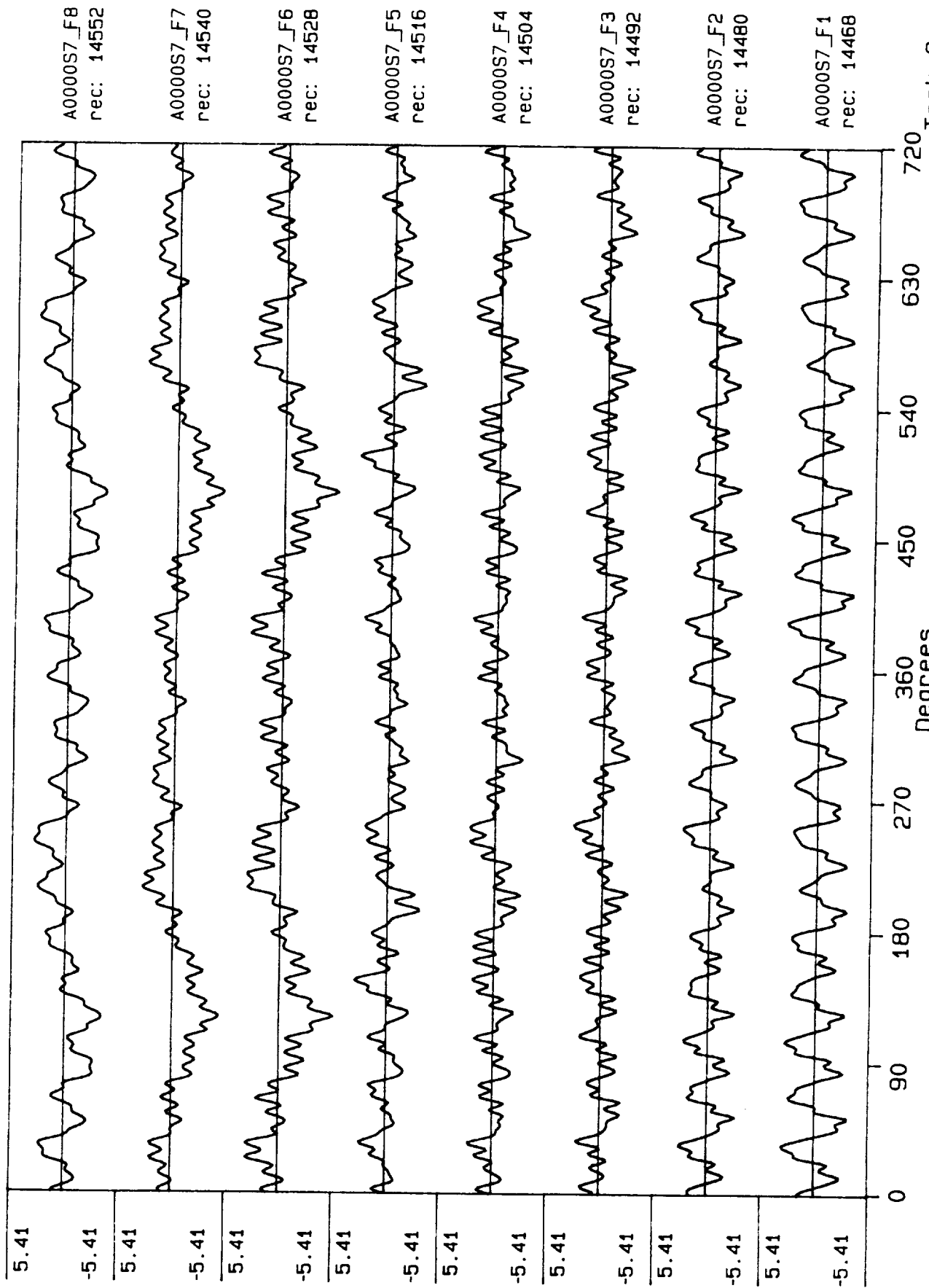
Process included: Calibration, Phase correction and DC filtering. Published: 06,07,89



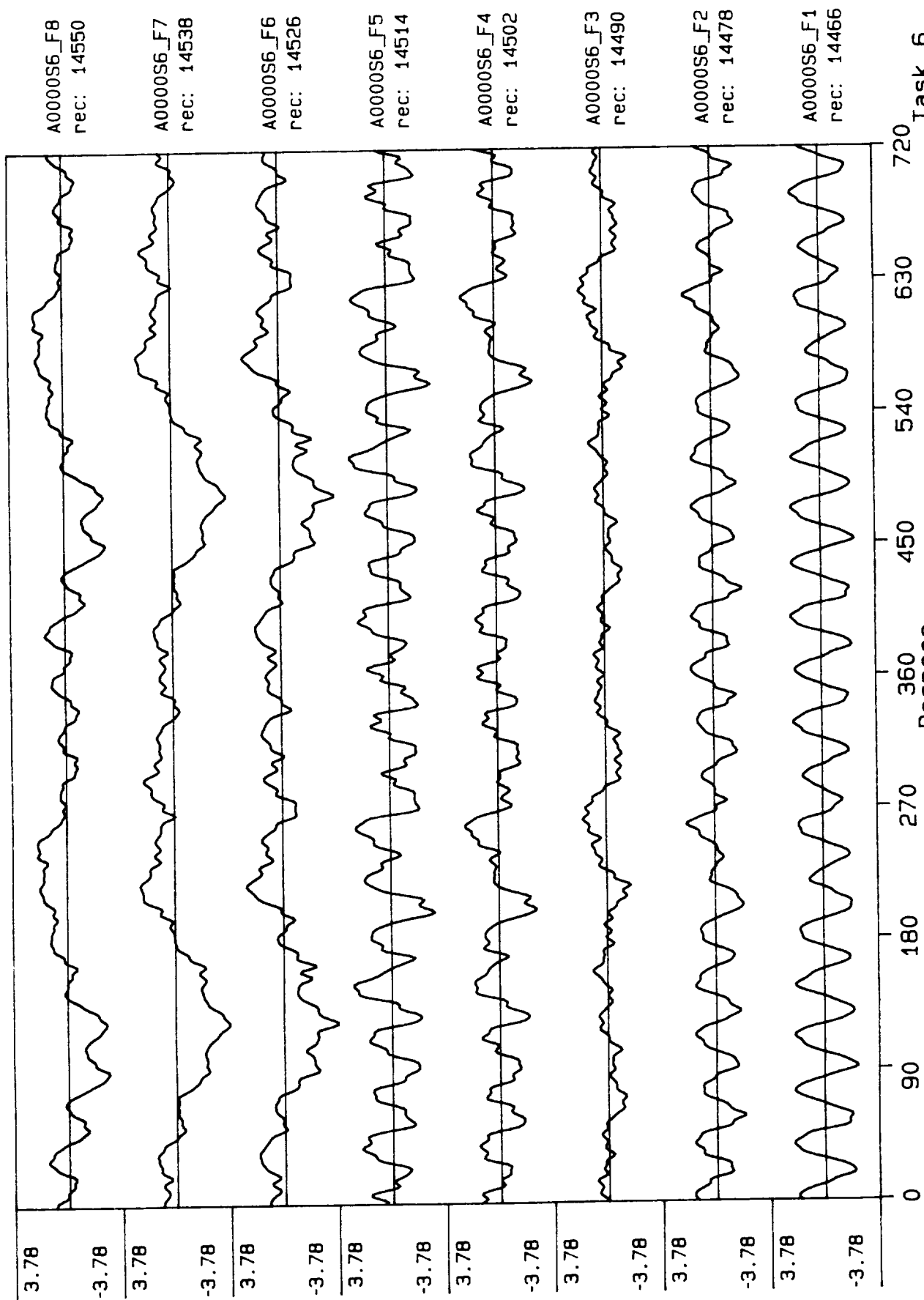
Process included: Calibration, Phase correction and DC filtering. Published: 06,07,89



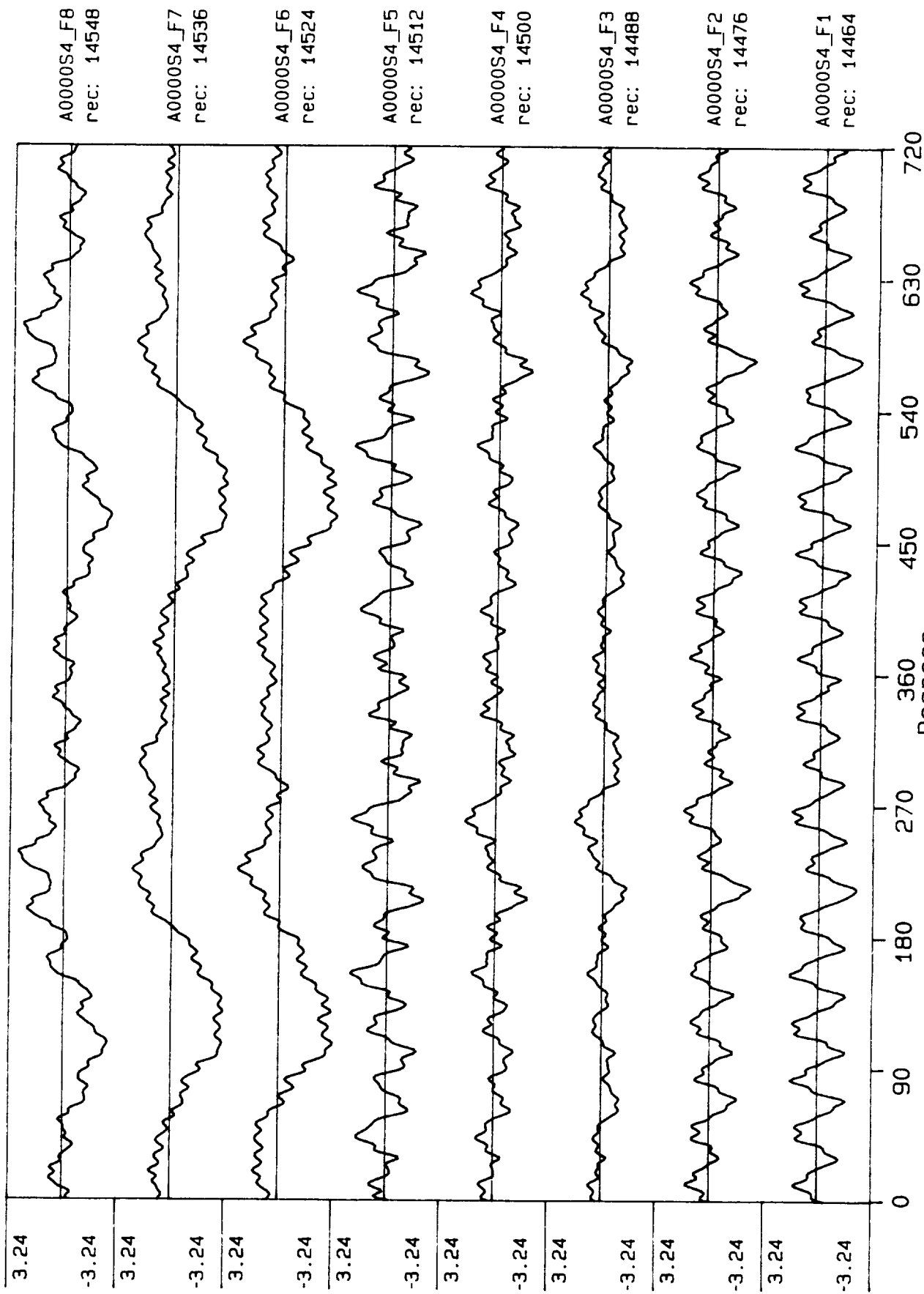
Process included: Calibration, Phase correction and DC filtering. Published: 06.07.89

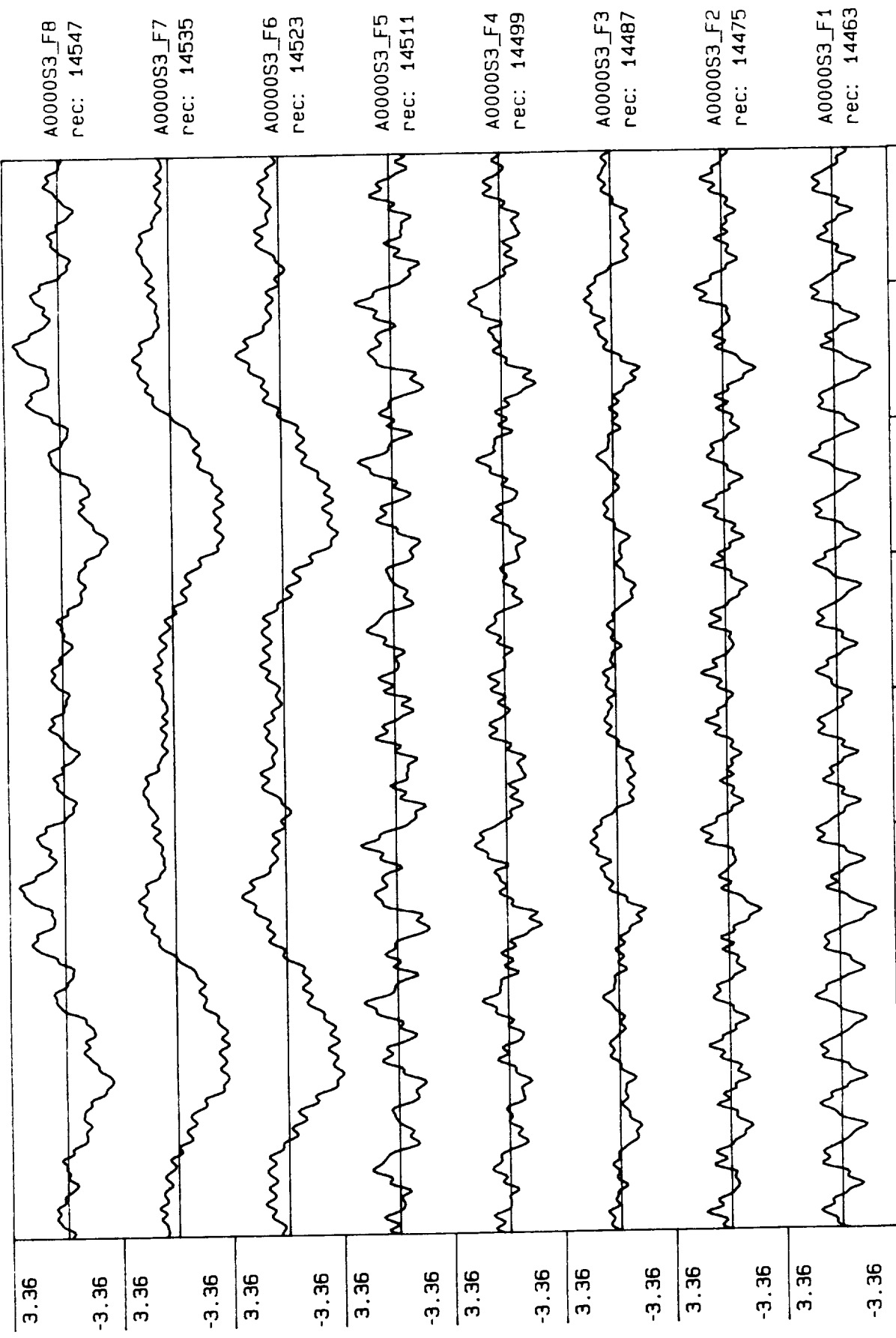


Process included: Calibration, Phase correction and DC filtering. Published: 06/07/89



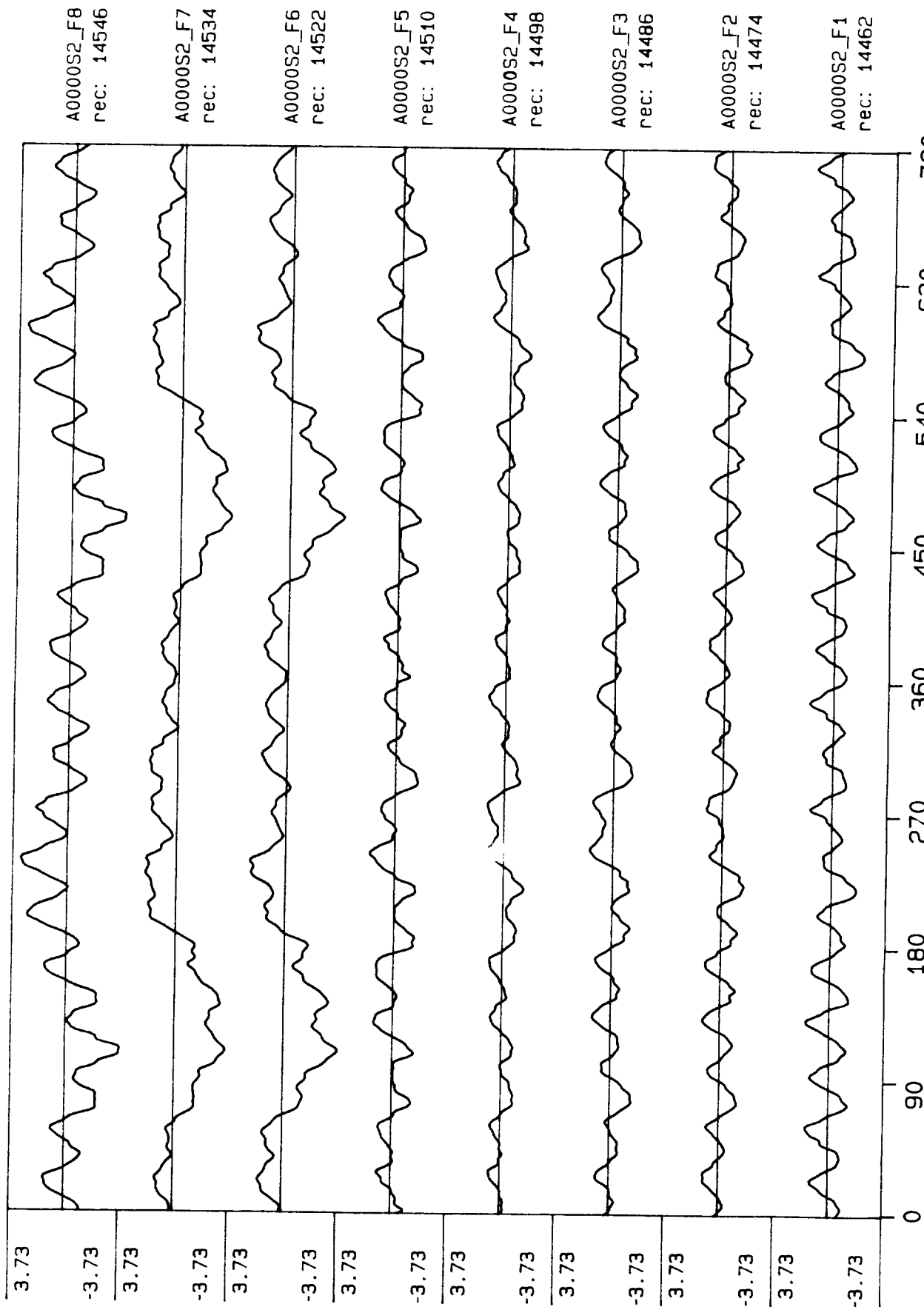
Process included: Calibration, Phase correction and DC filtering. Published: 06/07/89



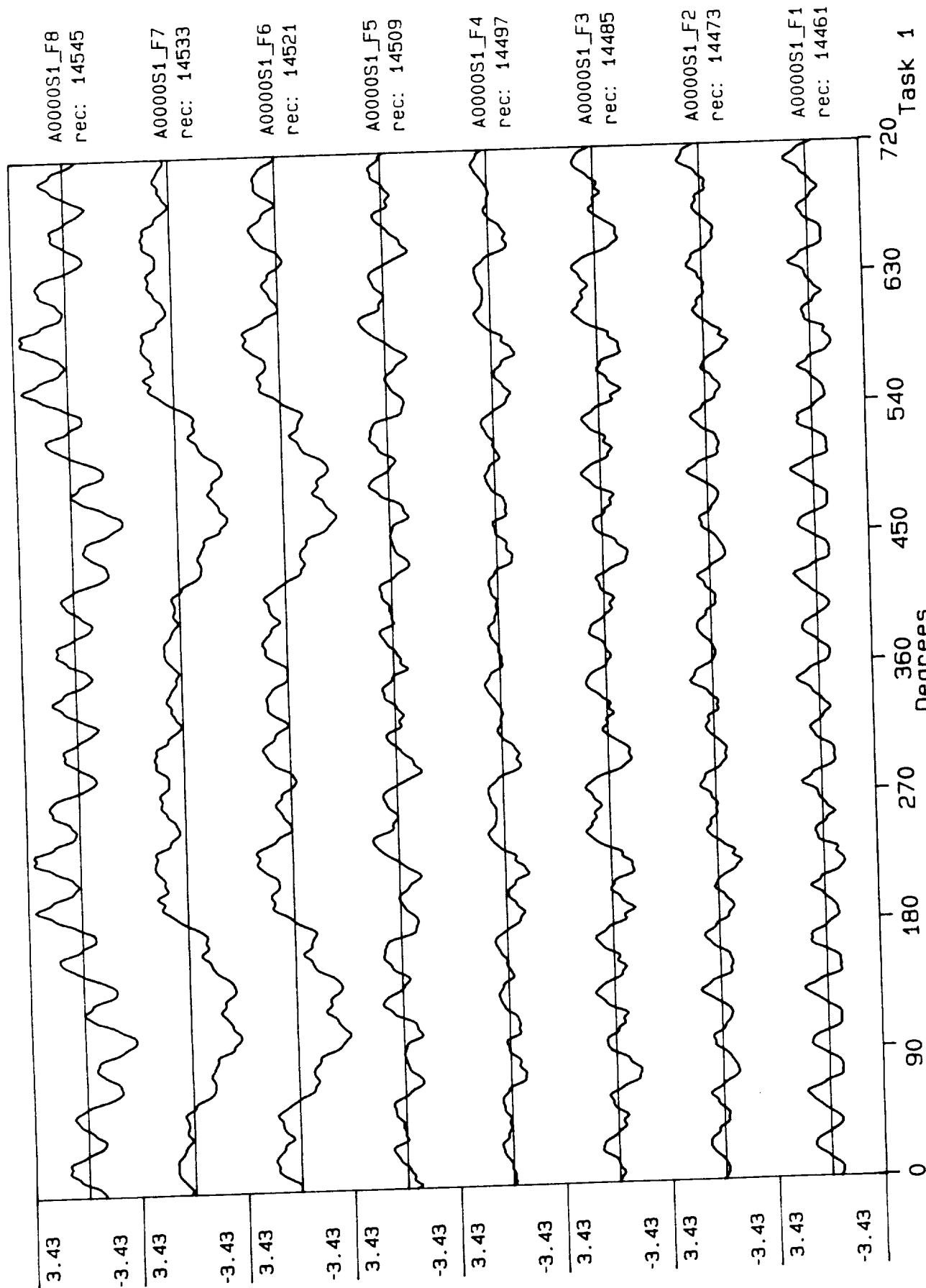


Task 3

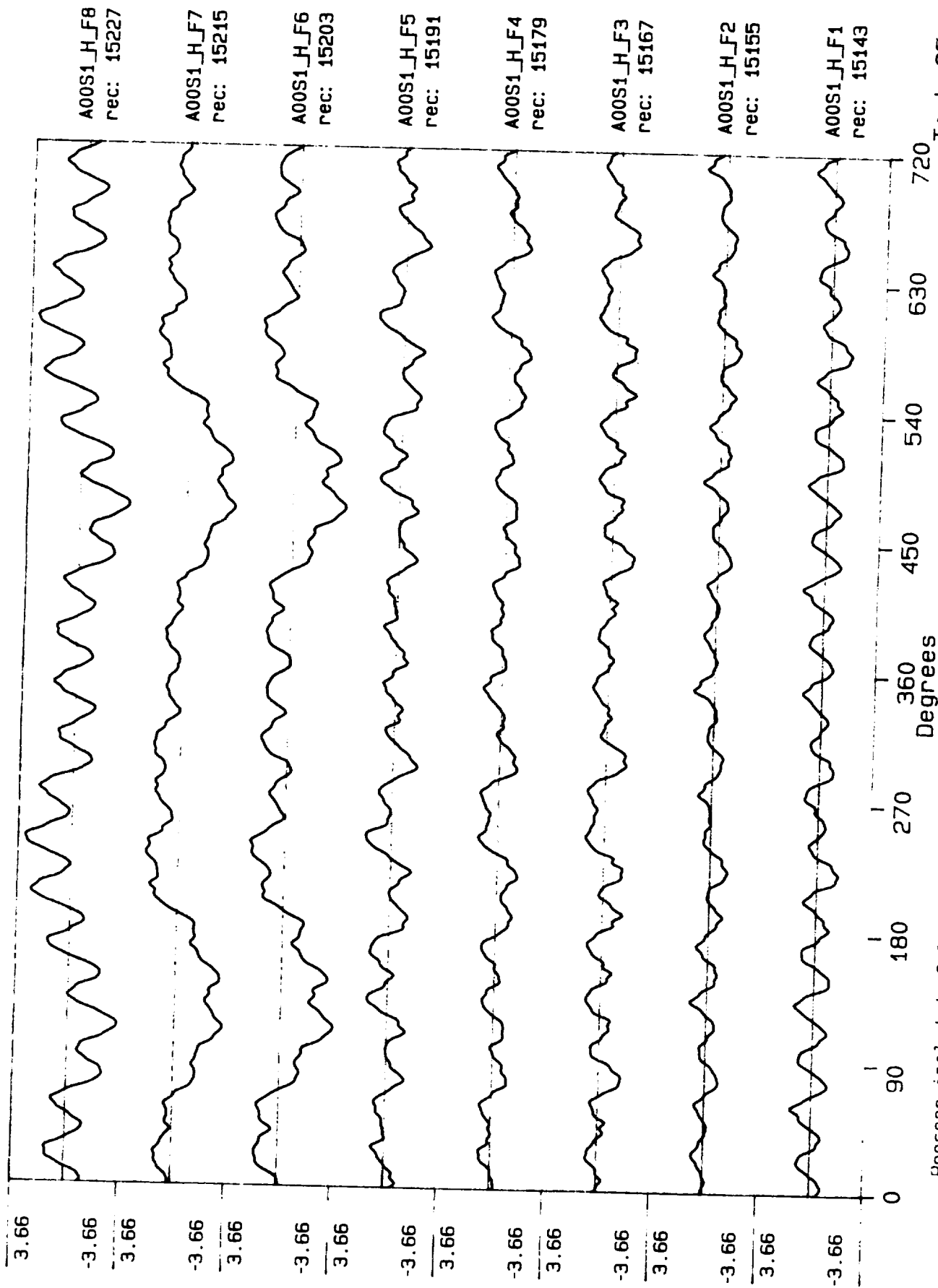
Process included: Calibration, Phase correction and DC filtering. Published: 06/07/89

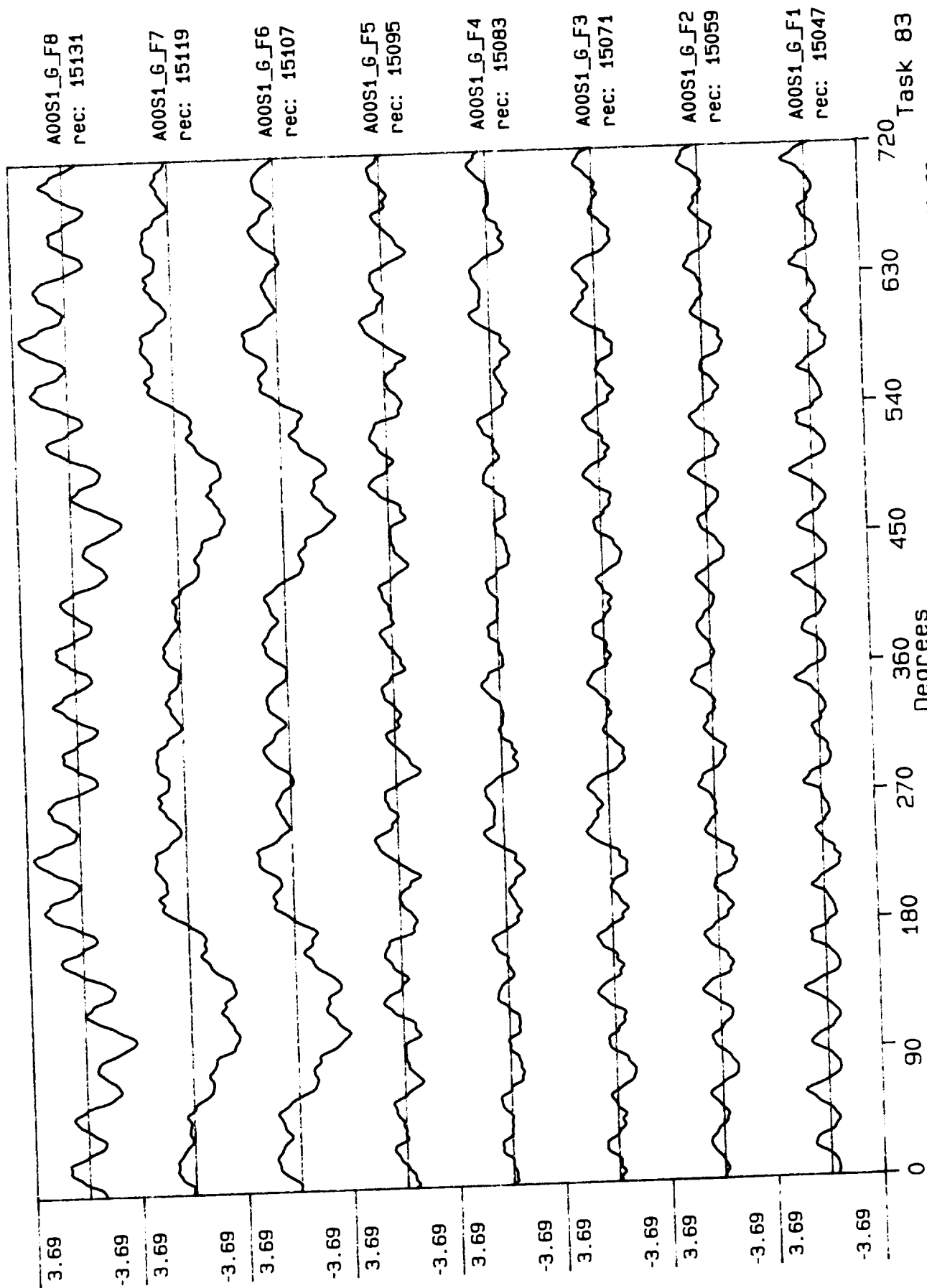


Process included: Calibration, Phase correction and DC filtering. Published: 06/07/89

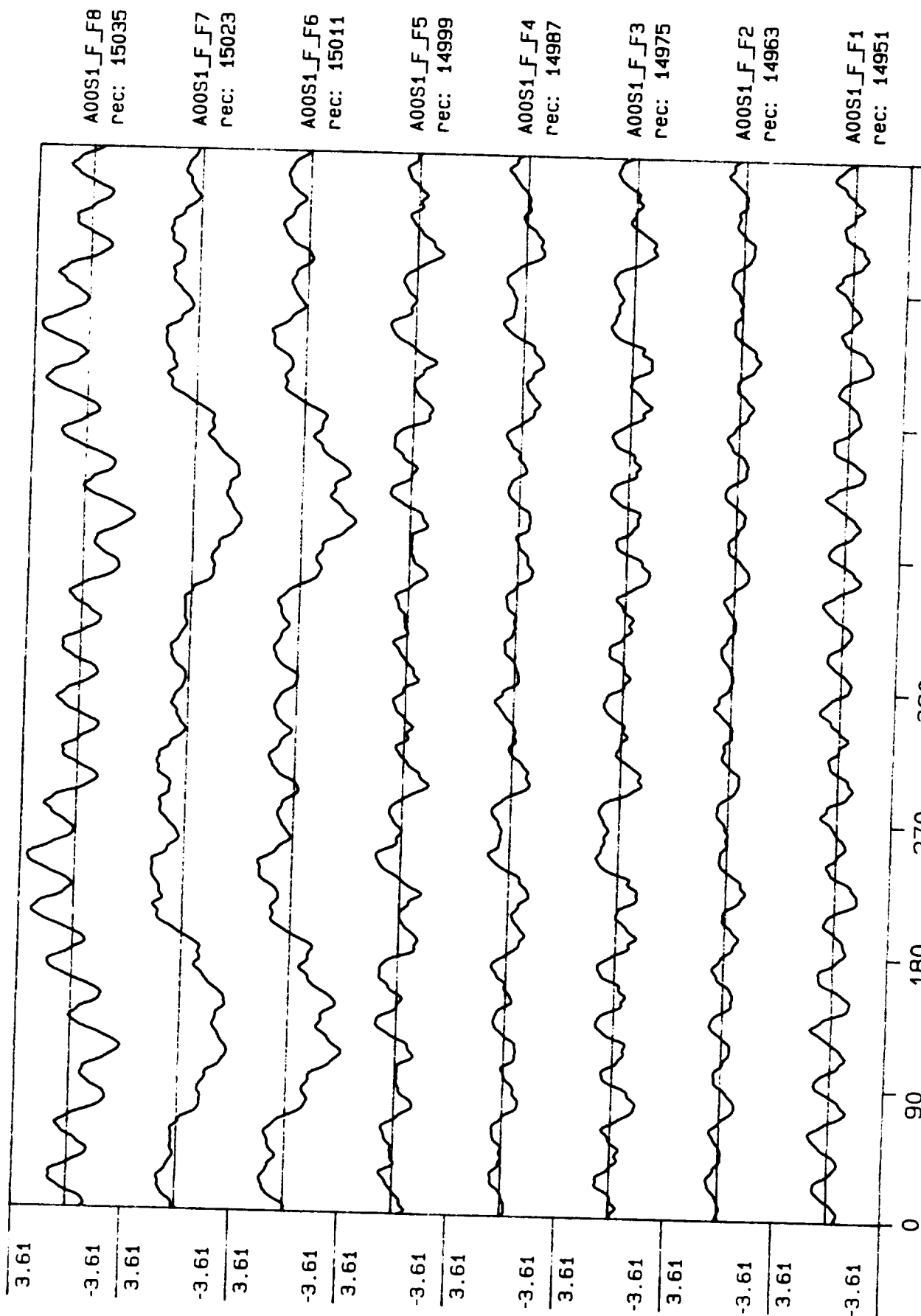


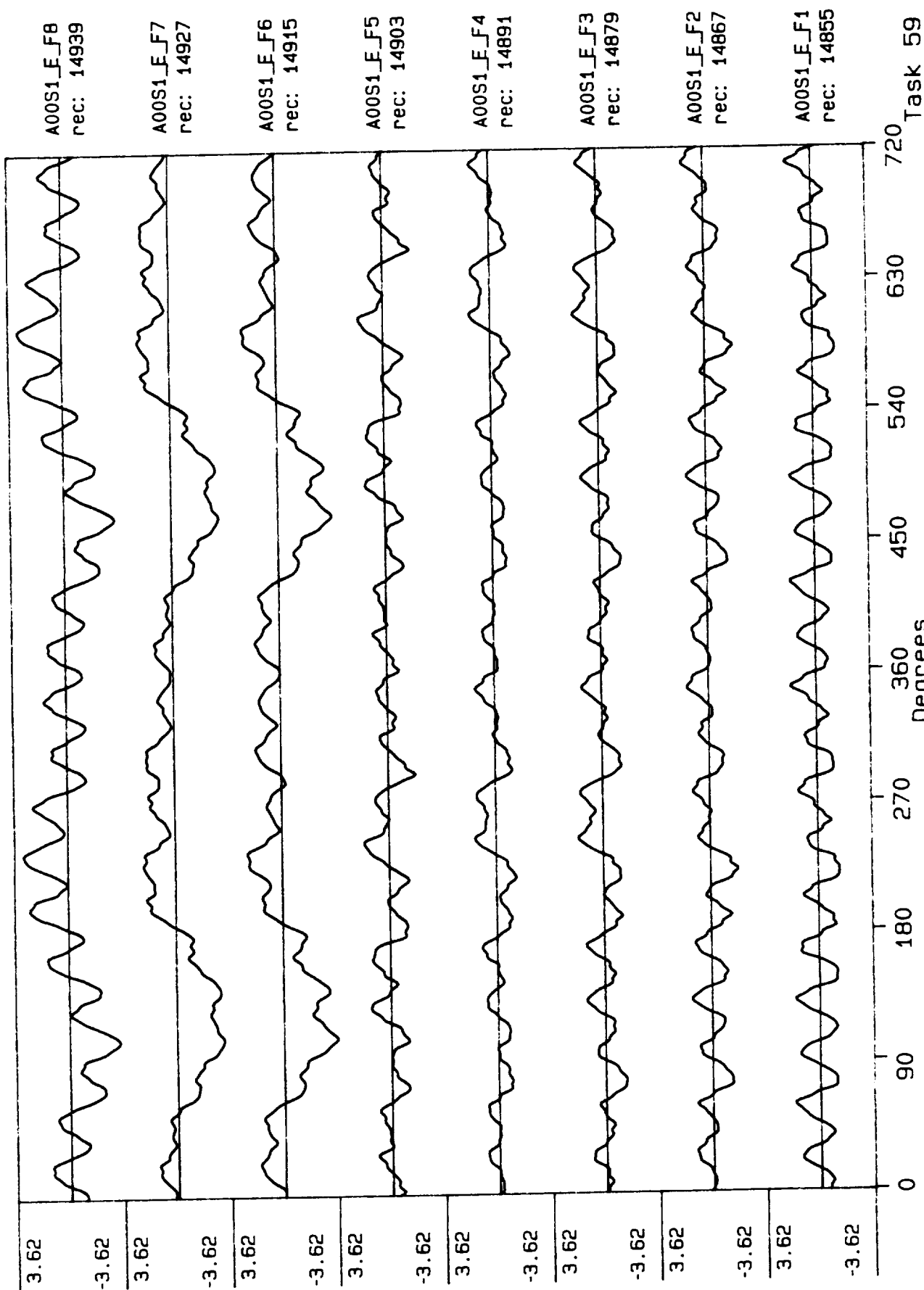
Task 1
Published: 06/07/89
Process included: Calibration, Phase correction and DC filtering.



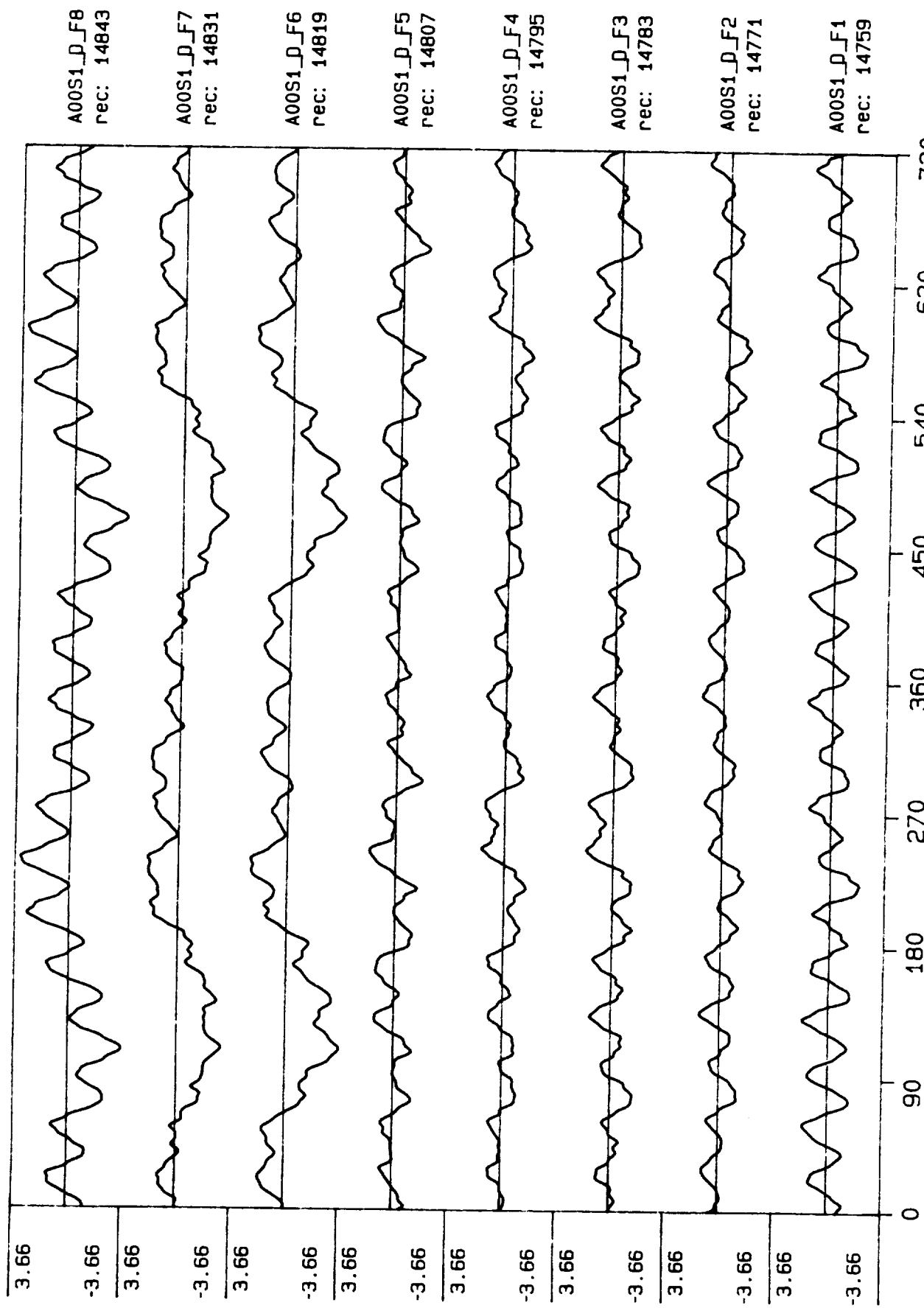


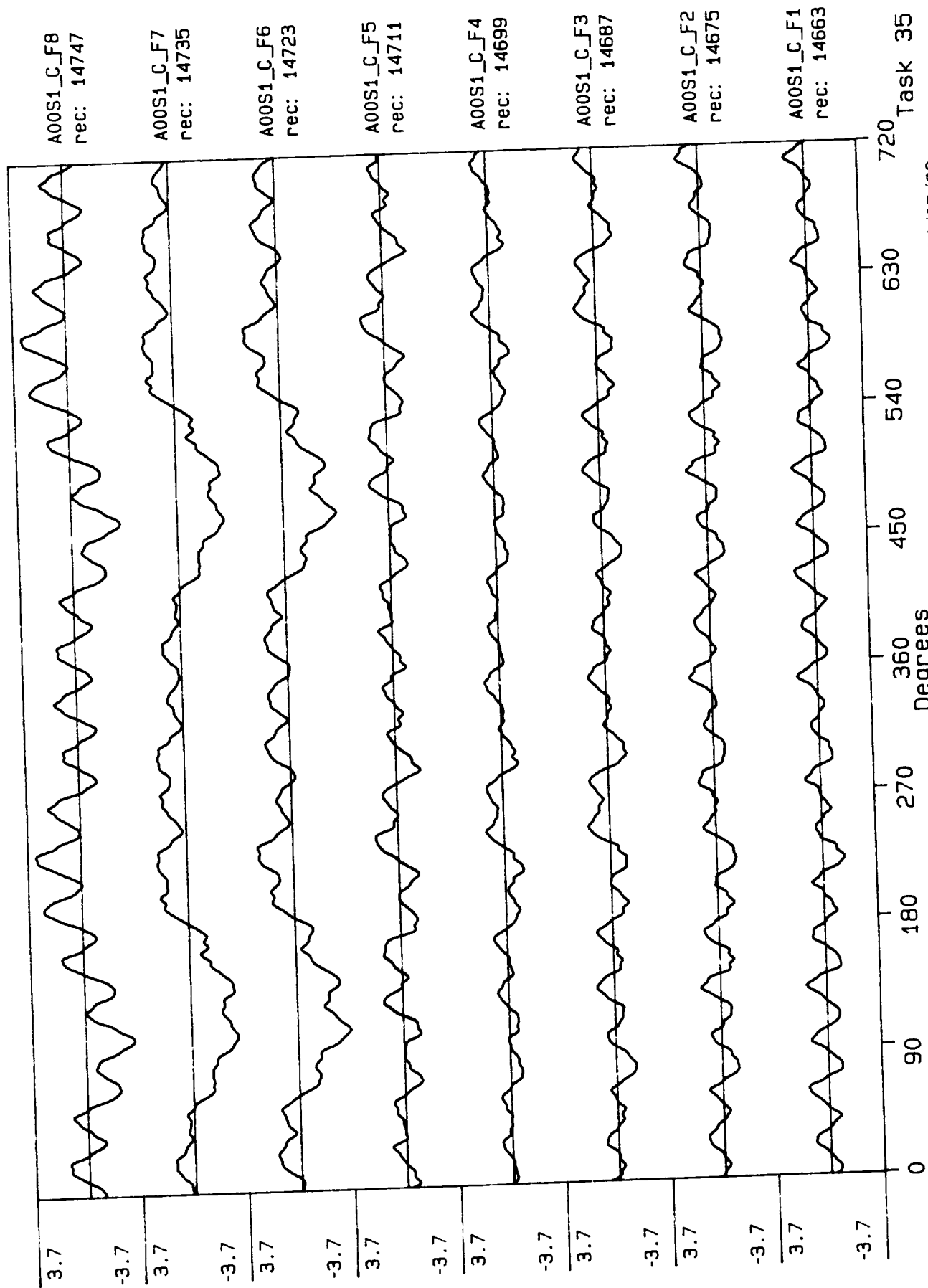
Process included: Calibration, phase correction and DC filtering. Published: 06,07,89



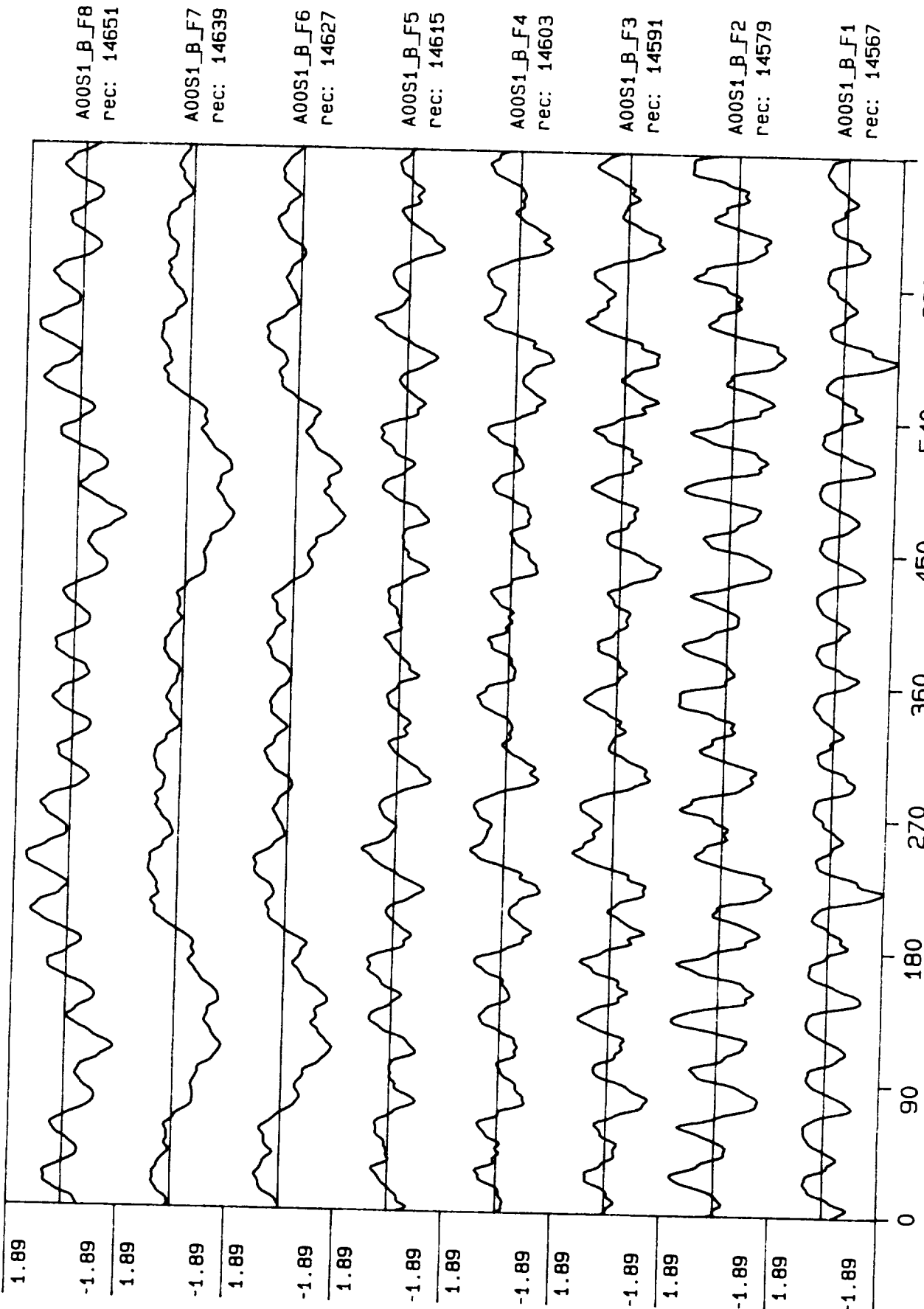


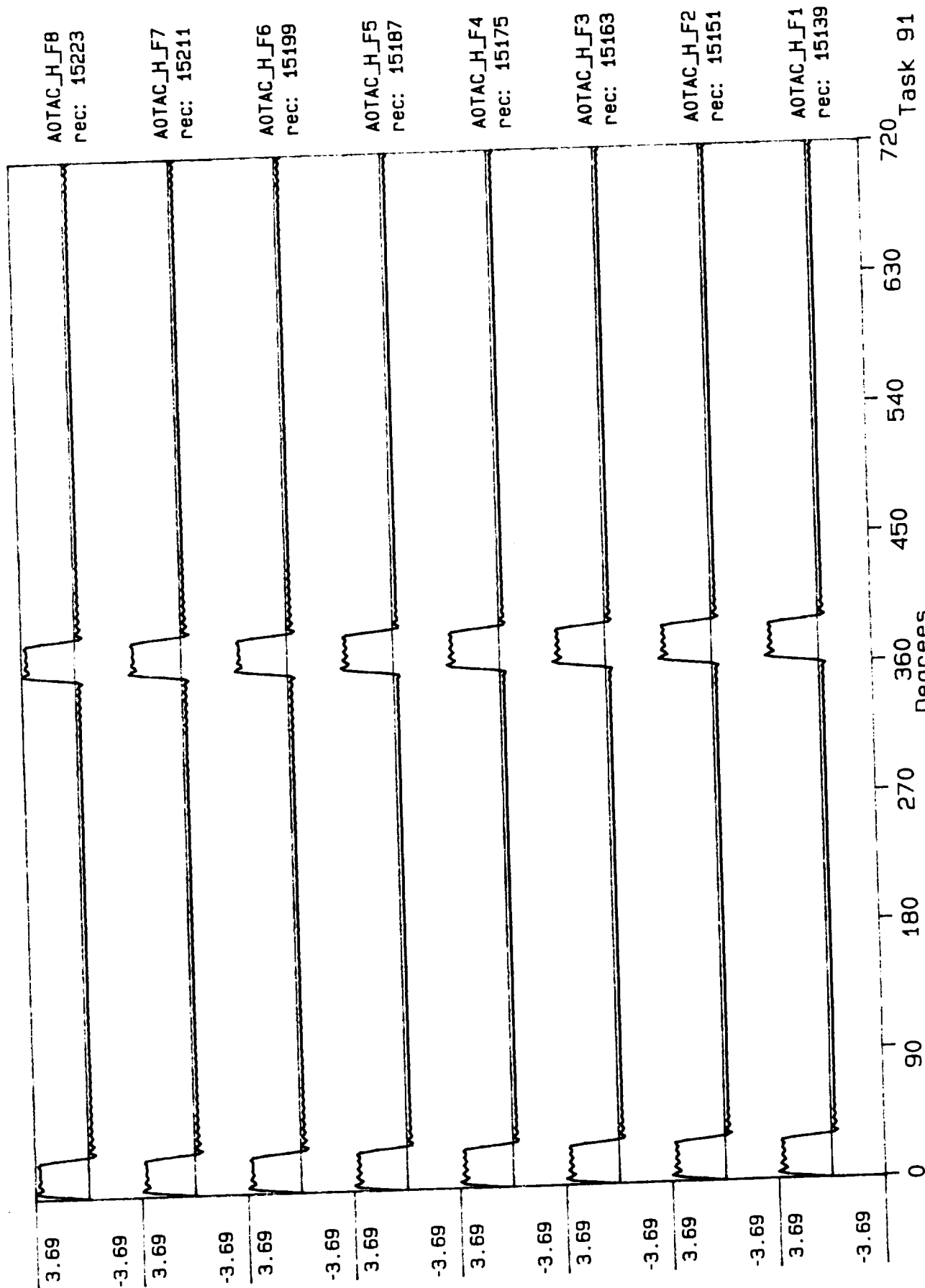
Process included: Calibration, Phase correction and DC filtering. Published: 06,07,89



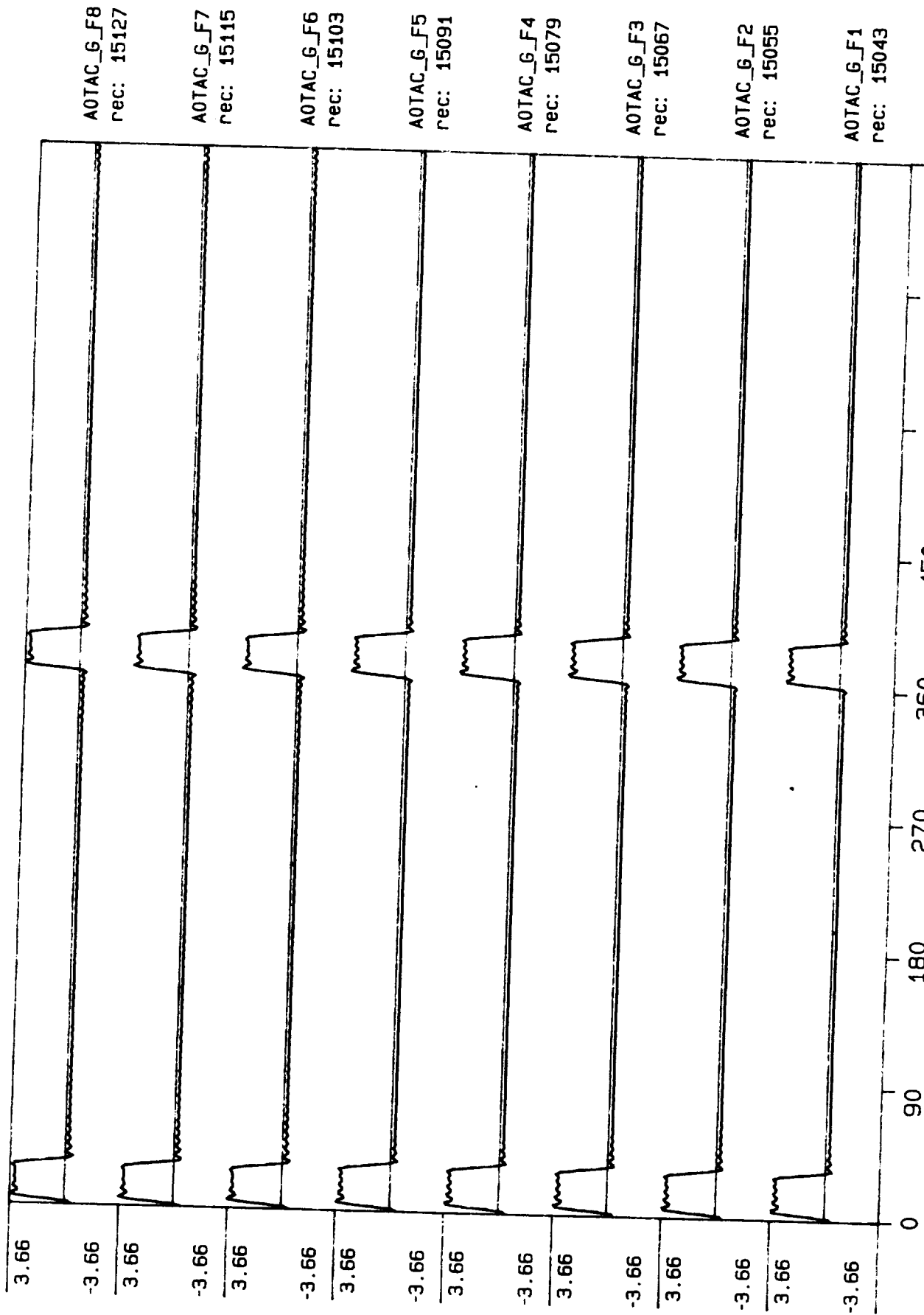


Process included: Calibration, Phase correction and DC filtering. Published: 06/07/89

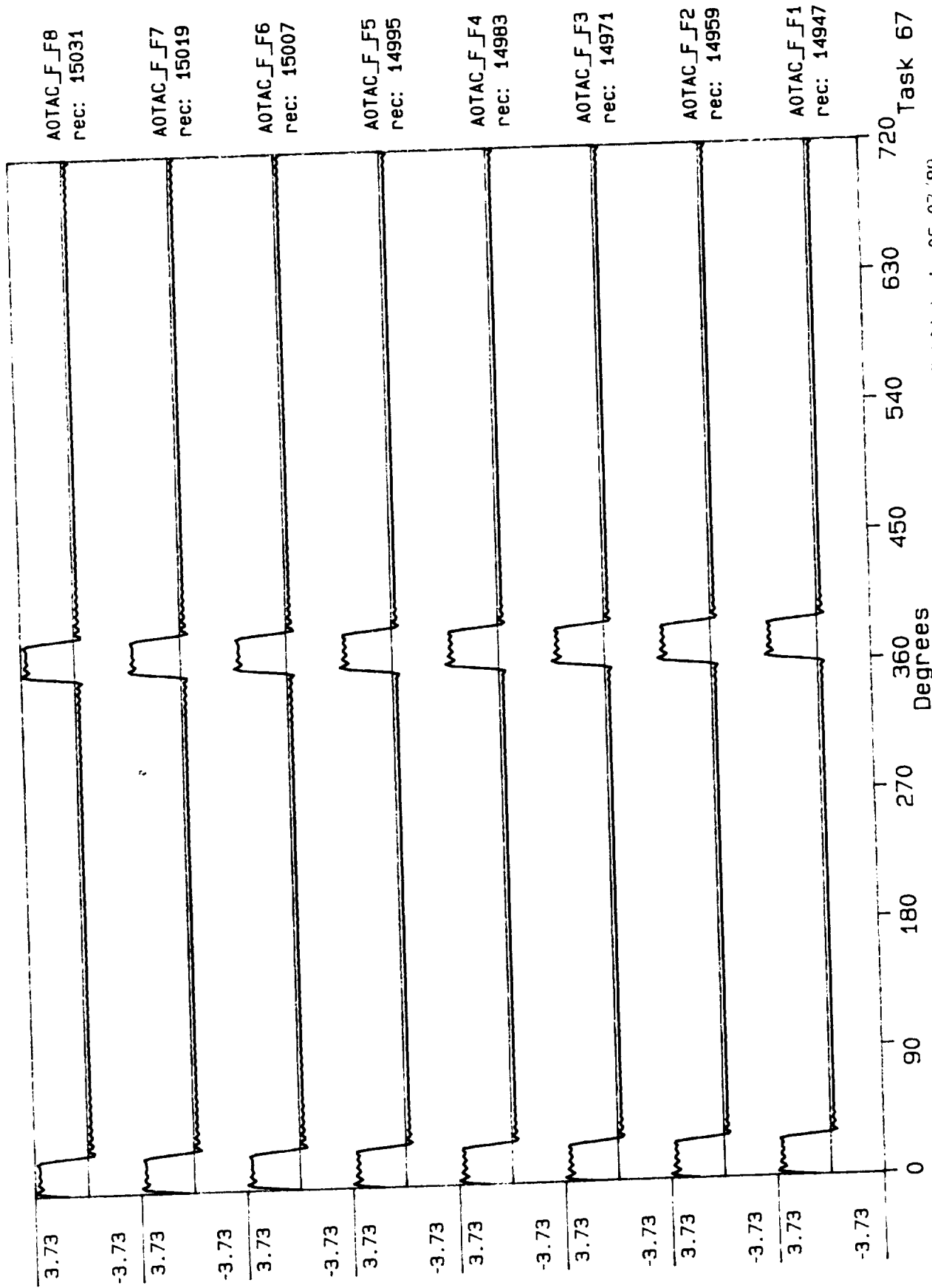




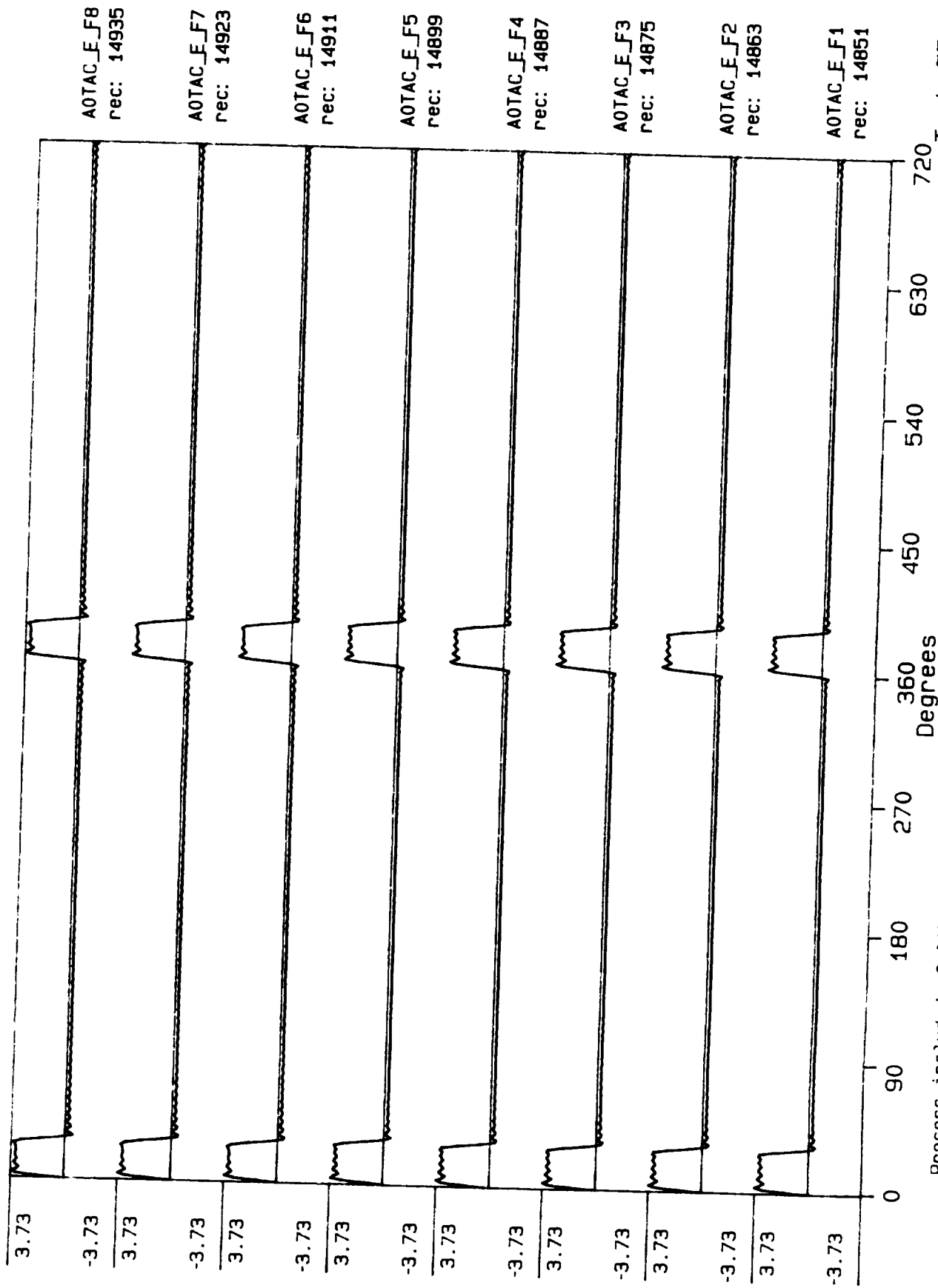
Process included: Calibration, Phase correction and DC filtering. Published: 06,07,89



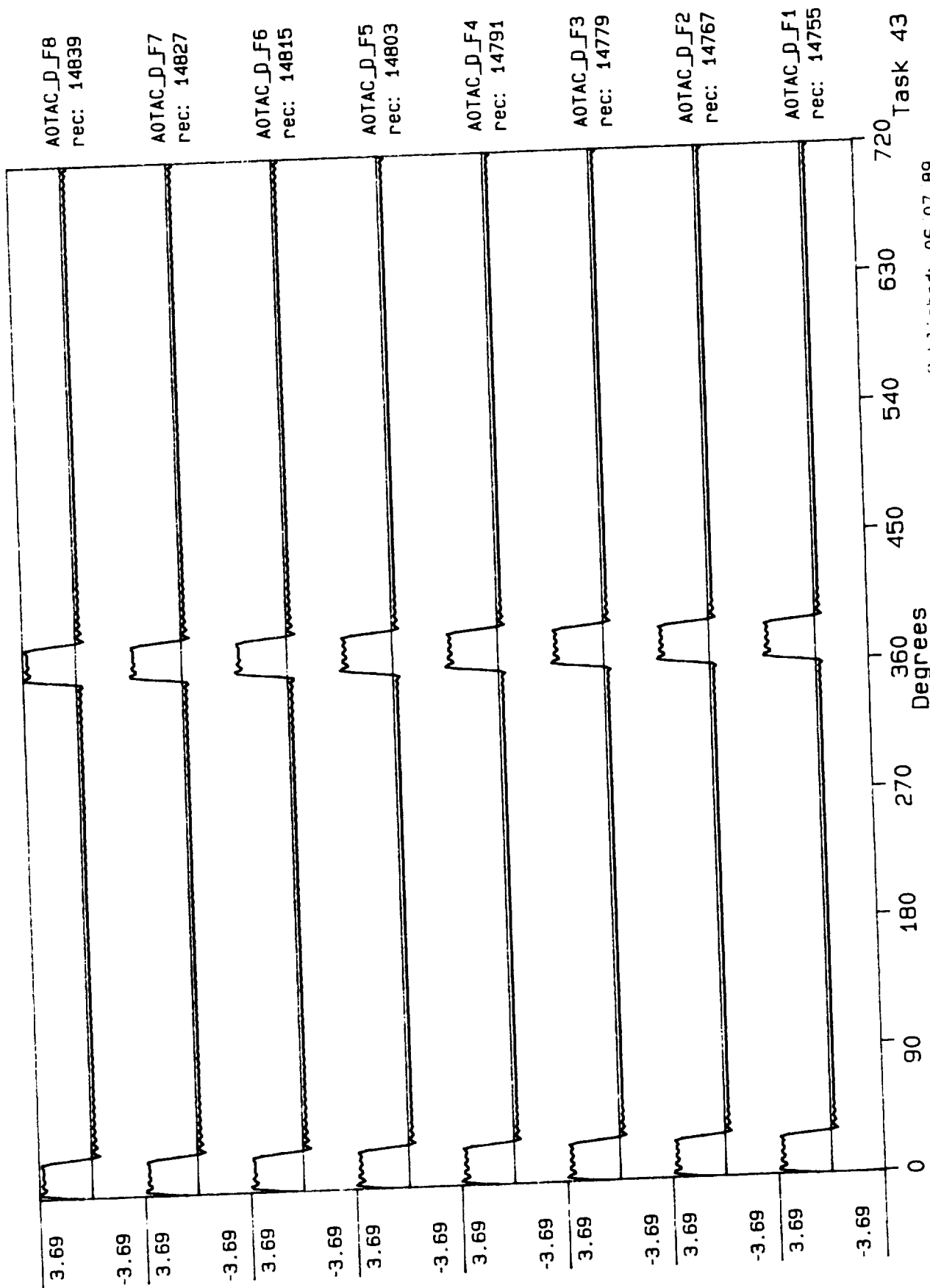
Process included: Calibration, Phase correction and DC filtering. Published: 06,07,89



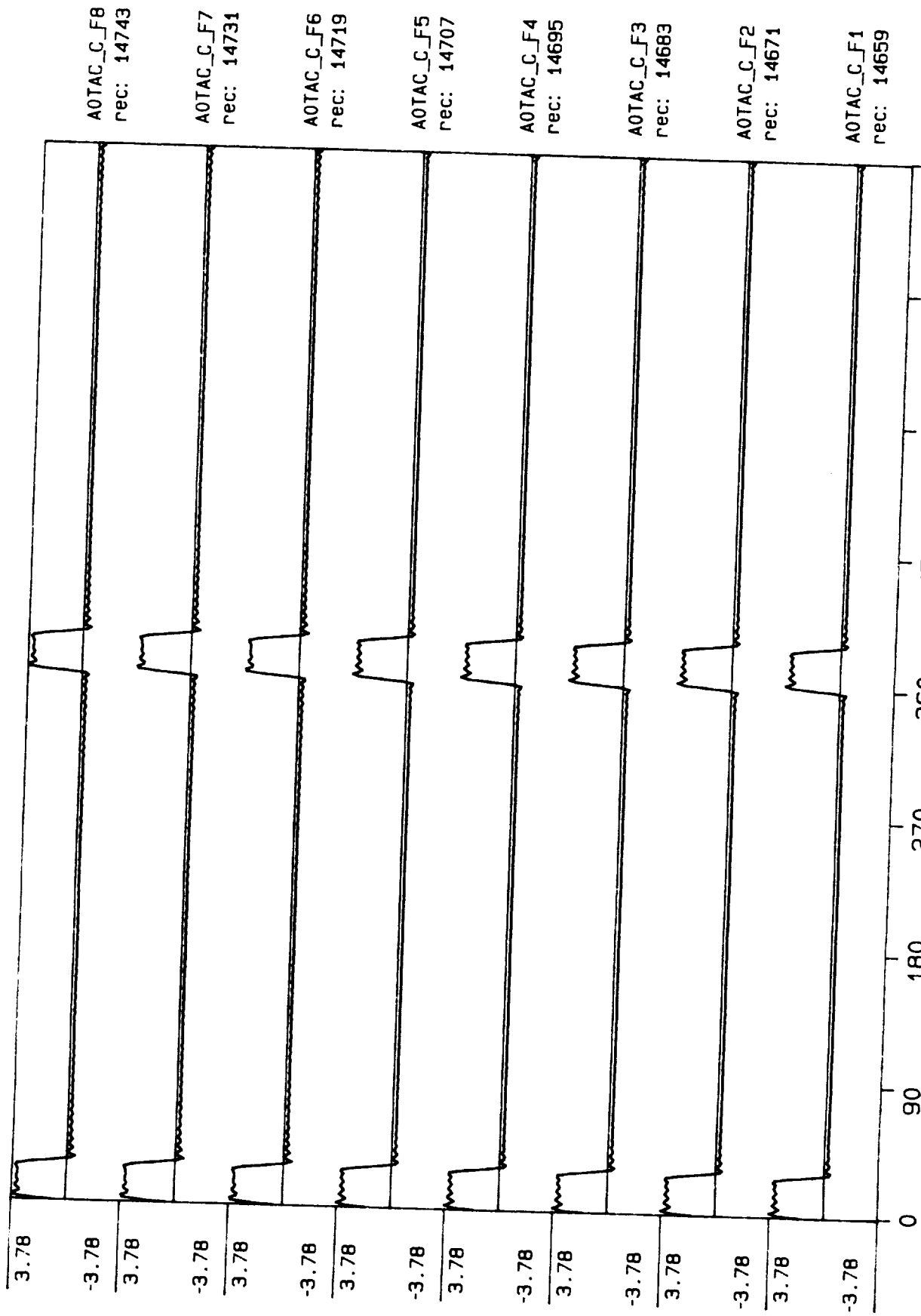
Process included: Calibration, Phase correction and DC filtering. Published: 06, 07, '89

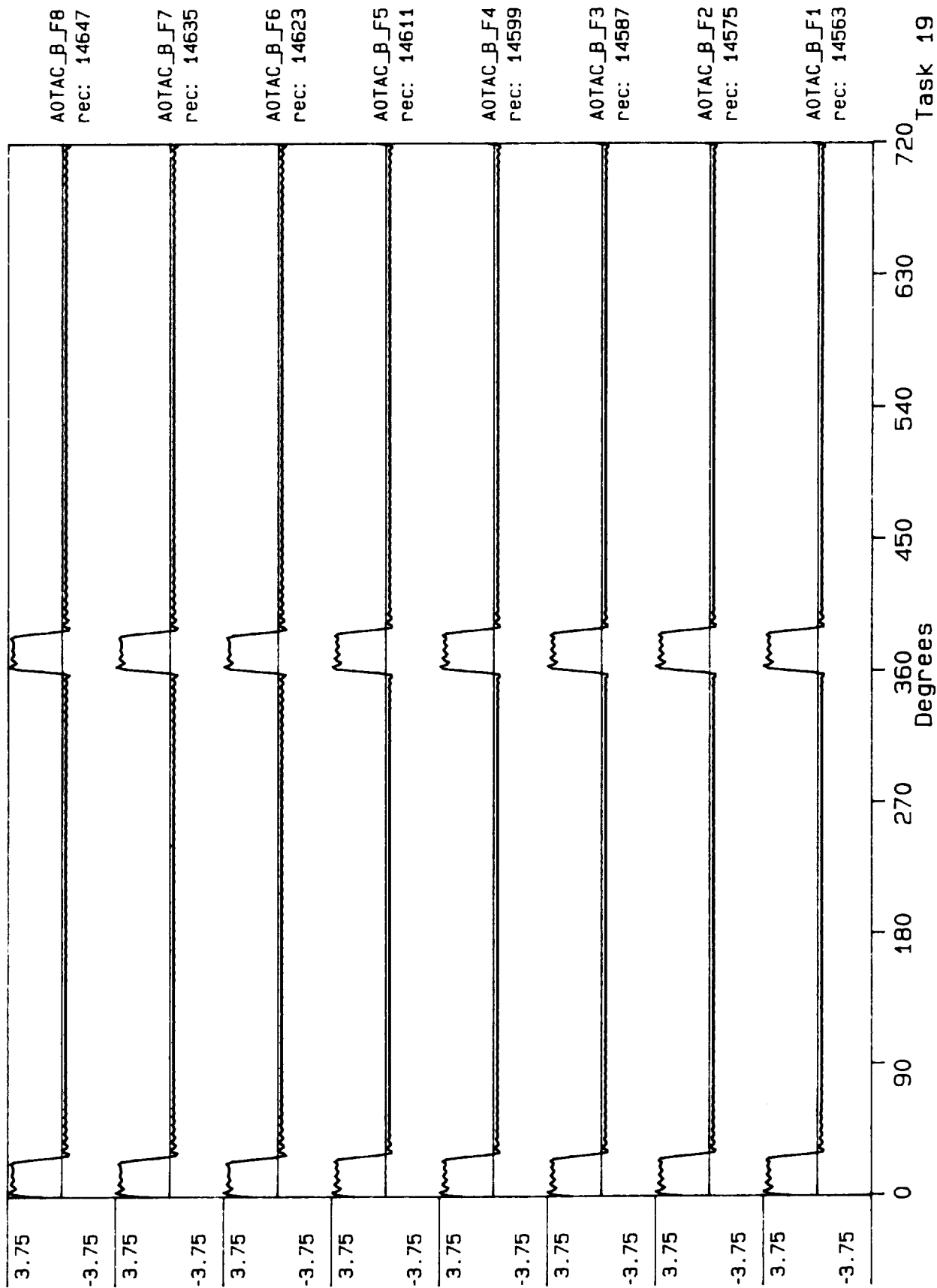


Process included: Calibration, Phase correction and DC filtering. Published: 06,07,89

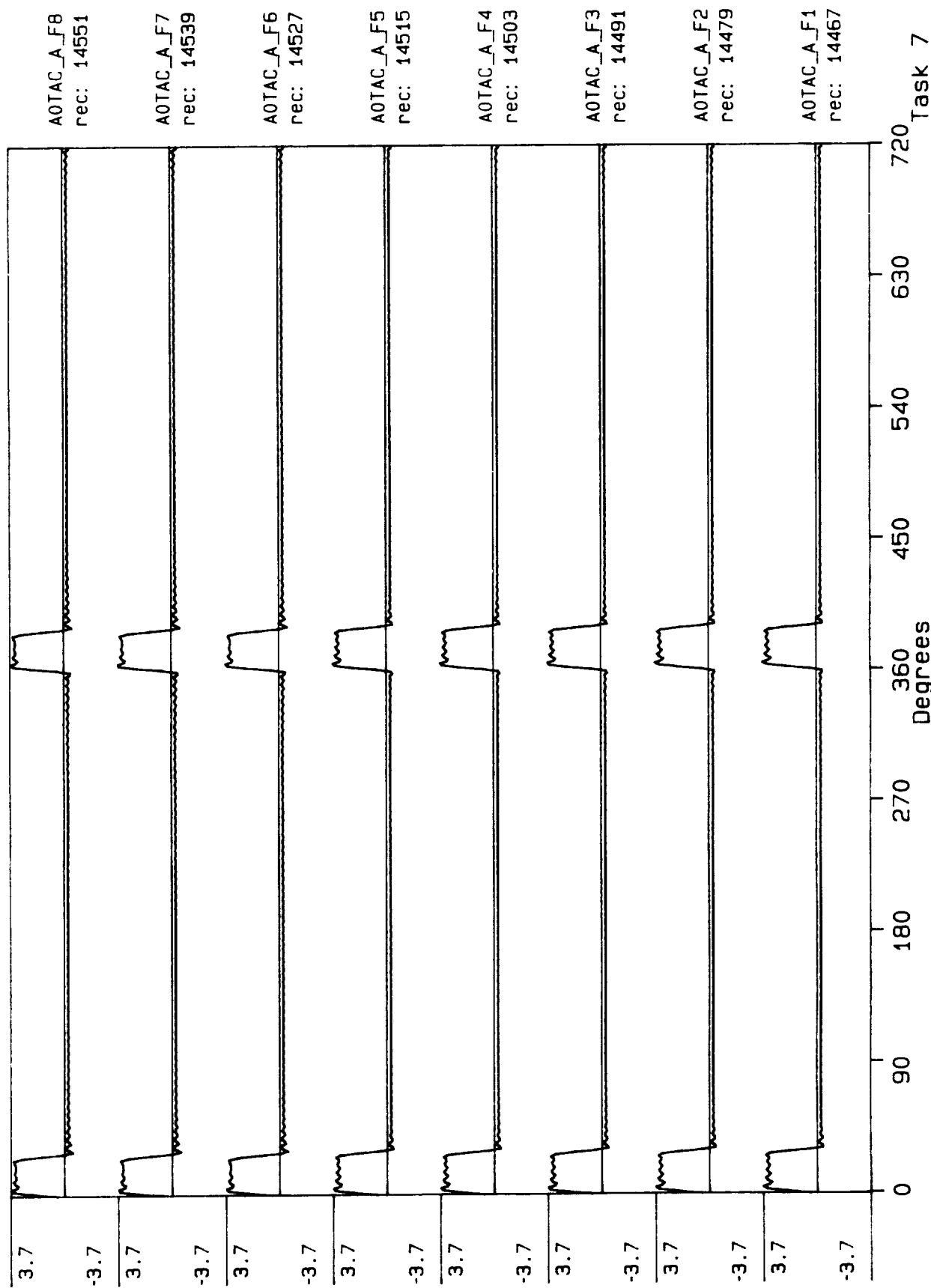


Process included: Calibration, Phase correction and DC filtering. Published: 06,07,89

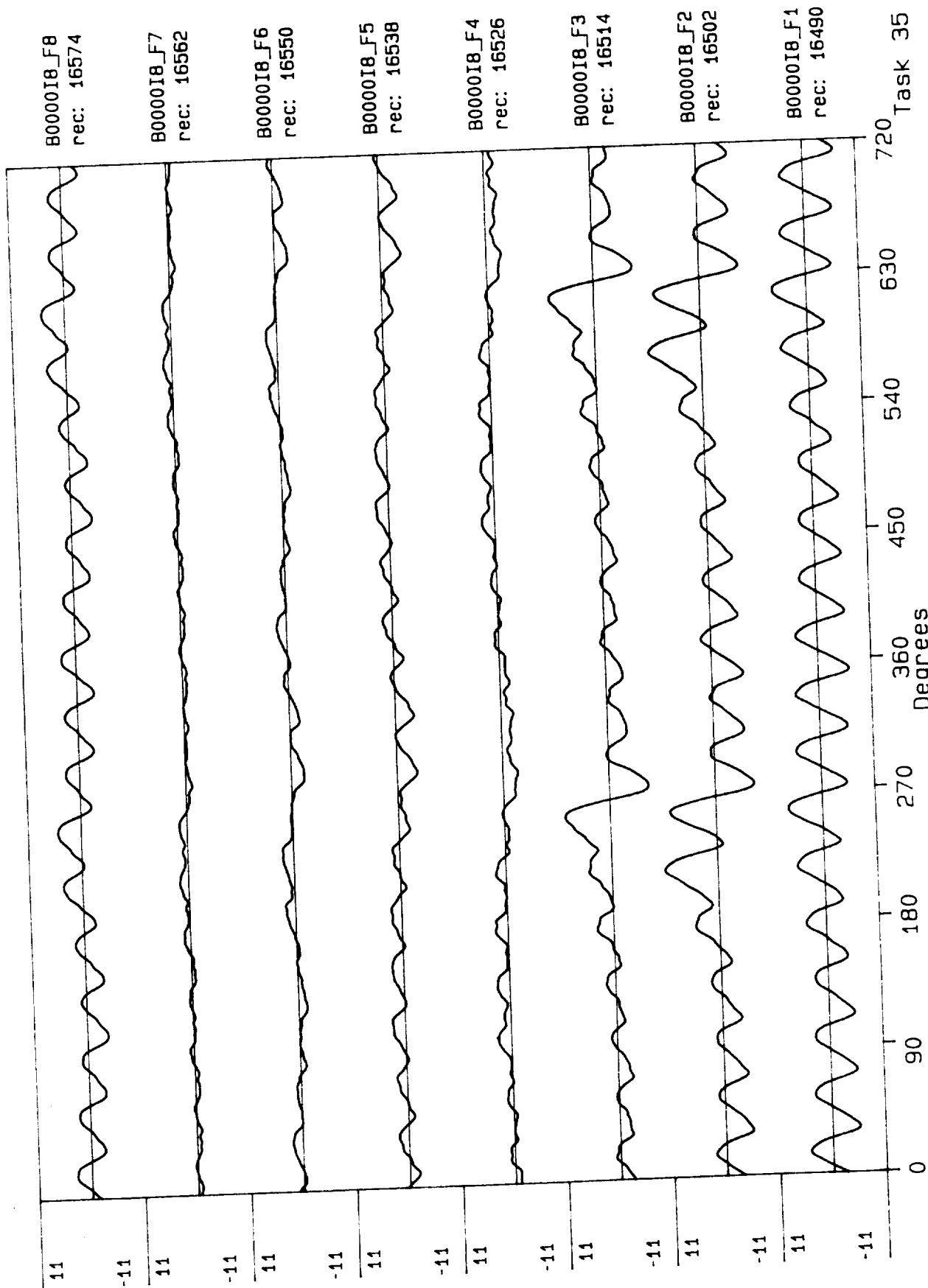




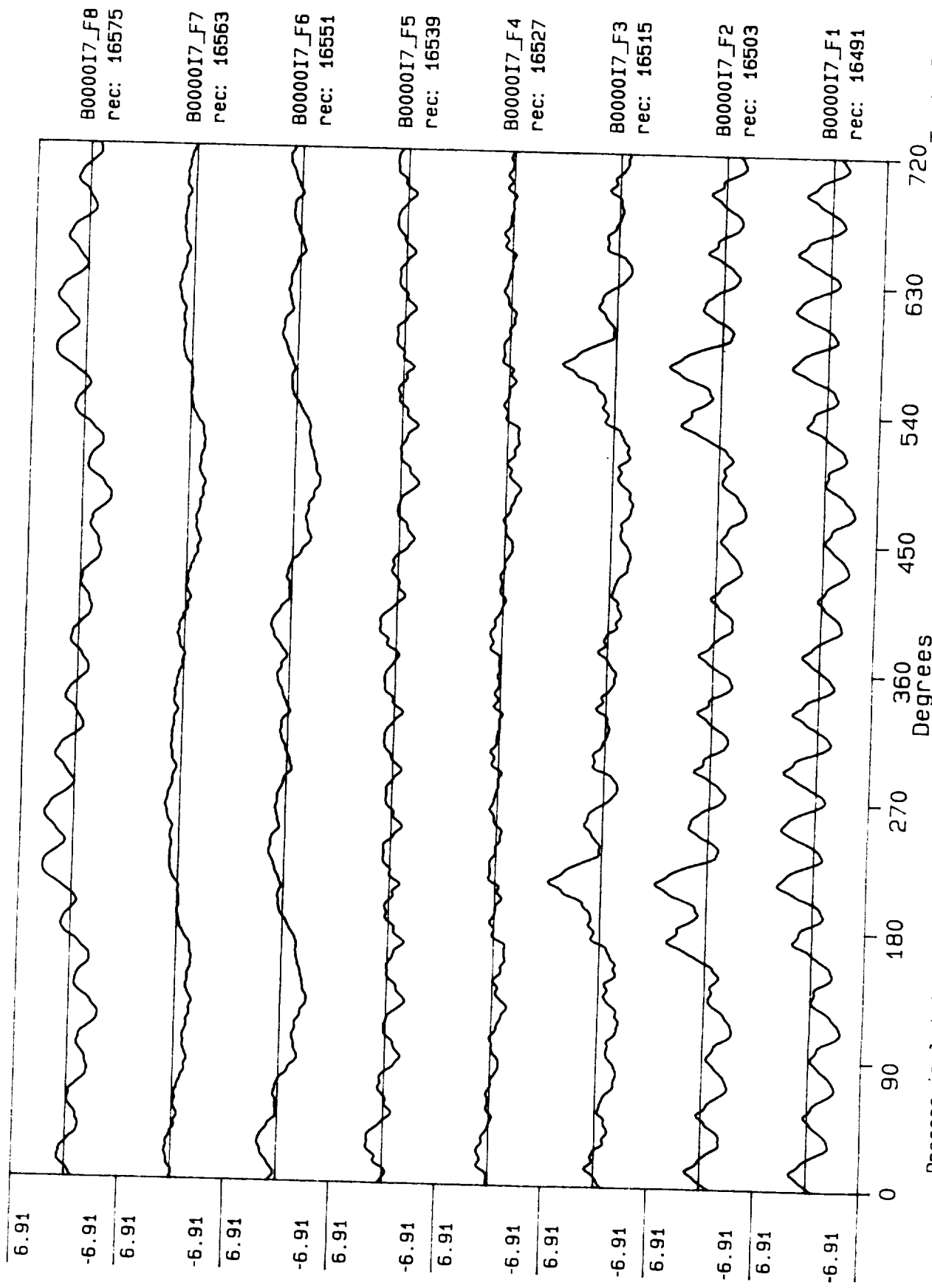
Process included: Calibration, Phase correction and DC filtering. Published: 06/07/89



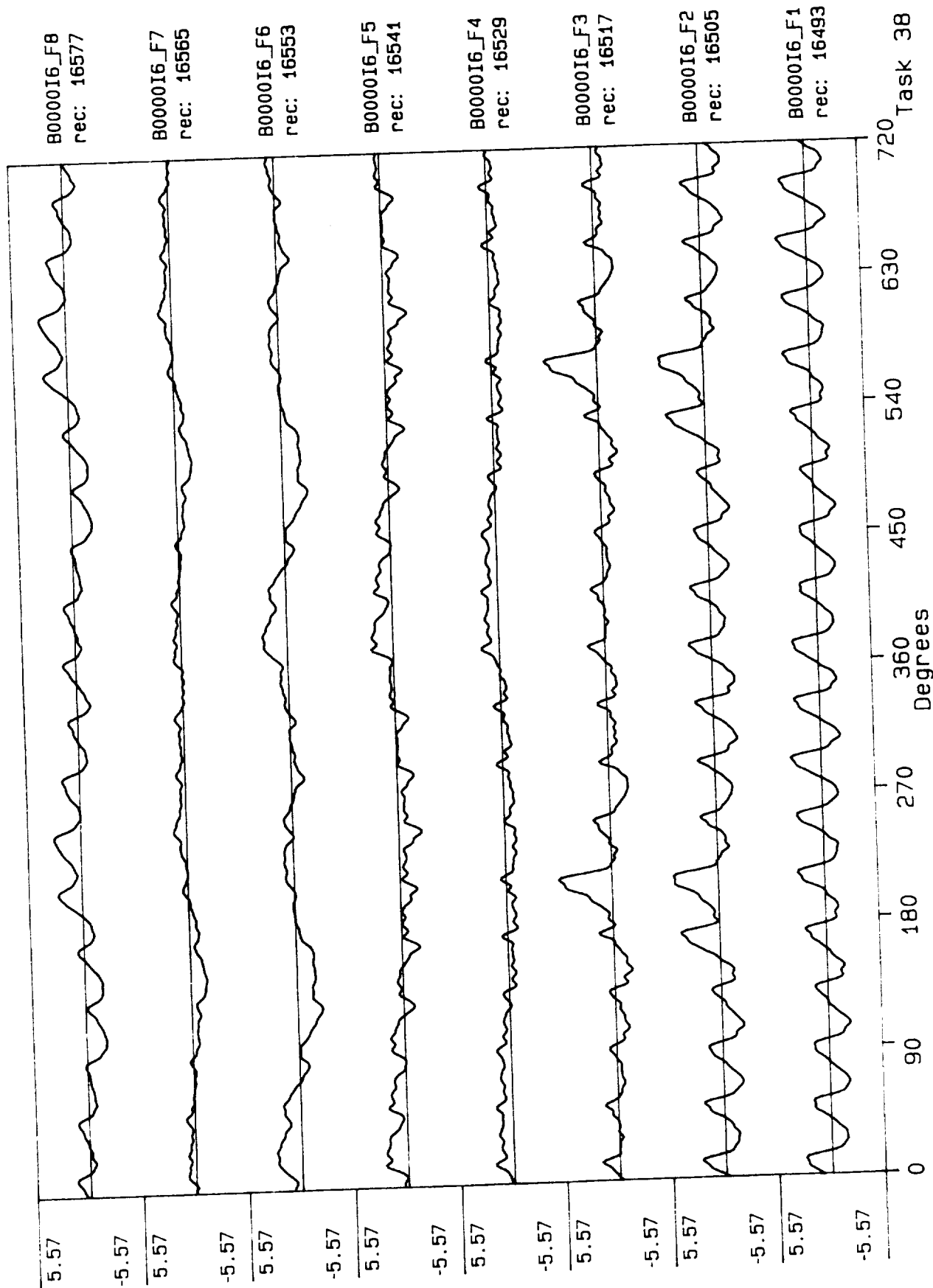
Process included: Calibration, Phase correction and DC filtering. Published: 06/07/89



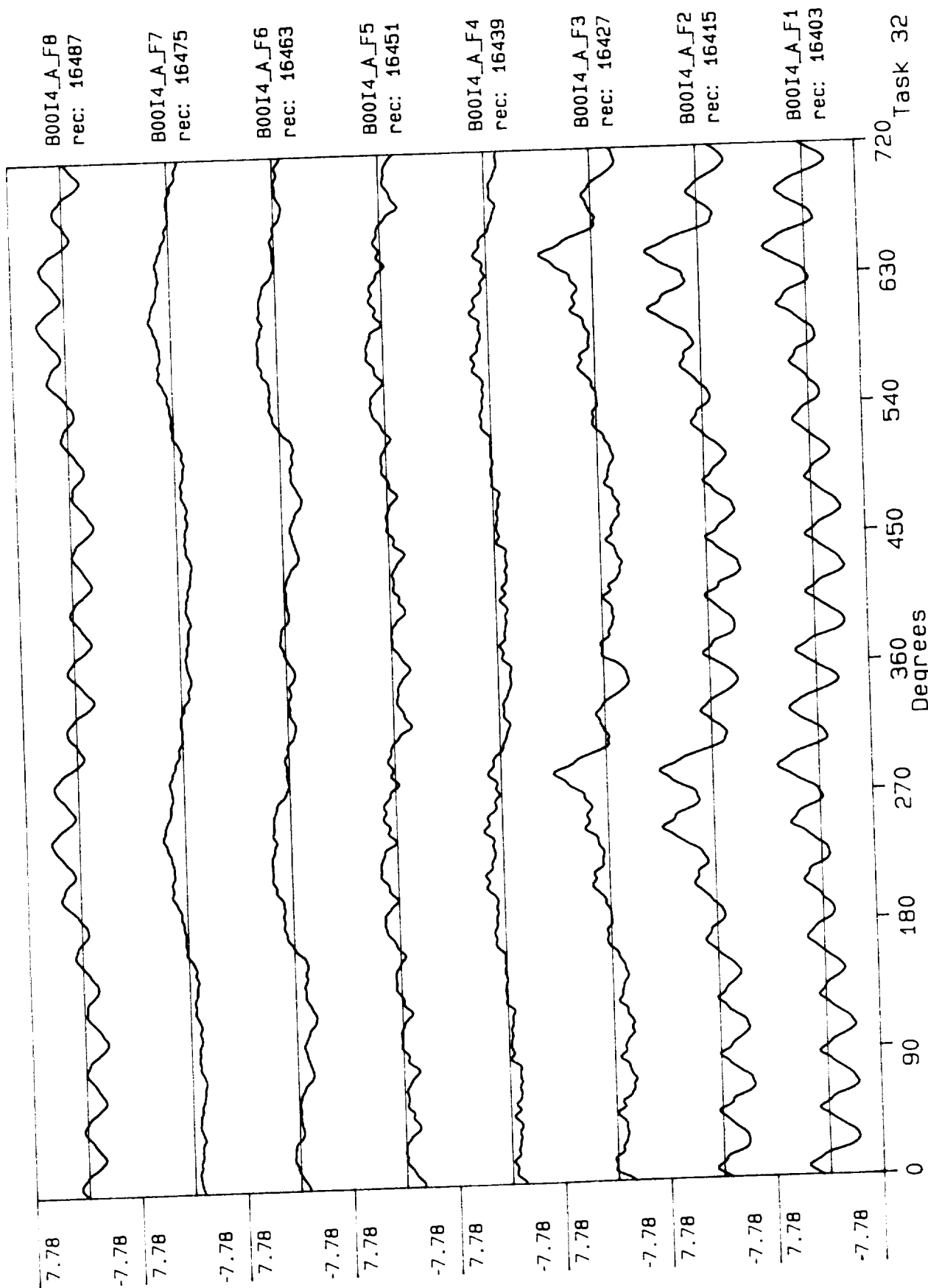
Process included: Calibration, Phase correction and DC filtering.



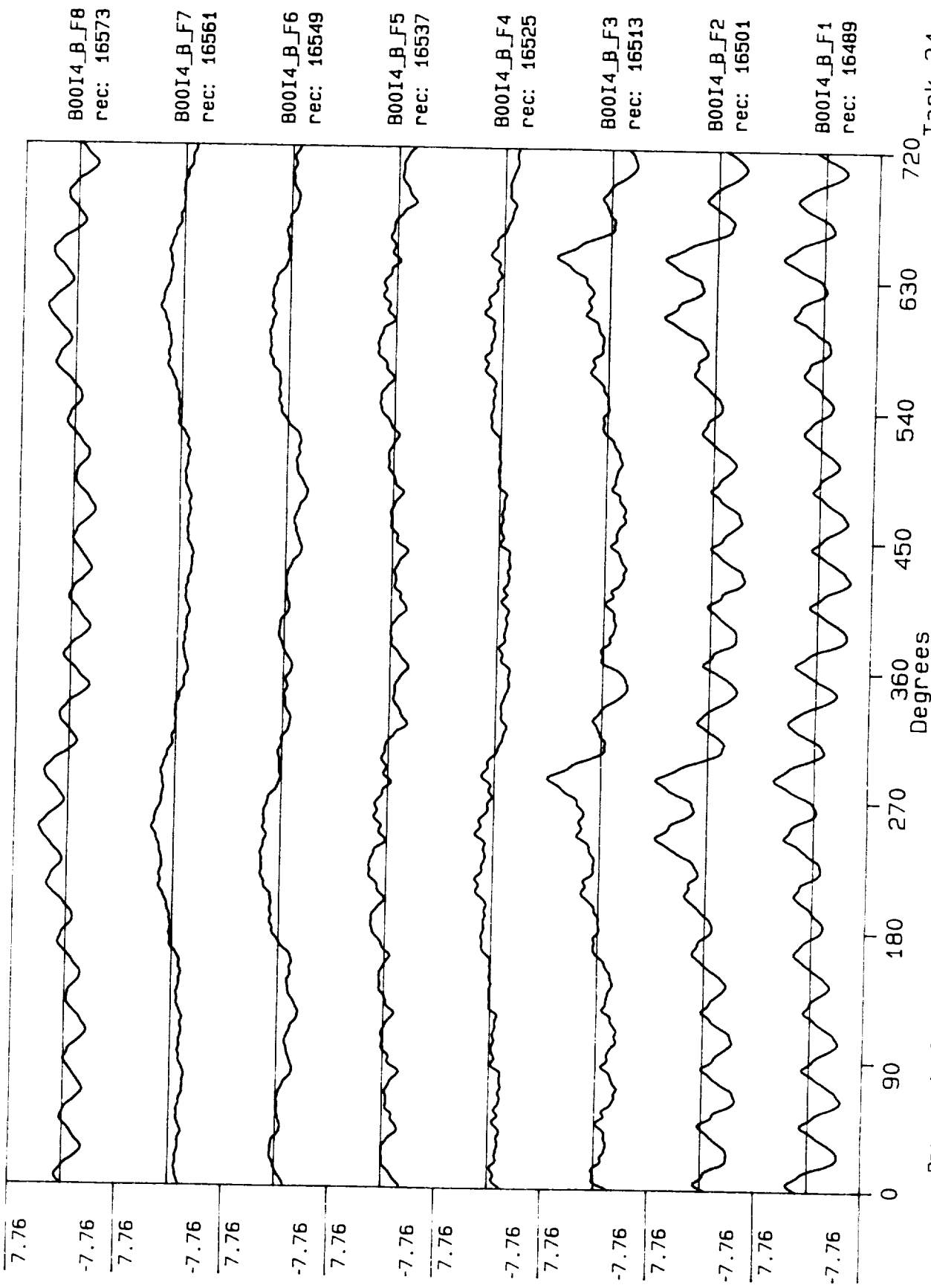
Process included: Calibration, Phase correction and DC filtering.



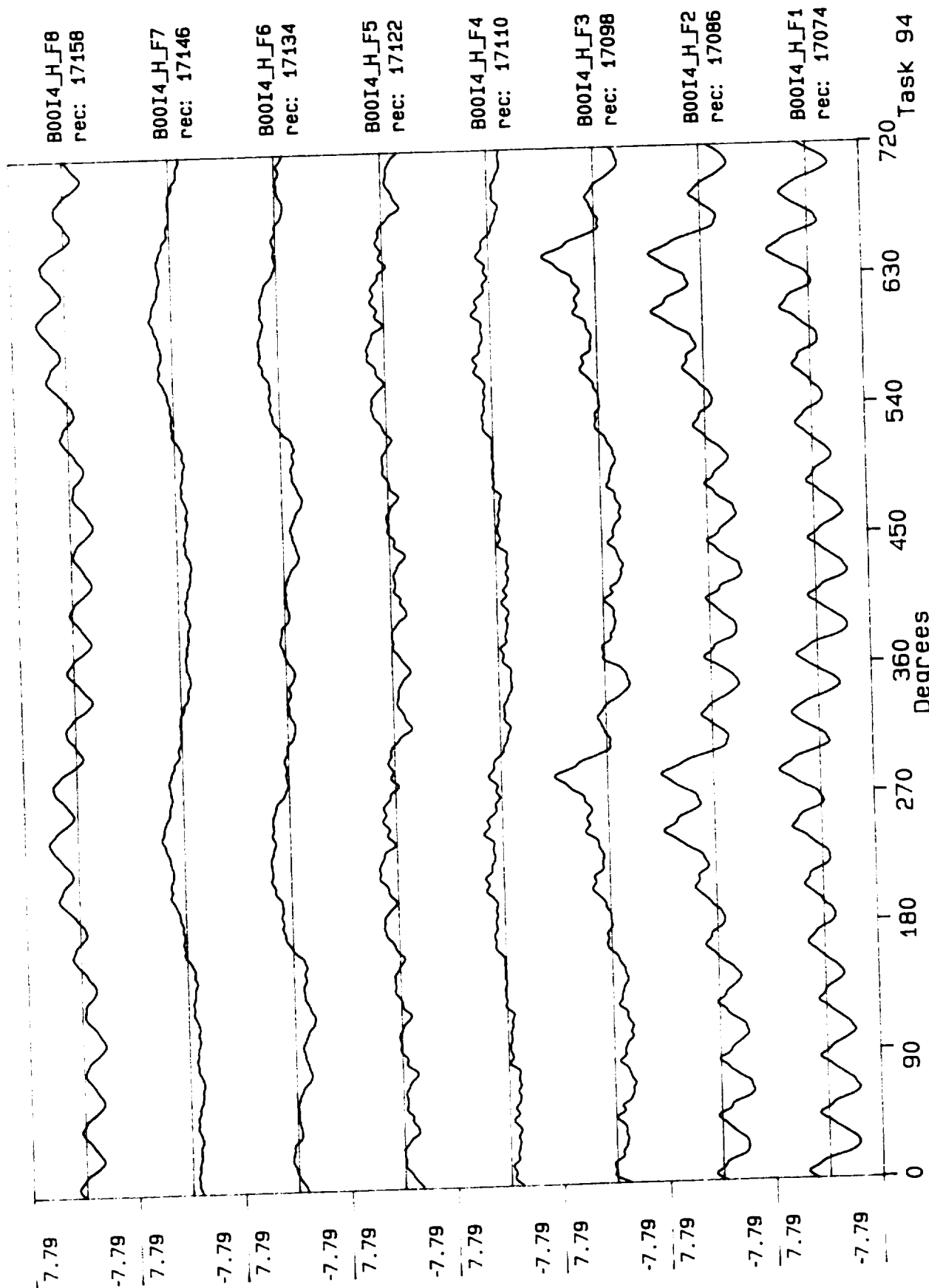
Process included: Calibration, Phase correction and DC filtering.



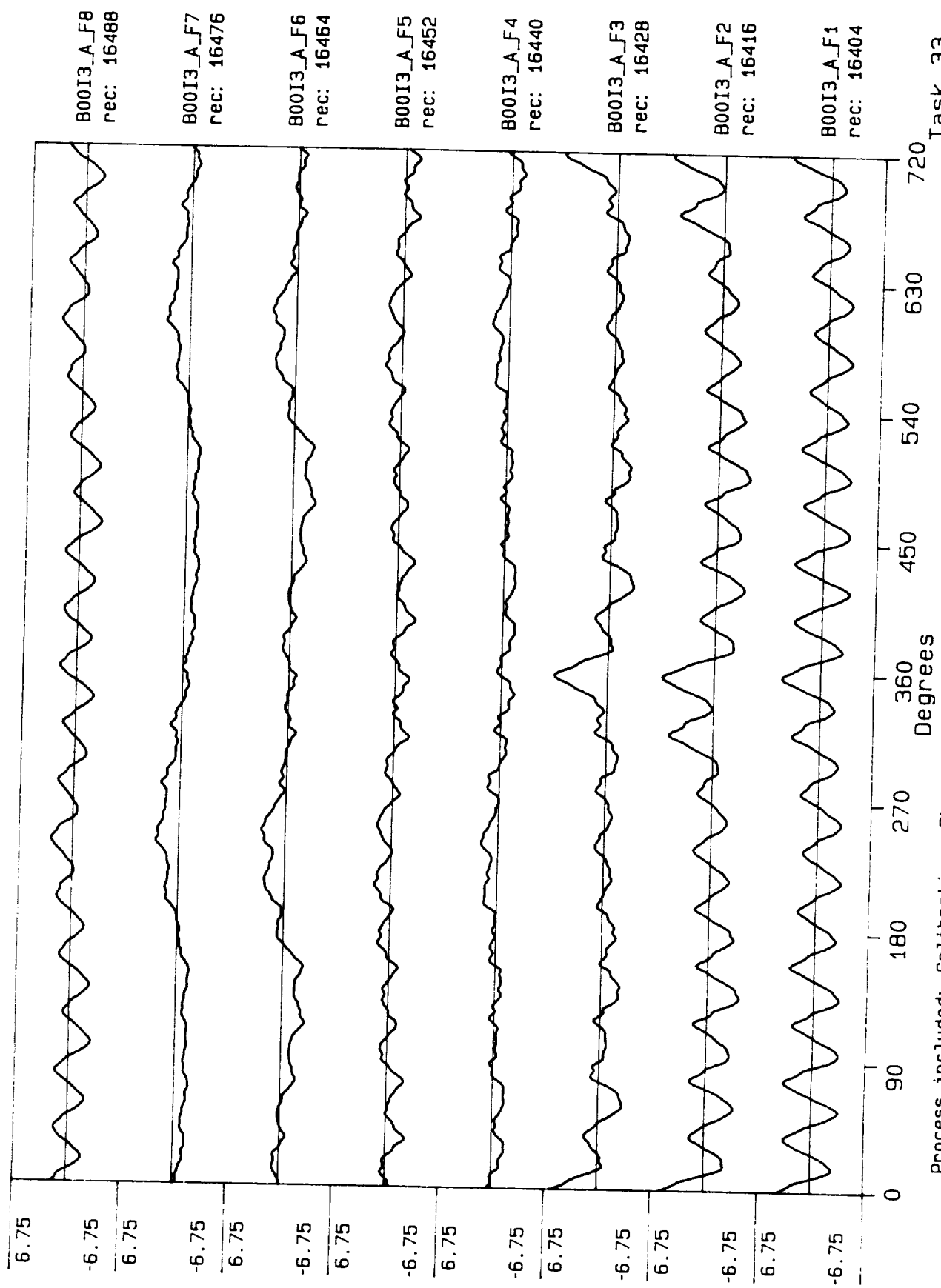
Process included: Calibration, Phase correction and DC filtering.

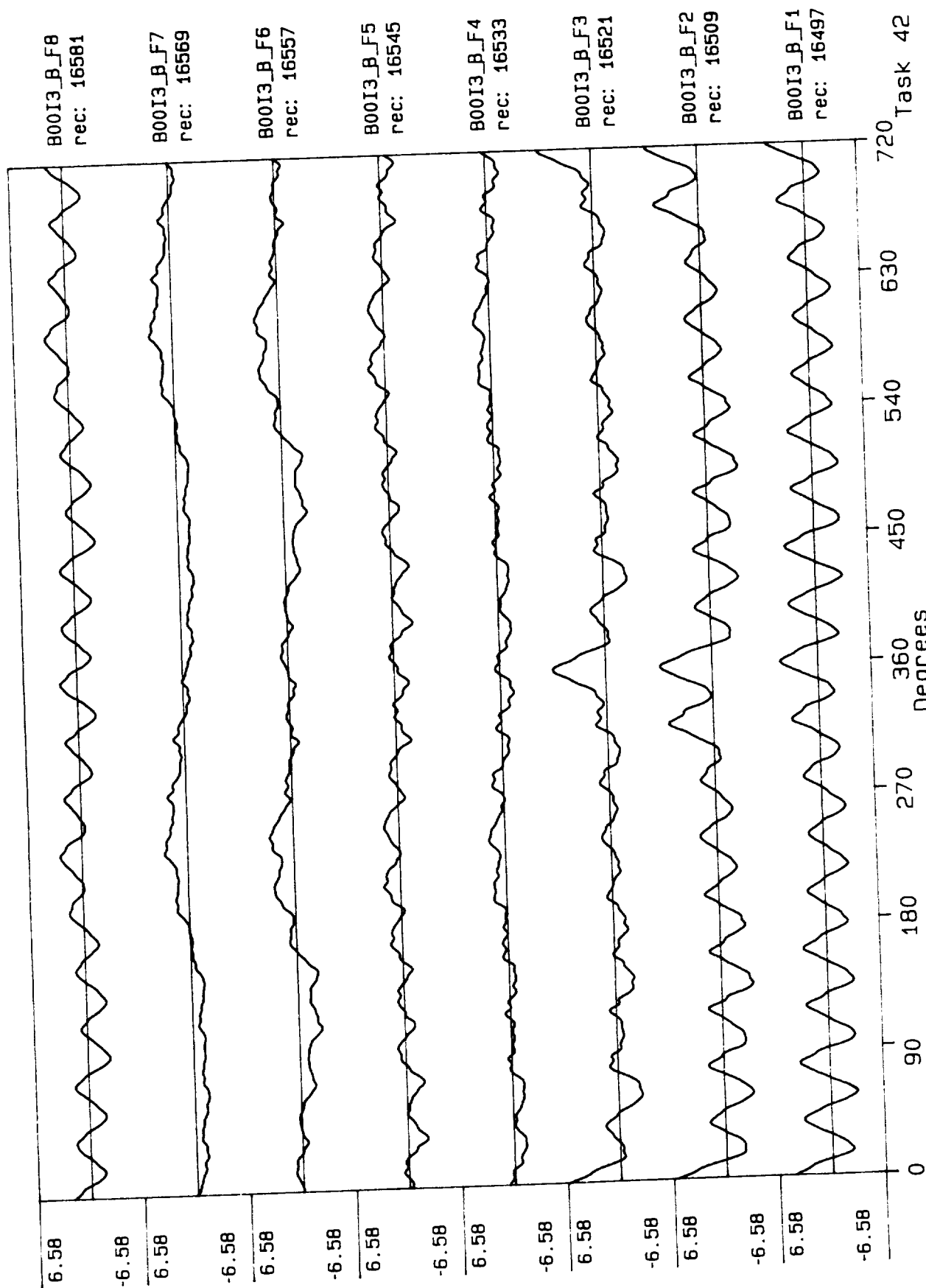


Process included: Calibration, Phase correction and DC filtering.

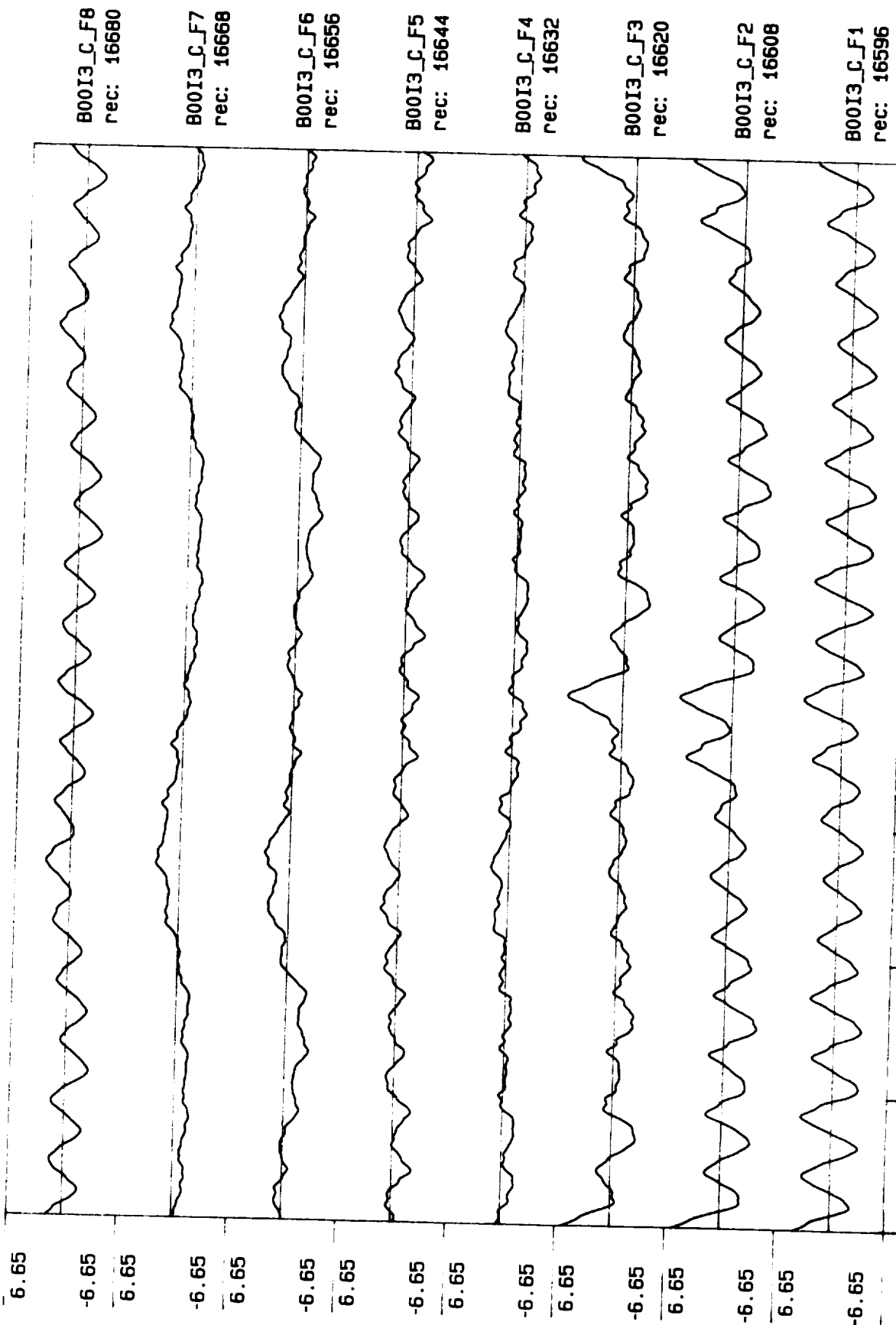


Process included: Calibration, Phase correction and DC filtering.

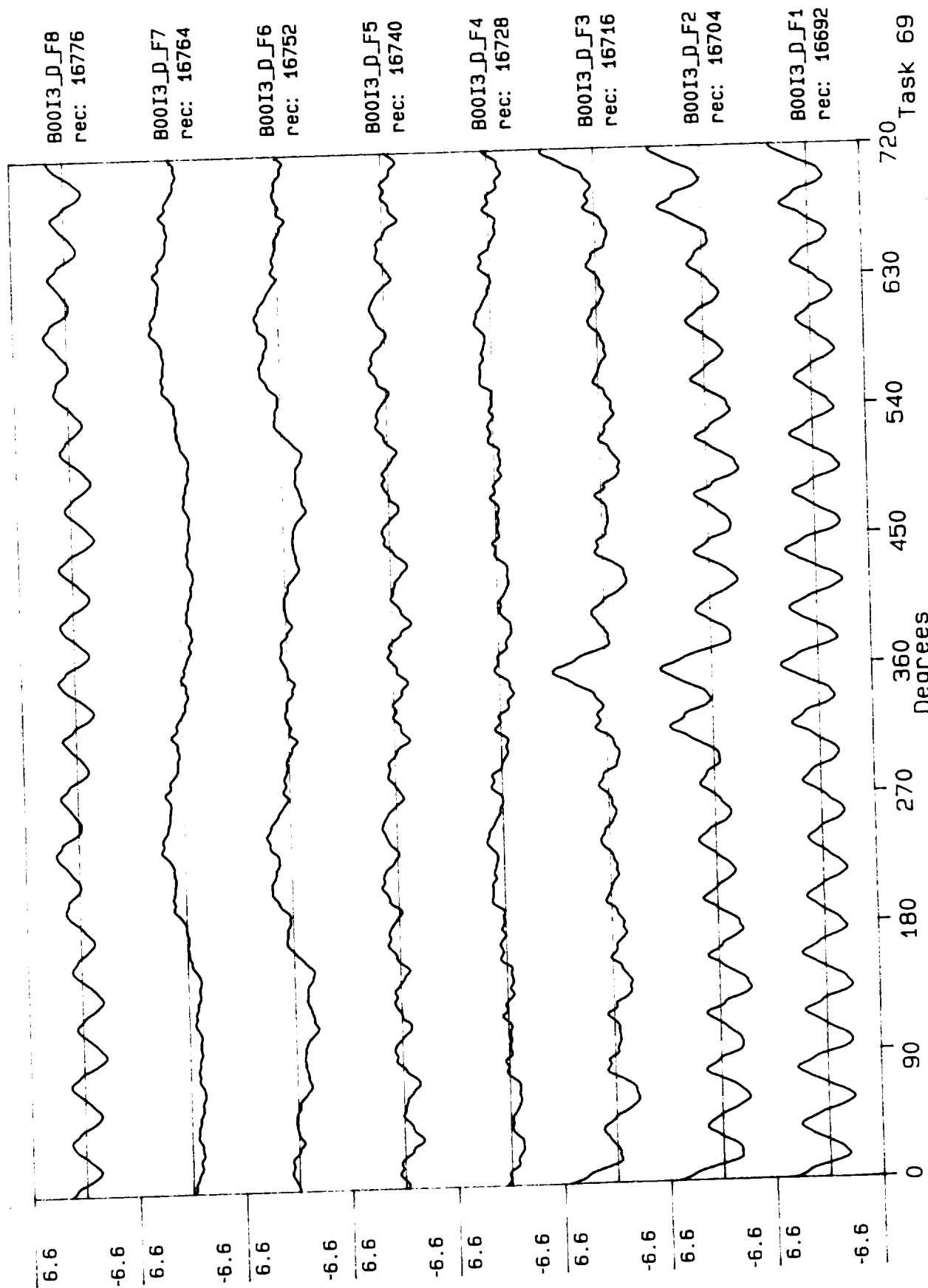




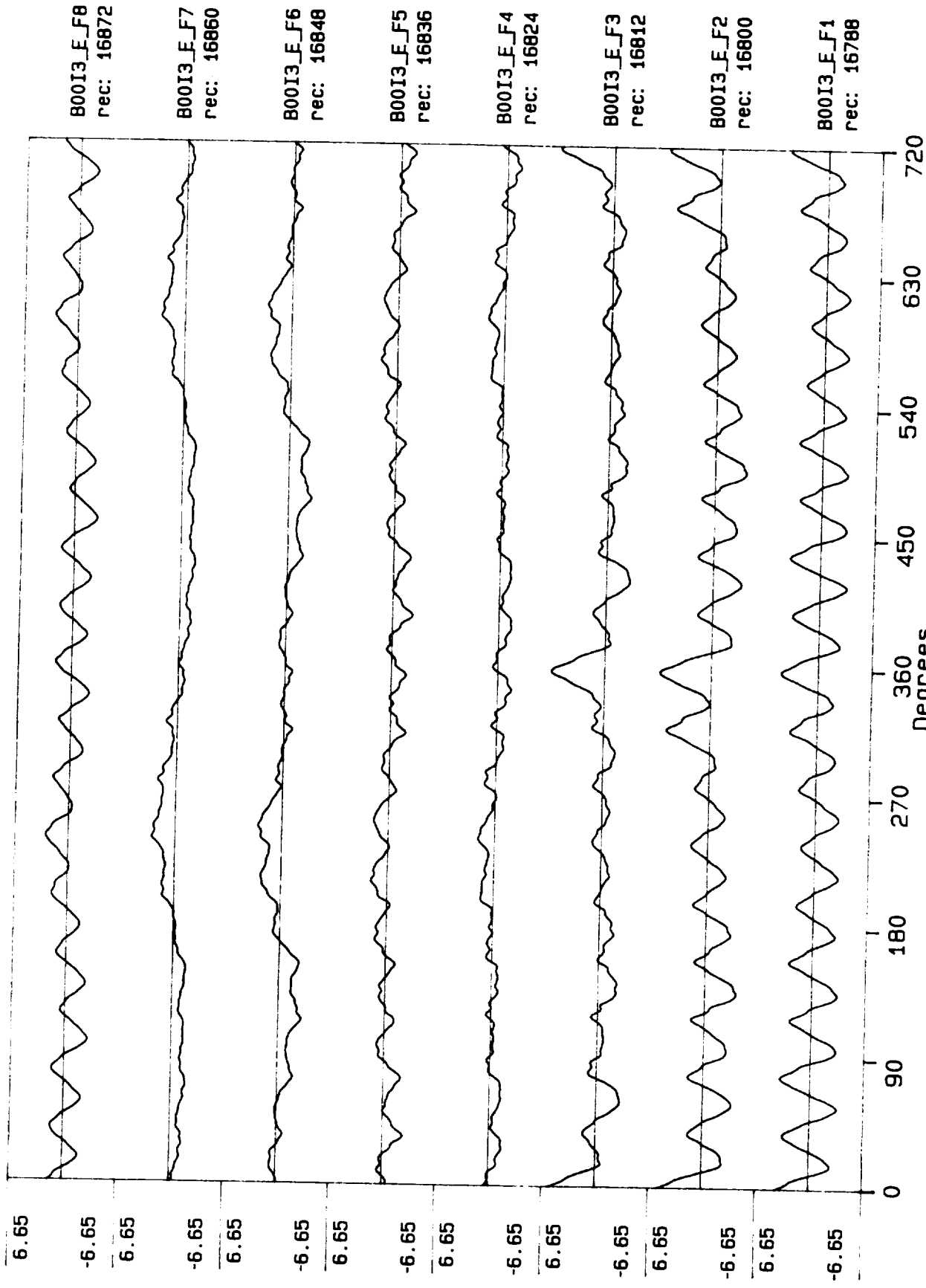
Process included: Calibration, Phase correction and DC filtering.



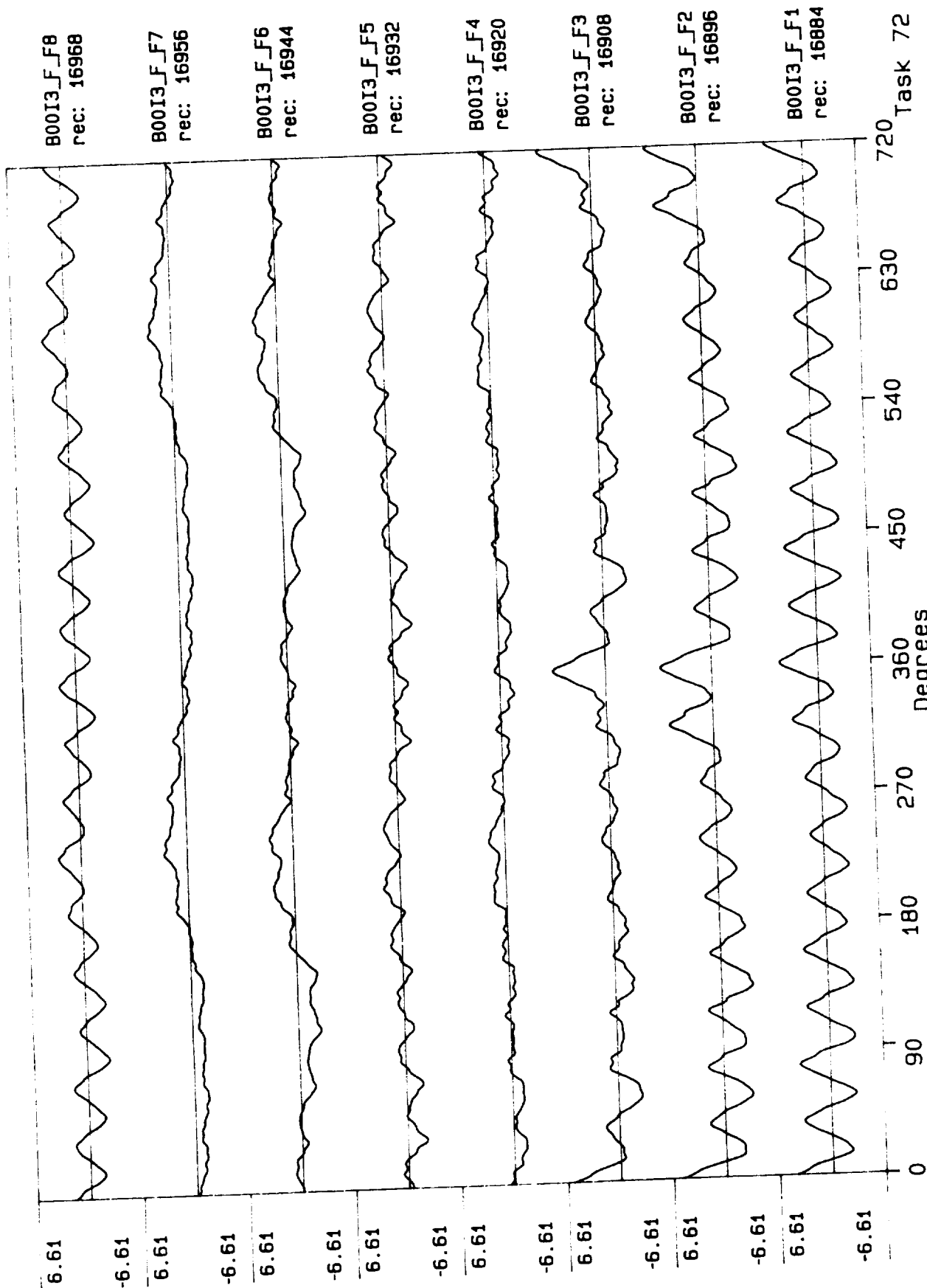
Process included: Calibration, Phase correction and DC filtering.



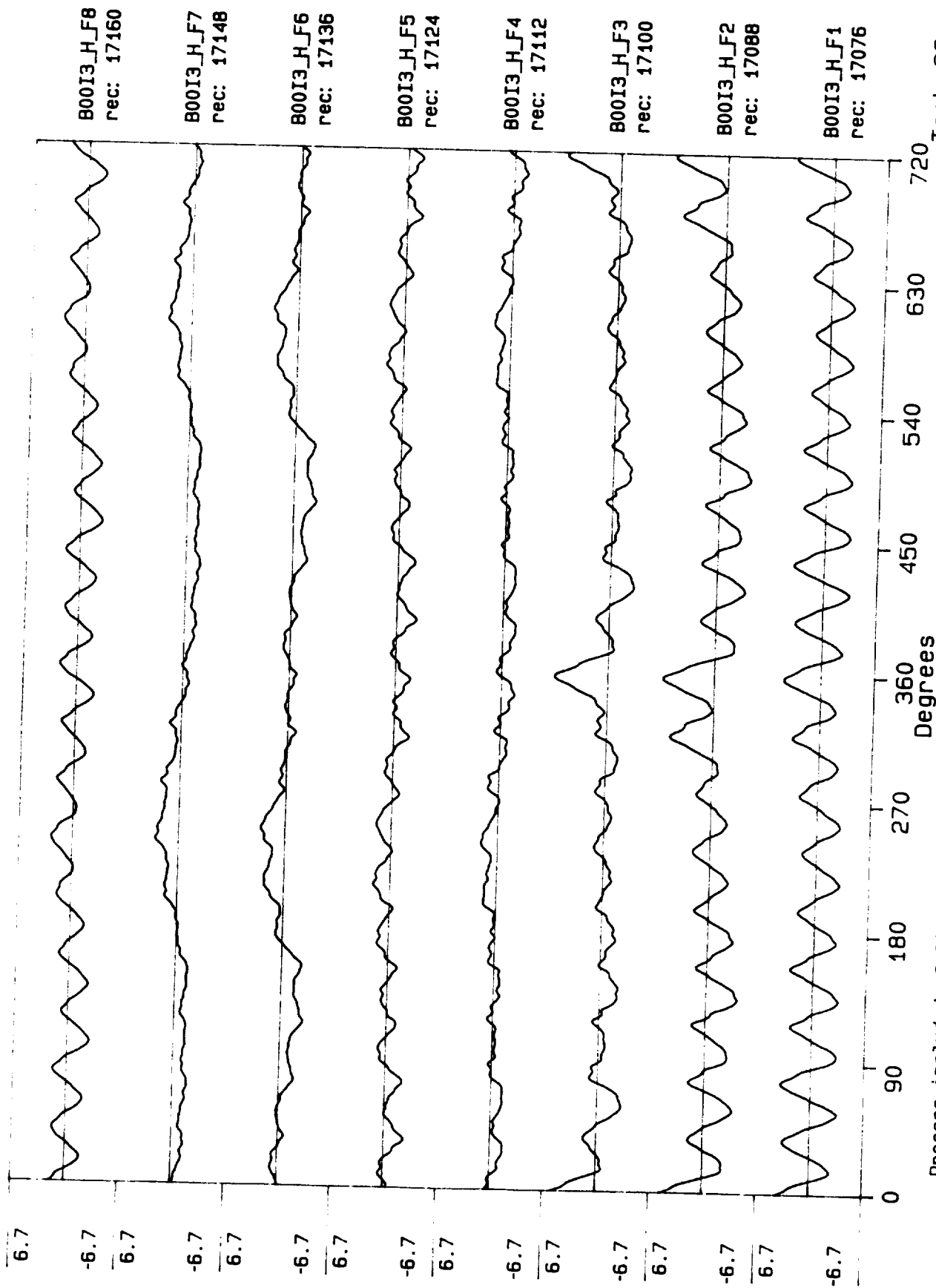
Process included: Calibration, Phase correction and DC filtering.



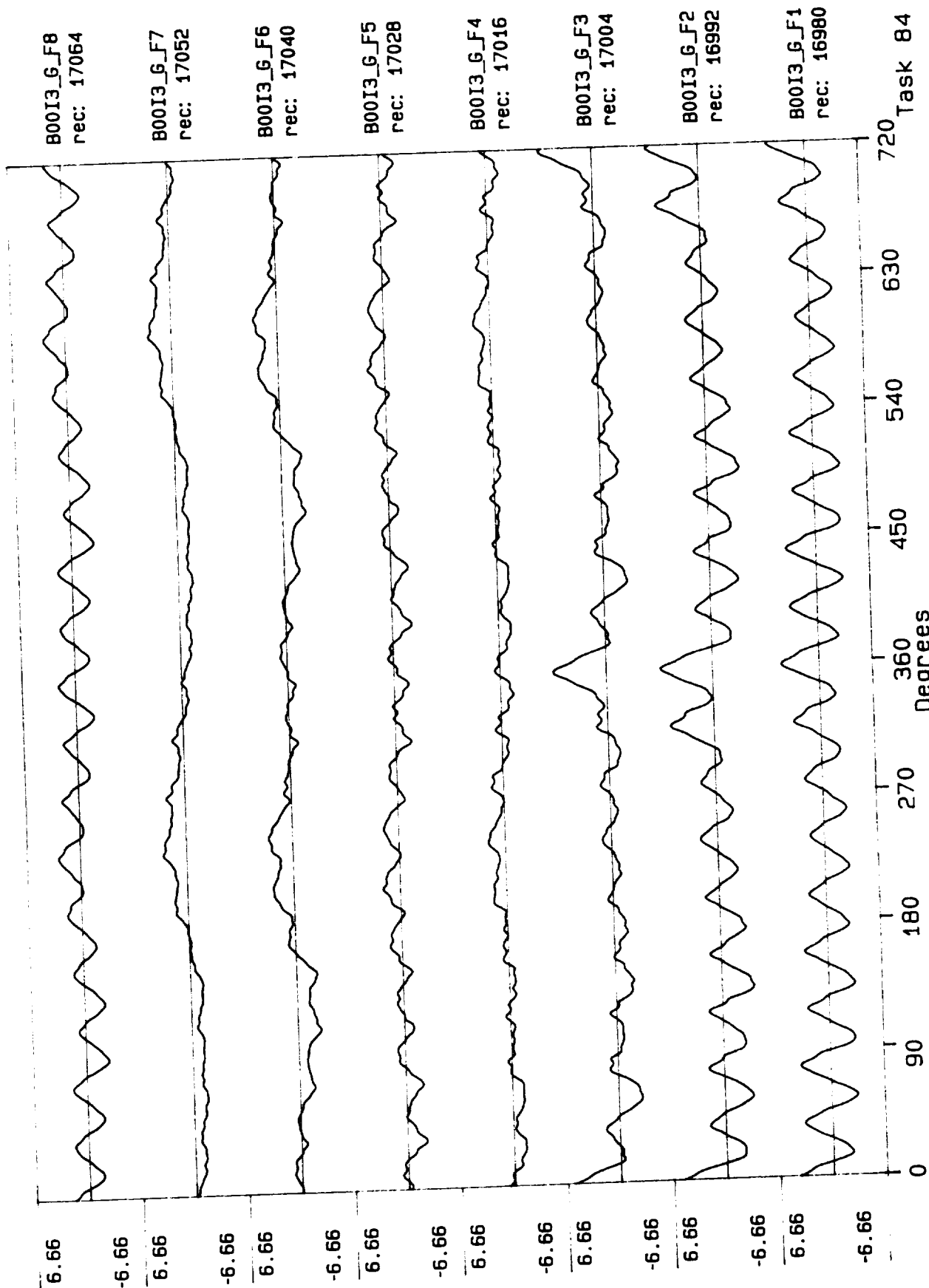
Process included: Calibration, Phase correction and DC filtering.



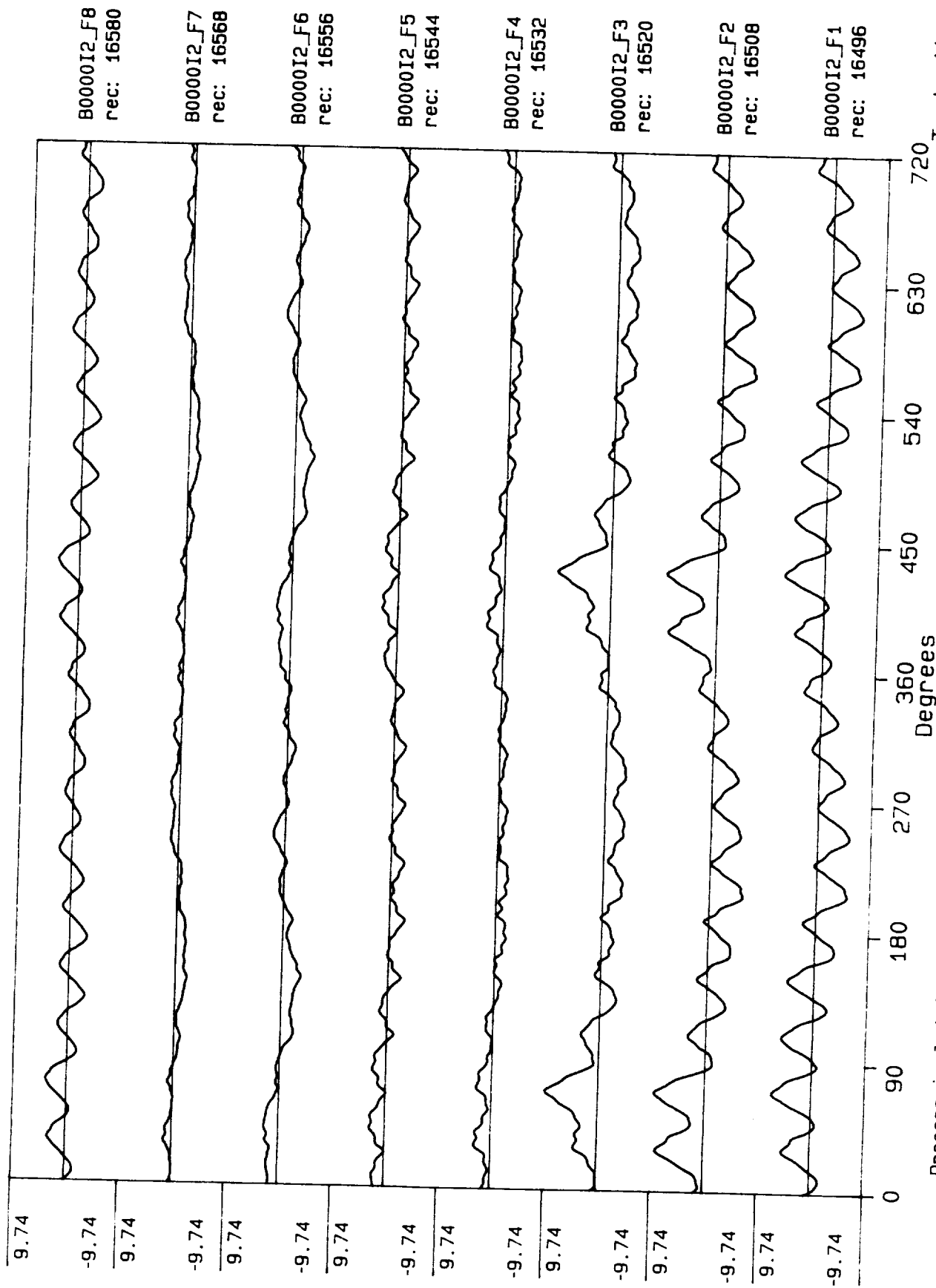
Process included: Calibration, Phase correction and DC filtering.



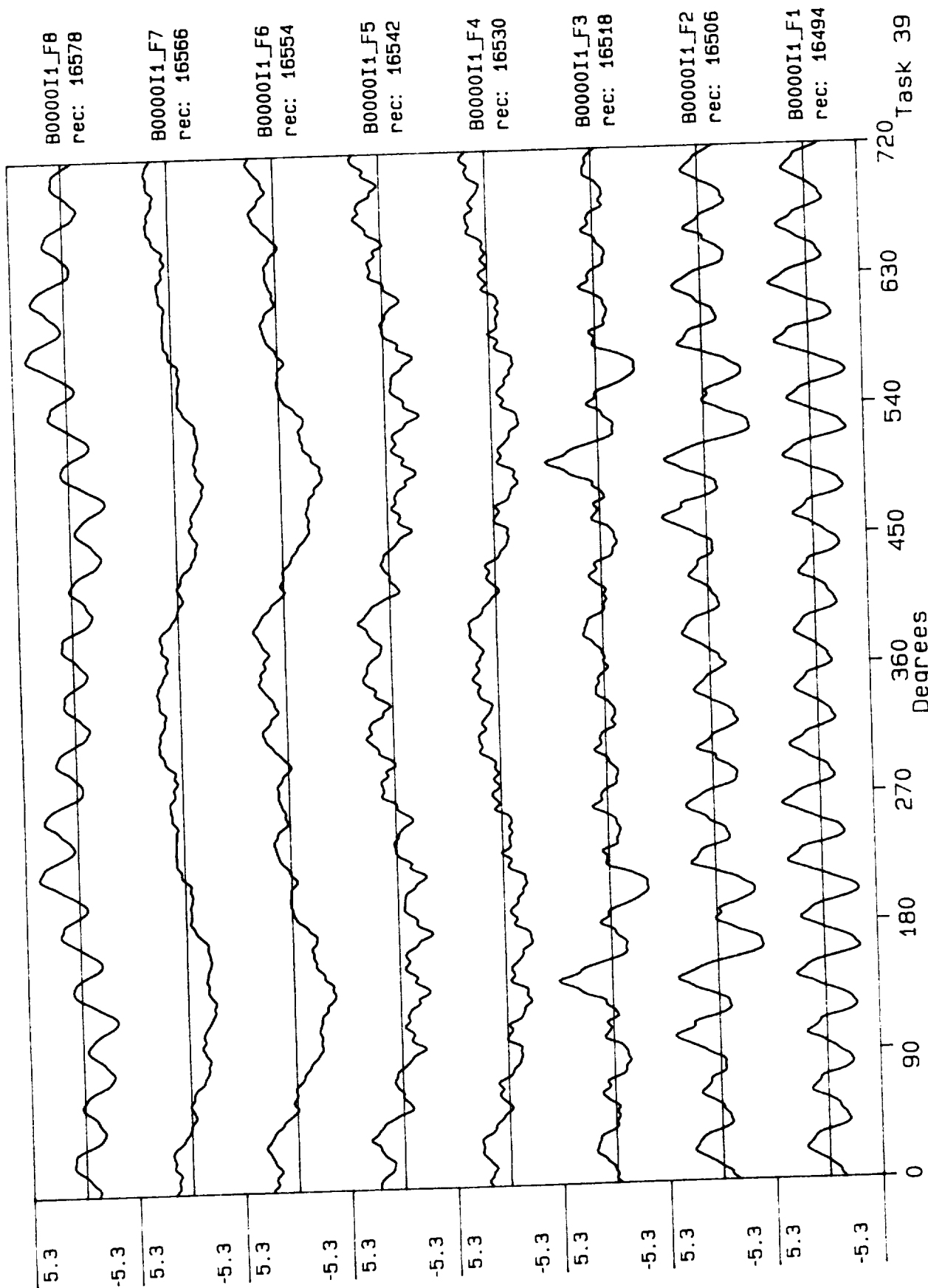
Process included: Calibration, Phase correction and DC filtering.



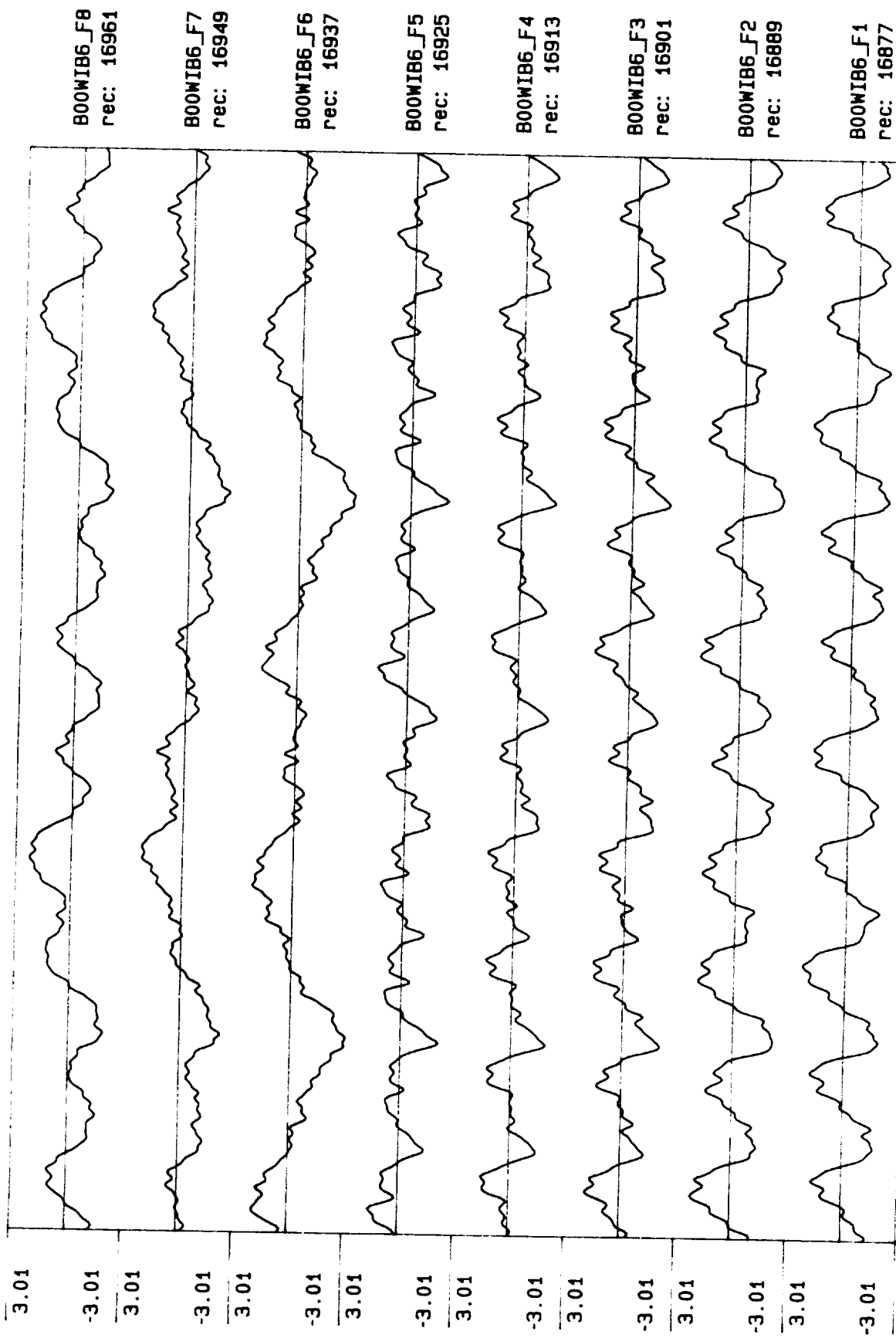
Process included: Calibration, Phase correction and DC filtering.



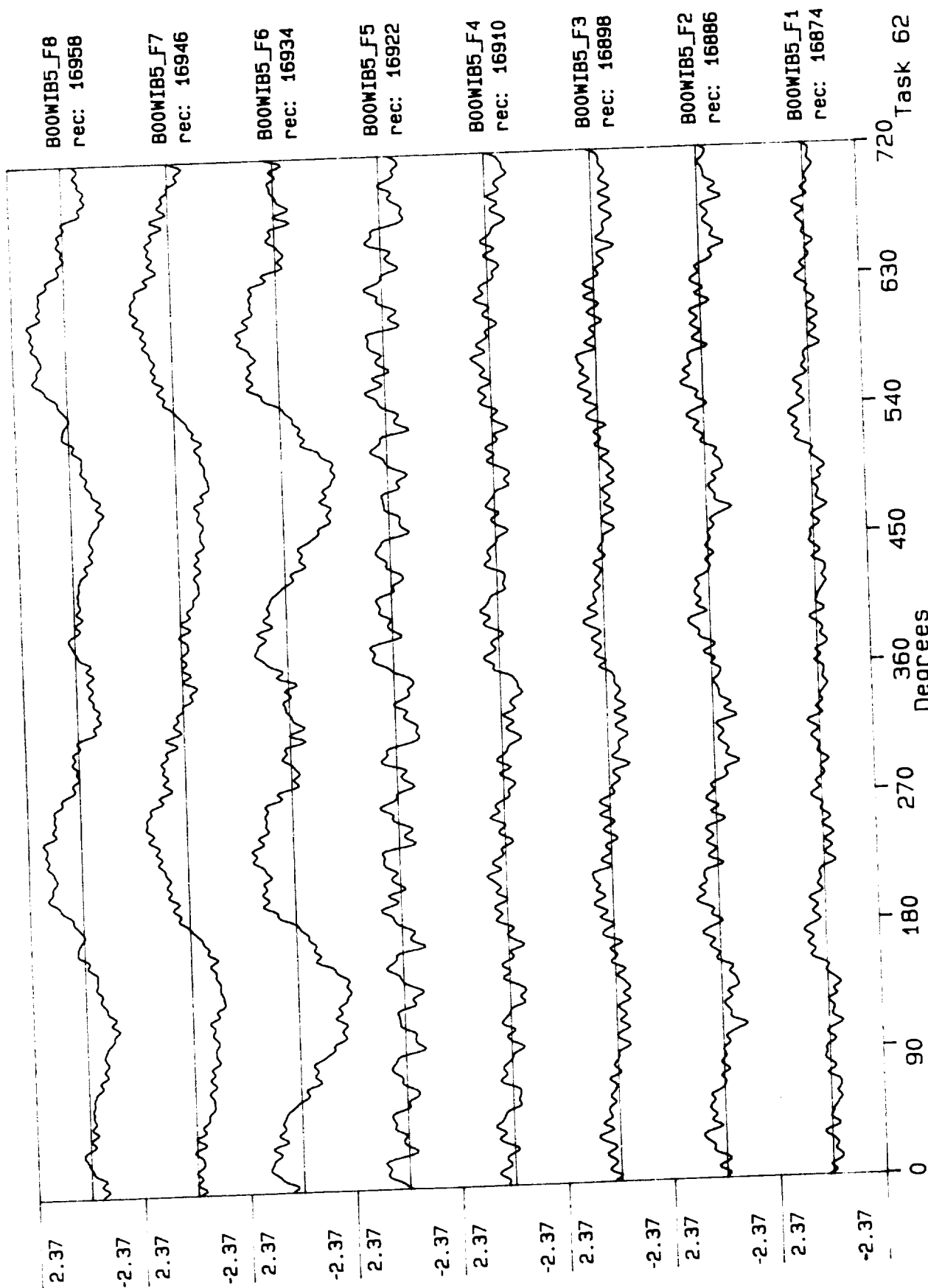
Process included: Calibration, Phase correction and DC filtering.



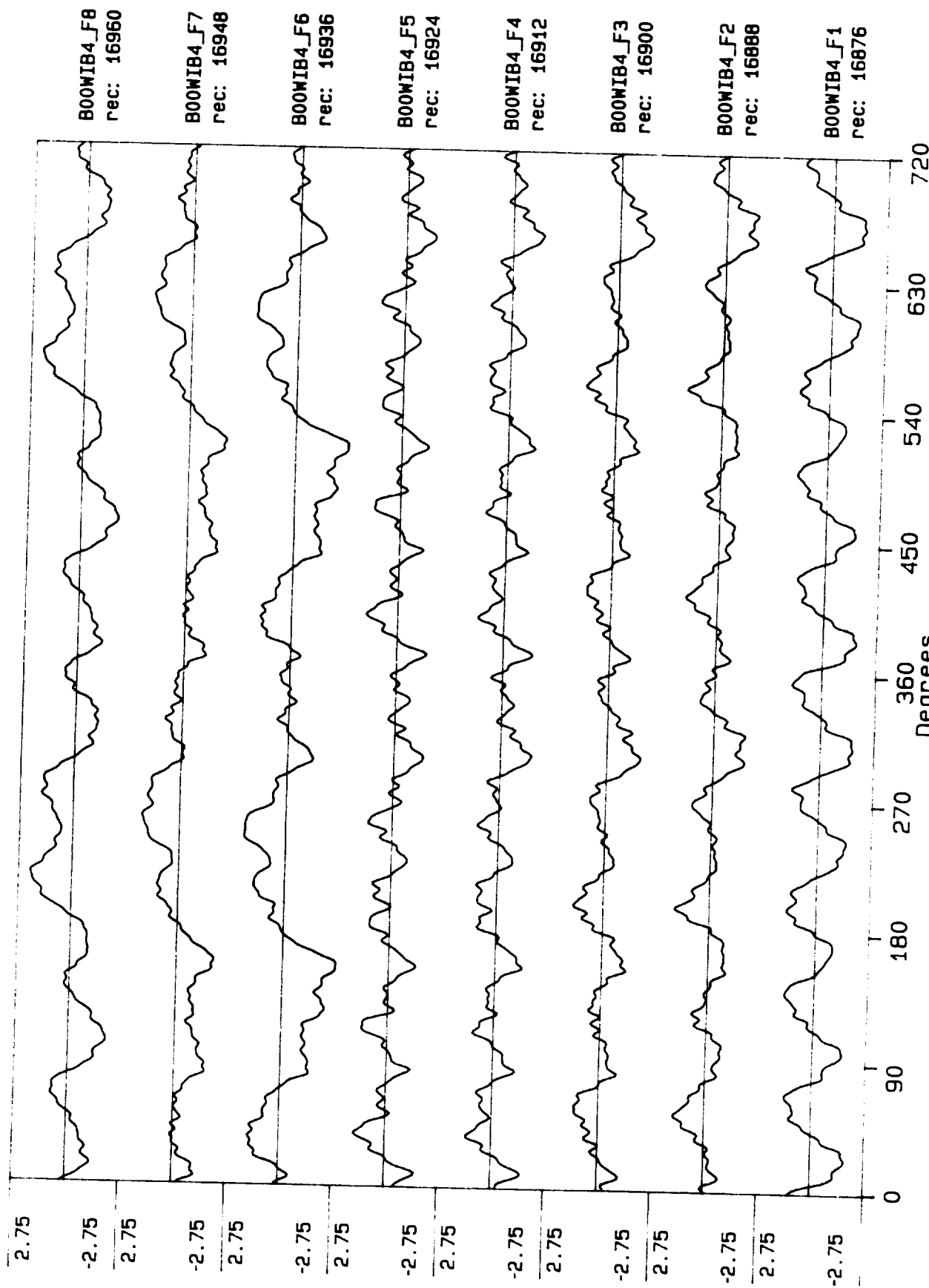
Process included: Calibration, Phase correction and DC filtering.



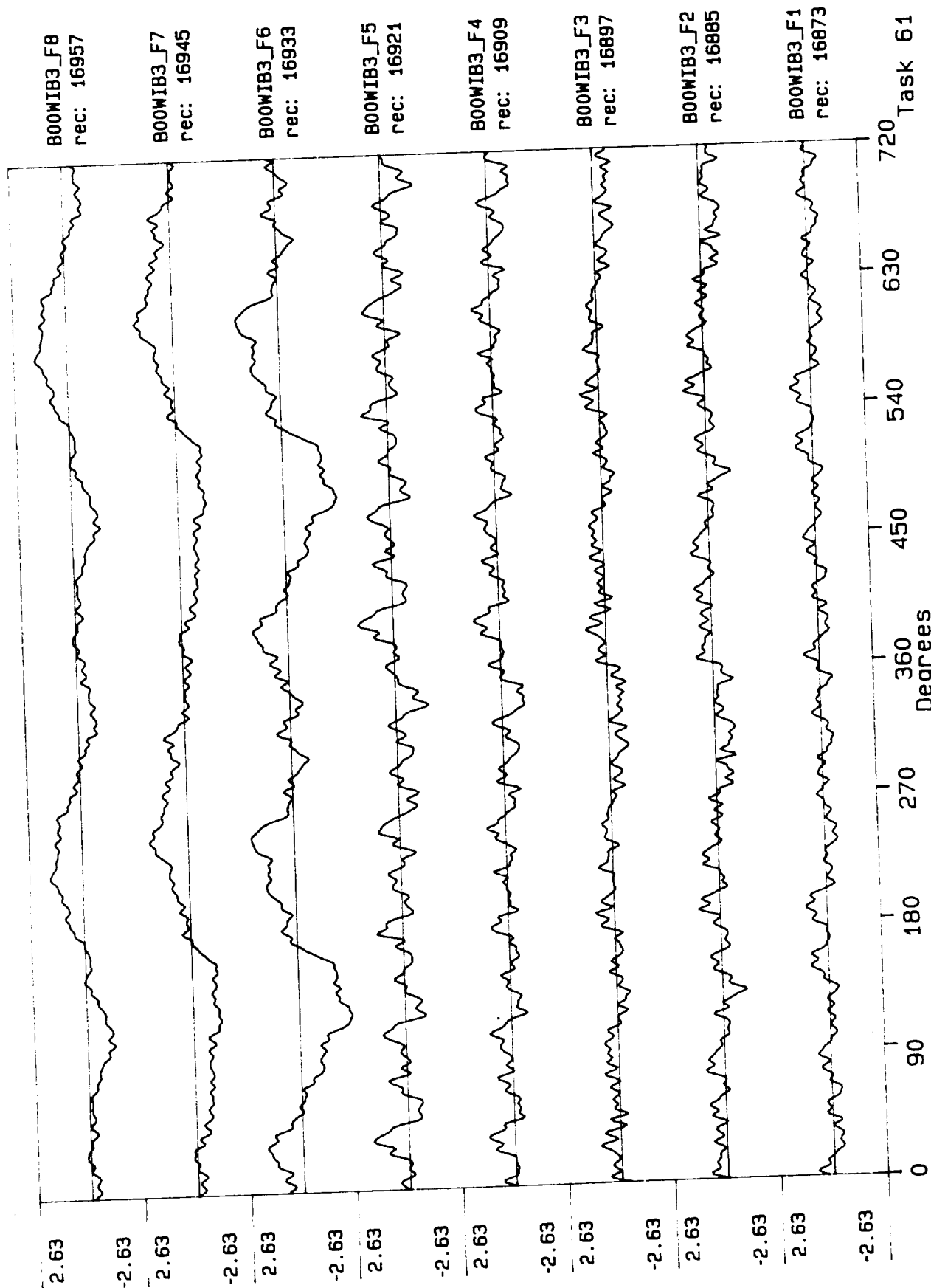
Process included: Calibration, Phase correction and DC filtering.

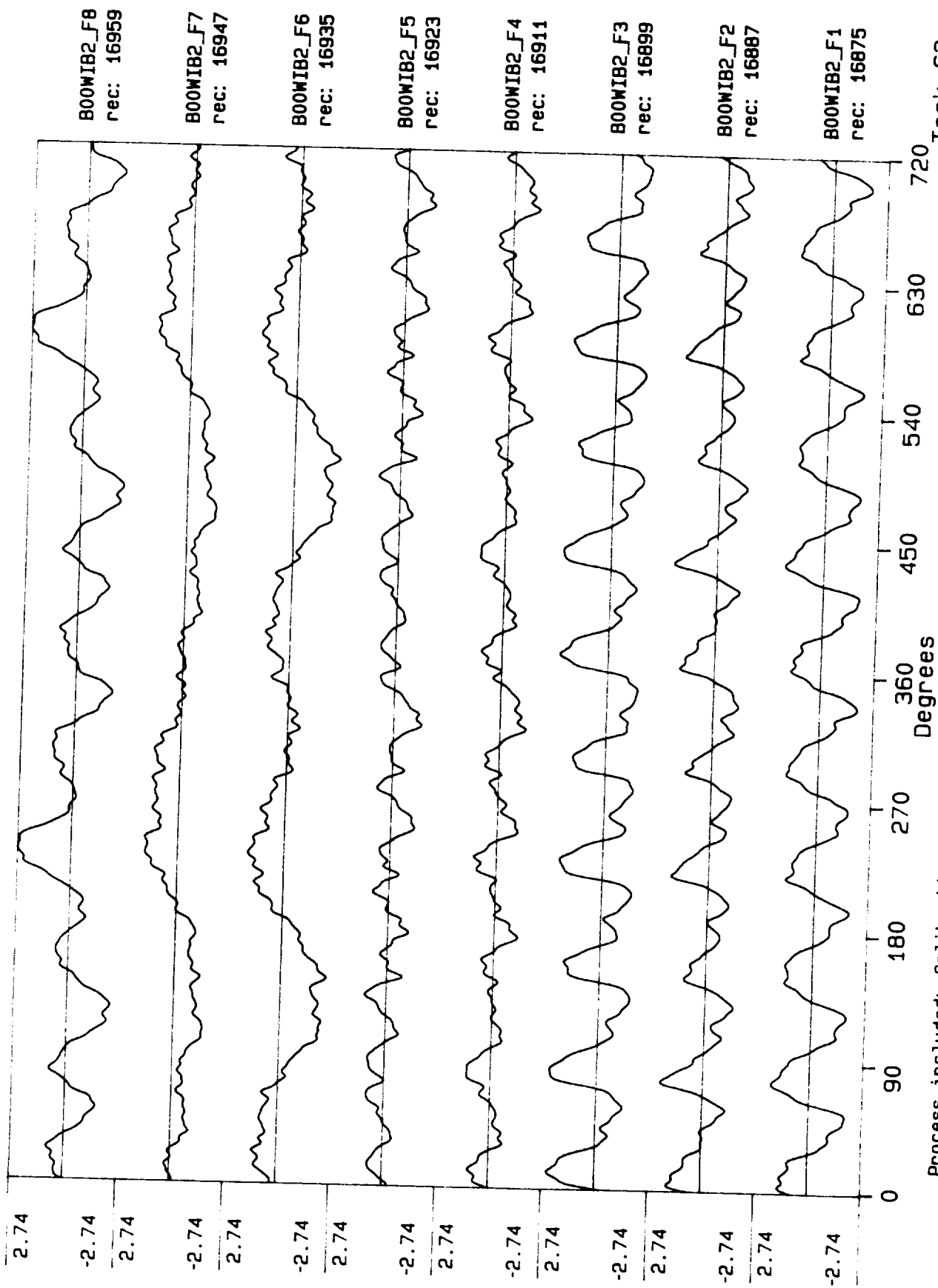


Process included: Calibration, Phase correction and DC filtering.

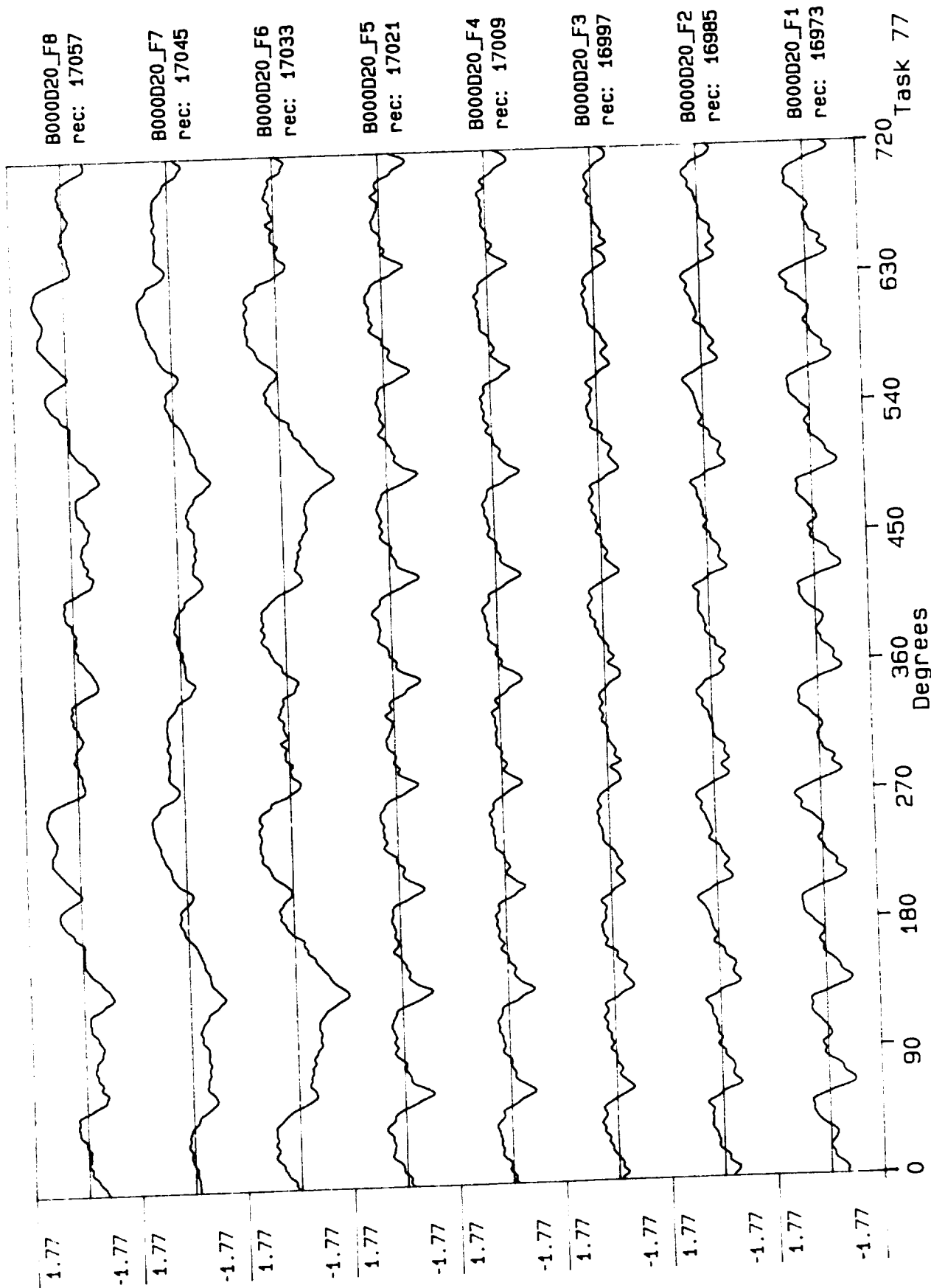


Process included: Calibration, Phase correction and DC filtering.

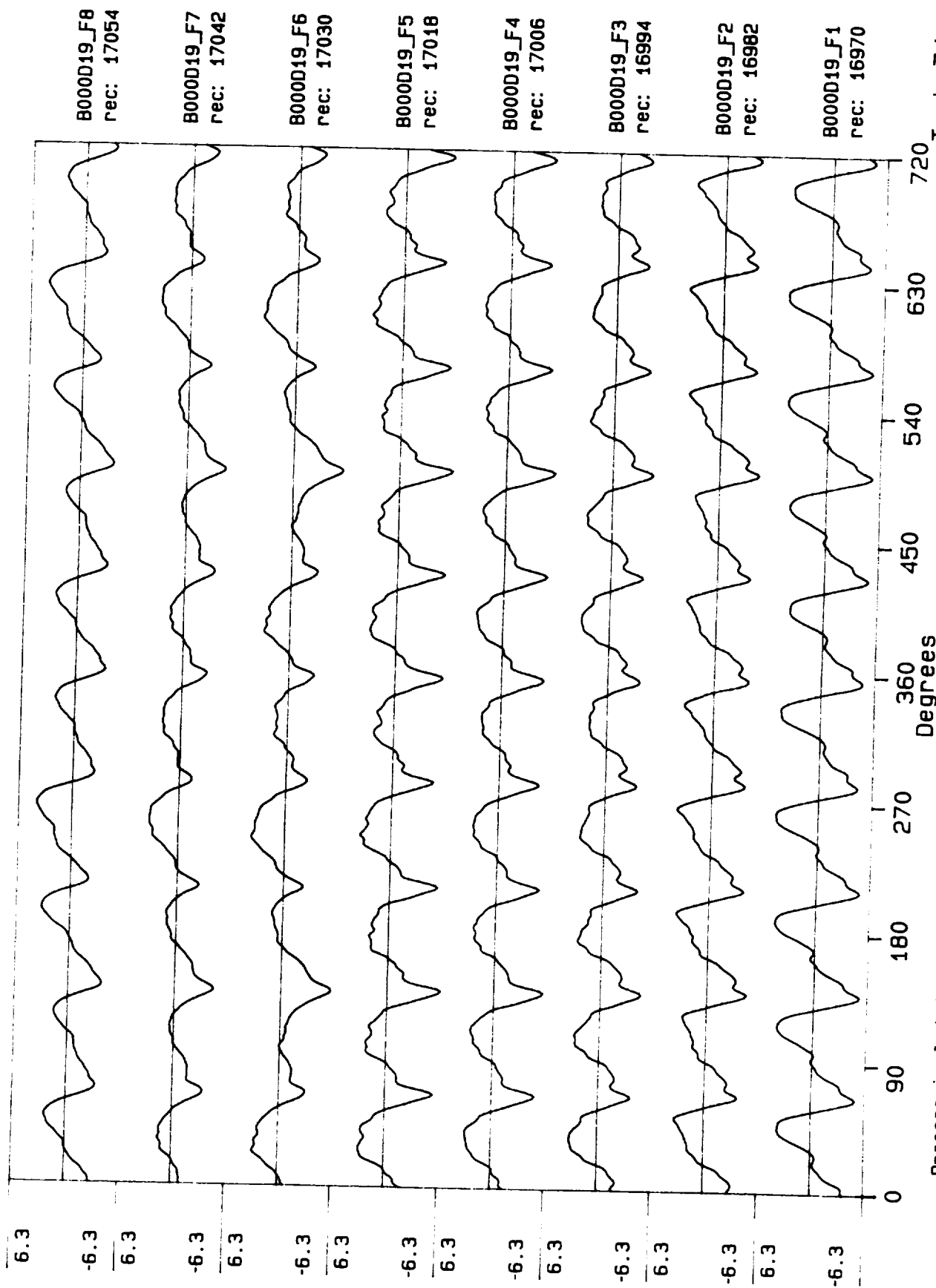




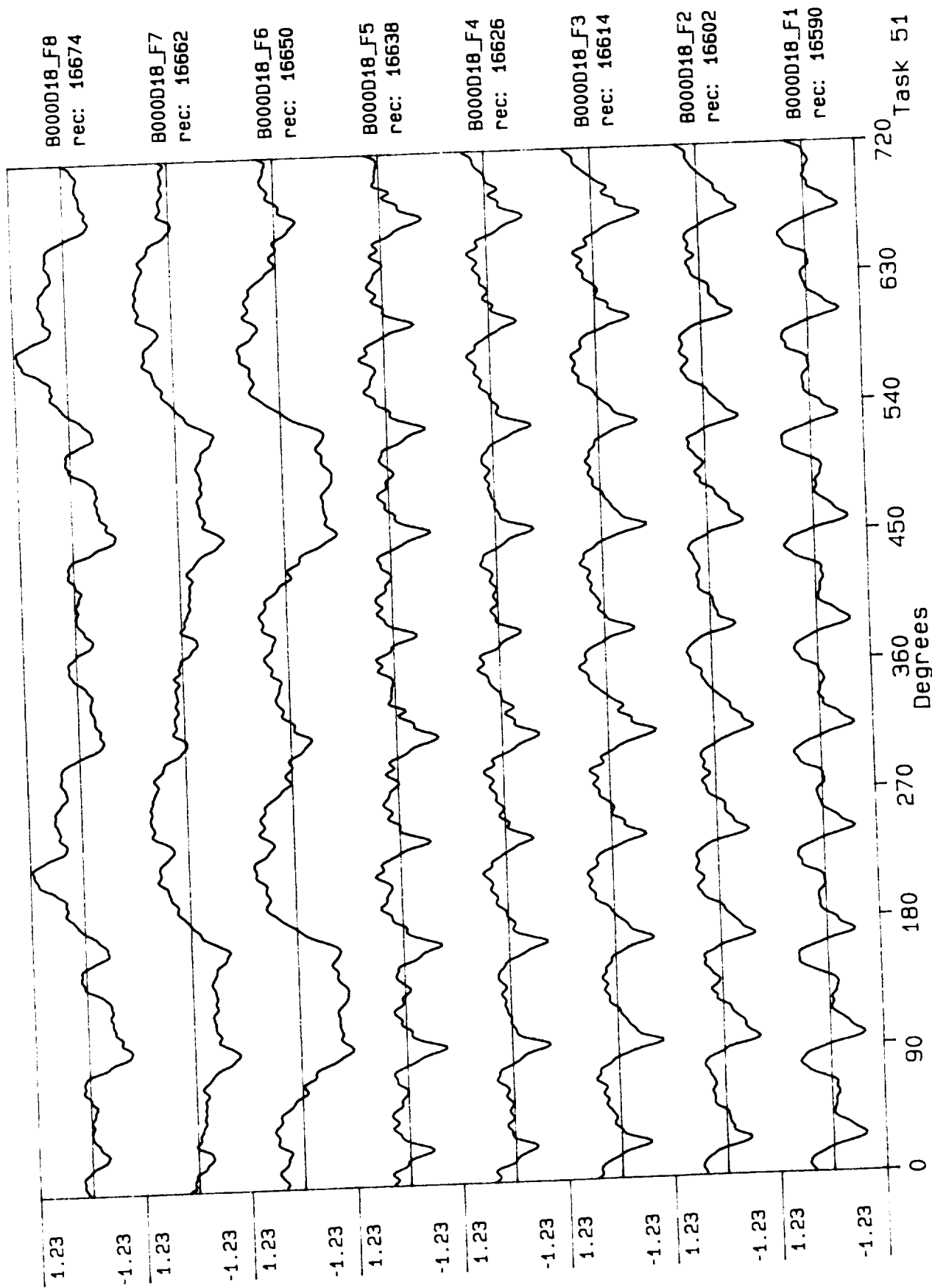
Process included: Calibration, Phase correction and DC filtering.



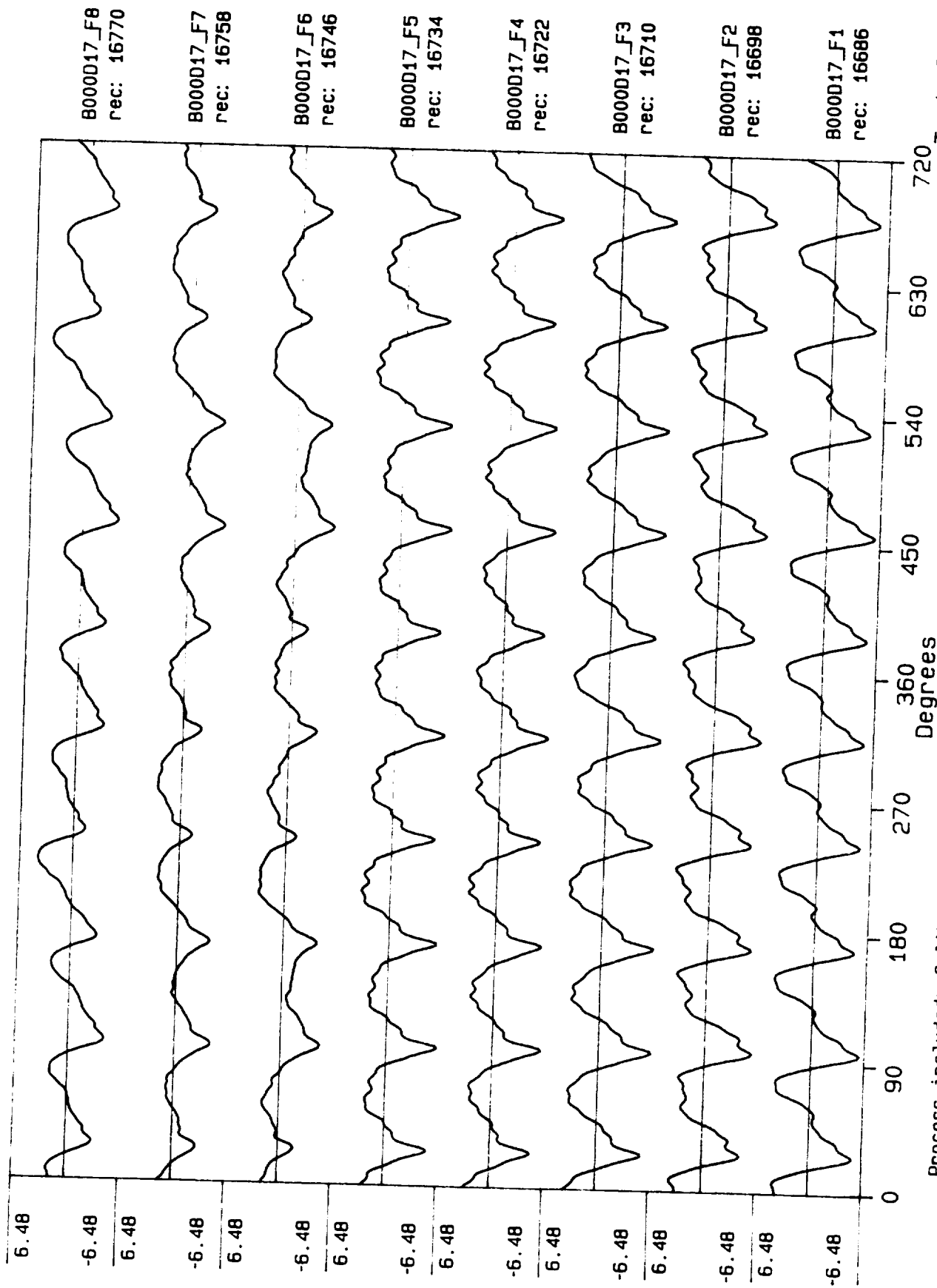
Process included: Calibration, Phase correction and DC filtering.



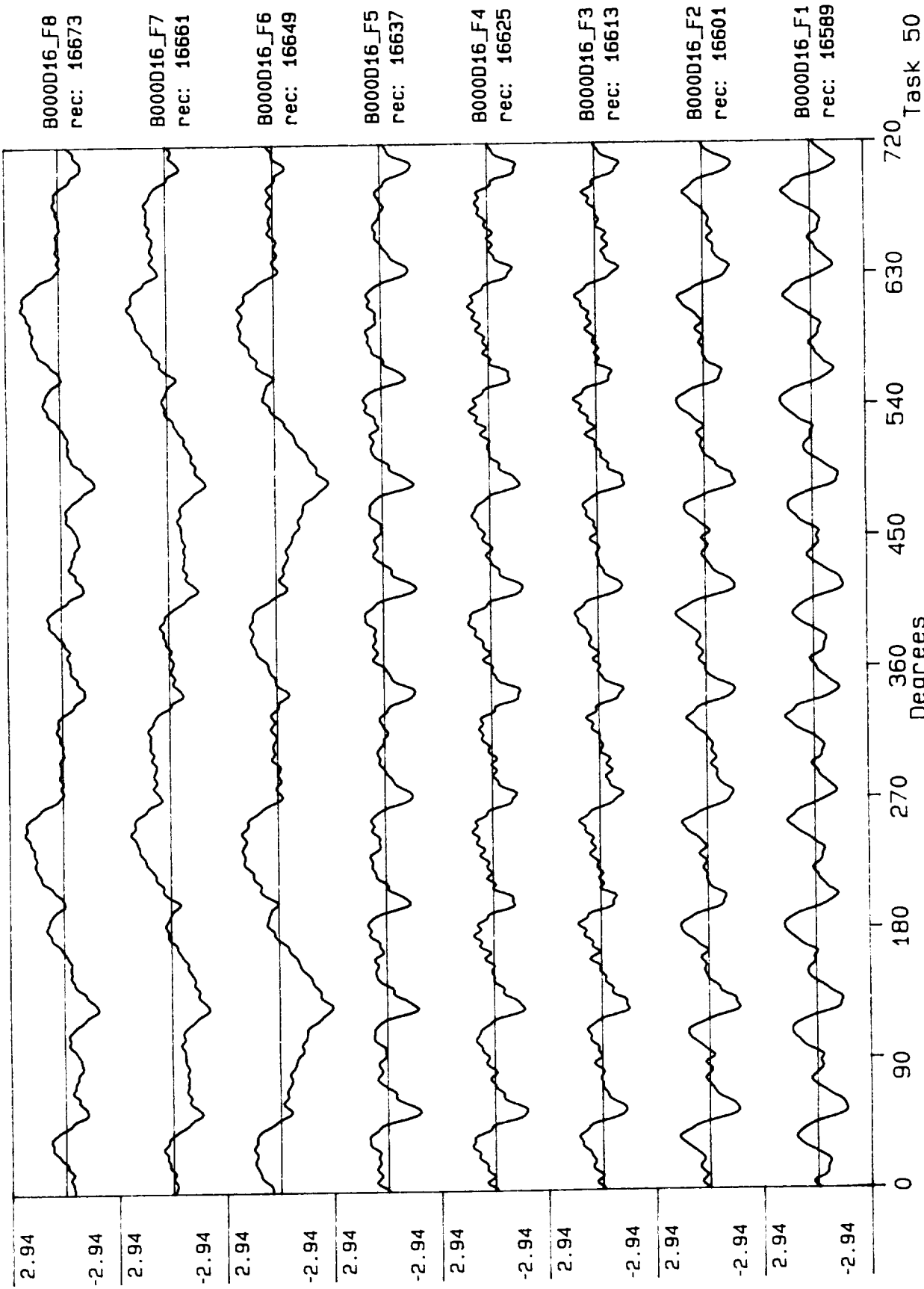
Process included: Calibration, Phase correction and DC filtering.



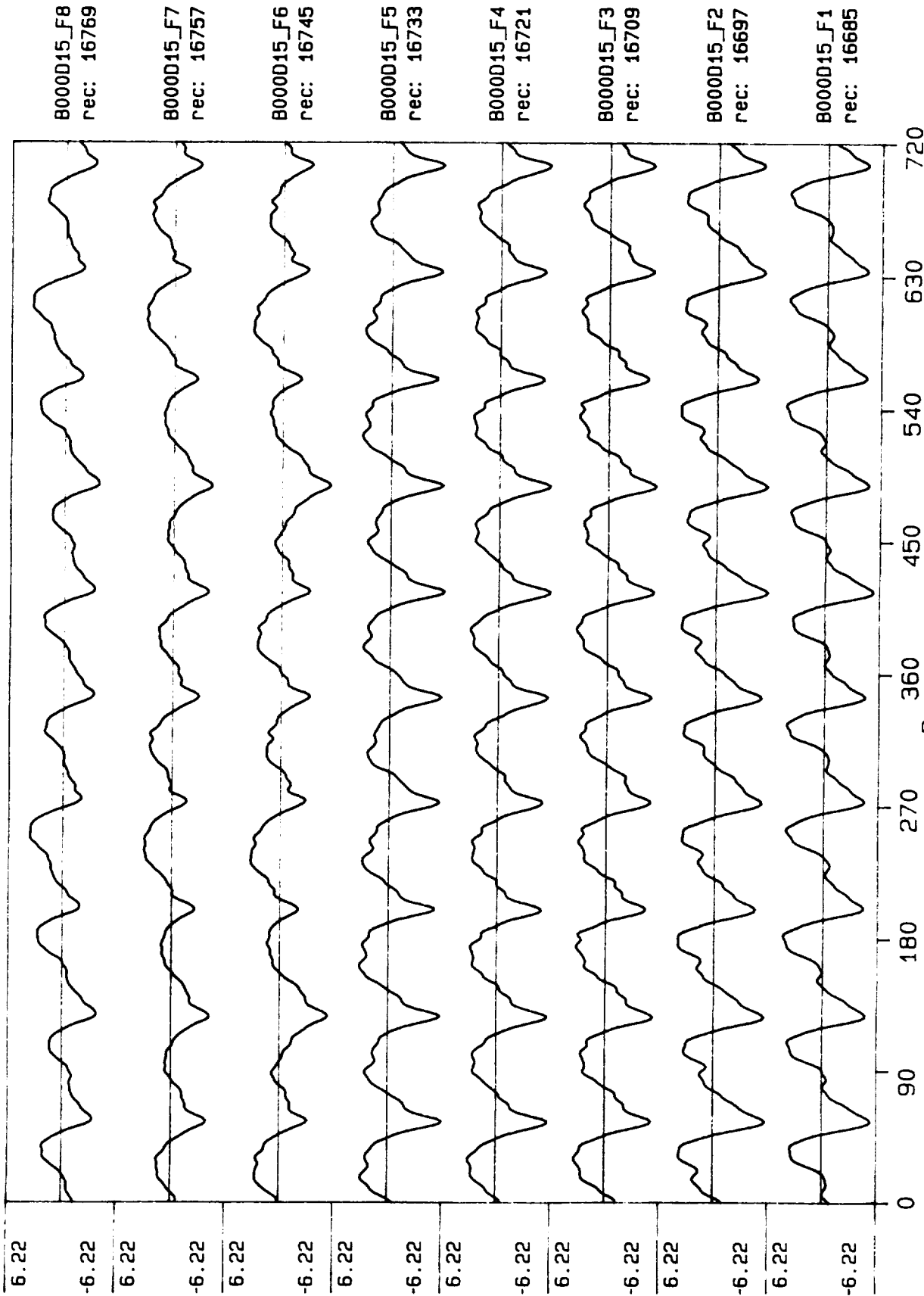
Process included: Calibration, Phase correction and DC filtering.



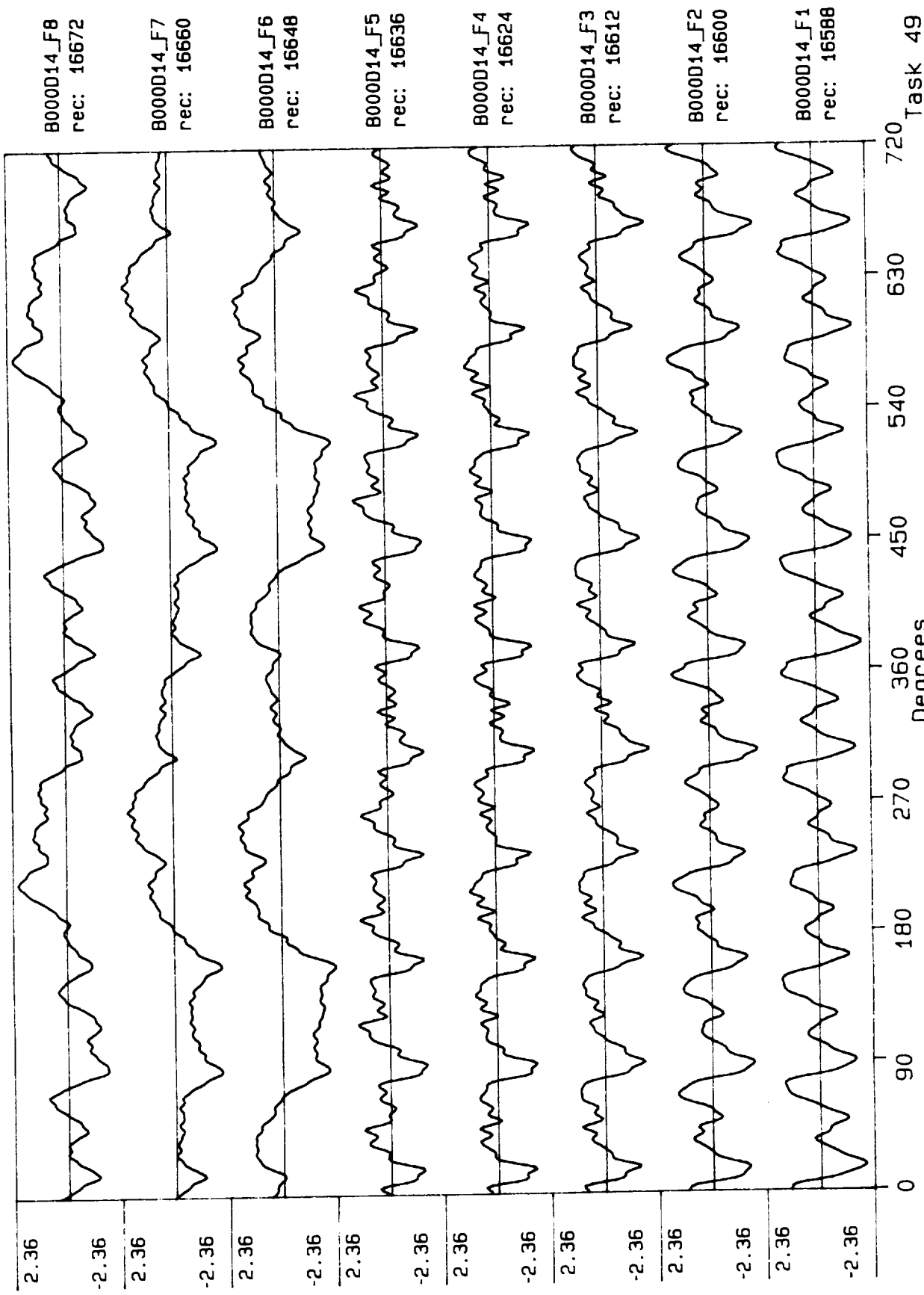
Process included: Calibration, Phase correction and DC filtering.



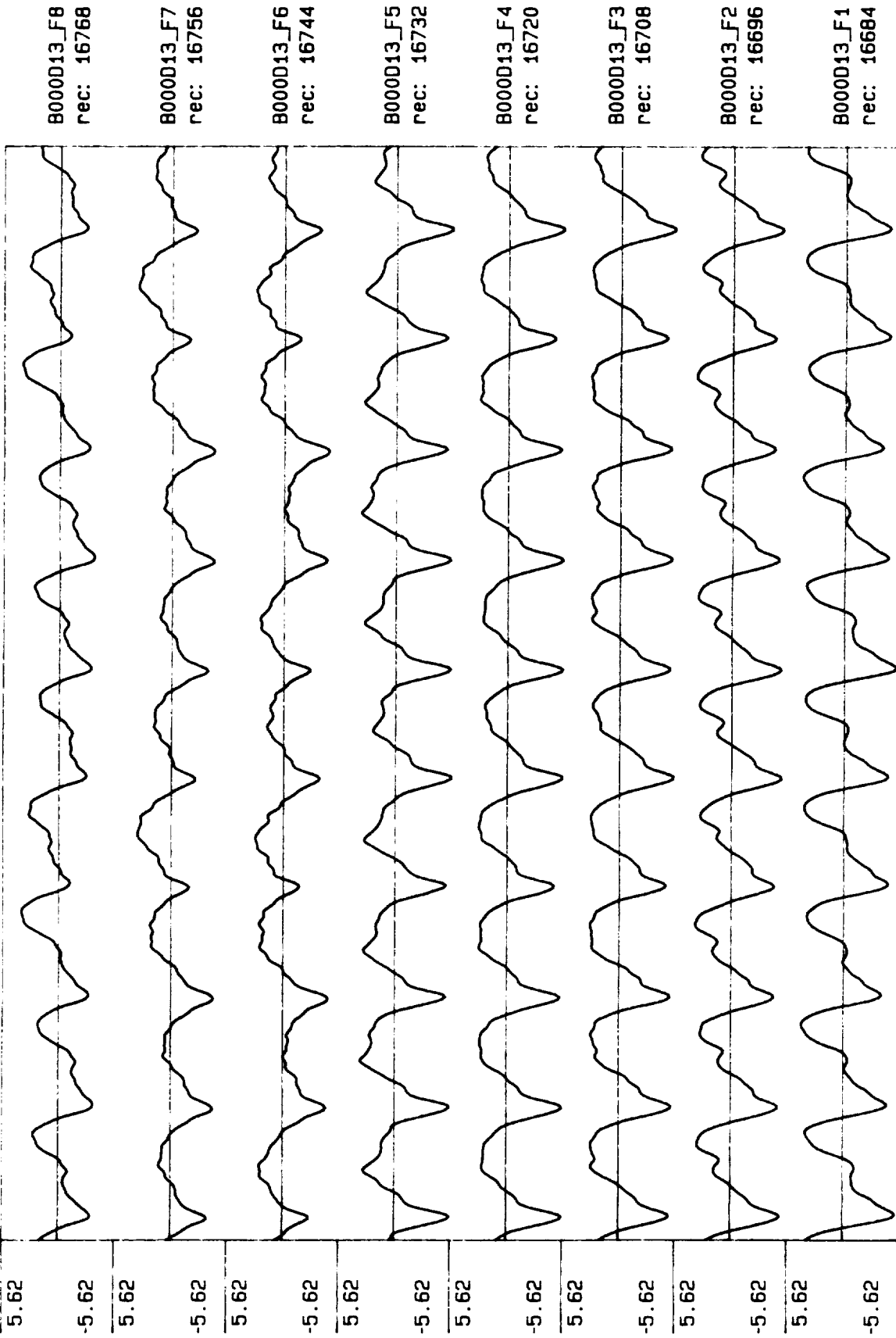
Process included: Calibration, Phase correction and DC filtering.



Process included: Calibration, Phase correction and DC filtering.

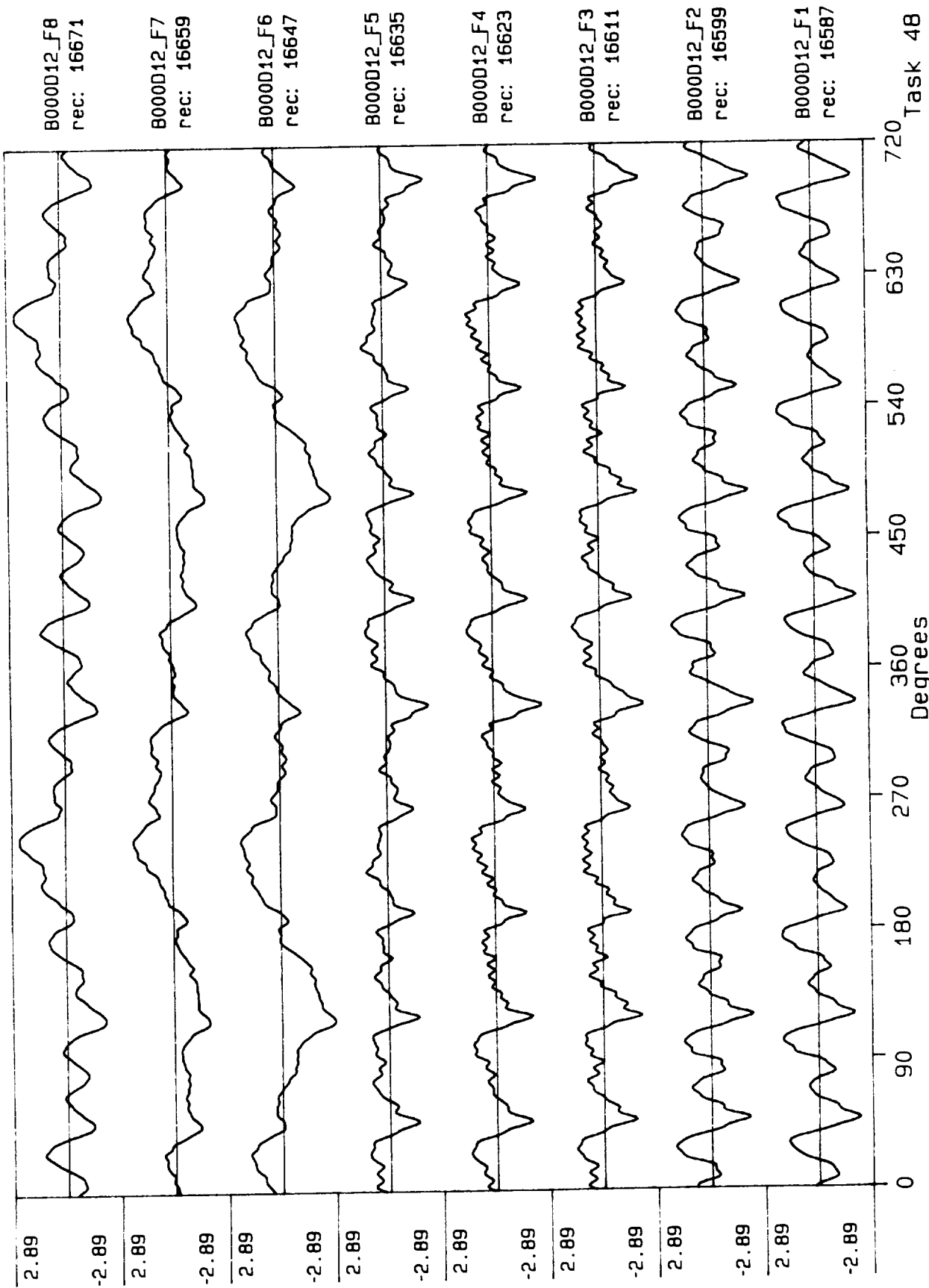


Process included: Calibration, Phase correction and DC filtering.

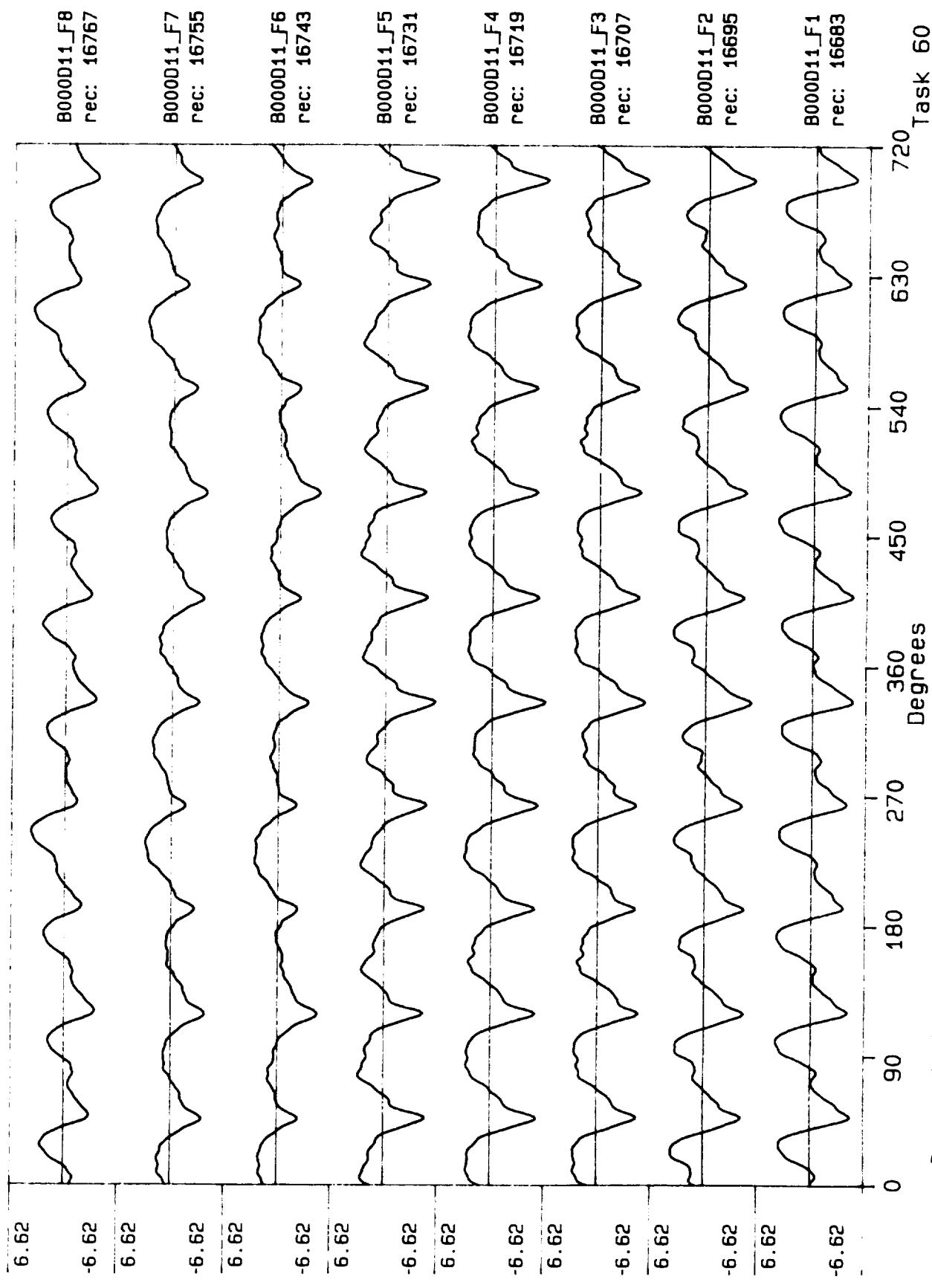


Process included: Calibration, Phase correction and DC filtering.

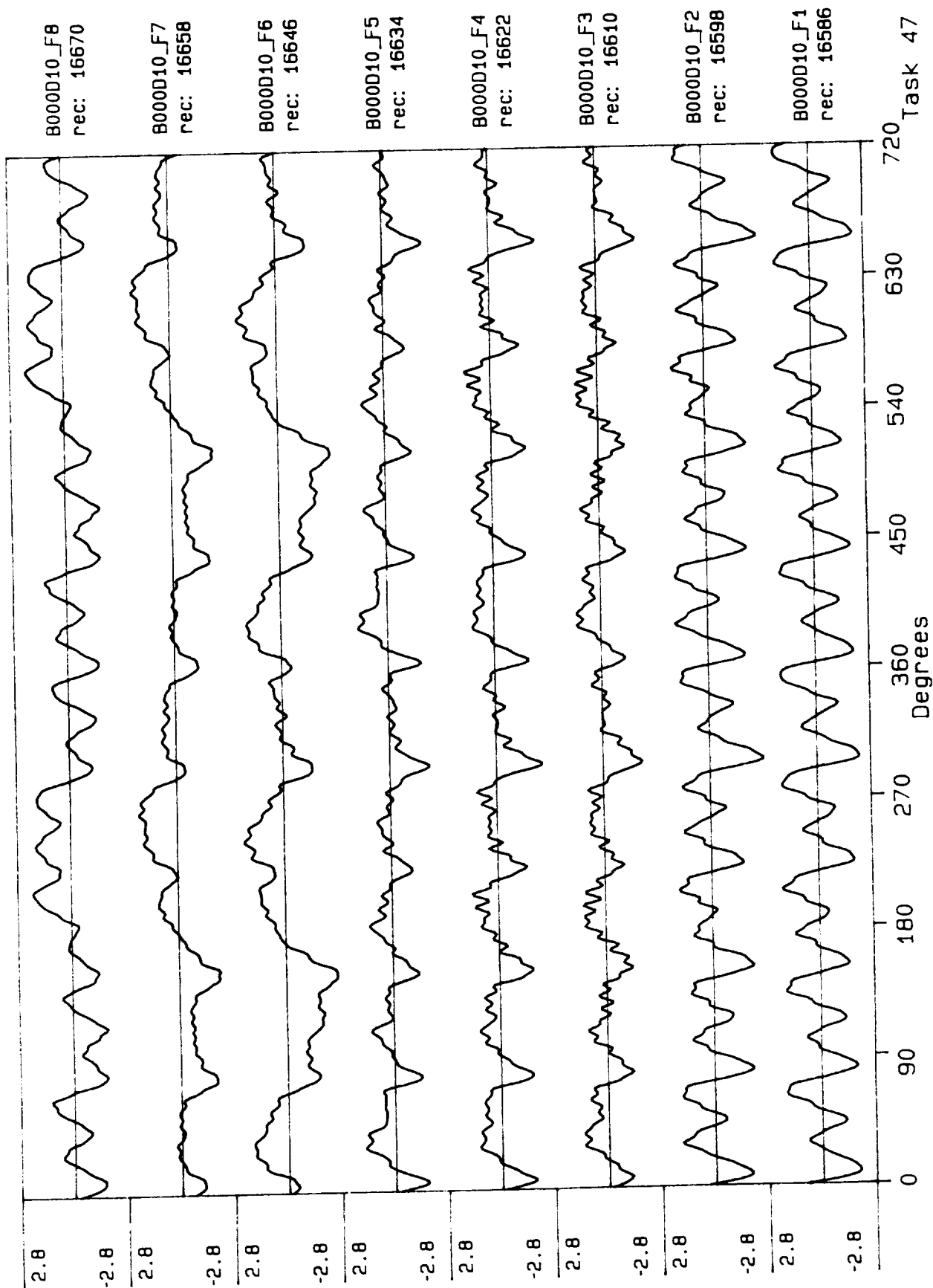
Task 61



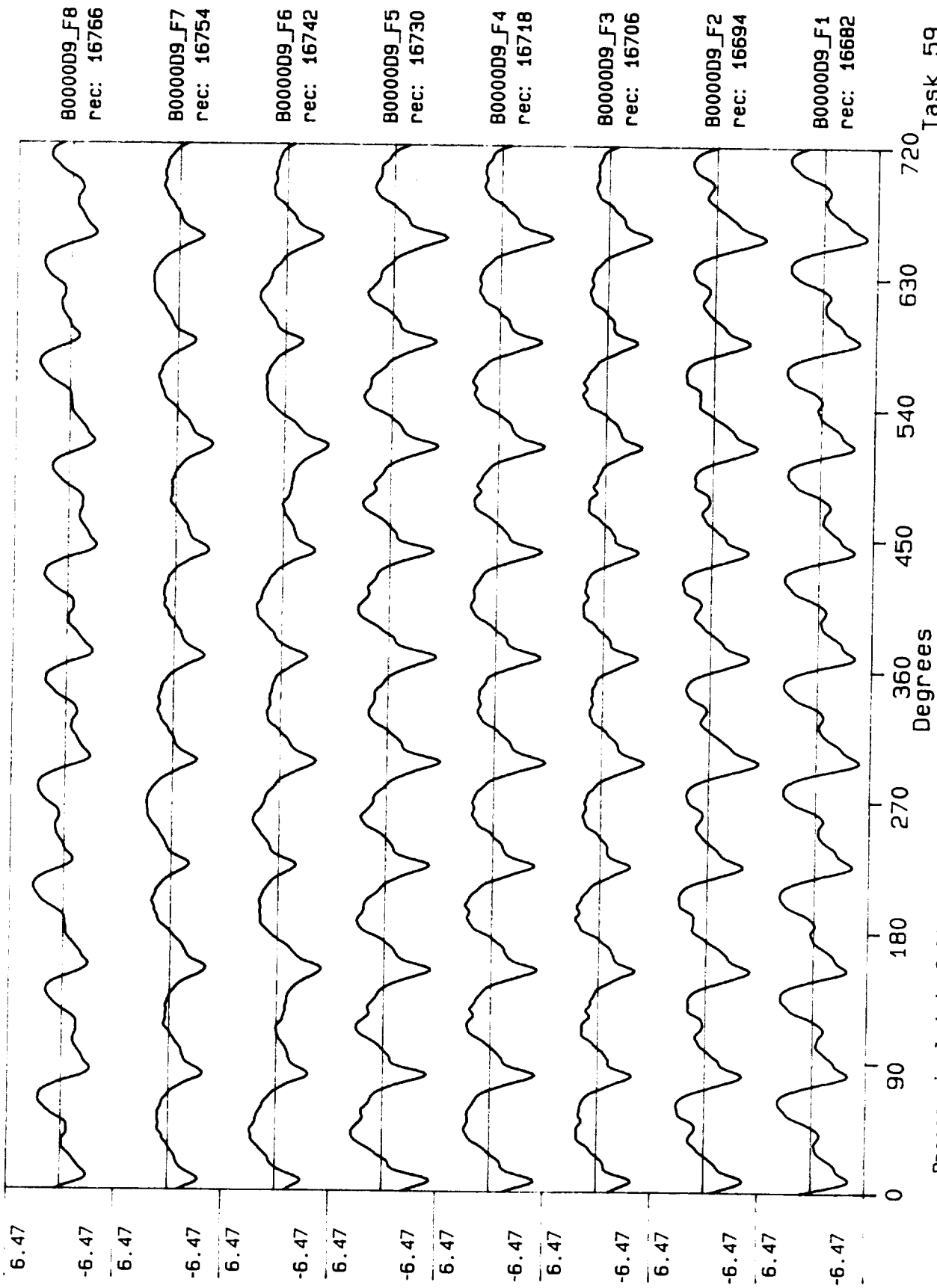
Process included: Calibration, Phase correction and DC filtering.



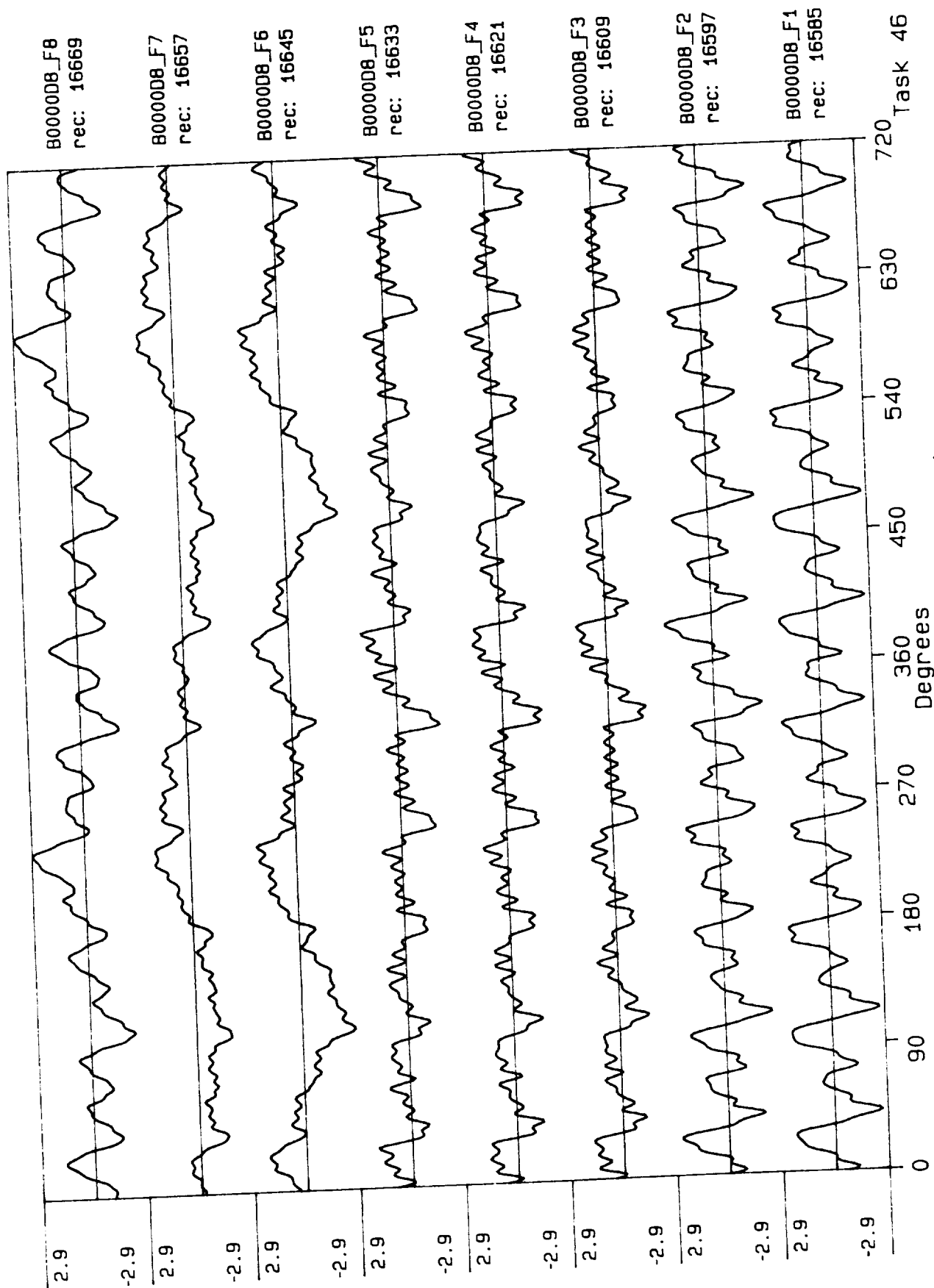
Process included: Calibration, Phase correction and DC filtering.



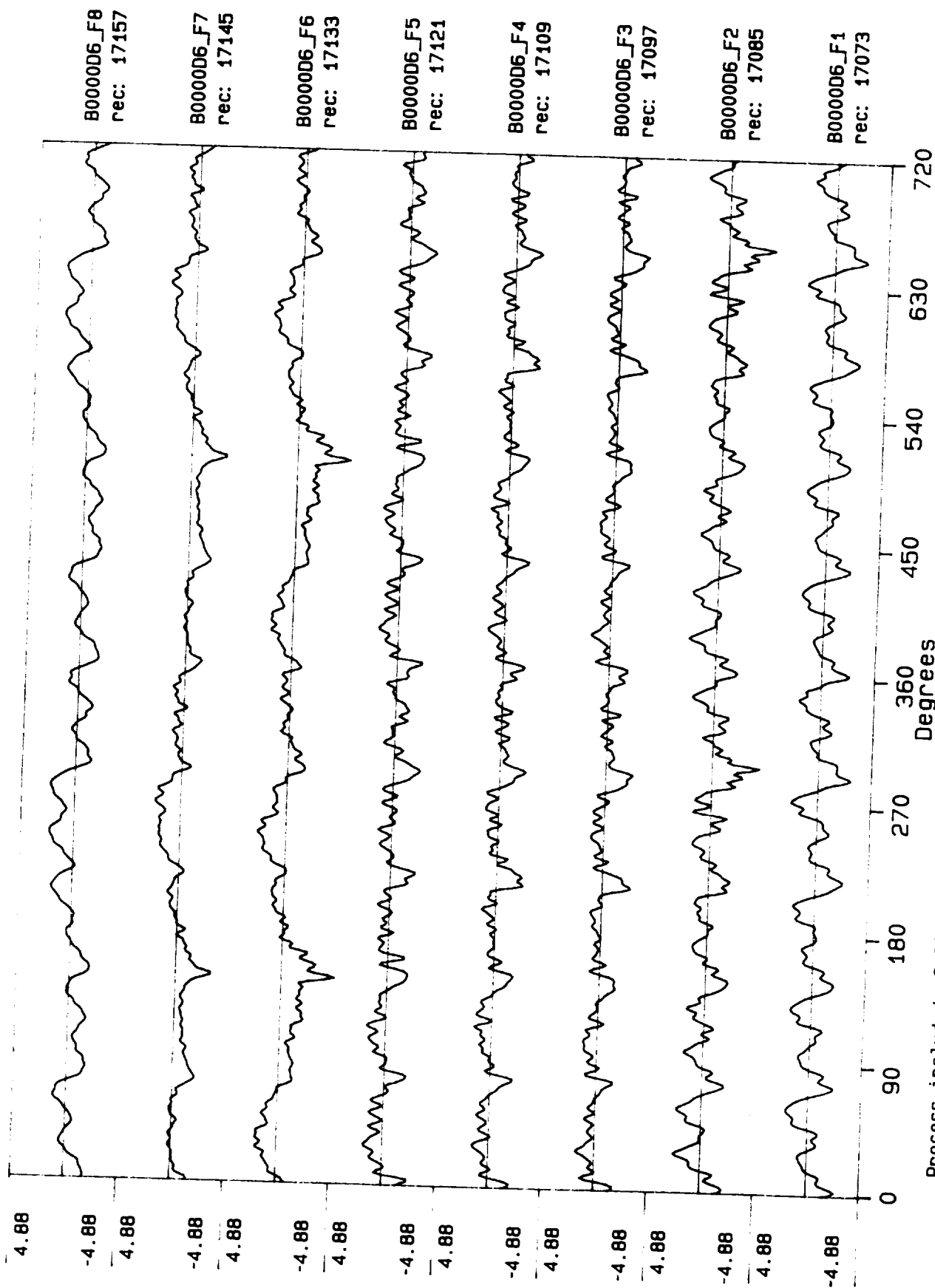
Process included: Calibration, Phase correction and DC filtering.



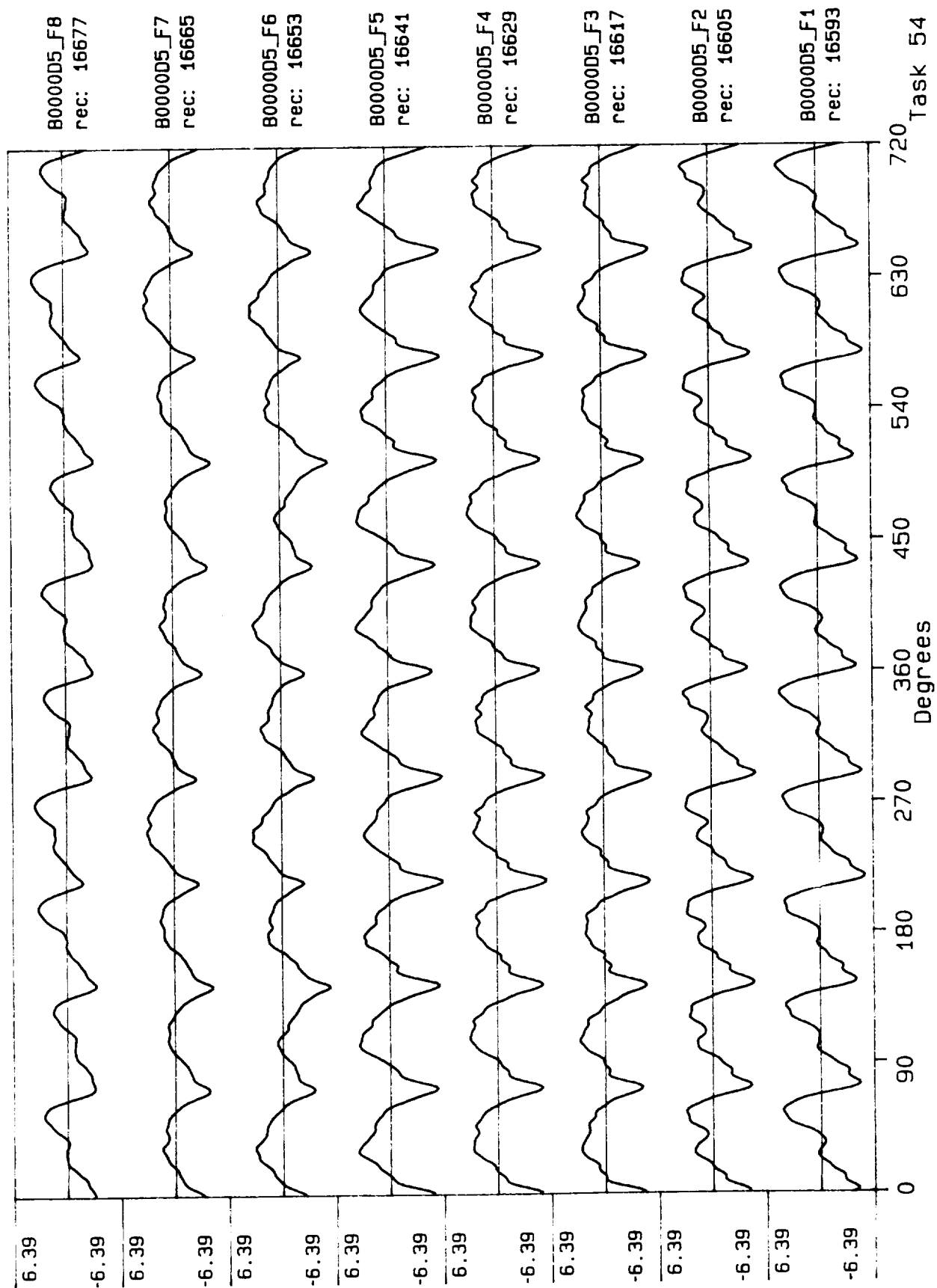
Process included: Calibration, Phase correction and DC filtering.



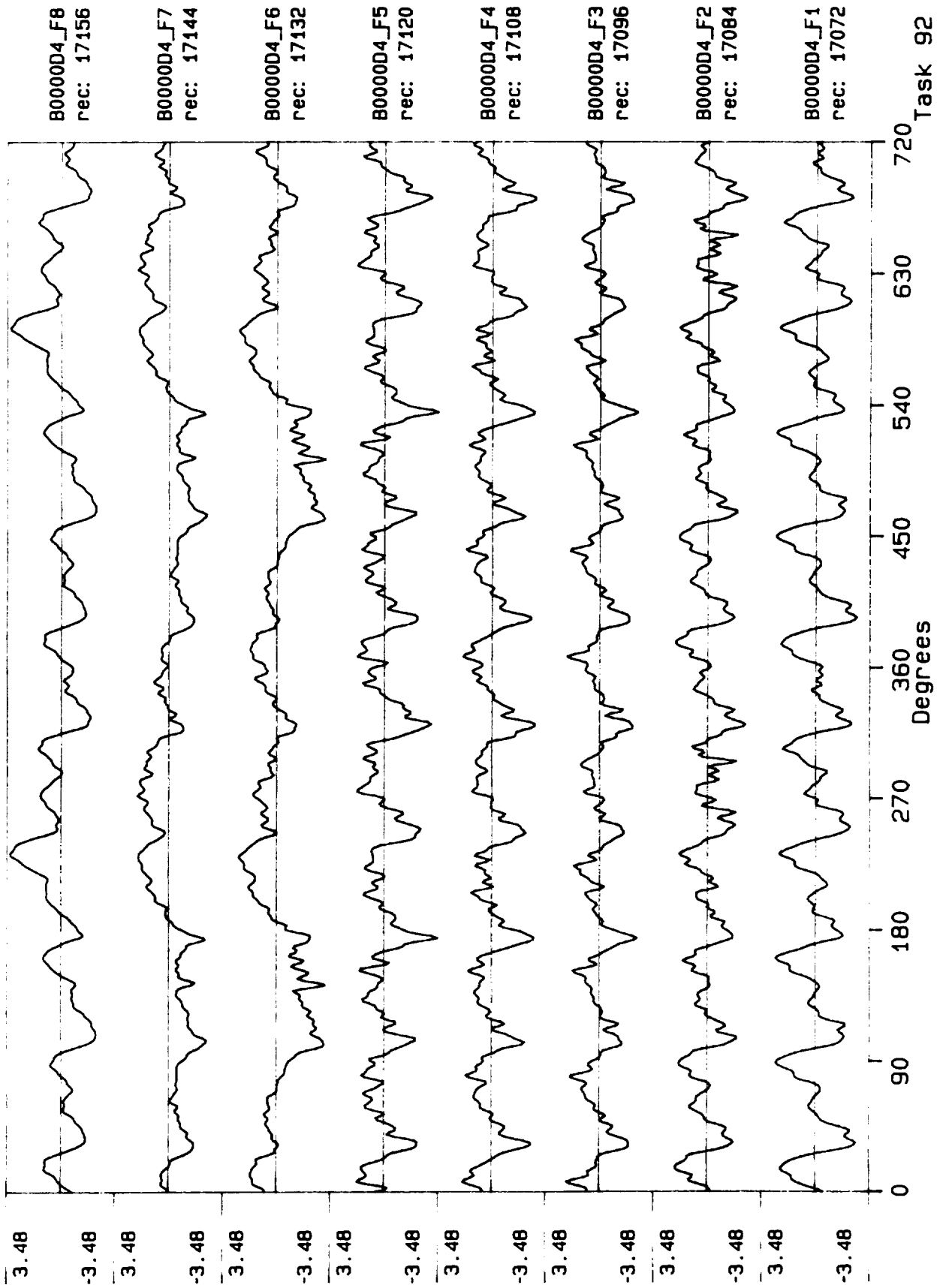
Process included: Calibration, Phase correction and DC filtering.

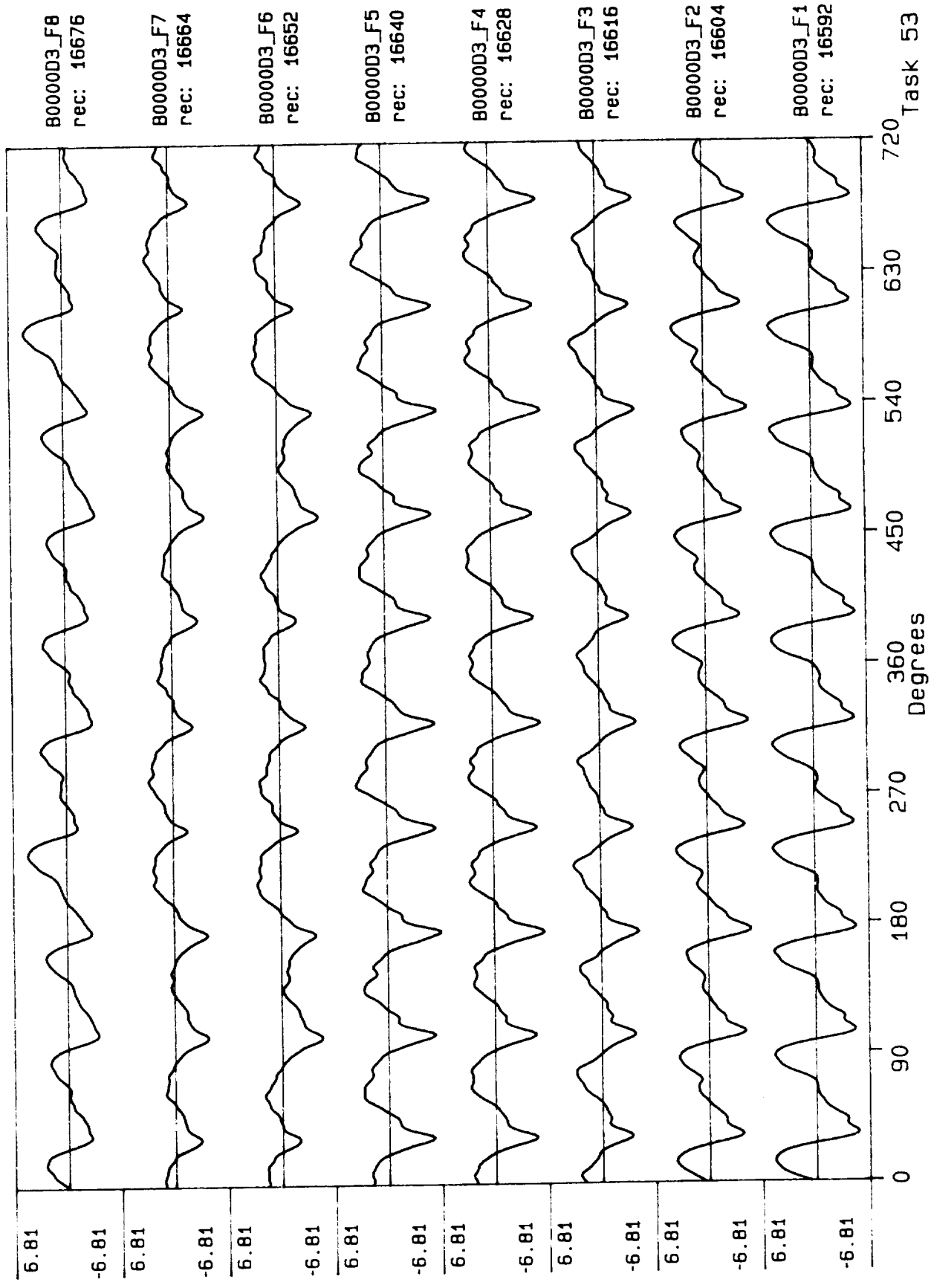


Process included: Calibration, Phase correction and DC filtering.

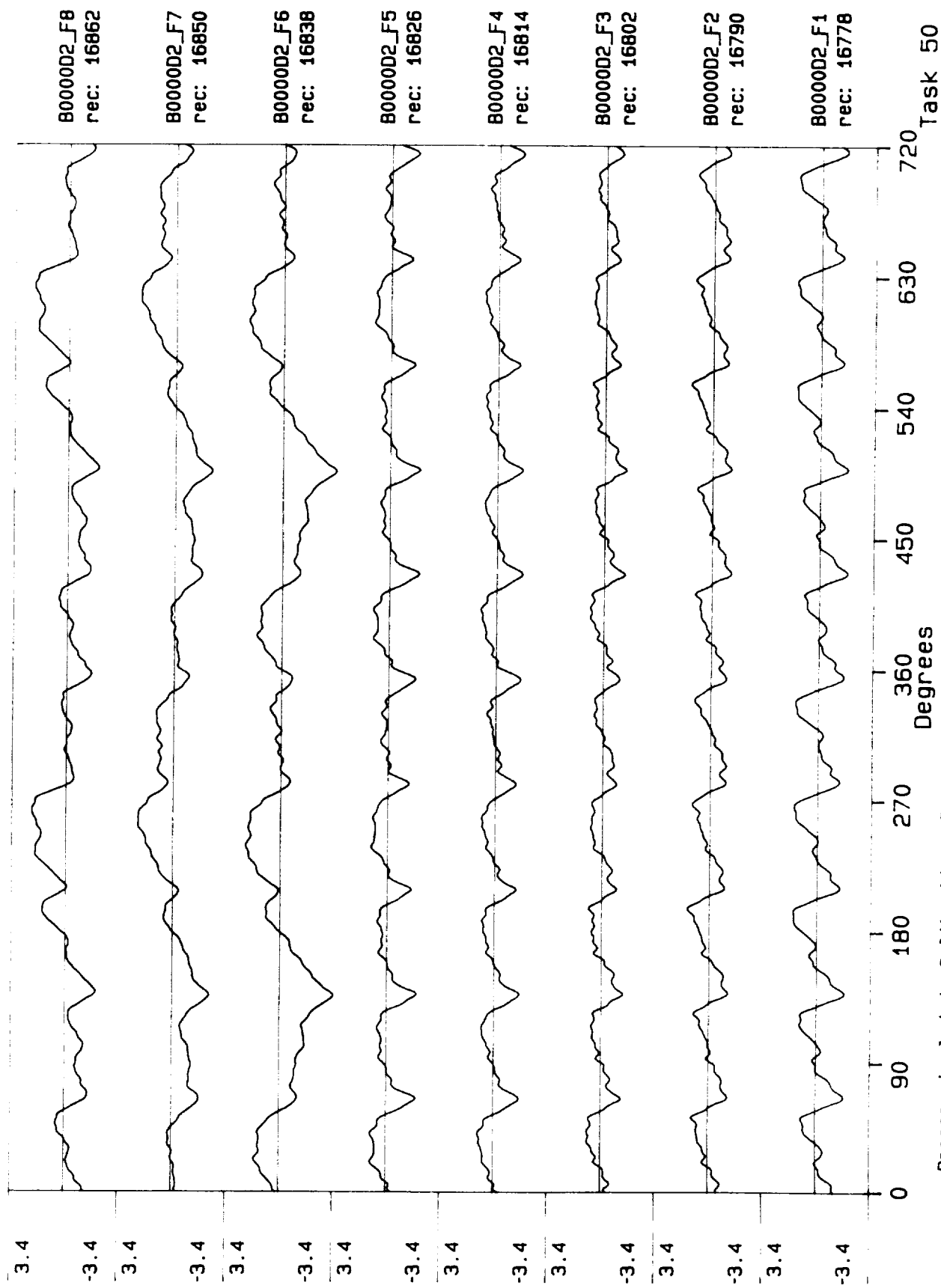


Process included: Calibration, Phase correction and DC filtering.

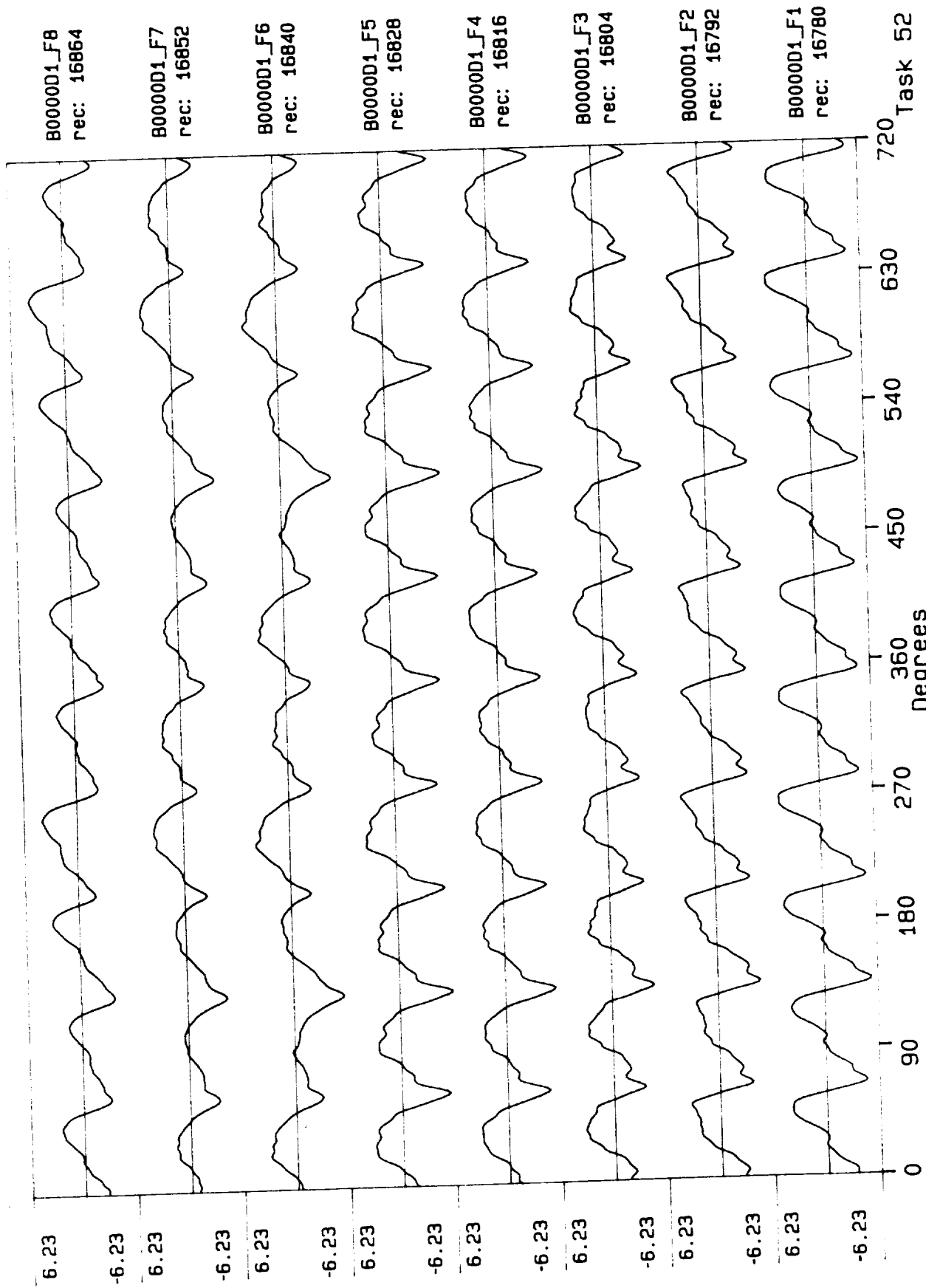




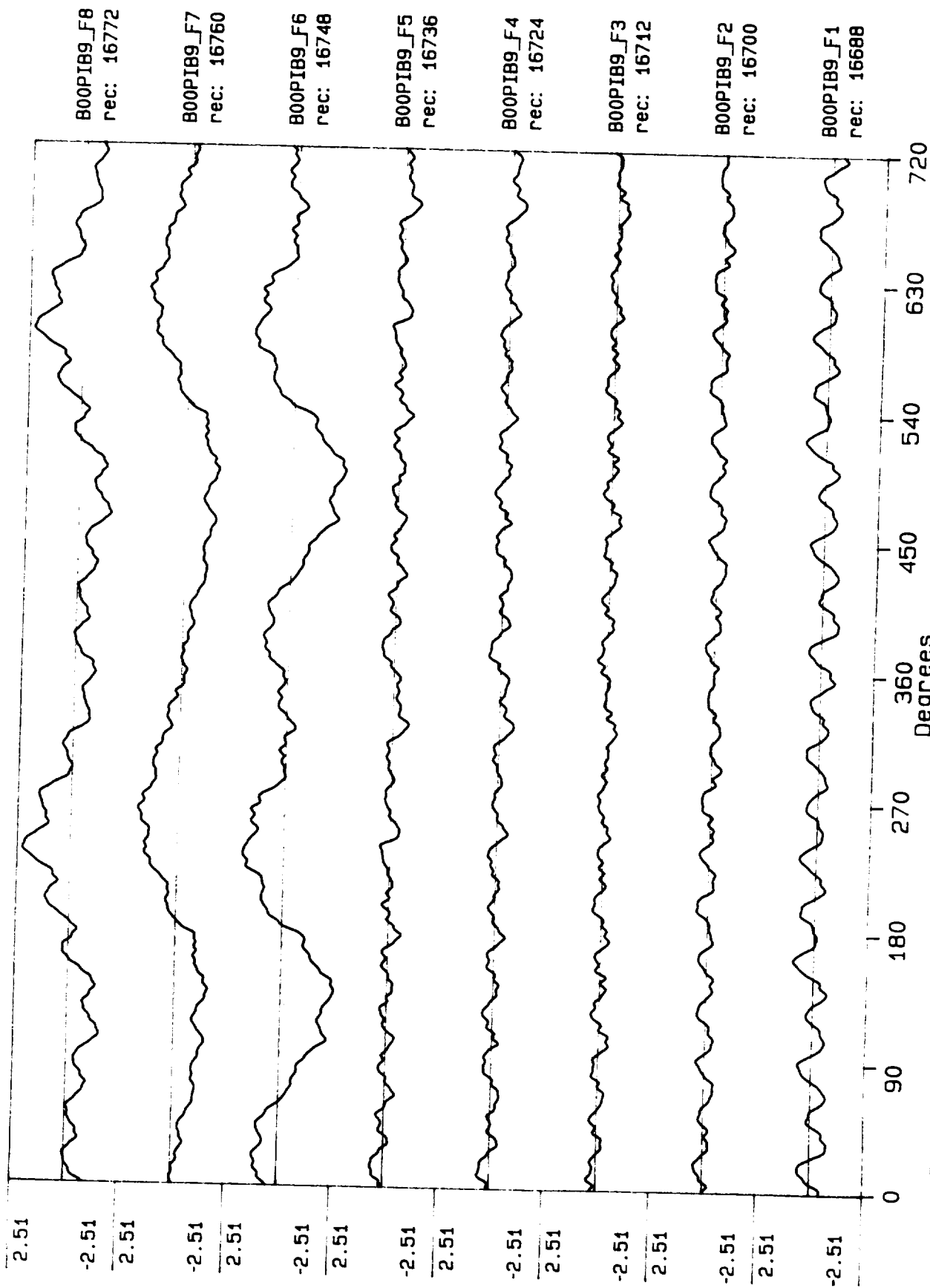
Process included: Calibration, Phase correction and DC filtering.

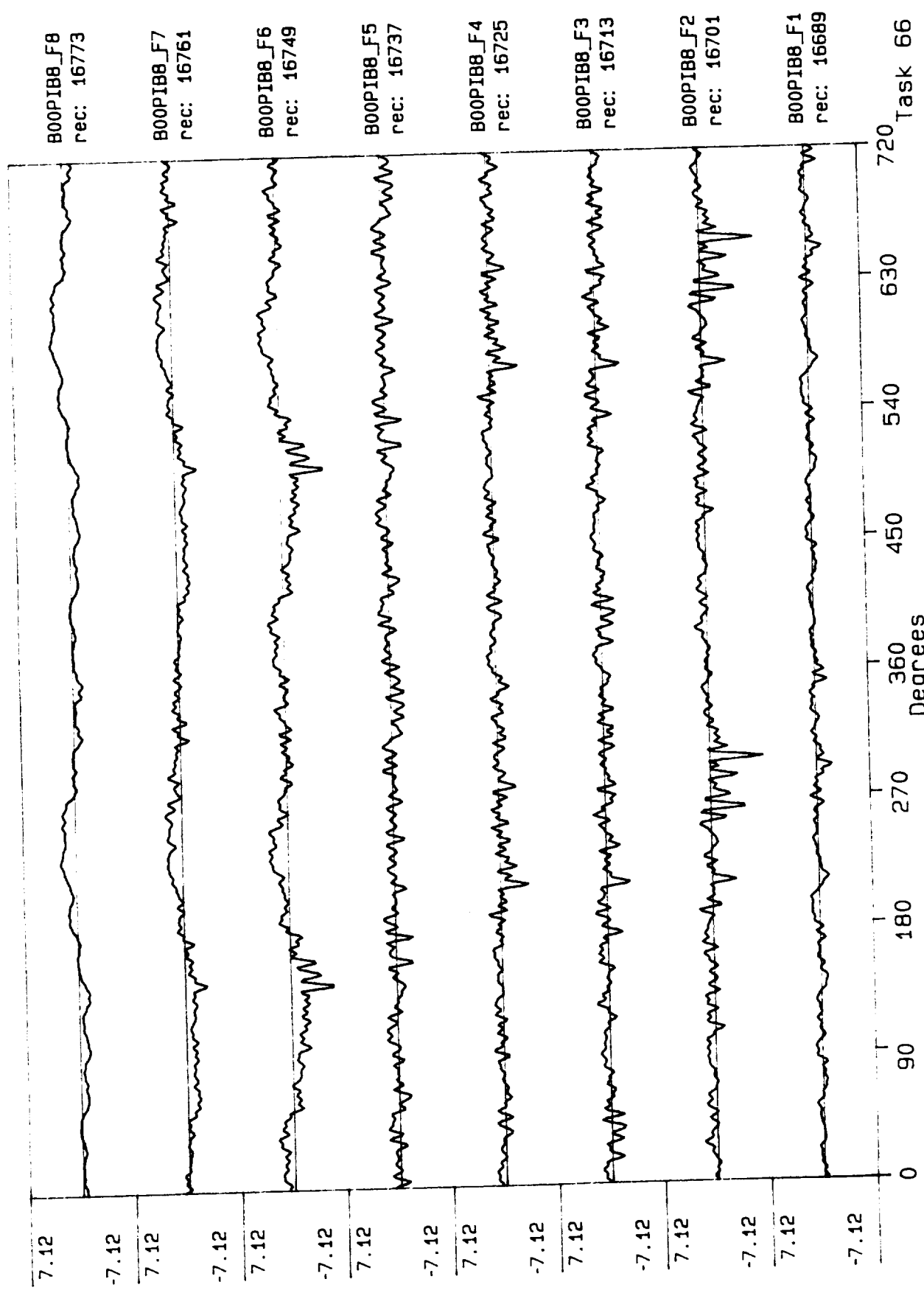


Process included: Calibration, Phase correction and DC filtering.

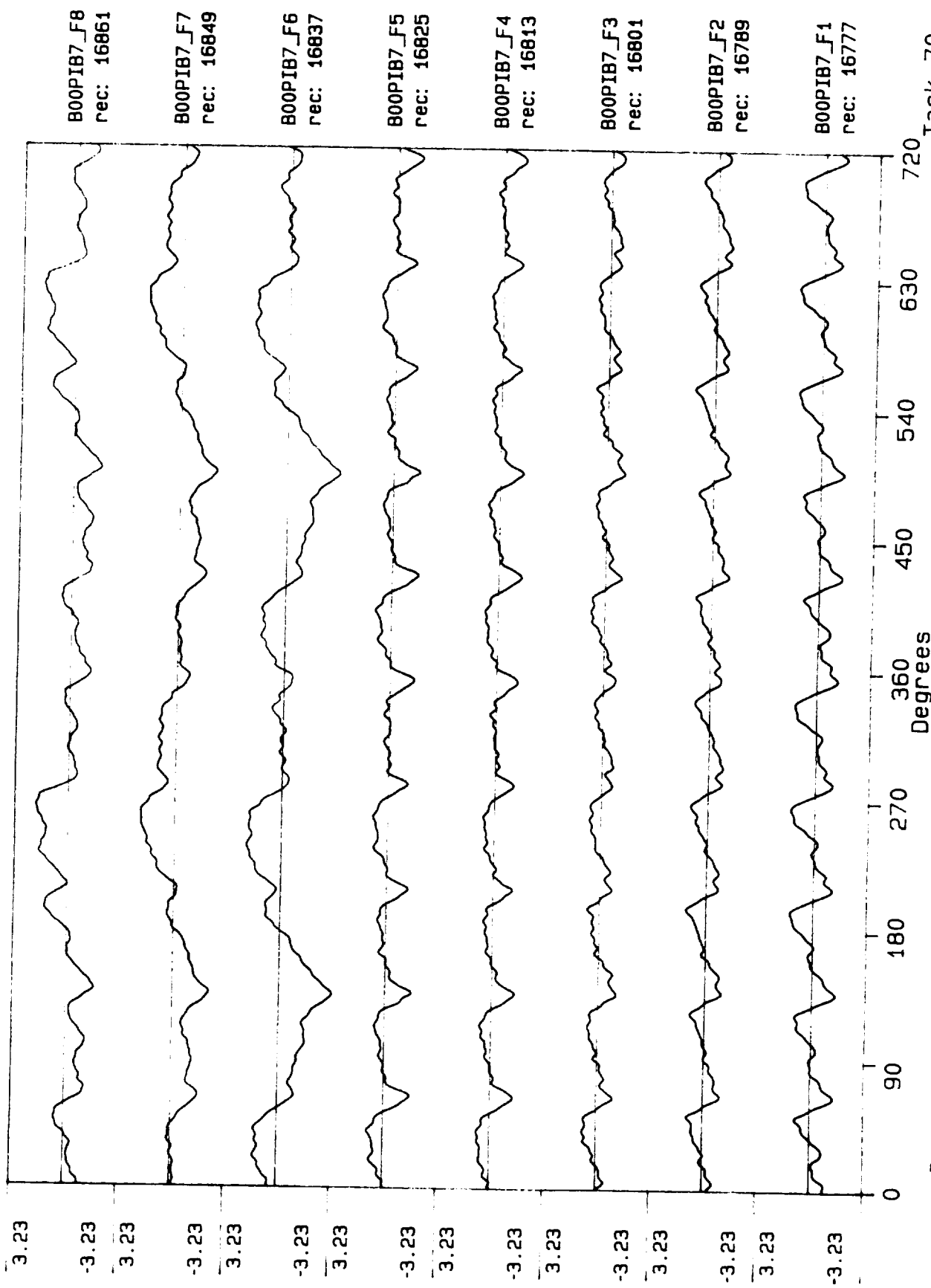


Process included: Calibration, Phase correction and DC filtering.

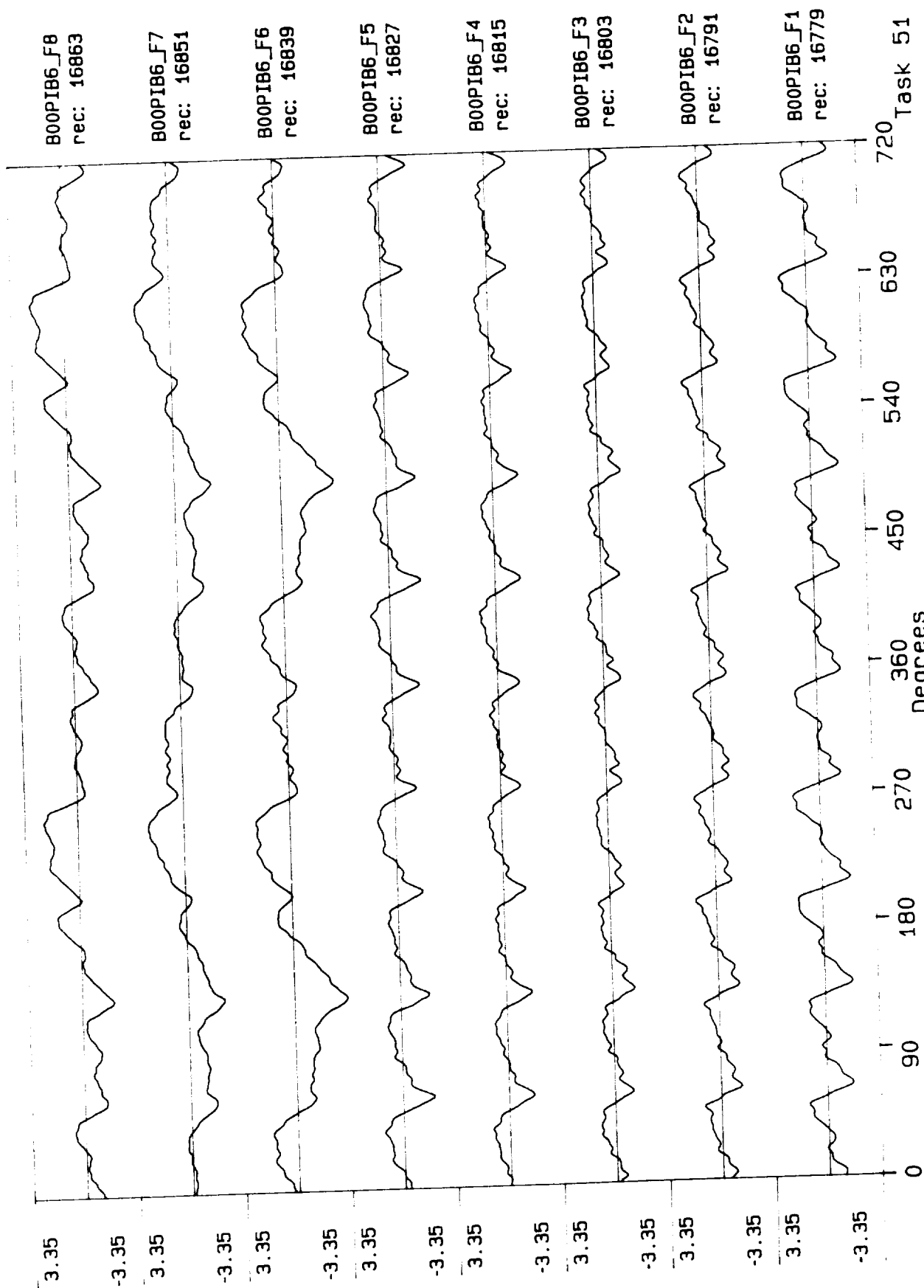




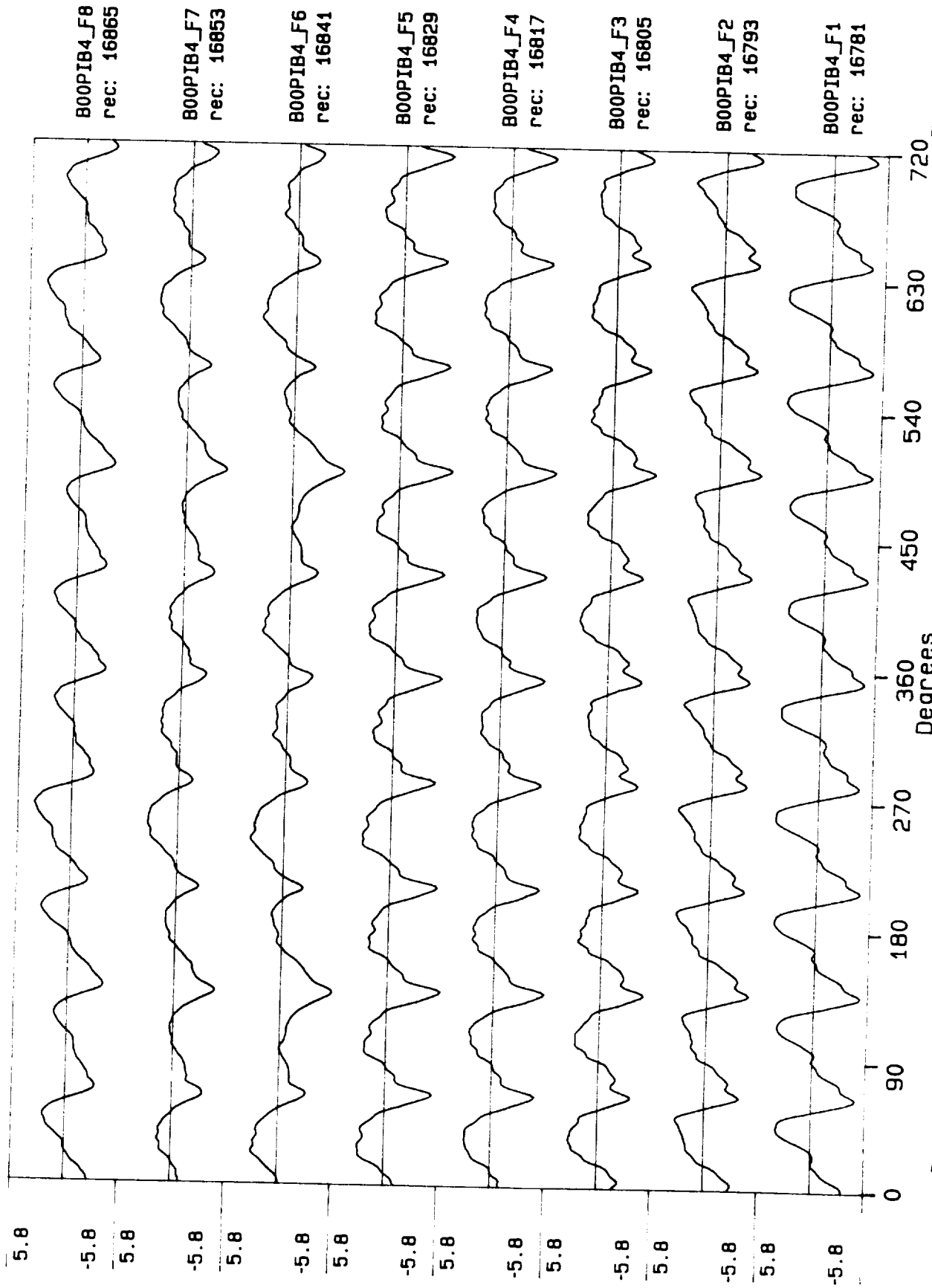
Process included: Calibration, Phase correction and DC filtering.



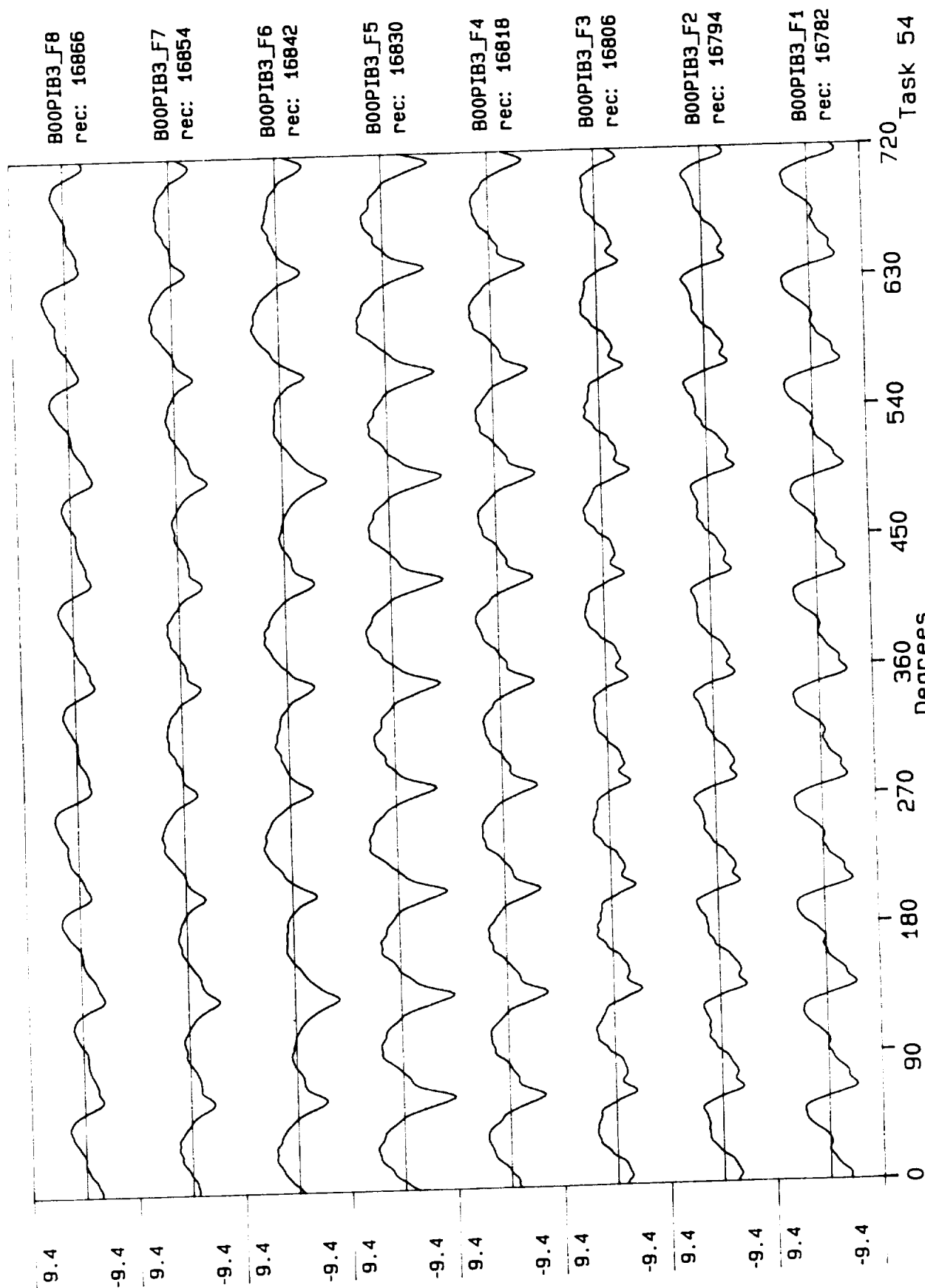
Process included: Calibration, Phase correction and DC filtering.



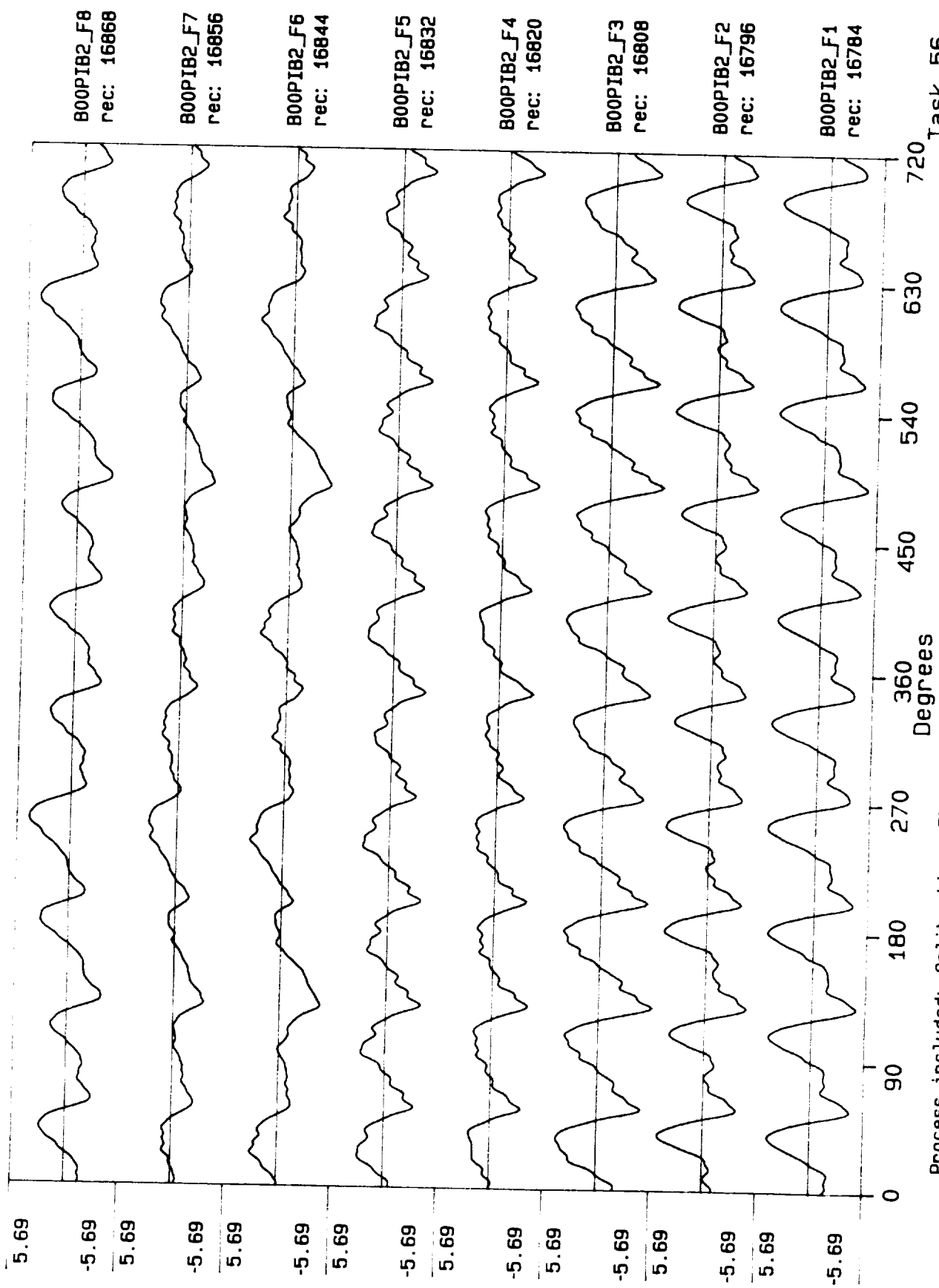
Process included: Calibration, Phase correction and DC filtering.

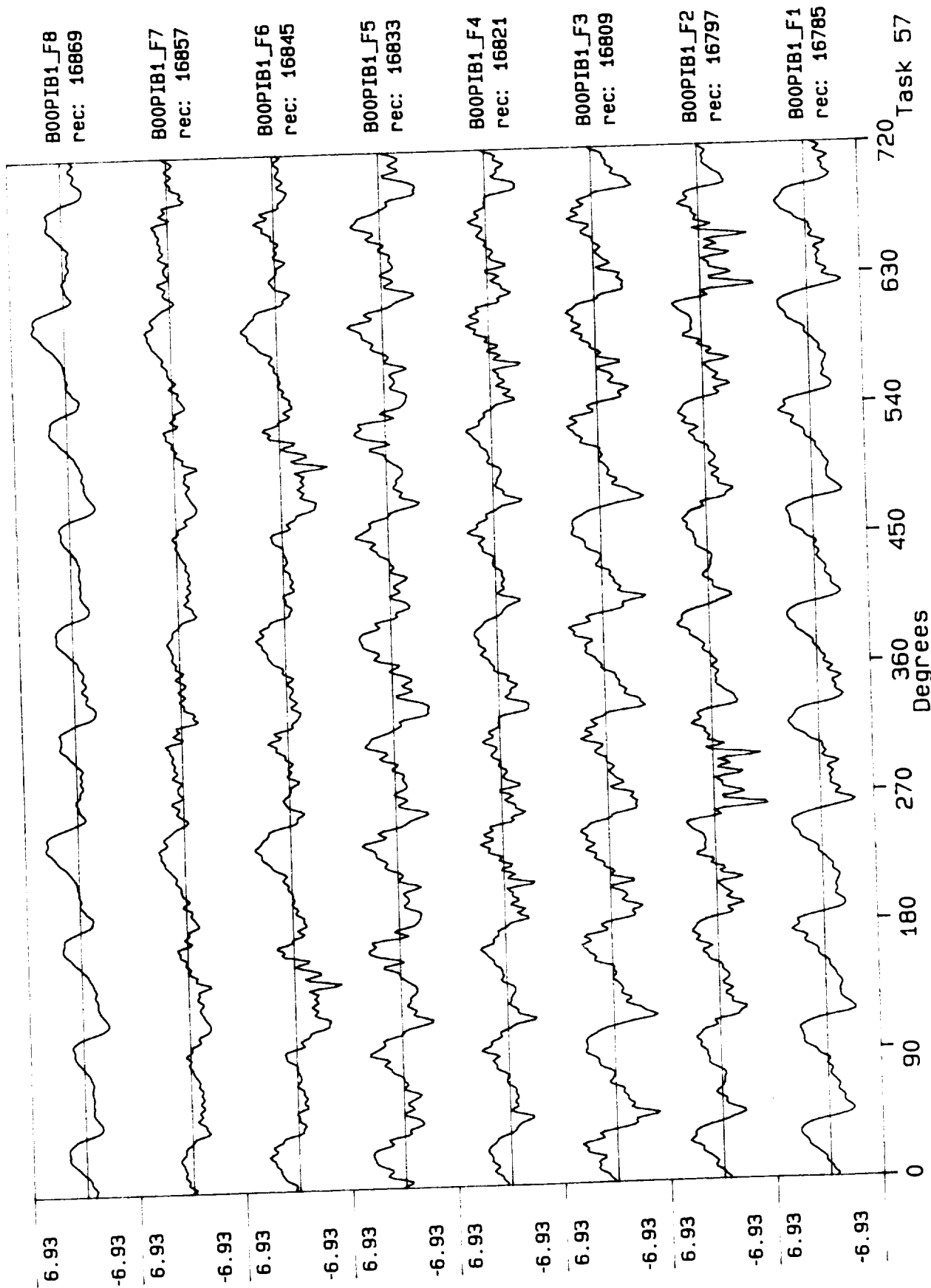


Process included: Calibration, Phase correction and DC filtering.

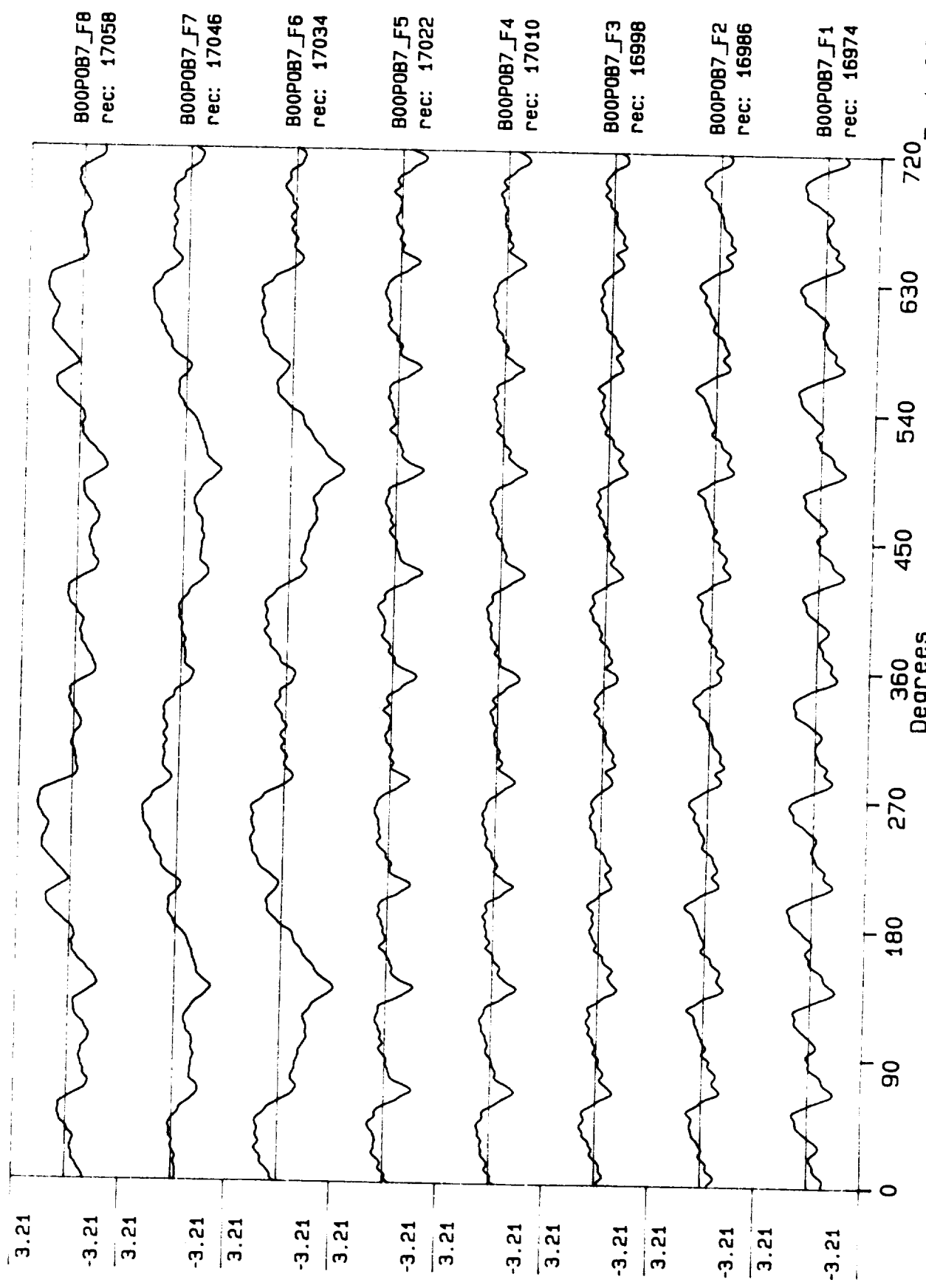


Process included: Calibration, Phase correction and DC filtering.

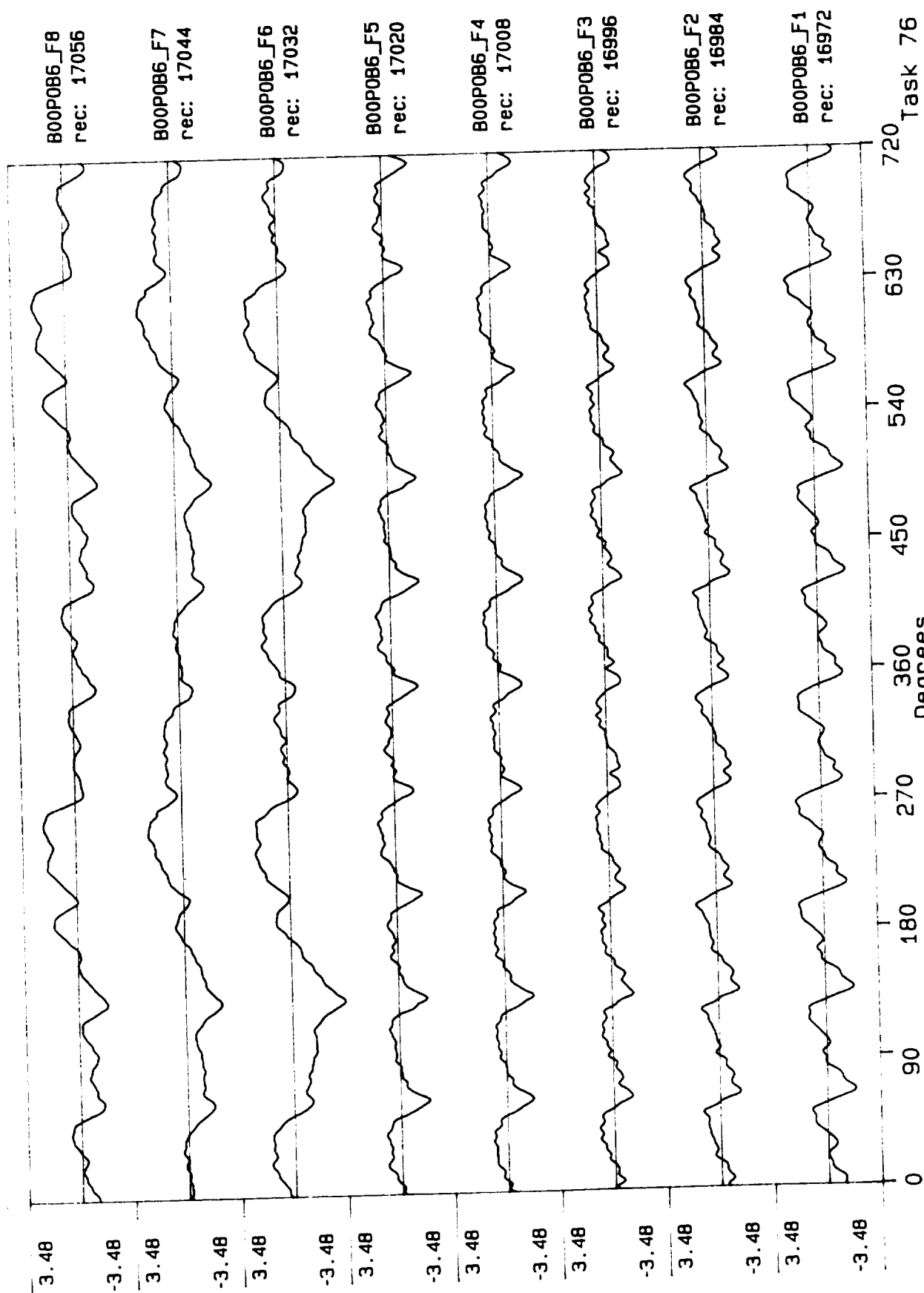




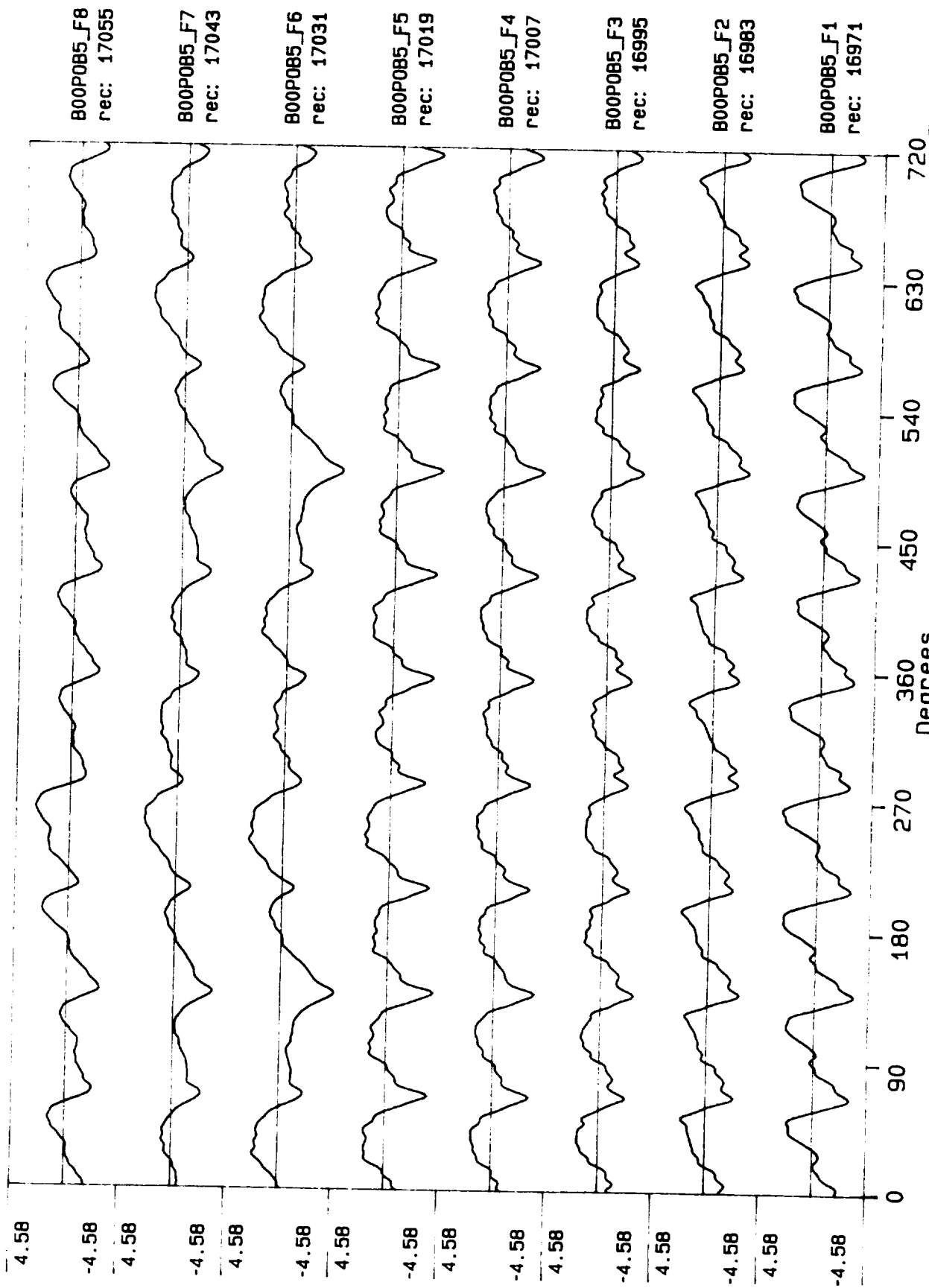
Process included: Calibration, Phase correction and DC filtering.



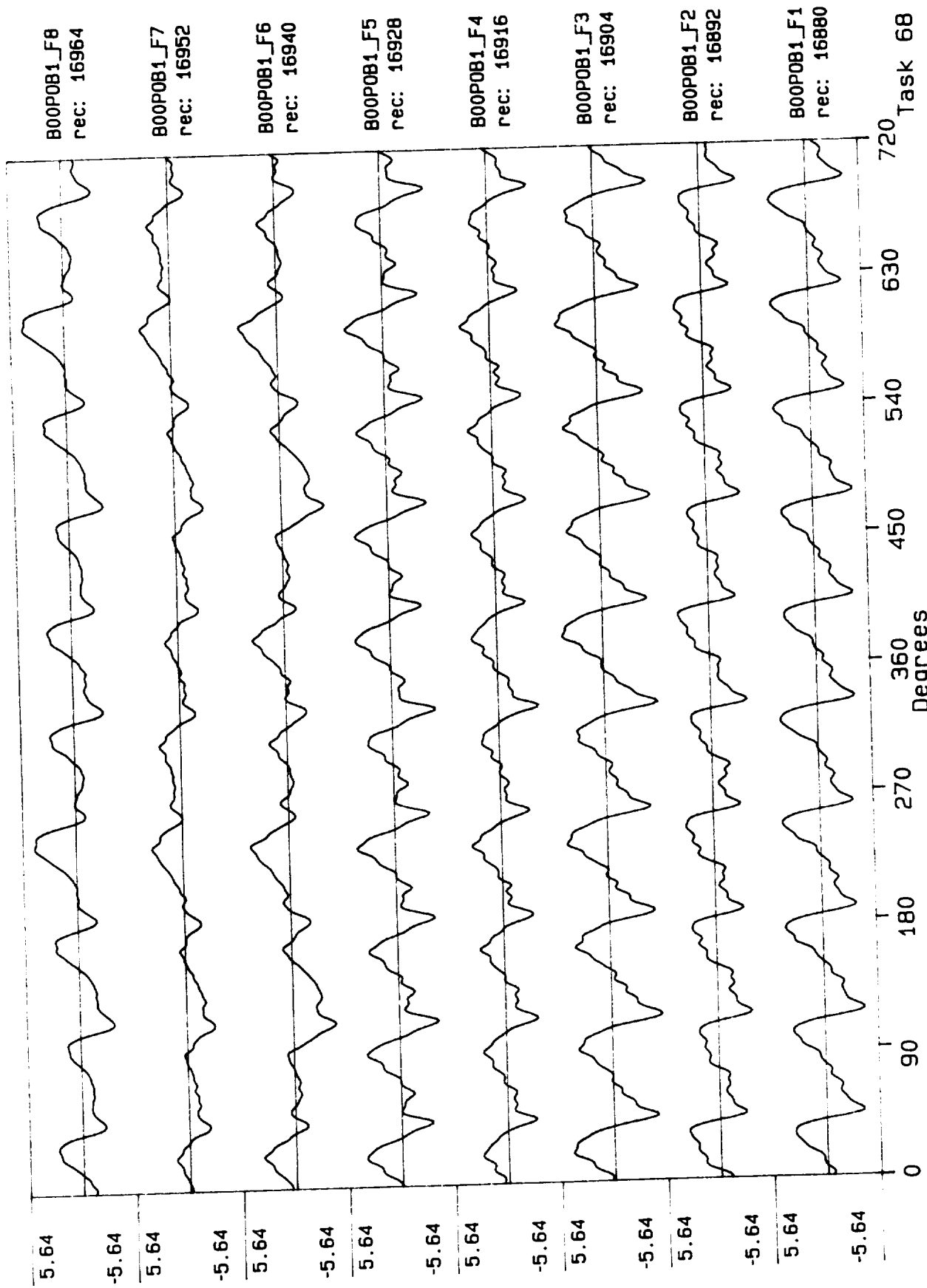
Process included: Calibration, Phase correction and DC filtering.



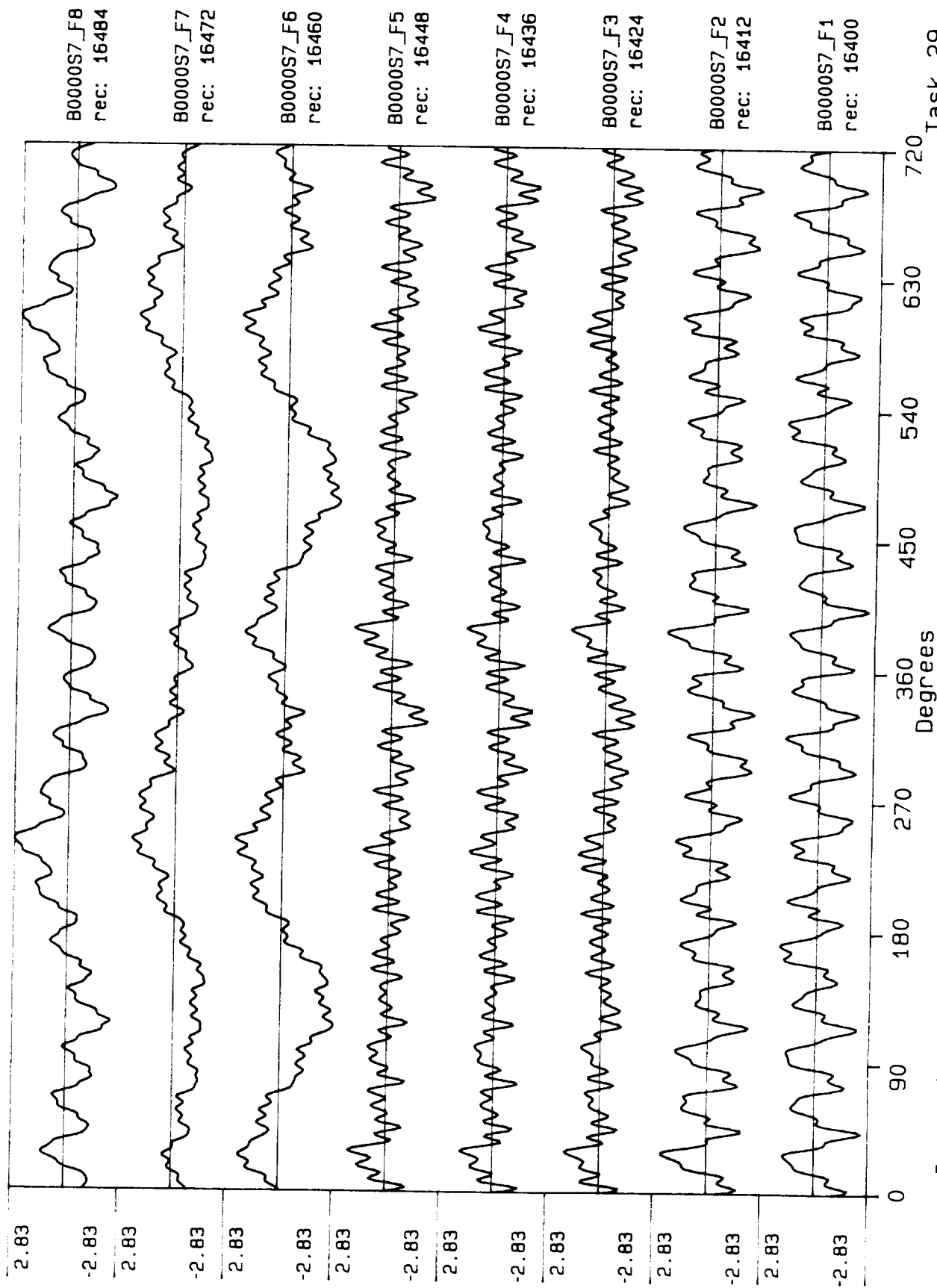
Process included: Calibration, Phase correction and DC filtering.



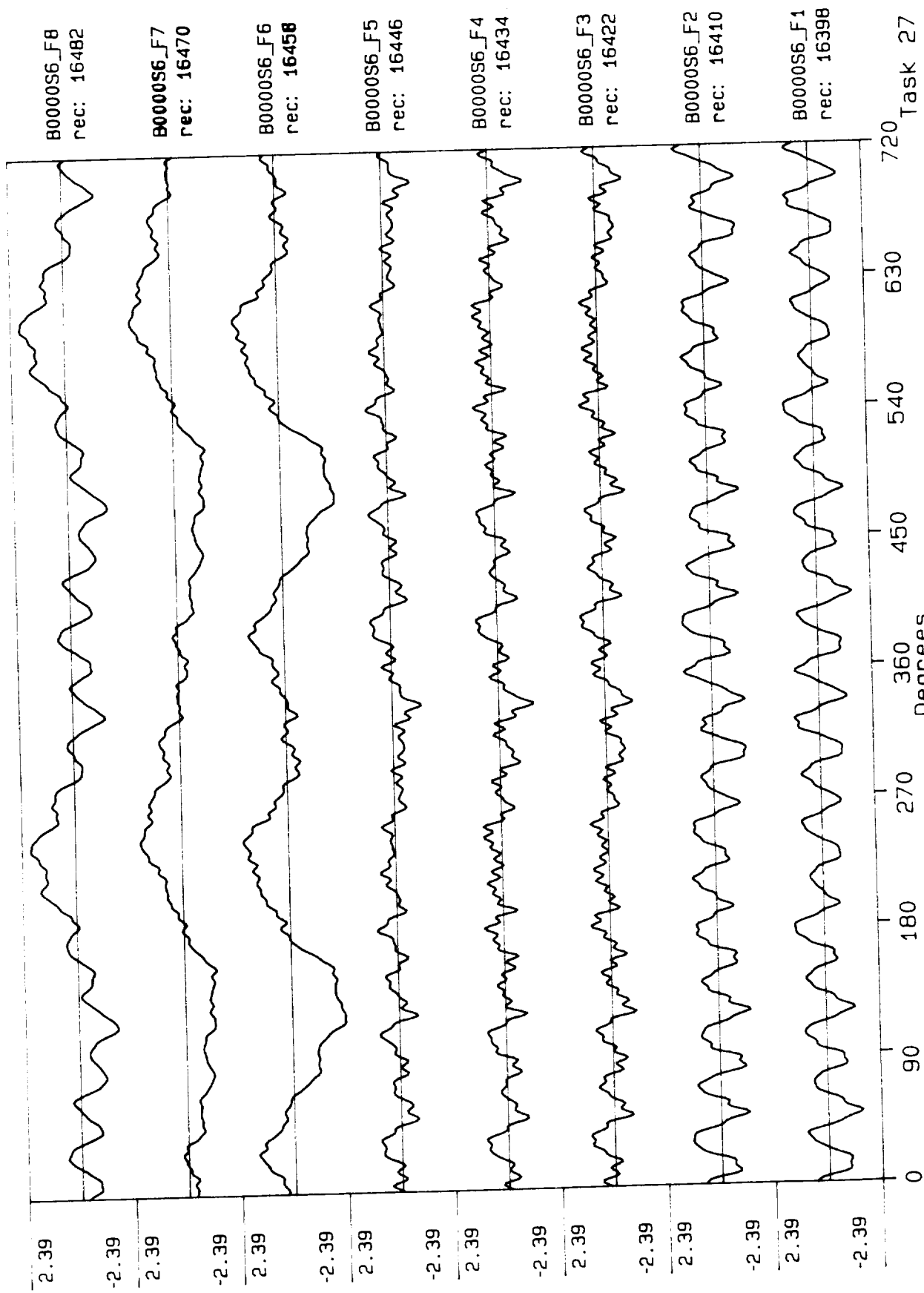
Process included: Calibration, Phase correction and DC filtering.



Process included: Calibration, Phase correction and DC filtering.

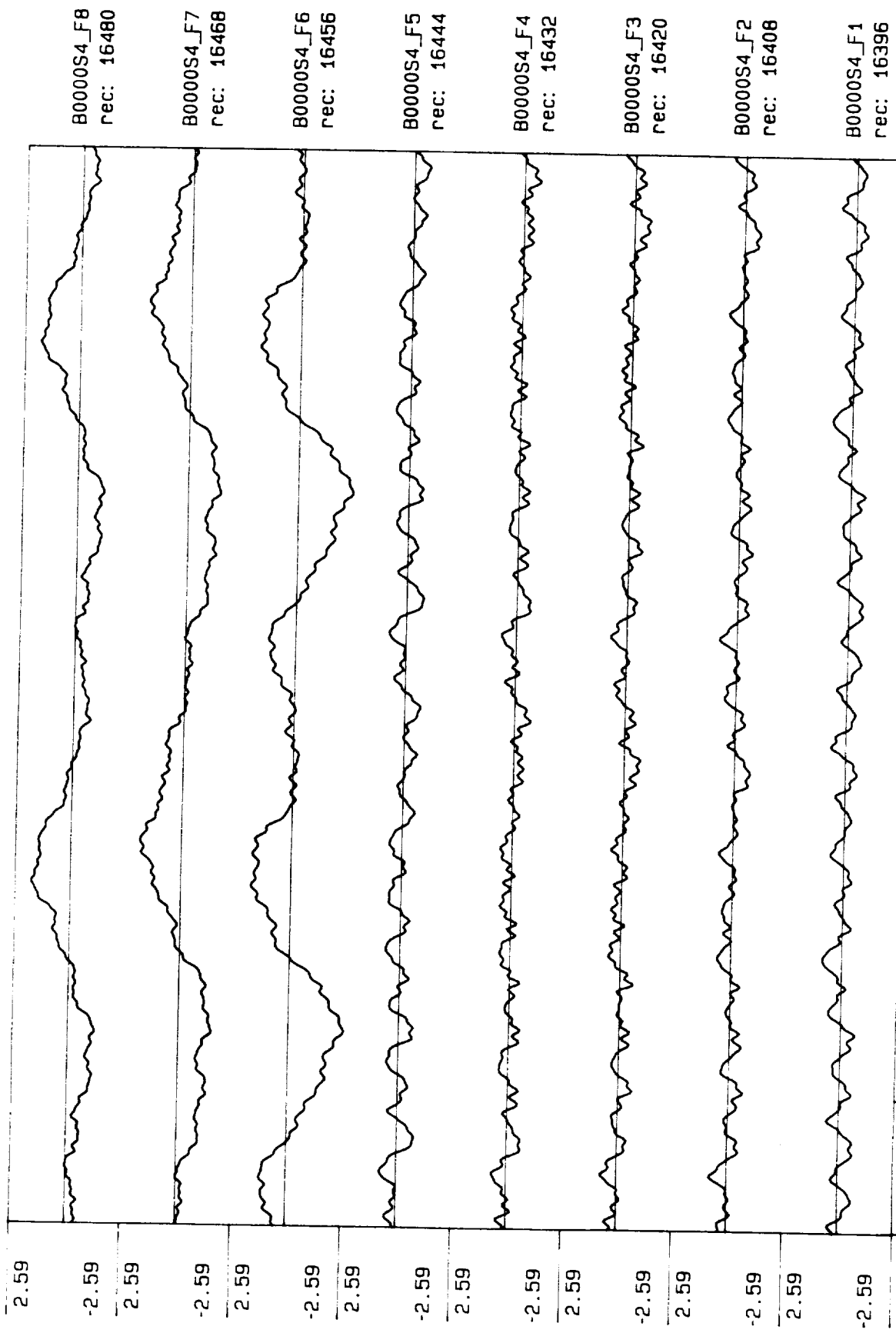


Process included: Calibration, Phase correction and DC filtering.



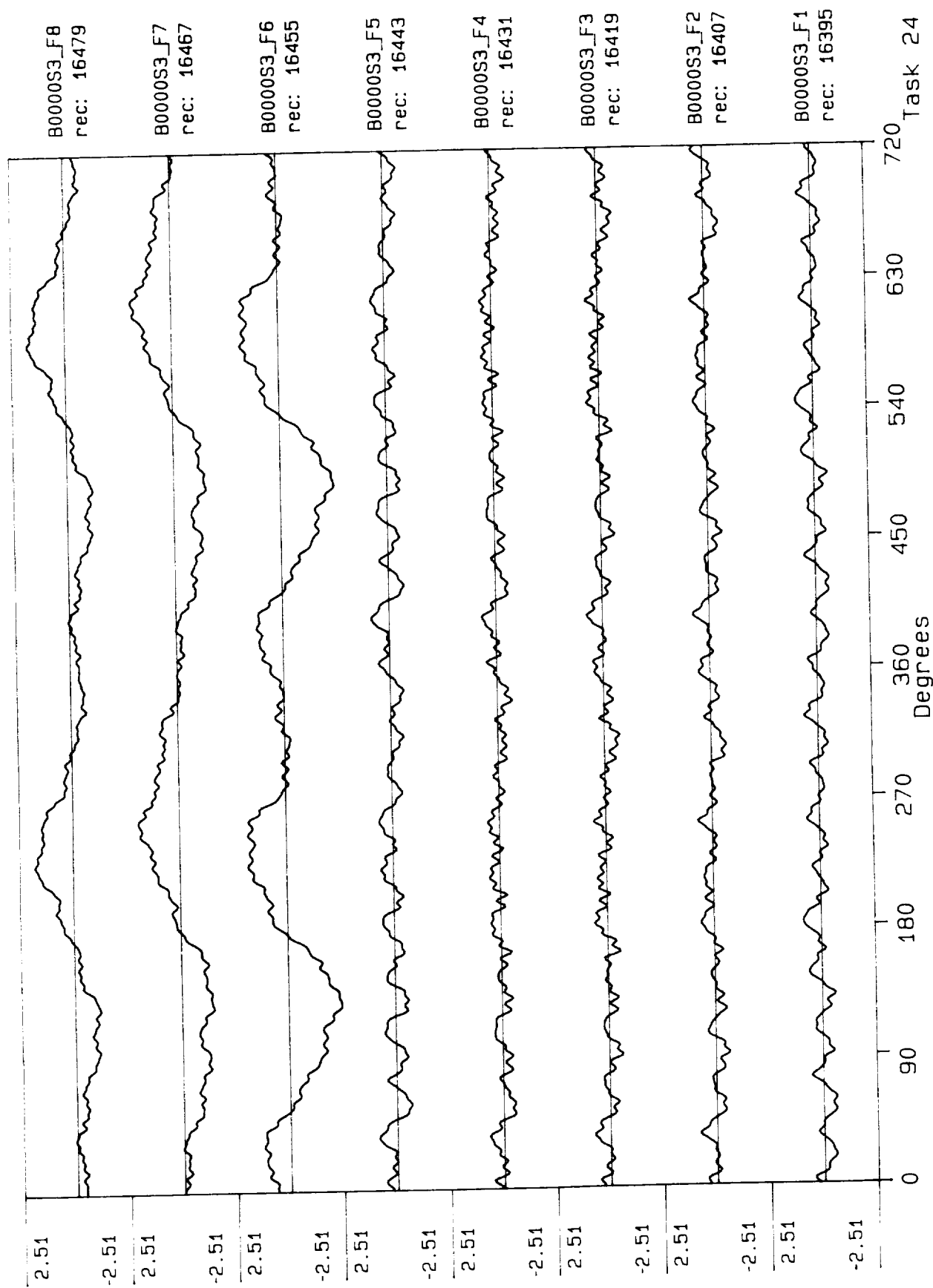
Task 27

Process included: Calibration, Phase correction and DC filtering.

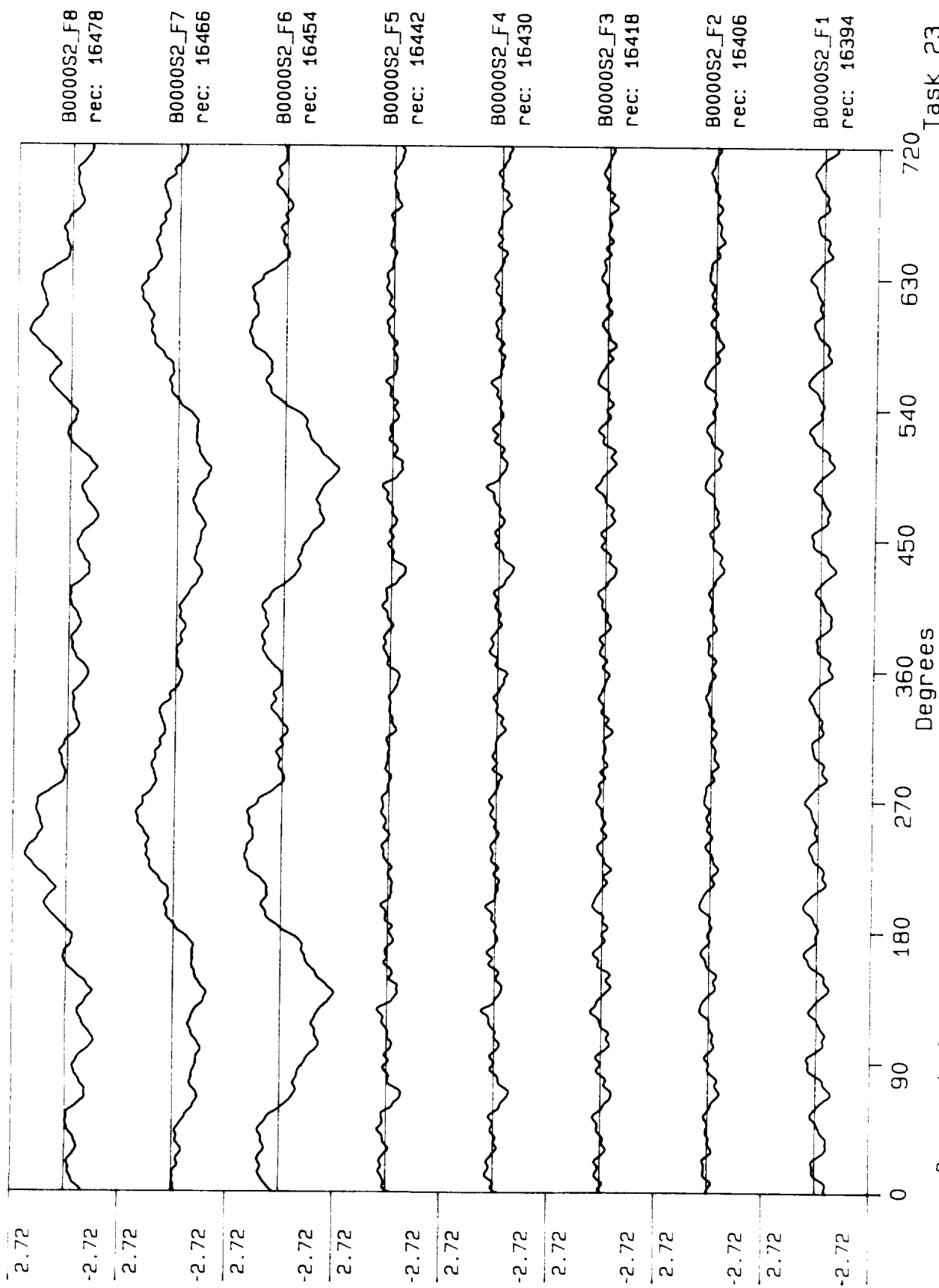


Process included: Calibration, Phase correction and DC filtering.

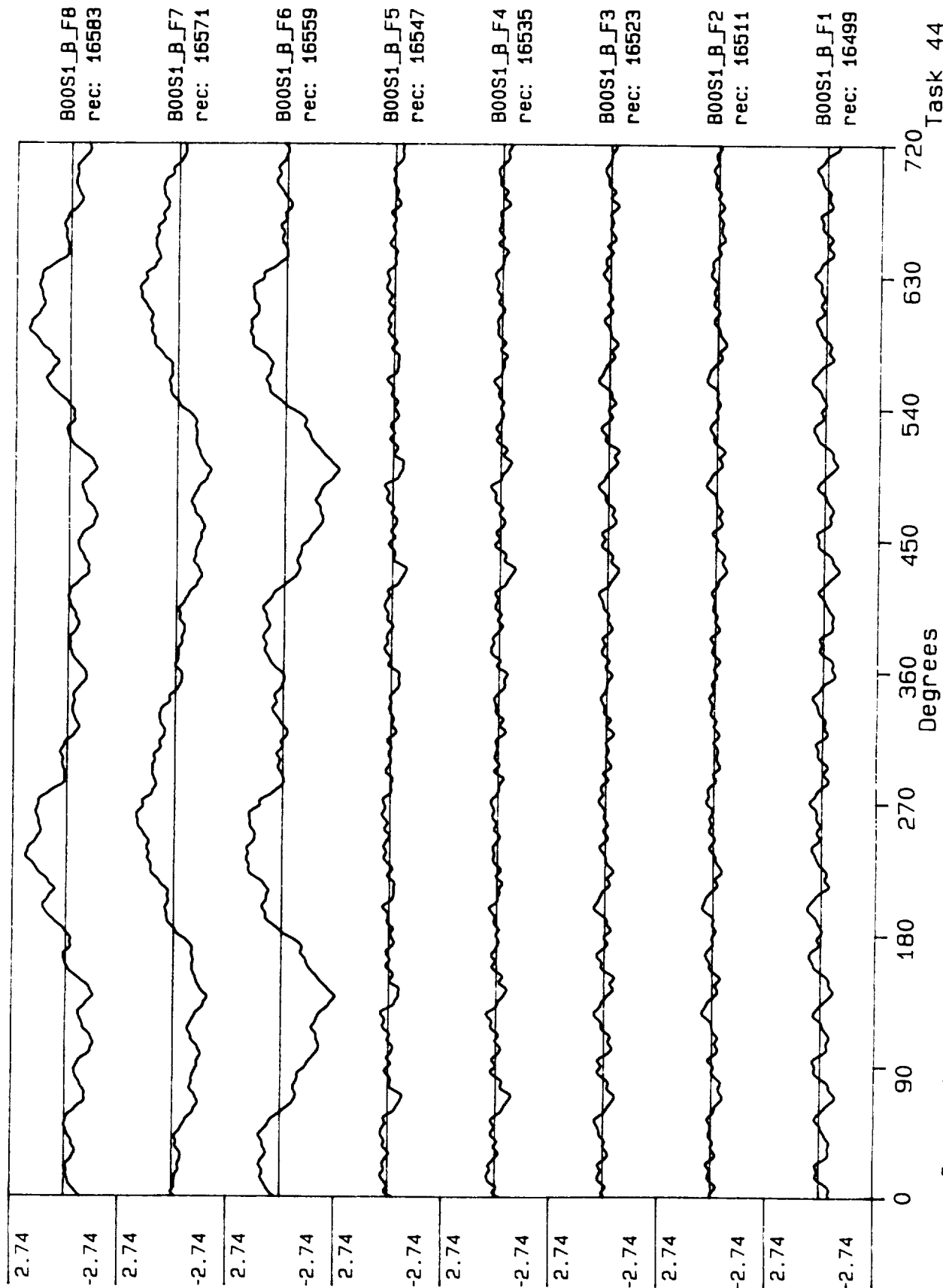
Task 25

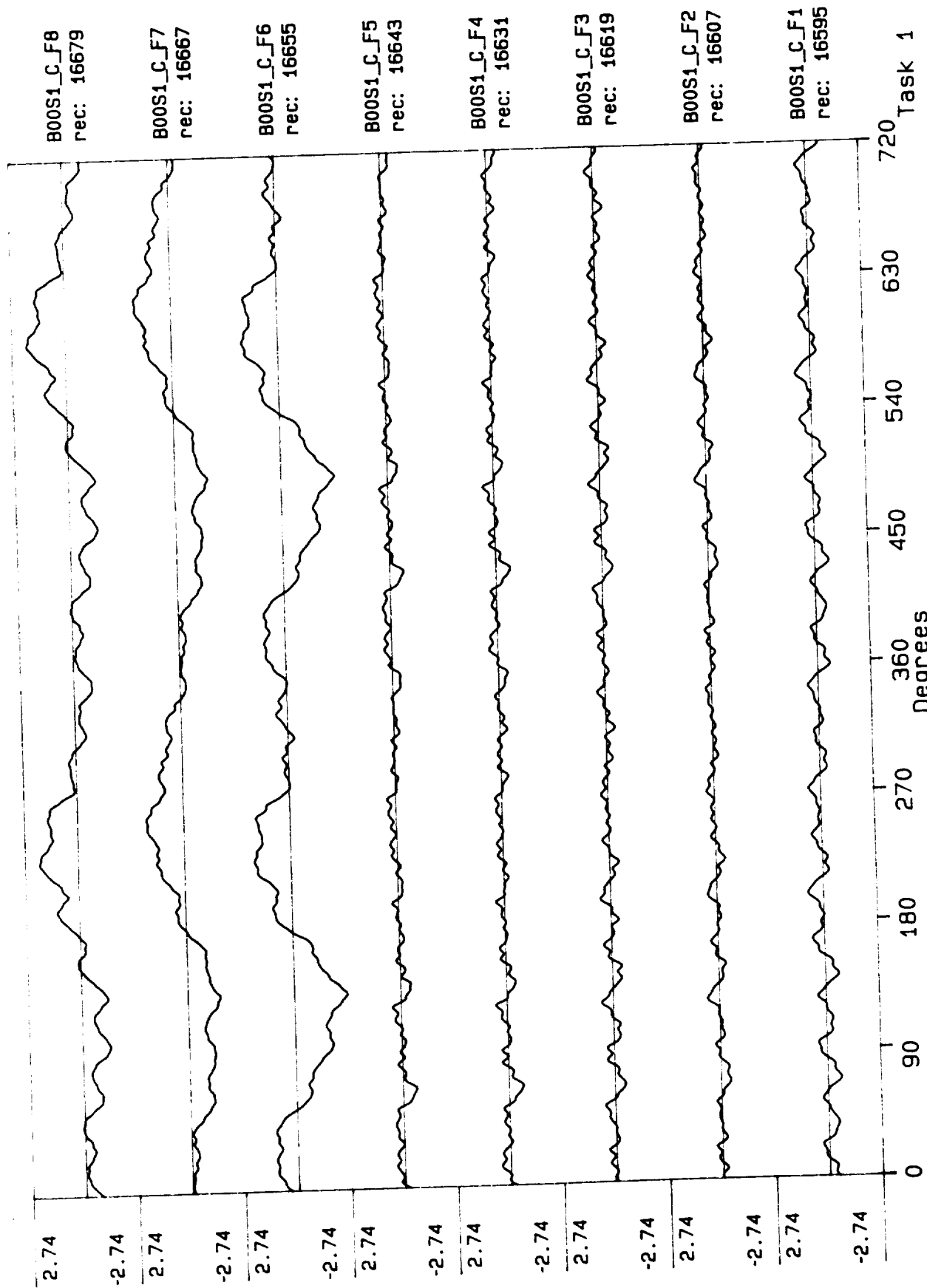


Process included: Calibration, Phase correction and DC filtering.



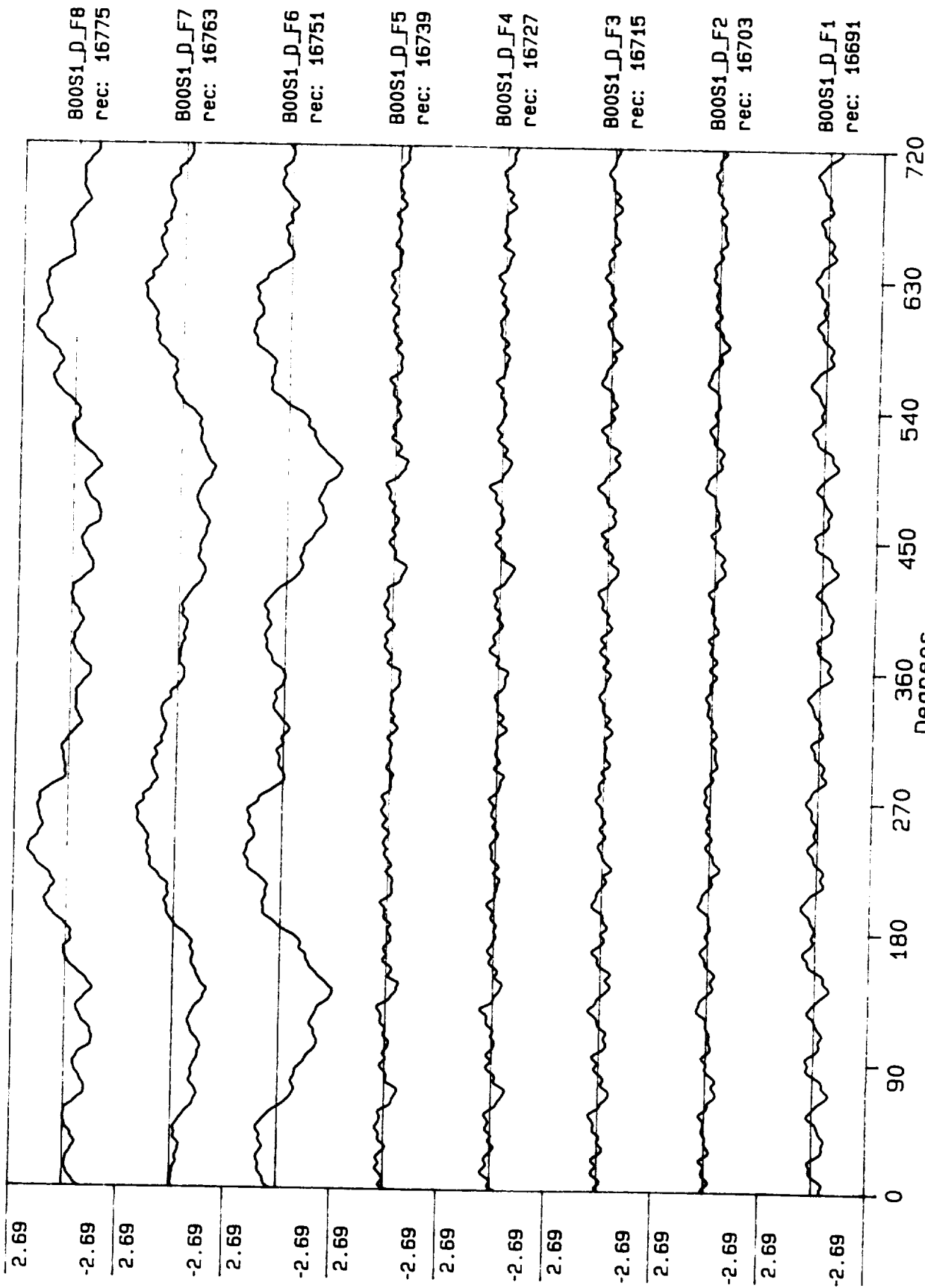
Process included: Calibration, Phase correction and DC filtering.



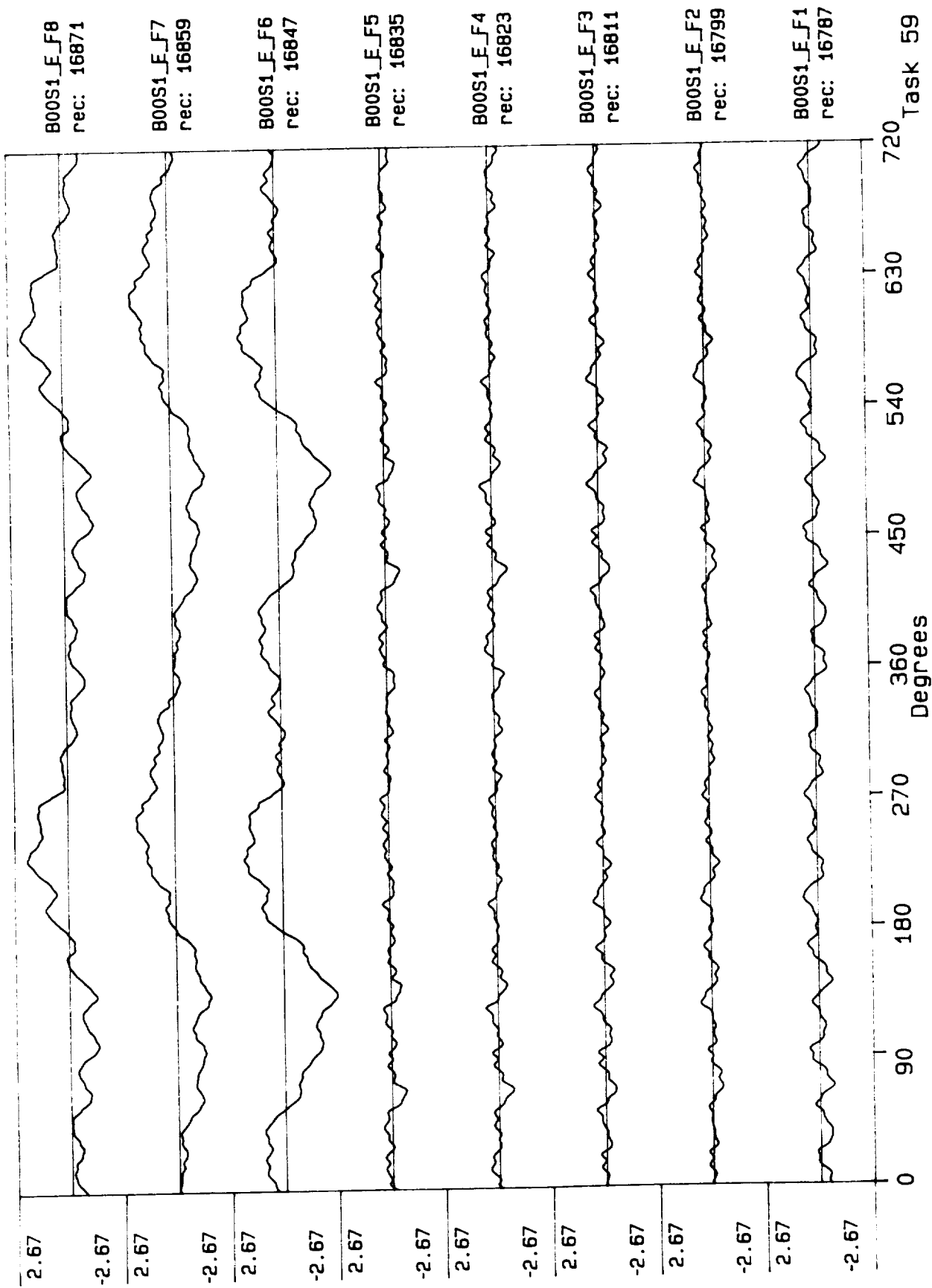


Process included: Calibration, Phase correction and DC filtering.

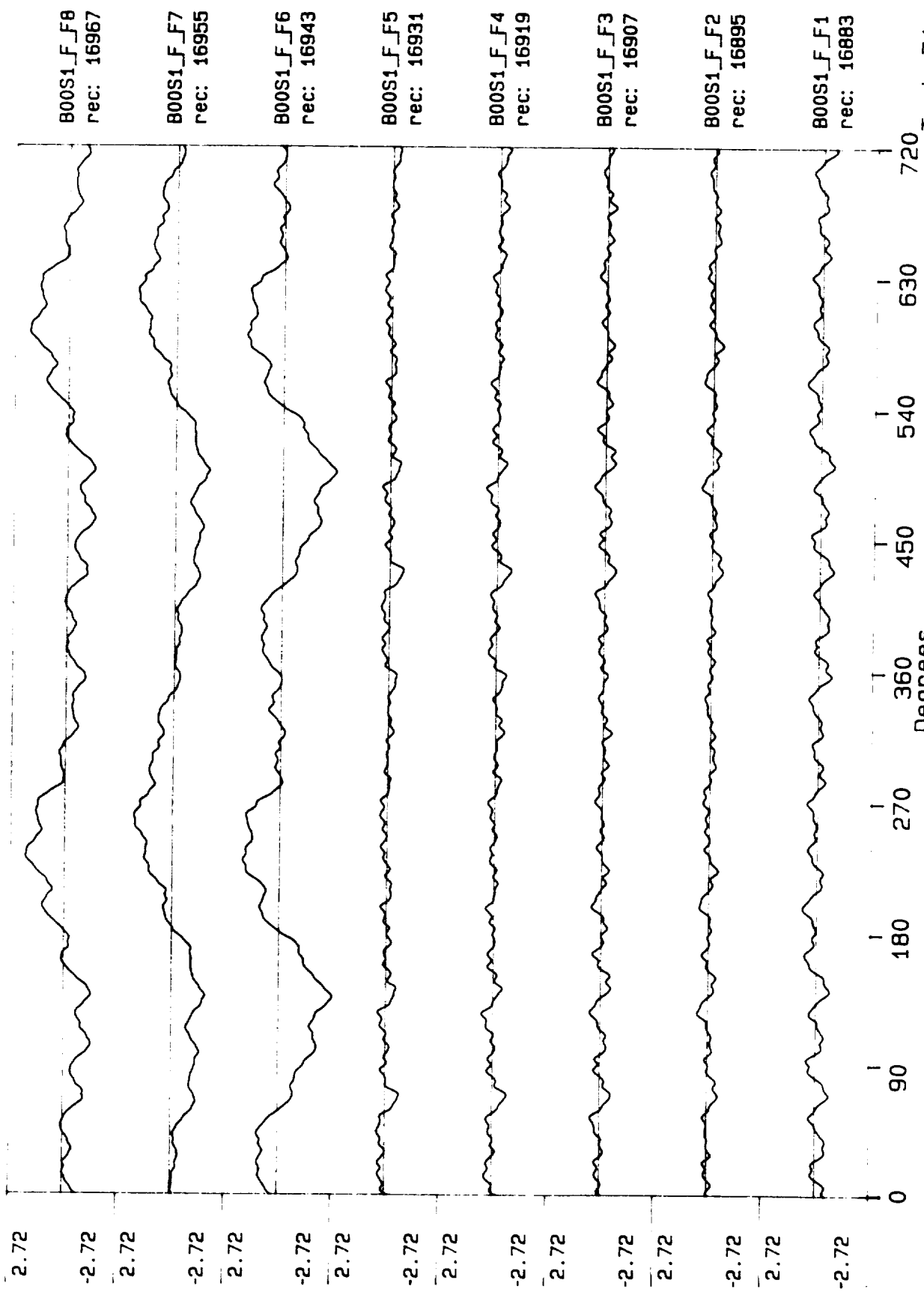
Task 1



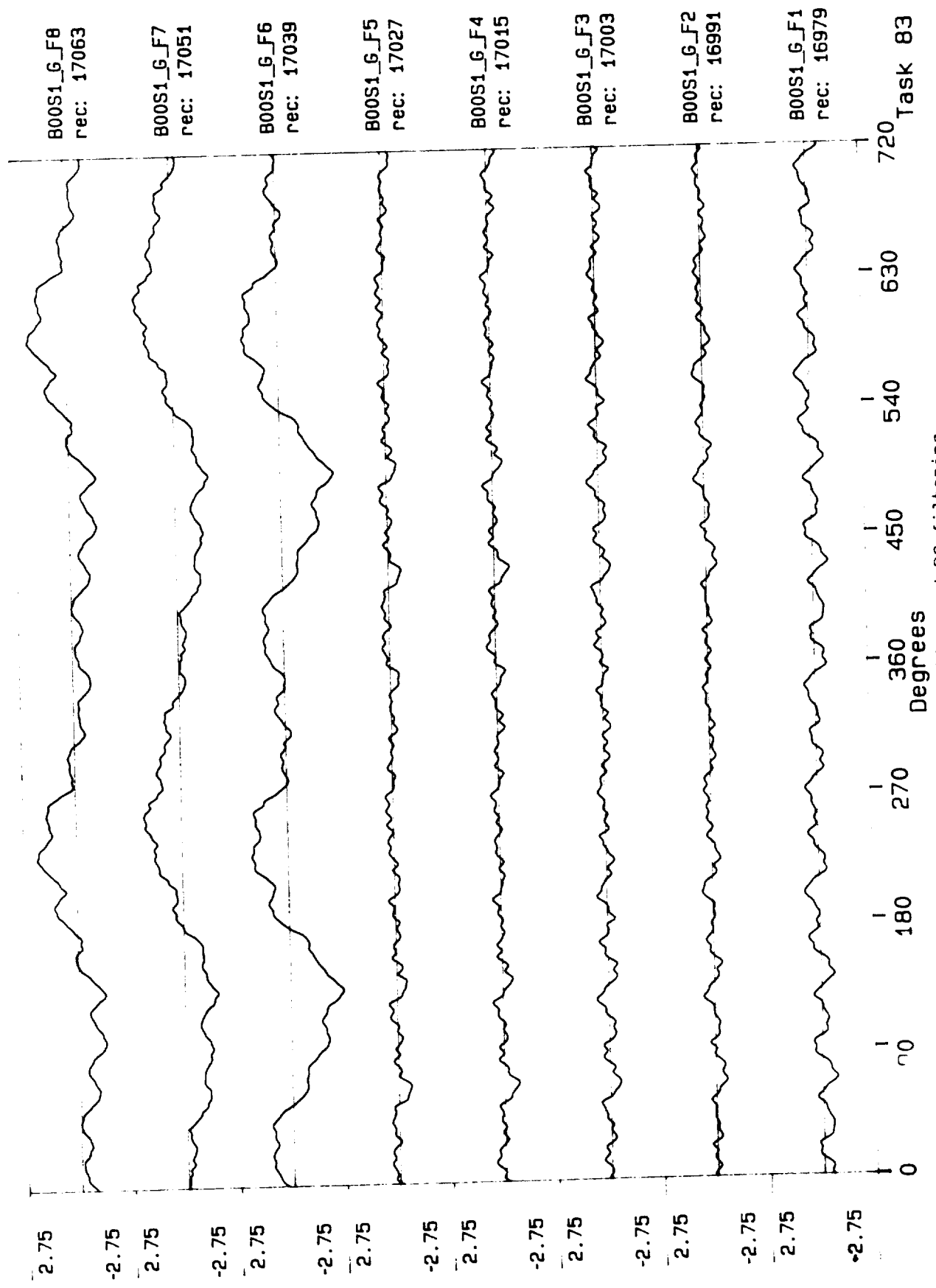
Process included: Calibration, Phase correction and DC filtering.



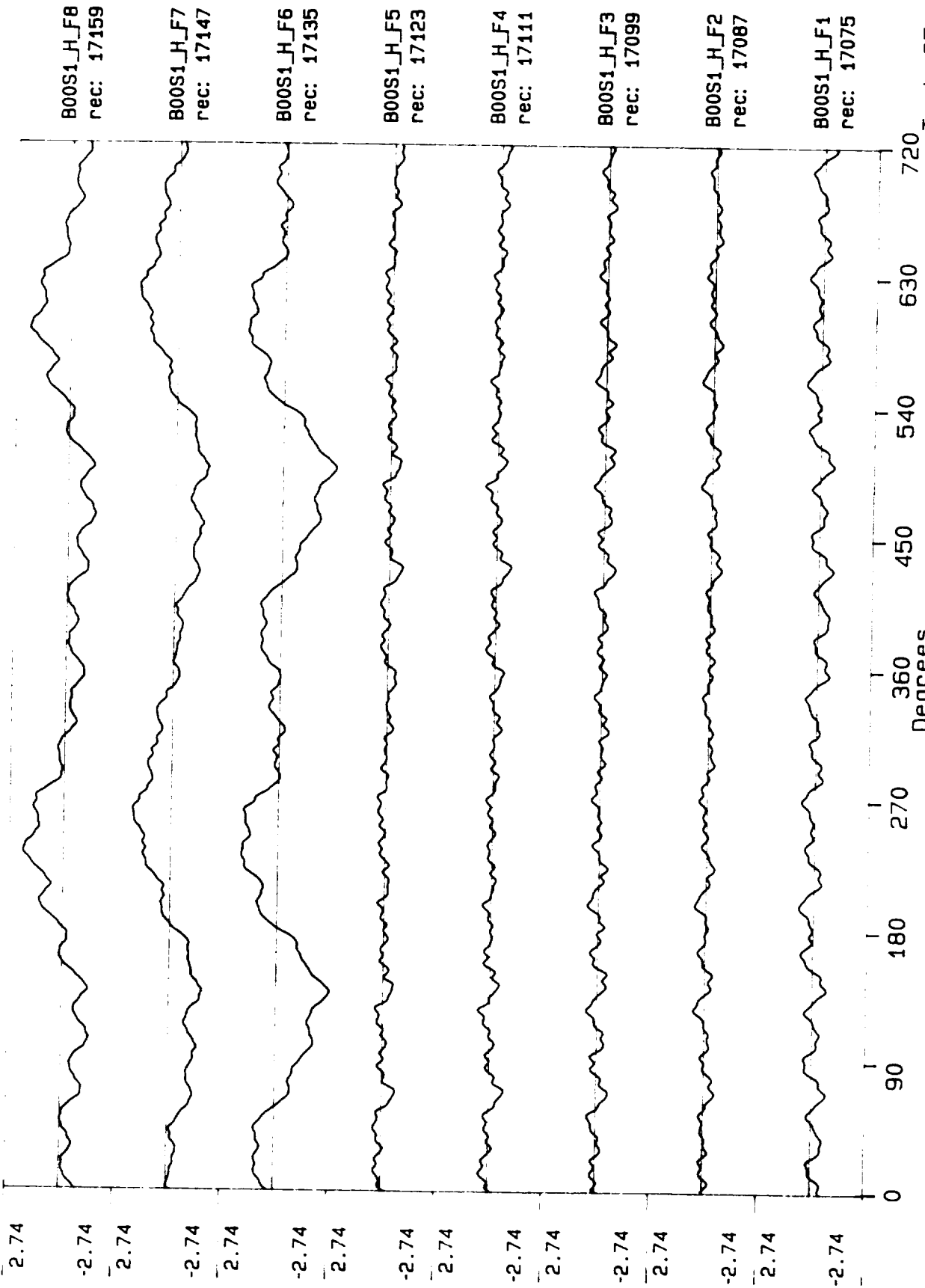
Process included: Calibration, Phase correction and DC filtering.



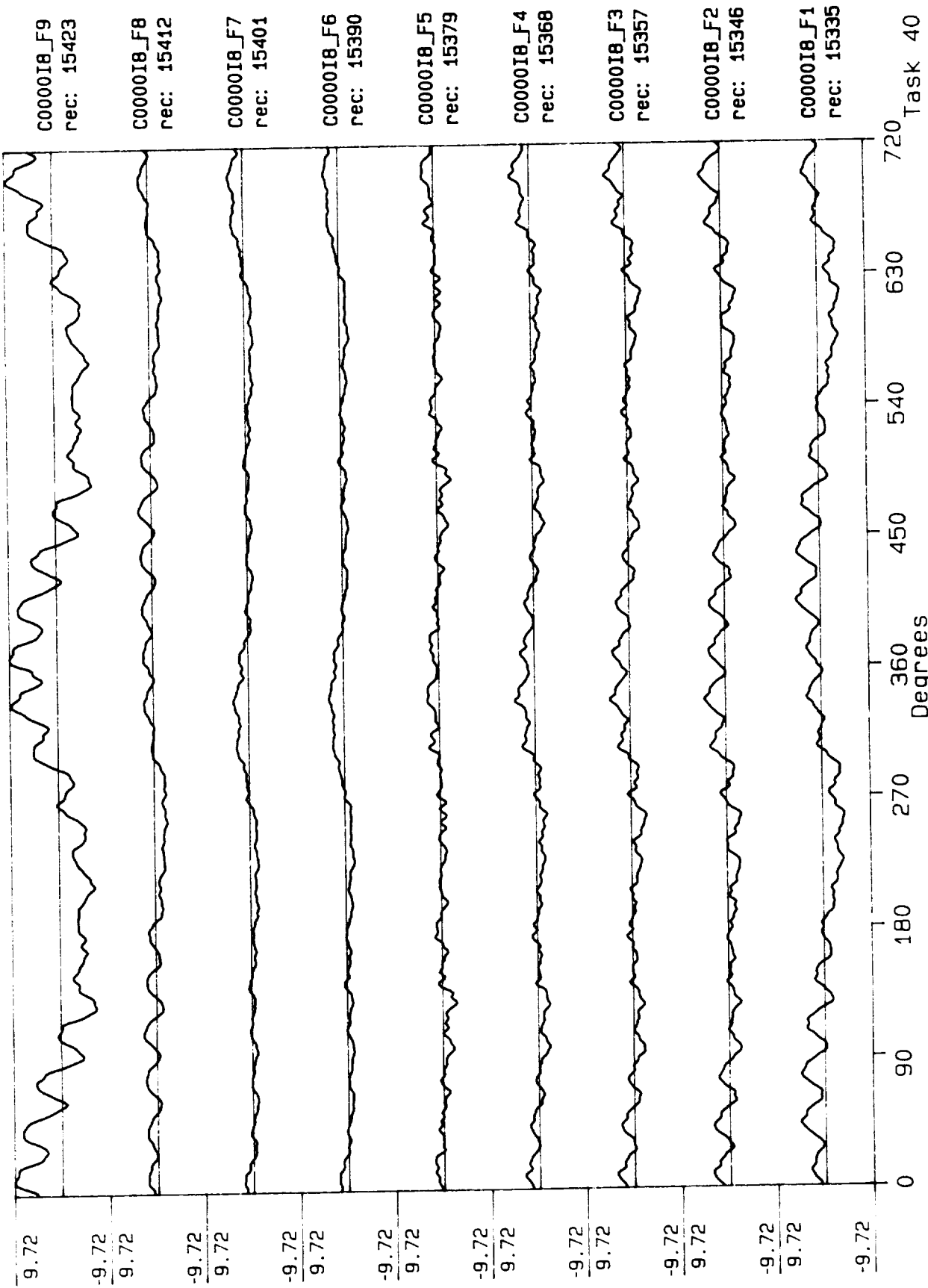
Process included: Calibration, Phase correction and DC filtering.



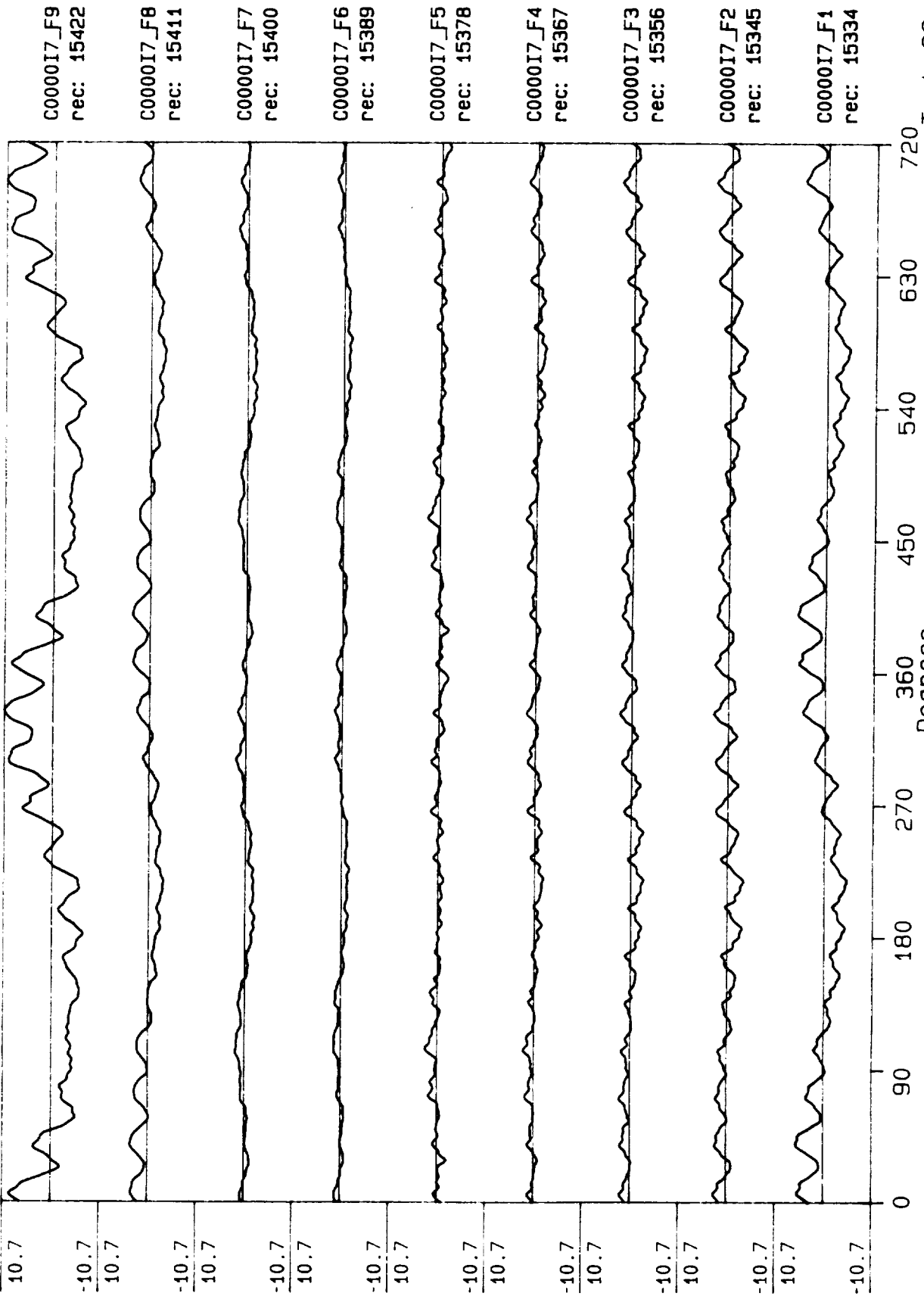
Process included: Calibration, Phase correction and DC filtering.



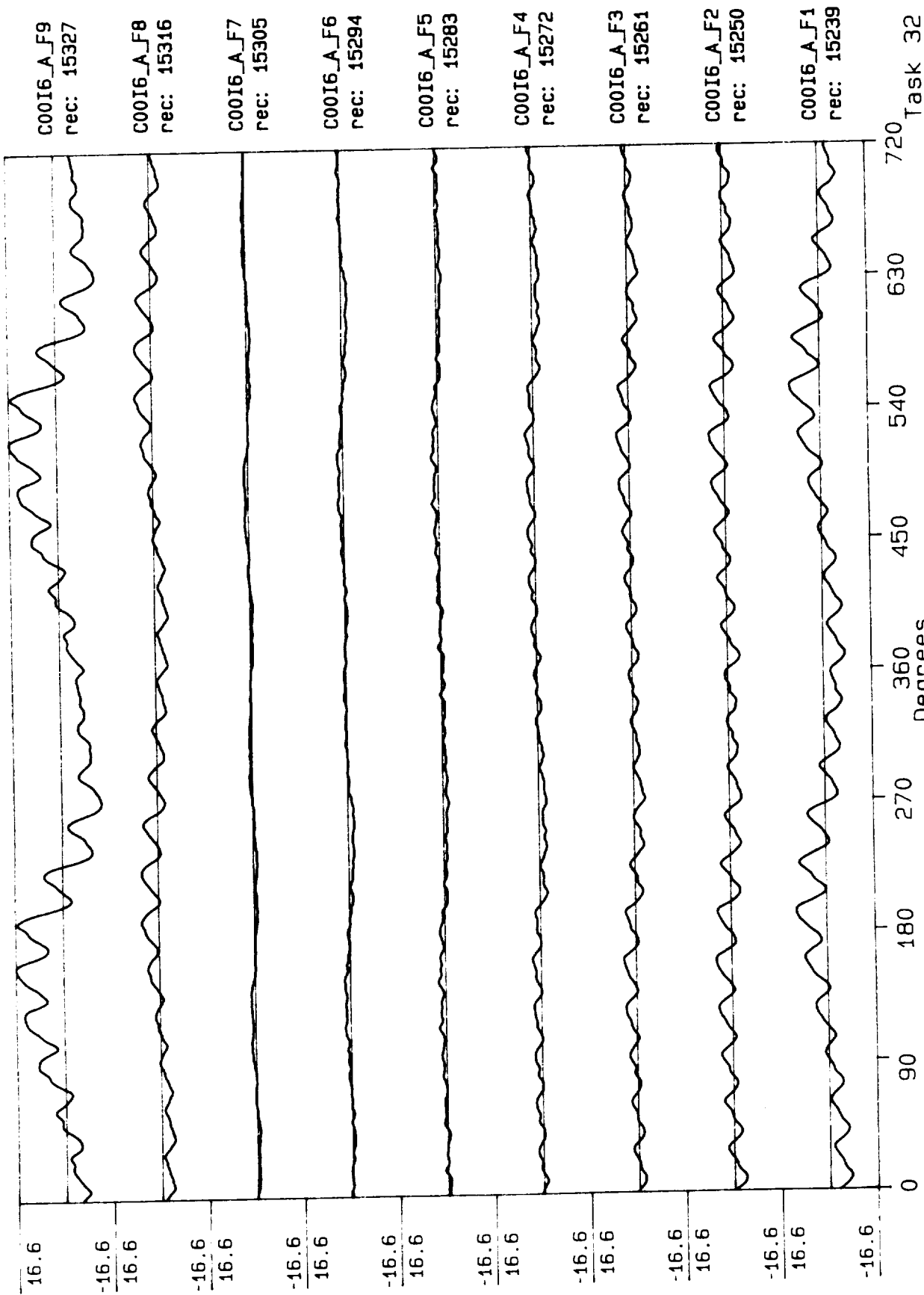
Process included: Calibration, Phase correction and DC filtering.



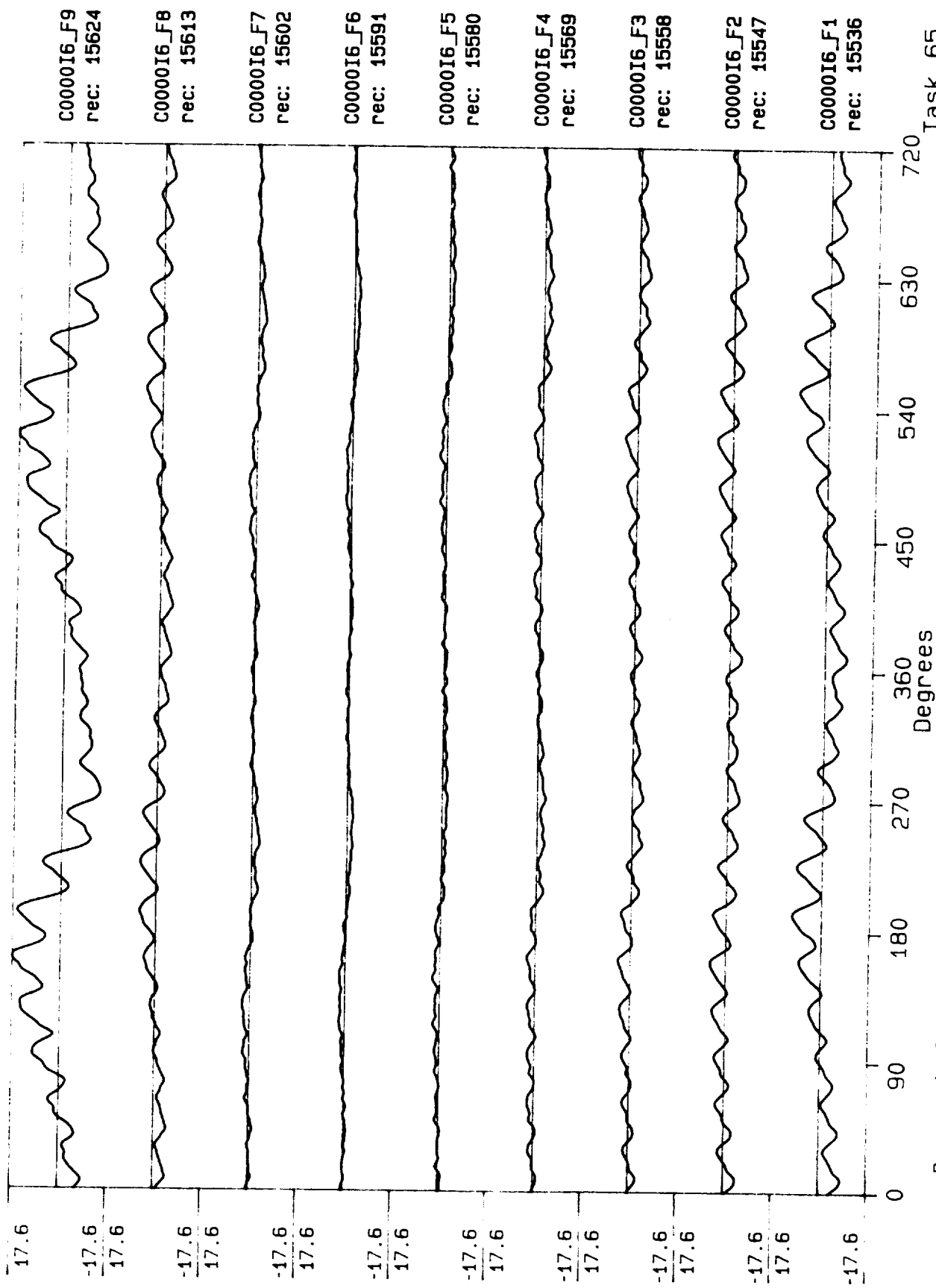
Process included: Calibration, Phase correction and DC filtering. Published: 06/20/89



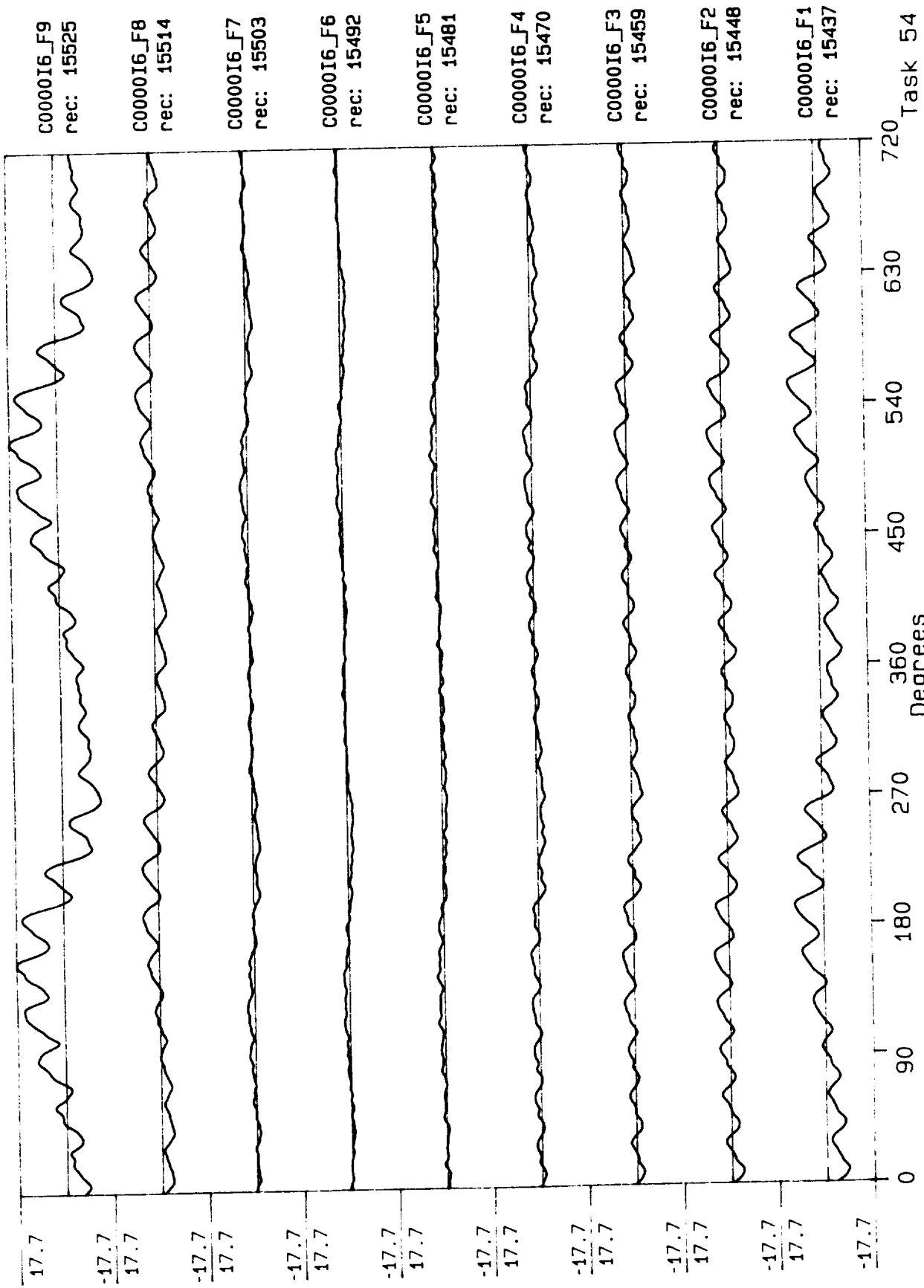
Process included: Calibration, Phase correction and DC filtering. Published: 06/20/89



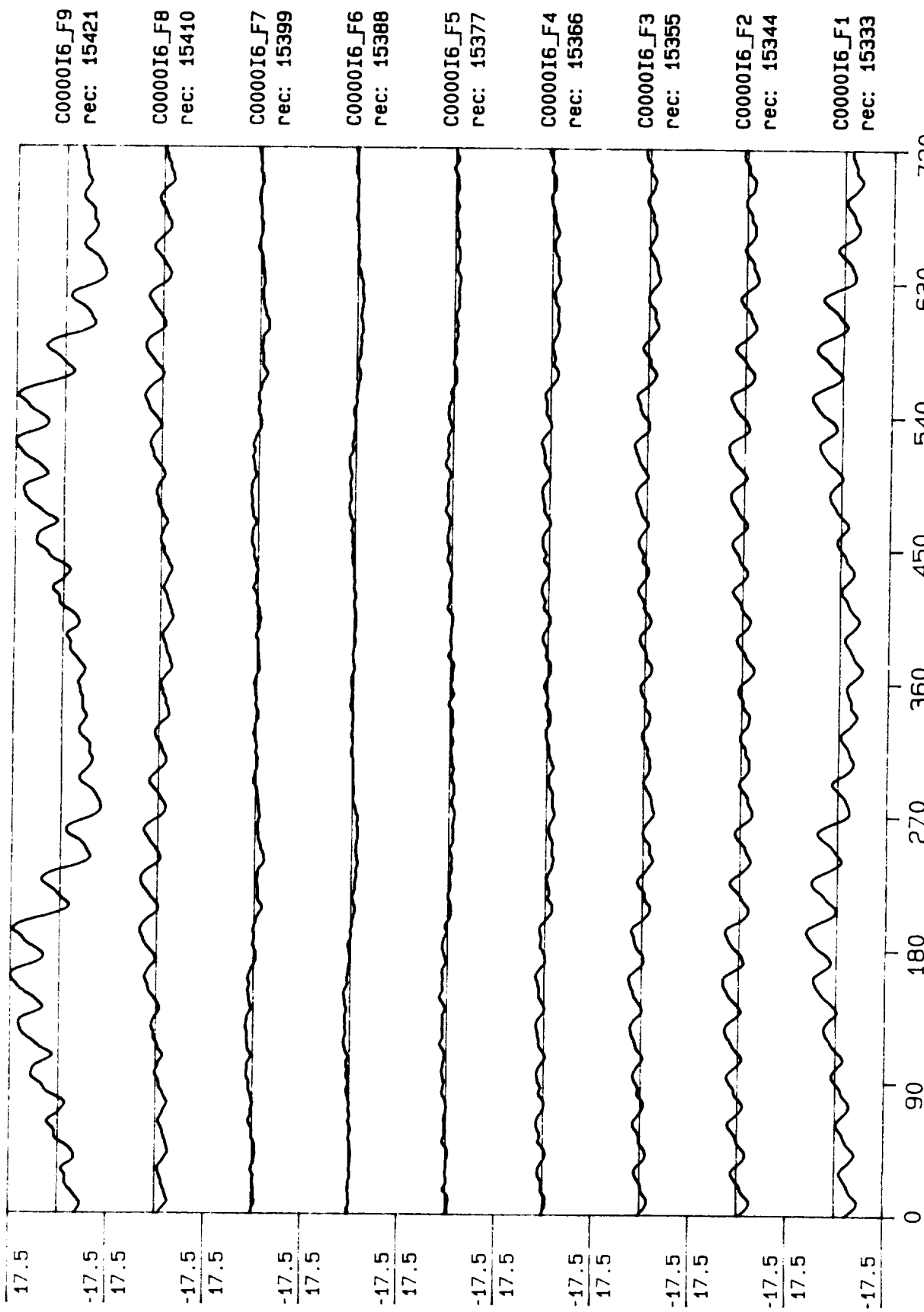
Process included: Calibration, Phase correction and DC filtering. Published: 06/20/89



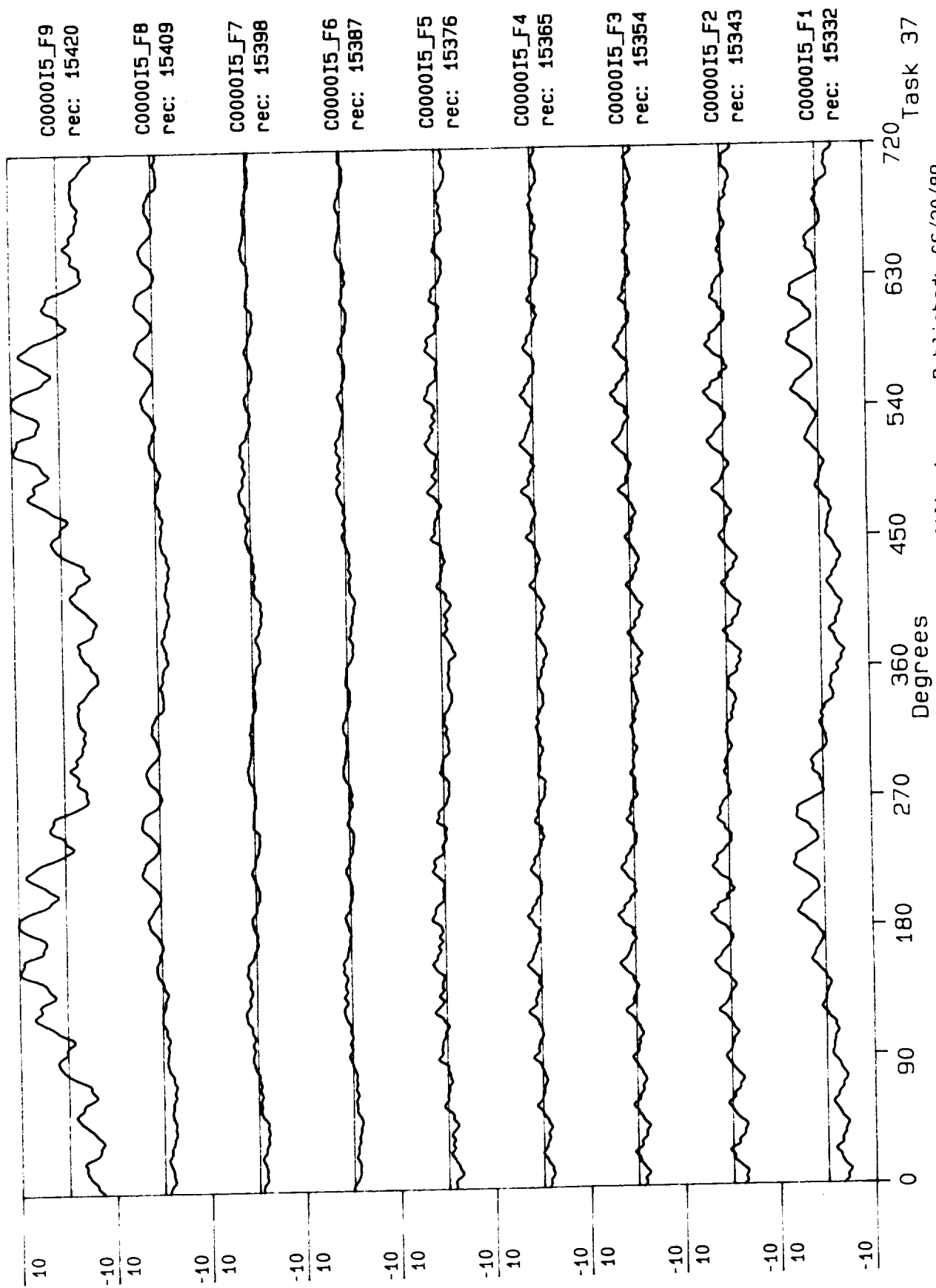
Process included: Calibration, Phase correction and DC filtering. Published: 06/20/89

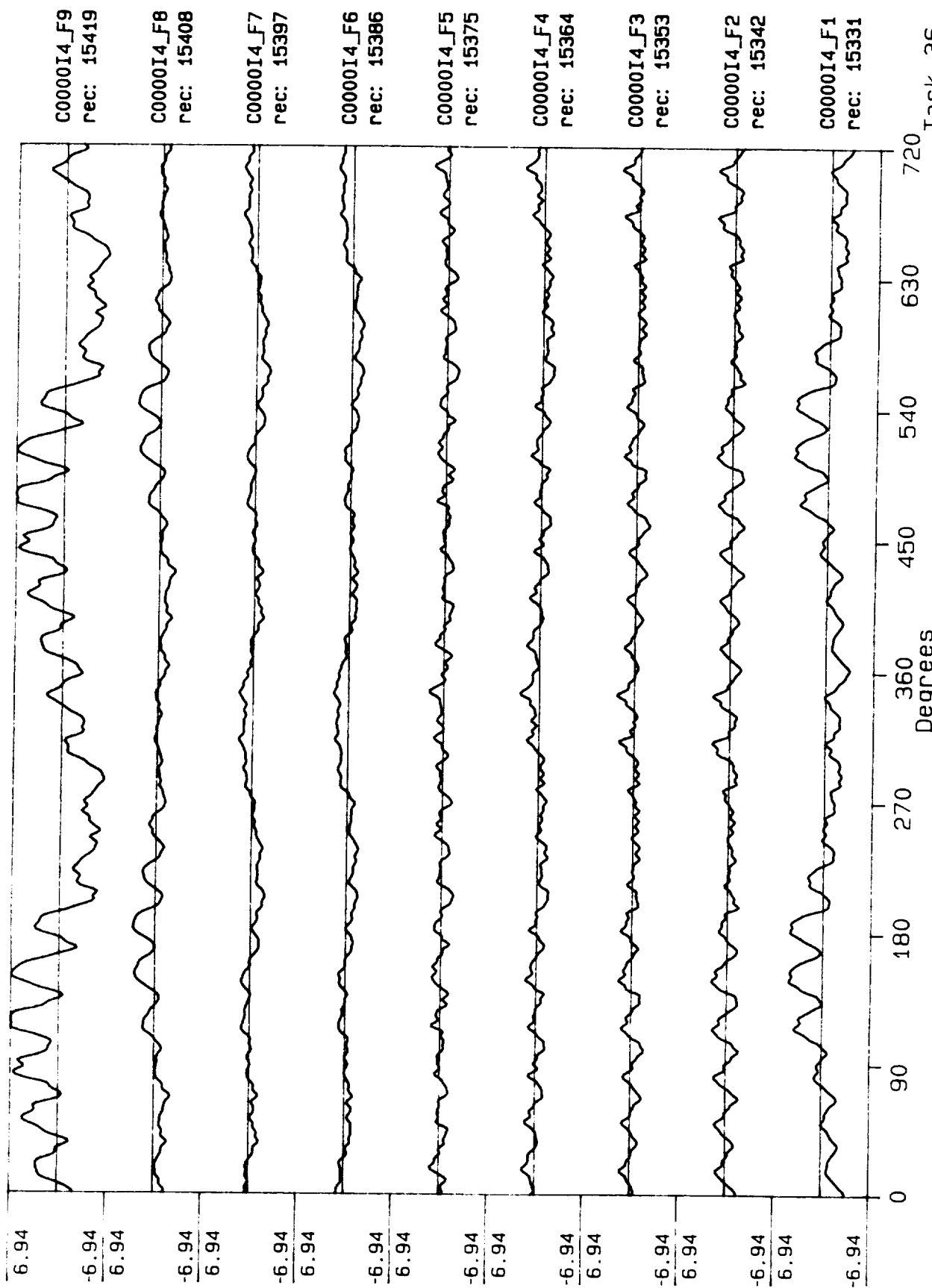


Process included: Calibration, Phase correction and DC filtering. Published: 06/20/89

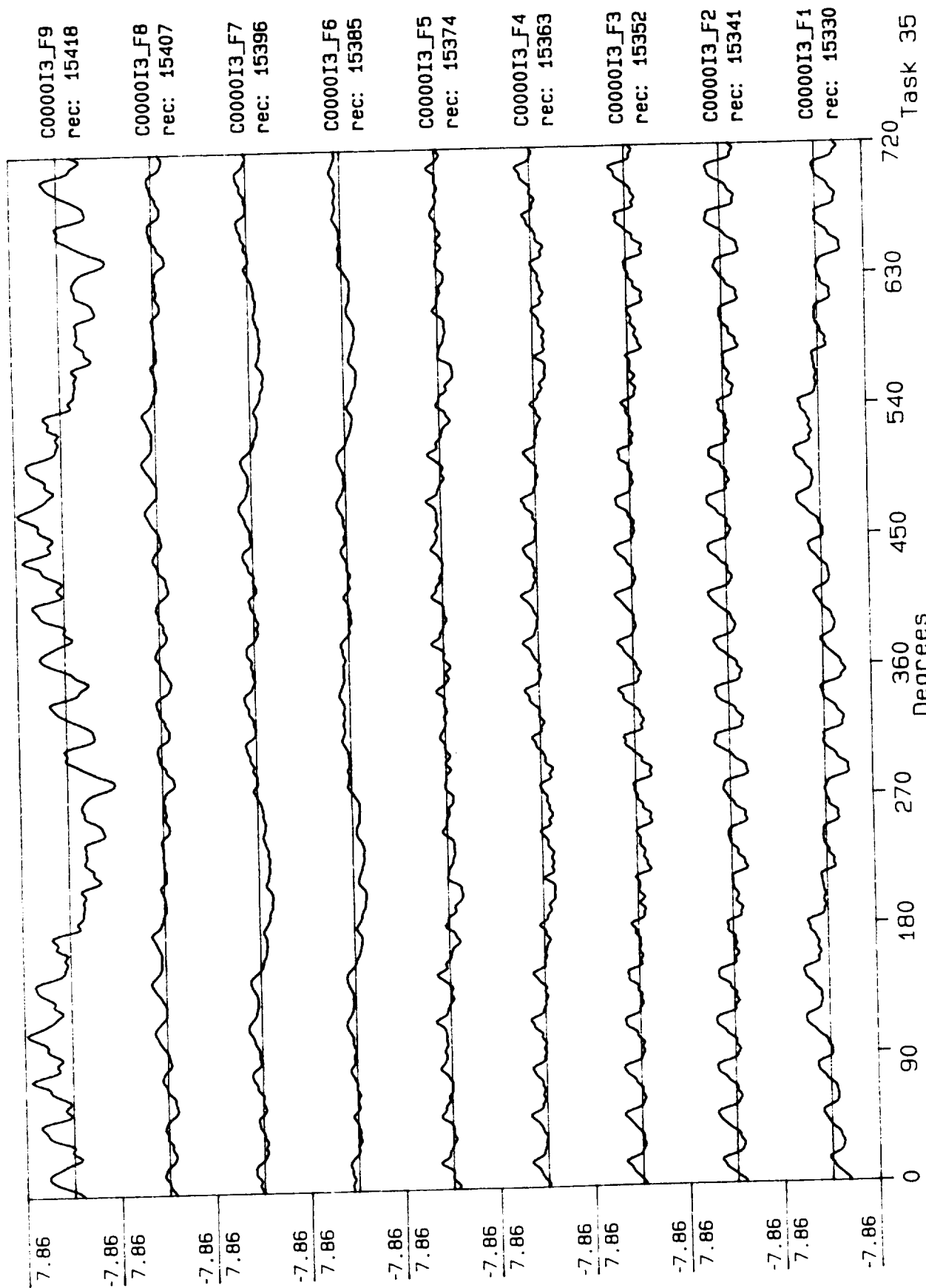


Process included: Calibration, Phase correction and DC filtering. Published: 06/20/89

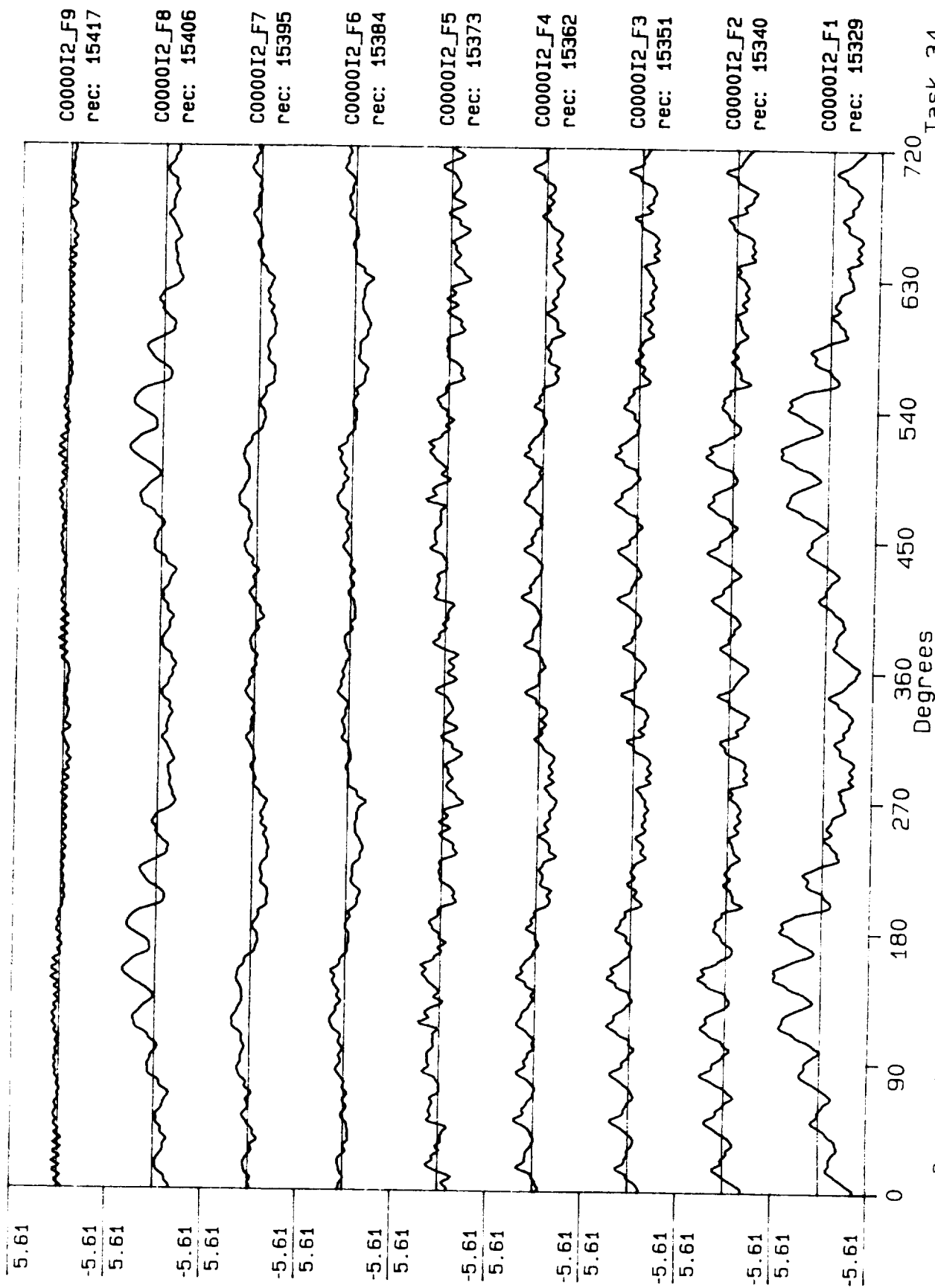




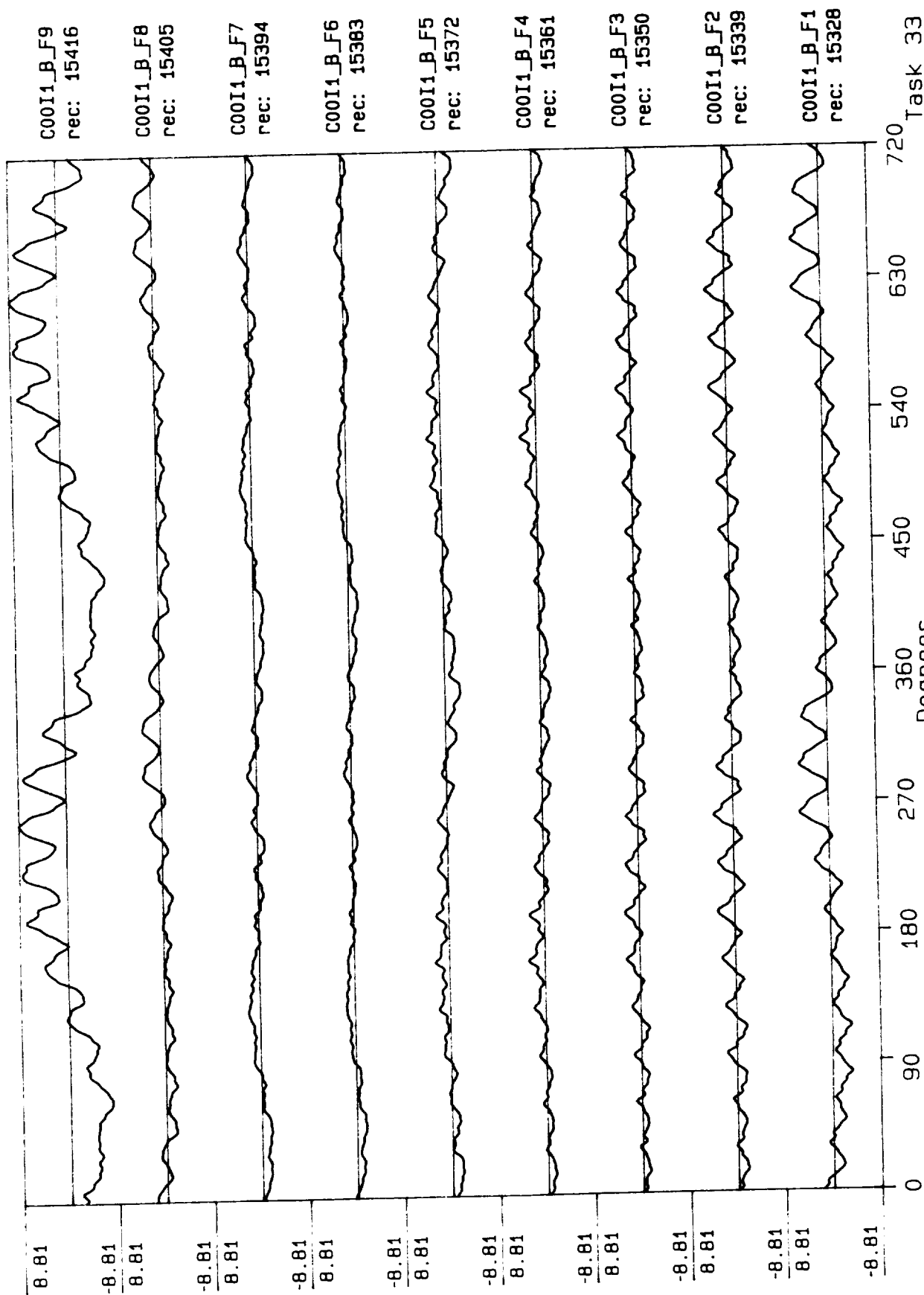
Process included: Calibration, Phase correction and DC filtering. Published: 06/20/89



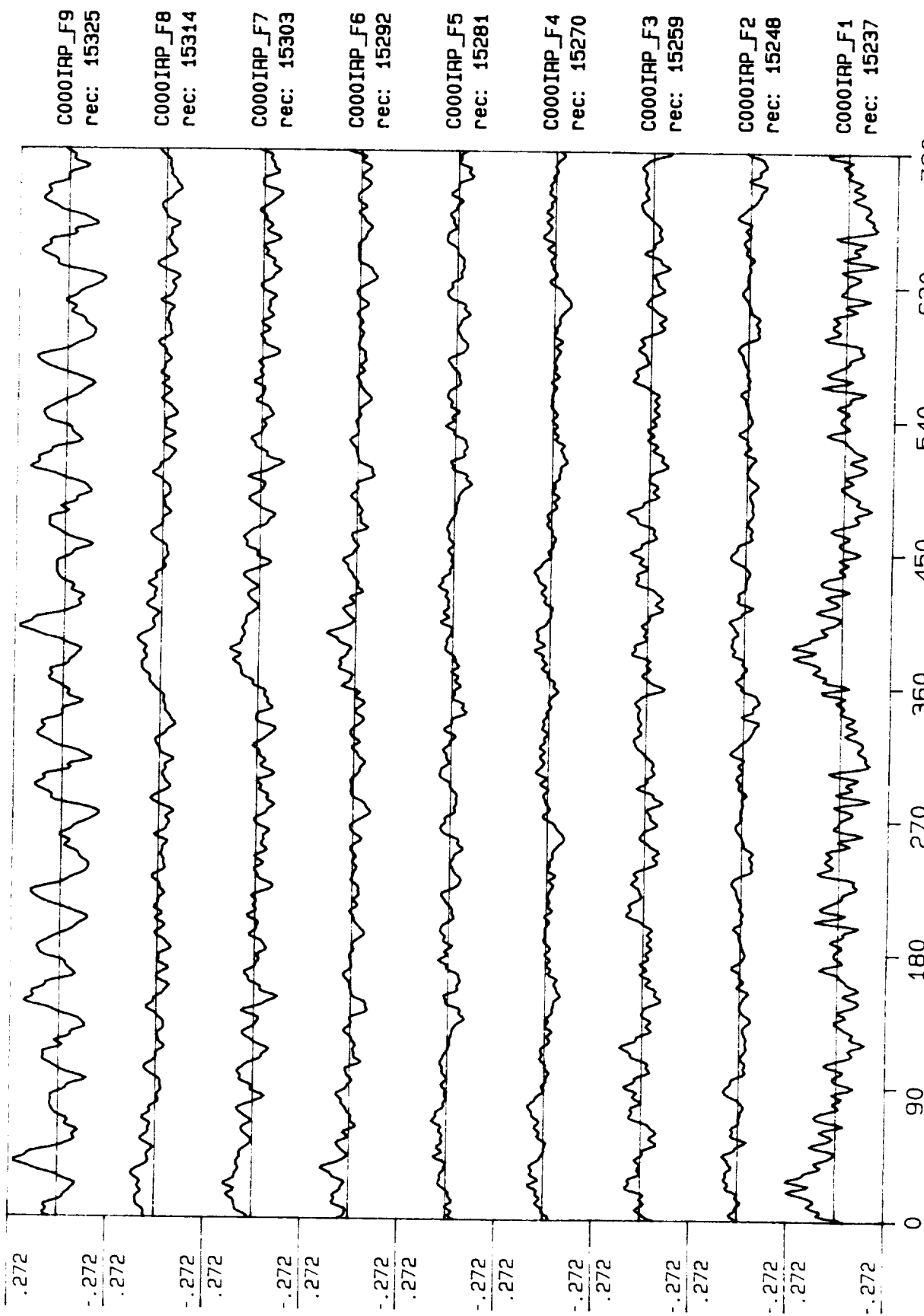
Process included: Calibration, Phase correction and DC filtering. Published: 06/20/89



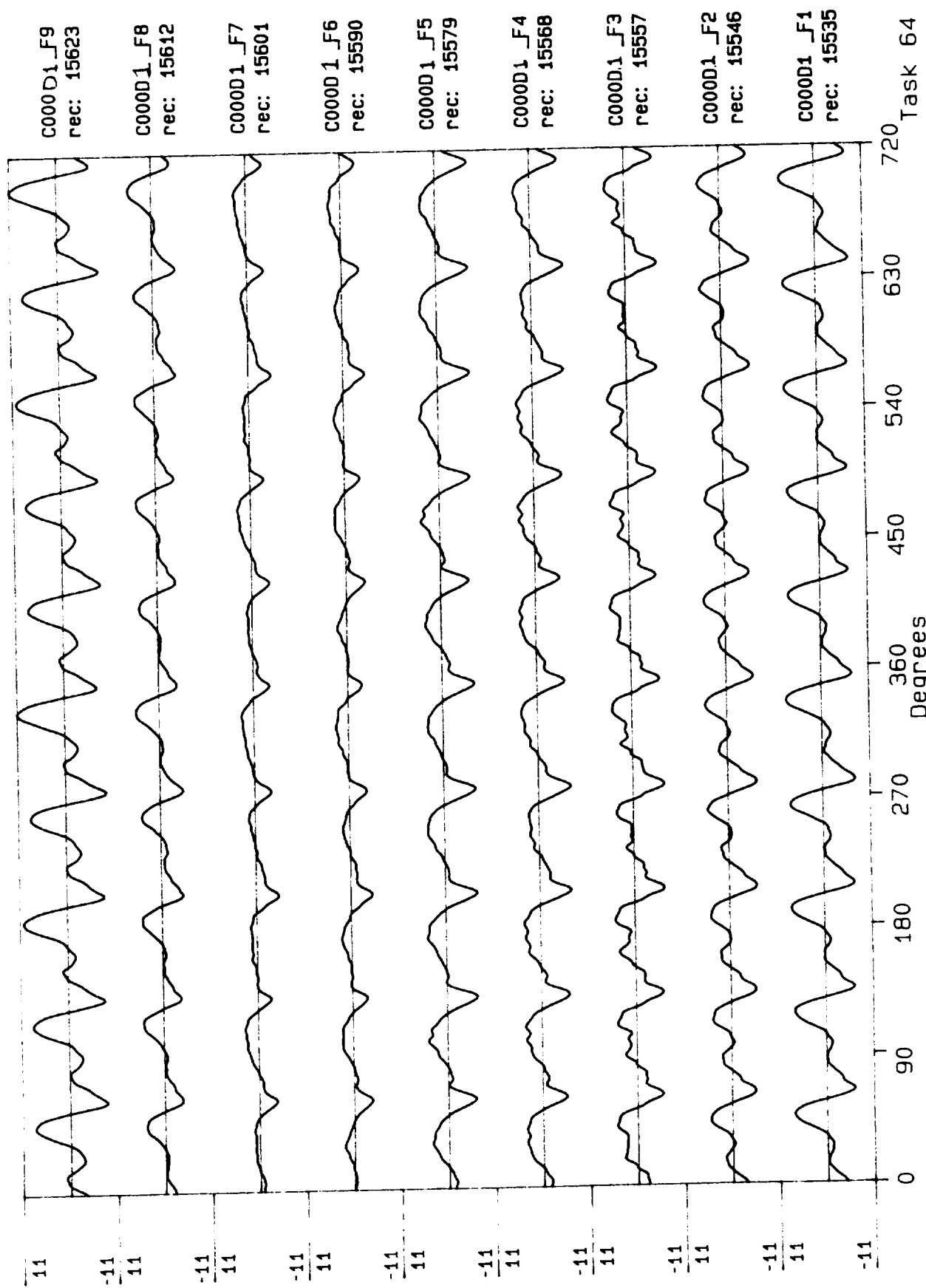
Process included: Calibration, Phase correction and DC filtering. Published: 06/20/89



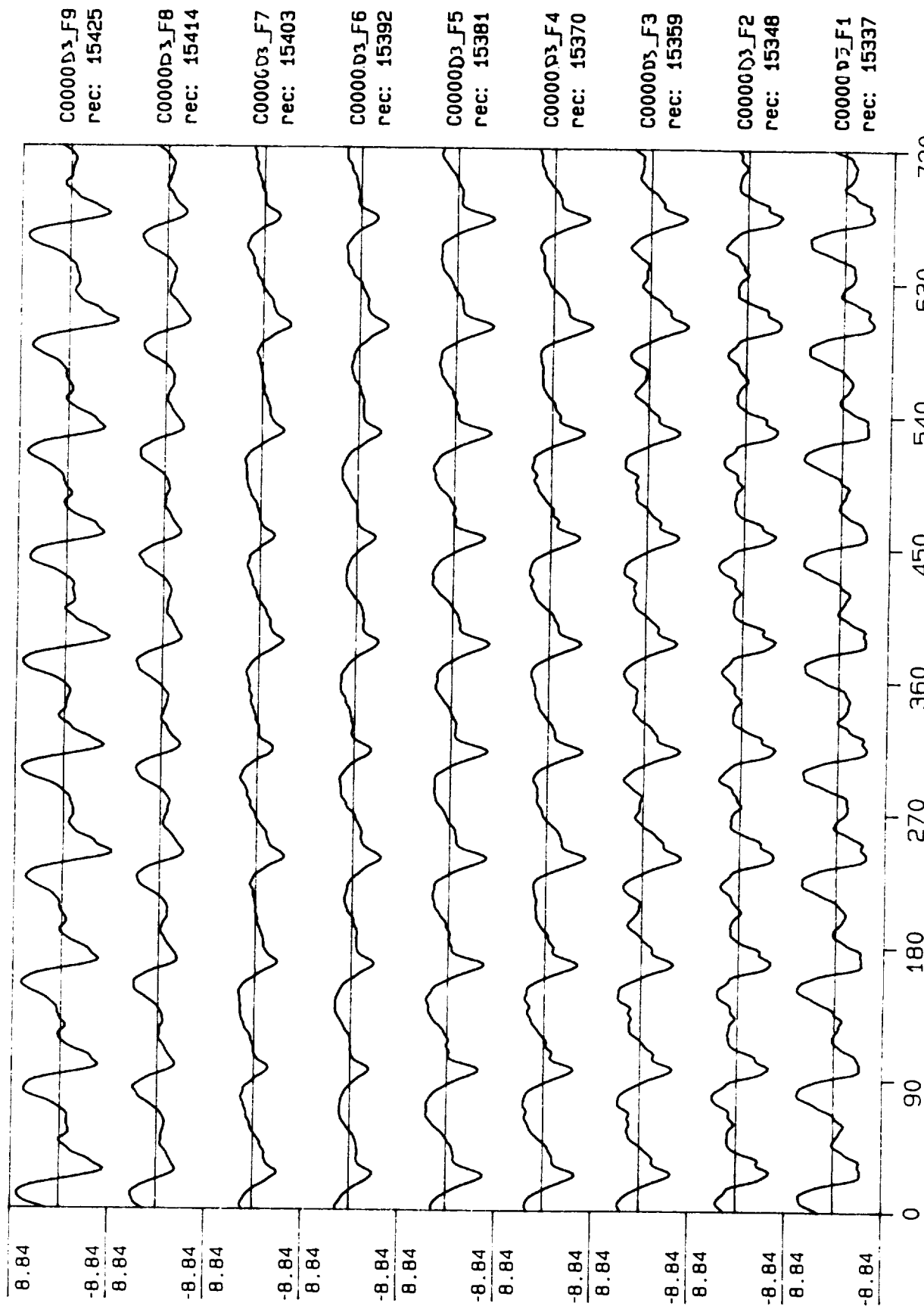
Process included: Calibration, Phase correction and DC filtering. Published: 06/20/89



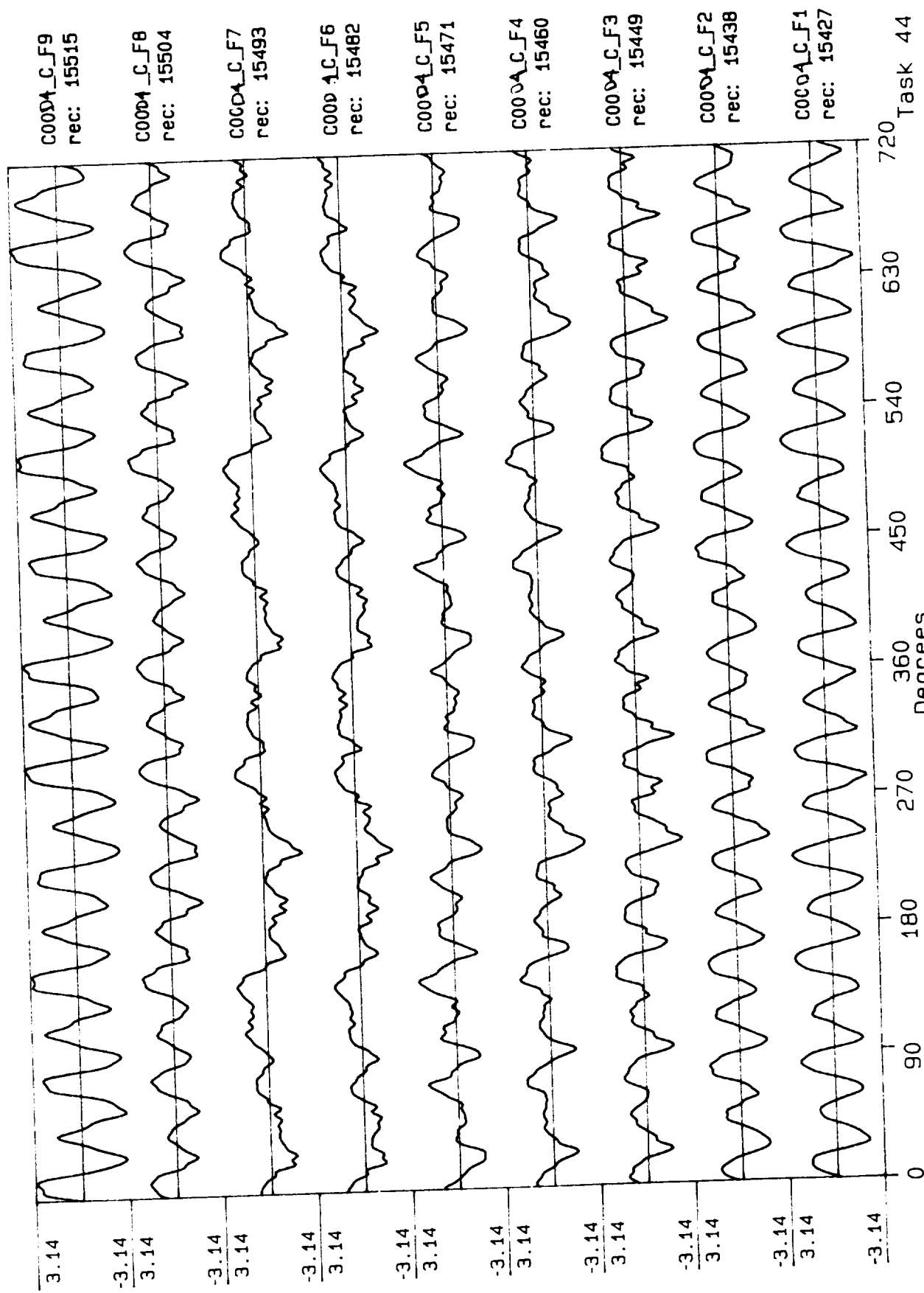
Process included: Calibration, Phase correction and DC filtering. Published: 06/20/89



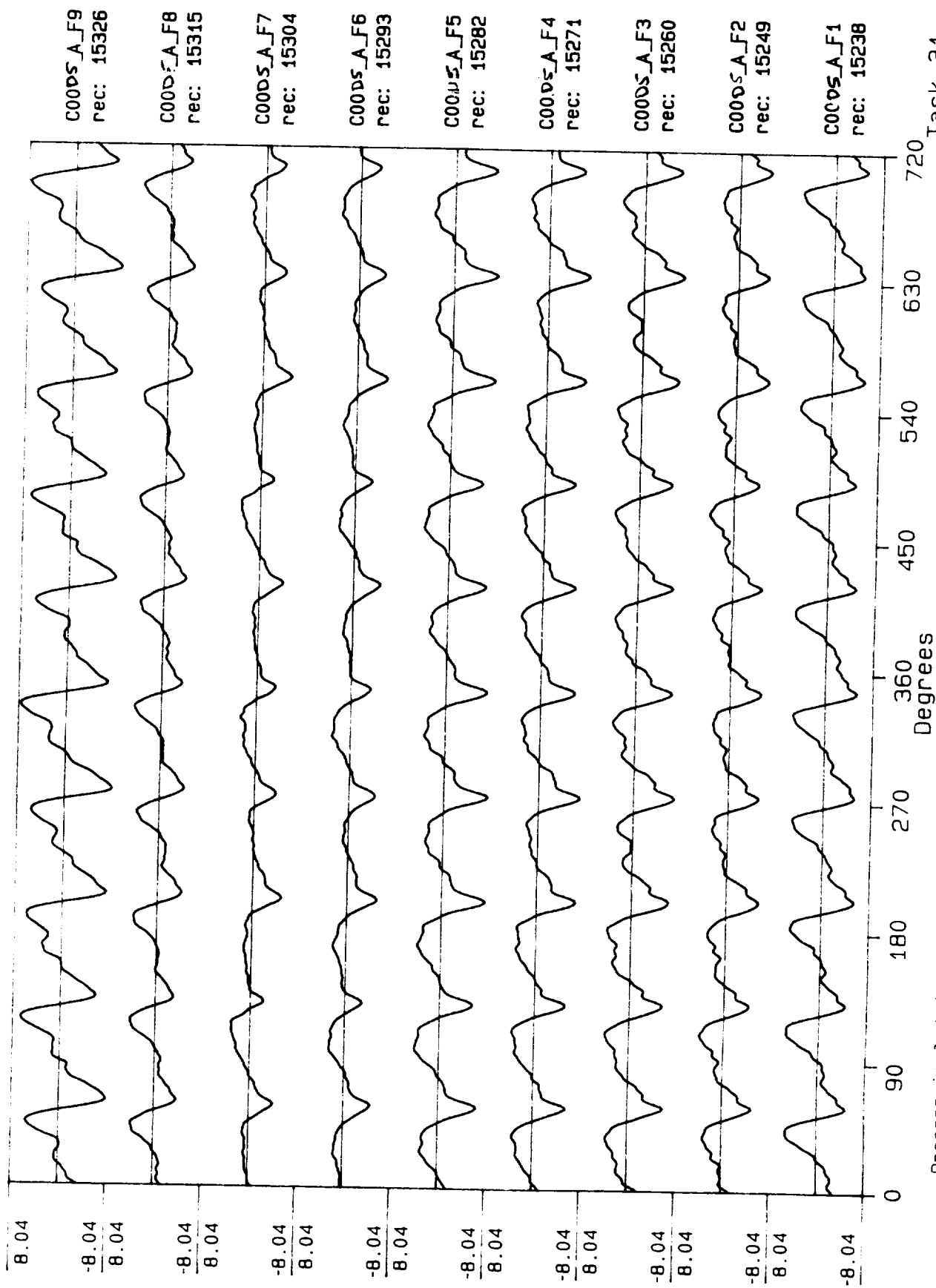
Process included: Calibration, Phase correction and DC filtering. Published: 06/20/89



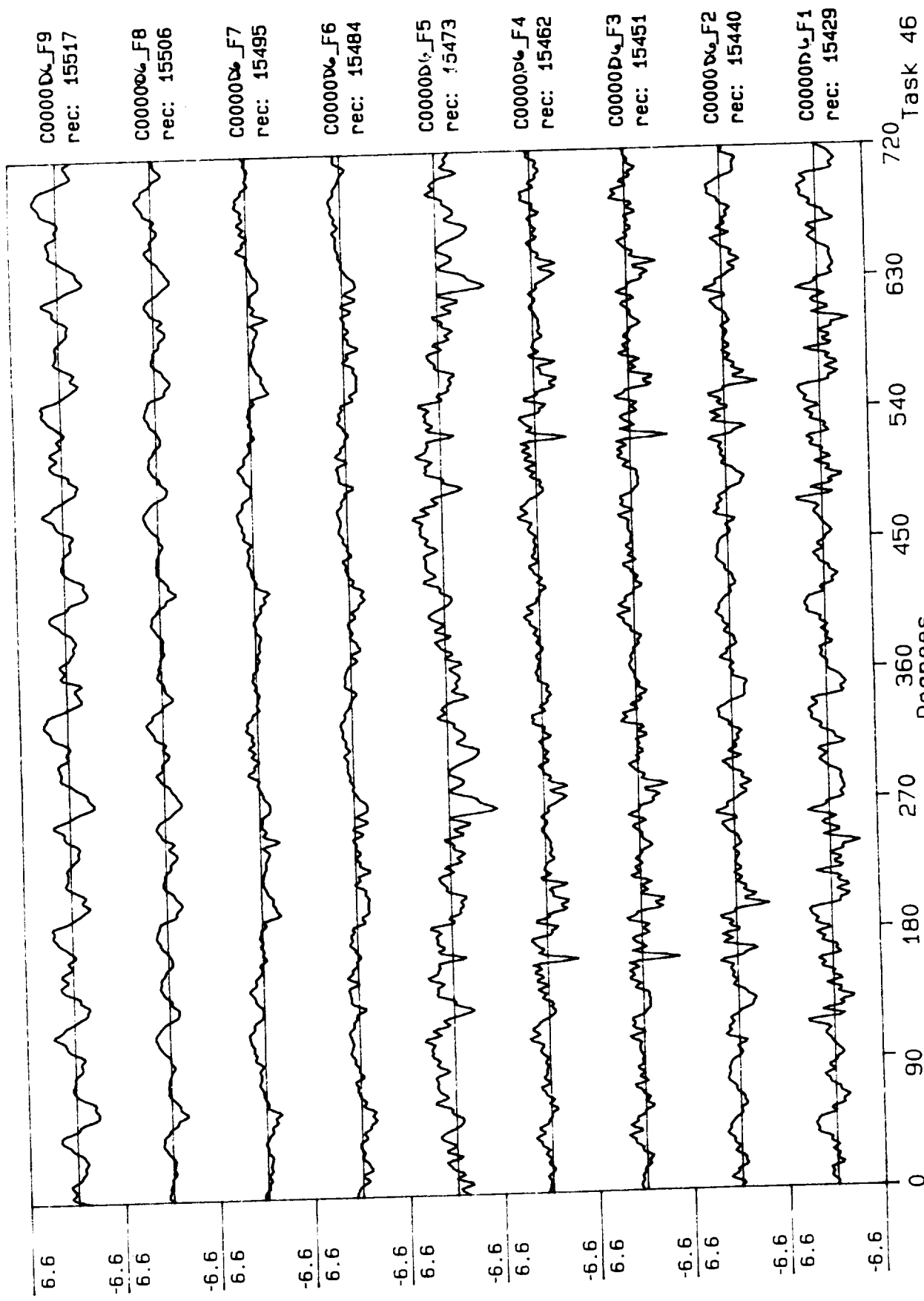
Process included: Calibration, Phase correction and DC filtering. Published: 06/20/89



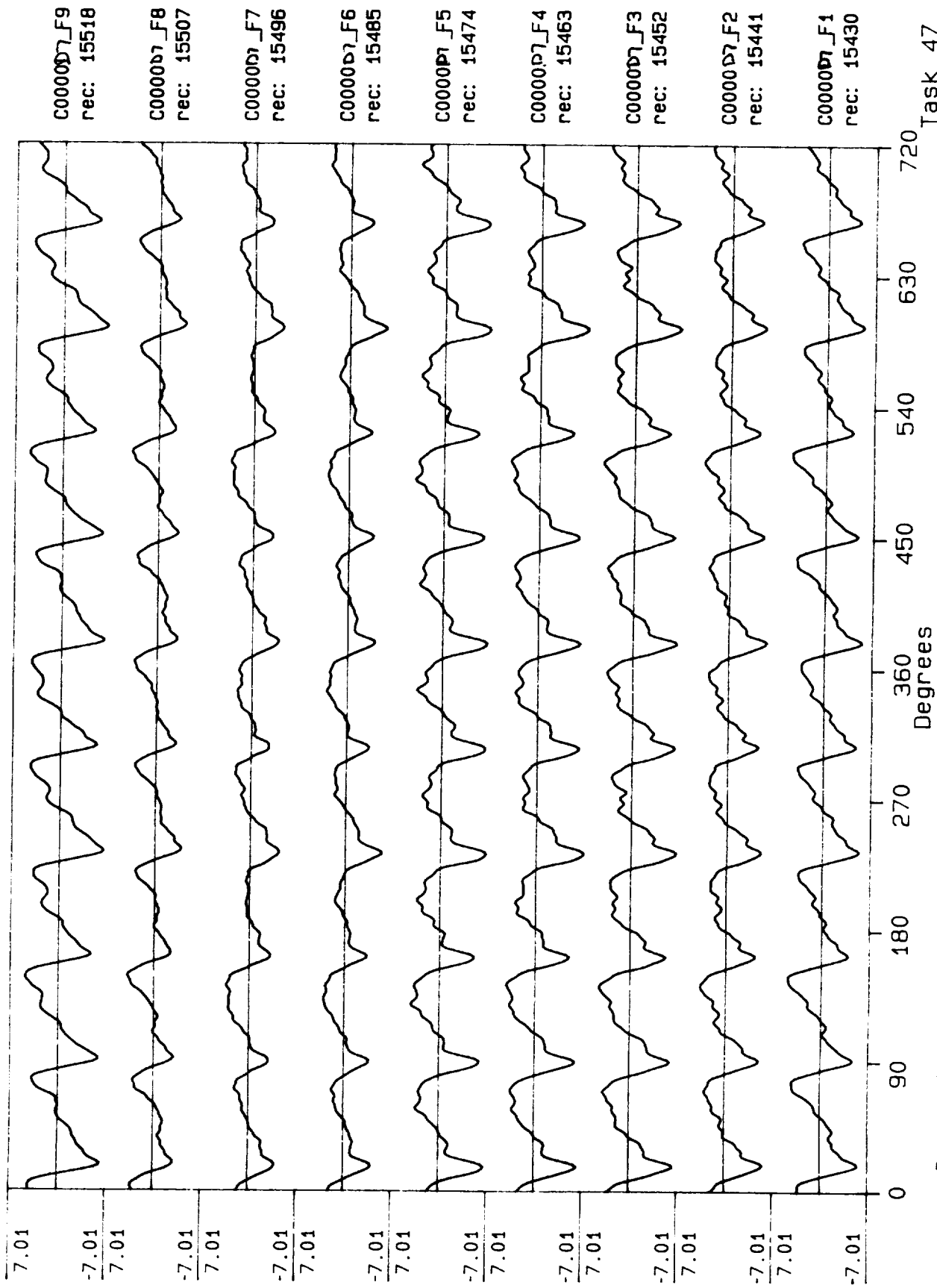
Process included: Calibration, Phase correction and DC filtering. Published: 06/20/89



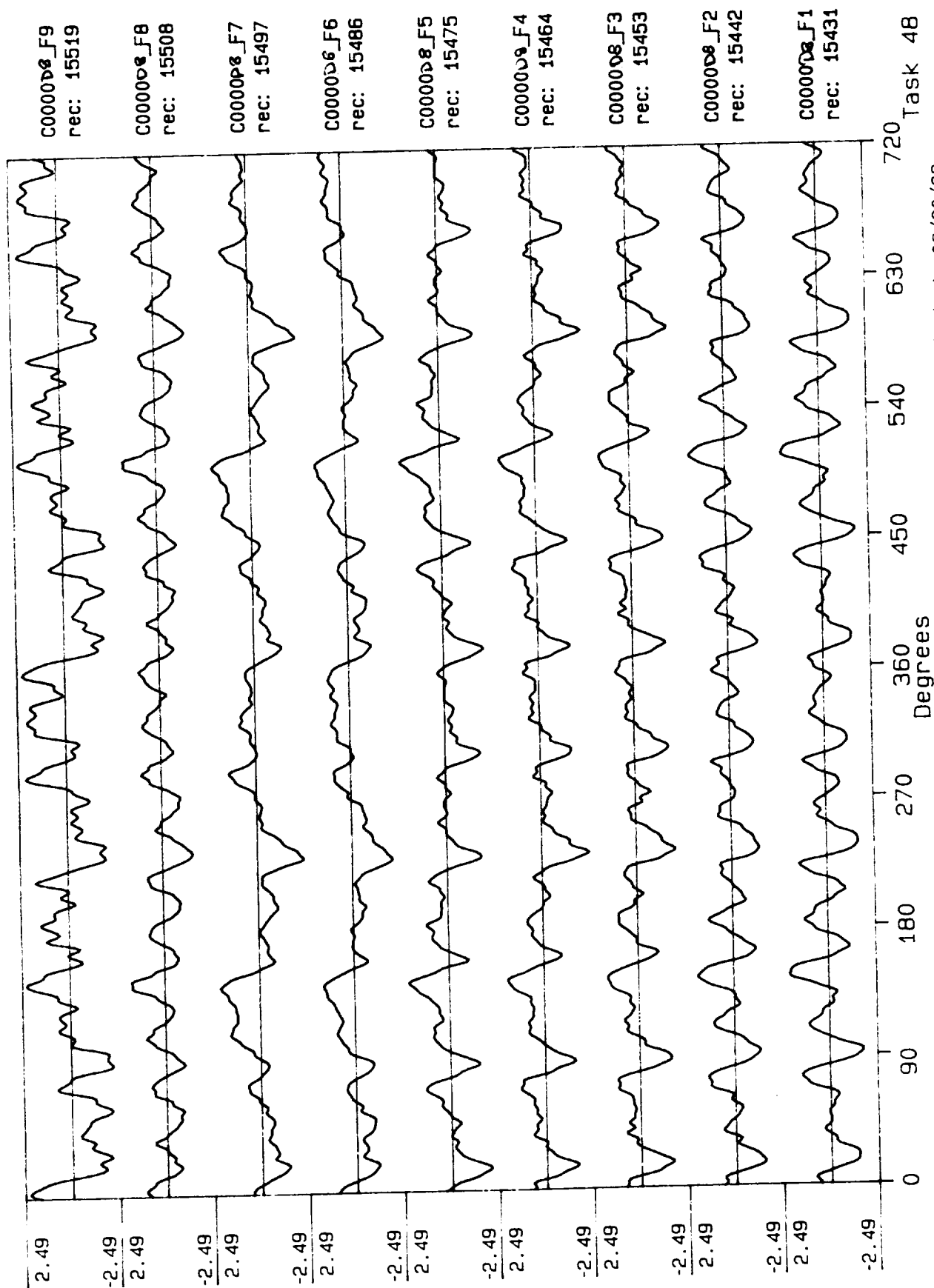
Process included: Calibration, Phase correction and DC filtering. Published: 06/20/89



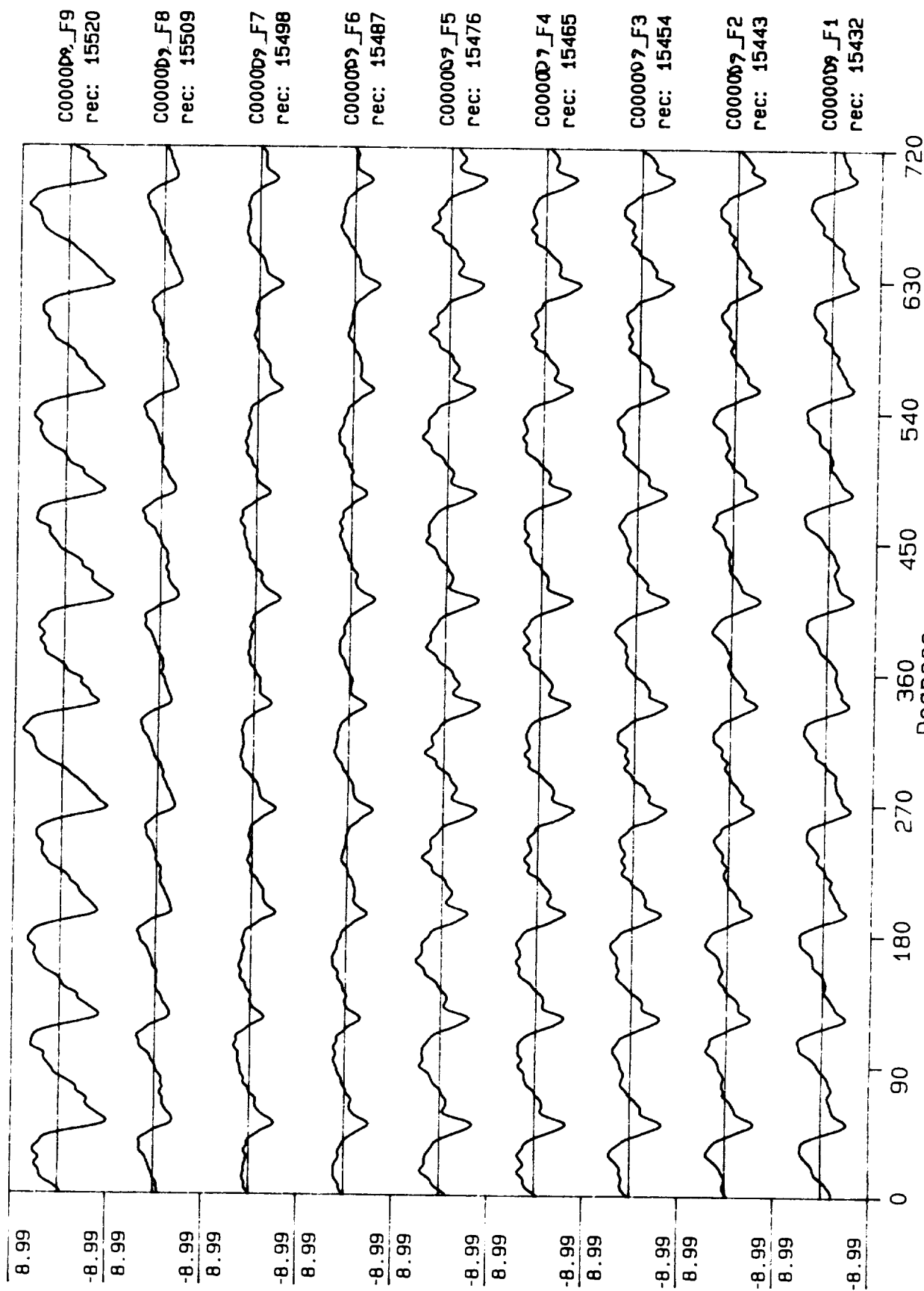
Process included: Calibration, Phase correction and DC filtering. Published: 06/20/89



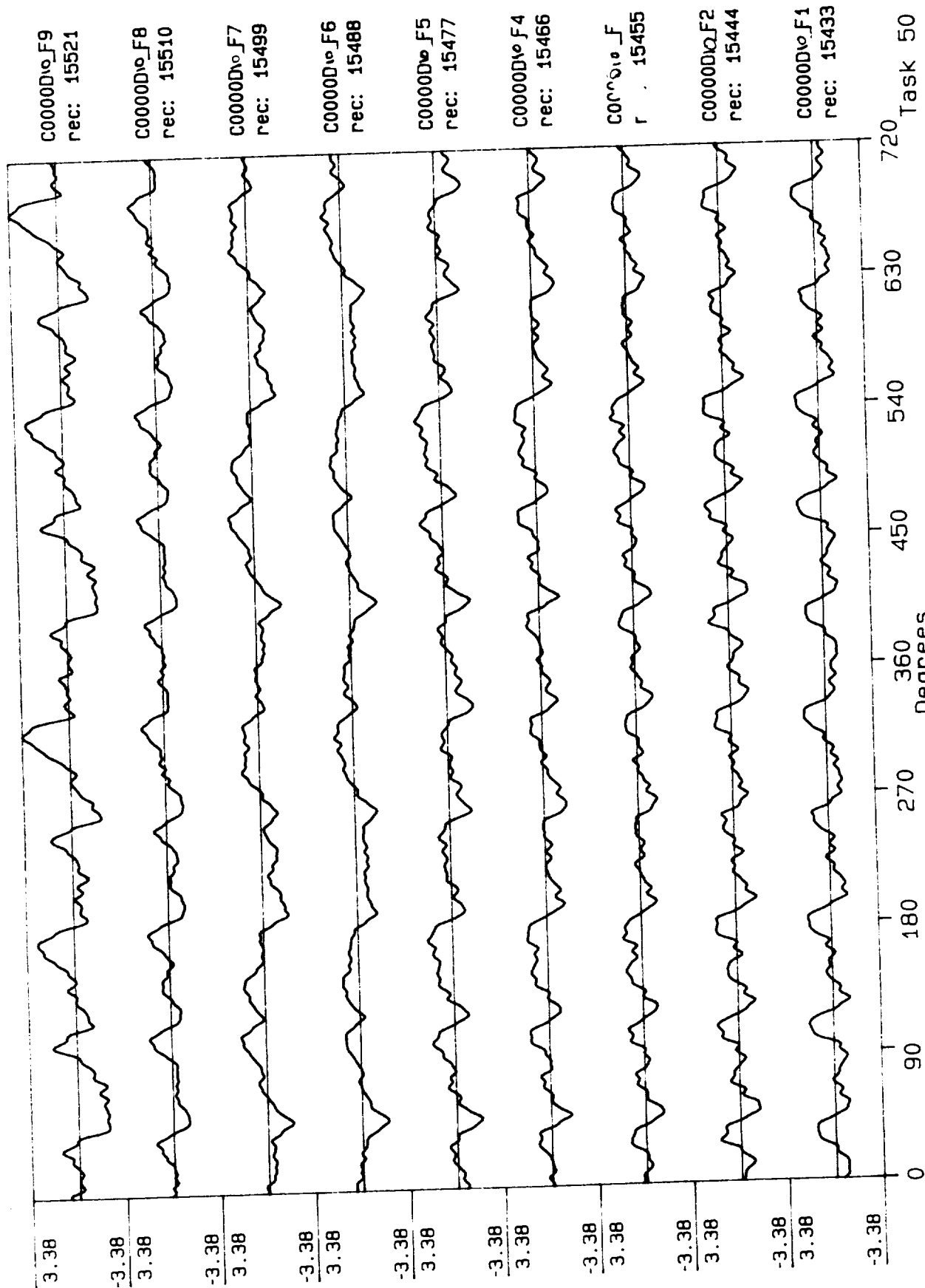
Process included: Calibration, Phase correction and DC filtering. Published: 06/20/89



Process included: Calibration, Phase correction and DC filtering. Published: 06/20/89

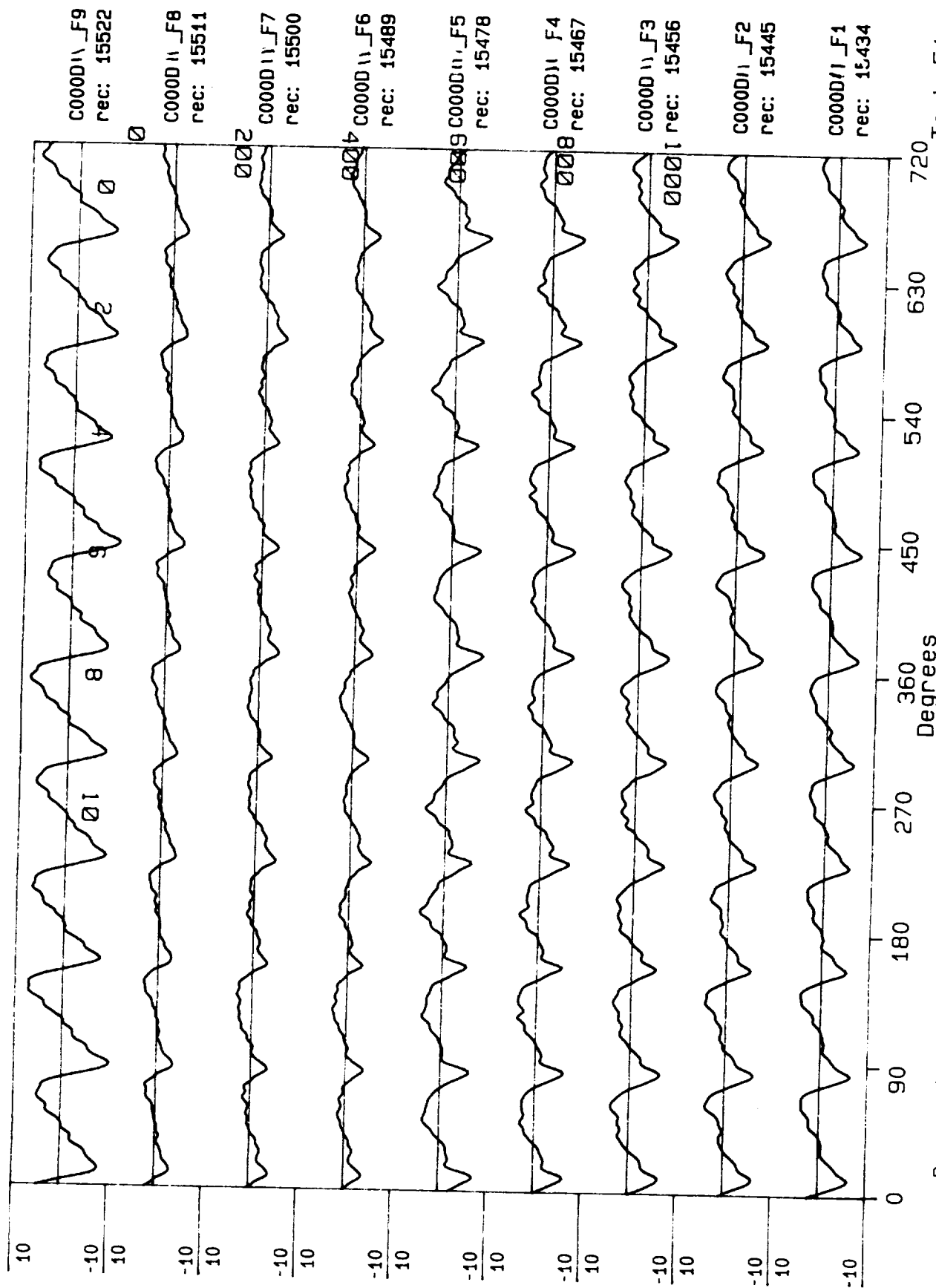


Process included: Calibration, Phase correction and DC filtering. Published: 06/20/89

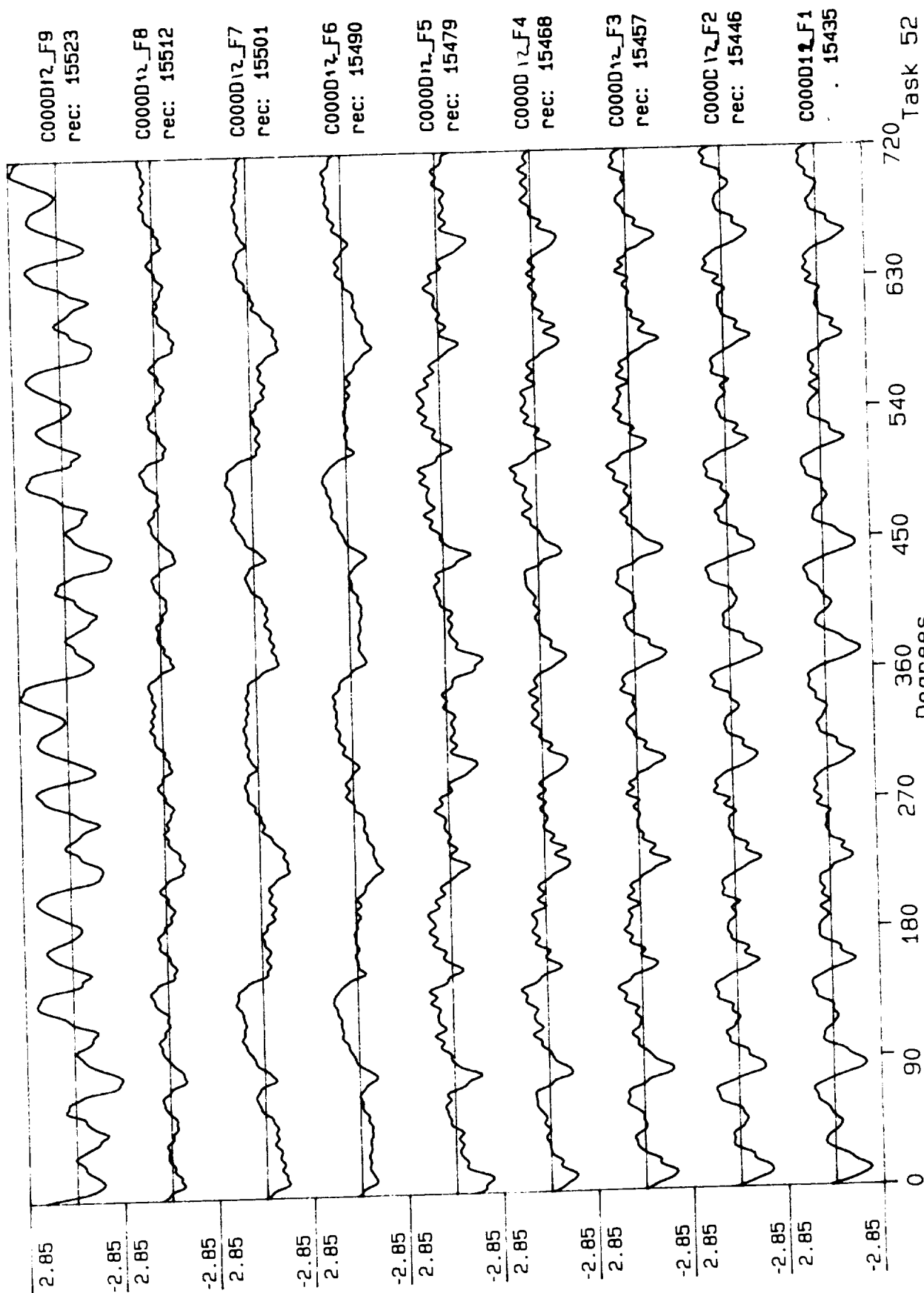


Task 50

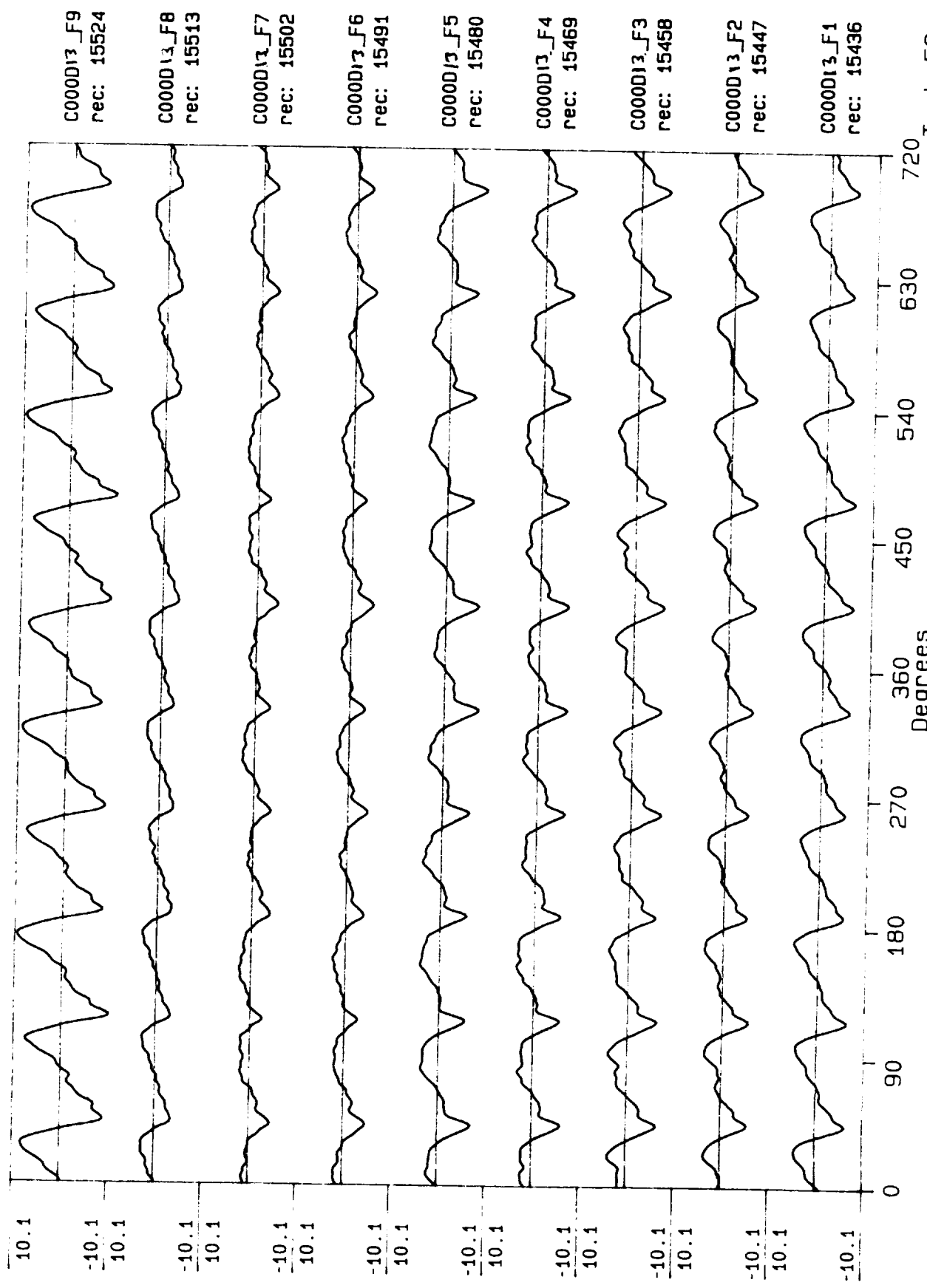
Process included: Calibration, Phase correction and DC filtering. Published: 06/20/89

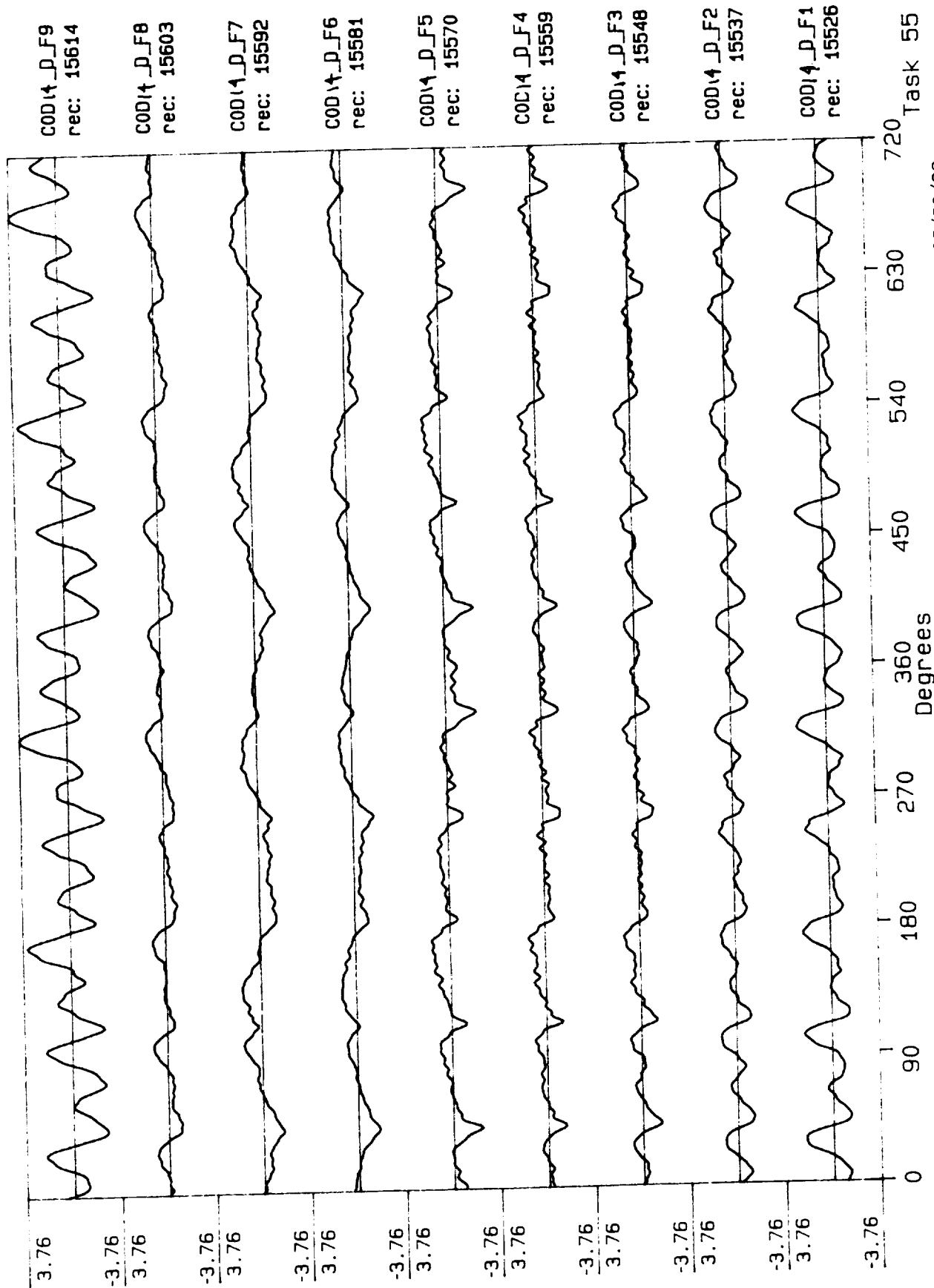


Process included: Calibration, Phase correction and DC filtering. Published: 06/20/89

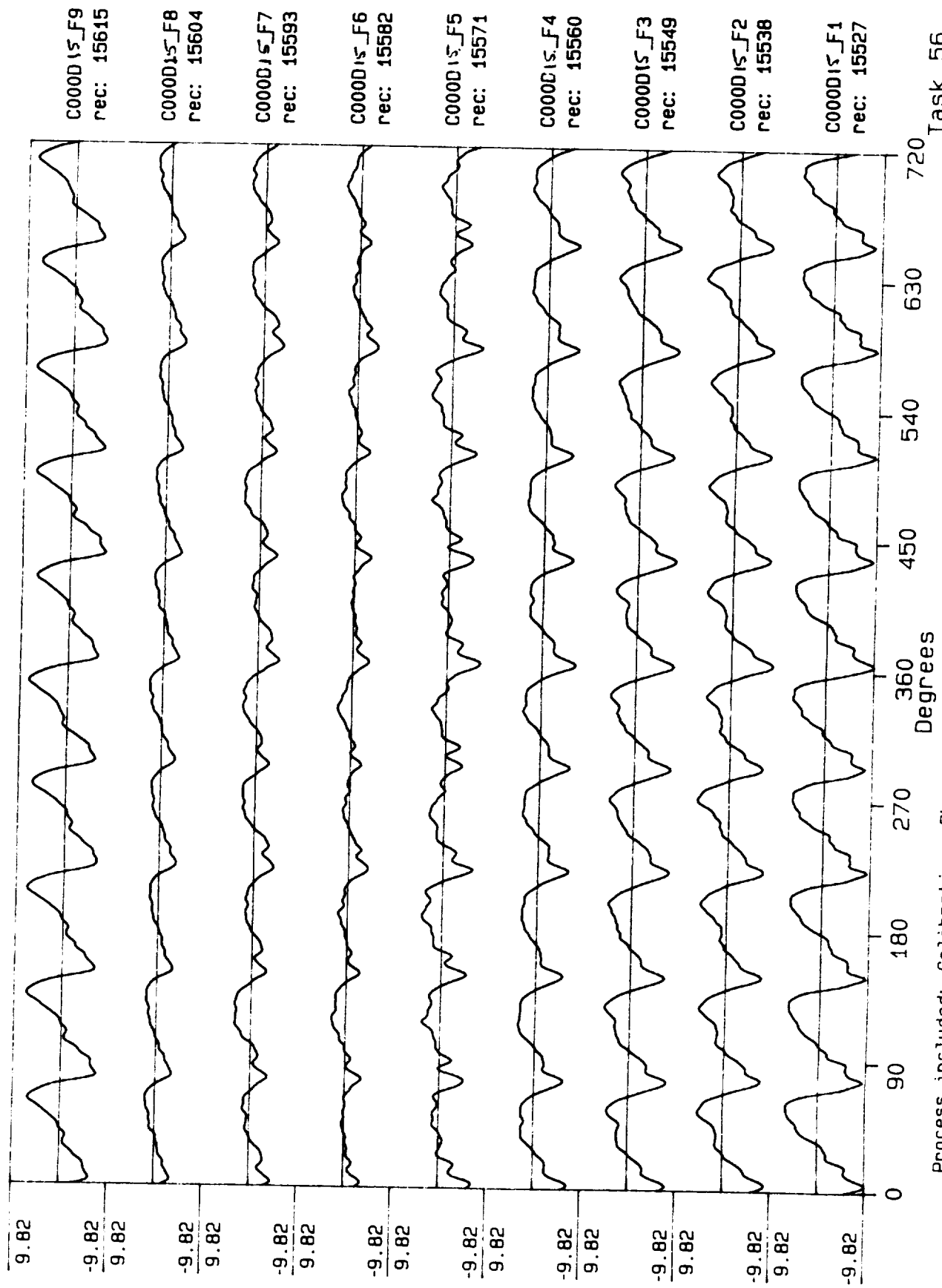


Process included: Calibration, Phase correction and DC filtering. Published: 06/20/89

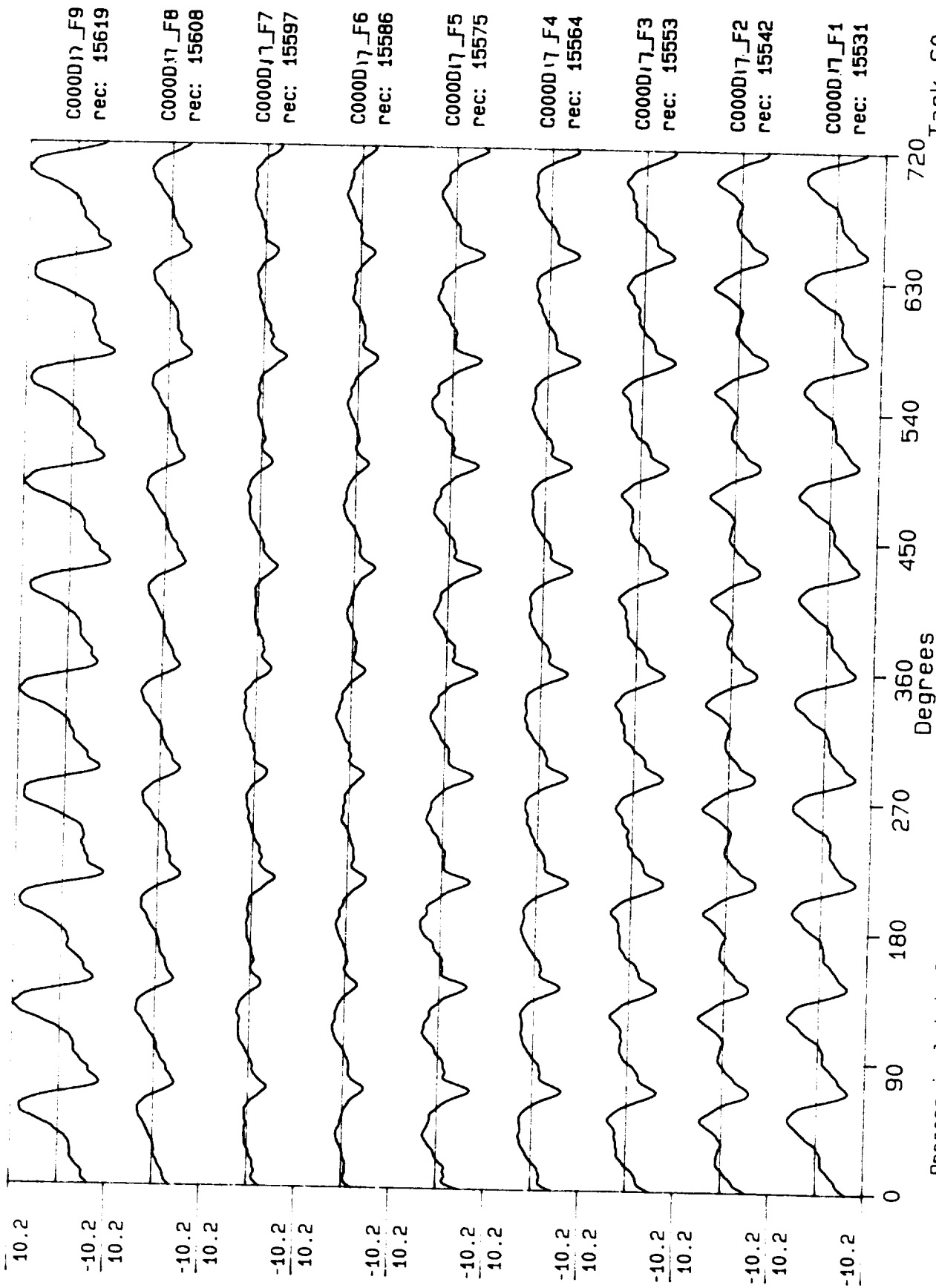




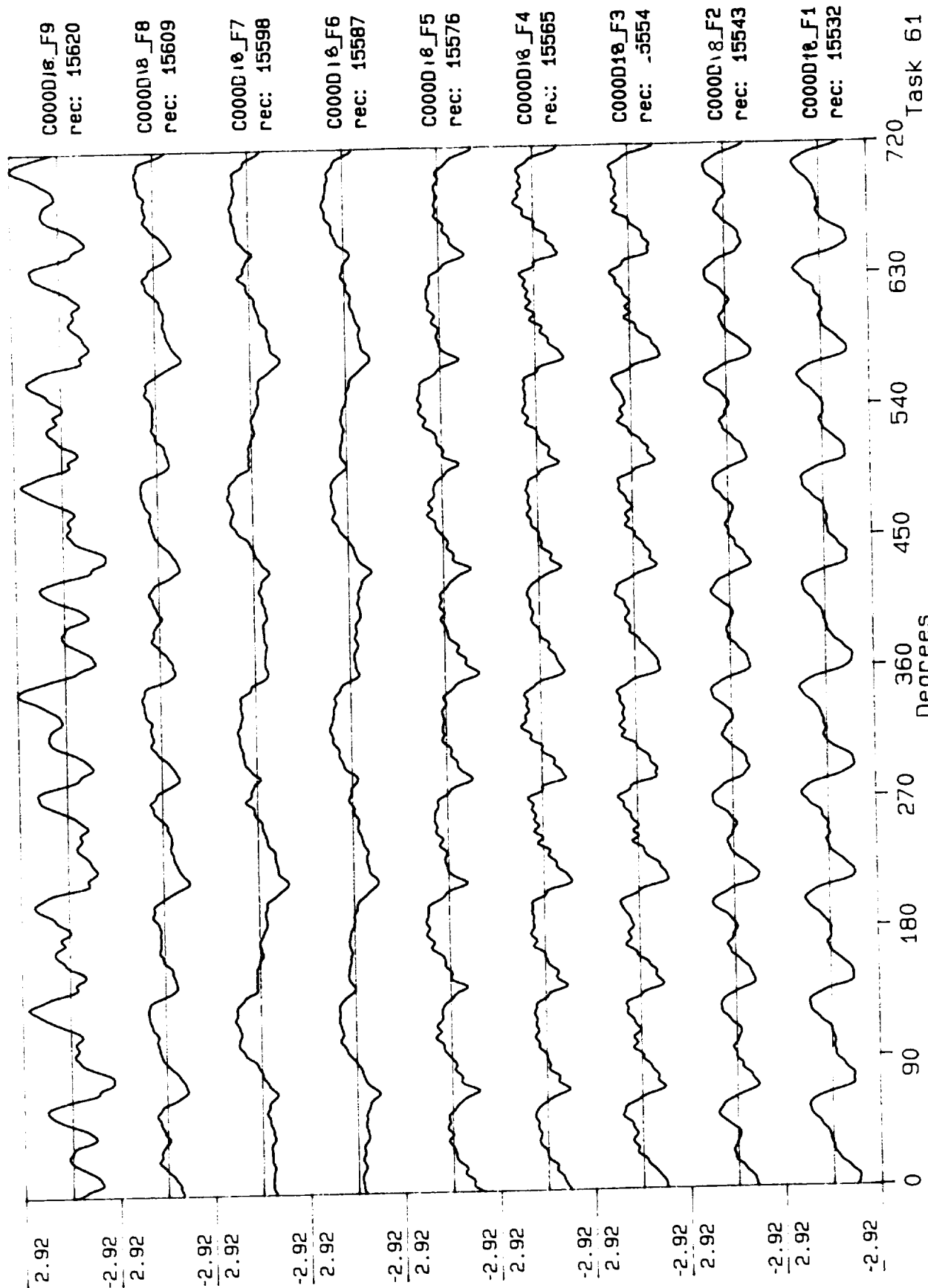
Process included: Calibration, Phase correction and DC filtering. Published: 06/20/89



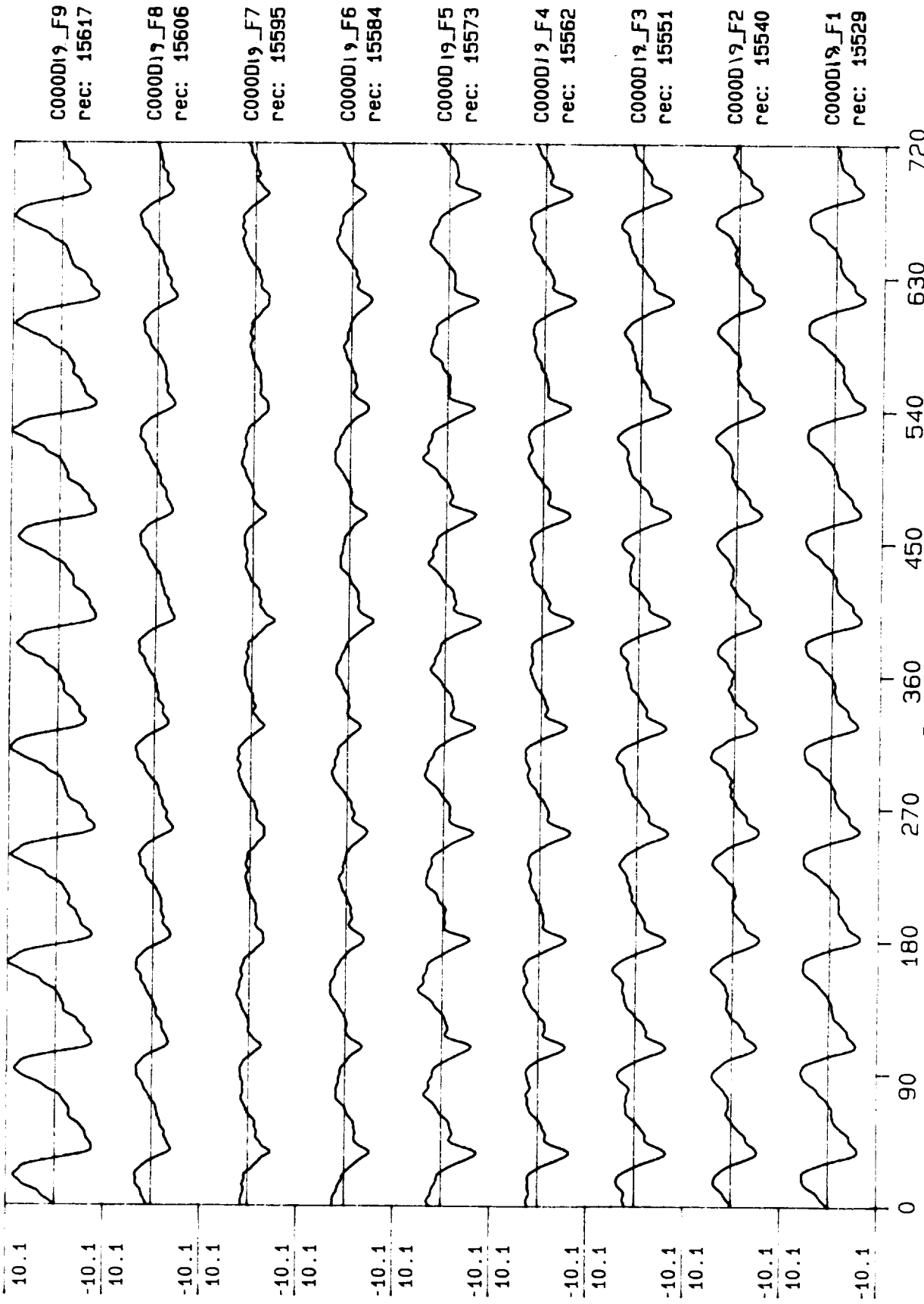
Process included: Calibration, Phase correction and DC filtering. Published: 06/20/89



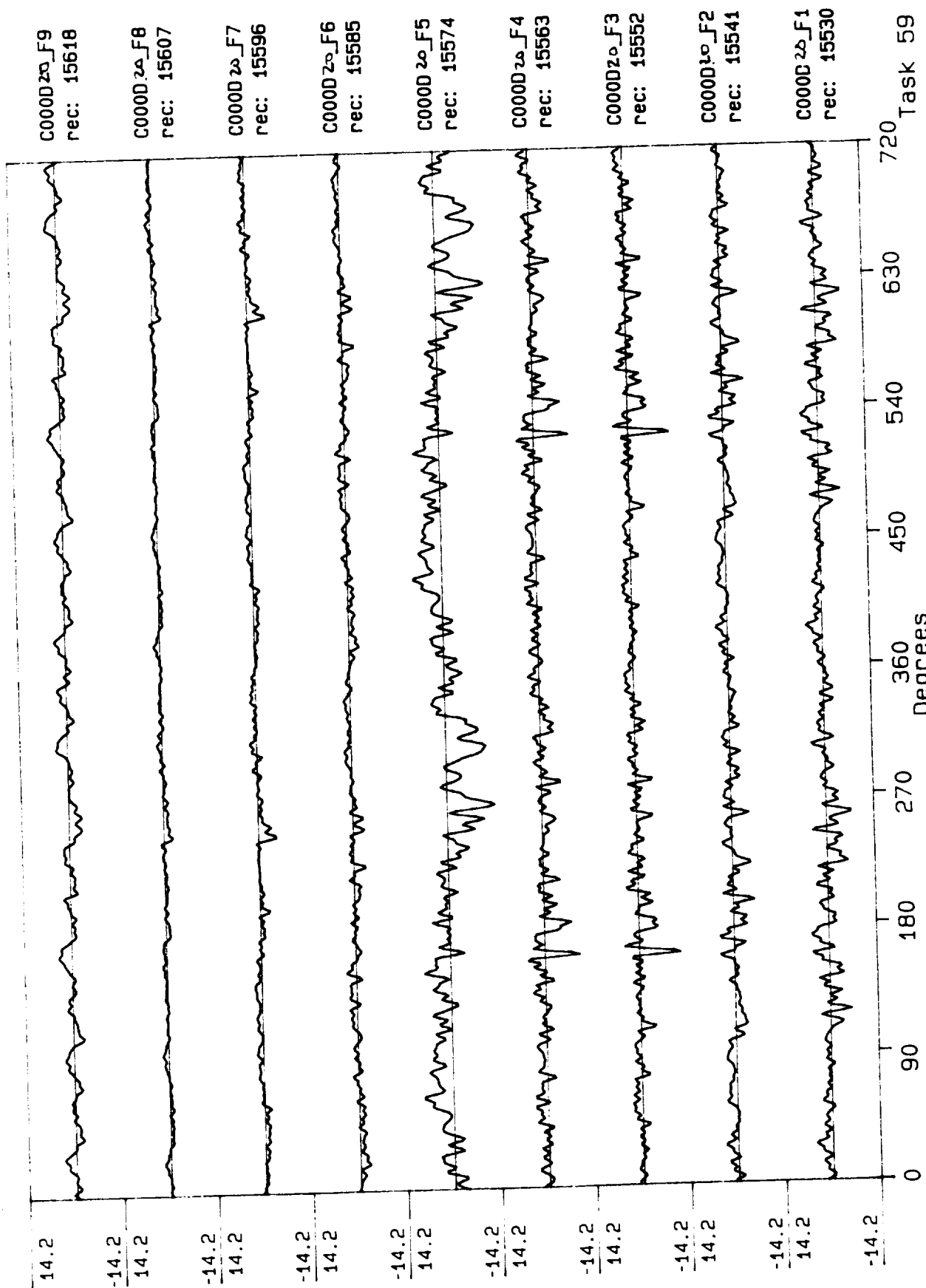
Process included: Calibration, Phase correction and DC filtering. Published: 06/20/89



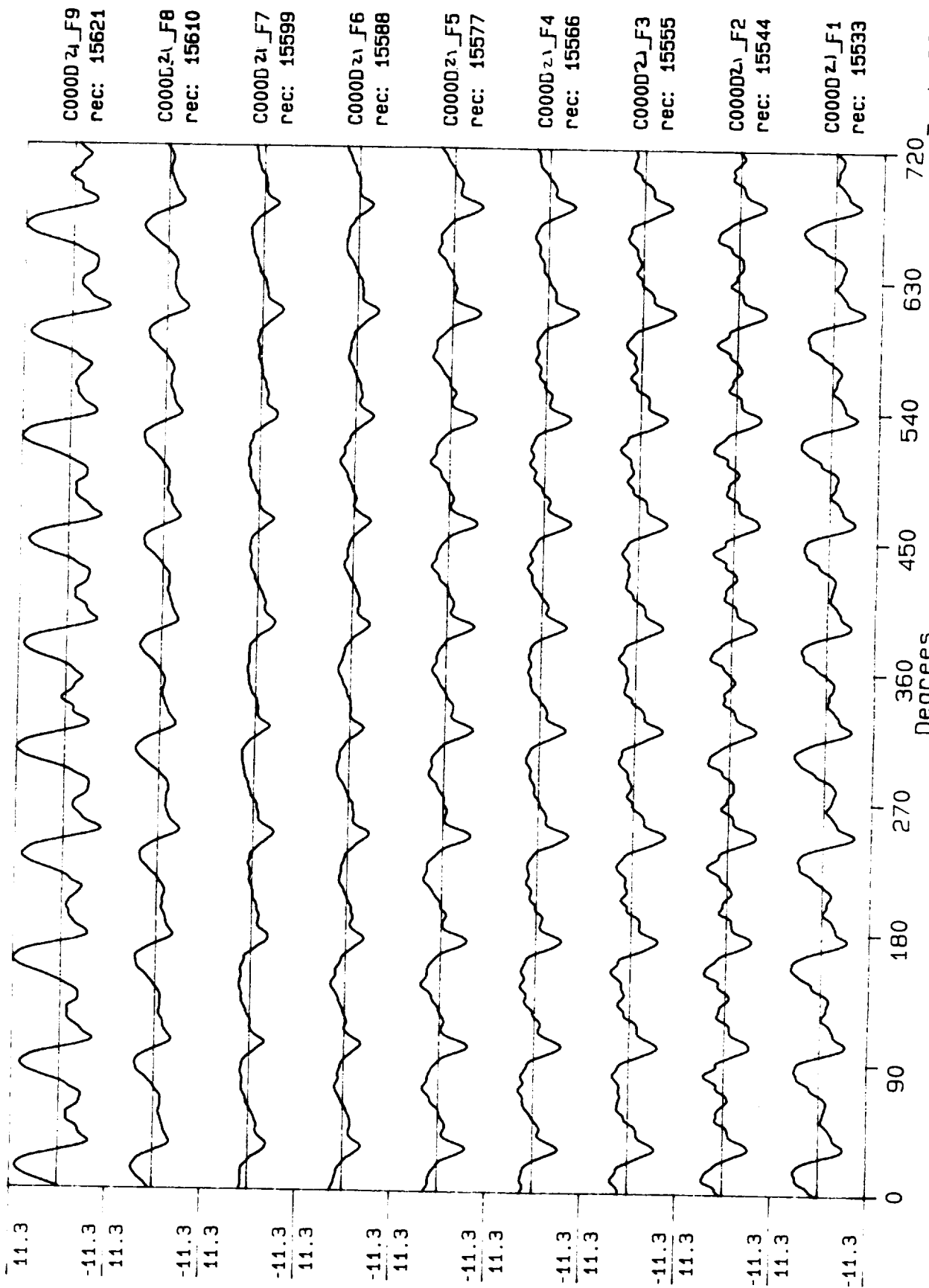
Process included: Calibration, Phase correction and DC filtering. Published: 06/20/89



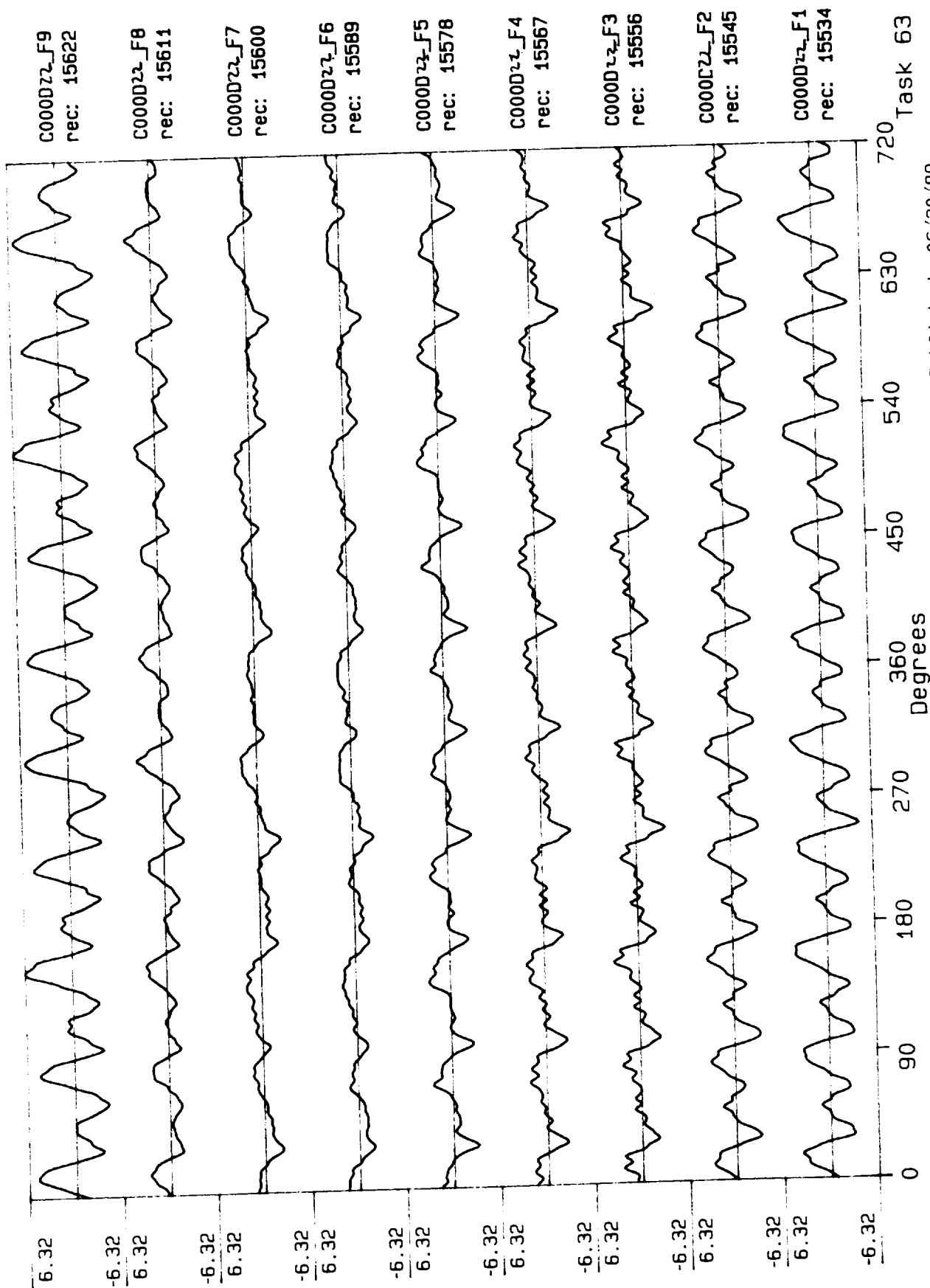
Process included: Calibration, Phase correction and DC filtering. Published: 06/20/89



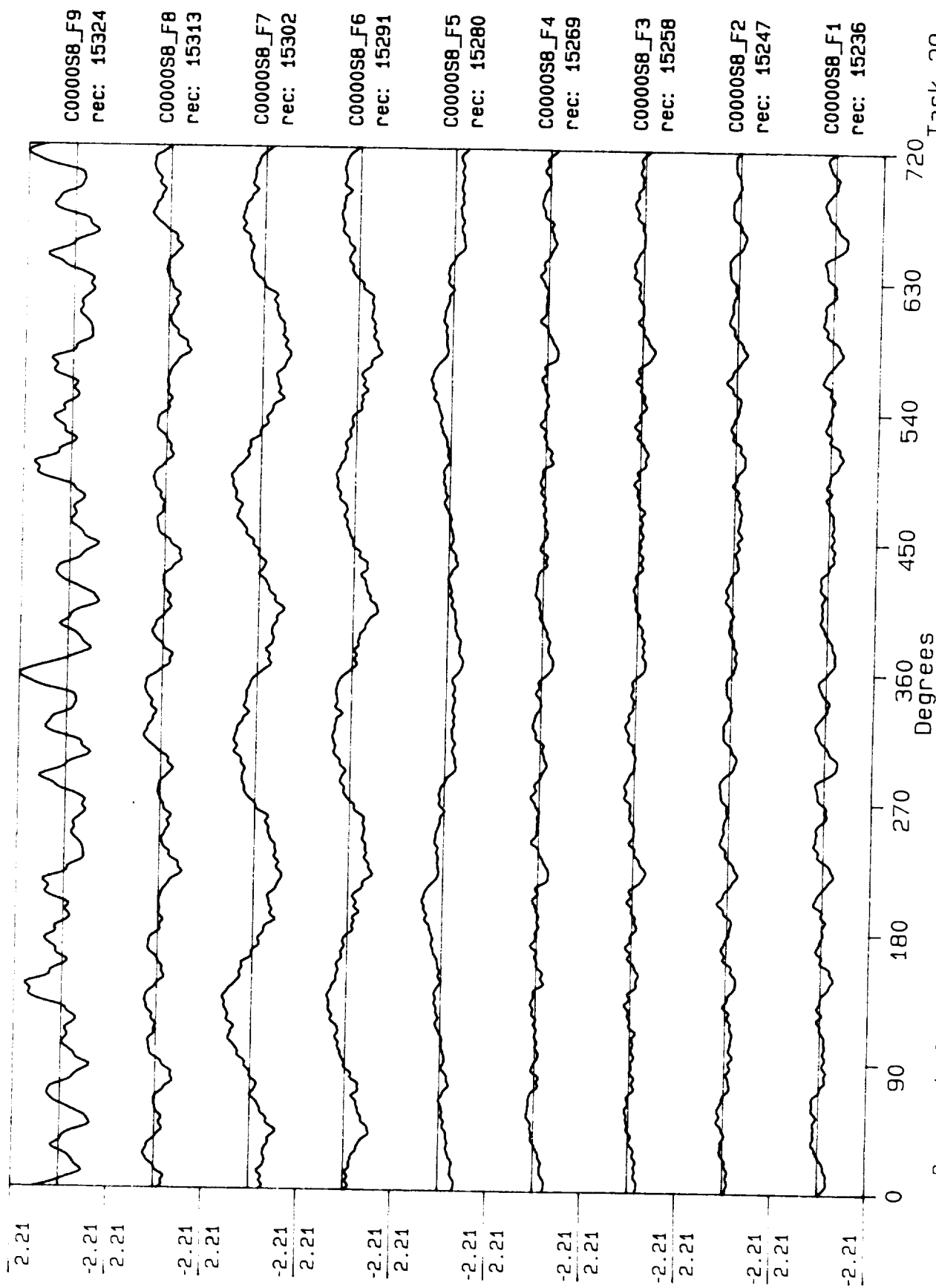
Process included: Calibration, Phase correction and DC filtering. Published: 06/20/89

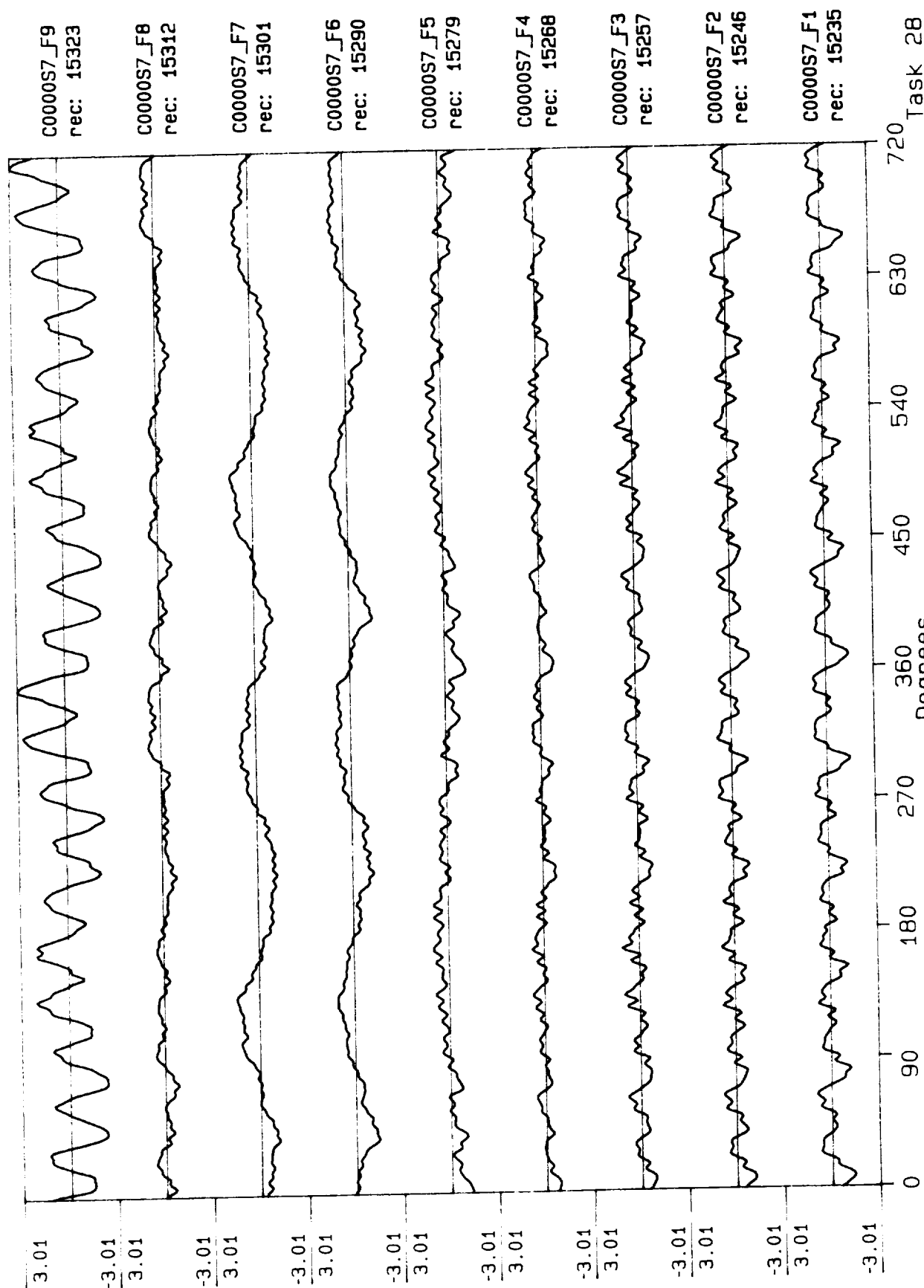


Process included: Calibration, Phase correction and DC filtering. Published: 06/20/89

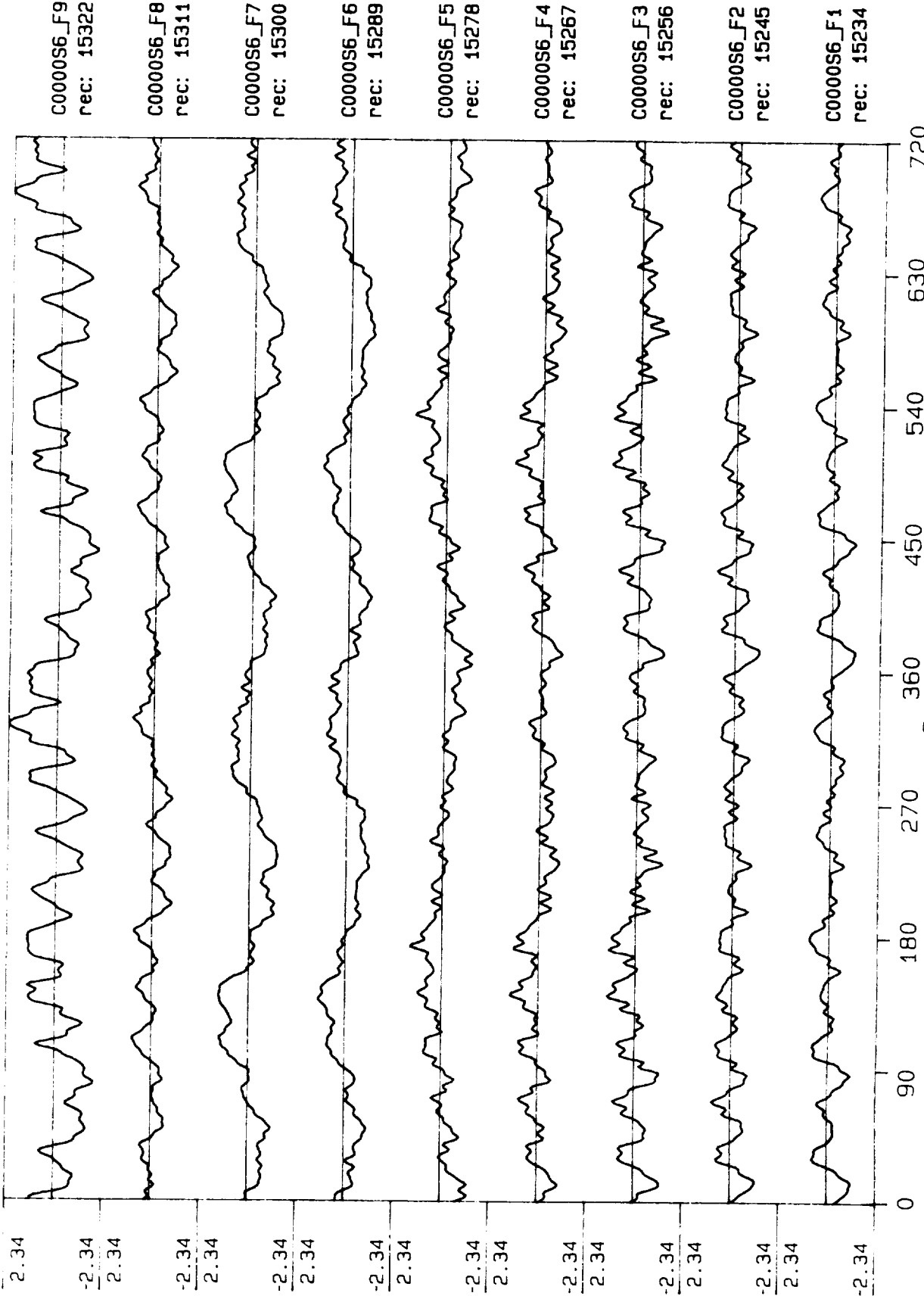


Process included: Calibration, Phase correction and DC filtering. Published: 06/20/89

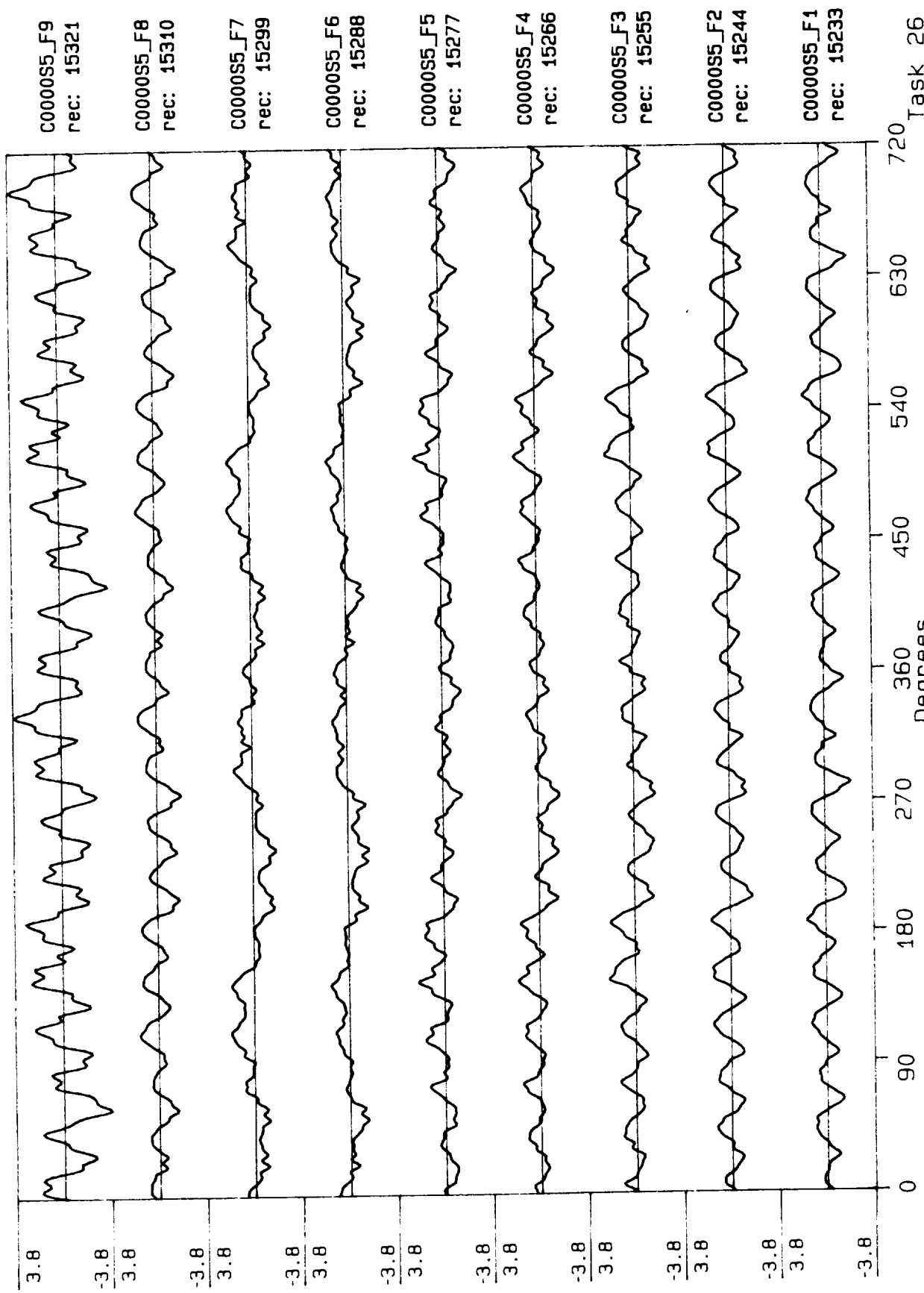




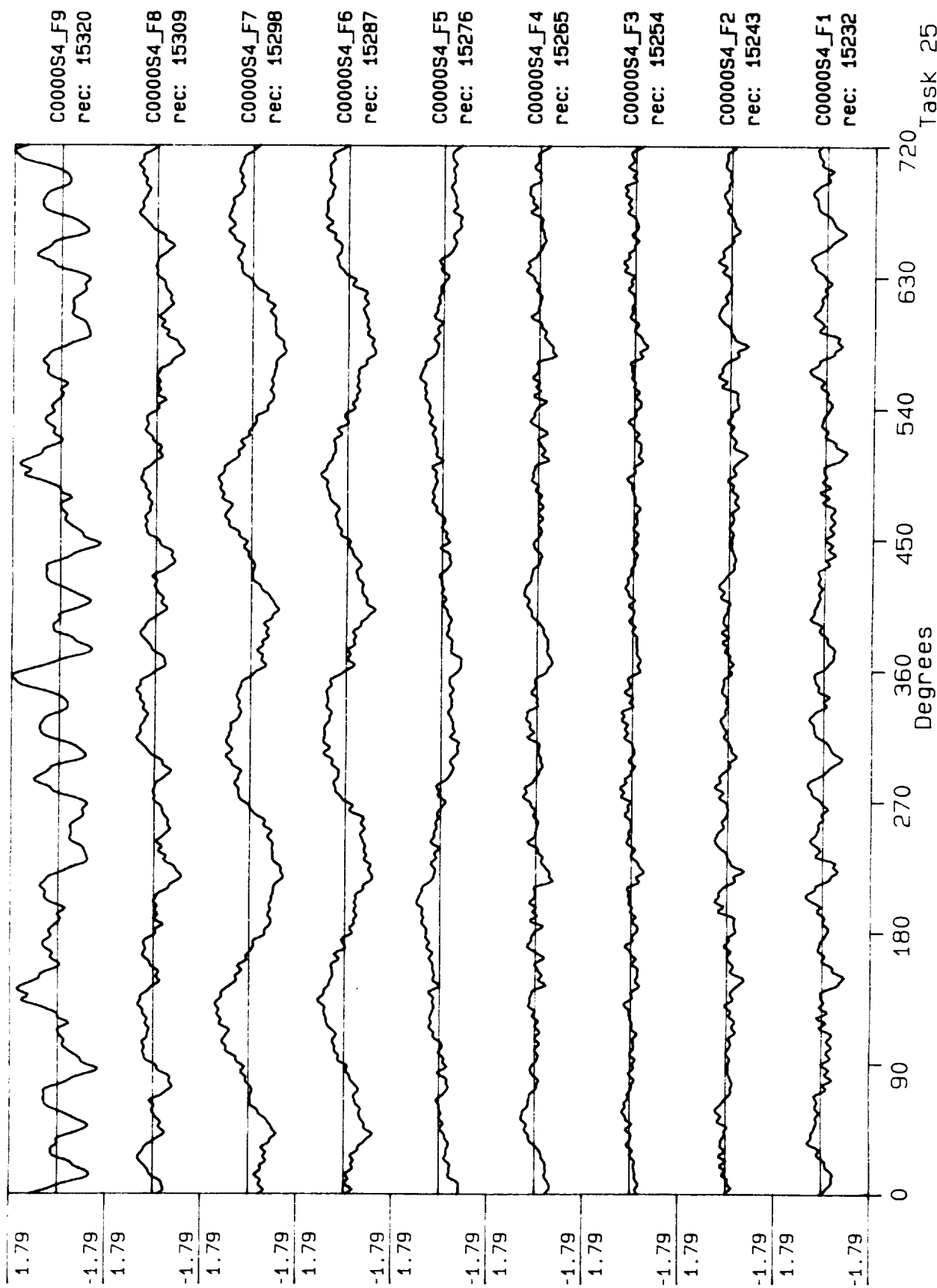
Process included: Calibration, Phase correction and DC filtering. Published: 06/20/89



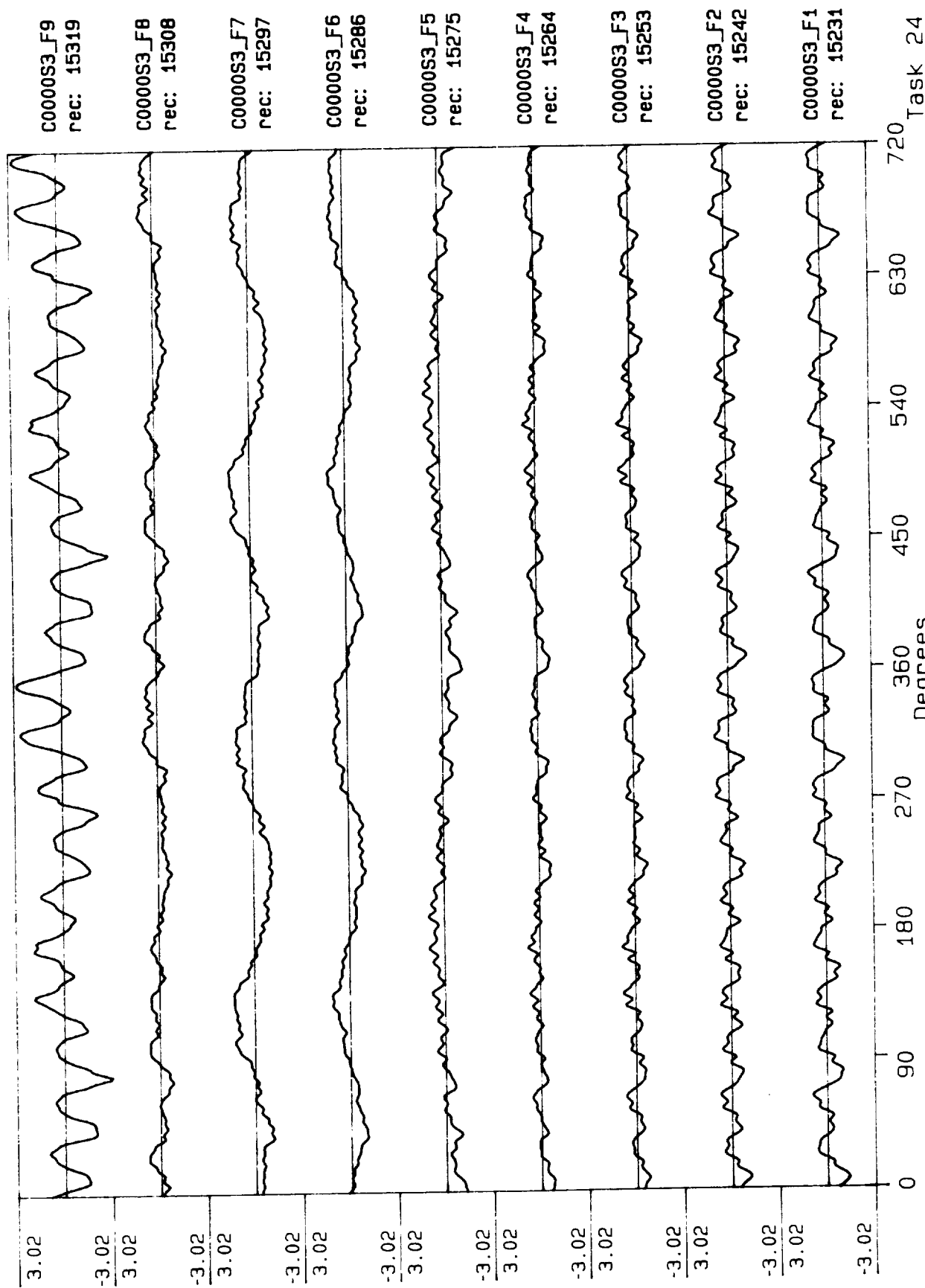
Process included: Calibration, Phase correction and DC filtering. Published: 06/20/89



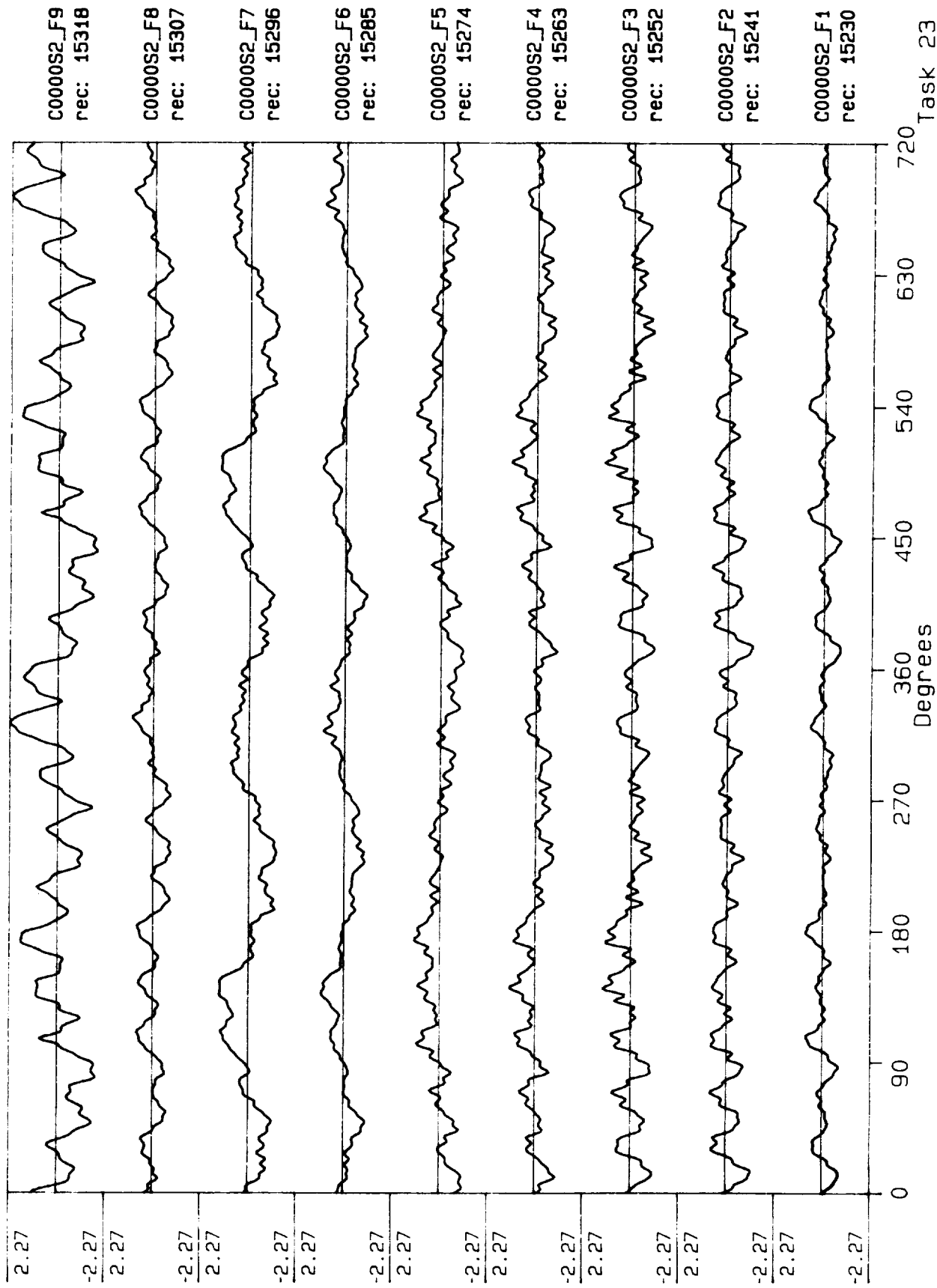
Process included: Calibration, Phase correction and DC filtering. Published: 06/20/89



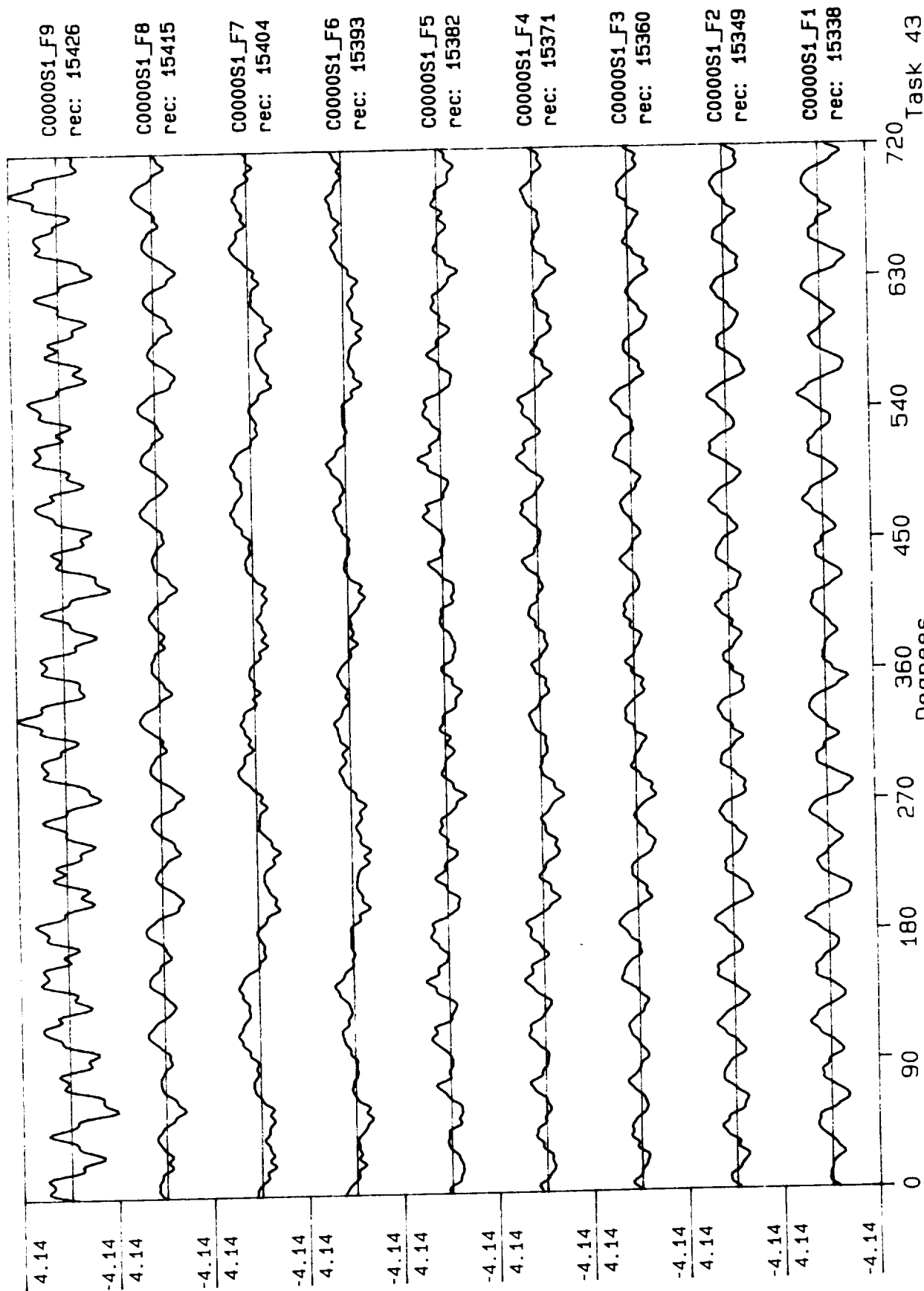
Process included: Calibration, Phase correction and DC filtering. Published: 06/20/89



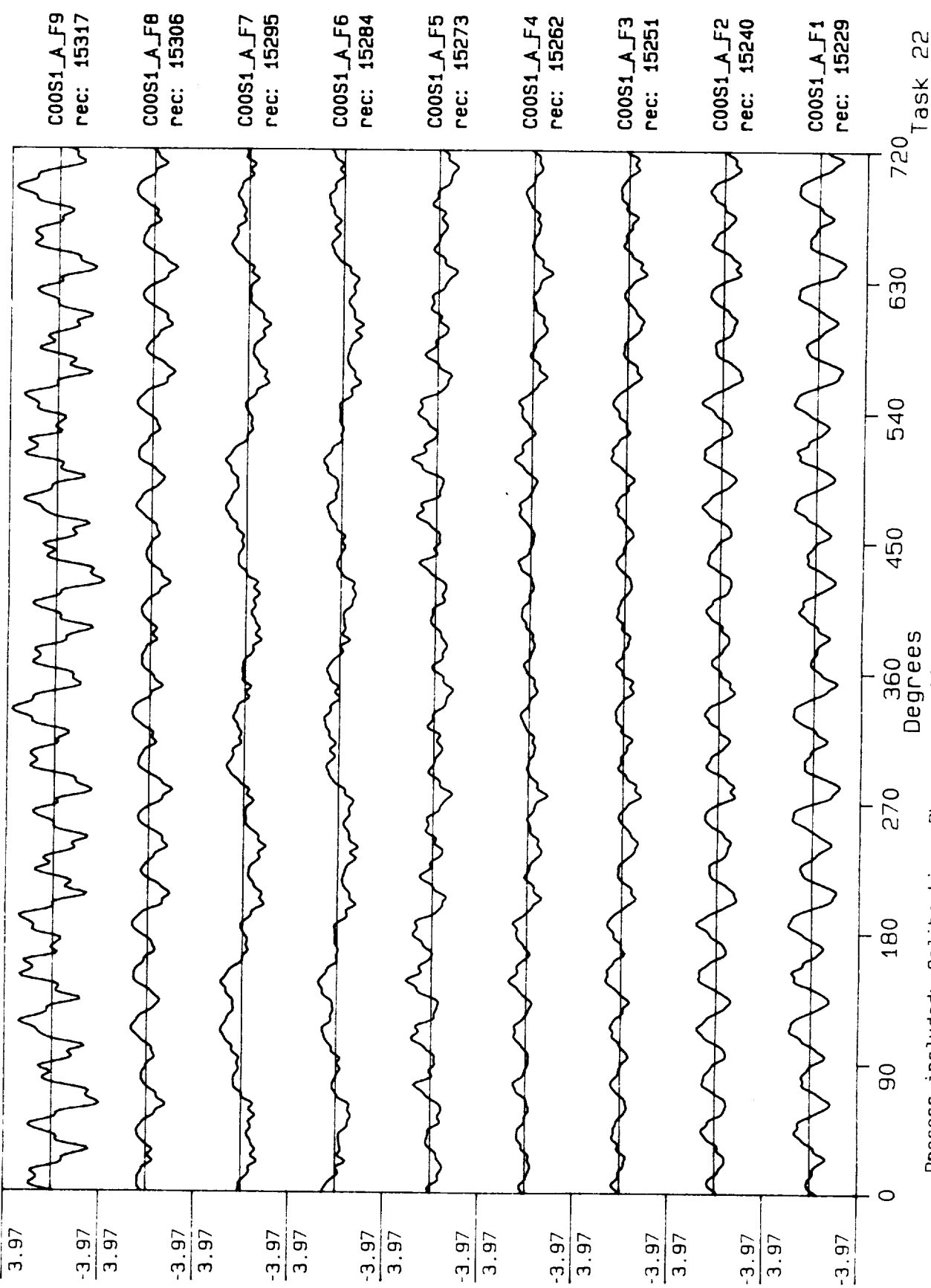
Process included: Calibration, Phase correction and DC filtering.



Process included: Calibration, Phase correction and DC filtering. Published: 06/20/89



Process included: Calibration, Phase correction and DC filtering. Published: 06/20/89



Process included: Calibration, Phase correction and DC filtering. Published: 06/20/89



Report Documentation Page

1. Report No.	2. Government Accession No.	3. Recipient's Catalog No.	
4. Title and Subtitle Fluctuating Pressures in Pump Diffuser and Collector Scrolls -- Final Report		5. Report Date August, 1989	
		6. Performing Organization Code	
7. Author(s) Donald P. Sloteman		8. Performing Organization Report No.	
		10. Work Unit No.	
9. Performing Organization Name and Address Ingersoll-Rand Company Research & Development Department 942 Memorial Parkway Phillipsburg, NJ 08865		11. Contract or Grant No.	
		13. Type of Report and Period Covered Final Report	
12. Sponsoring Agency Name and Address NASA George C. Marshall Space Flight Center Marshall Space Flight Center, AL 35812		14. Sponsoring Agency Code	
15. Supplementary Notes			
16. Abstract			
17. Key Words (Suggested by Author(s))		18. Distribution Statement "Unclassified-Unlimited"	
19. Security Classif. (of this report)	20. Security Classif. (of this page)	21. No. of pages	22. Price

PREPARATION OF THE REPORT DOCUMENTATION PAGE

The last page of a report facing the third cover is the Report Documentation Page, RDP. Information presented on this page is used in announcing and cataloging reports as well as preparing the cover and title page. Thus it is important that the information be correct. Instructions for filling in each block of the form are as follows:

Block 1. Report No. NASA report series number, if preassigned.

Block 2. Government Accession No. Leave blank.

Block 3. Recipient's Catalog No. Reserved for use by each report recipient.

Block 4. Title and Subtitle. Typed in caps and lower case with dash or period separating subtitle from title.

Block 5. Report Date. Approximate month and year the report will be published.

Block 6. Performing Organization Code. Leave blank.

Block 7. Author(s). Provide full names exactly as they are to appear on the title page. If applicable, the word editor should follow a name.

Block 8. Performing Organization Report No. NASA installation report control number and, if desired, the non-NASA performing organization report control number.

Block 9. Performing Organization Name and Address. Provide affiliation (NASA program office, NASA installation, or contractor name) of authors.

Block 10. Work Unit No. Provide Research and Technology Objectives and Plans (RTOP) number.

Block 11. Contract or Grant No. Provide when applicable.

Block 12. Sponsoring Agency Name and Address. National Aeronautics and Space Administration, Washington, D.C. 20546-0001. If contractor report, add NASA installation or HQ program office.

Block 13. Type of Report and Period Covered. NASA formal report series; for Contractor Report also list type (interim, final) and period covered when applicable.

Block 14. Sponsoring Agency Code. Leave blank.

Block 15. Supplementary Notes. Information not included elsewhere: affiliation of authors if additional space is re-

quired for block 9, notice of work sponsored by another agency, monitor of contract, information about supplements (film, data tapes, etc.), meeting site and date for presented papers, journal to which an article has been submitted, note of a report made from a thesis, appendix by author other than shown in block 7.

Block 16. Abstract. The abstract should be informative rather than descriptive and should state the objectives of the investigation, the methods employed (e.g., simulation, experiment, or remote sensing), the results obtained, and the conclusions reached.

Block 17. Key Words. Identifying words or phrases to be used in cataloging the report.

Block 18. Distribution Statement. Indicate whether report is available to public or not. If not to be controlled, use "Unclassified-Unlimited." If controlled availability is required, list the category approved on the Document Availability Authorization Form (see NHB 2200.2, Form FF427). Also specify subject category (see "Table of Contents" in a current issue of STAR), in which report is to be distributed.

Block 19. Security Classification (of this report). Self-explanatory.

Block 20. Security Classification (of this page). Self-explanatory.

Block 21. No. of Pages. Count front matter pages beginning with iii, text pages including internal blank pages, and the RDP, but not the title page or the back of the title page.

Block 22. Price Code. If block 18 shows "Unclassified-Unlimited," provide the NTIS price code (see "NTIS Price Schedules" in a current issue of STAR) and at the bottom of the form add either "For sale by the National Technical Information Service, Springfield, VA 22161-2171" or "For sale by the Superintendent of Documents, U.S. Government Printing Office, Washington, DC 20402-0001," whichever is appropriate.

